PROCEEDINGS OF THE IRE®

Published Monthly by

The Institute of Radio Engineers, Inc.

VOLUME 45 — *December, 1957* — NUMBER 12

Authors are requested to submit three copies of manuscripts and illustrations to the Editorial Department, Institute of Radio Engineers, 1 East 79 St., New York 21, N. Y.

CONTENTS

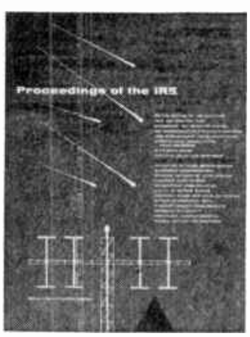

THE COVER—The outline of an antenna against a background of meteor trails symbolizes a new type of communication system which utilizes the ionization produced in these trails to transmit intermittent low-power vhf signals over greatly extended distances. The first complete discussion of propagation phenomena, system characteristics, types of equipment, and operating results is reported in a special series of 12 papers and 2 letters to the editor which start on page 1642 of this issue.

Change of address (with 15 days advance notice) and letters regarding subscriptions and payments should be mailed to the Secretary of the IRE, 1 East 79 Street, New York 21, N. Y.

PROCEEDINGS OF THE IRE

Published Monthly by

The Institute of Radio Engineers, Inc.

(Continued)

IRE News and Radio Notes:

Books:

ADVERTISING SECTION

Poles and Zeros

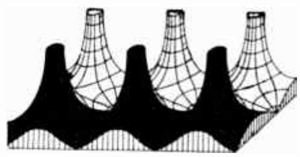

Meteors. This issue presents twelve papers and two letters on an unique form of radio communication, in which the ionization created by the flight of a meteor is an essential element of the propagation path. Ten years ago, no one would have suggested that so transient and unpredictable a phenomenon as a meteor trail could be used in communications. Since then our growing ability to cram large amounts of information into a short space of time has so altered the situation that a practical system has emerged.

The PROCEEDINGS in March, 1948 reported that the FCC monitoring staff at Grand Island, Nebraska had, as early as 1943, picked up short bursts of fm broadcast programs from Boston, at a distance of 1370 miles. The sporadic and transitory nature of the transmission suggested an intense and highly localized patch of ionization and it was then suggested that the impact of meteors might be the cause. For a while thereafter meteor bursts were considered a minor nuisance, a mere statistic in interference predictions. Following the war, propagation scientists in Canada, Great Britain and the United States made a systematic study of meteoric ionization. By 1950, enough was known to suggest work on a communication system. The initiative was taken by the Canadian Defense Research Board and Stanford University. By 1954 the Canadian group had the first closed-loop meteor circuit in operation. As seems unavoidable in probing new techniques in communication, this work was classified and the profession at large knew little about it.

About a year ago IRE President Henderson, who as Principal Research Officer of the Canadian National Research Council was in the know, passed the word to the Editorial Board that the Canadian work was being declassified and that a group of four papers would be forthcoming. We expressed interest in publishing them. Then followed an act of high professional courtesy. The Canadian workers, assuming (correctly) that we might not know that similar work was proceeding under security wraps in the United States, suggested that it might be well to delay publication of the Canadian papers pending negotiation for a series of U.S.A. papers. Following this lead, the editorial staff rounded up eight additional papers. Nearly all the information contained in these papers, Canadian and U.S., was declassified in 1957.

Interest in these papers extends well beyond the propagation effects on which the meteor system is based, since the techniques of high speed, wideband communication and storage of information are intimately woven into the system design. We particularly wish to thank the authors of the Canadian contributions for their good will, which has made it possible for us to bring all the information together in one issue.

Lefthanded. Since 1948 we have printed a black-and-white "barber pole" border on the front outside edge of the contents page of the PROCEEDINGS. Thereby, this most-often-turned-to page can be found by bending the issue so that the edges of the pages are exposed. We were recently reminded that this handy device has been of no use whatever to the left-handed, of which persuasion the Institute has over 2000 members. To assist this sinistral host, we now print the barber pole on both sides of the page.—D.G.F.

Language. It was with some surprise that we found on the editorial page of *The New York Times* (October 21, 1957) a highly technical description, complete with formulas, of the Doppler shift technique of determining how closely the earth satellite passes an observer. The *Times*, a little shaken by this experience with scientific lingo, went on to note* "... it isn't just the sputnik that is up in the air; it is most of the rest of us. The scientist, even when doing his best to be simple, speaks another language .... Perhaps we had all better learn that language."

Unfortunately, it is not only the layman who has difficulty understanding the scientist, but all too often, his fellow scientists as well. Specialized language no doubt causes some of the trouble. IRE Standards define some 3500 technical terms in our field alone and, as the *Times* suggests, it behooves us all to learn that language.

Too much of the trouble, though, lies in poor *use* of the language. Growing concern over the need for more effective communication between engineers has led to the formation of an IRE Professional Group on Engineering Writing and Speech, which in its first five months has already issued newsletters and held a highly successful national meeting. Most encouraging of all, 70% of its membership is made up of regular engineers, as opposed to publications people. We suggest that all members concerned with writing reports and giving talks would benefit by joining the PGEWS for only $2. —E.K.G.

Howard R. Hegbar

DIRECTOR, 1957-1958

Howard R. Hegbar was born in Valley City, N. D., in 1915. He received the degree of Bachelor of Science in electrical engineering at North Dakota State College in 1937, in 1938 the Master of Science degree, and the Ph.D degree in electrical engineering from the University of Wisconsin in 1941.

Employed by the Radio Corporation of America in 1941 as an electronic research engineer, Dr. Hegbar specialized in power tube and microwave magnetron development during five years at RCA's plants at Harrison and Princeton, N. J. He joined Goodyear Aircraft Corporation's Aerophysics Departments in Akron, Ohio, in 1946, working primarily in electronic guidance and control systems for missiles and aircraft, test equipment, and electronic computers. In 1957 he was placed in charge of Goodyear Aircraft's new Avionics and Electronics Engineering Division.

Dr. Hegbar is the inventor or co-inventor of patented devices in several fields, including magnetrons for pulsed operation, internally neutralized duplex tetrode uhf power tubes for television transmission, pulse-modulator circuits for parallel operation of thyratrons, and electronic ignition systems for jet engines.

In 1941, Dr. Hegbar joined the IRE as a Student Member; he became an Associate in 1942 and a Senior Member in 1946. He became a Fellow in 1957. He was chairman of the Akron Subsection in 1948–1949, and led the movement to establish the Akron Section. He served as first chairman of the Akron Section in 1949–1950. He is a member of the American Ordnance Association and of Sigma Xi.

Scanning the Issue

On the Nature of the Electron (Salpeter, p. 1588)—The average electronic engineer knows a good deal more about the uses of the electron than he does about the electron itself. What does it look like? What role does its spin play? Does an electron behave as a particle or a wave—or both? In this stimulating article, reprinted from the *Proceedings of the Institution of Radio Engineers Australia*, the reader is brought face to face with the electron and is shown its "private life" as revealed to us by fundamental concepts of modern physics.

A Thin Cathode-Ray Tube (Aiken, p. 1599)—A radically new type of cathode-ray tube has been developed which is only a few inches thick. The electron gun, instead of pointing directly at the face of the tube, is placed off to one side and aimed parallel to the bottom edge. Two sets of deflection plates bend the beam up and then into the tube face. The deflection plates can be made transparent by depositing transparent conducting material on the inside back of the glass envelope, thus making it possible to see the picture from the back as well as the front. When transparent phosphors are used on the tube face, the device is altogether transparent. This latter arrangement can be incorporated in an aircraft windshield for displaying on it flight information in bad weather without impairing the pilot's vision in good weather. A prototype model for TV receivers was demonstrated six weeks ago that was 2⅝ inches thick. Whether or not the thin tube becomes widely adopted for television, it represents the first major breakaway from conventional types of display tubes and, equally significant, involves new techniques that are finding important application in other fields.

New Microwave Repeater System Using a Single Traveling-Wave Tube as Both Amplifier and Local Oscillator (Kurokawa, *et al.*, p. 1604)—This paper describes a novel 480-channel microwave repeater system, now in use in Japan, which features the use of one traveling-wave tube for both power amplification and local oscillation. This arrangement does away with the need for afc circuits and a separate local oscillator, thereby reducing the total number of tubes required to 35, as compared to the previous 70, and the number of microwave tubes to only one instead of four.

IRE Standards on Graphical Symbols for Semiconducting Devices (p. 1612)—This Standard represents one of the most important additions to radio engineering symbology in the past decade, presenting for the first time some three score symbols for representing transistors and related devices.

The 1959 International Radio Conference (de Wolf, p. 1618)—In 1947 the International Telecommunications Union held an international radio conference in Atlantic City at which the international radio regulations now in force concerning the use of the radio spectrum were drawn up. A year and a half from now another such conference will be held in Geneva to review and revise the existing regulations. The preparation of the United States position at this important meeting is being carried forward by the State Department with the help of the FCC and the Office of Defense Mobilization and aided by numerous agencies, companies and organizations, including the IRE. In this article the chief of the telecommunications division of the State Department presents a timely account of the background of the forthcoming conference and the preparations for it.

The International Radio Consultative Committee (Cross, p. 1622)—The above named committee, perhaps better known as the CCIR, is an important arm of and advisor to the International Telecommunications Union on radio matters that are primarily technical in character. Its work provides technical information upon which the ITU may draw in establishing international regulations at conferences such as that described in the preceding article. The CCIR carries out its study of technical radio problems through 14 study groups and through tri-annual Plenary Assemblies, the last of which was held in Warsaw last year. In this article the chairman of the U.S. delegation to the Warsaw Assembly discusses the results of that meeting, the studies that are being undertaken in preparation for the next Assembly to be held in the United States in 1959, and the participation of the IRE.

A New Wide-Band Balun (Roberts, p. 1628)—This paper presents clearly and unpretentiously a handy device for matching the impedance of an unbalanced circuit to a balanced one over a wide range of frequencies. Although the balun described here was designed for 20 to 70 megacycles, it is adaptable to other frequency ranges of similar ratio. Because of the wide bandwidth, simple construction and substantially reduced size of this type of balun, it should prove useful to a substantial number of workers in the antenna and transmission line fields.

Synthesis of Lumped Parameter Precision Delay Lines (Kuh, p. 1632)—A technique is presented for designing delay lines for precision time domain applications, such as arise, for example, in analog to digital conversion. The problem is broken down into two parts, resulting in a delay line that consists of a tandem connection of a low-pass network which provides the required time response and an all-pass network which gives the desired time delay. The method is illustrated by an example of how to design a delay line with a 1 microsecond delay, a 0.05 microsecond rise time, and a maximum step response distortion of 1 per cent. The need for circuits of this type in many different communication and electronic systems makes this work of general significance to the art.

Series of Papers on Meteor-Burst Communication (starts on p. 1642)—It is estimated that the earth's atmosphere is bombarded by 10 billion dust-like meteoric particles a day. The collision of these rapidly moving particles with air molecules produces a trail of free electrons in the meteor's wake. The resulting meteor trail acts as a radio wave scattering mechanism by which a low power vhf signal may for a moment be transmitted over a long distance during the brief life of the meteor trail. By utilizing successive meteor trails, an intermittent type of communication system has recently been developed in which pre-recorded messages are transmitted at a very high rate of speed in brief bursts corresponding to the durations of the individual meteor trails. In a typical case, messages might be sent at 20 times the normal speed in bursts varying from 0.1 to several seconds. On the average the system might be transmitting only 5 per cent of the time and waiting for a meteor trail of proper orientation and ionization density 95 per cent of the time. Proper timing of the transmission bursts is accomplished by providing a transmitter and a receiver at both the sending and receiving stations. When a suitable meteor trail appears, the receiving station will detect the sender's carrier signal and will then automatically transmit an acknowledgment back to the sender, at which time the sender will transmit the message for as long as the receiving station indicates it is receiving it.

The latter part of this issue is devoted to a collection of twelve papers and two letters to the editor describing the recent work of several laboratories in Canada and the United States to develop and perfect meteor-burst communication systems. These papers discuss the nature of meteor trails, their propagation characteristics, the statistics of their occurrence and utility, characteristics of the system such as storage capacity and bandwidth requirements, actual equipment used, and operating results. These results point to the feasibility of this important new technique for low-power point-to-point communications (voice, teletype and facsimile) over distances of 1000 miles or more at 30 to 50 mc.

On the Nature of the Electron*

J. L. SALPETER†

Summary—**In this paper the concept of the electron as a fundamental particle of modern physics is discussed in relation to Pauli's exclusion principle, wave mechanics, the uncertainty principle, and relativity.**

Introduction

THE ELECTRON was discovered in 1897 by J. J. Thomson. By deflecting cathode rays in electric and magnetic fields he could determine the ratio of charge to mass (e/m = "specific charge") of the particles constituting cathode rays and found that this ratio remained the same, no matter what gas had been used to fill the cathode ray tube, or what material the electrodes had been made of. Assuming that the charge e is the same as found in electrolytic experiments, the mass m of the cathode ray particle could be determined. It was a great surprise to find that this mass was about 1/1800 of the mass of the lightest atom; *i.e.*, hydrogen. The conclusion drawn from these results was that electricity has an atomistic structure; *i.e.*, there exists a smallest amount of electric charge and any charge found in nature is an integral multiple of this elementary charge. This elementary charge, however, is inseparably combined with mass as found by Thomson in the new particles, the electrons. Apart from being the atom of electricity, the electron is a constituent of every "atom" of every element. Normally it is bound to the atom, but by special processes it can be liberated from the atom and become a "free electron." Actually the "bound electron" was discovered slightly earlier (in 1896) by Zeeman, a Dutch physicist, who found that it is possible to split the spectral lines of a light emitting element if this element is placed in a magnetic field. The interpretation given by Lorentz to the "Zeeman effect" was briefly this—the emitted light is generated within the atom by an oscillating electric particle, endowed with charge and mass, which proved later identical with the particle found by Thomson. The first one was in the "bound," the latter in the "free" state.

With the discovery of the emission of electrons by hot metals the "electronic age" was inaugurated. It is not necessary to tell the electronic engineer what part the free electrons played and are playing in vacuum tubes, radio valves, rectifiers, and so on. With the discovery of transistors and conduction by "holes" the bound electron (valency electron) became interesting to the electronic engineer too. However, in this article we are not going to discuss the engineering applications of the free and bound electron. We are going to meet the electron not professionally but—as it were—in its private life. What does it really look like? How does it behave when nobody looks and what is its social life (if any)?

Admittedly, the answers to questions of this kind are not necessary for the efficient use of vacuum tubes and other electronic devices, but we do not offer apologies for discussing these matters in an article addressed to the electronic engineer. After all, man does not live by bread alone and at all times philosophy has drawn heavily on science in respect of questions concerning the nature of our surroundings. Knowledge of the nature of the fundamental particles may help us to obtain an answer to the eternal question, who are we? Science is often regarded as a means to help invent more and better gadgets, but scientists themselves rather wish science to be appreciated for its own sake, and for the sake of its philosophic consequences. Of all people who are not physicists themselves, the electronic engineer is the most familiar with the electron, although not on a personal footing. The aim of this article is to arouse his scientific curiosity.

Atomic Structure of Charge, Matter, Energy

The nineteenth century saw great successes in the physical sciences. The successes were so great indeed that some scientists believed that everything that could be discovered had been discovered already and in future it would be only necessary to consolidate the achievements. The disciplines of mechanics, hydrodynamics, elasticity, electrodynamics, optics, and so on were all rounded off and perfected, mainly in the language of partial differential equations. If the Creator of the world was a mathematician (as some maintained), He must have been very fond of partial differential equations. These equations are admirably suited to describe phenomena in continuous media and "fields," and the precision and beauty of those differential equations induced some students to adhere to the idea of continuous matter longer than was warranted. Still at the end of the century there were some prominent scientists (like the great chemist W. Ostwald) who regarded the atomic structure as an unproved hypothesis. Today we still treat space and time (or rather space-time) as continuous entities but everything that happens and proceeds in space-time does so atomistically. We no longer believe that God is particularly fond of partial differential equations and even the partial differential equation on which wave mechanics is based serves rather to conceal than to reveal the actual state of affairs.

The name "atom" is a Greek word (meaning indivisible) and the hypothesis of atomism is of Greek origin. The Greeks had no physical science to speak of and the

* Manuscript reprinted from *Proc. IRE* (*Australia*), vol. 18, pp. 183–193; June, 1957.
† Philips Electrical Industries Pty. Ltd., Hendon, S. A.

theory of atoms was built not on basis of observation and experiments, but on pure speculation. Some maintain that it was pure coincidence that their theory proved correct after more than 2000 years and would deny any merit to Democritos who is regarded as the father of the atom. However, Schroedinger tries to vindicate the ancient philosophers by showing that it is possible to arrive at the atomic hypothesis by pure speculation based only on the primitive observation that matter can be condensed and rarified. Suppose now we regard matter as continuous and let us try to imagine what happens when we condense matter. We could start by mentally subdividing the piece of matter into, say, 1000 pieces and condensing each of the 1000 pieces. But then we should have to subdivide each of the 1000 pieces again into 1000 pieces and continue doing so *ad infinitum*. Subdividing matter into finite pieces is of no use if matter is continuous. So let us single out a finite number (although a very large one) of geometrical points within the piece of matter and watch how those points come nearer to each other when the matter is condensed. Yet, since we started with a finite number of points, we left out some points between the selected ones. If we make a second finite selection, there will be still some more points omitted and the points in the condensed piece will never come in touch with each other. Just let us try and think in silence about the situation! The paradox encountered in this mental exercise can be illustrated by the following geometrical consideration. Let us visualize two straight lines, one 1 inch long, the other 10 inches long. We are going to establish a one-to-one correspondence between the points of the two lines. To begin with, the two end points of the 1-inch line correspond with the two end points of the 10-inch line. Then let us select arbitrarily any point on the 1-inch line, measure its distance from the left end, say, multiply the distance by 10 and mark on the 10-inch line a point at that distance from the left end. Conversely, we can select any point on the 10-inch line, measure its distance, divide it by 10 and mark it correspondingly on the 1-inch line. To each point of the 1-inch line corresponds a point on the 10-inch line and conversely to each point of the 10-inch line corresponds a point on the 1-inch line. The 1-inch line is as rich in points as the 10-inch line which is obviously paradoxical but uncontrovertible. These paradoxes crop up usually when we deal with infinities and we have seen that the concept of continuous matter involves infinities. A nice example of what happens if we treat infinities seriously is this. Let us imagine a hotel with an infinite number of rooms and let the hotel be fully occupied. Despite the fact that every room of the hotel is occupied, it is possible to accommodate many more guests in this hotel, in fact an infinite number of additional guests. All we have to do is to move the gentleman of room No. 1 to room No. 2, the guest of room No. 2 to the room No. 4, the guest of room No. 4 to the room No. 8, and so on. This process can be repeated without limits. We are not to be afraid that some people at the end of the hotel will be turned out, because there is no end.

All those disabilities connected with infinities are avoided if we conceive of matter as consisting of a finite number of ultimate, indivisible particles; *i.e.*, atoms. This reasoning is of course no substitute for the experimental proof of the existence of atoms, but we can give the ancient Greeks credit for arriving at the concept of the atom by a reasoning which still today has an appeal for us. This is not to say that the concept of the ultimate, fundamental particle does not involve philosophical difficulties of its own, but in dealing with them we are assisted by Nature itself, since all experimental evidence speaks in favor of the existence of ultimate, no longer divisible particles.

Fundamental Particles

The term "atom" is today a misnomer. We know that the atom consists of a positive nucleus and a number of negative electrons moving around it. The electrons that perform in vacuum tubes such useful functions for us, were originally constituents of the atoms of the cathode. The atom is then no longer indivisible; we can at least detach some electrons from it. Even the nucleus (with the exception of hydrogen) is not indivisible. The nucleus of hydrogen is a fundamental particle, *i.e.*, the "proton," while the nuclei of all heavier elements consist of protons and neutrons. The neutron is a fundamental particle of approximately the same mass as the proton, but without charge. There are a number of other fundamental particles, but we shall be concerned with the negative electron only and mention only that there exists a positive electron, termed "positron" (or antielectron), but this does not normally occur in matter. We may also mention that an antiproton and an antineutron (*i.e.*, a negative proton and a neutron with a reversed magnetic moment) are conceivable and have been discovered already.

How is the electron to be imagined? In the early days of electron theory it was an acceptable procedure to assume some shape of and charge distribution within the electron, for instance sphere or ellipsoid, to regard it rigid or deformable and so on, and calculate its behavior accordingly. Today we would regard this procedure as naive. We might as well imagine the electrons as tiny hard billiard balls, painted blue and red, blue standing for negative, red for positive charge. If we consider charge distribution within the electron, the question obtrudes itself, how does this charge manage not to explode (or are perhaps the charge elements within the electron glued together with some cement)? Today we are not encouraged to try and explore the structure of the electron itself. An ultimate particle has no structure, and we have to stop somewhare exploring structure. To begin with, there is charge and mass connected with the electron, but we are not to picture charge and mass as separate entities embraced by the electron. We should rather regard charge and mass as properties of the electron. Needless to say, even if we could see the electron, we could not discern its color, because its diameter would be so much smaller than the wavelength of visible light that it could not possibly reflect any visible light.

Although the electron is one of the constituents of visible and tangible matter, it differs from ordinary matter by virtue of its indivisibility. This indivisibility is not only to be accepted as a fact, but even in our imagination we are not to try and subdivide the electron, otherwise we shall be confronted with difficulties of a similar character as, for example, while dealing with infinities. As Dirac puts it, the smallness of an ultimate particle is absolute, not relative. In the process of subdividing matter, once we reach the ultimate particle we have to be prepared to encounter behavior and properties quite unlike those connected with ordinary matter.

Properties of the Electron

The electron is characterized by three properties, charge, mass, and spin. We have discussed already charge and mass. Apart from charge and mass the electron is endowed with spin; *i.e.*, it rotates around its diameter with some specific unchangeable velocity. By no means is it possible either to speed up or retard this rotation. Spin was postulated by Uhlenbeck and Goudsmit in order to explain spectral lines in accordance with quantum theory. Later Dirac derived spin by applying the principle of relativity to the theory of the electron and has shown the spin of fundamental particles to be a consequence of the symmetry of the universe with respect to space and time. Although nobody has ever observed the electron in the act of spinning, the spin seems well founded in basic theory. It is responsible for the magnetic behavior of the electron; in fact, due to the spin, the electron, apart from incorporating elementary charge, represents an elementary magnetic dipole.

So far we have been talking of a single electron and its three properties. As soon as we consider an aggregate consisting of two or more electrons, a property becomes apparent that has no meaning for a solitary electron. This property is the "indistinguishability" of electrons. One electron is exactly like its fellow electron and it is absolutely impossible to tell one from another. This is a very remarkable property with some very important consequences. We have warned before that in the process of subdividing matter as soon as we arrive at the ultimate particles, we are bound to encounter behavior very much different from the behavior of macroscopic, visible, and tangible matter. Some of those new features, like the dual aspect (wave particle aspect) are very difficult to visualize, but others like indistinguishability, although not occurring in our everyday experience, are possible of comprehension by the process of going to the limit. In our everyday experience there are no two objects equal in every respect. Among the two and a half billion inhabitants of the earth there are no two individuals absolutely alike. This would be the case even if we allowed for the differences in age or if we took into consideration all people that ever lived on earth. The greatest similarity we encounter are among twins, but even among twins who cannot be told apart by their own mother, we would detect differences by careful examination (finger prints, weight, size). Or let us take balls for ball bearings as an example. They may look alike, but by weighing on a sensitive scale, we would most certainly detect small differences.

Let us see what classical physics had to say in this matter. Even in classical physics it was assumed that mass and charge of all electrons were equal, but there was no emphasis on this equality. Within the errors of measurement, mass and charge proved to be equal for all electrons and there was no phenomenon known which would call for fluctuations in the values of charge and mass as an explanation. It will be realized that only a theory can postulate equality, because measurements alone, no matter how accurate, are encumbered by unavoidable errors and we could always assume—if we wanted—that there are small fluctuations which however are masked by the errors. No measurements could ever prove absolute equality. But in classical physics the matter was of no importance, because there were no effects known which could be explained either by accepting or rejecting the notion of absolute equality.

It is different in quantum mechanics. Here the indistinguishability of electrons generates a new kind of interaction, a new kind of nondynamic force which explains such things as chemical valency, cohesion of crystals, ferromagnetism in iron, nickel, and cobalt, and many others.

Apart from that, indistinguishability throws some light on the nature of fundamental particles. We remember the story of the little girl who got two pennies from her mother with the request to buy with one penny, salt, and with the other, pepper. After a while the girl returned with the pennies because she forgot which of the pennies was meant for salt and which for the pepper. For her the pennies were distinguishable and she did not understand that the values incorporated in the two pennies were indistinguishable.[1] In the realm of energy we have no difficulty in realizing that two equal units of energy are indistinguishable—we could hardly tell apart the kilowatt hour we consumed yesterday from the kilowatt hour we consume today. And yet, according to Einstein, mass and energy are mutually convertible into each other. It should not be surprising then that entities that were indistinguishable in form of energy remain indistinguishable in form of matter. However, we shall see that indistinguishability can be regarded as confirmed by experience.

[1] Anticipating these difficulties the English language introduced the term "pennyworth," but this is not the case in other languages.

Perfection—Imperfection

The indistinguishability of fundamental particles could be also expressed by saying: they are perfect. There are only a few numbers that characterize an electron or a proton, but there are absolutely no deviations whatsoever from those numbers. It is different in the realm of macroscopic objects or objects of our everyday experience. "Nothing on earth is perfect," we often say. The human body is nominally symmetrical, but we know that the organs within the body are not arranged symmetrically. Even the face is never quite symmetrical. If we cut a photograph of a face vertically in two halves and replace one of them by a mirror image of the other, we obtain a symmetrical face, but such a face, surprisingly enough, looks unnatural. Perhaps we have a better chance to find perfection among nonliving objects. A diamond crystal may look like a near approach to perfection. A man in the street values in the diamond its optical properties and its hardness. The physicist is more impressed by the regularity of the arrangements of its atoms in a space lattice. The surfaces of a crystal may have a pretty appearance and shape (configuration of the external surfaces). We rather appreciate the crystalline nature of an object by inspecting its internal arrangement in form of a space lattice of perfect periodicity. But is this periodicity really perfect? Since the discovery by Laue of X-ray diffraction by a space lattice, thousands and thousands of crystals have been investigated regarding their space lattice, but none of them was perfect. Recently a symposium was held with the title "Imperfections in Nearly Perfect Crystals." This title implies a regret and resentment that but for a few incidental imperfections the crystals would have been perfect. However, the imperfections were not incidental. They are in fact unavoidable and the extent of any kind of imperfection can be determined thermodynamically.

The most common imperfection in a crystal is chemical impurity. Minerals found in nature are always contaminated but we can purify them by chemical and other methods in the laboratory. Methods are now available (for instance the melted zone method of purifying germanium) which achieve a purity that would have been considered impossible a few years ago. However an absolute absence of foreign atoms is impossible, not just for practical reasons but in principle.

Briefly, the reason is this: let us say, we have one impurity atom per cubic millimeter of the crystal. This impurity atom may occupy one of the sites occupied ordinarily by one of the atoms of the substance, of which the crystal is composed. Since there are roughly 10^{19} atoms in one cubic millimeter there are 10^{19} ways in which the contamination of the crystal can be realized. On the contrary there is only one way in which a perfectly pure crystal can be realized. Hence the probability of the occurrence of a contaminated crystal is many orders of magnitude larger than for a perfect crystal. On the other hand the impurity atom within the crystal lattice may involve more energy than an atom of the host substance and so a compromise will eventuate between the requirements of a minimum energy and maximum entropy. This is essentially the basis of the thermodynamic reasoning which leads to a quantitative evaluation of the extent to which contamination is to be expected.

Macroscopically nothing is perfect; on the level of fundamental particles everything is perfect.

Pauli's Exclusion Principle

The electronic engineer is familiar with the free electron; *i.e.*, the electron outside the atom. We know that the density of free electrons in vacuum or in an ionized gas never exceeds, say 10^{15} per cm^3 (at least in terrestrial laboratories). This means that the mutual distance of free electrons is on the average never less than 10^{-5} cm (which means 1000 interatomic distances in a solid). At these distances the only interaction to be considered between the electrons is the electrostatic repulsion due to the charges of the electrons. It is not even necessary to be aware of the electron spin; we shall see later why there is little chance to observe spin of a free electron. Likewise the indistinguishability of electrons or otherwise does not play any prominent part with free electrons.

Within an atom (or molecule or crystal) the electron density is of the order of 10^{23} to 10^{25} per cm^3 and the mutual distances are of the order of 10^{-8} cm or less. At these distances the electrons no longer behave simply as ordinary particles of small size: they show features characteristic of fundamental particles. One of them is a peculiar mutual dislike of electrons of the same sign spin. We avoid deliberately the term "force" or "repulsion," because it is more than a repulsion. According to Pauli's Exclusion Principle, we shall never find two electrons of the same sign spin in the same orbit of an atom. Now, it would not be correct to say: let us place two electrons of the same spin in the same orbit and we shall see that due to an enormous short range mutual repulsion one of them will leave the orbit. This would not be correct to say, because no power on earth would be able to place two equivalent electrons in the same orbit to begin with. We shall later discuss this curious impossibility, but let us first describe more fully this fundamental exclusion principle.

This principle is best described in its historical context. We have mentioned previously that the Zeeman effect (splitting of spectral lines in presence of a magnetic field acting on the emitting atom) had been interpreted by Lorentz on the assumption that an electric particle bound to the atom by a quasi-elastic force is oscillating around its equilibrium position. But what does this particle (electron) do when it is not oscillating (*i.e.*, when the atom is not emitting light)? It could not be at rest, because nothing would prevent it then from falling into the nucleus. The planets do not fall into the sun because they have sufficient kinetic energy enabling them to cruise around the sun on a circular or elliptical orbit. Electrons are attracted to the positive nucleus by Coulomb's forces (inverse square law) just as the planets are attracted to the sun by gravitation and accordingly, if endowed with sufficient kinetic energy, they can avoid falling into the nucleus by cruising around it. However, unlike the planets, an electron following a curved orbit emits electromagnetic radiation and so a cruising electron would continually lose energy, the diameter of its orbit would decrease, and eventually it would fall into the nucleus. Whether we assume the electron at rest or in motion, the classical theory saw no way of preventing the collapse of the atom. At this stage Niels Bohr proclaimed his revolutionary theory of the atom according to which the electron can move around the nucleus without radiating and losing energy, provided its total energy is one of a set of discrete energy levels, characteristic for the element concerned. There exists for each chemical element a set of permitted energy levels, the lowest of which belongs to the "ground state." In the ground state the electron or electrons are nearest the nucleus. If the atom absorbs a certain amount of energy, the electron can be lifted to the next higher level and the atom is said to be in an "excited state." On dropping from an excited to the ground state, the electron loses energy, which is radiated as light. No intermediate energy levels are permitted. This is at complete variance with the behavior of a free electron and with the classical theory of electromagnetism. In classical theory we can endow an electron with any amount of energy and according to classical theory any acceleration of the electron is accompanied by radiation. (Motion on a curved orbit involves acceleration.) These two rules were broken by Bohr's theory, but the theory proved successful in explaining the numerical relationships of spectral lines and was accepted enthusiastically by physicists.

The hydrogen atom is the simplest of all. It consists of a positive nucleus (proton) of unit charge and with one electron moving on an orbit of radius 0.53 Å. The next in the periodic system of elements is helium with two electrons moving on an orbit of radius 0.30 Å. The third element is lithium with three electrons for which the orbit shell should have a radius 0.20 Å. (The radii become smaller with increasing charge of the nucleus, because the attraction becomes greater.) However, it was known that the diameter of the lithium atom must be much larger than 0.4 Å because the "atomic volume" of lithium was known to be large. For this reason it seemed unlikely that all three electrons were located on the same shell. It is here that Pauli's Exclusion Principle came into its own. This principle postulated that no electron shell shall contain more than one pair of electrons of the same state of motion—exactly as in Noah's Ark there was only one couple of each kind of animal. Only, in the case of electrons the couples are not distinguished by sex but by spin. According to this principle the third electron in the lithium atom has to go to a new shell (of 1.50 Å radius). The beryllium atom has four electrons and the fourth electron goes to the second shell, the third and fourth electrons having opposite spins. The second shell is hereby closed and the fifth electron in the boron atom goes to a new shell. As we progress in the periodic system of elements, new electrons (shells and subshells) are formed and so we can say that Pauli's Exclusion Principle is responsible for the electron shell structure of the chemical elements. Without this principle all electrons would go to the first shell and it is impossible to say how the world would look in that case.

The exclusion principle is generally expressed in the following way: no two electrons of the same spin shall be in the same space and have the same state of motion. The "same space" refers in the case of atoms to the electron shells, but otherwise it refers to a system in which the electrons can interact. In old textbooks of physics we can find a principle of impenetrability—no two bodies can occupy the same place. The exclusion principle is less demanding, it only requires that no two electrons of the same spin shall occupy the same place and be in the same state of motion. On the other hand the words "the same place" are not to be taken literally. The electrons occupy the same place, if they can interact.

With the advent of wave mechanics the exclusion principle has been incorporated in it and has been reformulated in a much more precise and quantitative manner. We are now going to discuss wave mechanics to the extent necessary for the understanding of the exclusion principle and its consequences.

Wave Mechanics

The twentieth century revolution in physics is best shown in the wave or quantum theory. The experimental basis on which wave mechanics was founded is electron diffraction by a crystal (say of mica). Let us direct an electron beam on to a crystal plate and place behind the crystal plate a photographic plate. After exposure and developing of the photographic plate we notice first of all a black circle corresponding to the cross section of the electron beam, but apart from this circle, we shall notice around it a regular diffraction pattern, quite similar to the diffraction pattern as obtained by X rays. Diffraction is a clear demonstration of the wavelike character of the electrons and yet their origin in the electron gun points to their particle aspect. The diffraction pattern does not depend on the intensity of the cathode ray. We can use a beam of very low intensity and expose the plate for a very long time and obtain the same pattern as with high intensity and short time. We can make the electron beam intensity so low that only one electron passes through the crystal at a time. How do the electrons know which point of the pattern each of them has to hit? There is only one answer to this question—each electron is itself a wave and each electron creates the whole pattern, but energy can be absorbed only in finite quanta and so the electron hits the photographic plate in one point only, the distribution of those points being given by a probability function. We are then faced with the following situation. The electron originates in the gun as a particle and is being absorbed by the photographic emulsion as a particle, but in between it behaves like a wave. This dual aspect of the electron "wave-particle" caused many people great concern and was the subject of numerous discussions and controversies. (A suggestion has been made to call the electron a "wavicle" but the term alone does not of course solve any problems.)

In this article we wanted only to discuss a few properties of the electron, in particular "indistinguishability," because this is not beyond common sense apprehension and yet has far-reaching consequences. Indistinguishability is closely connected with the exclusion principle and this in turn is best expressed in the language of wave mechanics.

We have seen that the phenomenon of electron diffraction suggests the wave nature of the electron. What exactly is it that vibrates in the electron wave? The answer is quite different from the answers to the same question for any other kind of wave. The intensity of the electron wave indicates the probability that we shall find the electron at a particular point x, y, z in space. As with any other kind of wave, the intensity is equal to the square of the amplitude and the amplitude is a function of the space coordinates, but the amplitude itself has no physical meaning. It is only an auxiliary quantity, whose sole purpose is to enable us to compute the intensity.

Apart from the amplitude, the shape of the wave is an important characteristic, and particularly the wavelength of the fundamental. In wave mechanics the wavelength λ is connected with the observable electron velocity v by the following relation,

$$h/\lambda = mv$$

where h stands for a constant (Planck's constant) and m for the electron mass.

Let us now see how the wave nature of the electron helps us to understand the structure of the atom. As a preliminary experiment let us put the electron into a box, not literally a box with walls of cardboard or steel, but a box whose walls are potential barriers. The potential walls are high enough to prevent the electron from escaping, which means in the language of wave mechanics that the probability of finding the electron outside the box or even at the walls is zero. Consequently the wave representing the electron is a standing wave within the box. Assuming the length of the box to be L, then the wavelength of the standing wave will be $2L$, or L, or $2L/3$, and so on, or generally

$$\lambda = 2L/n$$

where $n = 1, 2, 3, 4, \cdots$. Remembering now the relation connecting λ with the electron velocity v, we see that this velocity can have only one value of a set of discrete values. This is a very strange and very important result. In classical mechanics an electron confined in a box can have any value we want to endow it with; we can change the velocity continuously. In wave mechanics only certain velocities are possible and if we want to increase or decrease the velocities we have to do it in finite jumps. What we have said about velocities applies in our case to the energies equally well, because the energy of the electron in the box is made up entirely of its kinetic energy. We arrive at the result that the energy of an electron in a box is capable of assuming only certain values of a set of discrete levels given by the length of the box.

To some rough approximation we can regard the atom as a kind of a potential box in which the electron is held captive by the attraction of the nucleus and we can transfer the results just mentioned to the atom. In this way we arrive at the postulates of Bohr's theory of the atom, but with this difference. While in Bohr's theory the postulates of discrete energy levels appear suddenly from nowhere, they are here the natural outcome of identifying the electron with a standing wave. However, our aim was to express Pauli's Exclusion Principle in a more rigorous manner, so let us return now to this principle.

Symmetrical and Antisymmetrical Wave Functions

The original wave equation, derived by Schroedinger in 1926, refers to a single electron. We are not going to discuss its mathematics, but shall describe only the meaning of the wave parameters. We have mentioned already how the wavelength is linked with the electron momentum (product of mass and velocity), while the frequency is proportional to the total energy of the electron. The quantity corresponding to the refractive index in case of light waves is determined in the case of electron waves by the electrical potential at a given point (x, y, z). The wave amplitude has no physical meaning, but the wave intensity indicates the probability of finding the electron at a given point. Originally the wave intensity was interpreted as charge density and this is still true today, if we consider the time average of the charge density over an appropriate period of time. If for instance we let a weak electron beam penetrate a thin crystal of mica and watch blackening of a photographic film placed behind the mica, the pattern of blackening will be given by the wave intensity.

The wave equation for a single electron has been applied successfully to the hydrogen atom, where we have a single electron in the field of the positive proton. However, in the next element, helium, we have already two electrons, in lithium three electrons and so on (and in uranium as many as ninety-two electrons). The first rule to be observed in case of a system containing more than one electron is Pauli's Exclusion Principle—no more than one electron of the same spin in one orbit. Pauli's principle is quite independent of wave mechanics and in fact overrides it; the wave equation for two electrons has to be formulated in such a way as to exclude automatically the simultaneous presence of two electrons of the same spin in the same place.

If $\zeta_1(x_1, y_1, z_1)$ and $\zeta_2(x_2, y_2, z_2)$ are the two wave functions of the two electrons, it would be tempting to write the wave function for the case of two electrons as the sum of $\zeta_1(x_1)$ and $\zeta_2(x_2)$

$$\psi = 0.71(\zeta_1(x_1) + \zeta_2(x_2))$$

where $\zeta_1(x_1)$ and $\zeta_2(x_2)$ stand as abbreviations for $\zeta_1(x_1, y_1, z_1)$ and $\zeta_2(x_2, y_2, z_2)$. The factor 0.71 will be explained presently. The function $\psi = \zeta_1 + \zeta_2$ would take account nicely of interference and diffraction phenomena of electron waves and would be in strict analogy to other waves encountered in physics, like optical and accoustical waves. However, we have said before that the wave intensity expresses the probability of finding the electron at a given point. Similarly the intensity of a two-electron wave function should stand for the probability of finding electron 1 in point 1 and electron 2 in point 2. With the requirement of representing the probability, the functions ζ_1 and ζ_2 are as a rule written in "normalized" form, *i.e.*, provided with such a factor as to make the integral of ζ_1^2 and ζ_2^2, respectively, over the whole space equal to unity. A probability of one means certainty, and since we are certain to find the electron *somewhere* in the whole infinite space, the integral (*i.e.*, the sum of all probabilities) must be equal to unity. Let us now similarly integrate ψ^2 over the whole space. If we form the square of ψ we obtain

$$\psi^2 = 0.5(\zeta_1^2 + 2\zeta_1\zeta_2 + \zeta_2^2).$$

The integral of ψ^2 over the whole space will then be equal to unity plus the integral of $\zeta_1\zeta_2$. Now by analogy with optical waves we realize that the integral of $\zeta_1\zeta_2$ over the whole space must be zero. In optics the wave intensity stands for the energy and if we let two waves interfere we know that whatever happens the energy will be conserved; *i.e.*, integral of $(\zeta_1+\zeta_2)^2$ must be equal to integral of $\zeta_1^2+\zeta_2^2$, or the integral of $\zeta_1\zeta_2$ must be zero. With electron waves it is the charge that is being conserved, which is quite all right, but what about probability? The sum $0.5(\zeta_1^2+\zeta_2^2)$ stands for the probability of finding *either* electron 1 in point 1 *or* electron 2 in point 2, but this is not what we were after. We wanted an expression for the probability of finding electron 1 in point 1 *and* electron 2 in point 2. The probability that two events will take place is equal to the product of the probabilities of the single events. Let us then write

$$\psi = \zeta_1\zeta_2$$

and we shall then have, as required

$$\psi^2 = \zeta_1^2\zeta_2^2.$$

At the same time we realize that the integral of ψ^2 over the whole space will be equal to unity. (We keep firstly point 2 constant and integrate ζ_1^2 over the whole space obtaining thus ζ_2^2 as a result and then integrate ζ_2^2 over the whole space and obtain unity.) This would be quite all right but we remember that electrons are indistinguishable and therefore it is not permissible to label electrons as we did in the reasoning leading to $\psi = \zeta_1\zeta_2$. As long as we have to do with single electrons, it is a matter of course to establish a function ζ_1 for one electron and a function ζ_2 for another electron. As soon however as we have a system consisting of two electrons, the wave function is required to be formulated in such a manner that interchanging of the two electrons does not alter the function (or rather, its meaning). We can arrive at such a formulation in the following way. Given $\zeta_1(x_1)$ and $\zeta_2(x_2)$ we know that $\zeta_1(x_1)\cdot\zeta_2(x_2)$ leads to the probability of finding electron 1 in point 1 and electron 2 in point 2. By exchanging electron 1 with electron 2 we obtain the product $\zeta_1(x_2)\cdot\zeta_2(x_1)$ which leads to the probability of finding electron 2 in point 1 and electron 1 in point 2 (this is really the same probability as the previous one since the electrons are not distinguishable). The wave equation is a *linear* differential equation and consequently, if we have two solutions of the equation, any linear combination of the two solutions will be a solution again. To find a solution which is invariant in respect of interchange of the two electrons, we put

$$\psi = 0.71(\zeta_1(x_1)\cdot\zeta_2(x_2) \pm \zeta_1(x_2)\cdot\zeta_2(x_1)).$$

We see that interchanging of electrons 1 and 2 leaves ψ unaltered in case of the plus sign and reverses the sign of ψ in case of the minus sign; however, reversing of the sign of ψ is irrelevant because only the square of ψ has significance. It can be shown that the expression put down for ψ is the only linear combination satisfying the equation of which ζ_1 and ζ_2 are solutions and making the function invariant in respect of electron exchange. The function with the plus sign is referred to as "symmetrical"; the function with the minus sign is an antisymmetrical function.

What happens if the two points x_1 and x_2 coincide; *i.e.*, if $x_1 = x_2$? In the case of the symmetrical function $\psi = \zeta_1\zeta_2$; in the case of the antisymmetrical function the wave function ψ vanishes. Let us now choose the symmetrical function for the case of two electrons of opposite spin and the antisymmetrical function for the case of two electrons of the same spin. In doing so we achieve automatic fulfilment of Pauli's principle, because $\psi = 0$ (and consequently $\psi^2 = 0$) means that the probability of finding two electrons of the same spin in the same place is zero. We see now how wave mechanics of a two-electron system has been formulated so as to embrace the exclusion principle. At the same time it has to be emphasized that wave mechanics goes beyond the exclusion principle. While the exclusion principle tells us what the electrons are forbidden to do, wave mechanics tells us what they are actually doing. Since its inception in 1926 wave mechanics has made an enormous contribution to progress in physics. One is reminded of a saying of Einstein—"God may be secretive, but He is not malicious." It may be difficult to gain access to a certain region of knowledge, but once we have pierced a small hole through the curtain, we are often permitted to see more than we hoped for.

Exchange Energy

One of the most interesting and important consequences of wave mechanics (including indistinguishability of electrons and the exclusion principle) is the existence of a new kind of nondynamic force, *i.e.*, exchange forces and exchange energies. Exchange forces being responsible for the chemical bond form the basis of theoretical chemistry, and similarly, exchange forces underlie the phenomena of ferromagnetism quite apart from the role exchange energy plays in the interpretation of atomic and molecular spectra. It is quite possible to obtain even without mathematics a qualitative understanding of the origin of exchange forces in the following way. Let us visualize two hydrogen atoms, each with a positive nucleus (proton) and an electron cruising around the proton. If the two electrons are of opposite spin, the exclusion principle permits them to be close to each other. Not only are they permitted to be close together, but since they are represented by a symmetrical wave function, the probability of where we shall find them, has a maximum for $x_1=x_2$, *i.e.*, the same point. Here it is time to mention that the notion of the orbit of an electron around the nucleus—as we often see it pictured on the covers of popular books on atomic physics and even in advertisements on electronic devices—is obsolete today, although the term "orbit" is still used in a loose sense for the sake of convenience. The wave function permits us to compute the probability of finding the electron at a particular point at any one time, but does not permit us to draw a continuous orbit along which the electron travels (this will be discussed at some length in the next section). While now for a single hydrogen atom the probability of finding the electron has a maximum at some particular distance (0.53)Å from the nucleus but otherwise does not depend on the direction, it is different in the case of two hydrogen atoms. If the two electrons are of opposite spin, the probability has a maximum for both electrons at the midpoint between the two protons. We have then at the midpoint a double electronic (negative) charge attracting on each side a single positive proton charge. (The charge on the proton is of the same magnitude but opposite sign to that on the electron.) The double electron charge serves as a cement between the two protons and in this way the hydrogen molecule is formed. No molecule is formed if the two electrons have spin of the same sign. We can also see easily why a hydrogen molecule does not attract a third hydrogen atom. Since the two electrons in the molecule have opposite spins, the electron of a third atom would have the same spin as one of the two electrons of the molecule and according to the exclusion principle would avoid the vicinity of this electron; hence, the lack of attraction.

The reasoning so far is of a purely qualitative nature. In particular we disregarded the electrostatic repulsion of the two electrons of opposite spin (the magnetic interaction is so small that it can be neglected for the time being). Two electrons of opposite spin like each other despite their mutual electrostatic repulsion, but this attractiveness cannot be described in such simple terms as Coulomb's electrostatic forces. Coulomb's law was established for charges (and charged particles) and is valid in wave mechanics without any modification. The new "exchange forces" however can be applied to electrons only on the basis of the wave nature of the electron. Briefly it could be said that the exchange energy is due to the fact that generally $(A+B)^2$ is not equal to A^2+B^2. If A and B stand for wave amplitudes, then—as we have seen before—$(A+B)^2$ is equal to A^2+B^2 (if we integrate over the whole space) because the integral of AB over the whole space cancels out. The physical meaning of $(A+B)^2=A^2+B^2$ is the conservation of energy. In wave mechanics, however, the wave intensity stands for charge density rather than for energy density. Energy is given, as we know, by elementary electrostatics, by the product of charge and electric potential V. In this case the integral of $(A+B)^2V$ will not be equal to the sum of the integrals of A^2V and B^2V, because the integral of ABV does ***not*** cancel out.

Let us consider as an example the two electrons in the helium atom. The simplest case is the ground state of the atom, where the two electrons are of opposite spin and therefore both can be in the same, the lowest energy orbit. Yet this case is not interesting for us, because the two electrons being in the same orbit have the same wave function and if the wave function of a single electron is $\zeta_1(x_1)$, the wave function ψ for two electrons will be simply $\psi=\zeta_1(x_1)\zeta_1(x_2)$. The next case of higher energy is where one electron is in the ground state, the other in an excited orbit. Here the two wave functions are different: $\zeta_1(x_1)$ and $\zeta_2(x_2)$ and the wave function of the two electrons ψ will be either a symmetrical or an antisymmetrical function, depending on whether the two electrons have opposite or the same spin:

$$\psi(x_1, x_2) = 0.71(\zeta_1(x_1)\zeta_2(x_2) \pm \zeta_1(x_2)\zeta_2(x_1)).$$

Let us inquire about the energy of the system. There is first the electrostatic energy of the nucleus, then the electrostatic energies of the two electrons taken each separately, and lastly the interaction energy of the two electrons. This last term is of particular interest to us. To obtain the interaction energy we have to multiply the charge density (or rather its time average) by the electric potential and integrate the product over the whole space. The charge density is given by ψ^2, while the electric potential is equal to e^2/r_{12}, where e stands for the electronic charge and r_{12} for the mutual distance of the two electrons. Let us put for short $\psi = A + B$, then we shall see that the integral of $0.5(A^2+B^2)\cdot(e^2/r_{12})$ over the whole space includes e^2/r_{12} which is just the Coulomb interaction energy as in classical electrostatics. Apart from that, however, we have a term $AB\cdot e^2/r_{12}$ integrated over the whole space, which does not occur in the classical theory. This term is what is referred to as "exchange energy." Let us inspect more closely the product AB, that is

$$AB = \pm \zeta_1(x_1)\zeta_2(x_2)\zeta_1(x_2)\zeta_2(x_1).$$

We see at once that this product has a finite value only if the orbits of the two electrons overlap to some extent. If there were no overlapping $\zeta_1(x_2)$ would be equal to zero and so would be $\zeta_2(x_1)$. It follows that exchange forces are only short range forces which explains why there is little chance of coming across exchange forces while observing free electrons. Then we see that the exchange energy is proportional to e^2/r_{12}, *i.e.*, to the electrostatic energy but can occur with a plus or minus sign. We cannot say then that exchange energy is a kind of extension of electrostatic energy. We have to reconcile ourselves to the fact that exchange energy is the outcome of the wave nature of the electron (more specifically of the interpretation of wave intensity as charge density and not energy density). The term "exchange" energy indicates the indistinguishability of electrons and hence their exchange in the formulation of the wave function ψ as the prime source of exchange energy.

Uncertainty Principle

There is something incongruous between a wave and an electron. There is a story about an actor who was looking for a job and asked by the producer about his past achievements answered that he had played a wave (a sea wave produced by rattling of a mechanical contraption). Now we can imagine how an actor can play a wave, but how can a wave play the part of an electron? Let us take the simple case of a plane sinusoidal wave, extending from $-\infty$ to $+\infty$. Frequency and wavelength (or rather wave number) define accurately energy and momentum of an electron, but otherwise this wave gives no information about the electron, in particular no information about the position of the electron. The question is sometimes asked whether electron is "in reality" a particle or a wave. It is doubtful whether physics is at all able to give an answer to this kind of question. The job of the physicist is to devise methods of enabling us to predict physical occurrences. For free electrons the particle aspect is very well suited to describe the phenomena (like the electron tracks in a Wilson cloud chamber or in a photographic emulsion); for an electron in an atom the wave picture is better suited. The electron is neither a particle nor a wave, both are only modes of description. But is it possible to bridge over the span between an infinite wave and a tiny particle? Fortunately this is possible. Superposing a number of sinusoidal waves gives us a "wave packet" or—as the communications engineer would rather say—a "pulse." A Fourier analysis may give us the "spectral" components of the pulse and they may be all solutions of a given wave equation. What is the difference between an infinite wave and a pulse? Of course, the pulse is confined in space and its propagation simulates the motion of a particle. The sharper the pulse the more it resembles a moving particle. Then why not represent an electron by an extremely sharp pulse rather than by an extended wave? The answer is, that in representing the electron by a sharp pulse we have to pay a price for the "sharpness." We know the sharper the pulse the broader the spectrum in the Fourier analysis of the pulse. The spectrum of the pulse shows us the distribution of the wavelengths (or wave numbers) among the components of the pulse and we know that the wave number stands in wave mechanics for the momentum of the electron (product of mass and velocity). This means the sharper the pulse the larger will be the range of wave numbers among which we can choose the momentum of the electron. An infinite wave gives us precisely the wave number (electron momentum or velocity) but no position of the electron. An infinitely sharp pulse gives us exactly the position of the electron but no velocity. We cannot know exactly both the position and velocity of the electron; the product of the sharpness of the pulse and the sharpness of its spectrum is constant. If we denote the range of position by Δx and the range of velocity by Δv, then we shall have

$$\Delta x \cdot \Delta v = h/m$$

where h stands for Planck's constant and m for the mass of the particle. This is the celebrated "uncertainty principle" first put forward by Heisenberg.

It follows immediately from the uncertainty principle that we cannot imagine an electron being at rest. Being at rest means $v = 0$ and accordingly $\Delta v = 0$, but if Δv is zero then Δx must be infinite and vice versa, if $\Delta x = 0$ then Δv must be infinite and accordingly $v = \infty$ too. This gives us another explanation why an electron cruising around the nucleus can never fall into it. Falling into the nucleus would give the electron a definite position and therefore an infinite velocity. The actual orbit is a compromise between the large value of energy the electron would have very near the nucleus and the large energy if completely detached.

The uncertainty principle tells us, too, why there is little chance to observe the spin of the free electron directly. The spinning electron represents a magnetic dipole whose field intensity is inversely proportional to the cube of the distance. According to the uncertainty principle, there is no hope of being able to observe the spin of an electron at rest. It must be moving. Yet a moving electron generates a magnetic field of its own around its path whose intensity is given by the reciprocal of the square of distance. Obviously the field intensity due to the spin should be larger than the "uncertainty" of the field intensity due to the motion of the electron. If we write down the formulas for both magnetic field intensities, this requirement leads to $\Delta r \cdot \Delta v < h/m$, yet according to the uncertainty principle this product cannot be smaller than h/m, hence it is impossible to observe the spin of the free electron directly. The spin of electrons bound in the atom is not observed directly either, but in the case of the atom the splitting of spectral lines in presence of a magnetic field gives a good clue as to the spin of the electrons responsible for the spectrum.

Another way to regard the uncertainty principle is to consider the way we observe the electron. To observe a macroscopic object, say, a chair, we let an image of the chair be formed on the retina of our eye. Of course, we can see the chair only if it is illuminated, but we know that the chair does not suffer in any way by the illumination. An electron is so small that we could not see it, either with the naked eye or with an ordinary microscope. In an imaginary experiment we could use an X-ray microscope, because the wavelength of the X rays, could be chosen small enough to be reflected from the electron. Yet this would be a pretty hard X ray, of very high energy, and as a result the electron hit by the X ray would be dislocated. The very act of measurement would disturb the quantities to be measured. A similar phenomenon occurs in psychology: for instance, if we want to watch how our own mind behaves when we fall asleep, we either fail to make the observation or fail to fall asleep. Only to some approximation is the observation possible and the uncertainty principle states quantitatively how near we can come to the assessment of the quantities to be measured. The uncertainty principle applies not only to the electron but to larger particles as well. However, we notice that the right-hand side of the relation is equal to h/m, which means that the uncertainty is inversely proportional to the mass of the particle. For a proton it is about 2000 times smaller than for an electron and for a tiny (just perceptible) grain of sand it is practically zero. That is the reason why in ordinary mechanics it is not necessary to consider uncertainties.

A consequence of the uncertainty principle is the impossibility of drawing the "orbit" of an electron. We can ascertain the position of the electron as often as we want, but we could not be certain that the "orbit" of the electron would be the same if we did not disturb it by our measurements. Perhaps it may even be meaningless to ask what the orbit would be if we did not observe the electron. Nor can we be sure that in two successive observations we observe "the same" electron, since electrons are indistinguishable. All this is philosophically disquieting; it is the first time in history of physics that we have a theory in which the observer and the observed enter on equal footing. In all other branches of physics the phenomena are described regardless of whether there is an observer or not. In wave mechanics the phenomenon observed is partly created by the act of observation.

The uncertainty principle gives us a new angle from which to regard indistinguishability. Let us say two identical twins are walking on the street. We could not tell one from another, but we could label the one on the right-hand side Tom and the other Dick. They may change places, engage in a brawl, but as long as we keep an eye on them, we can tell which one is Tom and which is Dick. With two electrons it is different, because we cannot watch them continuously and as soon as we shut our eyes they might change their identities if they have identities. All this is not pure speculation and we can put these considerations to test in the following way. We bombard a sample of matter by means of negatively charged, high energy particle beams and inquire after the maximum energy that can be transferred from the bombarding particle to an atom, or rather to an electron of an atom of the sample. For a given energy of the incident particle a formula can be derived for the maximum transferable energy as a function of the mass of the hitting particle. It is true we cannot vary the mass of the incident particle at will, but since cosmic rays provide us with such a variety of fundamental particles of various masses, it is not quite unrealistic to consider this transferable energy as a function of the mass of the incident particle. Starting with infinite mass for which the value of the function is zero, the function increases with decreasing mass, but at the moment the mass of the incident particle equals the mass of the particle, struck, *i.e.*, when both are electrons, the maximum transferable energy drops suddenly to half the value indicated by the formula. This happens because we could not tell which of the two electrons was hitting and which hit, which the donor and which the acceptor of energy, hence the factor 1/2. This result has been confirmed by experiment.

Shooting high energy particles at a fluorescent screen makes the effect of a single particle observable. The light output in the form of a scintillation indicates the energy of the incident particle and at the same time we can observe the spot on the screen where the particle has impinged. This would be a contradiction to the uncertainty principle, so let us consider how we do observe the spot where the screen has been hit. We may observe the screen by means of a microscope in which case the limit of resolution is of the order of 2000 Å, *i.e.*, about 100 million times the size of a fundamental particle. We see the light generated by the impact of a single particle all right, but to say we also see *where* the particle has hit the screen would be tantamount to saying: I know exactly where Mr. Smith is at the moment, he is somewhere on the surface of the earth.

The Relativistic Electron

We started with the aim of getting acquainted with the electron on a personal footing, but this turned out to be impossible, because a single electron has no personality, no individuality, no "sameness." If the fundamental particles have no individuality, but macroscopic objects have, they obviously owe their individuality not to the matter of which they consist, but to the pattern of their assembly. Nineteenth century physics seemed to confirm or even encourage the materialistic outlook in philosophy which attributed to matter an overriding importance. This is no longer true today. It was particularly the discovery of Rutherford of the nucleus of the atom that dealt a severe blow to the materialistic outlook. Rutherford found that the nucleus in which more than 99 per cent of the matter of the atom is concentrated occupies only a minute fraction of the total volume of the atom. The atom consists mainly of empty space, while the density of the nucleus is such that a matchbox full of nuclear substance would weigh millions of millions of pounds. This is not how the nineteenth century man imagined matter. If we grip with our hand a piece of steel, we may feel that the matter of our palm comes into intimate contact with the matter of the steel. Actually the best we can hope to achieve is that the electron clouds of the atoms of the palm come into touch with the electron clouds of the atoms of the steel. Since matter is mainly concentrated in the nucleus, intimate contact of matter with matter should involve contact of nuclei. While this is not impossible, it is a rare occurrence, usually involving nuclear reactions with sometimes rather conspicuous consequences. In gripping with our hand a piece of steel, "common sense" deceives us into believing that we come to grips with matter. Actually however the rigidity and hardness of steel is due not directly to any hardness of the fundamental particles but to the "fields" surrounding them. The fields surrounding the particles are in a way more real than the particles themselves.

We should like to conclude with a remark about what the theory of relativity has to say about the electron. One of the postulates of the theory of relativity concerns the velocity of propagation either of a particle or a field, *viz.*, nothing can propagate with a velocity higher than the velocity of light. Let us now visualize an electron facing the approach of an electromagnetic wave. If the electron has a finite size, one end of it will sooner be engulfed by the wave than the other and will be acted upon earlier. This means that one end will start to move while the other still knows nothing about the wave. As a result the electron would become deformed but this is something impossible for a fundamental particle. If we start imagining that a fundamental particle can be deformed, we might as well assume that a wave of sufficient strength would tear the electron apart which would be a contradiction to the concept of an ultimate particle. We cannot assume that the electron is absolutely rigid, because that would mean that any impulse reaching the electron at one end travels to the other end with infinite velocity, yet according to the theory of relativity there is nothing that travels with a velocity higher than the velocity of light. The only way out is to assume that the electron has no spatial extension at all, in other words that the electron is nothing but a geometrical point in which charge e and mass m are concentrated with infinite density. The third property of the electron, the spin, could not be now achieved by rotation of the electron around its axis, because this would require an infinite angular velocity. Instead it is assumed that the point-like electron revolves around the electron path with velocity of light, the diameter of the orbit being chosen such as to obtain the known value of the electron magnetic moment.

The electrostatic energy of a sphere of charge e is proportional to e^2/r (where r stands for the radius of the sphere) and accordingly the energy of a point-like electron is infinite. This is of course a great difficulty for the theory, although physicists have learned somehow to live with those infinities.

We have started by pointing out that the concept of continuous matter involves infinities which can be avoided by assuming finite, ultimate, indivisible particles. We have now come all the way round the circle and are once again facing infinities, even while working with ultimate particles. It seems that we face infinities whenever we arrive at frontiers of knowledge, or perhaps at the frontiers of our potentiality for knowledge.

Acknowledgment

The author would like to thank Philips Electrical Industries for permission to publish this paper.

A Thin Cathode-Ray Tube*

W. R. AIKEN†, MEMBER, IRE

Summary—A new type of cathode-ray tube typically only a few inches thick is described. The beam is injected parallel to one edge of the thin tube and caused to pass through two right-angle deflections: the first sends the beam into the region between the front and back tube surfaces, and the second turns it into the phosphor-coated front surface. A brief analysis of the deflection-focusing action is presented and the sweep-voltage requirements are described. The thin tube can be adapted to multicolor operation or to any other use to which cathode-ray tubes are put; it also has many unique features (in addition to small size), such as the capability of being viewed from both sides of the display screen or being rendered transparent.

Introduction

THE "thin" cathode-ray tube (crt) described below differs radically from conventional types in that the basic building blocks which comprise a crt (electron gun, accelerating and deflecting structures, and display screen) are here arrayed in a novel fashion. It is this departure from the usual "in-line" arrangement that makes the principal advantage of the thin crt possible—its reduced size. The importance of reducing the crt dimension perpendicular to the viewing screen (usually called *length*, but in the present case perhaps more appropriately called *thickness*) is selfevident in circumstances where space is at a premium, *e.g.*, in aircraft instrument panels. The reduction in bulk is obviously an attractive feature in many other applications also, as in home television receivers.

In comparison with conventional types the thin crt has several other inherent advantages, the chief among which is that the powerful deflection-focusing action makes it possible to utilize larger beam currents for a given "spot size," or to obtain a smaller spot size with the same current. Deflection focusing in the thin crt is not the defect usually associated with conventional crt's;[1] rather, the property of deflecting systems that causes initially parallel rays to converge after deflection actually constitutes the focusing system. This feature thus results in improved brightness or resolution (or both). Moreover, by relatively simple modifications of the basic model, the thin crt can be adapted to provide such special features as transparency, viewing of both sides of the display screen, and two or three primary color displays; the tube can be, of course, adapted to perform all the multifarious tasks that certain special display tubes can do, such as displaying characters and serving as a memory (storage) element.

* Original manuscript received by the IRE, January 16, 1956; revised manuscript received, June 13, 1957; second revised manuscript received, September 23, 1957.

† West Coast Electronics Lab., Kaiser Aircraft and Electronics Corp., Palo Alto, Calif.

[1] See for instance, J. R. Pierce, "Theory and Design of Electron Beams," 2nd ed., D. Van Nostrand Co., Inc., New York, N. Y., p. 45; 1954.

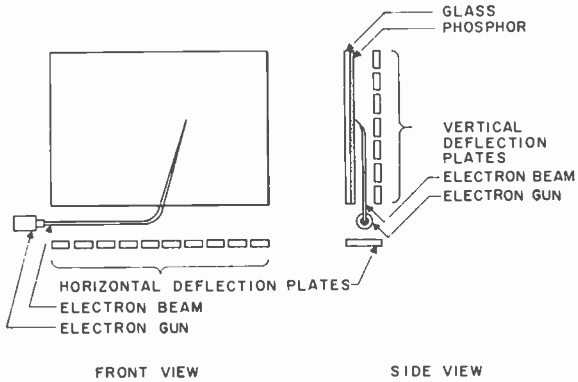

Fig. 1—Schematic diagram of thin crt.

Principle of Operation

Only one of a large number of possible configurations will be described, shown schematically in Fig. 1. The electron beam is injected along the bottom edge of the display screen, and travels in a field-free region between a set of electrodes designated as "horizontal deflection plates" and the bottom edge of the screen. If this edge and the horizontal deflection plates are all at the same (gun anode) potential, the beam continues all the way to the right. However, if the voltage on one of the deflection plates is lowered, the beam is deflected upward. The position at which this deflection occurs can thus be moved in a continuous manner from right to left (or left to right) by sequentially lowering the voltage on adjacent horizontal deflection plates in the appropriate direction.

The upward deflected beam enters another field-free region, bounded on one side by the phosphor screen and on the other by a set of strip electrodes ("vertical deflection plates"), each of which extends all the way across the tube. If the vertical deflection plates are all at the same potential as the phosphor, the beam continues all the way to the top. However, if the voltage on one of the deflection plates is lowered, the beam is deflected into the phosphor. Again, the position at which the deflection occurs can be varied continuously by sequential variation of the voltage on adjacent deflection plates. By choosing the appropriate sequence for each of the two sets of deflection plates (horizontal and vertical), the spot at which the beam strikes the phosphor can thus be made to sweep out a raster.

For practical reasons, the region of the horizontal deflection plates ("primary section") is usually isolated from the region between the vertical deflection plates and the display screen ("secondary section") by a transition section. The transition section also comprises electrostatic lenses, so that it not only isolates the primary section from the secondary, but provides an additional means of controlling beam focusing as well. The main reason why a transition section is necessary, however, is that the primary section is operated at potentials of the order of the accelerating (anode) potential of the electron gun, *i.e.*, about 1 kv, whereas the secondary section is of necessity operated at the potential of the display screen, which with present-day phosphors must be of the order of 15 kv. Under these circumstances the bottom edge of the display screen cannot serve simultaneously as part of both the primary and secondary sections, and a transition section must be provided. An additional lens system is often made part of the transition section to counteract the action of the effective convergent lens on the beam as it passes from the low-voltage primary to the high-voltage secondary section and also to provide additional beam focusing controls after the first deflection.

When an electron beam of finite thickness is deflected by a uniform electrostatic field, the beam is also focused. In conventional crt's, so-called "deflection defocusing" results if the beam actually comes to a crossover as a result of this action and then diverges before arriving at the display screen. In the thin crt, on the other hand, deflection focusing is turned to advantage by judicious juxtaposition of the deflecting plates with regard to the beam and to the display screen.

Upon deflection by the horizontal deflection plates (primary section), the beam is brought to a focus in a plane parallel to the display screen, and if the transition section is properly designed, the cross section of the beam is changed from circular to elliptical as the beam enters the secondary section with the major axis of the ellipse oriented normal to the display screen. The cylindrical beam traveling horizontally along the primary section thus becomes more or less a ribbon beam as it begins its upward travel. Upon deflection by the vertical deflection plates (secondary section), the process is repeated and the beam is again focused, this time in a vertical plane perpendicular to the display screen; the ribbon beam becomes a pinpoint as it tends toward a crossover. If the display screen is located at a plane just before this doubly focused beam actually comes to the second crossover, a relatively small spot size at the display screen can be achieved. (The beam is not permitted to diverge after passing through the crossover toward which it tends as a result of the *first* deflection in the primary section; in fact, it may not even reach this crossover. The combined action of the transition section and of the effective lens through which the beam passes as it travels from the low-voltage primary to the high-voltage secondary section is to offset any tendency of the beam either to diverge or to converge; this action can be optimized in practice by transition-section design and by adjustment of voltages to correct for any adverse effects, including to some extent that of space-charge beam spreading.)

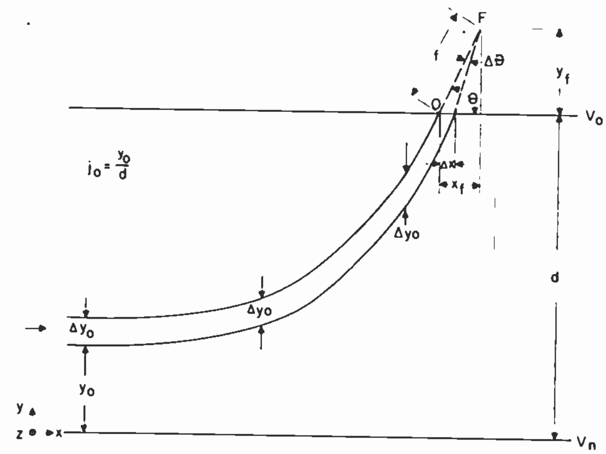

Fig. 2—Trajectories of two adjacent electrons separated by a distance ΔY_0.

Analysis of Deflection Action

In the following analysis, fringing at the edge of the deflection plates is neglected for simplicity, and the field is considered to be quite uniform. Consider two adjacent electrons separated by a distance Δy_0 (Fig. 2) entering a uniform electrostatic field between parallel plates at different potentials ($V_n < V_0$) with a velocity v_x. In a uniform field the vertical elemental separation Δy_0 remains constant as the electrons are deflected by the field, but there will be a focusing effect if we consider a horizontal plane such as $y = d$ since one of the electrons will have fallen through a larger potential than the other. This difference in potential is

$$\Delta V = \frac{dV}{dy}\Delta y_0 = \frac{V_0 - V_n}{d}\Delta y_0 = (V_0 - V_n)\Delta j_0 \tag{1}$$

where $j \equiv y_0/d$. One of the electrons thus achieves a greater y component of velocity than the other, and if the two electrons leave the uniform field at $y = d$ to enter a field-free space, they converge rectilinearly (dashed lines) toward a focal point in the xy plane. The focal length f is given by

$$f\Delta\theta = \Delta x \sin\theta \tag{2}$$

where $\Delta\theta$ is the angular convergence of the two electron paths and Δx is their horizontal separation at $y = d$. The rectangular coordinates x_f, y_f of the focal (crossover) point F with respect to an origin at the exit point O can be derived from (2) to be

$$\begin{aligned} x_f &= f\cos\theta = (\Delta x/\Delta\theta)\sin\theta\cos\theta \\ y_f &= f\sin\theta = (\Delta x/\Delta\theta)\sin^2\theta \end{aligned} \tag{3}$$

which can be rewritten with the help of the expression $\tan\theta = dy/dx$ for the slope as

$$x_f = \frac{1}{\sec^2\theta}\frac{\Delta x}{\Delta\theta}\tan\theta = \tan\theta\frac{\Delta x}{\Delta(\tan\theta)}$$

$$= \left[\frac{dy/dx}{d^2y/dx^2}\right]_{y=d}$$

$$y_f = \frac{1}{\sec^2\theta}\frac{\Delta x}{\Delta\theta}\tan^2\theta = \tan^2\theta\frac{\Delta x}{\Delta(\tan\theta)}$$

$$= \left[\frac{(dy/dx)^2}{d^2y/dx^2}\right]_{y=d}. \tag{4}$$

These expressions thus relate the coordinates of the crossover point with slope (or slope squared) and curvature of the beam path at the exit point. In order to determine the position of the crossover, we must therefore first determine the electron trajectories, either experimentally or analytically. The analytic approach is not prohibitively difficult in the relatively simple geometrical configuration under consideration, provided that we can safely make certain simplifying assumptions. For instance, if we consider a multiplate deflection system (*i.e.*, if we break up the lower plate at a potential V_n in Fig. 2 into a series of short adjacent plates at different potentials $V_1, V_2, \cdots, V_n$), the analysis remains quite simple if we only assume that the electrostatic fields in the region of each plate are uniform (*i.e.*, change abruptly at the boundaries between adjacent plates without fringing) and that the horizontal separation between adjacent plates is negligibly small compared with their lengths.

Under these assumptions the acceleration d^2x/dt^2 in the x direction is zero and the acceleration in the y direction can be written (in terms of the x component of velocity $v_x = dx/dt$) as

$$\frac{d^2y}{dt^2} = v_x^2\frac{d^2y}{dx^2}. \tag{5}$$

This relationship can then be used in conjunction with (4) to determine the position of the crossover point.

It should be pointed out that under the above-mentioned assumption of abrupt changes in the value of the electric field, the acceleration—and hence the curvature d^2y/dx^2 of the beam path—will be discontinuous at the boundaries between adjacent deflection plates. However, the beam path itself and its slope both remain continuous at these transition points. Moreover, the deflection potentials on adjacent plates are usually varied (in a time-correlated fashion, as described below), thus creating additional transitions. Both effects can be taken into account for a given geometrical and voltage configuration in performing a computation of the crossover position x_f, y_f and of the exit angle θ. Conversely, for desired values of these parameters, optimum values of the injection velocity v_x and relative initial position j_0 can be determined.

Effect of Exit Slot

In order to enable the deflected beam to leave the primary section, the upper plate (Fig. 2) at potential V_0 must be slotted in the x direction. The effect of this slot, which can be considered as part of the transition section, is that of a thin lens of focal length given approximately by[2]

$$f_{yz} = \frac{2V}{E_2 - E_1} \tag{6}$$

where V is the acceleration voltage (in the y direction) of the incident particles, and E_1 and E_2 are the scalar magnitudes of the electrostatic fields on the incident and exit sides of the apertured plate, respectively. The subscripts yz are used to indicate that the lens focusing action takes place in the yz plane, in contrast to the deflection-focusing action described by (2)–(4), which takes place in the xy plane. Upon passing through the slot lens, the electron thus acquires a z component of velocity in addition to the x and y components produced by the electron gun and by the deflection plates, respectively. The deflection in the yz plane can be described in terms of an angle α as follows:

$$\tan\alpha = v_z/v_y \tag{7}$$

where α and f_{yz} are related (from analogy with geometrical optics) by

$$\tan\alpha = z/f_{yz} \tag{8}$$

where z is the distance of the entering parallel ray from the axis.

In the configuration represented by Fig. 2, if $E_1 = (V_0 - V_n)/d$ is the magnitude of the uniform electrostatic field in the primary section and E_2 that of the field in the region above the primary section, (6) can be reduced to

$$f_{yz} = \frac{2E_1(d - y_0)}{E_2 - E_1} = \frac{2d(1 - j_0)}{\dfrac{E_2}{E_1} - 1} \tag{9}$$

since the accelerating voltage V (in the y direction) is given by

$$V = Ey = E_1(d - y_0) \tag{10}$$

and $j_0 = y_0/d$ as before.

The slot acts as a divergent lens (defocusing) if $E_1 > E_2$, so that f_{yz} is negative; and as a convergent lens if $E_1 < E_2$. Moreover, (9) enables us to make a quick estimate of the magnitude of f_{yz} in any special case, as in the two following cases.

Case 1—$E_2 = 0$

The beam diverges and

$$f_{yz} = -2d(1 - j_0) < 0.$$

[2] C. J. Davisson and C. J. Calbick, "Electron lenses," *Phys. Rev.*, vol. 38, p. 585; 1931 and vol. 42, p. 580; 1932.

For instance, for an electron entering at the midpoint between the parallel plates ($j_0=0.5$), $f_{yz}=-d$.

Case 2—$E_2/E_1 \gg 1$

The beam converges and

$$f_{yz} \doteq \frac{E_1}{E_2} 2d(1-j_0) > 0.$$

For $j_0=0.5$, $f_{yz} \doteq (E_1/E_2)d \ll d$.

It will be perceived that the exit slot thus represents an important part of the transition section and must be taken into consideration in the design of this section. One practical arrangement, for instance, is to provide an almost field-free region between the primary and secondary sections. In that case, the focusing action is as follows. In the yz plane the beam *diverges* (since $E_2=0$) on passing through the slot, but this divergence is offset by the action of the effective convergent lens represented by the passage from the low-voltage field-free transition section to the high-voltage secondary section. In the xy plane the beam converges as a result of the deflection-focusing action; it is unaffected by the slot, approaches a crossover, and would begin to diverge if it were not for the offsetting action due to the transit from low to high voltage. In the detailed electron-optical design of the transition section, factors such as space-charge spreading and the noncircular beam cross section resulting from astigmatic focusing must be taken into consideration. It should be emphasized that the excellent practical results obtained to date have not depended on the design of the electron gun, which was usually of a conventional, commercially available type; further improvements may well result from modifications which would serve to adapt the gun to the special application under consideration (such as providing a noncircular beam on entry to the primary section). But even with standard guns, the deflection-focusing action of the thin crt yields considerably greater definition without a sacrifice of brightness than can be attained with conventional crt's, and only a slight variation in focus from top to bottom is observed.

Sweep Voltages

The number of deflection plates used to produce a commercial tv raster is of the order of 10 in both the primary and secondary sections. It is not necessary, as might appear at first glance, to provide, let us say, 525 deflection plates to produce a 525-line raster. Instead, the voltage on each deflection plate is varied monotonically from full voltage to near zero in such a way that as one plate approaches zero potential, the next one begins to decrease from its full value. It is expedient to allow the voltage waveforms to overlap in time, *i.e.*, the voltage on the second plate is caused to begin decreasing considerably before the first plate has reached zero potential with a resultant averaging of the deflecting forces acting on the beam. Various combinations of waveforms and amount of overlap can be used to get good linearity.

A number of possible schemes for achieving such sequential operation has been developed. Perhaps the simplest scheme consists of connecting the deflection plates to the anodes of a multianode triode provided with a single variable-mu grid wound in such a way that the several anodes are located opposite a progressively tighter grid mesh, as shown schematically in Fig. 3. A positive-going sawtooth voltage applied to this grid will cause the tube to conduct progressively from top to bottom, so that the requisite sequential operation is obtained; the resistors serve to return the plates to their initial voltage during the retrace pulse. Alternately, a series of separate triodes can be used, the several tubes differently biased to require a progressively larger grid pulse to cause conduction; a sawtooth pulse is then applied to all the grids in common. This is the method that has been most often used to date.

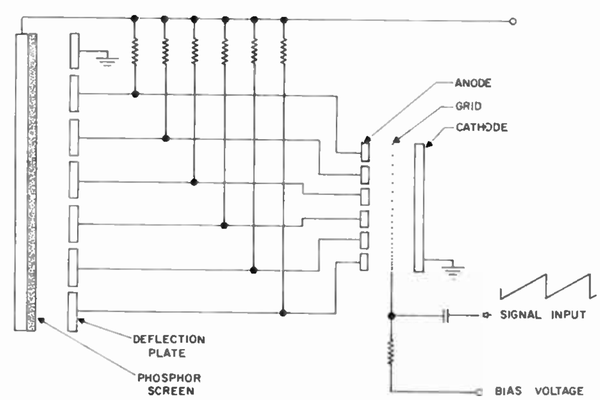

Fig. 3—Variable-mu voltage-sweep tube for secondary section.

In another scheme a sweep tube comprising a cathode-ray gun in conjunction with a series of targets is used, each target connected to a deflection plate. Sequential operation is obtained by deflecting the beam so that it sweeps across the targets in sequence. Resistors are again used to return the several deflection plates to their initial voltage, except that here they can do so without waiting for the retrace.

Still other arrangements that come to mind involve tapped pulse lines, radial beam-switching tubes, and other special devices. It should be pointed out that any electronic device intended for voltage switching in the secondary section must be rated for operation at voltages up to 20 kv. One problem that arises in this connection is the design of tubes in which the effect of high-voltage positive-ion bombardment of the cathode is eliminated to provide long life. One tube, the 6IT6, developed especially for this purpose, which will be described in a companion paper,[3] includes an electrostatic ion trap for the protection of the cathode.

[3] W. R. Aiken and R. E. Heller, "A high-voltage ion-trap pentode," *Electronics Mag.*, (to be published).

Practical Results

A number of models of the thin crt have been constructed, both continuously pumped and sealed off, and comprising various electrode configurations. Fig. 4 shows an experimental television receiver which was first exhibited at WESCON in August, 1956, and under the sponsorship of the U. S. Information Service at the International Trade Fair held in West Berlin in the fall of 1956. The display tube in this particular device is a sealed-off model that measures 12×12 inches (Fig. 5) with a display area covering about 60 per cent of the available glass area; in more recent models of comparable size, the relative display area is about 80 per cent. The horizontal (primary) deflection section contains 10 deflection elements, each approximately 1 inch long. The vertical (secondary) section consists of 8 plates about 1 inch wide, which are made of conducting material deposited on the inside of the back surface. Primary and secondary operating voltages are approximately 1 and 12 kv, respectively. A televised signal displayed on a similar tube is shown in Fig. 6.

In the laboratory, thin crt's up to 24 inches (diagonal) have been constructed, and resolutions as great as 2000 lines (at nearly acceptable brightness levels) have been achieved. In general, the substitution of an electrostatic for a magnetic deflection system makes it possible to achieve deflection with the expenditure of less power than in conventional crt's, especially if care is taken in selecting a deflection-control scheme by which a minimum number of deflection plates is maintained in a lowered voltage condition at any instant; by this method, a minimum amount of power is wasted in those plate resistors which are not active in beam deflection at that instant.

The deflection-focusing action proves to be relatively insensitive to quite substantial variations in the deflection voltages; the percentage changes in both deflection angle and final spot size as the primary- and secondary-section voltages are varied turn out to be very small compared with these voltage changes. Operation of the thin crt is therefore relatively insensitive to power-supply instabilities. Moreover, since the beam is deflected through the same two angles regardless of the ultimate spot position, no aberrations such as are inherent in the variable-angle deflection systems of conventional crt's are present; nor can the effects of other aberrations or fabrication errors become very prominent since the beam travels only a very short distance after the second deflection, so that there is virtually no "lever arm" to magnify such distortions.

There is neither pin-cushion nor barrel-type distortion. One source of aberration is inherent in the variation of the total length of the beam path for various spot positions. Beam spreading results in slightly nonuniform focusing over the area of the screen. In practice, this effect is to a considerable extent compensated by the deflection-focusing action described above.

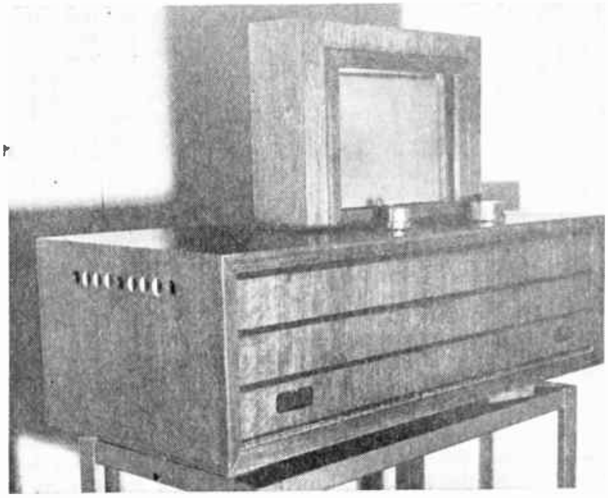

Fig. 4—Experimental television receiver incorporating a thin tube.

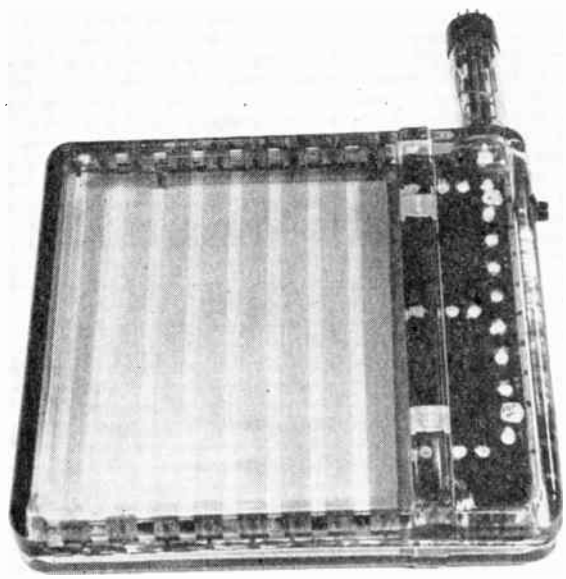

Fig. 5—Experimental sealed-off model (back view). The strips are the vertical deflection plates made from conducting material deposited on the inside of the glass envelope.

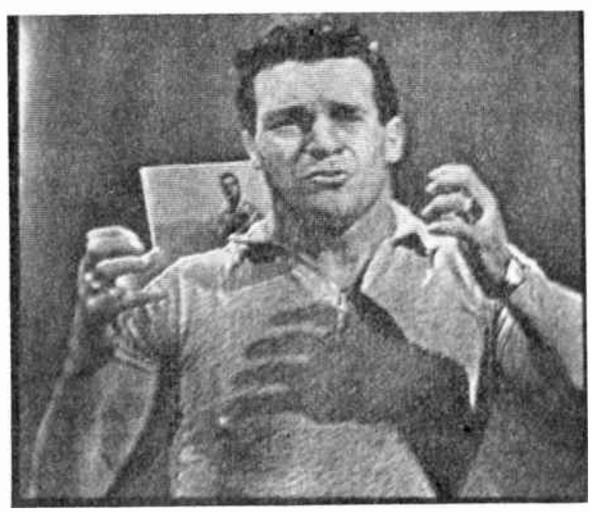

Fig. 6—Video signal received with the thin tube.

One other aberration that must be corrected in the model described in the present paper is that which arises from the finite value of the injection velocity v_x (Fig. 2). The deflection angle θ is given by tan $\theta = v_y/v_x$, and approaches 90° as v_x is made small compared with the deflection velocity v_y. However, since the electrons must be injected with a finite velocity v_x, θ is not quite a right angle, so that an uncorrected rectangular raster appears as a parallelogram skewed at an angle θ that in practice falls around 80°. This aberration can be corrected by a number of methods, including positioning the gun and transition section at an angle θ with respect to the bottom edge of the display area; making a correction in the controlling signal; or immersing the primary section in a localized transverse magnetic field, such as can be obtained by means of a very simple magnetic circuit (a U-shaped bar pole piece) located outside the vacuum envelope.

Methods of adapting the thin crt to two or there primary color operation have been worked out, and experimental models show very promising results, especially with regard to linearity and raster registration. Finally, by the use of transparent vertical deflection plates (such as can be obtained by depositing strip layers of a transparent conducting material on the back plate of the glass vacuum envelope), the thin-crt display can be viewed from both sides simultaneously; if a transparent phosphor is used, the device can be made altogether transparent.

Acknowledgment

The author gratefully acknowledges the contribution of Dr. R. Madey (Brookhaven National Laboratory) to the analytical portions of this paper and the aid of Dr. C. Süsskind (University of California) in the preparation of the manuscript.

New Microwave Repeater System Using a Single Traveling-Wave Tube as Both Amplifier and Local Oscillator*

H. KUROKAWA†, ASSOCIATE MEMBER, IRE, I. SOMEYA†, AND M. MORITA‡, SENIOR MEMBER, IRE

Summary—**This paper describes a new microwave repeater system using one traveling-wave tube as both amplifier and local oscillator. The new system uses a minimum number of vacuum tubes and requires no afc because of the inherent stability of the local oscillator frequency due to the use of a high-Q cavity resonator in the feedback circuit of the traveling-wave tube. The result is marked simplicity in the over-all circuit composition of the repeater equipment.**

Output power, frequency stability, crosstalk, and other characteristics of the new system are examined. Over-all characteristics are also illustrated by examples, and application of the new system to the 480 telephone channels is mentioned.

Introduction

As MICROWAVE repeater equipment for the super-multichannel telephone or television trunk line, the all-traveling-wave-tube-type repeater has some problematic points, such as switching-over to the standby circuit and branching of the circuit, and also cannot be considered economical with increase in the number of microwave tubes. For these reasons, throughout the world the heterodyne repeater system has been used mostly. Nevertheless, this system has some difficulties in that it requires the local oscillator (LO) and its automatic frequency control (afc) or the frequency multiplier circuit following the crystal oscillator, besides the main circuits (IF amplifier, mixer, and power amplifier) through which the signal passes.

The authors have studied and developed a new system of microwave repeater equipment [1, 2] which uses one traveling-wave tube for a combined purpose of both power amplification and local oscillation, and does away with the LO klystron and its afc. Some of the more important points of the new repeater system are given below.

Principle and Composition of New Repeater System [5]

The new system, as far as the signal passing through is concerned, is similar to the conventional heterodyne repeater equipment. As shown in Fig. 1, the band-pass filter (BPF), receiving mixer (MIX), IF amplifier (IFA), high-power mixer (MIX), and traveling-wave tube power amplifier (TWT) are connected in tandem. The LO power is shifted in frequency corresponding to the difference between the sending and receiving frequencies be-

* Original manuscript received by the IRE, February 8, 1957; revised manuscript received, September 24, 1957.
† Nippon Telephone and Telegraph Corp., Tokyo, Japan.
‡ Nippon Electric Co., Ltd., Kawasaki, Japan.

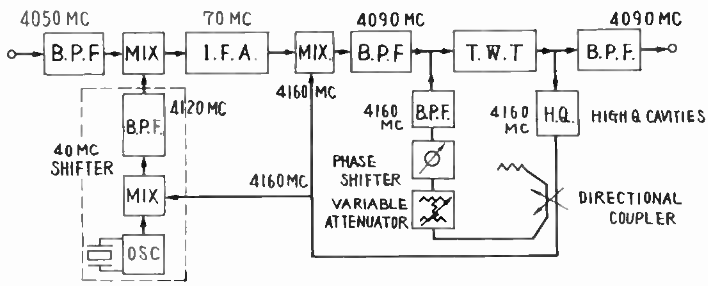

Fig. 1—Block diagram of the new system.

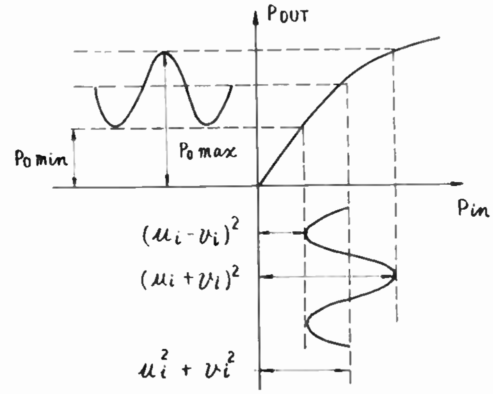

Fig. 2—Working condition of a traveling-wave tube when two frequencies are simultaneously amplified.

fore it is applied to the receiving mixer. This is also similar to the conventional repeater equipment.

As mentioned, the uniqueness of the new repeater system lies in the use of the traveling-wave tube as both power amplifier and local oscillator with provision of a proper filter at either side of the traveling-wave tube input and output. Through these filters the sending frequency is separated from the LO frequency, and only the latter is fedback from the output side of the traveling-wave tube to its input side. The feedback circuit is provided with a resistance attenuator and a phase shifter; and by properly adjusting an amount of the feedback, the traveling-wave tube is made to oscillate at the LO frequency.

A major part of the LO power produced is fed to the high-power mixer and is modulated by the IF into the sending frequency, which is then passed back to the traveling-wave tube. The traveling-wave tube, by virtue of its broad-band characteristics, amplifies the sending frequency while it is generating the local frequency. The amplified sending frequency is separated from the LO frequency at the output side of the traveling-wave tube and is delivered to the antenna system. This is the operating principle of the new system. In practice, the directional coupler is employed to separate the feedback power from the LO output, and high-Q cavity resonators are provided in the feedback circuit to stabilize the LO frequency. (This resonator also serves as a branching filter.) Two cavity resonators are coupled together to provide the band-pass characteristics and thereby avoid variation in oscillation strength.

Transmitting Power Output

Before discussing the power output of the new repeater system, the general output characteristics when two frequencies are amplified simultaneously at a traveling-wave tube will be studied. Let u_i and v_i be the input amplitudes of two frequencies. The composite input of two frequencies produces beat, and pulsates from a minimum instantaneous input $(u_i - v_i)^2$ to a maximum instantaneous input $(u_i + v_i)^2$. Against this variation, since the traveling-wave tube generally has a saturation characteristic as shown in Fig. 2, the output pulsates from $P_{0\,\min}$ to $P_{0\,\max}$, as the curve in the diagram shows. Although the precise calculation is difficult, if the following rough approximate equation for the saturation characteristic is assumed, the output powers for two frequencies, u_0^2 and v_0^2, can be calculated [3].

$$O = 1 - e^{-I}, \tag{1}$$

where O = output amplitude in relative value, and I = input amplitude in relative value. If we substitute the composite wave of u_i and v_i for I in the above equation, we obtain the output composite wave including various frequencies.

Now, for simplicity, we assume that: 1) The frequency characteristics of the gain of the traveling-wave tube amplifier is flat in the frequency band considered. 2) The harmonics in the output composite wave are negligible. Then we obtain

$$(u_0 + V_0)^2 = 1 - e^{-(u_i+v_i)^2} \tag{2}$$

$$(u_0 - V_0)^2 = 1 - e^{-(u_i-v_i)^2}. \tag{3}$$

Fig. 3 shows such calculated results, which can be translated further as Fig. 4. From Fig. 4 the following may be said qualitatively:

1) When a composite input is constant, gain of the composite output vs composite input is at a minimum when the amplitudes of two frequencies are equal. As the ratio of u_i to v_i becomes separated from 1, the more apart, the larger the gain until it approaches the gain of a single frequency.
2) When the ratio of u_i to v_i is constant, the smaller the composite input, the nearer the gain approaches that of a single frequency. As the composite input becomes larger, and the average operating point nears the maximum saturation point, reduction in gain due to the two frequencies becomes marked.

When the above phenomena are applied to the new repeater system, the following may be said from 1). Namely, reduction in gain of the sending frequency due to the use of the traveling-wave tube for both amplification and local oscillation, decreases abruptly as the power required for the LO becomes small. If the gain of

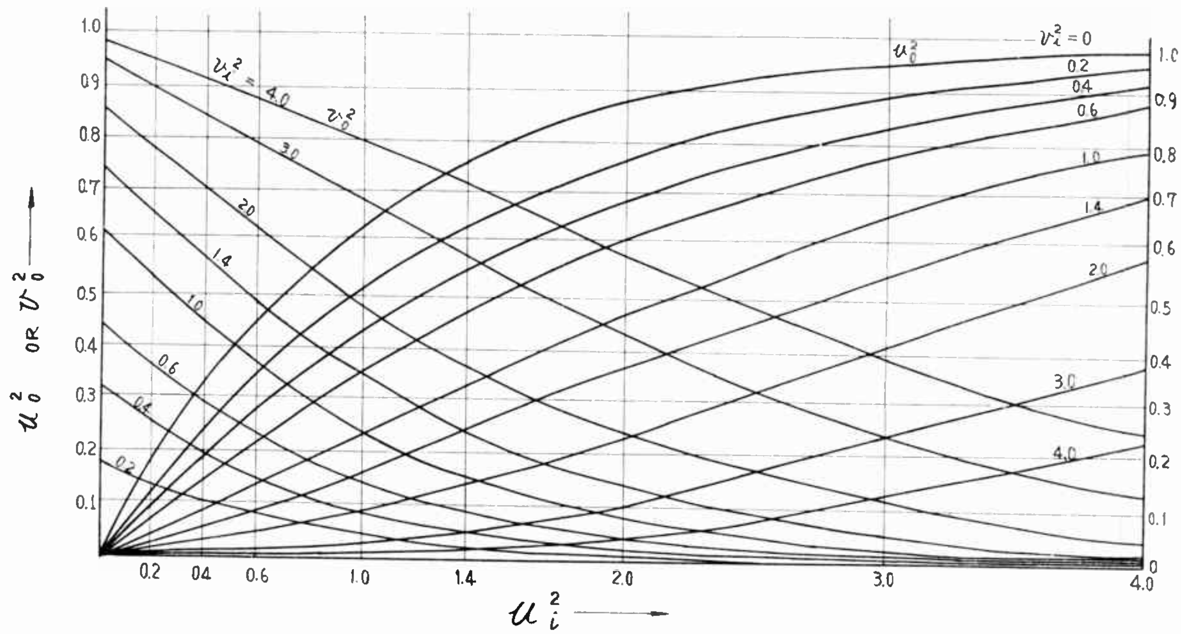

Fig. 3—Characteristics of a traveling-wave tube when two frequencies are simultaneously amplified (calculated).

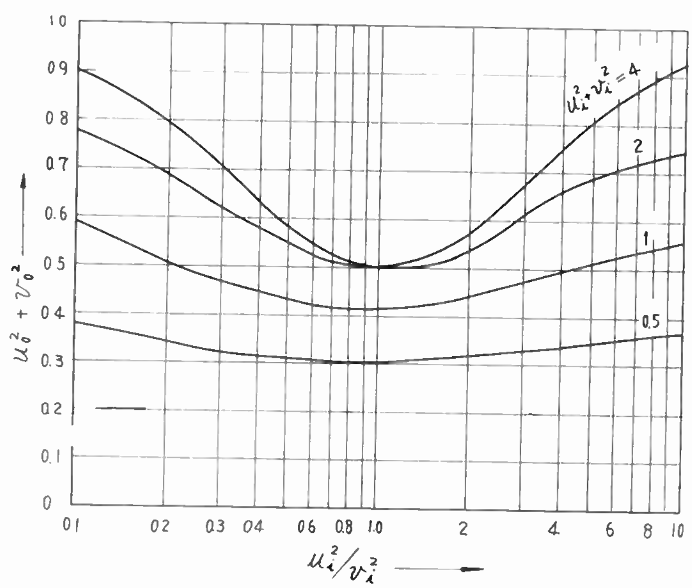

Fig. 4—Total output power vs input power ratio (calculated).

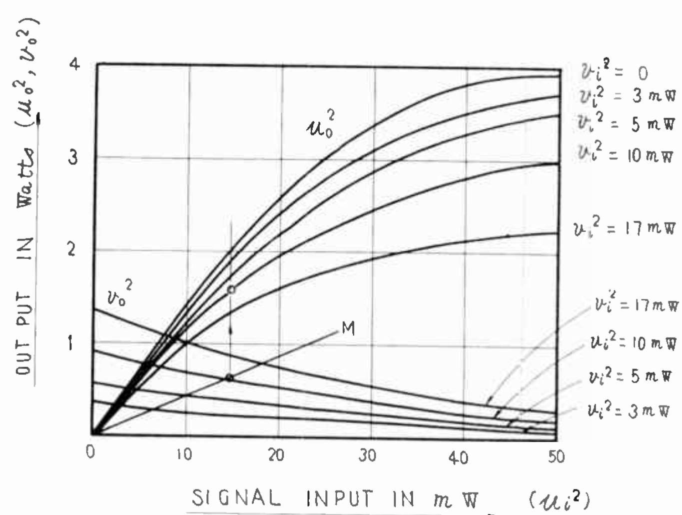

Fig. 5—Measured characteristics of a traveling-wave tube when two frequencies are simultaneously amplified.

the traveling-wave tube is sufficiently large, only a small amount of the high-power mixer output would be required; therefore, a small amount of the LO output would be sufficient for the high-power mixer. Thus considered, reduction in gain of the traveling-wave tube due to the new system becomes a negligible factor. From 2), it is also seen that the traveling-wave tube used in this system should have preferably a high maximum saturation point.

In practice, however, since the adjustment of the helix voltage and the matching between the waveguide and tube are aimed at obtaining the optimum condition of the sending frequency, gain for the two frequencies would not be identical in each case. Fig. 5 shows the measured value of the amplification characteristics using a type 4W75 4000-mc band traveling-wave tube [11].

The abscissa represents the sending frequency input (u_i^2); the ordinate, the sending frequency (u_0^2) and LO frequency output (v_0^2); the parameter, the LO frequency input (v_i^2). Straight line M represents the characteristics when the conversion loss (LO→signal) of the high-power mixer is made constant. The sending output for each LO input is represented by an output on curve u_0^2, which corresponds to the signal input at the intersection of line M and curve v_0^2. When the LO input is varied successively (in practice, the resistance attenuator in the feedback circuit is varied), the characteristics shown in Fig. 6 are obtained. It will be noted in the diagram that, with increase in the LO input, the mixer output increases, while the amplification of the traveling-wave tube decreases. Eventually, there exists a peak for the sending output, which is about 1.6 watts in this example. When this is compared with an output of 2

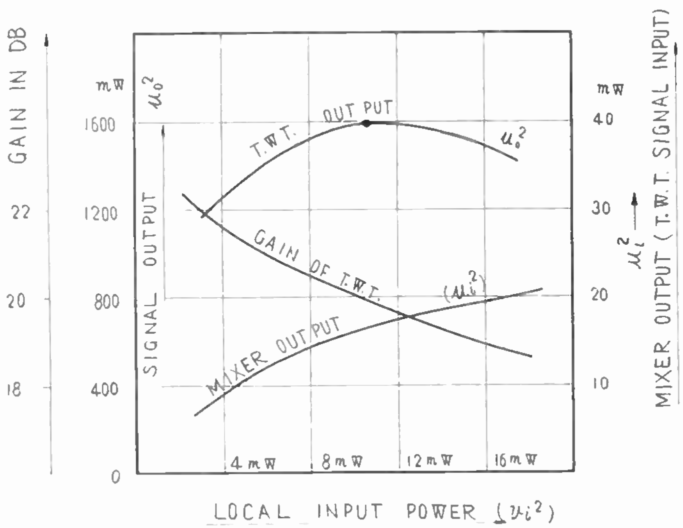

Fig. 6—Relations between output power vs LO power.

watts which would be gained with an identical input by a single-frequency amplifier, the output is about 1 db down. However, an output loss of this extent is considered to be quite permissible because of the large advantage that this system offers.

As described, the operating point of the traveling-wave tube in this system can be readily set to its peak by varying the resistance attenuator in the feedback circuit. However, since a marked variation in this operating characteristic might cause cutoff of the local oscillation, the helix voltage of the traveling-wave tube is stabilized by the series tube. The supply circuit design also considers possible reduction in gain of the traveling-wave tube due to decrease in the cathode emission current during a prolonged tube use. To remedy this, the first anode voltage is controlled to keep the cathode current constant at all times.

From a number of past showings, it has been made clear that the repeater equipment thus designed and constructed, retains the initially selected operating condition for a long period of time.

Frequency Stability

Initial Drift of Oscillation Frequency

In each of the conventional microwave oscillators such as klystron oscillator, light-house tube oscillator, and magnetron, a part or entire resonance cavity which determines the oscillation frequency is made up of its tube electrodes; and because of deformation of these electrodes from temperature rise in the initial period of oscillation, frequency drift at the start of oscillation cannot be avoided. In the traveling-wave tube which has high-Q cavity resonators inserted in the feedback circuit, the main element which determines the frequency is outside the traveling-wave tube and is not influenced by temperature rise.

Fig. 7 shows a value actually measured. When the heater is connected in advance, frequency drift at the start of oscillation is of order less than 4×10^{-6}, and

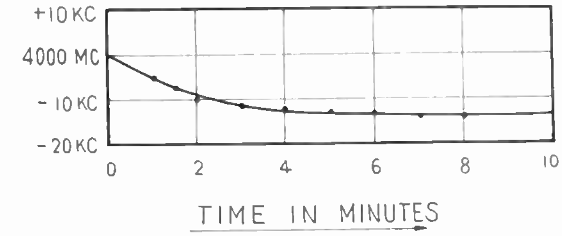

Fig. 7—Frequency drift of the twt oscillator.

immediately after the throwing of the main switch, the system is in perfect readiness for normal operation. The above drift, in the meantime, is considered to be attributed to the expansion of the helix and the change of dielectric constant of support rods due to the temperature rise at the start of oscillation.

Frequency Variation Due to Supply Voltage Variation

In general, the following relation [6, 7] holds true:

$$\frac{d\theta}{dV} \doteqdot \frac{\pi}{2}\cdot\frac{N}{V} \text{ radian}/V \tag{4}$$

where

V = helix voltage
dV = amount of variation in helix voltage
N = length of helix expressed in the number of waves
$d\theta$ = amount of phase variation in amplified wave.

Also, when the traveling-wave tube is given a feedback, it becomes an oscillator.

Then, if the amplified wave in the traveling-wave tube changes its phase θ by $d\theta$, the oscillation frequency f is changed by df and the entire phase ϕ in the loop circuit is changed by $d\phi$. The relations between $d\theta$, $d\phi$, and df are given by

$$d\theta + d\phi = 0 \tag{5}$$

$$\frac{df}{f} = \frac{d\phi}{\phi}. \tag{6}$$

Therefore, the next equation between the phase variation in the traveling-wave tube and the variation of the oscillation frequency is obtained:

$$\frac{df}{f} = \frac{-d\theta}{\phi} = \frac{-d\theta}{2\pi(N + N_Q + N_\beta)}, \tag{7}$$

where

N_Q = equivalent length of frequency reference cavity (expressed in the number of waves)

N_β = equivalent length of feedback circuit (expressed in the number of waves).

And when there are n cavities, the following relation exists:

$$N_Q = \frac{nQ}{\pi}, \tag{8}$$

where

Q = loaded Q for one cavity.

From (4) and (7), the relation between voltage variation and frequency variation becomes

$$\frac{df}{f} = \frac{N}{4(N + N_Q + N_\beta)} \cdot \frac{dV}{V}. \tag{9}$$

The traveling-wave tube tested was of the type 4W75, $N = 35$, the reference resonator used consisted of two cavities, each of whose $Q = 4000$, and it was assumed that $N_\beta \doteq 570$. These values were substituted in (9), the obtained value of the frequency variation was about 330 kc for 3 per cent variation in supply voltage at 4000 mc. As shown in Fig. 8, the measured value agreed approximately with the above calculated value. Variation of this extent is permissible for a transmitter and receiver equipment operating at 4000 mc. In actual equipment, however, the helix voltage is stabilized to avoid the oscillation amplitude variation with the supply voltage. Since the feedback gain for the stabilizing circuit is sufficient (more than 40 db), variation of oscillation frequency with the ac supply voltage is not experienced at all. Eventually the temperature coefficient for the frequency reference cavity will remain as the final problem. Presently, the reference cavity is made from invar metal and provides sufficient accuracy for practical purposes.

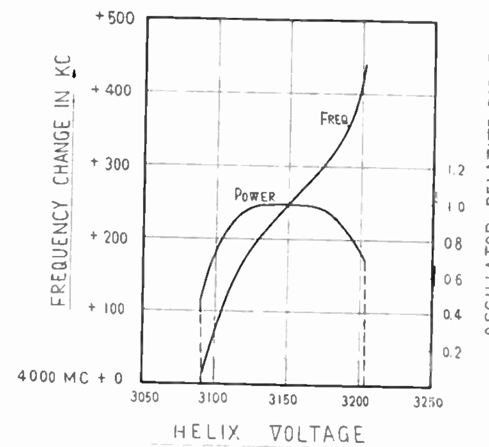

Fig. 8—Frequency and power variations caused by the variation of the helix voltage.

Unintelligible Crosstalk

In this system, the frequency-modulated signal from the high-power mixer and the LO frequency are simultaneously amplified at the same traveling-wave tube. In this case, cross modulation phenomenon from the transmitting signal to the LO frequency was a matter of concern. This study showed that the cause of cross modulation primarily lies in the phase modulation of the output wave due to the amplitude variation in the traveling-wave tube input, and that other factors are negligible.

If the frequency/amplitude characteristic for the IF amplifier, mixer, and waveguide filter, etc. are not flat throughout, the high-power mixer output suffers amplitude modulation during frequency modulation. The undesirable amplitude modulation thus produced is passed to the traveling-wave tube where it is converted to the phase modulation [12].

This phase modulation occurs in the transmitting frequency and is also present in the LO frequency. Among these effects on the signal are the phenomena experienced as long as the traveling-wave tube is used as an output tube, even in the conventional heterodyne repeater equipment in which the local oscillator is provided separately. When this fact is considered, the amplitude characteristic of the IF amplifier, of course, should be sufficiently flat. However, the point which needs special consideration [4] is that the LO frequency, which should be fundamentally free from modulation, is frequency-modulated, since this is a distortion due to the feature of the new system. On this point it can be said that unintelligible crosstalk may be explained as follows: when the frequency deviation of the signal and that of the LO are linearly related, no distortion is produced and accordingly no unintelligible crosstalk is present. However, when amplitude-frequency characteristics for the IF amplifier and mixer have to be expressed by the quadratic, cubic, or still higher order curves, the LO frequency is frequency modulated by the harmonic components of the modulation frequency of the signal. These are mixed up at the high-power and receiving mixer stages and added to the signal as unintelligible crosstalk.

In the above explanation, cross modulation was referred as "phase modulation" or as "frequency modulation." Strictly speaking, the correct use of either term depends on the modulation frequency being considered. When a very low modulation frequency is considered, the LO frequency which undergoes phase modulation at the traveling-wave tube is frequency-modulated, since phase change is proportional to frequency deviation in the feedback circuit. In a usual traveling-wave tube oscillator, it is clear that when the phase of the amplified wave in the traveling-wave tube is changed by some means, its phase variation equals the variation of the phase in the feedback loop including helical line in the tube and cavity resonators because of the variation of the oscillation frequency. The above mechanism is similar when the phase in the traveling-wave tube oscillator is affected by the low-modulation frequency, the sidebands of which are not cut down by the cavity resonators in the feedback circuit. Thus, if a small deviation range is considered, the deviation of the LO frequency is proportional to the phase variation in the traveling-wave tube, which relates the amplitude variation of the signal frequency and does not relate its modulation frequency. Therefore, in the low-modulation frequency, the deviation can be measured by the method in which the signal amplitude changes statically.

Fig. 9 shows statically measured values of frequency variation. In this measurement, the IF output applied

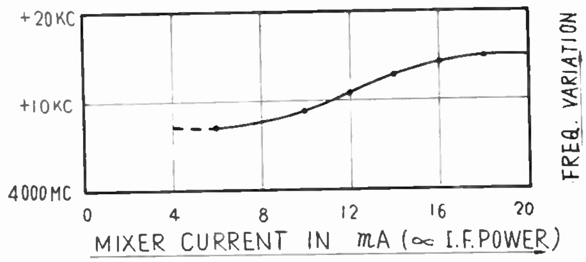

Fig. 9—Variation of local oscillator frequency caused by the variation of input power.

to the high-power mixer was varied successively to give corresponding variation in signal input to the traveling-wave tube, and each LO frequency variation was measured. The results showed that for a variation of 20 per cent in signal input, the corresponding variation in the oscillation frequency was 2 kc. Accordingly, when it is assumed that the amplitude/frequency characteristic up to the traveling-wave tube is a single-peak characteristic of the 0.1-db deviation in ± 4-mc band, the second harmonic distortion becomes 92 db, which is quite negligible for practical purposes.

Let us next consider the case of higher modulation frequency. With a higher-modulation frequency component, its sideband waves are fully attenuated in passing through the cavity resonators and are hardly fed back to the traveling-wave tube input side. It is more reasonable, then, to assume that the phase modulation occurs at the traveling-wave tube output side.

Under the above circumstance, if the LO frequency supplied to the high-power and receiving mixers is branched off at the output side of the traveling-wave tube, the modulated component cross-modulated at the tube is also passed out to the mixers. But if branching to the mixers is made after the two high-Q cavity resonators, the cross-modulated component reaching the mixers is reduced exceedingly and suppressed in amount as to be harmless for practical purposes. Attenuation of sideband waves by two high-Q circuits increases at a rate of about 12 db per octave, and becomes about 33 db at a modulation frequency of 2 mc which corresponds to the highest subcarrier of 480 channels. Although distortion developed through phase modulation increases at a rate of 6 db per octave, when the above attenuation is subtracted, distortion decreases substantially at high-modulation frequencies. At low-modulation frequencies, cross modulation shows up in the form of frequency modulation as stated previously, and results in frequency deviation unrelated to the modulation frequencies themselves.

Thus, the new system provides two-frequency simultaneous amplification completely free from cross modulation using the same traveling-wave tube, due to the fact that one of the frequencies is the LO frequency without modulation, which permits the use of high-Q cavities. On this point, the new system differs distinctly from the all-traveling-wave tube repeater system using reflex principle [12], which produces cross modulation.

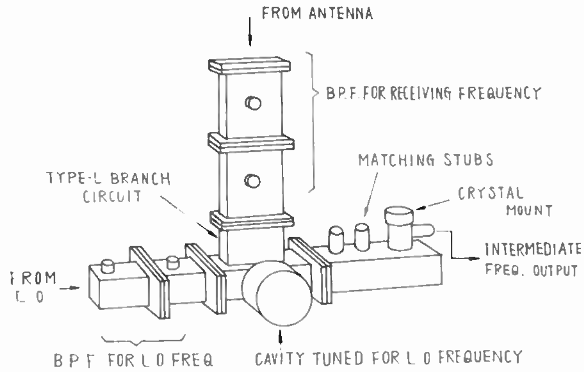

Fig. 10—Single mixer using the type-L branch circuit.

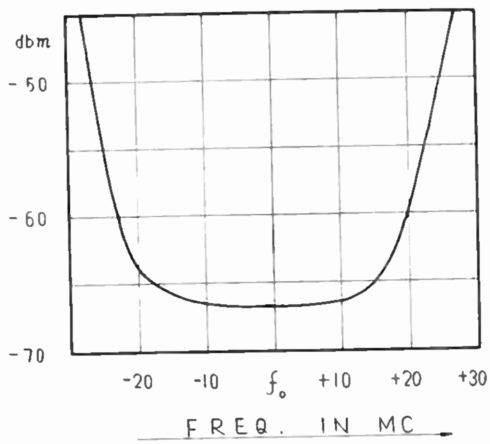

Fig. 11—Amplitude-frequency characteristic of receiver section of the repeater.

Over-all Characteristics of New-System Repeater Equipment [9]

Receiver Section Characteristics

The receiver section of the new-system repeater equipment consists of a single mixer, four stages of inverted-type amplifier following the mixer, and a main IF amplifier operating in 70 mc$\pm$20 mc band. As shown in Fig. 10, the single mixer employs an L-type branching circuit [10] specially designed to eliminate the leak of the LO output to the receiving antenna side. Noise figure of this section averages 12 db. At the top of the receiver input, the matching and adjusting circuit is provided, and it keeps the vswr value below 1.1 in the bandwidth of 20 mc. This circuit is inserted to prevent the generation of echo distortion in the fm wave. Fig. 11 shows the amplitude/frequency characteristic curve of the over-all receiver section, the deviation of which is within 0.2 db in ± 10 mc band. In the agc characteristics, the output variation is suppressed to about 0.5 db for the input variation between -25 dbm and -60 dbm.

Transmitter Section Characteristics

The transmitter section consists of an IF amplifier unit operating in 70 mc$\pm$20 mc band, a high-power mixer using the germanium diodes, and a traveling-wave tube which follows the mixer. Because of the non-

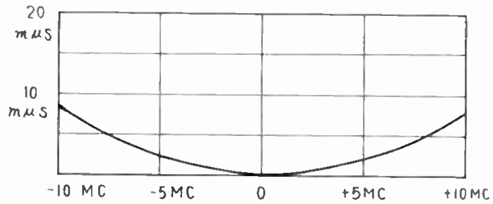

Fig. 12—Delay distortion of the repeater.

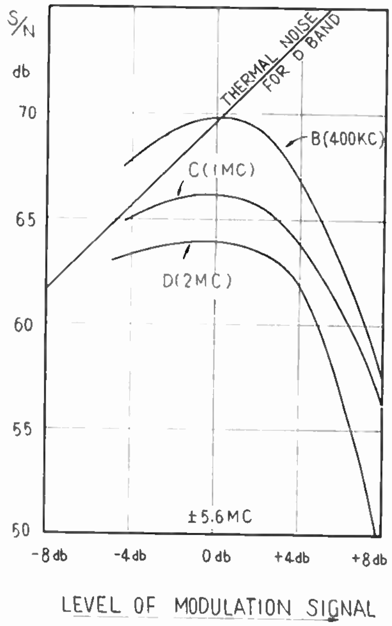

Fig. 13—Noise loading test results when modulator-2 repeaters-demodulator are connected in tandem.

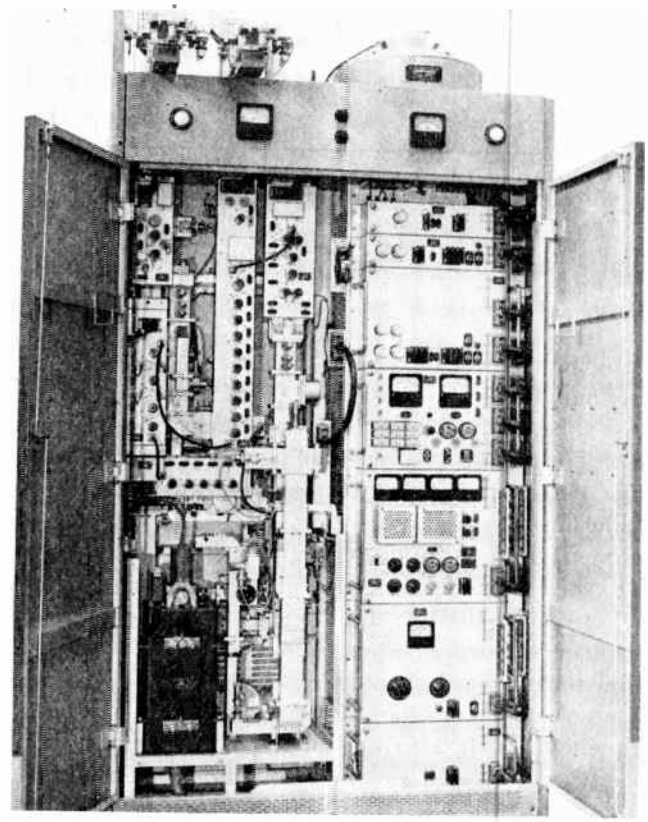

Fig. 14—Front view of new repeater (4 kmc), used for trunk line in Japan.

linearity of the traveling-wave tube, this system produces spurious frequencies at intervals of 70 mc, for which a band-pass filter (bpf) is provided at the output side of the tube. As in the case of the input side of the receiver equipment, a directional coupler for matching adjustment is provided at the output side of the transmitter equipment. The traveling-wave tube amplifier unit also provides the agc function. Because of the saturation characteristic of the traveling-wave tube, when the IF output varies and in turn varies the converted microwave signal, the LO output increases or decreases inversely to vary the conversion loss at the mixer, and suppresses variation in mixer signal input.

Transmitter and Receiver Over-All Characteristics

Over-all delay distortion of the transmitter and receiver in this system is about 8 mμsec in ±10-mc band, a typical example of which is shown in Fig. 12. As the above measurement shows, the value measured between the receiver input and transmitter output agrees with that measured between the receiver input and high-power mixer output. Therefore, delay distortion at the power amplifier of the traveling-wave tube is a negligible factor.

For testing the over-all characteristics of this repeater equipment as applied to the super-multichannel circuit, two repeater equipments were tandem-connected. To this an fm modulator-demodulator equipment was connected, and a noise loading test corresponding to that for the 480 channels was made. The result was expressed in terms of signal-to-noise ratio (snr) per channel as show in Fig. 13. In the diagram, the ordinate shows the composite frequency deviation; and parameters *B*, *C*, and *D* represent snr of channels whose subcarriers are 400 kc, 1 mc, and 2 mc, respectively. According to the diagram, the signal-to-noise value of curve *D*, representing the worst snr channel of the 480 channels at the standard modulation depth (ordinate 0 db) of 280 kc per channel, is 64 db. Since the snr of the fm modulator-demodulator itself is 65 db, the signal-to-noise deterioration due to distortion of two repeater equipments is better than 70 db, which is considered to meet the requirements for the CCIF 2500-km circuits. This distortion is made up mainly of delay distortion. It has been proved, after all, that the use of the traveling-wave tube for the dual purpose of amplification and oscillation presents no problem, except that a slight lowering of its output is encountered. Fig. 14 shows a front view of one of the new repeaters. Fig. 15 shows a photograph of an improved model. This model is considerably more simplified in circuitry and miniaturized in size, exhibiting full advantages of this system; it is 210 cm high by 52 cm wide by 22.5 cm deep, including power units. Fig. 16 shows a package type traveling-wave tube, type 4W75 [11], used in the improved model.

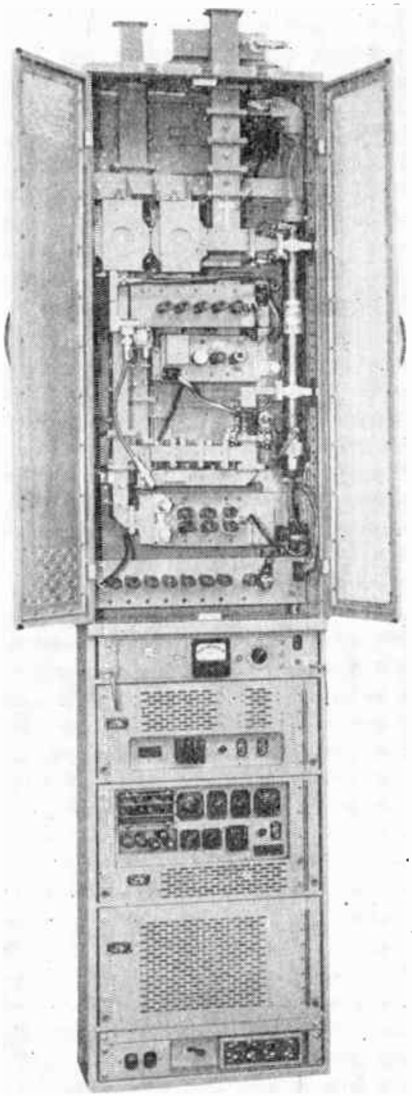

Fig. 15—Front view of improved and miniaturized new repeater (4 kmc).

Fig. 16—Package type traveling-wave tube (type 4W75), used for improved repeater shown in Fig. 15.

Conclusion

This new repeater system, compared with the conventional heterodyne system, provides the following features: 1) a separate LO is not required, 2) an afc is not required, and 3) as a result, the entire equipment has been markedly simplified.

The following are some of the concrete advantages gained through the use of this repeater equipment on such circuits. In the conventional system route between Osaka and Fukuoka, the number of vacuum tubes used per repeater equipment is 70, of which four are microwave tubes. In the new system installed along Tokyo, Sendai, and Sapporo, the number of vacuum tubes used per repeater equipment is 35, of which only one is the microwave tube. The difference between the two arises from the absence of the LO tubes and the automatic frequency control circuit for the oscillator in the new system.

It is expected, then, that, because of the simplified circuitry of the new system, sharp reduction of maintenance labor, of failure percentage, and of vacuum tube replacement costs can be realized. Already 240 such repeater equipments have been made and installed in many stations along the trunk line, and are now regularly operating with excellent results. The fact that percentage failure for the above trunk line is markedly low in comparison with those of the conventional circuits is considered proof of the merits of this system.

Acknowledgment

This study has been completed after several years of joint research by the Nippon Telephone and Telegraph Public Corporation and Nippon Electric Company. The authors wish to express their deep gratitude for various valuable contributions made by I. Konishi, T. Matsumoto, T. Fukami, and T. Masuda of the Nippon Telephone and Telegraph Public Corporation, and T. Kawahashi and M. Kenmoku of Nippon Electric Company, and for the helpful guidance and encouragement received from our supervisors.

Bibliography

[1] Morita, M. "Problems of Super-Multichannel Telephone Repeater Equipment," *Proceedings of the Institute of Electrical Communication* (Japan), Vol. 37 (September, 1954), pp. 608–612.

[2] Morita, M. "New Microwave Repeater System," *Joint Convention Record of the Institute of Electrical Communication and the Institute of Electrical Engineer* (Japan), (October, 1954), pp. 604.

[3] Masuda, T., Takata, M., Yamamoto, R., and Noda, K. "On Nonlinearity and 2-Frequency Amplification of Traveling-Wave Amplifier," *Joint Convention Record of the Institute of Electrical Communication and the Insittute of Electrical Engineer* (Japan), (April, 1955), p. 719.

[4] Fukami, T., Takata, M., and Yamamoto, R. "Unintelligible Crosstalk Produced When Traveling-Wave Tube Is Used for Both Amplification and Local Oscillation," *Joint Convention Record of the Institute of Electrical Communication and the Institute of Electrical Engineer* (Japan), (April, 1955), p. 843.

[5] Hayashi, S., Yokoi, D., and Morita, M. "On Composition of New Type Micro-Wave Repeater Equipment," *Convention Record of the Institute of Electrical Communication* (Japan), (October, 1955), p. 95.

[6] Beam, W. R. and Blattner, D. J. "Phase Angle Distortion in Traveling-Wave Tubes," RCA Review, Vol. 17 (March, 1956), pp. 86–99.

[7] Johnson, H. R. and Whinnery, J. R. "Traveling-Wave Tube Oscillators," IRE Transactions, PGED-2 (January, 1953), pp. 11–35.

[8] Sawazaki, N. and Homma, T. "New Microwave Repeater System Using Traveling-Wave Tubes," Proceedings of the IRE, Vol. 44 (January, 1956), pp. 19–24.

[9] Konishi, I., Matsumoto, T., Fukami, T., and Kawahashi, T. "On The Characteristics of New Type Microwave Repeater Equipment," *Convention Record of the Institute of Electrical Engineer* (Japan), (October, (1956), p. 96.

[10] Kawahashi, T. "L-type Branching Circuit," *Joint Convention Record of the Institute of Electrical Communication and the Institute of Electrical Engineer* (Japan), (1954), p. 512.

[11] Mishio, H., Nemoto, T., and Yasuda, S. *A Package-Type Traveling-Wave Amplifier For 4000 Megacycle Band*, presented at the Congres International on Tubes Hyperfrequences, Paris, France, 1956.

[12] Laico, J. P., McDowell, H. L., and Moster, C. R. "A Medium Power Traveling-Wave Tube for 6000-Mc Radio Relay," *Bell System Technical Journal*, Vol. 25 (November, 1956), pp. 1285–1346.

IRE Standards on Graphical Symbols for Semiconductor Devices, 1957*

57 IRE 21. S3

COMMITTEE PERSONNEL
1957–1958

Symbols Committee

H. R. Terhune, *Chairman*
R. T. Haviland, *Vice-Chairman*

H. W. Becker
E. W. Borden
D. C. Bowen
M. C. Cisler
W. A. Ford
I. L. Marin
C. D. Mitchell
E. W. Olcott
M. B. Reed
C. F. Rehberg
R. V. Rice
M. P. Robinson
M. S. Smith
R. M. Stern
H. P. Westman

The Symbols Committee gratefully acknowledges the valuable assistance rendered during the preparation of these Standards by the Semiconductor Device Symbols Task Group, 28.4.8. The membership of the task group was:

S. K. Ghandhi, *Chairman*
J. M. Goldey
B. J. Rothlein

Standards Committee

M. W. Baldwin, Jr., *Chairman*
C. H. Page, *Vice-Chairman*
R. F. Shea, *Vice-Chairman*
L. G. Cumming, *Vice-Chairman*

J. Avins
W. R. Bennett
J. G. Brainerd
D. R. Brown
T. J. Carroll
P. S. Carter
A. G. Clavier
G. A. Deschamps
S. Doba, Jr.
J. E. Eiselein
D. Frezzolini
E. A. Gerber
A. B. Glenn
H. Goldberg
V. M. Graham
R. A. Hackbusch
H. C. Hardy
D. E. Harnett
A. G. Jensen
I. M. Kerney
J. G. Kreer, Jr.
W. A. Lynch
A. A. Macdonald
W. Mason
D. E. Maxwell
H. R. Mimno
G. A. Morton
J. H. Mulligan, Jr.
W. Palmer
R. L. Pritchard
P. A. Redhead
R. Serrell
H. R. Terhune
W. E. Tolles
J. E. Ward
E. Weber
W. T. Wintringham

Foreword

These Standards are supplementary to, and should be used in conjunction with, IRE Standards on Graphical Symbols for Electrical Diagrams, 1954 (54 IRE 21. S1). The following are some points of general philosophy underlying their development.

1) The symbol structure should reflect the past; *i.e.*, the symbols should, within a logical framework, revert in their simplest forms to those commonly in present use.
2) The symbol structure should look to the future; *i.e.*, it should be capable of extension to the many new semiconductor devices that may become available.
3) The symbol structure should indicate physical properties, when this is possible, without overcomplication.

The Symbols Committee feels that these Standards comply with the general philosophy expressed above. Section 2.0 illustrates the application of the ancillary symbols of Section 1.0 to a variety of semiconductor devices.

1.0 Basic Rules and Symbol Elements

This section sets forth the basic rules and symbol elements for the construction of graphical symbols for semiconductor devices. See *1.17* for full details of graphical construction.

* Approved by the IRE Standards Committee, July 11, 1957. Reprints of this Standard, 57 IRE 21. S3, may be purchased while available from the Institute of Radio Engineers, 1 East 79th Street, New York, N. Y., at $.60 per copy. A 20 per cent discount will be allowed for 100 or more copies mailed to one address.

1.1 Semiconductor region with one ohmic connection. (In the illustration, the horizontal line indicates the base region and the vertical line indicates the ohmic connection.)

1.2 Semiconductor region with a plurality of ohmic connections. (In the illustrations, the horizontal lines indicate base regions and the vertical lines indicate ohmic connections.)

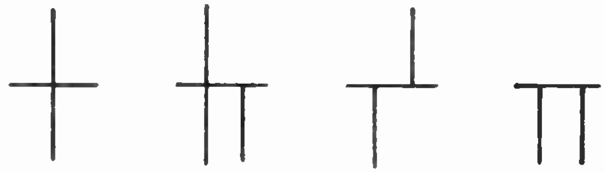

1.3 Transition between *P* and *N* regions (either *P* to *N* or *N* to *P*). (Slant lines indicating transitions shall be appreciably shorter than collector and emitter lines. Note that the transition is along the horizontal line and that no ohmic connection is made to the slant line. See *2.9* and *2.11* as examples.)

1.4 Intrinsic (*I*) region between regions of dissimilar conductivity type. (Slant lines indicating transitions shall be appreciably shorter than collector and emitter lines. Note that the transition is along the horizontal line and that no ohmic connection is made to the slant line. See *2.14* and *2.15* as examples.)

1.5 Intrinsic (*I*) region between regions of similar conductivity type. (Slant lines indicating transitions shall be appreciably shorter than collector and emitter lines. Note that the transition is along the horizontal line and that no ohmic connection is made to the slant line. See *2.16* and *2.17* as examples.)

1.6 *P* region on *N* region (rectifying junction).

(a) (b)

1.7 *P* emitter on *N* region. (The slant line with arrowhead represents the emitter and the horizontal line represents the *N* region.)

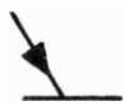

1.8 Plurality of *P* emitters on *N* region. (When possible, the electrodes on the symbol drawing should have the same relative order as the electrodes on the device.)

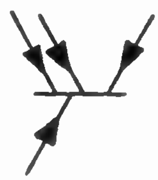

1.9 *N* region on *P* region (rectifying junction).

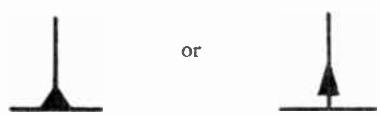

(a) (b)

1.10 N emitter on P region. (The slant line with arrowhead represents the emitter and the horizontal line represents the P region.)

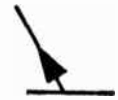

1.11 Plurality of N emitters on P region. (When possible, the electrodes on the symbol drawing should have the same relative order as the electrodes on the device.)

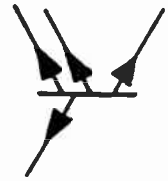

1.12 Collector on semiconductor region of dissimilar-conductivity type. (The slant line represents the collector, and the horizontal line does *not* undergo a transition at the point where the slant line meets it.)

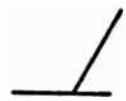

1.13 Plurality of collectors on semiconductor region. (When possible, the electrodes on the symbol drawing should have the same relative order as the electrodes on the device.)

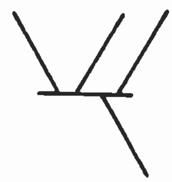

1.14 Collector separated from a region of opposite-conductivity type by an intrinsic region. The intrinsic region is the region between the slant lines, and the collector connection is made to the long solid slant line.

1.15 Collector separated from a region of the same conductivity type by an intrinsic region. The intrinsic region is the region between the slant lines.

1.16 The line enclosing the device symbol is for recognition purposes and its use is recommended.

1.17 Arrowheads on both N- and P-emitter symbols shall be of 45° included angle. They shall be filled and approximately half their length away from the semiconductor-region symbol. The emitter and collector symbols as well as the transition lines shall be drawn at approximately 60° to the semiconductor-region symbol.

1.18 The following device properties may be indicated with the aid of identifying letters placed within the enclosure or adjacent to the symbol.

B = breakdown device
τ = storage device
T = thermally actuated device
λ = light-actuated device.

It is recognized that all semiconductor devices are light and temperature sensitive and exhibit breakdown and storage characteristics. The letters listed above are to be used only if these properties are essential to the operation of the circuit.

2.0 Glossary of Device Symbols

In this section, a listing is made of some semiconductor devices, together with their graphical symbols. It is recognized that in many cases it is possible to develop other device symbols using the standard symbol elements shown in Section 1.0. In general, the angle at which a connecting lead is brought to a graphical symbol has no particular significance. Orientation, including a mirror-image presentation, does not change the meaning of a symbol.

2.1 *P-N-P* transistor (also *P-N-I-P* transistor, if omitting the intrinsic region will not result in ambiguity).

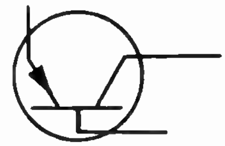

2.2 *N-P-N* transistor (also *N-P-I-N* transistor, if omitting the intrinsic region will not result in ambiguity).

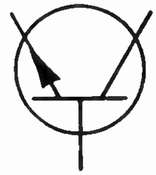

2.3 *P*-type unijunction transistor (sometimes called double-base diode or filamentary transistor).

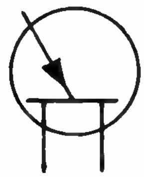

2.4 *N*-type unijunction transistor (sometimes called double-base diode or filamentary transistor).

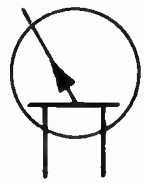

2.5 *P*-type field-effects transistor.

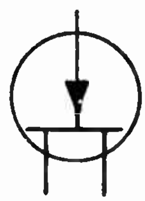

2.6 *N*-type field-effects transistor.

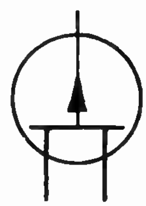

2.7 *P-N-P-N* transistor (hook or conjugate-emitter connection).

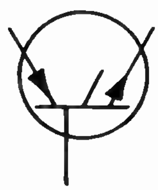

2.8 *N-P-N-P* transistor (hook or conjugate-emitter connection).

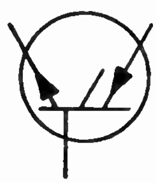

2.9 *P-N-P-N* transistor (remote base connection).

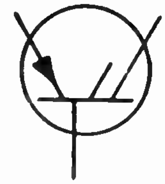

2.10 *N-P-N-P* transistor (remote base connection).

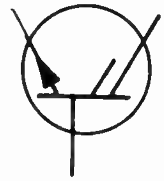

2.11 *P-N-P-N* transistor without base connection.

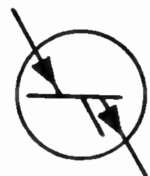

2.12 *P-N-P* tetrode.

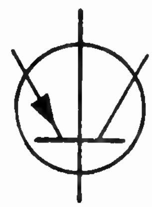

or

2.13 *N-P-N* tetrode.

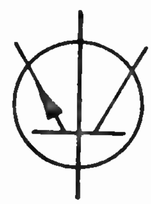

or

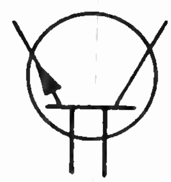

2.14 *P-N-I-P* transistor with ohmic connection to the intrinsic region.

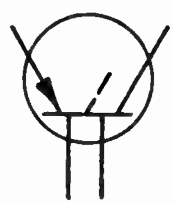

2.15 *N-P-I-N* transistor with ohmic connection to the intrinsic region.

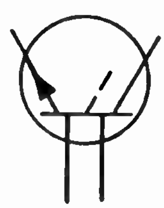

2.16 *P-N-I-N* transistor with ohmic connection to the intrinsic region.

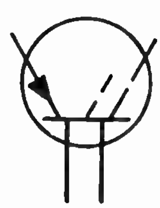

2.17 *N-P-I-P* transistor with ohmic connection to the intrinsic region.

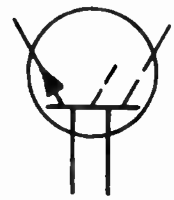

2.18 *P-N* diode. (The arrowhead shall be of 60° included angle; the point of the arrowhead shall touch the adjacent element symbol.)

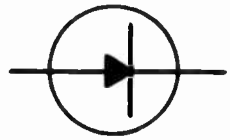

2.19 Breakdown *P-N* diode. (The arrowhead shall be of 60° included angle; the point of the arrowhead shall touch the adjacent element symbol.)

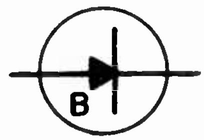

2.20 Bipolar voltage limiter. (The arrowhead shall be of 60° included angle; the point of the arrowhead shall touch the adjacent element symbol.)

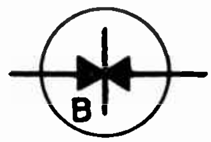

2.21 *P-I-N* triode.[1]

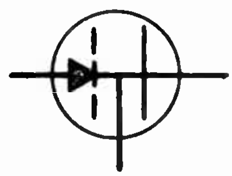

2.22 *P-I-N* diode.[1]

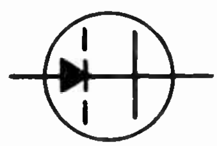

[1] It will be noted that these symbols do not exactly conform to the rules of Section 1.0. They are, in effect, the transition between the diode and the multielement-device symbols. Arrowheads shall be of 60° included angle; the point of the arrowhead shall touch the adjacent element symbol.

The 1959 International Radio Conference*

FRANCIS COLT DE WOLF†

THE International Radio Conference of the International Telecommunication Union will be held in Geneva from July 1 to October 30, 1959. The conference will review and revise as necessary the currently effective International Radio Regulations drawn up at Atlantic City in 1947. The review of the Regulations by the Conference is certain to include lengthy study of the frequency allocation plan and will doubtless result in certain revisions.

Background

Before describing specifically what has been done in the United States in preparation for the forthcoming International Radio Conference, it may be useful to review the history, organization, and operation of the International Telecommunication Union (ITU), although the organization and its functions have previously been more completely described in the IRE Transactions and Proceedings.[1]

The need for international cooperation and regulation in the field of telecommunications has long been established. Austria and Germany recognized such a need as early as 1850 when they joined in a Regional Telegraph Union. Actually the ITU had its origin as the International Telegraph Union under a Convention drawn up in Paris in 1865.

The Paris Convention was revised by a Conference in Vienna in 1863, which created what is now known as the General Secretariat of the ITU. It became the Union's permanent liaison organ. Its headquarters were located in Berne until 1948 when they were moved to Geneva.

The first provisions concerning international telephone services were drawn up in Berlin in 1885 and the first International Radio Telegraph Convention was signed in Berlin in 1906. The interrelation of international telegraph and telephone regulations became apparent with the increasing use of these services and the development of radio. Therefore, two plenipotentiary conferences, the Telegraph and Telephone Conference and the Radio Telegraph Conference, were held in Madrid in 1932 out of which emerged a single International Telecommunications Convention, with annexes called the Telegraph Regulations, the Telephone Regulations, and the Radio Regulations. Countries which signed or acceded to it formed the ITU, and constituted its membership.

The stated purposes of the ITU are to maintain and establish international cooperation for the improvement and rational use of telecommunication of all kinds; to promote the development of technical facilities and their most efficient operation with a view to improving the efficiency of the telecommunication services, increasing their usefulness, and making them, so far as possible, generally available to the public; and to harmonize the actions of nations in the attainment of those common ends.

The ITU Conferences at Atlantic City in 1947 and the Plenipotentiary Conference at Buenos Aires in 1952 introduced substantial changes in the organization and structure of the ITU to provide for the establishment and maintenance of permanent organs to deal with telecommunication matters at an international level. The decisions of those conferences were supplemented by more recent actions of the ITU Administrative Council, particularly at its Tenth Session in 1955. The Convention at present in force, which is actually the constitution of the Union, was drawn up by the Buenos Aires Conference in 1952. Its provisions are completed by the Radio Regulations and the additional Radio Regulations of Atlantic City 1947, the Telegraph Regulations of Paris 1949, and the Telephone Regulations of Paris 1949. It is the review and revision of the Radio Regulations and the additional Radio Regulations of Atlantic City 1947 with which the forthcoming conference will deal and with which this article is concerned. The conference also will be concerned with the work and activities of two of the ITU permanent organs, the International Frequency Registration Board (IFRB), and the International Radio Consultative Committee (CCIR). Detailed provisions regarding these organs are included in the Radio Regulations. Both of them have their headquarters at Geneva with the General Secretariat of the ITU.

The International Frequency Registration Board

The functions of the IFRB are to effect an orderly recording of frequency assignments notified to the Board by the different countries so as to establish, in accordance with the procedure provided for in the Radio Regulations and in accordance with any decisions which may be taken by competent conferences of the Union, the date, purpose, and technical characteristics of each of these assignments, with a view to insuring formal international recognition thereof; to furnish advice to members and associate members with a view to the

* Original manuscript received by the IRE, August 26, 1957.

† Chief, Telecommunications Division, Dept. of State, Washington, D. C.

[1] F. C. de Wolf, "The ITU and global communications," IRE Trans., vol. CS-2, pp. 18–21; November, 1954.

E. W. Allen, "The seventh plenary assembly of the International Radio Consultative Committee," Proc. IRE, vol. 43, pp. 132–139; February, 1955.

operation of the maximum practical number of radio channels in those portions of the spectrum where harmful interference may occur; to perform any additional duties, concerned with the assignment and utilization of frequencies, prescribed by a competent conference of the Union, or by the Administrative Council with the consent of the majority of the Members of the Union in preparation for or in pursuance of the decisions of such a conference; and to maintain such essential records as may be related to the performance of its duties.

The members of the Board, who are independent international officials, are elected by the International Radio Conference according to the present provisions of the Radio Regulations. The conference will have the task of considering the membership provisions and of electing Board members.

The International Radio Consultative Committee

The CCIR studies technical radio questions and operating questions, the solution of which depends principally on considerations of a technical radio character and issues recommendations on them. Countries that are members of the Union are, as of right, members of the CCIR. The Secretariat of the CCIR at Geneva is headed by a Director, and a Vice-Director specializing in broadcasting, both of which positions are filled by election. The CCIR works through Plenary Assemblies, which meet approximately every three years, and review and approve the results of the work of its various Study Groups, making recommendations where appropriate. The Study Groups, of which there are fourteen under the chairmanship of experts from various countries, work in the interim between Plenary Assemblies on specialized assigned technical radio problems to develop recommended solutions. The Study Groups conduct their work by correspondence but hold international meetings when necessary.

Besides being concerned with the provisions of the Radio Regulations covering the organization and structure of the CCIR, the forthcoming Radio Conference will consider the recommendations and the results of the studies of the CCIR on technical radio question for guidance in its deliberations on international radio problems and for possible inclusion in the revised Radio Regulations where appropriate.

Responsibility for Preparatory Work

The foregoing may bring into focus some of the matters which have to do with the United States preparation for, and later United States participation in, the Radio Conference at Geneva beginning July 1, 1959. Radio engineers, as well as others connected with telecommunication companies and organizations, or the government agencies concerned, are aware of the intense interest in the comparatively recent growth in the use of radio internationally as well as domestically; consequently, this interest becomes of intensified concern when new international agreements or regulations are to be promulgated.

In the United States Government structure, the Secretary of State is responsible to the President for the conduct of foreign affairs, including negotiations of international agreements in the field of telecommunications. There are extensive and detailed agreements in this field and such matters are therefore of considerable concern to the Department of State. Domestically, the Office of Defense Mobilization is responsible for the coordination of the radio requirements of the civil and military agencies of the Federal government; the Federal Communications Commission (FCC) is responsible for the coordination and regulation of the frequency requirements of the other users of out radio services. In the preparation of the United States position on various international telecommunication questions for presentation at an international level, there is what amounts to a triangle, with the Department of State at the apex having final authority for making United States policy on international questions, supported jointly at the base by the FCC and the users licensed by it on one side and, on the other, the Office of Defense Mobilization and the Government users of radio.

To assist it in the formulation of policy decisions, the Department of State has established a standing advisory committee known as the Telecommunications Coordinating Committee (TCC). The TCC was created in 1946 by an exchange of letters among the Secretary of State and the heads of four other government departments and the Federal Communications Commission. The Committee is composed of one representative of the Departments of State, Treasury, Commerce, the FCC, and the Departments of the Army, Navy, and Air Force. TCC representatives are designated by the heads of each agency. The Committee, as a matter of practice, includes in its meetings and in the composition of any working committees representatives of any nonmember agencies having a special interest in the work in hand.

Preparatory Committee Structure

In addition to this standing committee, the Department of State establishes special preparatory committees to develop factual and policy information for use in connection with specific conferences in the international telecommunication field. Such a committee has been established to formulate proposals and to recommend United States policy for the International Radio Conference.

The first meeting of the full preparatory committee for the International Radio Conference was called by the Department of State on November 8, 1956. At this meeting it was agreed to establish five working committees comprised of an Executive Committee and four technical committees. The Executive Committee has the responsibility for over-all coordination, guidance, and approval of the work of the technical committees described below, which deal with various categories of technical work.

The Department of State undertook to obtain chairmen for the four technical committees from certain of the interested Government agencies. The various committees and their chairmen are as follows:

Committee I—Executive Committee
F. C. de Wolf, Chief,
Telecommunications Division,
Department of State.

Committee II—Organizational Regulations
Rear Admiral J. N. Wenger,
Joint Chiefs of Staff,
Communications-Electronics Office.

Committee III—Frequency Allocations
Commander T. A. M. Craven,
Commissioner, FCC

Committee IV—Technical Regulations
Dr. F. W. Brown, Director,
Boulder Laboratories,
National Bureau of Standards.

Committee V—Operating Regulations
Rear Admiral F. T. Kenner,
U. S. Coast Guard.

The members of Committee I, who are the principal representatives designated by government agencies, private companies, or organizations for the preparatory work, are responsible for coordinating the participation of all persons from their agencies, companies, or organizations in the various technical committees in order that such participants may have a unified position; for obtaining the approval of their respective agencies or companies for the proposals prepared by the various technical committees; for reviewing and approving the results of the work of the technical committees; for representing the views of their agencies on questions of policy which may arise; and for resolving conflicts which cannot be resolved within a technical committee. In the case of any such conflict, the matter may be referred to the Executive Committee by any member of the Executive Committee.

The general work assignments of the various technical committees, that is, the provisions of the Radio Regulations, 1947, or the subjects with which they deal, are as follows:

Committee II—Organizational Regulations

Art. 18 and App. C—Monitoring
Art. 20 and App. 6 and 7—Service Documents
Art. 21—Secrecy
Art. 22—Licenses (Station)
Art. 42—Amateur Stations
Art. 43—Experimental Stations
Art 44 and App. 15—Radiolocation Service
Art. 45—Special Service
Art. 46—Proposals Regarding CCIR
Art. 47—Effective Date
Recommendation No. 3—International Monitoring
App. 13—Hours of Service for Ships.

Committee III—Frequency Allocations

Art. 3—General Rules for Assignment and Use of Frequencies
Art. 4—Special Arrangements
Art. 5—Table of Frequency Allocations
Art. 6—Classes of Emissions
Art. 7—Special Rules for Assignment and Use of Frequencies
Art. 9—Special Rules Relating to Particular Services
Art. 10, 11, 12—Proposals Regarding the IFRB
App. 1—Form of Notice to IFRB
App. 2—Report of Irregularity or Infringement of Convention on Radio Regulations
Resolutions—Preparation of the new International Frequency List, Directives for the Provisional Frequency Board, and Participation in the Provisional Frequency Board
App. 6 (List I)—International Frequency List EARC Agreement.

Committee IV—Technical Regulations

Art. 1—Definitions
Art. 2—Designation of Emissions
Art. 13, 14, 15—Interference
Art. 16—Choice of Apparatus
Art. 17—Quality of Emissions
App. 3—Table of Frequency Tolerances
App. 4—Table of Tolerances for Intensity of Harmonics
App. 5—Band of Frequencies Required for Certain Types of Radiocommunications
App. A—Radio Propagation
Recommendation No. 1—International Coordination of Studies of Radio Propagation
Recommendation No. 4—Review of Appendices 3, 4, and 5 of the Radio Regulations
Recommendation No. 7—Performance Requirements for Radiophoto Equipment
Recommendation No. 8—Signal Ratios and Frequency Tolerances
Recommendation—Specifications of Performance for the Automatic Alarm Receiving Device.

Committee V—Operating Regulations

Recommendation No. 2—Standard Frequency Broadcasts and Time Signals
Recommendation No. 5—Distress Signals
Recommendation No. 6—Watch on Distress Frequency 2182 kc
Recommendation—International Code of Signals
Recommendation—Coded Passive Reflectors
Recommendation—New Method of Generating Call Signs
Resolution—Preparatory Committee of Experts

Art. 8—Protection of Distress Frequencies
Art. 19—Call Signs
Chapters XI, XII, and XIII (Art. 23–35) and App. 8 and 9—Radio Communications in the Maritime and Aeronautical Services
Chapter XIV (Art. 36 and 37)—Distress, Alarm, and Safety Signals
Chapter XV (Art. 38–41)—Radiotelegrams (routing, priorities, accounting, etc.)
Art. 45 (II) and App. B—Standard Frequencies and Time Signals.

United States Proposals

The Technical Committees held their organizational meetings and formed subcommittees as required for various subjects. The committees and the subcommittees are well under way on their deliberations of technical questions and will continue their work until they have prepared final reports. After a document has been cleared in the individual Technical Committee, it will then be referred to the Executive Committee for over-all coordination and final approval. It is contemplated that the United States position as approved by the Executive Committee will be reviewed by the Telecommunications Coordinating Committee (TCC), the membership of which will be enlarged to include representation from those interested Government agencies that are not presently members of this organization, after which the United States proposals will be forwarded to the ITU for distribution to the various countries that are members of the Union.

According to ITU administrative rules, proposals for revision of regulations to be considered by a conference must be in the hands of the Secretary General of the ITU eight months before the conference opens in order to allow him ample time to distribute them prior to the start of the conference. The International Radio Conference will open on July 1, 1959, and it is necessary for the United States proposals to reach the Secretary General by November 1, 1958, at the latest. Working back from this date, it appears that the final U. S. position should be established by the various technical committees and should be ready for final review by the Executive Committee as of July 1, 1958.

The committees and subcommittees, which, as indicated above, are meeting regularly, have received and are working on definite proposals from the private companies participating in the preparatory work and from the various interested Government agencies, particularly the FCC and the Interdepartment Radio Advisory Committee (IRAC). In this connection, it may be well to mention that the FCC has recently announced and commenced proceedings in the matters of the Allocation of Frequencies in the Bands Above 890 mc (Docket No. 11866) and a Statutory Inquiry into the Allocation of Frequencies to the Various Non-Government Services in the Radio Spectrum Between 25 mc and 890 mc (Docket No. 11997). Data and information obtained from these proceedings will be used in formulating the Commission's position which in turn will be reflected in the United States position for the Conference.

Considering the progress that has been made up to the present and the interest and ability of the participants in the preparatory work, it can safely be assumed that the United States position for the forthcoming International Radio Conference will be fully established and will be ready for transmission to the ITU by the anticipated deadline.

The response to the Department's invitation to participate in the work of the Preparatory Committees has indeed been gratifying. In the Executive Committee, of which the membership consists of principal representatives of each interested agency, company, or organization, there are approximately 55 agencies, companies, or organizations represented. As a matter of information, the Institute of Radio Engineers (IRE) is represented on the Executive Committee by L. G. Cumming, Technical Secretary of the IRE. Registration in the Technical Committees ranges from about sixty persons in Committee II to well over 100 persons in Committee III, the Frequency Allocation Committee. Membership in the Committees is open to any United States agency, company, or organization and its representatives who have an interest in the development of the United States position. Announcement of the formation of the preparatory committee was given as wide circulation as possible. If any person, who has not previously known of the preparatory committee, is interested in contributing to the work, he may obtain further information by writing to the Telecommunications Division, Department of State, Washington 25, D. C.

The International Radio Consultative Committee*

JOHN S. CROSS†

Summary—**The International Radio Consultative Committee (CCIR) will hold its Ninth Plenary Assembly in the United States beginning April 1, 1959. The Eighth Plenary Assembly was held in Warsaw, Poland, from August 9 through September 13, 1956. It was attended by approximately 400 delegates, representatives, experts, and observers from some forty countries that are members of the International Telecommunication Union (ITU), sixteen recognized private operating agencies, eight international organizations, and seven scientific or industrial organizations.**

At the Eighth Plenary Assembly all the fourteen Study Groups of the CCIR held meetings in Warsaw, and the Plenary Assembly adopted 83 Recommendations, 58 Reports, and 19 Resolutions which were put forward by the Study Groups. The program of work for the next three years was also established. This program consists of 71 Questions and 57 Study Programs dealing with all aspects of radio communication, including programs of the transmission, propagation, and reception of electromagnetic waves which arise in the operation of all radio services.

The Eighth Plenary Assembly at Warsaw accepted unanimously an invitation to hold the Ninth Plenary Assembly of the CCIR in the United States. This article relates to the results of the Warsaw Assembly in terms of the studies to be undertaken in preparation for the Ninth Plenary Assembly.

Background

The CCIR, which initials incidentally are of the French name, Comité Consultatif International des Radiocommunications, had its beginnings with the Radio Conference of Washington, D. C. in 1927. It was operated as an independent organization by the member governments which were interested in the coordinated study of international radio problems. In the period from 1927 until 1947, four plenary assemblies were held where studies were pursued and recommendations were drawn up on technical and operating radio questions. The International Telecommunication and International Radio Conferences at Atlantic City in 1947 reconstituted the CCIR within the ITU as a permanent organ of the Union, with a permanent Secretariat. The general terms of reference of the CCIR remained the same: that is, its purpose is to study technical and operating radio problems of international interest and to recommend solutions for those problems. However, principally in consequence of the tremendous advancements in electronics and the art of telecommunications, the scope of the studies of the CCIR necessarily became greatly broadened, and the countries that are members of the ITU have become increasingly more dependent on its recommendations or the results of its work otherwise in their decisions on international telecommunication regulations and operating procedures.

* Original manuscript received by the IRE, August 26, 1957.
† Asst. Chief, Telecommunications Div., Dept. of State, Washington, D. C. Chairman of the United States Delegation to the Eighth Plenary Assembly, Warsaw, Poland.

The results of the work of the CCIR Plenary Assemblies since 1947 followed a similar pattern. A number of recommendations were adopted on completed studies, and questions or study programs were formulated for future study by the CCIR Study Groups in the interim until each succeeding assembly. Study Groups have been established as necessary by the CCIR Assemblies to deal with various categories of the work. There are at present fourteen Study Groups, and their chairmen and vice-chairmen, who serve in their international capacity without compensation, are appointed by the Assembly.

The Eighth Plenary Assembly

The Eighth Plenary Assembly was held in Warsaw in response to the invitation issued by the Polish Delegation at the Seventh Plenary Assembly in London in 1953. The participation in this Plenary Assembly was widely representative of the membership of the Union and of agencies and organizations engaged in technical radio work.

The members of the United States Delegation, 21 in number, were designated from the representatives of government agencies and private companies and organizations who had contributed to CCIR studies in the United States and who assisted with the final United States preparatory work.

Work of the Plenary Sessions

The pattern or plan of operation of the Assemblies has usually been to hold organizational plenary sessions in the opening days of the Assembly, after which the concentration of work centers in meetings of the various Study Groups for several weeks. The results of the Study Groups' deliberations are then channeled back as proposed recommendations, reports, resolutions, or proposed new questions and study programs for consideration and adoption in plenary sessions in the final period of the Assembly. In addition to the considerations of technical matters under study, the Plenary Assembly deals with organizational and administrative matters, setting up special committees as necessary or handling such matters directly in plenary session. At the Eighth Plenary Assembly these questions concerned finances, the election of a new director for the CCIR, the reorganization of the operational structure of the CCIR, and technical assistance. The decisions on such matters affect to some extent the conditions and atmosphere in which the technical studies and activities are carried on.

At the Eighth Plenary Assembly at Warsaw, the chairman of the Assembly was selected, as is customary, from the delegation of the inviting Government, Poland. The formal opening plenary session on August 9, 1956 was followed on the same day by the first working plenary session. The Assembly appointed four vice-chairmen who also served as chairmen of committees handling work of the Assembly not falling within the purview of the Study Groups. These committees were Election, Finance, Technical Assistance, and Editorial.

The results of the work of these committees, as well as of the Study Groups, became valid as CCIR decisions only after consideration and acceptance or approval in full plenary sessions.

Organizational Decisions

Aside from the election of a new Director of the CCIR, Dr. Ernest Metzler, and the appointment or reappointment of Study Group chairmen and vice-chairmen, possibly the decisions affecting Study Group activities most closely were those arising from recommendations of the Organization Committee. This committee was actually constituted as the result of action of the Seventh Plenary Assembly. It resulted from proposals of the United States for certain changes and improvements in the composition of Study Groups. The Committee was established to provide a forum for the exchange of views about the effectiveness of the CCIR structure as it has operated, and for the formulation of recommendations looking toward a more effective organization.

The results of its work appear in four basic documents. The categories of studies to be undertaken by the Study Groups were realigned in some cases and the terms of reference and titles of the Study Groups are now more precisely defined. The high concentration of Study Group work in the weeks immediately preceding and at the Plenary Assembly in the past has created some difficulty in full coverage of the over-all field by delegations at assemblies. New procedures were therefore adopted and are now being followed, the purpose of which is to spread the activity over the three-year interval between assemblies more evenly, providing for much of the work to be done by correspondence or, if necessary, by interim meetings.

Briefly, the schedule provides that, in addition to the Study Group meetings held at the Plenary Assembly, interim meetings be scheduled by the Director in collaboration with the Study Group chairmen with the approval of their administrations at the latest practical date prior to the convening of the Plenary Assembly. These meetings are to be arranged in the interim between Assemblies over a period so as to avoid the conflicts which have previously existed in the meetings held during the Plenary Assembly period. A deadline for the receipt of documents from administrations is set at four months prior to such meetings and documents received between that time and the assembly will not be approved by the Study Group chairmen concerned unless they are of exceptional merit and influence.

A Study Group chairman must submit to the Director at least four months prior to the assembly his report of the interim meeting and any necessary draft questions, study programs, resolutions, reports, and recommendations. These will constitute the preliminary documentation for the Plenary Assembly. These draft documents are to be examined again and brought up to date at final Study Group meetings held immediately preceding and in connection with the assembly, in the light of any new contributions by administrations which have been approved as meritorious by the Study Group chairmen. This should greatly limit the work of the Study Groups at the final meetings and shorten them considerably.

At the same time, the new procedures should provide opportunity for more thorough discussion of problems and result in better actions and better understanding between administrations. Even so, it is expected that the final meetings of the Study Groups and the Plenary Assembly together, although shorter in the aggregate, will still require approximately twenty-five calendar days. Deadlines are not set for receipt of Study Group documents when no interim meeting is held and must be set later by correspondence with the Director.

In connection with proposals or documents submitted for consideration by Study Groups and the assembly, limits are now placed on the length of the documents, approximately 2500 words or five pages, and the number of drawings or charts attached, about three pages for each document. However, it has been left to the Study Group chairman, as the expert in the field, to relax these limits in exceptional circumstances.

These new procedures, if proven to be practical and effective, should greatly promote the efficiency of Study Group operation.

The Eighth Assembly also studied the question of ways and means of granting technical assistance to countries where telecommunication services are not sufficiently developed to fit into the harmonious development of international telecommunication services. An ad hoc group was created to work jointly with the International Telegraph and Telephone Consultative Committee (CCITT) to go into the question further of what forms of assistance the CCIR and the CCITT may offer in such cases.

CCIR Study Groups

To give a more complete picture of the current activities in the United States on CCIR technical studies in preparation for the Ninth Assembly, as related to the acts and decisions of the Eighth Assembly, the various Study Groups, their terms of reference, their international chairmen, and chairmen of the United States Committees for the various Study Groups are outlined below.

Study Group I—Transmitters

Chairman—Colonel J. Lochard (France).

Vice-Chairman—Prof. S. Ryzko (Poland).

(Dr. Ernest Metzler of Switzerland, the new Director of the CCIR, was formerly Chairman of this Study Group.)

Terms of Reference:

1) To make specific studies and proposals in connection with radio transmitters and generally to summarize and coordinate proposals for the rational and economical use of the radio spectrum.
2) To study a number of problems concerning telegraphy and telephony from the transmission point of view.
3) To study spurious radiation from medical, scientific, and industrial installations.

The Chairman, in his report to the Plenary Assembly on the work in the interim period, proposed the basis for the work of the Study Group. This was approved as follows:

I-A—Bandwidths.
I-B—Telegraphy.
I-C—Frequency Stability and Undesired Emissions.

On the question under study regarding harmonics and parasitic emissions, a new recommendation was approved which recommended that the maximum level of 200 mw be reduced to 25 mw for spurious radiation above 60 mc for transmitters with a fundamental frequency between 10 kc and 30 mc.

New recommendations were approved regarding frequency stabilization of transmitters, bandwidths of emissions, preferred standards for 4-frequency diplex telegraph systems, and designation for multichannel telegraph systems.

A questionnaire was prepared to obtain information on the occupied bandwidth of the various multiplex telegraph systems in use. This questionnaire is to be sent by the Director of the CCIR to administrations and recognized private agencies.

Further study was recommended on frequency shift keying and the limitation of unwanted radiation from industrial installations.

Chairman of the U. S. Committee for Study Group I—J. B. Coleman, Radio Corporation of America, Camden, N. J.

Study Group II—Receivers

Chairman—P. David (France).
Vice-Chairman—P. Abadie (France).
Terms of Reference: Measurement of the characteristics of receivers and tabulation of typical values for the different classes of emission and the various services. Investigation of improvement that might be made in receivers in order to solve problems encountered in radio communication.

At the Assembly, the work of the Study Group was divided under two general headings:

II-A—Sensitivity, Selectivity, and Stability.
II-B—Undesired Emissions from Receivers and Receiver Response to Quasi-Impulsive Interference.

In general, new reports and recommendations were drawn up to reflect advances in receiver techniques during the past few years and new questions were formulated on subjects requiring further study. A new question was adopted for study concerning the undesired emissions from frequency modulation receivers. Significant advances were made since the Seventh Plenary Assembly on the problem of undesired emissions from receivers, and a recommendation has been drawn up to reflect these advances, which should serve as a good start in reducing interference to several services.

Chairman of the U. S. Committee for Study Group II—J. H. Gough, Bureau of Ships, Navy Department, Washington, D. C.

Study Group III—Fixed Service Systems

Chairman—Dr. H. C. A. van Duuren (Netherlands).
Vice-Chairman—A. Cook (United Kingdom).
Terms of Reference:

1) To study questions relating to complete systems for the fixed and allied services and terminal equipment associated therewith (excluding radio relay systems). Systems using the so-called ionospheric-scatter mode of propagation, even when working on frequencies above 30 mc, are included.
2) To study the practical application of communication theory.

The work falls into four general categories:

III-A—Technical Performance Level for Complete Systems: (a) Bandwidth, field intensity and transmitter stability (Atlantic City Recommendation No. 4); (b) Directivity of antennas; (c) Maximum interference levels tolerable in complete systems.
III-B—Communication Theory.
III-C—Use of Radio Circuits in Association with 5-Unit Start-Stop Telegraph Apparatus.
III-D—Phototelegraphy and Facsimile on Radio Systems.

New reports, recommendations, study programs, and questions were adopted at the Warsaw Assembly concerning the above subjects and continuing studies are being carried on.

Chairman of the U. S. Committee for Study Group III—R. C. Kirby, Central Radio Propagation Laboratory, National Bureau of Standards, Boulder, Colo.

Study Group IV—Ground-Wave Propagation

Chairman—Prof. L. Sacco (Italy).
Vice-Chairman—G. Millington (United Kingdom).
Terms of Reference: To study the propagation of radio waves over the surface of the earth, taking into account changes in the electrical constants of the earth and irregularities of terrain, and including the effect of a standard radio atmosphere.

The Chairman recommended in his report to the Plenary Assembly the following breakdown of the studies:

IV-A—Mixed Paths.
IV-B—Irregular Terrain.

A new question was adopted on the subject "Determination of the Electrical Characteristics of the Surface of the Earth." A new recommendation was prepared to replace Recommendation 108—Presentation of Antenna Radiation Data. The use of cymomotive force is not removed from the new recommendation but is put in as an alternate but not mandatory method for presenting antenna radiation data on all frequencies.

A resolution was adopted concerning the examination of methods to extend the CCIR atlas curves to higher heights and frequencies for use in planning for vhf and uhf air-to-air and air-to-ground communications.

The previous study program as regards the effects of tropospheric refraction on frequencies below 10 mc was modified slightly and an additional aspect for study was introduced—phase changes due to abnormal refraction effects.

A report was adopted on the effects of tropospheric refraction on frequencies below 10 mc. The report indicates that more experimental work is necessary to establish the importance of the refractive index gradient of the atmosphere on field strengths observed at very low frequencies.

On the subject of ground wave propagation over mixed paths, a recommendation on the subject was approved for the use of simplified theoretical methods where they may be applied, and continued use of semi-empirical methods in other cases.

Chairman of the U. S. Committee for Study Group IV—J. W. Herbstreit, Central Radio Propagation Laboratory, National Bureau of Standards, Boulder, Colo.

Study Group V—Tropospheric Propagation

Chairman—Dr. R. L. Smith-Rose (United Kingdom).
Vice-Chairman—E. W. Allen (United States).
Terms of Reference: To study the influence of the troposphere on radio-wave propagation insofar as it concerns radio communication.

The work falls into the following categories:

V-A—Measurement of Field Strength.
V-B—Tropospheric Propagation Curves.

Various new recommendations and questions were prepared and old ones reaffirmed at Warsaw. A resolution was prepared providing for an interim working group to examine and to redraft, if necessary, the vhf tropospheric curves of Recommendation 111 (Tropospheric-Wave Propagation Curves). This work is to be centralized at the National Physical Laboratory of the United Kingdom, under the direction of Dr. Smith-Rose. Both the Central Radio Propagation Laboratory (CRPL) and the Federal Communications Commission (FCC) will participate actively in this work.

Recommendation 110 (Presentation of Data in Studies of Tropospheric-Wave Propagation) was revised to include a method of statistical study of the variation of tropospheric field strengths which in some cases is more precise than the single method previously specified.

A new question and a new study program were drafted to provide for a broader study of tropospheric propagation, including over-the-horizon or "tropospheric scatter" systems.

The Study Group proposed a new question on the "Measurement of Field Strengths for VHF and UHF Broadcast Services." This problem is under active study in the United States, both by the CRPL and FCC, and by television broadcast stations and consulting engineers.

Chairman of the U. S. Committee for Study Group V—E. W. Allen, Chief Engineer, Federal Communications Commission, Washington 25, D. C.

Study Group VI—Ionospheric Propagation

Chairman—Dr. J. H. Dellinger (United States).
Vice-Chairman—D. K. Bailey (United States).
Terms of Reference: To study all matters relating to the propagation of radio waves through the ionosphere insofar as they concern radio communications.

The work of this Study Group is divided into the following areas for study:

VI-A—Ionospheric Predictions—Short-Term Forecasts—and Indices.
VI-B—Propagation Topics.
VI-C—Noise Topics.
VI-D—Fading Topics.
VI-E—IFRB Matters.
VI-F—The Use of Standard Frequency Transmissions for Propagation Studies in Liaison with Study Group VII.

Among the major contributions which resulted were an extensive set of world-wide radio noise charts, specifications for a standard lightning-flash counter (for the WMO), and information on the new implications of long-distance scatter propagation.

The Study Group's work resulted in seven recommendations, twelve reports, four resolutions, and nine study programs. A total of twenty-seven topics were placed on the Study Group's agenda for future study.

Dr. Dellinger is also Chairman of the U. S. Committee for Study Group VI; his address is: RCA Frequency Bureau, 1625 K Street, N. W., Washington, D. C.

Study Group VII—Standard Frequencies and Time Signals

Chairman—Dr. B. Decaux (France).
Vice-Chairman—Prof. M. Boella (Italy).

Terms of Reference: Organization of a world-wide service of standard-frequency and time-signal transmissions. Improvement of measurement accuracy.

At the Eighth Plenary Assembly two new questions were formulated and adopted for study. One entitled "Standard Frequency Transmissions and Time Signals in Additional Frequency Bands" asks for recommendations for transmissions above 30 mc and below 100 kc. The second, "Stability of Standard Frequencies and Time Signals as Received," related to stability and accuracy of the services as received by the users.

Additionally, the questions, reports and recommendations assigned for study during the interim period were either revised or replaced. One of the principal problems is determination and adoption of methods of avoiding interference to enlisting bands allocated for these services.

Chairman of the U. S. Committee for Study Group VII—W. D. George, Radio Standards Laboratory, National Bureau of Standards, Boulder, Colo.

Study Group VIII—International Monitoring

Chairman—J. D. Campbell (Australia).
Vice-Chairman—George Turner (United States).
Terms of Reference: To study problems relating to the equipment, operation, and methods of measurement used by monitoring stations established for checking the characteristics of radio-frequency emissions. Examples of such measurements are: frequency, field-strength, bandwidth, etc.

The work assignments of the Study Group were organized under the following headings:

VIII-A—Automatic Monitoring of Occupancy of the Radio Frequency Spectrum; Frequency Measurements above 50 MC by Monitoring Stations.
VIII-B—Frequency Measurements above 50 MC by Monitoring Stations; Spectrum Measurements by Monitoring Stations.

The Eighth Assembly adopted several new questions, reports, and recommendations prepared by the Study Group, as well as certain revisions of standing studies.

Chairman of the U. S. Committee for Study Group VIII—G. Turner, Chief, Field Engineering and Monitoring Division, Federal Communications Commission, Washington, D. C.

Study Group IX—Radio Relay Systems

Chairman—H. Stanesby (United Kingdom).
Vice-Chairman—G. Pedersen (Denmark).
Terms of Reference: To study all aspects of radio relay systems and equipment operating at frequencies above about 30 mc, including systems using the so-called tropospheric-scatter mode of propagation.

The work of this Study Group deals generally with international wide-band radio relay systems. An interim meeting of the Study Group had been held in Geneva in 1954. At the Warsaw Assembly, the Study Group deliberations were divided into the following four categories:

IX-A—Transmission of telephony and television alternatively or simultaneously on the same system, and Radiotelephone systems using frequency-division multiplex.
IX-B—Hypothetical reference circuit, frequency tolerances for transmitters used in radio relay systems, and computation of intermodulation noise due to nonlinearity in radio-relay systems.
IX-C—Interconnection of multiplex radio-relay systems, maintenance of radio-relay systems, and interconnection of radio-relay systems with different characteristics.
IX-D—Radiotelephone systems using time-division multiplex, and operational characteristics of long distance radio-relay systems.

Two new questions were formulated by the Group and adopted by the CCIR. One is entitled "Preferred Characteristics of Radio Relay Systems for the Transmission of Monochrome Television." The second question is entitled "Radio Relay Systems Employing Tropospheric Scatter Propagation." The Study Group is currently continuing its work on these as well as its other assigned studies.

Chairman of the U. S. Committee for Study Group IX—E. W. Bemis, Operation and Engineering Dept., American Telephone and Telegraph Co., 195 Broadway, New York, N. Y.

Study Group X—Broadcasting

Chairman—A. P. Walker (United States).
Vice-Chairman—Kenneth Miller (United States).
Terms of Reference: To study the technical aspects of transmission and reception in the sound broadcasting service (except for tropical broadcasting), including standards of sound recording and sound reproduction to facilitate the international exchange of programs.

The work of the Study Group divides into two parts:

X-A—High Frequency Broadcasting: (a) Antennas for hf broadcasting; (b) Use of synchronized transmitters for covering overlapping and non-overlapping service areas; (c) Standards for fm broadcasting, particularly required field strengths for allocation of stations, and pre-emphasis characteristics.
X-B—Recording and Rebroadcasting: (a) Standardization of physical dimensions of cine-type spools; (b) Possible revision of surface induction of magnetic tape; (c) Brief discussion of sound recording on film for international exchange of television programs.

New questions and study programs were adopted on the above subjects for study by this Study Group in the interim until the next Assembly.

Chairman of the U. S. Committee for Study Group X—A. P. Walker, Manager, Engineering Department, National Association of Radio and Television Broadcasters, Washington, D. C.

Study Group XI—Television

Chairman—E. Esping (Sweden).
Vice-Chairman—G. Hansen (European Broadcasting Union).
Terms of Reference: Television.

Although the Study Group has very broad terms of reference under the heading of television, its studies have been on the following subjects:

XI-A—Color Television Standards.
XI-B—Requirements for the Transmission of Television Over Long Distances.
XI-C—Monochrome Television Standards.
XI-D—Television Picture Quality.
XI-E—Monochrome Television Interference Ratios.

On the subject of requirements for the transmission of television over long distance, it was decided that further studies should be carried out by a joint group of the CCIR and the CCITT; the U. S. representative named for this joint group is E. W. Bemis, who is chairman of the Committee for Study Group IX.

Several reports were prepared in this Study Group dealing with these subjects, and the assigned studies of the Group are currently under active consideration in the United States.

Chairman of the U. S. Committee for Study Group XI—C. J. Hirsch, Hazeltine Research Corporation, 59-25 Little Neck Parkway, Little Neck, Long Island, N. Y.

Study Group XII—Tropical Broadcasting

Chairman—B. V. Baliga (India).
Vice-Chairman—Dr. M. B. Sarwate (India).
Terms of Reference: To study standards required for good quality service in the tropical zone, and for tropical broadcasting systems; interference in the shared bands; power requirements for acceptable service; design of suitable aerials for short-distance tropical broadcasting; optimum conditions for the utilization of frequency bands used for broadcasting in the tropical zone; other associated questions.

In the discussion of the work of the Study Group at the Assembly, considerable controversy arose over the appropriate signal to interference ratio for tropical broadcasting; values of between 40 and 50 db were proposed but were not approved. A recommendation was approved for maximum powers for tropical broadcasting for frequencies below 5060 kc; it is 1) 10 kw for service range of 400 km, and 2) 30 kw for service range of 800 km. Further studies are necessary on much of the work of this Study Group and are presently being pursued.

Chairman of the U. S. Committee for Study Group XII—C. Pease, International Broadcasting Service, United States Information Agency, Washington, D. C.

Study Group XIII—Mobile Services

Chairman—Dr. J. D. H. van der Toorn (Netherlands)
Vice-Chairman—N. J. Soeberg (Norway).
Terms of Reference: To study technical questions regarding the aeronautical, maritime, land mobile, and radio location and navigation services, and miscellaneous operating questions of concern to several services.

The studies of the Study Group are in the following categories:

XIII-A—Identification of Radio Stations.
XIII-B—Marine Identification Devices, Bearing Classifications and Related Matters.
XIII-C—Technical Characteristics of FM VHF Maritime Equipment.
XIII-D—500 KC Auto Alarm Testing.
XIII-E—Codes.

In addition to revisions of questions and study programs resulting from contributions and discussion of the assigned studies, a number of new questions were prepared and adopted at Warsaw. These include a question in respect to the use of single side-band equipment by the aeronautical and maritime mobile services, and a question relating to the practices in assignment and use of frequency channels and required equipment characteristics employed in the vhf and uhf frequency bands for the land mobile service.

Chairman of the U. S. Committee for Study Group XIII—W. Mason, RCA Frequency Bureau, 60 Broad Street, New York 4, N. Y.

Study Group XIV—Vocabulary

Chairman—T. Gorio (Italy).
Vice-Chairman—R. Villeneuve (France).
Terms of Reference: To study in collaboration with the other study groups and, if necessary, with the CCITT, the radio aspect of the following: vocabulary of terms and list of definitions, lists of letter and graphical symbols and other means of expression, systematic classification, measurement units, etc.

In the course of the work at Warsaw, it was decided to postpone further work on vocabulary and letter and graphical symbols in the CCIR, to obtain from IEC the vocabulary recently prepared by them, and to circulate this vocabulary to all the members of this Study Group for comment.

It was also decided not to adopt officially the decimal classification system for the CCIR at this time but to review later the work of other international groups in this field to determine whether the CCIR should adopt the decimal classification system sometime in the future.

Chairman of the U. S. Committee for Study Group XIV—A. G. Jensen, Bell Telephone Laboratories, Murray Hill, N. J.

More complete information on the technical subjects under study by the CCIR, *i.e.*, its program of work for the next three years, may be found in Volume I of the results of the Warsaw Assembly which contains the texts of all recommendations, reports, questions, study programs, and resolutions adopted or reaffirmed at Warsaw. This volume may be obtained from the General Secretariat of the International Telecommunication Union at Geneva, Switzerland. Payment for the publication should accompany this order and should be made in Swiss francs. The price of the volume is 37.25 Swiss francs.

Information in more detail on the United States activities for the Warsaw Assembly on technical questions under study is available in the report of the U. S. Delegation to the Assembly and may be obtained, free of charge, by writing to Mr. Francis Colt de Wolf, Chief, Telecommunications Division, Department of State, Washington 25, D. C.

The coordination of the preparatory work in the United States for the Ninth Plenary Assembly, both on the technical studies under consideration and on organizational planning for the Assembly in the United States, is centralized in the Telecommunications Division of the Department of State. Mr. de Wolf is Chairman of the over-all U. S. Preparatory Committee and the U. S. Executive Committee for the CCIR. The members of the Executive Committee and of the U. S. Committees for the various Study Groups are, for the most part, representatives of government agencies and private telecommunication companies or organizations having an interest in the work. The Department of State welcomes the participation of any person wishing to contribute to the studies. If further information on the United States committee structure is required, it will be furnished in response to written requests to Mr. de Wolf. On the other hand, any company or person not already participating in the work of the various Study Group Committees and wishing to do so, should get in touch with either Mr. de Wolf or with the United States chairman of the appropriate Study Group Committee whose name and address is shown herein.

As a further item of interest, the Institute of Radio Engineers is represented in the CCIR preparatory committee work by A. G. Jensen, by Professor Ernest Weber of the Brooklyn Polytechnic Institute, and by L. G. Cumming, Technical Secretary of the IRE, who will be able to provide further detailed information about the participation of the IRE in the technical studies.

A New Wide-Band Balun*

WILLMAR K. ROBERTS†, MEMBER, IRE

Summary—**This paper describes a form of balun which is useful for matching a balanced circuit to an unbalanced circuit of nearly the same impedance over a wide frequency range. The bandwidth increase is obtained by the use of a quarter-wave transmission line section which is placed inside one of the balanced arms, thereby minimizing the over-all physical length. It is shown that a practical balun of this type, designed to match a 50-ohm unbalanced line to a balanced 70-ohm antenna, has a voltage standing-wave ratio of 1.4 or better over a frequency band of about 2.8 to 1. The wide bandwidth, simplicity, and reasonable physical dimensions make the balun particularly useful in connection with the adjustable-length dipole antennas which are generally used for vhf and uhf field-strength measurement.**

Introduction

A BALUN is a device intended to act as a transformer, matching an unbalanced circuit to a balanced one, or vice versa. The balun described here was developed to meet a need for a low-loss impedance-matching device to connect a balanced dipole antenna to an unbalanced coaxial transmission line. It was desirable that the balun have a wide-band characteristic so as to make unnecessary any adjustments on the balun over a range of frequencies covered by adjusting the telescoping elements of the dipole antenna. Certain previously described wide-band transformers,[1,2] require a considerable amount of space because of the use of the frequency-compensating effects of one or two quarter-wave transmission line sections connected between the balun and the balanced load. The balun described here employs a single quarter-

* Original manuscript received by the IRE, June 17, 1957; revised manuscript received September 17, 1957.

† Federal Communications Commission, Laurel, Md.

[1] Radio Res. Lab. Harvard Univ., "Very High-Frequency Techniques," vol. 1, 1st ed., McGraw-Hill Book Co., Inc., New York, N. Y., pp. 85–91; 1947.

[2] E. G. Fubini and P. J. Sutro, "A wide-band transformer from an unbalanced to a balanced line," Proc. IRE, vol. 35, pp. 1153–1155; October, 1947.

wave length of transmission line for compensation over a wide band, but the construction is arranged to allow this line to be housed inside one of the arms of the balun. Thus, the over-all physical length is only one-quarter wavelength.

Description of the Balun

A diagram of the balun is shown in two forms in Figs. 1 and 2. The sketches represent two variations of the same arrangement. The device is composed of two lengths of coaxial transmission line, a and b, suitably connected. The symbols Z_a and Z_b represent the characteristic impedances of lines a and b, respectively, considering the waves propagated within each line. Z_{ab} is the characteristic impedance of the balanced transmission line ab composed of the *outer* conductors of transmission lines a and b.

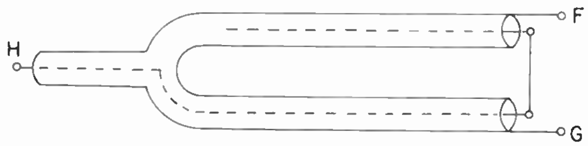

Fig. 1—The new balun. The balanced terminals are at F and G, and the unbalanced connection is made at H.

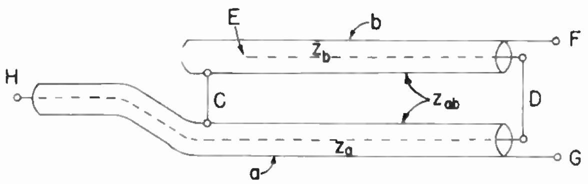

Fig. 2—A slight variation of the balun for the purpose of description.

The coaxial terminal H is the connection for the external unbalanced source (or load), while the terminals F and G are the points of attachment of the balanced load (or source). Center conductors of lines a and b are connected at D, while outer conductors of a and b are connected at C. The center conductor of line b ends at E.

Impedance Analysis

Fig. 3 shows an equivalent circuit of the balun for the purpose of studying the impedance. The terminals F, G, and H are the same as in Figs. 1 and 2. S and R are external impedances which may be connected to the balun. M is the impedance looking into coaxial line b toward the open circuit at E. N is the impedance looking from FG along the open transmission line ab toward the short-circuit at C.

If the transmission line losses are neglected,

$$M = -jZ_b \cot \theta_b$$

$$N = jZ_{ab} \tan \theta_{ab}, \qquad (1)$$

where θ_b and θ_{ab} are, respectively, the electrical lengths of transmission lines b and ab, taking into account their respective physical lengths and velocities of propagation.

From the equivalent circuit,

$$Z = \frac{RN}{R+N} + M \qquad (2)$$

$$Z = \frac{jRZ_{ab} \tan \theta_{ab}}{R + jZ_{ab} \tan \theta_{ab}} - jZ_b \cot \theta_b \qquad (3)$$

$$Z = \frac{R}{\dfrac{R^2}{Z_{ab}^2 \tan^2 \theta_{ab}} + 1} + \frac{jR^2 Z_{ab} \tan \theta_{ab}}{R^2 + Z_{ab}^2 \tan^2 \theta_{ab}} - jZ_b \cot \theta_b. \qquad (4)$$

Let the electrical lengths of line segments b and ab be equal, making $\theta_b = \theta_{ab} = \theta$, and let characteristic impedance $Z_{ab} = R$ and $Z_b = Z_a = S$. Then

$$Z = R \sin^2 \theta + j(\cot \theta)(R \sin^2 \theta - S). \qquad (5)$$

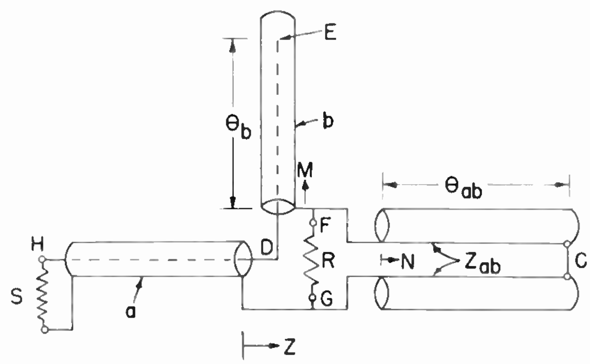

Fig. 3—An equivalent circuit of the balun for the purpose of studying its impedance characteristics. The lettering is the same as that of Fig. 2.

The reactive component of the impedance is zero when $\cot \theta = 0$, (for which Z equals R) and also when $\sin^2 \theta = S/R$ (for which Z becomes S). Fig. 4 is a sketch of the variation of resistance and reactance in the neighborhood of the lowest-frequency band of interest. The physical lengths being fixed, θ varies directly with frequency. The region $\theta_2 - \theta_1$ locates a frequency band $f_2 - f_1$ over which the balun has impedance matching characteristics of a desirable nature. Cot $\theta = 0$ establishes the center of the band and corresponds to an electrical length of 90°. From Fig. 4 it appears that the balun serves to transform from a resistance R to another resistance S with a perfect impedance match at frequencies f_1 and f_2. There is an approximate match in the band of frequencies within this interval and also at frequencies somewhat outside. The midband standing wave ratio increases with the ratio of R/S, hence the balun is particularly interesting for balanced to unbalanced transformations where the desired impedance transformation ratio is low.

An example is a balun for matching a 70-ohm balanced source to a 50-ohm unbalanced load. In this case let $Z_a = Z_b = 50$ ohms, $Z_{ab} = 70$ ohms, and $\theta_{ab} = \theta_b$. The values of θ for which a perfect match is expected are given by

$$\sin^2 \theta = \frac{S}{R} = \frac{50}{70}$$

$$\theta = 58°, 122°.$$

Since θ is linearly proportional to frequency, the frequency band between points of perfect match has a ratio of 2.1. The mismatch at the worst point in this band (namely, at the center frequency) corresponds to a voltage standing wave ratio of 1.4.

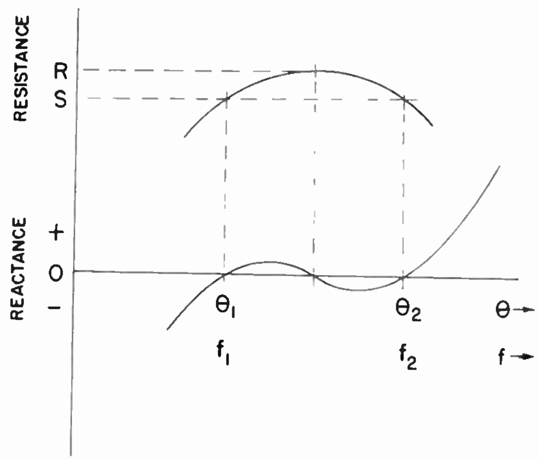

Fig. 4—The input resistance and reactance at the point Z of Fig. 3.

Physical Details of Construction

A number of baluns have been made in the form shown in Fig. 5. In practice, this balun is mounted inside a bakelite tube supporting a dipole antenna used in field strength measurements. The balun shown is made of two lengths of RG-58/U coaxial cable, whose shield braids form a 70-ohm parallel transmission line ab. The length of the parallel section, measured from the point C, where the two braids are connected together, to the points F and G, where the balanced circuit is to be connected, is made one-quarter wavelength at the center frequency of the operating range. For the determination of this length, it is necessary to take account of the propagation velocity, which is somewhat higher than that of the waves moving along the inside of the coaxial cables. The center conductor of the coaxial line b is cut by drilling a hole into the cable at the point E, which (considering the velocity of propagation inside the cable) corresponds to a quarter wavelength from the balanced terminals F and G at the center frequency of the band.

The construction of this version of the balun is based upon the realization of a characteristic impedance of 70 ohms in the parallel transmission line composed of the two lengths of cable held together by a wrapping of plastic tape. Because of variations in composition, diameter, or eccentricity of the outer insulation, the characteristics of parallel lines formed from certain coaxial cable samples may differ appreciably from the desired value. It is generally necessary, therefore, to determine the characteristic impedance and velocity of propagation by testing sample parallel line sections made of the intended material.

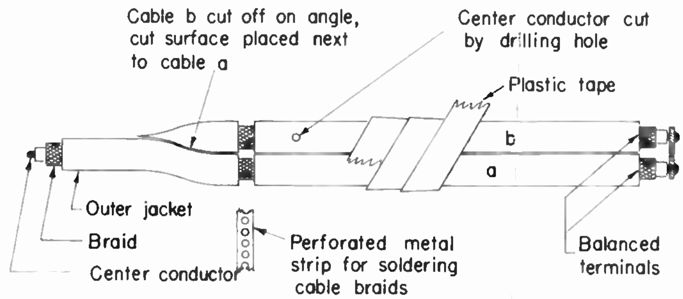

Fig. 5—The construction of a balun for matching a 50-ohm coaxial cable to a 70-ohm balanced load. The balun is made of two lengths of RG-58/U cable, held together by a wrapping of plastic tape. In use, this balun is housed inside an insulated tubing which supports the center of a half-wave dipole antenna. Alternatively, a metal housing could be employed to shield the balun.

Performance of the Balun

Fig. 6 shows the measured vswr looking into the unbalanced connector of a practical 70- to 50-ohm balun, made according to Fig. 5, when the balanced terminals were terminated by a 70-ohm noninductive resistor. This same figure gives the measured loss. The loss was measured through two identical baluns, their balanced terminals being joined through a 70-ohm balanced resistive attenuator for isolation. The loss of one balun is considered to be one-half the total attenuation, subtracting first the loss of the attenuator. The baluns have excellent symmetry, in that no appreciable change in measured values resulted from reversal of the balanced terminals of either balun. The curves in Fig. 6 are typical of those which have been measured on other baluns of the same construction covering frequencies as high as 1000 mc.

To verify the performance of the balun when associated with a dipole antenna, two identical balun-dipole assemblies were constructed to cover the range 400 to 1000 mc. Signals at a number of frequencies across this range were fed to one assembly, radiated, and picked up by the other. The attenuation through this path was compared with that obtained when the coaxial transmission lines were disconnected from the baluns and connected to each other. The propagation path between the antennas was approximately equivalent to free-space conditions. On the assumption that the resonant

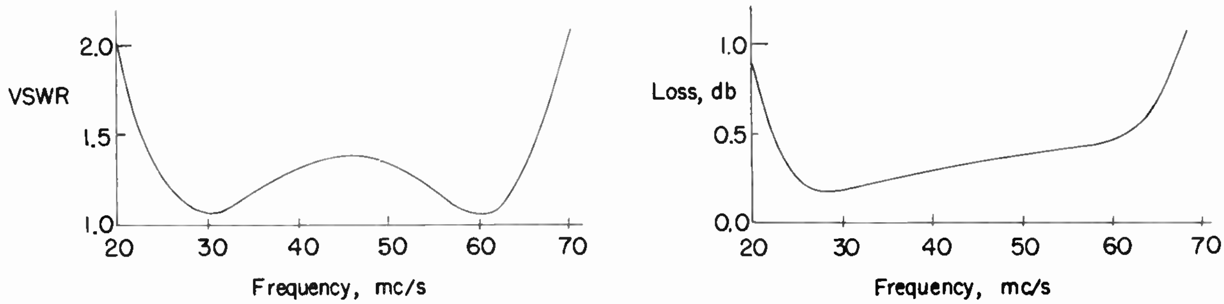

Fig. 6—The measured performance of the balun of Fig. 5 when the balanced terminals are connected to a 70-ohm noninductive resistance.

dipole antennas had a power gain over isotropic antennas of 1.64 (the theoretical value for an infinitely-thin dipole), and taking into account the distance between the dipoles, the loss attributable to the sum of dipole loss and balun loss for one assembly was found to be 0.6 db ± 0.4 db at the frequencies of test. This is considered to be an acceptable verification of the loss of the balun.

Conclusion

A new form of balun has been described. It has low loss and excellent impedance characteristics over almost a 3 to 1 frequency band, without any adjustments. The dimensions of the balun make it suitable for use at vhf and uhf, particularly in association with the adjustable dipole antennas widely used for field strength measurements in these frequency ranges.

Correction

Dr. Janis Galejs, of the Applied Research Laboratory, Sylvania Electric Products, Inc., Waltham, Mass., has called the following to the attention of the editor.

The comments of Strom[1] on the recent remarks by Goldstein[2] appear to be incorrect. In deriving (11) from (10) Strom states that the second integral on the right-hand side of (10) vanishes. Following Goldstein,[3] the band-pass filter output of the radiometer $v(t)$ is a sum of a periodic and of a random voltage

$$v(t) = A \cos \omega_q t + Bm(t),$$

where $m(t)$ is a random voltage. Substituting $v(t)$ in (10) the term proportional to A^2 in the second integral

$$\lim_{T\to\infty} \frac{1}{T} \int_0^T v(t)v(t+\tau) \frac{\cos \omega_q(2t+\tau)}{2} dt$$

gives a contribution to the constant term of $R_3(\tau)$, that is, equal to the contribution of the term proportional to A^2 in the first integral

$$\lim_{T\to\infty} \frac{1}{T} \int_0^T v(t)v(t+\tau) \frac{\cos \omega_q \tau}{2} dt.$$

The sum of these two terms is equal to the constant term in the $R_3(\tau)$ expression of Goldstein,[4] but is twice the constant term in (12) of Strom.

Strom considers his (8) to (12) as a special case of a more general treatment.[5] With the special case in error, a similar error may be expected in the development leading to (5) and (7). In order to make (5) and (7) compatible with the revised (12) and with the results of Goldstein,[2] a constant 16 should be substituted for the constant 32 in (5) and (7) of Strom.[1]

[1] L. D. Strom, "The theoretical sensitivity of the Dicke radiometer," Proc. IRE, vol. 45, pp. 1291–1292; September, 1957.
[2] S. J. Goldstein, Jr., "A comparison of two radiometer circuits," Proc. IRE, vol. 45, pp. 365–366; March, 1957.
[3] S. J. Goldstein, Jr., private communication.
[4] S. J. Goldstein, Jr., "A comparison of two radiometer circuits," Proc. IRE, vol. 43, pp. 1663–1666; November, 1955.
[5] L. D. Strom, "The theoretical sensitivity of the Dicke radiometer," dissertation, University of Texas; February, 1957.

Synthesis of Lumped Parameter Precision Delay Line*

E. S. KUH†, ASSOCIATE MEMBER, IRE

Summary—In the design of delay lines one can break down the problem into two parts, namely: 1) to provide the required time delay and bandwidth with a least complicated network and 2) to have a good time response. This paper presents such a design technique for precision time domain applications. The network obtained is a tandem connection of a low-pass ladder which provides the shape of time response and an all-pass bridge structure which gives the desired time delay.

The approximation to the ideal delay function is based on the potential analog method in both cases. A method of estimating the time domain error from the frequency domain error is used to determine the maximum permissible phase distortion of the all-pass network.

Introduction

The lumped parameter delay line has been designed mostly on the image theory basis. Usually, M-derived sections are used in a limited bandwidth to achieve the linear phase characteristics. However, for precision time domain applications, such as analog to digital conversion, this design is undesirable because of the unavoidable amount of distortion (overshoots or undershoots) in the time response.

With modern synthesis techniques available, a direct approach can be made. First, one approximates an ideal delay function by a physically realizable transfer function and then realizes the delay network from the approximated function. Storch[1] uses such a technique to realize low-pass networks with a maximally flat delay function and good time response. However, his method is useful only when the ratio of delay to rise time is very small and becomes extremely inefficient and impractical when the ratio is a little larger than unity.

The method proposed here is intended for an efficient design of delay lines with an arbitrarily large delay-rise time ratio, which satisfy a strict transient response requirement. A cascade connection of a low-pass and an all-pass network is used. The approximation is done on the potential analog basis which is shown to be more efficient than the maximally flat design in the sense that a wider bandwidth is covered for a given number of singularities to realize the same amount of delay. Moreover, the method is flexible enough to handle delay lines with a less stringent transient requirement simply by trading the quality of the time response with the efficiency obtained. Finally, a method of estimating time domain error from frequency domain error is discussed and illustrated.

An ideal delay line has a transcendental transfer function, e^{-pt_0}, where p is the complex frequency variable and t_0 the time delay. On the real frequency axis, the loss is zero and the phase linear (*i.e.*, the delay is constant). For a lumped parameter network, a rational approximation to e^{-pt_0} is needed. Two types of approximation are possible. In the first one, a low-pass network is realized. The linear phase approximation is good at low frequencies and the associated minimum phase loss is realized. In the second case, an all-pass network is realized. The phase approximation is as before, yet the loss is zero over the complete frequency band. From time-domain point of view, a good delay line should have fast rise time and no overshoots or undershoots. The low-pass network can be designed to have finite rise time and essentially no overshoots or undershoots. On the other hand, an all-pass network has an infinite bandwidth or zero rise time, yet the time response is completely distorted for the simple reason that the delay through the network approaches zero as the frequency approaches infinity. Hence a high-frequency signal gets through without any delay.

For linear phase low-pass networks, the bandwidth (in cycles per second) and rise time bear a simple relationship as given by

$$B\tau = \tfrac{1}{2}. \tag{1}$$

If $T(p)$ represents the transfer function of a delay line, on the real frequency axis,

$$T(j\omega) = A(\omega)e^{-j\beta(\omega)} \tag{2}$$

where $A(\omega)$ is the magnitude and $\beta(\omega)$ the phase. The bandwidth B to be used in (1) is defined as

$$B = \frac{1}{2\pi A(0)}\int_0^\infty A(\omega)d\omega, \tag{3}$$

and is approximately equal to the 6-db bandwidth. The rise time is defined in terms of the step response as shown in Fig. 1. To characterize a delay line, one defines a phase factor,

$$u = 2\pi B t_0 = \frac{\pi t_0}{\tau} \tag{4}$$

measuring the usable phase. Let m represent the total number of finite singularities (poles and zeros) of $T(p)$, then it is clear that the theoretically available amount of phase is $m\pi/2$ radians. Thus one can define the efficiency of a delay line as

$$E = \frac{u}{m\pi/2}\,. \tag{4a}$$

* Original manuscript received by the IRE, April 1, 1957; revised manuscript received, September 23, 1957.

† University of California, Berkeley, Calif.

[1] L. Storch, "Synthesis of constant-time-delay ladder networks using Bessel polynomials," Proc. IRE, vol. 42, pp. 1666–1675; November, 1954.

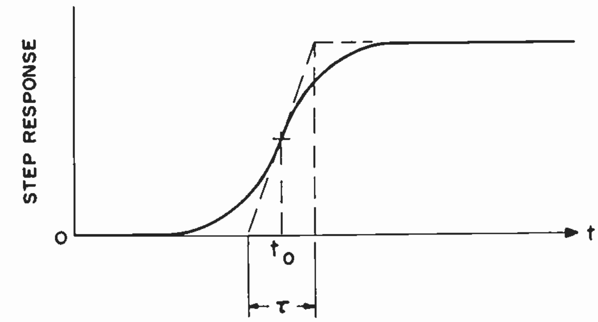

Fig. 1—Rise time definition.

For the low-pass delay line with a maximally flat delay the efficiency is proportional to $1/\sqrt{m}$, as shown by Storch,[1] while the all-pass network with a given bandwidth has an efficiency independent of m (since the phase factor, u, is directly proportional to the number of all-pass sections). In Fig. 2 the efficiency of the maximally flat delay line is plotted vs m. It is clear that such a design is far from practical when m is larger than 12 for the reasons of poor efficiency and the difficulty of finding the element values and building the actual ladder network.

As noted, a low-pass network can be designed with excellent time response, such as illustrated by Storch, by using the maximally flat delay functions. (A more efficient design is shown in the next section, using the potential analog method.) The remaining problem is to improve the efficiency when u is large and while maintaining the quality of the time response. This can be achieved simply by cascading a low-pass network N_1 with a constant resistance all-pass network N_2 as shown in Fig. 3. Thus the low-pass network is designed to have a good time response and the all-pass network contributes only to the delay. Let $h_1(t)$ be the impulse response of N_1, then the over-all output $h_2(t)$ is desired to be

$$h_2(t) \sim h_1(t - t_2) \tag{5}$$

where t_2 represents the delay contributed by N_2. The remaining problem is to obtain a good approximation in (5). To accomplish this, one must design the all-pass network carefully such that the phase remains linear over a wide frequency band at least that over which the loss of the low-pass network is low. The approximation problem in general is treated in the next section; the design details and time domain considerations are given afterwards.

It should be pointed out that the discussion given above assumes an ideal impulse or step input function, *i.e.*, the frequency spectrum is from dc to infinity. For practical applications in pulse transmission systems, the input wave may contain only low-frequency signals; hence only an all-pass network is needed. To summarize, two distinct problems are solved in this paper:

1) The design of low-pass networks which yields a good time response to ideal impulse or step inputs. The transfer function obtained is an improvement over the maximally flat delay function.
2) The design of all-pass networks which give a good time response to a practical finite rise time input function.

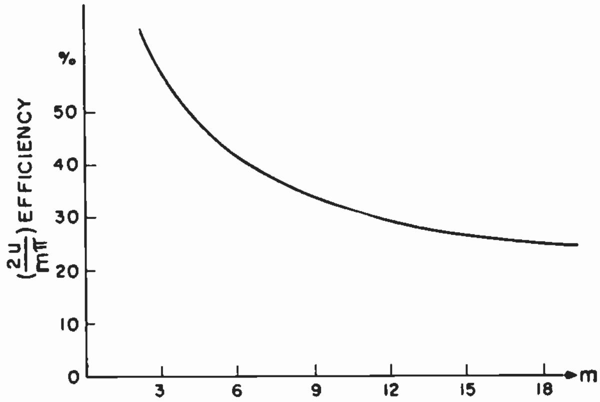

Fig. 2—Efficiency vs number of poles of the maximally flat delay low-pass network.

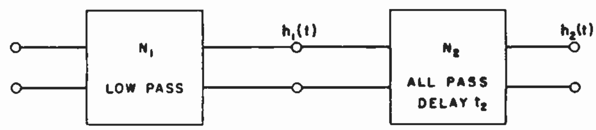

Fig. 3—Cascade connection of a low-pass and an all-pass network.

The Approximation Problem

A low-pass network with all the transmission zeros at infinity has a transfer function

$$T_1(p) = \frac{K}{Q_1(p)} \sim e^{-pt_0}. \tag{6}$$

An all-pass network with poles and zeros at mirror images with respect to the $j\omega$ axis has a transfer function

$$T_2(p) = \frac{Q_2(-p)}{Q_2(p)} \sim e^{-pt_0}. \tag{7}$$

Hence the problem here is to find a polynomial $Q(p)$ to approximate the function e^{pt_0}. Thus if the low-pass and all-pass networks have the same poles, the delay of the former is just half as much as the latter.

The Bessel polynomial approximation which yields a maximally flat delay is not efficient for the same reason that the Butterworth filter is not efficient as compared to the Tchebycheff filter. Since the equal ripple approximation to a flat delay has not been solved, the other two general approximation methods due to Darlington[2,3] can be used. The potential analog method is chosen here rather than the Tchebycheff polynomial method for two reasons: 1) The delay ripple obtained

[2] S. Darlington, "The potential analogue method of network synthesis," *Bell Sys. Tech. J.*, vol. 30, pp. 315–365; April, 1951.
[3] S. Darlington, "Network synthesis using Tchebycheff polynomial series," *Bell Sys. Tech. J.*, vol. 31, pp. 613–665; July, 1952.

can be controlled very easily so that the phase deviation is small at low-frequencies where its effect on the time response is most critical and 2) the singularities can be determined easily without solving any high degree polynomials.

The potential analog method requires the selection of a contour on which the charges will be located. A condenser plate design is not desirable because of the large truncation error. To eliminate such a difficulty, an elliptic contour is chosen. The eccentricity of the ellipse may be varied to obtain various approximations. Since, in the potential analog, the delay is represented by the electric field normal to the $j\omega$ axis, it is clear intuitively that the narrower the contour, the more efficient the design. However, one must also realize that a quantization procedure is always needed to obtain the network singularities after the potential problem is solved, and quantization causes granularity error. Hence the contour should not be so close to the $j\omega$ axis as to cause excessive ripples due to quantization and therefore distort the time response. In the next few paragraphs some empirical formulas are derived to obtain the best compromise in choosing the eccentricity.

As shown in Fig. 4, let ξ_0 and $\sqrt{\xi_0^2-1}$ represent the major and minor axes of an ellipse and let

$$r = \frac{\xi_0}{\sqrt{\xi_0^2 - 1}} \tag{8}$$

characterize the ellipse eccentricity. To obtain a flat delay approximation the location of the poles are found to be

$$\begin{aligned} \sigma_i &= -\sqrt{\xi_0^2 - 1}\cos y_i \\ \omega_i &= \pm\,\xi_0 \sin y_i \end{aligned} \tag{9}$$

where

$$\sin y_i = \frac{1}{n}, \frac{3}{n}, \frac{5}{n} \cdots \frac{n-1}{n} \text{ for } n \text{ even}$$

and

$$\sin y_i = 0, \frac{2}{n}, \cdots \frac{n-1}{n} \text{ for } n \text{ odd.} \tag{10}$$

n represents the number of poles only. y_i represents the angle measured from the positive-σ axis as shown in Fig. 4 and n designates the total number of poles used. The derivation of the potential analog method is given in Appendix I. Thus, given r and n, the poles can be found immediately from (9) and (10). The zeros for an all-pass network are simply at the mirror images of the poles.

The next question is to determine r and n from the prescribed information on bandwidth and time delay. First one finds, as shown in the Appendix, the flat delay (or the electric field intensity normal to the $j\omega$ axis) as a function of n for a given ellipse. From (41) in Appendix I

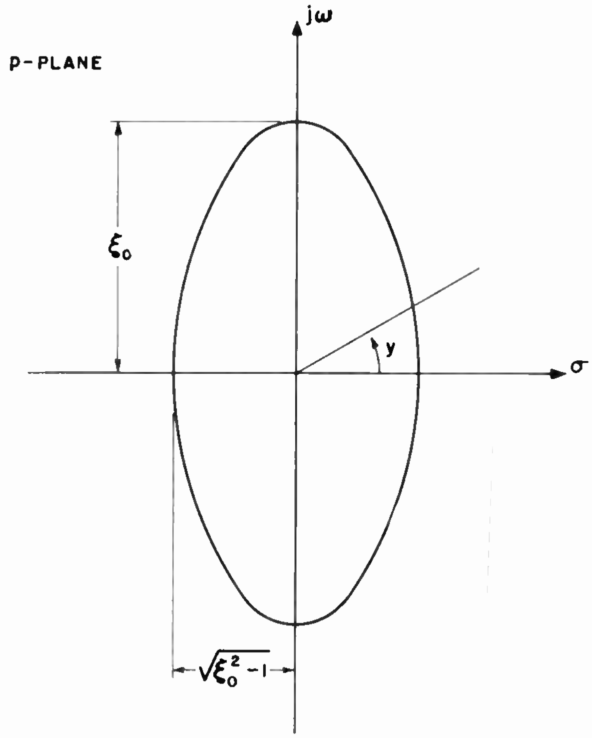

Fig. 4—Elliptic contour.

$$t_0 = \frac{n\pi}{\xi_0 + \sqrt{\xi_0^2 - 1}}. \tag{11}$$

This formula includes the effect of negative charges in the right half plane and hence corresponds to the delay of an all-pass network. The total available phase (*i.e.*, the product of the flat delay and the available bandwidth, ξ_0)[4]

$$\beta_{av} = t_0\xi_0 = \frac{n\pi}{1 + \sqrt{\dfrac{\xi_0^2 - 1}{\xi_0}}} = \frac{n\pi}{1 + \dfrac{1}{r}}. \tag{12}$$

It is seen that the larger r is, or the narrower the ellipse is, the larger is the available phase. As r reaches infinity, the available phase reaches the theoretically available amount $n\pi$ for n pairs of poles and zeros. In the design of the all-pass network one needs to know β_{av} required and from which n is determined. Once r and n are chosen, β_{av} is fixed; a standard frequency normalization is needed to give the desired bandwidth and flat delay.

The remaining problem is to find a suitable relation between r and n. This relation is determined by the granularity error due to quantization. Because of the shape of an elliptic contour, it is clear that the error is small at low frequency near the origin and gets larger near the cutoff frequency. To get an estimate of this error vs frequency as a function of r, the following approximation is made. The granularity error of an

[4] In terms of potential analog, this is the total flux crossing the $j\omega$ axis inside the chosen contour.

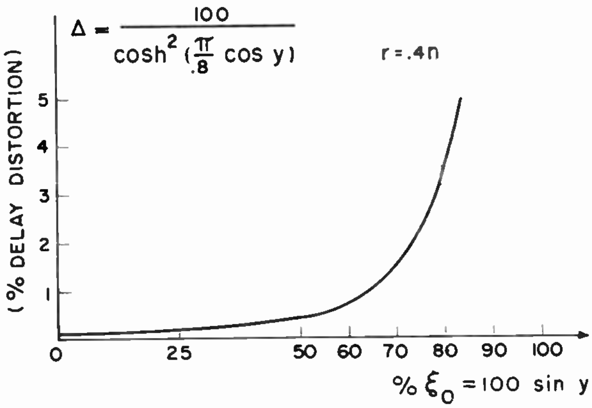

Fig. 5—Estimate of per cent delay distortion vs per cent available bandwidth for the case $r=0.4n$.

elliptic contour is assumed equal to that due to an infinite array of charges parallel to the $j\omega$ axis at a variable distance $\sqrt{\xi_0^2-1}\cos y$ away from the $j\omega$ axis. The spacing between successive line charges is constant and is equal to $2\xi_0/n$. In Appendix II it is derived that the maximum granularity error due to an array of filamentary charges is on a percentage basis

$$\Delta = \frac{100}{\cosh^2\left(\frac{\pi a}{b}\right)} \tag{13}$$

where b is the spacing between charges and a their distance from the $j\omega$ axis. Using the distances given above for the elliptic contour,

$$\Delta = \frac{100}{\cosh^2\left(\frac{n\pi\cos y}{2r}\right)} \tag{14}$$

where $\sin y=\omega/\xi_0$ represents the ratio of ω at which the error is estimated and the normalized available bandwidth ξ_0. Using (14) it is found at $\omega=70$ per cent ξ_0, $\Delta<1.5$ with a choice of

$$r \sim .4n. \tag{15}$$

This is a useful empirical formula for both the all-pass and the low-pass design. It turns out that with such a choice of $r\sim 0.4n$, the time response of the low-pass network is usually excellent.[5] Eq. (14) is plotted in Fig. 5 for the $r=0.4n$ choice. The estimate is usually good in the range of $\omega \leq 85$ per cent ξ_0.

Some Design Considerations

Low-Pass Network

The low-pass network is designed on the basis of obtaining good time response and efficiency. It is clear that using the potential analog method, the larger the number n is, the better the approximation and the better the time response. From experimental results obtained from analog computers, it is found that with $n\geq 9$ and the eccentricity of the ellipse defined by $r\sim 0.4n$, there is essentially no visually detectable distortion of the impulse response. In this section, some results are shown for the case $n=11$. Various r are selected for comparison. In Table I, the phase factor

TABLE I

$n=11,\ t_0=1$	$u=2\pi Bt_0$	eff $=2\mu/n\pi$
max. flat	5.39	0.312
$r=0.283n$	5.69	0.330
$r=0.318n$	5.75	0.333
$r=0.354n$	5.78	0.335
$r=0.389n$	5.81	0.337
$r=0.424n$	5.85	0.338

and the efficiency are given for various r and also for the maximally flat function. It is seen that the $r=0.424n$ case is about 9 per cent more efficient than the maximally flat case. The step and impulse responses of all six cases are good. The $r=0.424n$ case is shown in Fig. 6.

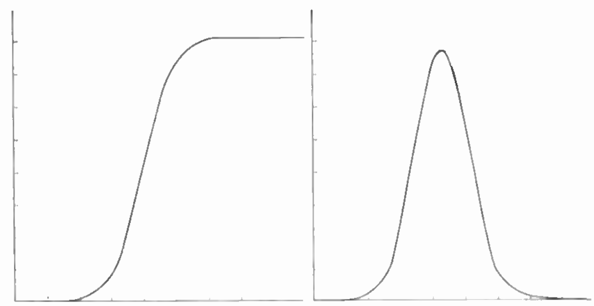

Fig. 6—Step and impulse responses of low-pass network with $n=11$, $r=0.424n$.

Once the poles are located, the network can be determined from existing well-known techniques.[6,7] A low-pass ladder with series inductances and shunt capacitances is realized. In this case of $n=11$, one gets five inductances and six capacitances. Networks can be realized both for termination at one end (Z_{21} or Y_{21} design) and terminations at both ends (transmission coefficient design). In the first case the network elements can be obtained very easily by finding the continued fraction expansion of z_{22} or y_{22}, while in the second case, one has to find the reflection coefficient and the input impedance. The details can be found in Guillemin[6] and Darlington.[7] It should be mentioned that for given n and r, the element values are determined once for all, subject only to the trivial impedance and fre-

[5] It should be pointed out that the shape of the time response depends on the *phase* deviation from linearity; however, since the delay contributed by the low-pass network is usually small in this proposed method, $\Delta=1.5$ usually corresponds to a tolerable *phase* deviation from linearity.

[6] E. A. Guillemin, "Modern Methods of Network Synthesis," in "Advances in Electronics," Academic Press, New York, N. Y., vol. III, pp. 275–303; 1951.

[7] S. Darlington, "Synthesis of reactance 4-poles," *J. Math. Phys.*, vol. 18, pp. 257–333; September, 1939.

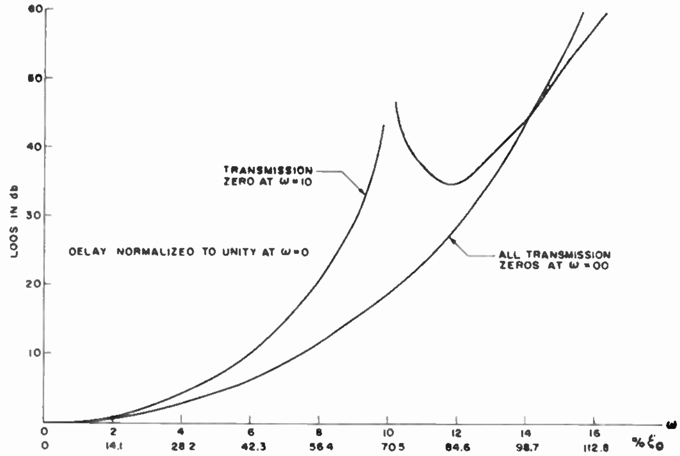

Fig. 7—Low-pass network loss in db vs frequency.

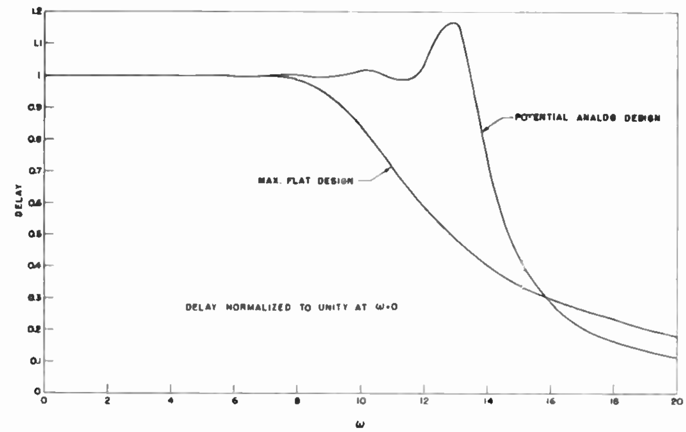

Fig. 9—Comparison of delay vs frequency for $n=11$ maximally flat and elliptic contour $r=0.424n$ case.

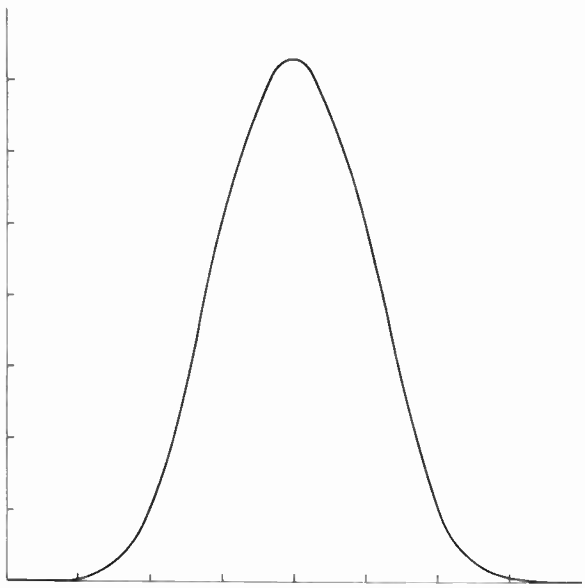

Fig. 8—Impulse response of low-pass network with transmission zero at $\omega=10$.

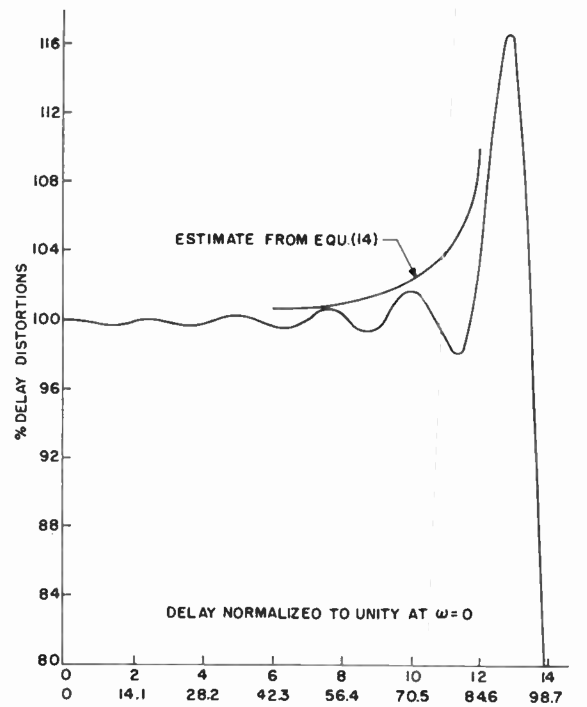

Fig. 10—Estimate of granularity error of (15) and actual delay vs frequency plot for $n=11$, $r=0.424n$.

quency normalizations. As a practical consideration, the $n=11$ case represents almost an upper bound for a ladder that can still be designed, built, and aligned to a given accuracy.

A variation of the low-pass design is to have one or more pairs of transmission zeros on the $j\omega$ axis. Series or parallel tuned circuits are introduced in the ladder realization. This is sometimes useful when the overall time response error is not too strict. The additional loss introduced at lower frequencies makes the design of the all-pass network easier. It is also true that the bandwidth of the low-pass network is reduced by the transmission zeros. The loss curve for the $r=0.424n$ case with a transmission zero at $\omega=10$ is plotted in Fig. 7 along with the case with all zeros at infinity. It is seen that the 6-db bandwidth is reduced from $\omega=5.8$ to 4.75. The impulse response is shown in Fig. 8. Thus a pair of transmission zeros at finite frequencies does not impair the quality of the time response.

All-Pass Netowrk

If the required phase shift of the all-pass network is given, r and n can be determined immediately using (12) and (15). To compare the result obtained with that of the maximally flat network, the delay for $n=11$, $r=0.424n$ is plotted vs frequency along with the $n=11$ maximally flat case in Fig. 9. It is seen that a much wider flat delay bandwidth is realized using the elliptic contour, yet the flatness of the delay at low frequency is just as good.

In Fig. 10 the same delay curve is plotted in a larger scale to show the relative accuracy of the estimate of the granularity error given by (14). It is also possible to estimate the amount of phase distortion from linearity.

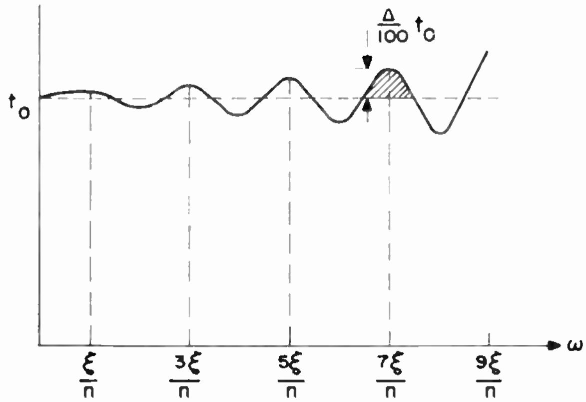

Fig. 11—Assumed delay distortion curve for estimating the phase distortion.

Assuming that each delay ripple is sinusoidal, then the maximum phase distortion $\theta(\omega)$ can be found directly from the percentage delay distortion, Δ. As shown in Fig. 11, the shaded area represents $\theta(\omega)$ and is given (in radians) by

$$\theta(\omega) = \frac{2}{\pi}\frac{\xi_0}{n}\frac{\Delta}{100}t_0 = \frac{2}{\pi}\frac{\xi_0}{n}\frac{\Delta}{100}\frac{n\pi}{\xi_0\left(1+\frac{1}{r}\right)}$$

$$= \frac{\Delta}{50\left(1+\frac{1}{r}\right)}. \tag{16}$$

The time response of the over-all network depends on $\theta(\omega)$ and the magnitude function $A(\omega)$ of the low-pass network. In the next section, the relationship is derived on a theoretical basis. In this section, some experimental results obtained from an analog computer are shown. Referring to Fig. 3, a low-pass network N_1 with $n=12$, $r=0.357n$ is used to cascade with an all-pass network N_2, with $n=12$, $r=0.357n$. Let the flat delay of N_1 and N_2 be t_1 and t_2. By keeping t_2 constant and varying t_1, different time responses are obtained. They are tabulated in Table II for three distinct cases.

TABLE II

t_2	t_1	$t_0=t_1+t_2$	$u=\pi(t_0/t)$	eff	Overshoot (Impulse response)	Overshoot (Step response)
2	1		18.8	0.336	none	none
2	0.7		23.8	0.421	4.3 per cent	1 per cent
2	0.7	(With transmission zero at $\omega=12$)	20	0.336	0.5 per cent	negligible amount

This actually amounts to changing the bandwidth of the low-pass network while keeping the all-pass network with the same phase. The step responses for the last two cases are shown in Figs. 12 and 13. Thus, it is seen that the efficiency of the over-all delay line can be traded easily with the quality of the time response. Compared to the results shown in Table I, it is clear that the cascading connection can improve the efficiency or keep the efficiency constant while realizing a much larger phase factor u. The time response can also be controlled easily.

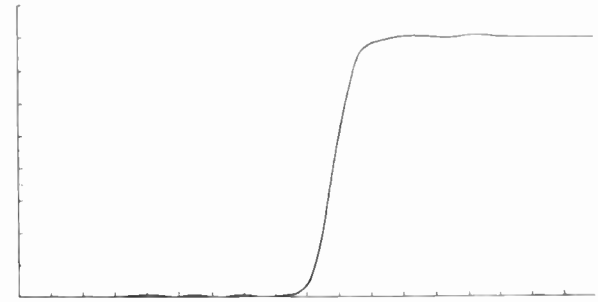

Fig. 12—Step response of case 2 of Table II.

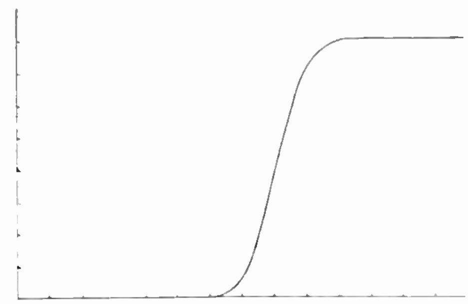

Fig. 13—Step response of case 3 of Table II.

The structures to be realized for the all-pass network are all of the constant resistance bridge-T type. Because of the specific choice of eccentricity of the ellipse as given by (15), all but two of the bridge-T sections contain all positive elements and can be realized in the form as shown in Fig. 14. For the remaining two with singularities closest to the σ axis, one requires negative coupling as shown in Fig. 15, and the other can be realized as a twin T as shown in Fig. 16.

Time Domain Considerations

In the design of all-pass network for the delay line problem, it is important to know some relationship between the distortions in the frequency and time domains. Since for time domain applications the requirement of the line is usually given in terms of time response and the design of the all-pass network is based on the delay or phase specification in the frequency domain, it is necessary to have some method to determine one from the other. A useful formula used here, due to C. A. Desoer, is derived in Appendix III. It states that

$$|e(t)| \leq \max_{0\leq\omega\leq\infty}\frac{\omega_0}{2}\left[1+\left(\frac{\omega}{\omega_0}\right)^2\right]|\epsilon(j\omega)| \tag{17}$$

where $e(t)$ is the error in time domain, $|\epsilon(j\omega)|$ is the error in frequency domain, and ω_0 is a parameter to be chosen such that the maximum value in the bracket is a mini-

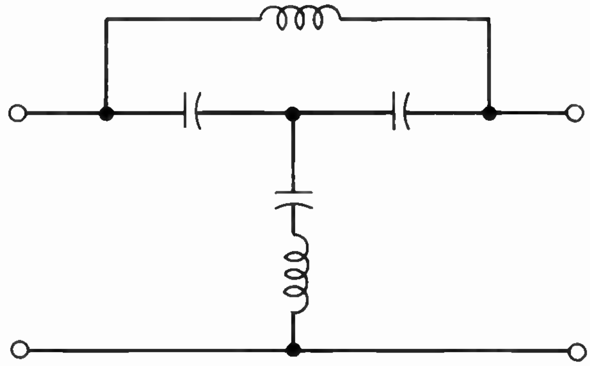

Fig. 14—All-pass constant-R bridge-T structure.

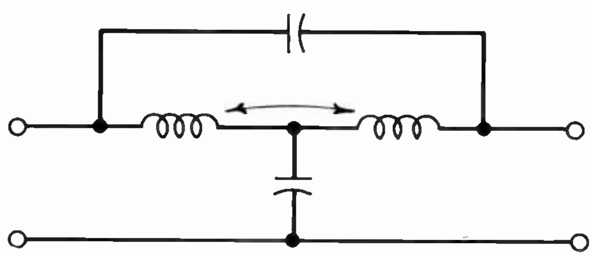

Fig. 15—Bridge T with negative coupling.

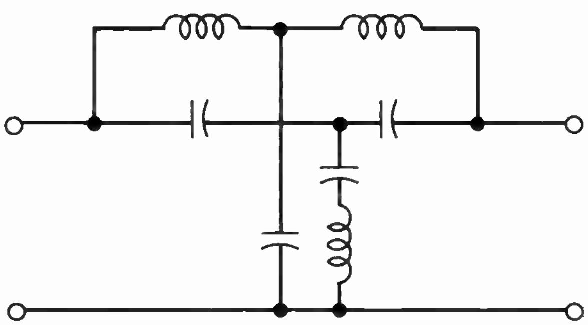

Fig. 16—Constant-R twin-T structure.

mum. This inequality gives an estimate of the upper bound of time domain error from a given frequency domain error. To apply this formula, the following terms are defined. From Fig. 3, let the transfer function of the low-pass network be

$$T_1(j\omega) = A(\omega)e^{-j\beta_1(\omega)} \tag{18}$$

and the all-pass network

$$T_2(j\omega) = e^{-j\beta_2(\omega)} = e^{-j(\omega t_2+\theta)} \tag{19}$$

where $\theta(\omega)$ denotes the phase deviation from linearity. It follows that impulse responses

$$h_1(t) = \mathcal{L}^{-1}[T_1(p)] \tag{20}$$

$$h_1(t - t_2) = \mathcal{L}^{-1}[T_1(p)e^{-pt_2}] \tag{21}$$

and

$$h_2(t) = \mathcal{L}^{-1}[T_1(p)T_2(p)] \tag{22}$$

where $\mathcal{L}^{-1}$ designates the inverse Laplace transform.

Since $h_1(t)$ represents a desired impulse response and $h_2(t)$ the over-all impulse response, the error in the time domain can be represented as

$$e(t) = h_1(t - t_2) - h_2(t). \tag{23}$$

The corresponding error in the frequency domain is therefore

$$\epsilon(p) = T_1(p)e^{-pt_2} - T_1(p)T_2(p). \tag{24}$$

On the real frequency axis,

$$\epsilon(j\omega) = A(\omega)e^{-j(\beta_1+\omega t_2)}(1 - e^{-j\theta}). \tag{25}$$

The absolute value is

$$|\epsilon(j\omega)| = 2A(\omega) \sin \frac{\theta(\omega)}{2}. \tag{26}$$

Using (17) one has

$$|e(t)| \leq \max_{0\leq\omega\leq\infty} \omega_0\left[1 + \left(\frac{\omega}{\omega_0}\right)^2\right]A(\omega) \sin \frac{\theta(\omega)}{2}. \tag{27}$$

This equation allows one to determine the requirement on $\theta(\omega)$ from the permissible time domain error $e(t)$ and the magnitude $A(\omega)$ of the transmission of the low-pass filter. Since $A(\omega)$ is close to unity at low frequency and approaches zero at high frequency, from (27) it can be seen that $\theta(\omega)$ must be small at low frequency and may become increasingly large as ω increases. ω_0 can be assumed any arbitrary value to start with and changed in the succeeding estimate so that the previous maximum is reduced. It is found that an optimum choice of ω_0 is to start with 6-db bandwidth. An illustrative example is given in the next section to show the application of this estimate.

Illustrative Design

A delay line with 1-μsec delay and 0.05-μsec rise time is needed. The maximum allowable step response distortion is 1 per cent.

From (1) one finds the required bandwidth (6 db)

$$B = \frac{1}{2 \times 0.05} = 10 \text{ mc}.$$

Assuming an $n=11$, $r=0.424n$, low-pass network is used, the contribution of delay due to the low-pass network is

$$t_1 = \frac{u_1}{2\pi B} = \frac{5.85}{2\pi \times 10 \times 10^6} = 0.093\ \mu\text{sec}$$

where u_1, the phase factor of the low-pass network, can be found in Table I. Hence the required delay for the all-pass network is

$$t_2 = 1 - 0.093 = 0.907\ \mu\text{sec}.$$

The problem now is to determine the bandwidth of flat delay or linear phase of the all-pass network such that the over-all step response satisfies the given requirement. First, one has the magnitude function $A(\omega)$

of the low-pass network from Fig. 7. The 6-db point in the figure is normalized to a frequency of $B=10$ mc. Therefore at

frequency	$\frac{B}{3}$	$\frac{2B}{3}$	B	$1.5B$	$2B$	$2.5B$	$3B$
loss in db	$=0.5$	2.8	6	14.5	22	44	75
A	$=0.945$	0.725	0.5	0.188	0.0795	0.0063	0.000178.

The corresponding formula for error in frequency domain for the step response can be obtained from (26) simply by dividing the expression by ω

$$|\epsilon(j\omega)| = 2\frac{A(\omega)}{\omega}\sin\frac{\theta(\omega)}{2}.$$

Thus the time domain error is

$$|e(t)| \le \max_{0\le\omega\le\infty}\left(\frac{\omega_0}{\omega}\left[1+\left(\frac{\omega}{\omega_0}\right)^2\right]A(\omega)\sin\frac{(\omega)}{2}\right).$$

Assuming $\omega_0=2\pi B$, the following terms are calculated:

frequency	$\frac{B}{3}$	$\frac{2B}{3}$	B	$1.5B$	$2B$	$2.5B$	$3B$
$\frac{\omega_0}{\omega}\left[1+\left(\frac{\omega}{\omega_0}\right)^2\right]$	$\frac{10}{3}$	$\frac{13}{6}$	2	2.17	2.5	2.9	$\frac{10}{3}$
$\frac{\omega_0}{\omega}\left[1+\left(\frac{\omega}{\omega_0}\right)^2\right]A$	3.15	1.57	1	0.408	0.199	0.0183	0.00059.

Since $e(t)$ is to be smaller than 0.01, hence we obtain the following inequalities displayed in tabular form:

frequency	$\frac{B}{3}$	$\frac{2B}{3}$	B	$1.5B$	$2B$	$2.5B$	$3B$
$\sin\frac{\theta}{2}$	≤ 0.0032	0.0064	0.01	0.0245	0.05	0.54	16
$\frac{\theta}{2}$	≤ 0.0032	0.0064	0.01	0.0245	0.05	0.57	—.

From (16), it is found that the per cent delay distortion must satisfy the following inequalities at

frequency	$\frac{B}{3}$	$\frac{2B}{3}$	B	$1.5B$	$2B$	$2.5B$
Δ	≤ 0.39	0.78	1.21	2.98	6.1	69.

Knowing the allowable per cent delay distortion vs frequency, one can determine the available phase required from Fig. 5. In this example, it is found that if $1.5B$ corresponds to 75 per cent ξ_0, the inequality as shown above can be satisfied at all frequencies. Hence the available phase bandwidth (denormalized ξ_0)

$$= \frac{1.5B}{B}\times 10 \text{ mc} \times \frac{100}{75} = 20 \text{ mc}.$$

The availabe phase is therefore by (12)

$$\beta_{av} = 2\pi \times 20 \text{ mc} \times 0.907 = 18.14 \times 2\pi \text{ rad}.$$

Using (12), one finds the number of poles needed as

$$n = \frac{\beta_{av}\left(1+\frac{1}{r}\right)}{\pi} = 2\times(18.14)(1.214) = 44.$$

Hence the complete delay line has a low-pass network with $n=11$ and an all-pass network with $n=44$ or 22 bridge structures. The phase factor is from (4).

$$u = 2\pi B t_0 = 62.8$$

and the efficiency

$$\text{eff} = 62.8 \times \frac{1}{\frac{\pi}{2}(11+4\times 22)} = 0.404.$$

From this example, it is found that at frequencies where the low-pass filter provides more than 30 to 40-db loss, the phase distortion $\theta(\omega)$ is almost immaterial. A more efficient design can, be done therefore, if the low-pass network has a pair of transmission zeros at finite frequency as shown in Fig. 7. An improvement of about 10 per cent in efficiency is possible.

Appendix I

Approximation of the Ideal Delay Function Using Potential Analog Method

The transmission function is defined as the logarithm of the transfer function, thus for the ideal delay function

$$F(p) = \ln T(p) = -t_0 p = -t_0\sigma - jt_0\omega. \tag{28}$$

This desired transmission function is identified as a complex potential, F_i, inside a chosen contour on which the charges will be located. To determine the charge distribution, an exterior complex potential, F_e, is found based on the following two considerations:

1) The real parts of F_i and F_e must be continuous on the chosen contour.
2) The exterior complex potential must vanish at infinity at least as $1/p$ in order to obtain a unique solution. Therefore, the discontinuity of the imaginary parts of F_i and F_e fixes the single layer charge distribution needed on the contour. In terms of the network theory the real part of the complex potential (the real potential, V) is identified with the gain function, α, and the imaginary part (the stream function, ψ) is identified with the negative phase, $-\beta$. The charge distribution has to be quantized as filamentary charges to obtain the poles and zeros of the network transfer function.

Since an elliptic contour is selected for this problem, it is more convenient to use the elliptic coordinates (ξ, η) where

$$p = \sigma + j\omega = \sqrt{(\xi^2-1)(1-\eta^2)} + j\xi\eta. \tag{29}$$

The Cauchy Riemann conditions are given as[8]

$$\frac{\partial V}{h_1\partial\xi} = \frac{\partial\psi}{h_2\partial\eta} \quad\text{and}\quad \frac{\partial V}{h_2\partial\eta} = -\frac{\partial\psi}{h_1\partial\xi} \tag{30}$$

where

$$h_1 = \sqrt{\frac{\xi^2-\eta^2}{\xi^2-1}} \quad\text{and}\quad h_2 = \sqrt{\frac{\xi^2-\eta^2}{1-\eta^2}}.$$

In the present problem,

$$\begin{aligned} F_i(p) &= V_i + j\psi_i = -t_0 p \\ &= -t_0\left[\sqrt{(\xi^2-1)(1-\eta^2)} + j\xi\eta\right] \end{aligned} \tag{31}$$

and it is required to determine $F_e(p)$ such that $V_i = V_e$ at $\xi = \xi_0$. Using standard methods, the result is found as

$$F_e(p) = -t_0 \frac{1}{1 - \dfrac{\xi_0}{\sqrt{\xi_0^2-1}}}\left(p - \sqrt{p^2+1}\right). \tag{32}$$

By making a Taylor series expansion at infinity, one can see that F_e vanishes as $1/p$ at ∞. To manipulate (31) and (32), it is more convenient to introduce a transformation

$$p = \sinh z = \sinh x \cos y + j\cosh x \sin y. \tag{33}$$

Hence one obtains

$$\xi = \cosh x \qquad \sqrt{\xi^2-1} = \sinh x$$

and

$$\eta = \sin y \qquad \sqrt{1-\eta^2} = \cos y. \tag{34}$$

Substituting these relations in (31) and (32) one has

$$F_i = -t_0\sinh z = -t_0(\sinh x\cos y + j\cosh x \sin y) \tag{35}$$

and

$$\begin{aligned} F_e &= \frac{t_0}{1 - \dfrac{\xi_0}{\sqrt{\xi_0^2-1}}} e^{-z} \\ &= \frac{t_0}{1 - \dfrac{\xi_0}{\sqrt{\xi_0^2-1}}}\left(e^{-x}\cos y - je^{-x}\sin y\right). \end{aligned}$$

On the elliptic contour, $\xi = \xi_0$, it is seen that

$$V_i = V_e = -t_0\sqrt{\xi_0^2-1}\cos y, \tag{36}$$

$$\psi_i = -t_0\xi_0 \sin y \text{ and } \psi_e = t_0\sqrt{\xi_0^2-1}\sin y. \tag{37}$$

Therefore the charge distribution is found as

$$2\pi Q = \psi_i - \psi_e = -t_0\left(\xi_0 + \sqrt{\xi_0^2-1}\right)\sin y. \tag{38}$$

The ellipse is plotted in Fig. 4, where y represents the angle from the real σ axis. The charge Q is plotted vs angle y in Fig. 17. It is seen that negative charges are needed for $0 \le y < \pi/2$ and $(3\pi/2) < y < 2\pi$, positive charges at $(\pi/2) < y < (3\pi/2)$. The quantized filamentary charges are therefore on the contour $\xi = \xi_0$ at

$$y_i = \pm\sin^{-1}\frac{i-1}{n}, \quad \begin{array}{l} n \text{ odd} \\ i \text{ odd from 1 to } n \end{array} \tag{39}$$

and

$$y_i = \pm\sin^{-1}\frac{i}{n}, \quad \begin{array}{l} n \text{ even} \\ i \text{ odd from 1 to } n-1. \end{array}$$

The case of $n=3$ is shown in Fig. 18. In terms of the rectangular coordinates,

$$\begin{aligned} \sigma_i &= \pm\sqrt{\xi_0^2-1}\cos y_i \\ \omega_i &= \pm\xi_0 \sin y_i. \end{aligned} \tag{40}$$

[8] J. Stratton, "Electromagnetic Theory," McGraw-Hill Book Co., Inc., New York, N. Y.; 1941.

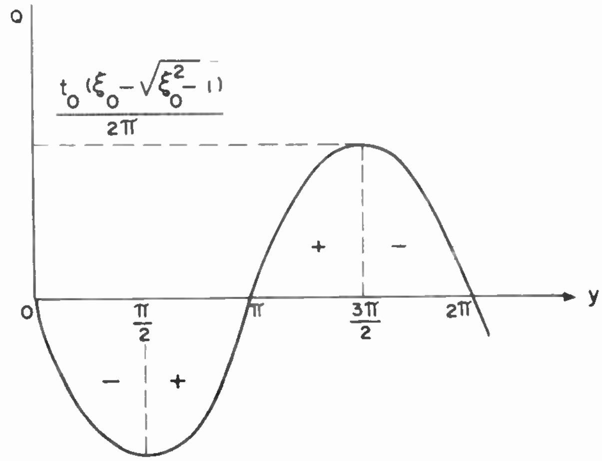

Fig. 17—Charge distribution vs angle y on the elliptic contour $\xi=\xi_0$.

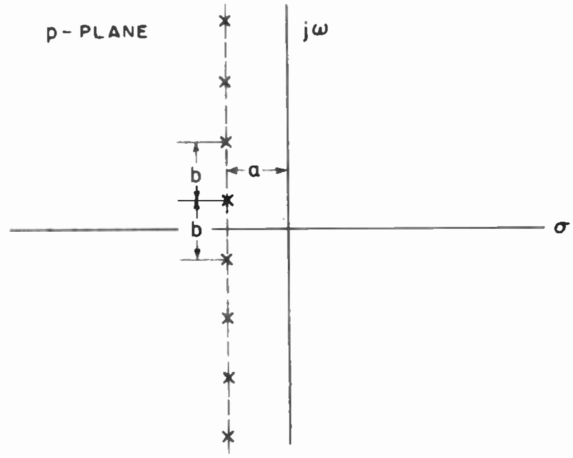

Fig. 19—An infinite array of filamentary charges.

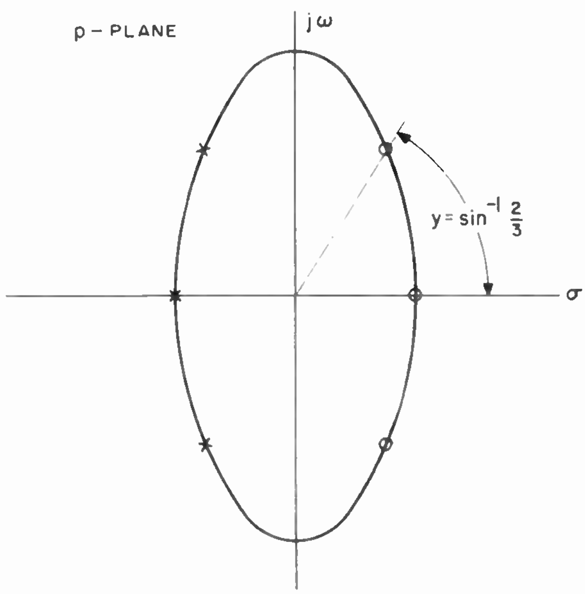

Fig. 18—Locations of poles and zeros for $n=3$.

It is clear that the delay is no longer constant after quantization. The average delay relating to the number of poles n can be obtained easily from (38) as

$$t_0=\frac{n\pi}{\xi_0+\sqrt{\xi_0^2-1}}. \qquad (41)$$

For a low-pass network with all the zeros at infinity, the delay is half as much.

Appendix II

Granularity Error Derivation

With an infinite array of filamentary charges parallel to the $j\omega$ axis as shown in Fig. 19, the complex potential is

$$F=\ln\cos\frac{\pi}{jb}(p+a). \qquad (42)$$

On the $j\omega$ axis,

$$F=\ln\cos\frac{\pi}{b}(\omega-ja)$$

$$=\ln\left[\cos\frac{\pi}{b}\omega\cosh\frac{\pi}{b}a+j\sin\frac{\pi}{b}\omega\sinh\frac{\pi}{b}a\right]. \qquad (43)$$

Hence the phase function is

$$\beta=-\tan^{-1}\left[\tan\frac{\pi}{b}\omega\tanh\frac{\pi}{b}a\right] \qquad (44)$$

and the delay function

$$\frac{d\beta}{d\omega}=-\frac{\frac{\pi}{b}\tanh\frac{\pi}{b}a}{1-\left[\frac{\sin\frac{\pi}{b}\omega}{\cosh\frac{\pi}{b}a}\right]^2}. \qquad (45)$$

At $\omega=0$

$$\frac{d\beta}{d\omega}(0)=-\frac{\pi}{b}\tanh\frac{\pi}{b}a, \qquad (46)$$

while

$$\left(\frac{d\beta}{d\omega}\right)\max=-\frac{\pi}{b}\coth\frac{\pi}{b}a \qquad (47)$$

occurs at $\sin(\pi/b)\omega=\pm 1$. Therefore

$$\frac{\left(\frac{d\beta}{d\omega}\right)_{\max}-\frac{d\beta}{d\omega}(0)}{\left(\frac{d\beta}{d\omega}\right)_{\max}}=\frac{1}{\cosh^2\frac{\pi}{b}a}. \qquad (48)$$

Hence the maximum error on a percentage basis is

$$\Delta = \frac{100}{\cosh^2 \frac{\pi}{b} a} \cdot \tag{49}$$

Appendix III

Inequality Relating Frequency and Time Domains

Let the frequency domain error $\epsilon(j\omega)$ be the difference between the desired transfer function $T_d(j\omega)$ and the realized transfer function $T_r(j\omega)$. In the application of the text $T_d(j\omega) = T_1(j\omega)e^{-j\omega t_2}$ and $T_r(j\omega) = T_1(j\omega)T_2(j\omega)$.

The only assumption necessary for the proof is that as $\omega \rightarrow \infty \left|\epsilon(j\omega)\right| \sim 1/\omega^n$ where $n \geq 2$. This assumption is not as restrictive as it seems since an example can be easily found such that if 1) for all ω's $\left|\epsilon(j\omega)\right| < \eta$ where η is a fixed number and if 2) $\left|\epsilon(j\omega)\right| \sim (1/\omega)$ the time domain error can be made larger than any prescribed number.

The relation between $e(t)$ and $\epsilon(j\omega)$ is

$$e(t) = \frac{1}{2\pi}\int_{-\infty}^{\infty} \epsilon(j\omega)e^{j\omega t}d\omega. \tag{50}$$

Let

$$\tan\theta = \frac{\omega}{\omega_0} \cdot \tag{51}$$

Hence

$$d\theta = \frac{\dfrac{d\omega}{\omega_0}}{1 + \left(\dfrac{\omega}{\omega_0}\right)^2} \tag{52}$$

$$e(t) = \frac{1}{2\pi}\int_{-\pi/2}^{\pi/2}\left(\epsilon(j\omega)\omega_0 \cdot \left[1 + \left(\frac{\omega}{\omega_0}\right)^2\right]e^{j\omega t}\right)_{\omega=\omega_0 \tan\theta} d\theta. \tag{53}$$

Now the absolute value of the integral is smaller or equal to the maximum value of the integrand times the length of the interval of integration. If, in addition, we use $\left|e^{j\omega t}\right| \leq 1$, we get

$$\left| e(t) \right| \leq \frac{1}{2\pi} \max_{0 \leq \omega \leq \infty} \left(\omega_0\left[\omega_0\left(\frac{\omega}{\omega_0}\right)^2\right]\left|\epsilon(j\omega)\right|\right) \times \pi \tag{54}$$

hence, for any t,

$$\left| e(t) \right| \leq \frac{1}{2} \max_{0 \leq \omega \leq \infty} \left(\omega_0\left[\omega_0\left(\frac{\omega}{\omega_0}\right)^2\right]\left|\epsilon(j\omega)\right|\right) \cdot \tag{55}$$

Acknowledgment

The author wishes to acknowledge the suggestions and criticisms of Dr. C. A. Desoer of the Bell Telephone Laboratories.

The Principles of JANET—A Meteor-Burst Communication System*

P. A. FORSYTH†, E. L. VOGAN†, ASSOCIATE MEMBER, IRE, D. R. HANSEN†, ASSOCIATE MEMBER, IRE, AND C. O. HINES†

Summary—**The JANET system of long-range communication employs vhf radio signals which are forward-scattered by the ionized trails of individual meteors. The propagation characteristics and design considerations of such a system are surveyed in this paper, and preliminary operating experience is summarized.**

I. Introduction

MORE than a quarter of a century ago, Eckersley[1] pointed out that scattering from inhomogeneities in the ionospheric ionization could be an important factor in the propagation of radio waves and could indeed provide a means of communicating with stations which otherwise would be inaccessible. Since that time, there have been many investigations aimed at the understanding and utilization of the various irregularities which occur in the ionosphere. The underlying hope in most of these studies has been that some means would be found whereby at least the lower part of the vhf band could be used for long distance communication. One of the most outstanding contributions in this field was the extensive work of Bailey, *et al.*,[2,3] which led to the development of practical communica-

* Original manuscript received by the IRE, March 22, 1957. This work was performed under project PCC No. D48-28-35-05.

† Radio Physics Lab., Defence Research Board, Ottawa, Can.

[1] T. L. Eckersley, "Studies in radio transmission," *J. IEE*, vol. 71, pp. 405–454; September, 1932.

[2] D. K. Bailey, R. Bateman, L. V. Berkner, H. G. Booker, G. F. Montgomery, E. M. Purcell, W. W. Salisbury, and J. B. Weisner, "A new kind of radio propagation at very high frequencies observable over long distances," *Phys. Rev.*, vol. 86, pp. 141–145; April 15, 1952.

[3] D. K. Bailey, R. Bateman, and R. C. Kirby, "Radio transmission at vhf by scattering and other processes in the lower ionosphere," PROC. IRE, vol. 43, pp. 1181–1231; October, 1955.

tion systems operating in this band.[4] This method of communication, which has come to be known as "ionospheric scatter," makes use of the small background signal which is present continuously at distances of several hundred kilometers from a powerful vhf transmitter.

In the past ten years, tremendous strides have been made in the detailed study of meteoric and auroral ionization by radio means. From time to time, suggestions have been made to the effect that the scattering from such ionization could be used for communication purposes. Since these suggestions were considered only casually for several years, it now seems impossible to establish their origin conclusively and no attempt will be made to do so here. Apparently, the possibility of using individual meteor signals for communication purposes was discussed by McKinley and others in Ottawa as early as 1950, and similar discussions took place at the Tenth General Assembly of URSI held in Sydney, Australia, during August, 1952. Certainly the suggestion was circulating widely during the autumn of 1952 when the work described in this paper started at the Radio Physics Laboratory of the Defence Research Board of Canada. Previously, various groups at the Radio Physics Laboratory had been interested in scattering from ionospheric irregularities but the experimental work had been confined mainly to back-scatter measurements. In 1952, largely because of the stimulus provided by the Cedar Rapids-Sterling experiment of the National Bureau of Standards, the emphasis was shifted to forward-scatter measurements. These measurements led to a detailed investigation of the forward scattering of radio signals from meteor trails and a study of the utility of these signals for communication purposes. By 1954, communication by means of the vhf signals reflected from individual meteor trails had been achieved and development of equipment designed specifically for this purpose was under way.

The initial studies of forward scattering from meteor trails at the Radio Physics Laboratory leaned heavily upon similar investigations which were already in progress at Stanford University.[5–7] From the outset it was evident that if the meteor trails were to be used efficiently for communication it would be necessary to operate in bursts, taking advantage of the relatively large signals when they were present and shutting down the system when no suitable trail was in existence. It was expected that this mode of operation would permit effective communication with transmitters of substantially lower power than would be required for continuous communication of the kind which has since been discussed by Eshleman and Manning,[8] and by McKinley.[9] The burst type of operation required that some means be devised to provide for detection of meteor trails and for the subsequent selection of those trails which were suitable for the transmission of information. In order to accomplish the detection and selection functions simultaneously, it was visualized that the system would incorporate both a transmitter and a receiver at each station, with the transmitters radiating carrier continuously. The reception of radio energy from the remote transmitter would indicate the presence of a suitable trail and information would then be transmitted at high speed to the remote station during the lifetime of the trail. The actual control of the system would be performed by "gating" units which would permit the transmission of information only when the received signal level was greater than some predetermined value. With the addition of the necessary information storage facilities at each end, this mode of operation would provide, inherently, a two-way communication system. The system which incorporates this technique was given the code-name JANET, after Janus, the Roman god of the doorway who looked both ways at once.

In order to establish the feasibility of the proposed system, three phases of experimentation were contemplated:

1) It was necessary to assess, at least approximately, the utility of the meteor signals themselves for communication purposes. To this end, relatively crude measurements of strength and duration were made on the signals received from transmitters at distances of 900 and 1200 km. These measurements, made late in 1952, indicated that a sufficient number of meteor signals were observed with a transmitter of modest power to support teletype communication at moderate rates.
2) It was necessary, also, to establish that reciprocal propagation conditions existed on two frequencies which were sufficiently separated to permit the adjacent operation of transmitters and receivers. In June, 1953 modulated signals were transmitted simultaneously in both directions over a path extending from Ottawa to Port Arthur, a distance of 1050 km (see the map of Fig. 1). The frequencies used were near 50 mc and were separated by about one mc. This occasion marked the first successful automatic operation of a two-way circuit, in which the modulation of the transmissions was initiated by the occurrence of a suitable meteor trail.
3) Finally, it was necessary to demonstrate that the meteor signals were capable of carrying coded information. For this purpose, a rudimentary tele-

[4] J. R. McNitt, "Practical considerations, for forward scatter applications," IRE TRANS., vol. CS-4, pp. 28–32; March, 1956.

[5] V. R. Eshleman, "Mechanism of Radio Reflection from Meteoric Ionization," Stanford University Electronics Res. Lab., Rep. 49; July, 1952.

[6] O. G. Villard, Jr., A. M. Peterson, L. A. Manning, and V. R. Eshleman, "Extended-Range Radio Transmission by Oblique Reflection from Meteoric Ionization," Stanford University Electronics Lab. Rep. 55; October, 1952.

[7] O. G. Villard, Jr., A. M. Peterson, L. A. Manning, and V. R. Eshleman, "Extended-range radio transmission by oblique reflection from meteoric ionization," *J. Geophys. Res.*, vol. 58, pp. 83–93; March, 1953.

[8] V. R. Eshleman and L. A. Manning, "Radio communication by scattering from meteoric ionization," PROC. IRE, vol. 42, pp. 530–536; March, 1954.

[9] D. W. R. McKinley, "Dependence of integrated duration of meteor echoes on wavelength and sensitivity," *Can. J. Phys.*, vol. 32, pp. 450–467; July, 1954.

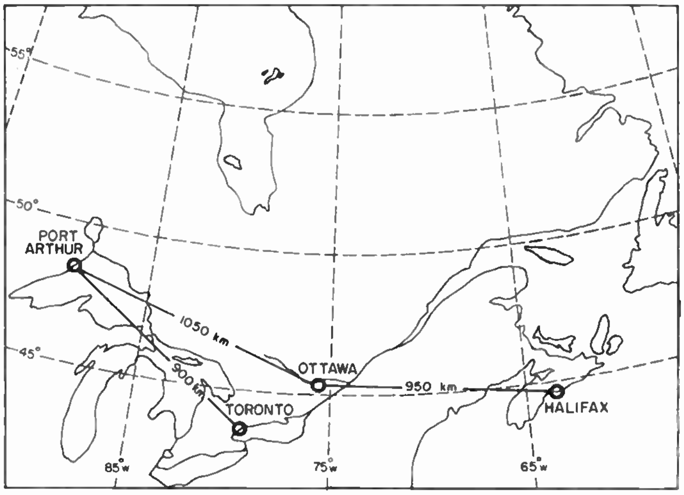

Fig. 1—Map of the various paths used in the development of the JANET system.

> type system was set up in which the occurrence of a suitable meteor trail caused teletype signals originating at Ottawa to be transmitted at high speed to Halifax and then retransmitted back to Ottawa where they were decoded and printed for comparison with the original. The system operated successfully in March, 1954.

At this point it was considered that the feasibility of the method was established, and a contract was placed with Ferranti Electric Ltd., of Canada for the development of equipment suitable for use in a communication system of the JANET type. The equipment which was developed under this contract has been in operation between Port Arthur and Toronto for about 18 months and is described in a companion paper.[10]

The JANET system exhibits many characteristics which differ significantly from those of more conventional communication systems. For example: its performance can be predicted only in a statistical sense; its capacity is a strong function of the geometric relationship between the incoming meteors and the particular communication path in use; the usual relationship which exists between communication capacity, transmitter power, and communication bandwidth is modified; there is no advantage in using antennas of very high gain, particularly if they are directed along the great circle path joining the two stations. These characteristics will be discussed in detail in the following sections.

There is still much to be done before the basic phenomenon and the potentialities of the communication technique are fully understood. In the meantime, the outline given in this paper will serve to acquaint the reader with the present state of the JANET development. Sections II to V provide background information concerning the propagation mechanism, while the system itself is discussed in Sections VI to IX.

[10] G. W. L. Davis, S. J. Gladys, G. R. Lang, L. M. Luke, and M. K. Taylor, "The Canadian JANET system," this issue, p. 1666.

II. Physical Characteristics of Meteors

The earth's atmosphere is bombarded continuously by large numbers of dust-like particles with very small mass.[11] Spectroscopic studies of the resulting meteors show that the particles are composed of substances commonly found on the earth, such as iron and calcium. The total number of particles of all sizes incident on the atmosphere in a single day has been estimated at about 10^{10}, representing a total mass of the order of a ton. Larger particles occasionally strike the earth, sometimes appearing as fireballs, but these are rare occurrences and need not be considered further. The number of particles entering the atmosphere decreases with increasing particle size, the relationship being roughly of the form

$$N \propto 1/M, \tag{1}$$

where N is the number of particles of mass greater than M.

When a meteoric particle enters the region of the ionosphere in the height range 80–120 km, it becomes heated as a result of many collisions with air molecules. Atoms evaporate from its surface with thermal velocities and undergo further collisions with the air molecules. Such collisions result in the release of heat to the surroundings and may cause the excitation or ionization of the atom.[12,13] Excited atoms may emit visible light of sufficient intensity to make the meteor perceptible to an observer on the ground. The ionization produces a trail of free electrons in the wake of the meteor, and it is this trail which is detected by radio methods. Although a single observer may see only two or three visible meteors per hour, hundreds of trails can be detected in the same period by sensitive radio equipment.

Meteoric particles enter the atmosphere from all directions with speeds which vary over a considerable range of values. Results of visual observations suggest that there is some concentration in the plane of the ecliptic, at least for the larger visible meteors.[14] The earth's rotation, together with its tilt and motion about the sun, cause the meteor rate to vary from hour to hour and from season to season. Fig. 2 (p. 1646) is a view of the earth as seen from the apex of its way. At 6 A.M., an observer on the earth's surface is being carried headlong into the meteoric particles, while at 6 P.M. the particles must overtake the earth in order to be seen by him. As a result, the observed meteor rate is enhanced near 6 A.M. and reduced near 6 P.M. The seasonal variation in meteor rate can be explained with the help of the same figure. The northern hemisphere is tilted away from the apex in spring and toward it in autumn. As a

[11] F. G. Watson, "Between the Planets," Blakiston Co., Philadelphia, Pa.; 1941.

[12] N. Herlofson, "The theory of meteor ionization," *Rep. Prog. Phys.*, vol. 11, pp. 444–453; 1946–1947.

[13] T. R. Kaiser, "Radio echo studies of meteor ionization," *Advances Phys.*, vol. 2, pp. 495–544; October, 1953.

[14] A. C. B. Lovell, "Meteor Astronomy," Clarendon Press, Oxford, Eng.; 1954.

result, the meteor rate observed in autumn is greater than that observed in spring. The same variation occurs in the southern hemisphere, six months out of phase with the northern cycle. The degree of diurnal or seasonal variation depends upon the latitude of the observer: the diurnal variation is greatest at the equator and least at the poles; the seasonal variation is greatest at the poles and least at the equator.

Up to this point the discussion applies particularly to the sporadic or background meteors. Since these are always present, they are of greatest importance from the point of view of communication. However, at certain times of the year, the meteor rate may be increased appreciably by the occurrence of showers which result when the earth sweeps through streams of particles travelling in well-defined orbits about the sun. The particles may be localized in the orbit, in which case the shower appears periodically (Leonids, Giacobinids), or they may be distributed more or less uniformly along the orbit, in which case the shower appears as an annual event (Perseids, Quadrantids). The well-known showers were discovered by visual observations made during the dark hours. Recently, using radar techniques, workers at the University of Manchester have discovered a series of showers which occur during May, June, and July and which produce maximum rates during the daylight hours.[14] All meteors of a given shower travel at the same velocity and appear to diverge from a fixed point located on the celestial sphere. This point is the radiant of the shower, and the shower receives its name from the constellation in which its radiant is situated.

For many years it was uncertain as to whether meteors belonged to our solar system or whether they came from interstellar space. In order to be a member of the solar system, a meteoric particle must travel in an elliptical orbit about the sun and its velocity relative to the earth when it enters the atmosphere must be less than 72 km. Any greater velocity would mean that the meteor was traveling in a hyperbolic orbit. The present feeling, based on recent photographic and radar measurements,[15,16] is that all meteors are members of our solar system.

III. The Characteristics of Signals From Individual Trails

The ionized trails generated by meteors contain large numbers of free electrons. Line densities of 10^{10} to 10^{16} electrons per meter, extending along many kilometers of length, may be cited to fix ideas. The electrons partially scatter any radio waves incident on a trail, and it is this phenomenon which is utilized in the JANET system. Some understanding of the characteristics of the scattered signals is necessary, if the problems encountered in such a system are to be recognized and overcome.

[15] F. L. Whipple, "Exploration of the upper atmosphere by meteoritic techniques," *Advances Geophys.*, vol. 1, pp. 119–156; 1952.
[16] A. C. B. Lovell and J. A. Clegg, "Radio Astronomy," Chapman and Hall, London, Eng.; 1952.

Many aspects of the scattering of radio waves by meteor trails have been studied in the past, originally for the back-scatter (radar) case[14,17,18] and more recently for the forward-scattered signals which are of importance here.[3,5–8,19–35] A complete discussion would involve many complicating factors, but the elementary features of present interest can be treated fairly simply. The summary is conveniently broken into two parts, which represent limiting cases but which are roughly valid for line densities below and above 10^{14} electrons per meter, respectively. Following the summary, at the end of the section, the complications are indicated and their practical consequences are illustrated.

Underdense Trails

Meteor trails with fewer than 10^{14} electrons per meter of length are often referred to as "underdense." Radio waves can pass through such trails with little modification, and the unmodified fields can be used in calculating

[17] D. W. R. McKinley and P. M. Millman, "A phenomenological theory of radar echoes from meteors," Proc. IRE, vol. 37, pp. 364–375; April, 1949.
[18] L. A. Manning, "Meteoric echo studies," IRE Trans., vol. AP-2, pp. 82–90; April, 1954.
[19] E. W. Allen, Jr., "Reflections of very-high-frequency radio waves from meteoric ionization," Proc. IRE, vol. 36, pp. 346–352; March, 1948. See also Proc. IRE, vol. 36, pp. 1255–1257; October, 1948.
[20] O. G. Villard, Jr., A. M. Peterson, L. A. Manning, and V. R. Eshleman, "Extended-range high-frequency radio communication at relatively low power by means of overlapping oblique reflections from meteor ionization-trails," *Science*, vol. 117, pp. 638–639; June, 1953.
[21] O. G. Villard, Jr. and A. M. Peterson, "Meteor scatter: a newly discovered means for extended range communication in the 15- and 20-meter bands," *QST*, vol. 37, pp. 11–15, 126; April, 1953.
[22] O. G. Villard, Jr., V. R. Eshleman, L. A. Manning, and A. M. Peterson, "The role of meteors in extended-range vhf propagation," Proc. IRE, vol. 43, pp. 1473–1481; October, 1955.
[23] G. H. Keitel, "Certain mode solutions of forward scattering by meteor trails," Proc. IRE, vol. 43, pp. 1481–1488; October, 1955.
[24] P. A. Forsyth and E. L. Vogan, "Forward-scattering of radio waves by meteor trails," *Can. J. Phys.*, vol. 33, pp. 176–188; May, 1955.
[25] C. O. Hines, "Diurnal variations in the number of shower meteors detected by the forward-scattering of radio waves: Part 1—theory," *Can. J. Phys.*, vol. 33, pp. 493–503; September, 1955.
[26] P. A. Forsyth, C. O. Hines, and E. L. Vogan, "Diurnal variations in the number of shower meteors detected by the forward-scattering of radio waves: Part 2—experiment," *Can. J. Phys.*, vol. 33, pp. 600–606; October, 1955.
[27] C. O. Hines, P. A. Forsyth, E. L. Vogan, and R. E. Pugh, "The dependence of meteoric forward-scattering on antenna patterns and orientations," *Can. J. Phys.*, vol. 33, pp. 609–610; October, 1955.
[28] P. A. Forsyth and E. L. Vogan, "The duration of forward-scattered signals from meteor trails," *Can. J. Phys.*, vol. 34, pp. 535–545; June, 1956.
[29] R. E. Pugh, "The number density of meteor trails observable by the forward-scattering of radio waves," *Can. J. Phys.*, vol. 34, pp. 997–1004; October, 1956.
[30] C. O. Hines and R. E. Pugh, "The spatial distribution of signal sources in meteoric forward-scattering," *Can. J. Phys.*, vol. 34, pp. 1005–1016; October, 1956.
[31] C. O. Hines, "Diurnal variation in forward-scattered meteor signals," *J. Atmos. Terr. Phys.*, vol. 9, pp. 229–233; October, 1956.
[32] C. O. Hines and M. O'Grady, "Height-gain in the forward-scattering of radio waves by meteor trails," *Can. J. Phys.*, vol. 35, pp. 125–127; January, 1957.
[33] E. L. Vogan and L. L. Campbell, "Meteor signal rates observed in forward-scatter," *Can. J. Phys.*, vol. 35; October, 1957.
[34] D. W. R. McKinley and A. G. McNamara, "Meteoric echoes observed simultaneously by back scatter and forward scatter," *Can. J. Phys.*, vol. 34, pp. 625–637; July, 1956.
[35] J. C. James and M. L. Meeks, "On the Relative Contributions of Various Sky Regions to Meteor-Trail Communication," Tech. Rep., No. 1, Georgia Inst. Tech., Eng. Exp. Sta., Atlanta, Ga.; June, 1956.

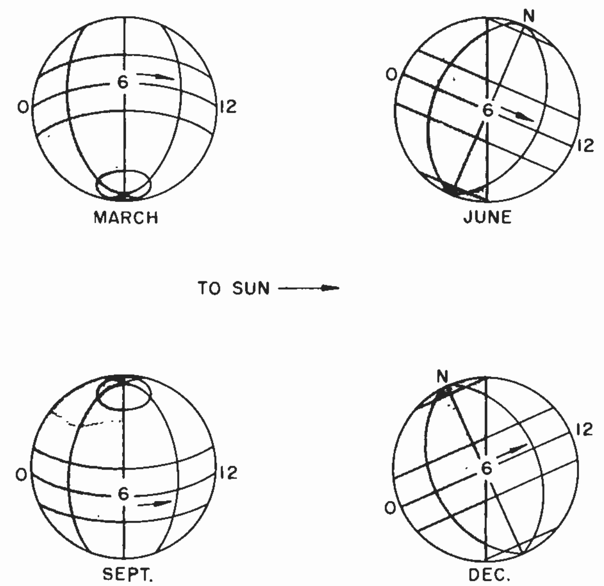

Fig. 2—Aspect of the earth as viewed from the forward side.

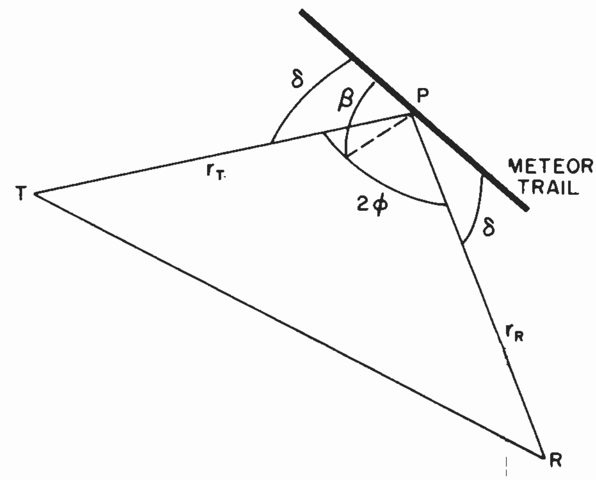

Fig. 3—Geometry of forward scattering from meteor trails.

the amount of scatter to be expected. The problem has been treated thoroughly by Eshleman,[5] who found that a simplified Fresnel description of the process is normally sufficient. On this picture, the scattering is specular for the majority of received signals—that is, the incident and scattered rays make equal angles δ with the axis of the trail (see Fig. 3)—and the received signal comes, in effect, from the principal Fresnel zone alone.

The principal Fresnel zone is centered on a point P on the trail, distant r_T and r_R from the transmitter T and the receiver R, respectively, such that r_T+r_R is a minimum for the trail in question. The zone has length

$$L = 2[\lambda r_T r_R/(r_T + r_R)(1 - \cos^2 \beta \sin^2 \phi)]^{1/2},$$

where λ is the radio wavelength, β is the angle between the trail axis and the plane TPR, and 2ϕ is the angle TPR. The received power rises rapidly in the fraction of a second taken by the meteor to traverse the principal zone, and reaches a peak value of

$$P_R(0) = \frac{P_T}{32\pi^4}\left(\frac{\mu_0 e^2}{4m}\right)^2 \frac{2\lambda^3 G_T G_R q^2 \sin^2 \alpha}{r_T r_R (r_T + r_R)(1 - \cos^2 \beta \sin^2 \phi)} \quad (2)$$

when the zone is fully formed. Here P_T is the transmitted power, μ_0 is $4\pi \times 10^{-7}$ henry/m, e and m are the electron charge and mass, G_T and G_R are the transmitting and receiving antenna gains for the directions TP and RP respectively, q is the electron line density at P, and α is the angle between the incident electric vector and the direction of the scattered ray PR.

Although the meteor trail is formed as a narrow column, a few centimeters in diameter, it immediately begins to expand by diffusion. As the diameter increases, the scattered signal suffers increasingly from a destructive interference of the fields scattered by individual electrons. In ideal circumstances, neglecting Fresnel ripples and initial diameter, the received power decays according to the formula

$$P_R(t) = P_R(0) \exp(-32\pi^2 Dt/\lambda^2 \sec^2 \phi), \quad (3)$$

where D is the ambipolar diffusion coefficient (of the order 1 to 10 m^2/s). The time constant

$$\tau = \lambda^2 \sec^2 \phi/16\pi^2 D, \quad (4)$$

which gives a convenient measure of the duration of signal amplitude, is of the order of a few tenths of a second for the relevant 30–50 mc radio waves.

Overdense Trails

Trails with more than 10^{14} electrons per meter are often termed "overdense." When treating them, it is no longer satisfactory to think of the incident wave as penetrating the trail without serious modification. Instead, coupling between individual electrons plays a prominent part, and the whole of the scattering process is conceived more simply in terms of reflection from a cylindrical surface.

The surface in question surrounds the axis of the trail at a radius ρ, where the electron volume density has the critical value normally associated with reflection of the incident wave (cf. reflection from the ionosphere). The volume density within ρ exceeds the critical value, and cannot support propagation in the usual sense at the pertinent frequency. As the electrons diffuse outwards, ρ increases from an initially small value, passes through a maximum, and falls to zero as the volume density at the axis of the trail decreases below the critical value. In the very latest stages the scattering reverts to the underdense type, but only after a time exceeding τ, and so only when the underdense scattering is extremely small.

The scattering process is again specular, the angles of incidence and reflection being equal. The received power is proportional to the radius ρ, so its time variation can be calculated under the assumption of diffusive expansion from an initial line distribution of electrons. In the back-scatter case, for a trail at distance r from the transmitter-receiver site, the signal is given by

$$\frac{P_T G_T G_R \lambda^2}{32\pi^2 r^3}\left[Dt \ln\left(\frac{\mu_0 e^2 q \lambda^2}{16 m\pi^3 Dt}\right)\right]^{1/2}.$$

There is no published account of forward scattering from overdense trails to provide formulas corresponding to those listed for the underdense case.[36] However, it is not difficult to justify the same type of geometric factors as those found in $P_R(0)$ and τ, and so to derive the received power variation

$$P_R'(t) = \frac{P_T G_T G_R \lambda^2 \cos\phi \sin^2\alpha}{16\pi^2 r_T r_R (r_T + r_R)(1 - \cos^2\beta \sin^2\phi)} \cdot \left[Dt \ln\left(\frac{\mu_0 e^2 q \lambda^2 \sec^2\phi}{16 m\pi^3 Dt}\right)\right]^{1/2} \tag{5}$$

for the forward-scattered signal. The total duration of such a signal is

$$\tau' = \mu_0 e^2 q \lambda^2 \sec^2\phi / 16 m\pi^3 D, \tag{6}$$

and the maximum received power is

$$P_R'(\tau'/\epsilon) = \frac{P_T}{32\pi^4}\left(\frac{\mu_0 e^2}{4m}\right)^{1/2}\left(\frac{\pi}{\epsilon}\right)^{1/2} \cdot \frac{\lambda^3 \sin^2\alpha\, q^{1/2}}{r_T r_R (r_T + r_R)(1 - \cos^2\beta \sin^2\phi)}, \tag{7}$$

where ϵ is the base of the natural logarithms.

The two sets of formulas and the variations which they imply are quite distinct (see Fig. 4), but they provide much the same values for duration and maximum power when $q \sim 10^{14}$ electrons/m. In fact, of course, there is a smooth transition from the one type of signal to the other, but this should be virtually completed as q varies through a single order of magnitude. It will be noticed that the "underdense duration" τ is independent of q, but the "overdense duration" τ' increases with q as the latter increases above 10^{14} electrons/m. Again, the "underdense signal" has a peak power $P_R(0)$ proportional to q^2, but this decreases to a $q^{1/2}$ dependence when the value $P_R'(\tau'/\epsilon)$ for an "overdense signal" comes into effect.

Meteor trails are subject to distortion by winds, and perhaps by small scale turbulence. The distortion is normally negligible for the first half second or so, and it therefore has little effect on the rapidly decaying underdense signals. Overdense signals, on the other hand, can deviate markedly from the idealized variation indicated above. Strong fading, characteristic of interference from more than one reflecting portion of the trail, is often present. Furthermore, trails whose initial orientation precludes specular reflection to the receiver may be re-

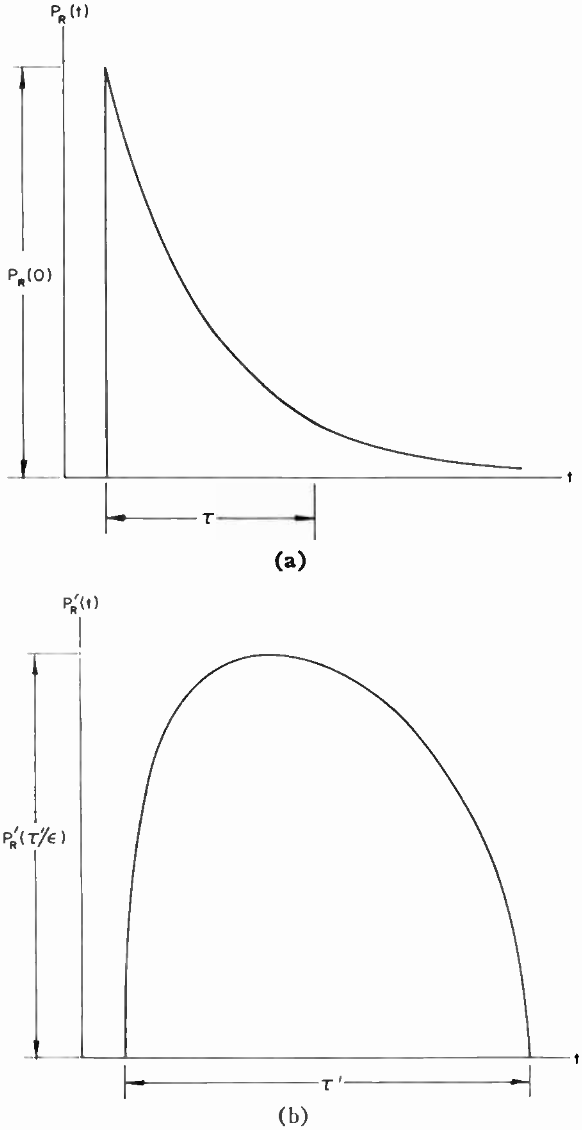

Fig. 4—Idealized time variations in signals from (a) underdense and (b) overdense meteor trails.

oriented by wind shear until the specular condition is achieved. This leads to yet another type of power variation in overdense signals.

The details of these and other complications are of interest primarily to the research radio astronomer.[37] They can be treated only empirically by the communication engineer, as experience with a particular system is accumulated. To provide some indication of the actual signal forms encountered in practice, several examples of high-speed recordings are displayed in Fig. 5. While the individual signals can usually be identified as belonging to the underdense class or to the overdense class, it is evident that there are wide variations from the idealized forms.

The wavelength dependence indicated by the preceding formulas is not supported in detail by the experimental data at present available,[28] although the

[36] This statement is no longer correct. See C. O. Hines and P. A. Forsyth, "The forward-scattering of radio waves from overdense meteor trails," *Can. J. Physics*, vol. 35, pp. 1033–1041; September, 1957.

[37] T. R. Kaiser, "Meteors," Pergamon Press, London, Eng., and New York, N. Y.; 1955.

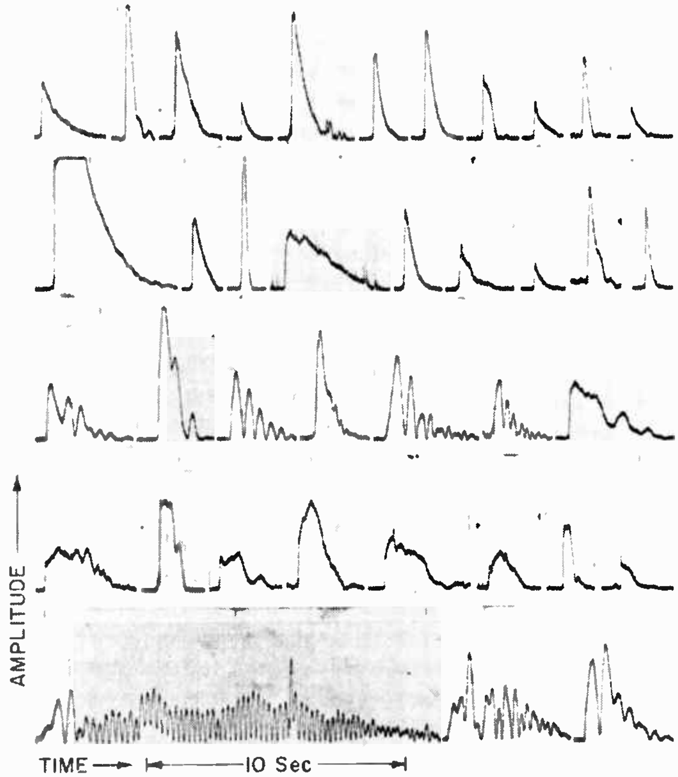

Fig. 5—Typical amplitude-time recordings of forward-scattered signals from meteor trails.

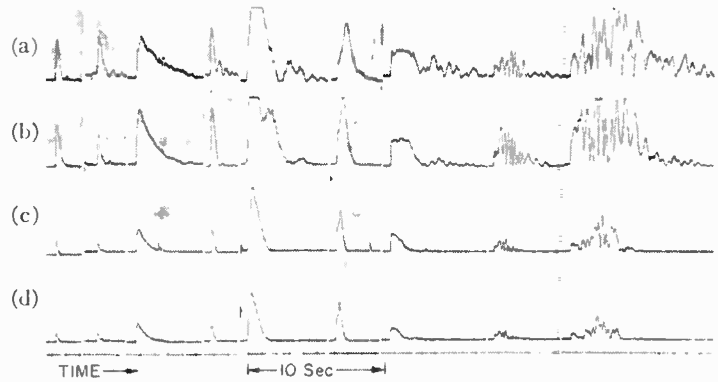

Fig. 6—Amplitude-time recordings obtained simultaneously at four frequencies: (a) 32.22 mc, (b) 39.22 mc, (c) 48.82 mc, (d) 49.98 mc.

general tendencies are confirmed. The important features are the decreases of signal strength and signal duration which accompany an increase in the operating frequency. Qualitatively, this variation may be seen on the records displayed in Fig. 6, which show several meteor signals as observed simultaneously on four frequencies. The variation ultimately introduces an upper limit to the range of useful operating frequencies, while a lower limit is introduced by excessive fading of the meteor signals and by competing modes of propagation. The most useful range seems to be 30–50 mc.

IV. The Statistical Characteristics of Meteor Propagation

It is apparent from the relationships listed in the preceding section that the signals scattered from successive meteor trails may vary greatly in strength as the orientation, position, and ionization vary from one trail to the next. This complicates the problem of assessing statistically the relative usefulness of meteors arriving from different directions, or of trails occurring in different regions of the sky, but such an assessment is of great value in the development of an efficient communication system. Its importance lies not only in the design of efficient antennas and the prediction of variations in communication capacity, but equally in the interpretation and understanding of the basic propagation characteristics. Past work in this field has been mainly theoretical and will be summarized in the first half of this section. The remainder of the section will be devoted to a second statistical problem of importance to the communication engineer, that concerning the distribution of signal amplitudes and durations. In this case, pertinent experimental data have been accumulated.

The assessment problem was first attacked by Eshleman and Manning,[8] who located theoretically the regions of the sky which are of greatest intrinsic importance in meteor scattering. The complementary approach was adopted by Hines,[25] who determined the most important directions of arrival of meteoric particles. The original approach was subsequently modified by James and Meeks,[35] and by Pugh,[29] while the two approaches have been correlated by Hines and Pugh.[30]

Basic to the whole problem is the incidence pattern of meteors—that is, the distribution of radiants over the observer's sky at the time in question. Unfortunately, this is one of the points of greatest controversy in meteor studies at the moment, and one which probably will not be resolved for some time to come. The issue may be ignored temporarily, by assuming a uniform distribution, but it will be reconsidered at a later stage.

Not all of the incident meteors produce useable trails, for the signals scattered from many will be below the operating threshold of the equipment. The useful fraction varies in size with the direction of incidence and with the region of the observer's sky in which the trail is formed. The variation can be analyzed into two distinct factors, each of which will be treated in turn.

The first restriction is imposed by a requirement for specular scattering. It may be assumed, for example, that at least half of the principal Fresnel zone must be formed within the length of the trail, if the trail is to scatter to the receiver a signal of any appreciable strength. Although arbitrary, this assumption could be justified by more realistic considerations. It confines attention to a certain fraction of the trails which are formed, the fraction being dependent on the orientation considered. It does more than that, for it restricts attention to a certain band of the sky where trails of the specified orientation do meet the specular condition: the position and orientation of useful trails are not wholly independent.

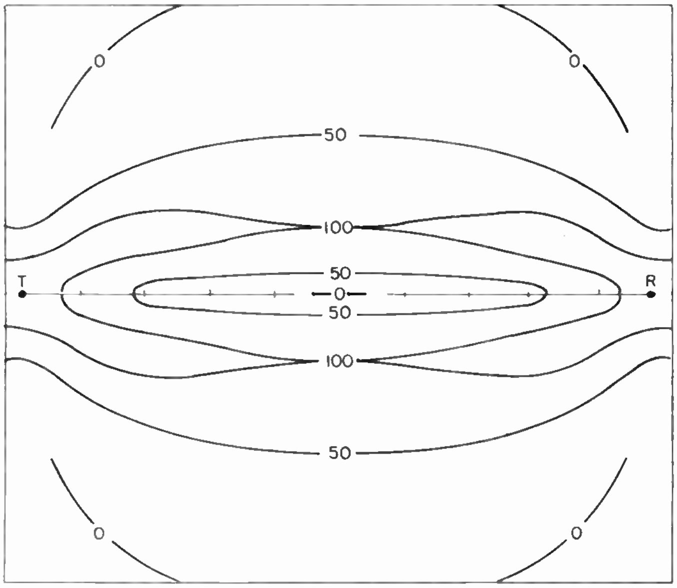

Fig. 7—Spatial distribution of useful meteor trails for a path length, TR, of 1000 km. Contours display relative densities.

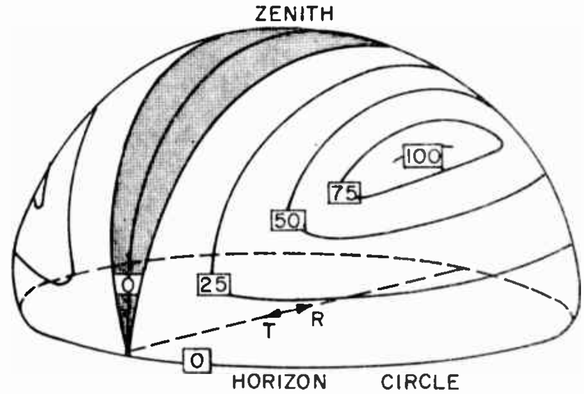

Fig. 8—Distribution of useful meteor radiants, displayed by contours on the celestial hemisphere.

Attention has now been confined to what may be termed, for communication purposes, potentially useful trails. By applying the formulas of the preceding section, it is possible to determine whether or not any one of these potentially useful trails does, in fact, provide a useful signal exceeding the operating threshold. For a trail of particular position and orientation, the question hinges on whether or not its line density of ionization is sufficient to yield, as peak received power, a value exceeding the operating threshold. Since the received power depends on the position and orientation, as well as on the ionization, the required degree of ionization must also depend on these parameters. Finally, the ionization is believed to vary as the mass of the parent meteoric particle and as the sine of the elevation angle of the radiant position. It is then possible, for trails of given position and orientation, to determine a limiting mass which the parent meteor must exceed if it is to provide a useful trail. The relative number of such meteors can then be determined from the distribution given in (1).

The results of such a calculation are of greatest value when the number of useful trails is given as a function of position or of orientation alone, rather than as a function of both. The two are linked by the specular condition, as already noted, so that one of the parameters describing position or orientation must be treated as a dependent variable. Its partner can then be removed by integration, to yield the required number of trails as a function of two position variables or of two orientation variables alone. (The third position variable is essentially fixed by the narrow height range of trail formation, and the third orientation variable is unnecessary by virtue of the axial symmetry of the trail.)

Almost all work in the past has been based on the underdense formula, a process which is justified if the operating threshold level is sufficiently low. Detailed results may be found in the papers previously cited, but the general effects are illustrated in two accompanying diagrams. The first of these, Fig. 7, shows the spatial distribution of useful meteors, plotted by contours on the horizontal plane which contains the transmitter and receiver; the actual distribution is, of course, at heights of 90 or 100 km. The second, Fig. 8, sketches the corresponding orientational distribution of useful trails, relative to the orientation of the transmitter-receiver axis. The hemisphere can be pictured as the celestial hemisphere of the sky, in which case the contours indicate the distribution of useful radiants, with the meteors impinging from points on the hemisphere onto the earth at the center.

Communication capacity in the JANET system depends more on the total time spent by the received signal above the threshold level than on the actual number of times the threshold is exceeded. With the assumption of underdense trails alone, and with the mass (or ionization) distribution (1), it is not difficult to show that this total time varies with position and orientation exactly as does the number, except for an additional $\sec^2 \phi$ factor introduced by the exponential decay constant (4). This extension has been incorporated in Fig. 9, which sketches the spatial distribution of potential usefulness of different regions of the sky, from the point of view of communication capacity. It is clear from this diagram that the most useful regions of the sky lie to the sides of the direct transmitter-receiver path, and this fact must receive consideration in the designing of efficient antennas.

The foregoing account summarizes the standard elementary treatment to be found in the papers mentioned above. Two elaborations should be noted.

The first concerns time variations and anisotropies in the meteoric incidence pattern, which have been ignored up to this point. It has been mentioned already that sporadic meteors tend to come from the apex of the earth's way, and further concentrations in their distribution may also exist. Such concentrations make the

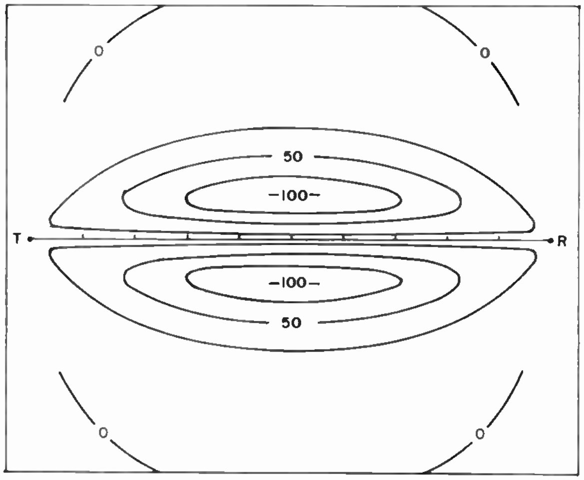

Fig. 9—Effective regions for a meteor communication system, displayed by contours which incorporate both numbers and durations of signals.

incidence pattern nonuniform over the celestial sphere and, when observed from the rotating earth, this pattern appears to sweep across the sky in the course of a day. Not only does this produce a diurnal variation in the communication capacity of a given system, but it also distorts the contours presented in the foregoing charts. Symmetry is lost, and each side of the path in turn provides the greater number of useful trails for a part of the day.[22,31,35] Further temporal changes occur as the earth passes into and through meteor shower streams, and such occasions provide the most direct experimental confirmation of the basic theory.[26,38]

The second elaboration concerns overdense trails. It is apparent that somewhat different variations occur when the limiting ionization lies in the overdense range, for the peak amplitude then varies as (meteor mass)^a with $a=\frac{1}{4}$ rather than $a=1$. The problem is complicated further when signal durations are considered, but the same principles do apply throughout and refined contour charts could, in principle, be deduced. It appears that detailed theoretical work involving distributions of overdense trails has, however, been limited to the second statistical problem under review, that of the distribution of signal amplitudes.

The basic point concerning this distribution has already been implied: the number, N_0, of peak amplitudes which exceed a counting level, A_0, would vary as A_0^{-1} if the underdense formula were valid for all signals, but as A_0^{-4} if the overdense formula were valid. This conclusion stems from the assumed proportionality of ionization and mass, and from the assumed distribution law (1). It follows directly when these relations are combined with the formulas (2) and (7) in turn, for a specified position and orientation of the trail, and it follows for all trails after position and orientation are removed by integration.

[38] C. O. Hines and E. L. Vogan, "Variations in the intrinsic strength of the 1956 Quadrantid meteor shower," *Can. J. Phys.*, vol. 35, pp. 703–711; June, 1957.

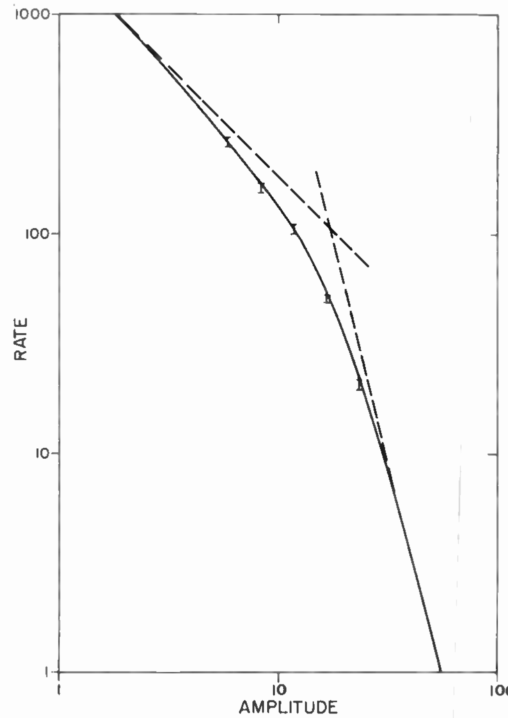

Fig. 10—Occurrence rate of signals exceeding a threshold amplitude, as a function of that amplitude. The solid line indicates the theoretical variation (with arbitrary scales), and has the broken lines as asymptotes; experimental data have been superimposed in the position of best fit.

In the actual circumstances, where both overdense and underdense signals must be taken into account, the dependence of N_0 on A_0 may be expressed simply when attention is confined to trails with a specified position and orientation: $N_0 \propto A_0^{-1}$ for $A_0 < A_T$ and $N_0 \propto A_0^{-4}$ for $A_0 > A_T$, where A_T is the amplitude appropriate to the transition between underdense and overdense ionizations. This transition is assumed to occur abruptly and (for continuity) at that value of ionization which leads to equal signal strengths when inserted in (2) and (7) in turn.

These simple pictures are ultimately complicated, however, when the net distribution relating to underdense and overdense trails of all positions and orientations is considered. The complication arises because A_T is itself dependent on position and orientation. The integration can be accomplished, however, by taking this dependence into account. The final result, for an isotropic incidence of meteors, is shown by the full curve in Fig. 10. This curve tends to the limiting forms (straight lines, on the log N_0 vs log A_0 plot, with slopes of -1 and -4, respectively) appropriate to underdense and overdense trails separately; the perceptible transition extends over a decade in amplitude. The exact shape and location of the transition region would be expected to vary throughout the day, as the actual (nonisotropic) incidence pattern sweeps across the sky, but the degree of distortion cannot be predicted. Extensive data have been accumulated, however, and have confirmed the shape shown here. Typical results have been superimposed on the diagram in the form of vertical bars, whose lengths indicate the random probable error of the data. The horizontal and vertical scales are arbitrary, and the experimental results were introduced in the position of best fit.

The distribution of signal durations is more difficult to obtain, both theoretically and experimentally, but it is of more direct importance to the communication capacity of a JANET system. The theory could be developed most readily for signal durations measured to $1/\epsilon$ of the maximum amplitude, by a routine extension of the methods indicated earlier in this section. The more relevant analysis, that required to obtain durations above a threshold level, would be much more involved but still possible in principle; the results would depend on the chosen threshold. In neither case would it be possible to take full account of variations in the diffusion coefficient, associated with the formation of trails at various heights, and neither analysis has yet been undertaken.

Experimentally, if the durations of signals from individual trails is desired, careful analysis is necessary because of the fading which is often present. Such analysis is required, however, when the basic characteristics of meteor propagation are under study, and reference may be made to details of such a study reported elsewhere.[28] For present purposes, it is sufficient to record the integrated distribution of durations, as measured by the number of signals whose duration exceeds a chosen value. The experimental distribution is shown in Fig. 11, for (a) durations to $1/\epsilon$ of the peak amplitude, and (b) durations above a counting level.

Experimental results can be obtained more readily if no attempt is made to interpret fading signals in terms of the individual trails which produce them. Instead, the durations of individual signal excursions above a threshold is obtained, and the measurement can be made automatically. The integrated distribution obtained in this way is shown in Fig. 11, curve (c), and it represents the most basic type of distribution required for communication design. Although curves (b) and (c) were obtained from different sets of data, a comparison of the two does give some indication of the effect of fading on the distribution of signal durations.

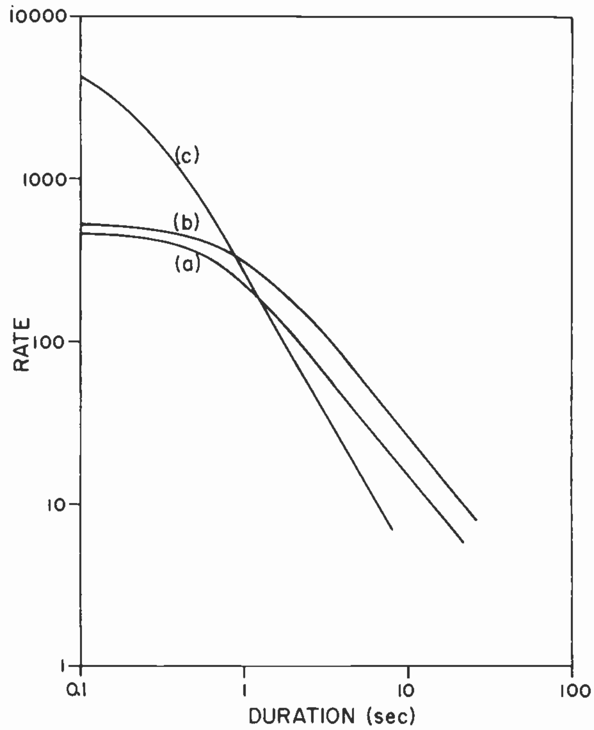

Fig. 11—Occurrence rate of signals exceeding a chosen duration, as a function of that duration: (a) total durations of signals measured to $1/\epsilon$ of the initial amplitude, (b) total durations of signals measured above a fixed level, (c) durations of individual excursions above a fixed level (see text). The vertical scale is arbitrary.

V. The Temporal Variation of Meteor Signals

The rate at which meteor signals are observed by means of forward scatter varies over wide limits from hour to hour and from one day to the next. In an effort to determine experimentally the extent of these variations, a forward-scatter recording program has been conducted over several paths in Canada. Path lengths varied between 800 and 1000 km, and frequencies were in the range 30–50 mc. Some results of this program have been reported elsewhere.[33] For present purposes, it will be sufficient to indicate the normal variations encountered on one of the paths, that from Greenwood, Nova Scotia to Ottawa, Ontario, a distance of 860 km.

The unmodulated transmission, at a frequency of 49.98 mc, was maintained continuously with a radiated power of about 100 watts. Records were obtained throughout the period June, 1955 to August, 1956. The receiving system consisted of a preamplifier, a commercial receiver, a peak-reading amplifier and a moving-chart recording milliammeter. The peak-reading amplifier maintained the peak signal amplitude for a sufficiently long time (about 3 sec) to compensate for the slow response of the recording meter. Five-element yagi antennas, arranged to illuminate the midregion of the path at a height of 100 km, were used for transmission and reception.

Meteor rates were obtained by counting those signals which provided an antenna voltage of 0.5 μv, representing an average snr of about 20 db in the bandwidth of 1.3 kc which was used. The records were scaled on an hourly basis and the resultant data were summarized for various periods.

The data obtained for July, 1956, are representative, though by no means typical, of all months. They are displayed by means of the scatter plot in Fig. 12, which illustrates the large spread normally encountered in hourly rates. The spread appears to be greatest in July and August when the rates are highest, and least in the spring months. The solid curve shows the mean diurnal variation for the month, obtained from the arithmetic means of the hourly data.

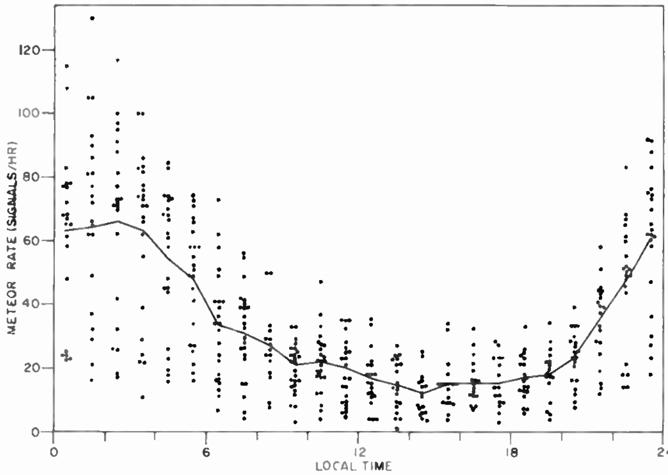

Fig. 12—Distribution of hourly signal counts obtained during July, 1956, on the Greenwood-Ottawa circuit, with curve of hourly averages superimposed.

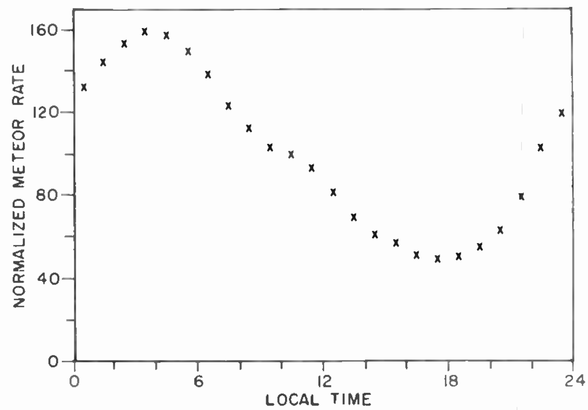

Fig. 13—Normalized mean diurnal variation of signal counts on the Greenwood-Ottawa circuit, obtained over a 12-month period, 1955–1956.

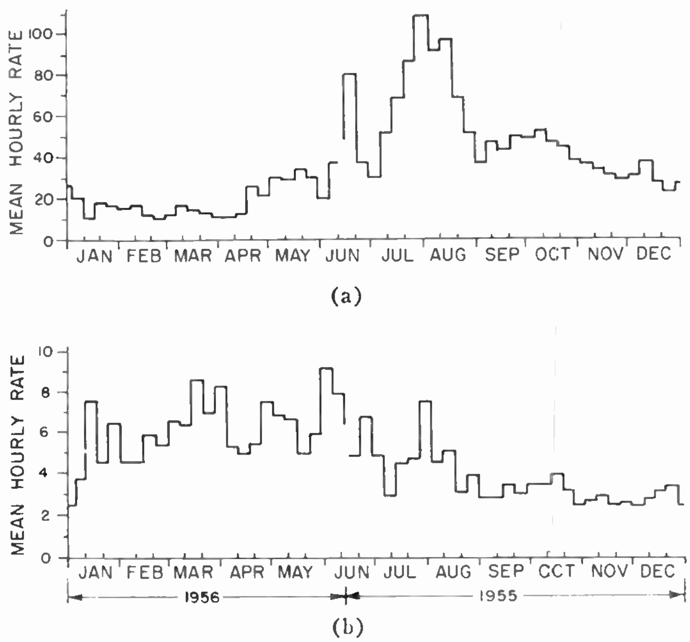

Fig. 14—Weekly averages of meteor data obtained on the Greenwood-Ottawa circuit over a 12-month period: (a) meteor rates, (b) max/min ratios.

All the data available from records obtained over a period of 12 months were averaged for each hour. The hourly averages are shown in Fig. 13, after normalization to a mean value of 100. The curve has a maximum at approximately 4 A.M. and a minimum at 6 P.M., with a slight enhancement just before noon. This enhancement is evident in the data for about half of the 12 months. The ratio of the maximum-to-minimum rate for the curve is 3.5.

Fig. 14(a) is the histogram of the average rate for each week of the 12-month period. The observed meteor rate is lowest in the spring, rises to a maximum during July and August, and falls off toward the end of the year. Excluding the summer months, the signal rate in the second half of the year is about twice that in the first half. The meteor rate in June, July, and August, is influenced by considerable shower activity, but the effects of individual showers are difficult to distinguish since the periods of increased activity overlap. On the other hand, the effects of the Quadrantid (January 3) and Geminid (December 12) showers are apparent in the figure.

The degree of diurnal variation in meteor signal rate is of some importance to the communication engineer. It can be expressed in terms of the ratio of the maximum to minimum rate over a 24-hour period. This ratio varies widely from one day to the next and may be as great as 20:1. In order to smooth the data somewhat, average diurnal variations were derived for weekly periods and the maximum-to-minimum ratio for each period was determined. The results are shown in Fig. 14(b). Even after this smoothing, the ratio varies over the range 2.5 to 9. Variation in the total signaling time, as distinct from the number of signals, is also of interest to the communication engineer, but it could not be determined with the peak-reading method of recording employed on this circuit. It may be noted, however, that individual signals tend to persist longer during the afternoon hours, and that this would compensate partially for the decreased number of signals then obtained. The practical consequences of this effect, as illustrated by results from a test run of the JANET system, will be indicated in a later section.

The results for a particular circuit and for a particular period have been presented here in order to illustrate typical behavior. It does not follow that they are applicable directly to any other circuit, since the number of meteor signals observed on a given circuit depends upon the latitude, path length, and orientation of the circuit, and on the antenna patterns employed. Also, meteor rates may differ from one year to the next, particularly during periods of shower activity. Nevertheless, this summary will serve to indicate the sort of variations which can be expected.

VI. Principles of a JANET System

The elements of a basic JANET communication system are shown in Fig. 15. Equipment at both terminals is identical (except for the operating frequencies of the transmitters and receivers, which are interchanged across the path) and consists of: transmitter, receiver, control unit, gated transmitting store, receiving store, and antenna system.

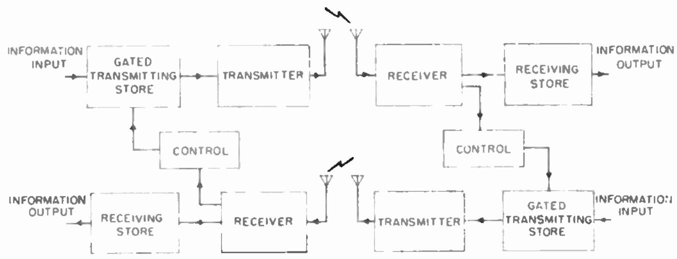

Fig. 15—A basic JANET communication system.

The transmitters radiate continuously on separate frequencies in the range 30 to 50 mc, a typical separation being 1 mc. Each receiver is tuned to the frequency of the distant transmitter. When a suitable meteor trail is formed, each receiver detects the carrier from the distant transmitter. The carrier level is monitored at the receiver by the control unit and, when it has risen to a value that assures an adequate snr, the transmitting gate is opened. This permits the transmitting store to discharge information and modulate the transmitter at a high rate. The transmission of information continues until the snr falls below the gating level, at which time the modulation is terminated. At the distant receiver, the signal is demodulated and inserted in the receiving store, whence it is discharged at conventional rates into the receiver terminal equipment.

During the operation of an ideal JANET system, information would flow into the transmitting store at one terminal and out of the receiving store at the other at a constant rate determined by the terminal equipment. The high instantaneous rate at which information would flow across the path intermittently would be related to this average rate by:

$$\text{average rate} = \text{instantaneous rate} \times \text{duty cycle}$$

where the duty cycle is defined as that fraction of the total time during which the received signal exceeds the gating level.

A basic object in JANET system design is the use of one meteor trail at a time, in order to minimize the fading of signals and the occurrence of multipath distortion. This, in turn, would appear to limit the practical duty cycle to values of 0.1 or less.

It should be noted that both duty cycle and instantaneous rate are dependent upon other parameters of the system and cannot always be varied independently. If the receiver bandwidth is broadened, to allow for an increased instantaneous rate, and if the gating snr is maintained constant, then only the stronger meteor signals can be used and the duty cycle decreases. It is fortunate that the usual amplitude distribution of meteor signals is such that a reduction of duty cycle achieved in this way leads to no loss, but rather to a net increase, in the average rate of information transfer.[39]

In the basic system described above, exact reciprocity in the reflecting mechanism is assumed, together with identical noise levels and equipments at both terminals. Only under these conditions could the snr existing at one terminal be used to control transmission to the other. Since such conditions are not found in practice, it is necessary that gating be controlled by the snr existing at the receiver to which the transmission is directed. The necessary control signals from this receiver can be returned in the reciprocal radio channel. The return channel may be used for this purpose alone, or may also be used for the passage of information. In the latter case, in which both channels are information channels, the receivers at both ends have the same pass band and require identical snr to operate. As a result, the information rate is controlled by the receiver with the higher noise level. In the former case, in which information is transmitted in one direction and control signals in the other, only a narrow bandwidth is required for control purposes. This permits one of the transmitters to be of lower power, or, if the transmitters are of equal power, it permits control of the operation to be governed by the noise level at the receiver to which information is directed.

VII. General Design Considerations

Gating

Probably the most important consideration in the design of a JANET system is that of gating—the operation of turning the system on and off as suitable meteor trails occur. The real problem is not one of instrumentation since satisfactory data handling and storage techniques are available. Instead, the problem is one of choosing the criteria to be used in determining when transmission is to be started and when stopped.

The principal requirements of the gating system are: 1) It should initiate (gate on) the transmission of information with the shortest possible delay after the occurrence of a suitable meteor trail. 2) It should terminate (gate off) the transmission before the signal level from that trail drops below a usable value.

The gate-on operation requires the measurement of the snr, and the identification of the carrier as that of the wanted transmitter. Although the signal and noise levels could be measured independently by conventional

[39] L. L. Campbell and C. O. Hines, "Bandwidth considerations in a JANET system," this issue, p. 1658.

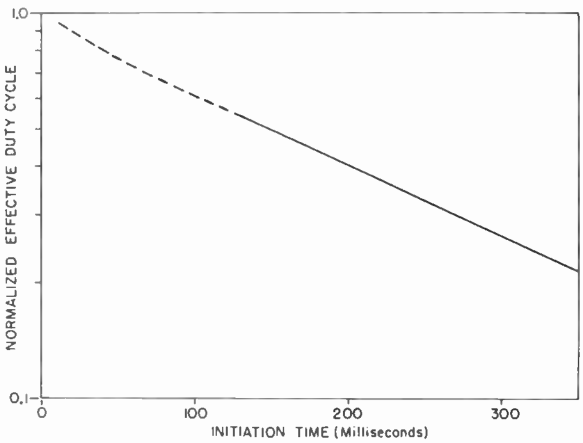

Fig. 16—Dependence of the effective duty cycle on the initiation time.

means, techniques have been developed for the direct measurement of their ratio. Carrier identification is necessary in order to prevent the premature discharge of information, initiated by the simultaneous occurrence of interfering signals at both receivers. Identification may be accomplished either by means of a distinctive modulation continuously applied to the carrier or by means of a brief identifying code transmitted at the start of each burst. Acknowledgement of receipt of this identifying signal is necessary in either case before information is transmitted. The first type of identification appears to be the more desirable of the two since it reduces the initial delay in starting transmission. This consideration is important because of the occurrence of a large number of signals of short duration, as illustrated in Fig. 16 which indicates the dependence of the effective duty cycle upon the initiation time. The solid portion of the curve was derived from operating experience with a JANET system, while the broken portion was derived by extrapolation and is supported by measurements of signal duration.

At the end of the burst, the system must be gated off before the snr drops below an acceptable value. Transmission cannot be stopped instantaneously since the "stop order" must be transmitted, received, interpreted, and acted upon. With most meteor signals, the resultant time delay is of little importance since it can be taken into account by setting the gating level somewhat higher than the value indicated above. However, in certain meteor signals, fading rates in excess of 0.2 db per millisecond have been encountered. In such cases it is possible for the signal level to drop 4 to 8 db in the time taken to shut down the system, and errors are likely if the snr is used as the only gating criterion. Other criteria may be introduced to compensate for this type of behavior, perhaps by incorporating the fading rate and its derivatives.

Storage

The storage problem in JANET is similar to that met in many computer applications. For a complete discussion of the techniques available, reference may be made to the literature.

The JANET system requires the sequential storage and discharge of information in a complementary set of stores at the transmitter and receiver. The function of the store may be exemplified by the magnetic tape "accordion" used in the present Canadian JANET system.[10] The input and output mechanisms, in this case, are separate magnetic recording and playback heads, and the actual store is a container capable of holding a quantity of magnetic tape. This arrangement facilitates the input and output operations proceeding at different rates.

Since the storage access time contributes to the initiation time, it should be kept as short as possible. Another consideration of importance is the storage capacity, the details of which are discussed in a companion paper.[40]

Modulation

The propagating mechanism appears to place few restrictions upon the choice of modulation for use in a JANET system, in contrast with scatter-communication systems which transmit continuously. This advantage results from the relative absence of the "Fresnel whistle" (the so-called Doppler whistle) which results from the mixing of the meteor signal with a continuous background signal as the meteor trail is formed. The phase variations which produce whistles in the presence of a background signal still occur in the meteor signal but exist only for the first few milliseconds, during the time normally used for initiation purposes.

Since a rapid variation of amplitude is characteristic of meteor signals, it might appear that the most appropriate modulation method would be one employing frequency or phase variation. Actually, however, double-sideband amplitude modulation is used successfully in the present Canadian JANET system. The advantage of this choice is that the carrier, which conveys no information, can be monitored in a narrow filter for gating purposes.

Antennas

The JANET technique does not require the use of extremely high gain antennas. Satisfactory results have been obtained using single, five-element yagi antennas both for transmission and for reception. For most purposes, it appears that increasing the antenna gain beyond some optimum value would, in fact, be disadvantageous if the antenna beam were directed along the great circle bearing of the distant station. The essential point, mentioned earlier, is that the useful meteors are formed in regions on either side of the great circle path and these regions must be illuminated if maximum efficiency is to be realized. In fact, antennas which suppress

[40] L. L. Campbell, "Storage capacity in burst-type communication systems," this issue, p. 1661.

the radiation along the great circle direction in favor of increased radiation to the sides may be used to advantage. Arrays consisting of two antiphased radiators, set on a line perpendicular to the great circle path, and spaced to give first-order lobes directed a few degrees to either side of this path, have been employed successfully. Theoretical work has been published which indicates the effect on "mean signal level" (communication capacity, in the JANET system) of lobe spacing and beam width in both single beam and split-beam arrays.[27] Because of the asymmetric variations indicated in Section IV, it appears desirable to use antenna beams directed to one side of the path for part of the day and to switch the radiation to the opposite side for the remainder.

If the sun or some noisy portion of the galaxy passes through the antenna beam, a considerable increase in background noise will occur. This increase may be as much as 6 db at a frequency of 40 mc. Under these conditions, it may be desirable to increase antenna gains to limit the time during which such effects will be experienced. Similarly, it is wise to suppress side and upper lobes in the antenna pattern.

The reflection process sets practical limits both on the physical separation of the transmitting and receiving antenna systems and on the separation of frequencies used in the two channels. This increases the danger of intermodulation between the signal from a meteor and that from the local transmitter. Careful shielding of equipment and intelligent placement of antennas may serve to minimize this unwanted coupling.

The desirability of obtaining identical transmitting and receiving antenna patterns makes attractive the use of a common antenna for transmission and reception. In this case, the necessary isolation may be obtained by the use of filters designed for common antenna working.

VIII. Operational Experience

While the major effort in the past has been directed toward improvement of the initial design of the system, a considerable amount of operating experience has been obtained, even in the development stage. This phase of the work is treated in some detail in a companion paper,[10] but representative results are summarized briefly here.

The equipment appears to operate quite satisfactorily. A sample of a message as received by a JANET system and printed by a teletype page printer is shown in Fig. 17(a). In order to illustrate the number of characters which are carried by each signal burst, the transmission was repeated and the letter group "XX" was inserted automatically at the end of each reception period, with the result shown in Fig. 17(b).

The most recent continuous test operation of satisfactory length extended from July 17 to August 17, 1956. Meteor activity is known to be high at this time of the year, but this advantage was partially offset by the use of antennas which were known to be less than

```
MORE THAN A QUARTER OF A CENTURY AGO,
ECKERSLEY POINTED OUT THAT SCATTERING FROM
INHOMOGENEITIES IN THE IONOSPHERIC IONIZATION
COULD BE AN IMPORTANT FACTOR IN THE PROPAGATION
OF RADIO WAVES AND COULD INDEED PROVIDE A MEANS
OF COMMUNICATING WITH STATIONS WHICH OTHERWISE
WOULD BE INACCESSIBLE. SINCE THAT TIME THERE
HAVE BEEN MANY INVESTIGATIONS AIMED AT THE
UNDERSTANDING AND UTILIZATION OF THE VARIOUS
IRREGULARITIES WHICH OCCUR IN THE IONOSPHERE.
THE UNDERLYING HOPE IN MOST OF THESE STUDIES
HAS BEEN THAT SOME MEANS WOULD BE FOUND WHEREBY
AT LEAST THE LOWER PART OF THE VHF BAND COULD
BE USED FOR LONG DISTANCE COMMUNICATION.
```

(a)

```
XX   MORE THAN A QUARTER OF A CENTUXXRY XXAGO,
XX
  ECKERSLEY POINTED OUT THAT SCATTERING FROM
INHOMOGENEITIES IN THE IONOSPHERIC IONIZATION
                                              XX
COULD BE AN IMPORTANT FXXACTXXOER IN THXXF PRXXOPAXX:ATION
OF RADIO WAVES AND COULD INDEED PROVIDT A MEANS
OT COMMUNICATING WITH STATIONS WHIXXCH OTHERWISE
WOULD BE INACCESSIBLT. SINCE THAT TIMT TXXHERE
HAVE BEEN XXMANY INVESTI:ATIONSXX AIMED AT THE
UNDERSTANDING AXXXXND UTIXXLXXIXXZATION OF THE VARIOUS
IRREGULARITIES WHICH OCCUR IN XXTHE IONOXXSPHERE.
THE UNDERLYING HOPE IN MOST OT THESE STUDIES
HAS BEEN THAT SOME MEANS WOULD BE FOUND WHEREBY
AT LEAST THE LOWER PART OT THE VHT BAND COULD
BE USEXXD FOR LONG DISTANCEXX CXXOMMUNICATXXION.
```

(b)

Fig. 17—Sample of a teletype message passed by a JANET system: (a) normal text, (b) with individual bursts followed by the letter group "XX."

optimum in design. The test was carried out by Ferranti Electric Ltd., between terminals 900 km apart, at Port Arthur and Toronto. The radiated power at each terminal was about 500 watts. During this test, an over-all average information rate of 34 words per minute was obtained. Individual hourly means of the information rate varied widely from this value. The distribution of the mean rates observed for individual hours is displayed in Fig. 18 where the number of hours, shown as a percentage of the total time for which the rate exceeded a given value, is plotted as a function of that value.

It was indicated earlier that the information rate obtained with a JANET system should undergo a large diurnal variation, but that the magnitude of this variation might not be as great as that observed in the number of meteor signals received. The diurnal variation of hourly mean information rates, derived from the test described above, is shown in Fig. 19. The maximum occurs near 4 A.M. and the minimum near 5 P.M. with a slight enhancement near noon. The max/min ratio is approximately four, somewhat less than the corresponding ratio for numbers during the same period [see Fig. 14(b)]. These trends, in addition to showing up in the averaged results, were apparent on most of the days individually.

As more experience has been gained with the system, the error rate has been reduced substantially. During the continuous test period in the summer of 1956 the average character error rate was approximately 1.5 per cent. It was noted at that time that most of the errors were occurring toward the end of individual transmissions. As a result, refinements have been introduced into the gate-off procedure and the system has been operating recently with an error rate of somewhat less than 0.1 per cent.

In the frequency range used for the JANET system it is not uncommon for the radio waves to be reflected by auroral or sporadic E ionization. There has been some concern regarding these nonmeteoric signals, since it

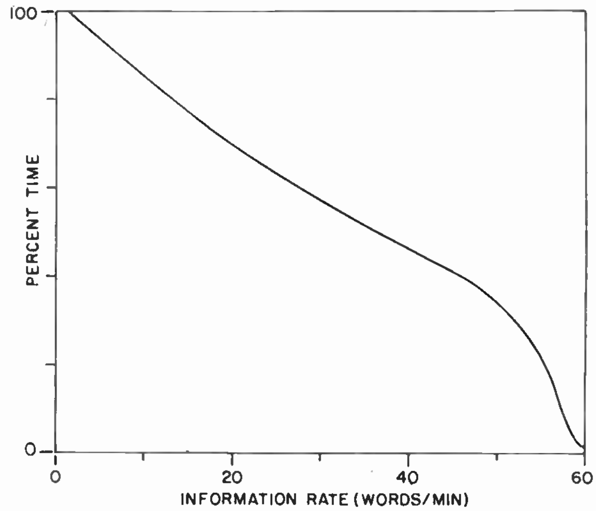

Fig. 18—Percentage of time the information rate exceeded a given value, as a function of that value, deduced from hourly averages obtained during a one-month test period on the Toronto-Port Arthur circuit.

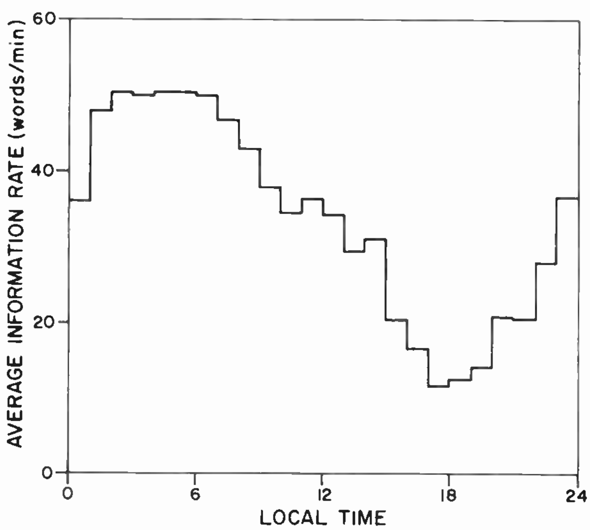

Fig. 19—Diurnal variation of average information rate, obtained during a test period on the Toronto-Port Arthur circuit.

is possible that they might interfere with the operation of the communication system. A strong nonmeteoric signal has been encountered only once during a test operation, on which occasion the system operated at maximum capacity for the whole period, with no noticeable increase in error rate.

IX. Further Characteristics of a JANET System

A unique feature of the JANET system, which may well prove attractive to the potential user, results from the use of meteor trails individually. The inherent directivity of the meteor-scattering process ensures that the signal reflected from a particular trail may be received within only a limited area on the ground. This reception area varies from one meteor to the next in size, shape, and position. The JANET system automatically selects those trails whose reception areas, for signals originating at the distant station, include the location of the local station. Any other receiver which might be present must lie within the same reception

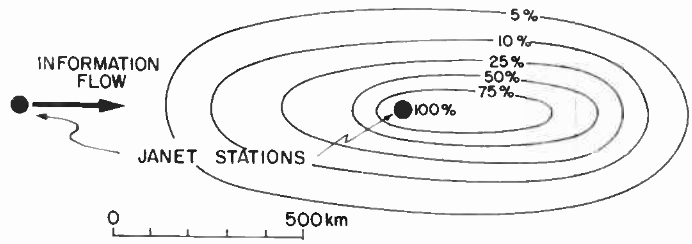

Fig. 20—Contours of information available to a receiver placed in the vicinity of a JANET system.

area if it is to detect a transmission and, in consequence, will receive only that fraction of the total information transfer for which this condition is satisfied. The condition is satisfied less frequently as the receiver is moved away from the JANET station until, at distances of the order of hundreds of kilometers, only a negligible fraction of the total transmitted information is available. The percentage information available at any location should not exceed the values indicated in Fig. 20 since these contours were calculated for the least favorable circumstances. (Similar theoretical curves have been published by the Stanford group,[41] together with experimental data.) This characteristic of the JANET system provides inherently a certain limited degree of privacy which is not available with more conventional techniques. The same characteristic provides a certain amount of protection from interference generated at some distance from either station. Further discrimination against a particular eavesdropping receiver, or against a particular source of interfering signals, may be obtained by suitable design of the antennas.

It may appear at first sight that the JANET technique is somewhat wasteful of spectrum space because of the relatively high instantaneous signalling rates which are required in order to achieve modest average information rates. This defect is offset by the fact that JANET systems, using the same frequency assignments, can be located much closer to each other than can other systems operating over comparable distances. As an extreme example, it is conceivable that two systems using identical frequencies could be operated under conditions where the two paths intersect at right angles near their midpoints. Each circuit would then suffer interference from the other for only a small part of the total time, and of this only a very small fraction would occur during actual periods of information transmission. It would, however, be necessary to use different identifying signals for the two circuits.

One of the strongest incentives toward utilization of the vhf band for long-range communication has been the hope that these frequencies might be immune to the ionospheric disturbances which plague hf communication circuits, particularly at high latitudes. To a very large extent this hope seems to have been justified. During most ionospheric storms the meteor signals are largely unaffected, although the experimental circuits

[41] O. G. Villard, A. M. Peterson, L. A. Manning, and V. R. Eshleman, "Some properties of oblique radio reflections from meteor ionization trails," *J. Geophys. Res.*, vol. 61, pp. 233–249; June, 1956.

have not yet been operated through a full sunspot cycle. For periods of a few minutes during intense auroral displays, quite strong absorption has been observed at frequencies up to 50 mc. An extreme example has been discussed elsewhere.[42] While such occurrences would reduce temporarily the average information rate of a JANET system, it does not seem likely, on the basis of present experience, that communication would ever be precluded for many hours as is frequently the case at lower frequencies.

During many ionospheric disturbances, the signal received from a distant vhf transmitter is subject to considerable enhancement due, presumably, to reflections from sporadic E or auroral ionization. Throughout the past two years, such enhancements have become more frequent as the sunspot activity has increased. Near the auroral zone these periods now account for a significant fraction of the total time. It remains to be seen whether it is possible to use all such enhanced signals as effectively as the single occurrence mentioned in the preceding section, or whether some of the enhanced signals exhibit fading of a type which would interfere with the operation of the JANET system. The complete answer to this question will be known only after a system has been operated in or near the auroral zone for an extensive period, preferably during a time of intense solar activity.

The discussion in the preceding sections has emphasized the characteristics of one type of JANET system suitable for point-to-point operation carrying a single teletype channel in each direction. This system by no means exhausts the uses to which the JANET principle may be applied. Several modifications appropriate to wide-band and multistation use have been considered in detail, but there seems to be little purpose in discussing them here since the most suitable development for any particular application depends markedly on the specific circumstances.

X. Conclusion

Much of the enthusiasm which has attended the development of the JANET communication technique has been due to its novelty. The feasibility of reliable communication by this method has been demonstrated, but it remains to be seen if it can compete with the more established techniques. In any immediate comparison, it should be noted that the JANET technique has not yet been applied in a system which approaches the maximum efficiency to be expected from the propagation mechanism. The development program has moved slowly because of the statistical nature of the meteor phenomenon. At each stage it has been necessary to conduct long tests in order to obtain statistically reliable results. A similar period of slow improvement likely will be required before a system is achieved which uses efficiently all of the available meteors. More detailed fundamental knowledge about meteors is a major requirement at the present time. While tremendous strides have been made in the past few years, much research of a basic nature is still needed.

An important consideration in assessing the utility of a practical communication system is the environment in which it is expected to operate. In Canada, with its sparsely settled north country bisected by the auroral zone, there exists a general requirement for a relatively low power, reliable, point-to-point communication system for use over ranges of the order of 500 to 1500 km. The JANET system, even at its present stage of development, gives every promise of filling this need. For such an application the disadvantages of complexity of storage and signalling equipment, of discontinuous communication with its attendant delays, and of limited ultimate range (about 2000 km) are offset by the fact that modest information capacity is obtainable with modest transmitter power and simple antenna systems. It would be presumptuous, if not foolhardy, to attempt a prediction of the eventual utility of so new a system even for Canadian use, but it is likely that future Canadian development will be aimed mainly at improved equipments of the type already described. For this program, a large amount of practical experience with operating JANET systems is required. This experience is being acquired currently.

In closing, it may not be inappropriate to mention a problem which, while not directly involved in the development of the technique under discussion, is of vital concern in its use. There are now at least two different communication systems, operating in the 30–50 mc region, which promise to provide alternative, or perhaps complementary, types of long range service. If these systems gain wide acceptance they will nearly double the amount of frequency spectrum space available for long distance communication. Unfortunately, there are still many transmitters in this frequency range which, although intended for purely local service, radiate the same order of power as that required by a JANET system. This problem exists both on this continent and, to an even greater degree, in Europe. It is to be hoped that as many as possible of the suitable frequencies may be either reserved or re-allocated for long range service.

Acknowledgment

The authors are indebted to a number of their colleagues at the Radio Physics Laboratory for assistance in the development of the JANET system. Specific mention should be made of Dr. L. L. Campbell who participated in many fruitful discussions, and C. Collins, J. K. Grierson, and J. W. Brown, who contributed much to the initial experiments. Thanks are due, also, to the many people at the laboratories of Ferranti Electric Ltd., who participated in the development. The work could not have been done without the continued encouragement of F. T. Davies, former Superintendent of the Defence Research Telecommunications Establishment, and the enthusiastic support of his successor, J. C. W. Scott.

[42] P. A. Forsyth and E. L. Vogan, "The frequency dependence of radio reflections from aurora," *J. Atmos. Terr. Phys.*, vol. 10, pp. 215–228; April, 1957.

Bandwidth Considerations in a JANET System*

L. L. CAMPBELL,† MEMBER IRE, AND C. O. HINES†

Summary—Some of the considerations which influence the choice of transmission bandwidth in a JANET system are discussed in this paper. It is shown that the mean rate of transfer of information increases with bandwidth, for bandwidths in the range currently contemplated, in spite of the consequent decrease in the duty cycle. A system designed to maintain a constant snr by varying the bandwidth with received signal power is discussed, and its advantage over a fixed bandwidth system is calculated.

I. Introduction

In conventional communication systems, an increase in transmitter power can be employed either to reduce the error rate through increased snr in a fixed bandwidth or to increase the signaling rate through the use of a wider bandwidth. In the JANET system, described by Forsyth *et al.*,[1] an increase in transmitter power can be used in either of these ways or it can be used to increase the duty cycle (fraction of time that communication is possible). In general, an increased duty cycle causes a decrease in the mean delay of a message in the system and an increase in the mean rate of information transfer, even without an increase in bandwidth. These advantages are offset to some extent by the increased possibility of multipath propagation. The dependence of duty cycle on sensitivity is discussed more fully in Section II.

An alternative approach is to consider the transmitter power fixed while the bandwidth and signaling rate are increased. In a conventional system this would normally lead to an increase in the error rate because of the increased noise accepted by the receiver in the broadened band. However, with a JANET system the bandwidth may be increased without an increase in error rate if, at the same time, the received signal level which is required to start transmission is increased proportionately, thereby maintaining the same threshold snr during transmission. The increased bandwidth allows an increased instantaneous signaling rate during transmission, but the increased signal level required for transmission reduces the duty cycle. Thus, in designing a system, it becomes important to decide whether to use a high instantaneous rate for a small fraction of time or a lower instantaneous rate for a larger fraction of time. This question will be discussed in Section III.

The approach adopted in the preceding paragraph may be extended. It is evident that a further advantage might be gained by the use of a variable bandwidth system capable of following the rapidly changing strength of useful signals. The object of such a system would be to vary the bandwidth in proportion to the signal power, keeping the snr constant, and so to make the most effective use of both strong and weak signals. The transmission rate could vary continuously or through several discrete steps. The improvement which may be expected from such a variable rate system and one possible method of achieving it will be indicated in Section IV.

II. Duty Cycle and System Sensitivity

The effect of the operating threshold level on the duty cycle can be derived simply, if it is assumed that all signals are of the underdense type.[1] The variation of signal amplitude is then given by

$$\begin{aligned} A &= 0 && \text{for } t < 0 \\ A &= A_p \exp(-t/\tau) && \text{for } t > 0, \end{aligned} \tag{1}$$

where A_p is the peak signal amplitude, τ gives a measure of the signal duration, and t measures time from the formation of the trail. For simplicity it will be assumed that a single value of τ is applicable to all signals, although the actual distribution could be taken into account by an appropriate integration. The variation of A_p from one signal to another is, however, of direct interest here, and a specific distribution of peak amplitudes must be adopted. It will be assumed that the number of signals per unit time, N_0 with peak amplitudes greater than some value A_0 is given by

$$N_0 = CA_0^{-2n}, \tag{2}$$

where n is some positive number.

The JANET system transmits information only when the received snr exceeds a suitable value. If this value corresponds to the amplitude level A_0, then the useful duration of a signal of the form (1) is given by

$$T_0 = \tau \ln (A_p/A_0) \tag{3}$$

for $A_p > A_0$. If $A_p < A_0$, the duration is zero and the signal is of no use. Thus the probability that the useful duration of the signal exceeds a value T is the same as the probability that the peak amplitude exceeds $A_0 \exp(T/\tau)$. From (2), the number of signals per unit time whose durations exceed T is $CA_0^{-2n} \exp(-2nT/\tau)$. The total number of useful signals per unit time is CA_0^{-2n} and hence, the probability that the duration of a useful signal will exceed T is $\exp(-2nT/\tau)$. Thus the probability distribution of the durations, and hence the mean duration, is independent of A_0. Now the duty

* Original manuscript received by the IRE, March 22, 1957. This work was performed under project PCC No. D48-28-30-05.

† Radio Physics Lab., Defence Research Board, Ottawa, Canada.

[1] P. A. Forsyth, E. L. Vogan, D. R. Hansen, and C. O. Hines, "The principles of JANET—a meteor-burst communication system," Proc. IRE, this issue, p. 1642.

cycle, or fraction of time that the received signal amplitude exceeds A_0, is given by

$$F = CA_0^{-2n}T_m, \tag{4}$$

where T_m is the mean duration of an individual signal. Eq. (4) is valid only when F is so small that the possibility of two suitable reflecting trails existing simultaneously may be neglected. Since C and T_m are independent of A_0, (4) may be written

$$F = KP_0^{-n}, \tag{5}$$

where P_0 is the threshold power corresponding to A_0 and K is independent of P_0.

McKinley[2] has proposed an empirical relation of the form (5), and has estimated the value of n to be 0.56. Some records have also been analyzed at this laboratory and they confirm that the relationship between F and P_0 is approximated well by an equation of this form, although the values of n which were obtained here range from 0.57 to 0.96. Forsyth and Vogan,[3] in an earlier analysis based on (2), obtained a value 0.72. The distribution of meteor masses which was indicated in the companion paper,[1] combined with the assumption of underdense trails, would have given as a theoretical estimate the value $n = 0.5$. The larger values found in practice can be attributed to the occurrence of overdense trails. In view of the simplifying assumptions which were necessary to derive (5) it seems best to regard this equation as a simple approximation to a much more complicated one.

The relation between duty cycle and mean rate of information transfer is a complex one which is discussed elsewhere.[4] In an important limiting case, however, it may be written

$$\text{mean rate} = \text{instantaneous rate} \times \text{duty cycle}. \tag{6}$$

The duty cycle, in turn, is directly proportional to the nth power of the transmitted signal power, as may be inferred from (5). Consequently, for a given bandwidth, the mean rate of transfer of information is proportional to the nth power of the transmitter power.

It should be emphasized that (5) must not be expected to hold for very large or very small values of P_0. When P_0 is small, considerable overlapping of signals must be expected and thus F will be smaller than (5) predicts. On the other hand, the transmitted power imposes an upper bound on P_0, above which the duty cycle must be identically zero. However, (5) does seem to be a good approximation for vaues of F between 0.005 and 0.1.

III. Fixed Bandwidth Systems

In the preceding section, the relation between mean rate of information transfer and transmitter power was discussed. In the present section, the relation between mean rate and receiver bandwidth will be examined on the assumption that the transmitter power is fixed. It will be assumed that the bandwidth is proportional to the instantaneous rate, that (5) and (6) hold, that the snr required for satisfactory operation is independent of the instantaneous rate and that the received noise power is proportional to the bandwidth. As a consequence of the last two assumptions, the required threshold power level, P_0, is seen to be directly proportional to the bandwidth and hence, (5) may be rewritten as

$$F = K_1B^{-n}, \tag{7}$$

where K_1 is independent of B. The mean rate of information transfer, R_f, is then given by

$$R_f = K_2BF = K_1K_2B^{1-n}, \tag{8}$$

where K_2 is another constant. Since n is normally less than unity it appears from (8) that the bandwidth and signaling rate should be chosen as large as possible if it is desired to make the mean rate large.

Operation of the system with a large bandwidth and small duty cycle may have one further advantage and at least one disadvantage. The favorable feature is that the number of characters per burst is increased as the signaling rate goes up. This reduces the number of errors which may be caused by start and stop procedures at the beginning and end of each burst. The unfavorable feature is the large delay of a message in the system when the duty cycle is small.

It is more difficult to estimate the effect on multipath errors of increasing the signaling rate and reducing the duty cycle. On the one hand, the higher signaling rate may mean more errors when multipath propagation occurs. On the other hand, a reduced duty cycle will mean that multipath propagation occurs less often. Multipath propagation occurs when two or more suitably oriented and suitably ionized meteor trails exist simultaneously in the antenna beams. In general, if communication is possible for a fraction F of the time, there will be multipath propagation for approximately a fraction F^2 of the time. However, much of this multipath propagation will be quite harmless, either because one reflected signal is much stronger than the other or because the path differences are such that the signals arrive in phase at the receiver. Experience indicates that multipath propagation does not cause serious difficulties for duty cycles up to 5 per cent.

IV. Variable Rate Systems

It has been suggested by Forsyth[5] that the performance of a JANET system could be improved by making

[2] D. W. R. McKinley, "Dependence of integrated durations of meteor echoes on wavelength and sensitivity," *Can. J. Phys.*, vol. 32, pp. 450–467; July. 1954.

[3] P. A. Forsyth and E. L. Vogan, "Forward-scattering of radio waves by meteor trails," *Can. J. Phys.*, vol. 33, pp. 176–188; May, 1955.

[4] L. L. Campbell, "Storage capacity in burst-type communication systems," PROC. IRE, this issue, p. 1661.

[5] P. A. Forsyth, unpublished report.

the bandwidth and signaling rate vary in direct proportion to the received signal power throughout each individual burst in order to use most efficiently all available signals. Such a variable rate system will be compared with a fixed rate system on the same assumptions as before.

It will be assumed that the bandwidth may be varied continuously between some lower limit, B_0, and some upper limit, B_1. When the received signal is so small that the snr in the bandwidth B_0 is below the threshold no transmission takes place; and when the snr in the bandwidth B_1 is above the threshold, the bandwidth remains fixed at the value B_1. Between these limits, the bandwidth varies so as to maintain the snr at the threshold value. The limits B_0 and B_1 would probably be determined by practical design considerations and for the present development must lie within the limits for which (7) is valid.

Now the fraction of time that communication is possible in a bandwidth B or greater is $F(B)$, where $F(B)$ is given by (7). Thus, if $B_0 < B < B_1$, the fraction of time that the variable rate system would operate with a bandwidth B to $B+dB$ is $F(B)-F(B+dB)$, or approximately $-F'(B)dB$. Hence, in the mode of operation described, the mean rate of transfer of information is given by

$$R_v = -K_2 \int_{B_0}^{B_1} BF'(B)dB + K_2 B_1 F(B_1). \tag{9}$$

When the value of $F(B)$ given by (7) is substituted in this, the result is

$$R_v = \frac{K_1 K_2 B_1^{1-n}}{1-n}\left[1 - n\left(\frac{B_0}{B_1}\right)^{1-n}\right]. \tag{10}$$

The best fixed bandwidth system with a bandwidth in the range B_0 to B_1 is the system with bandwidth B_1. The mean rate with this system is given by

$$R_{f_1} = K_1 K_2 B_1^{1-n}. \tag{11}$$

Thus, if an improvement factor, I, is defined by

$$I = R_v / R_{f_1}, \tag{12}$$

then

$$I = (1-n)^{-1}[1 - n(B_0/B_1)^{1-n}]. \tag{13}$$

If the bandwidth is varied in discrete steps, rather than continuously, the improvement will be somewhat less than that predicted by (13). If the typical value 0.75 is chosen for n, then for $B_0/B_1 = 1/10$, $I = 2.31$. If $B_0/B_1 = 1/100$, then $I = 3.05$.

Hansen[6] has proposed a technique which would provide a variable rate system and which might be feasible if the ratio B_1/B_0 is not great. Briefly, the technique is to convert digital information to modulation waveform at a fixed low rate and then store the modulation waveform. The modulation waveform would be discharged to the transmitter at a variable rate which is controlled by a signal from the receiving station. At the receiver the signal is demodulated and the modulation waveform is entered in the receiver store at the same rate as it is discharged from the transmitter store. Finally, the modulation waveform is discharged from the receiver store at a fixed low rate and is then converted to digital information. Now, if the snr is high enough that pre-detection filtering and post-detection filtering may be considered equivalent, a fixed audio frequency filter at the output of the receiver store is equivalent to a variable band-pass filter at the receiver input. Clearly this technique involves several problems of synchronization and the operation of servomechanisms which will control the speed of the storage units. It is not known yet whether the cost of surmounting these problems is low enough to make this a practical system.

In conclusion, it should be emphasized that the criterion used in this paper for comparing systems has been the mean rate of transfer of information. It is conceivable that other factors, for example the possible delay of a meassage, may be more important. In this case, one might wish to compare the variable rate system with a fixed rate system which has a lower mean rate than R_{f_1} but which has other desirable features. If the variable rate system retains these desirable features, as it would in the case of delays, the improvement factor over the given fixed bandwidth system might easily be much greater than that given by (13).

[6] D. R. Hansen, unpublished report.

Storage Capacity in Burst-Type Communication Systems*

L. LORNE CAMPBELL†, MEMBER, IRE

Summary—The relationship between storage capacity and mean rate of transfer of information is derived for a burst communication system of the JANET type. Specific probability distributions are then assumed for the durations of signals and the intervals between signals. An explicit formula for the mean rate as a function of storage capacity is calculated for these probability distributions. The specific distributions chosen are thought to approximate those which will be found in a typical JANET system.

I. Introduction

In a burst-type communication system, such as the JANET system described elsewhere by Forsyth, *et al.*,[1] it is necessary to employ storage units at the transmitting and receiving stations. The purpose of this paper is to examine the effect of the capacity of these storage units on the operation of the system.

The system to be considered here is one in which the transmission of information is intermittent. The durations of the transmissions and the intervals between transmissions are independent random variables whose probability distributions are known. In the JANET technique of communication, transmission begins when a suitably oriented meteor trail is formed in the upper atmosphere. Transmission continues until the trail diffuses to such an extent that it will no longer support communication.

The information which is to be transmitted is fed at a low rate to a storage unit at the transmitter. When conditions are suitable for transmission, the information is extracted from the storage unit and then transmitted at a high rate. At the receiving station the information is fed to another storage unit at the high transmission rate. The information is then extracted from this unit at the low input rate.

In the present JANET system, the low input and output rate is the rate at which commercial teletype readers operate. The high rate is chosen so that the outflow of information is nearly continuous. For example, if transmission takes place about five per cent of the time, then the high rate would be chosen to be about twenty times the low rate.

When the storage units hold only a finite amount of information, the above description must be modified slightly. If the storage unit at the transmitter is filled up, the inflow of information ceases until some of the information is transmitted from the store. Similarly, if the store becomes empty during transmission, the transmission rate drops and becomes equal to the input rate. Complementary conditions hold at the receiving station. However, if the storage unit at the receiving station has the same capacity as the one at the transmitting station, then it is not difficult to see that the effect of the receiver store on the operation of the system is exactly the same as the effect of the transmitter store. If at some instant the transmitter store is full and the receiver store is empty, then from that time on the sum of the amounts of information in the two storage units is equal to the capacity of one of them. Thus, when one becomes full the other becomes empty at the same instant and conversely. It will be assumed from this point on that this condition holds and hence that the receiver store does not affect the operation of the system, except through the additional delay it causes in the flow of information.

Clearly, if the capacity of the storage unit is too small, there will be many occasions where transmission is possible while the storage unit at the transmitter is empty. Hence, an unnecessarily small storage capacity leads to an inefficient system in which the mean rate of transfer of information is quite low. On the other hand, if the storage capacity is too great, the delay between delivery of a message to the store at the transmitter and its final reception at the output of the receiver store may become excessive. Thus, the demands of high rate and small delays impose conflicting demands on the storage capacity. The relative importance of rate and delays will depend on the way the system is to be used.

In Section II of this paper, general formulas are derived from which the effect of storage capacity on mean rate may be calculated. In Section III, specific probability distributions are assumed for the durations of transmissions and the intervals between transmissions. The dependence of mean rate on storage capacity is then calculated for these distributions. The specific distributions assumed in Section III are intended to approximate those which would obtain in a JANET system.

II. General Theory

List of Principal Symbols

$F_d(x)$ = distribution function of duration of a transmission.

$f_d(x)$ = probability density of duration of a transmission.

$F_i(x)$ = distribution function of length of interval between transmissions.

* Original manuscript received by the IRE, March 22, 1957. The work was performed under project PCC No. D48-28-35-05.

† Radio Phys. Lab., Defence Res. Board, Ottawa, Canada.

[1] P. A. Forsyth, E. L. Vogan, D. R. Hansen, and C. O. Hines, "The principles of JANET—a meteor-burst communication system," this issue, p. 1642.

$f_i(x)$ = probability density of length of interval between transmissions.

$F^J(x)$ = distribution function of amount of information in the transmitter store at the end of a transmission.

C = capacity of the storage unit; *i.e.*, the maximum quantity of information which the store will hold.

R_i = rate at which information is fed to the storage unit when it is not full.

R_0 = rate of decrease of amount of information in the storage unit during transmission equals difference between instantaneous transmission rate and R_i.

$\bar{d}$ = mean duration of a transmission.

$\bar{i}$ = mean interval between transmissions.

$A = (R_0\bar{d})^{-1}$.

$B = (R_i\bar{i})^{-1}$.

D = fraction of time the transmitter store is full.

R_m = mean rate of transfer of information in the system.

Amount of Information in the Storage Unit

In order to calculate the mean rate of transfer of information, it is necessary to know the distribution function of the amount of information in the storage unit at the end of a transmission. Once this distribution function is known, the other quantities can be calculated directly.

$$F_{n+1}{}^J(x) = \begin{cases} 0 & (x < 0), \\ H(x) + \int_0^{(C-x)/R_0} f_d(u)du \int_0^{(x+R_0u)/R_i} F_n{}^J(x + R_0u - R_it)f_i(t)dt & (x \geq 0), \end{cases} \tag{5}$$

Let I_n and J_n be the amounts of information in the storage unit at the transmitter at the beginning and end of the nth transmission. Let R_i be the rate at which information is fed to the store when the store is not full. Let R_0 be the rate at which the amount of information in the store decreases during transmission. Since information is fed to the store during transmission at the rate R_i, the instantaneous transmission rate is R_0+R_i. Let d_n be the duration of the nth transmission and let i_n be the duration of the interval between the end of the nth transmission and the beginning of the $(n+1)$th transmission. Then, if C is the capacity of the store,

$$J_n = \begin{cases} I_n - R_0d_n & (I_n - R_0d_n > 0), \\ 0 & (I_n - R_0d_n \leq 0), \end{cases} \tag{1}$$

and

$$I_{n+1} = \begin{cases} J_n + R_ii_n & (J_n + R_ii_n < C), \\ C & (J_n + R_ii_n \geq C). \end{cases} \tag{2}$$

The second half of (1) implies that once the store is emptied during a transmission period it remains empty until the end of the transmission period. Since the input to the store continues during transmission, this means that transmission continues at the low rate, R_i, after the store is emptied.

Let $F_d(x)$ and $F_i(x)$ be the probabilities that $d_n \leq x$ and $i_n \leq x$, respectively. It will be assumed that $F_d(x)$ and $F_i(x)$ vanish for $x \leq 0$ and that they possess derivatives $f_d(x)$ and $f_i(x)$, respectively, for $x \geq 0$. Let $F_n{}^J(x)$ and $F_n{}^I(x)$ be the probabilities that $J_n \leq x$ and $I_n \leq x$, respectively. Then

$$F_n{}^J(x) = \begin{cases} 0 & (x < 0), \\ \int_0^\infty F_n{}^I(x + R_0u)f_d(u)du & (x \geq 0), \end{cases} \tag{3}$$

and

$$F_{n+1}{}^I(x) = \begin{cases} \int_0^\infty F_n{}^J(x - R_iu)f_i(u)du & (x < C), \\ 1 & (x \geq C). \end{cases} \tag{4}$$

From (3) and (4),

where

$$H(x) = \int_{(C-x)/R_0}^\infty f_d(u)du = 1 - F_d\left(\frac{C-x}{R_0}\right). \tag{6}$$

The change of variables

$$\xi = x + R_0u - R_it$$
$$\eta = R_0u + R_it$$

reduces (5) to

$$F_{n+1}{}^J(x) = H(x) + \int_0^C F_n{}^J(\xi)K(x, \xi)d\xi \qquad (n = 1, 2, \cdots) \tag{7}$$

for $0 \leq x < C$, where

$$K(x, \xi) = \begin{cases} \dfrac{1}{2R_0R_i}\displaystyle\int_{x-\xi}^{2C-x-\xi} f_i\left(\frac{x-\xi+\eta}{2R_i}\right)f_d\left(\frac{\xi+\eta-x}{2R_0}\right)d\eta & (0 < \xi < x), \\ \dfrac{1}{2R_0R_i}\displaystyle\int_{\xi-x}^{2C-x-\xi} f_i\left(\frac{x-\xi+\eta}{2R_i}\right)f_d\left(\frac{\xi+\eta-x}{2R_0}\right)d\eta & (x < \xi < C). \end{cases} \tag{8}$$

The functions $F_n^J(x)$ $(n=1, 2, \cdots)$ are the same as the successive approximations to the solution of the Fredholm integral equation

$$F(x) = H(x) + \int_0^C F(\xi)K(x, \xi)d\xi. \tag{9}$$

It will now be shown that, if (9) has a solution $F(x)$, then $F_n^J(x)$ converges to $F(x)$ as $n\to\infty$ provided that

$$\int_0^C | K(x, \xi) | d\xi \le M < 1 \tag{10}$$

for $0 \le x \le C$. Let $F(x)$ be a solution of (9) and let

$$Q_n = \operatorname*{lub}_{0\le x<C} | F(x) - F_n^J(x) | \quad (n = 1, 2, \cdots), \tag{11}$$

where lub means least upper bound. It is a simple consequence of (7), (9), and (10) that

$$Q_{n+1} \le MQ_n. \tag{12}$$

Thus,

$$Q_{n+1} \le MQ_n \le M^2Q_{n-1} \le \cdots \le M^nQ_1. \tag{13}$$

Since Q_1 is finite and $M<1$, $Q_n \to 0$ as $n\to\infty$. Therefore,

$$\lim_{n\to\infty} F_n^J(x) = F(x) \tag{14}$$

for $0 \le x < C$.

Let

$$F^J(x) = \begin{cases} 0 & \text{for } x < 0, \\ F(x) & \text{for } 0 \le x < C, \\ 1 & \text{for } x \ge C, \end{cases} \tag{15}$$

where $F(x)$ is a solution of the integral (9). Since all the functions $F_n^J(x)$ are monotonic nondecreasing, $F^J(x)$ must be monotonic nondecreasing, since otherwise it would be impossible for Q_n to tend to zero. Thus, $F^J(x)$ is a monotonic nondecreasing function, is continuous on the right, and tends to 0 and 1 as x tends to $-\infty$ and $+\infty$, respectively. Therefore, $F^J(x)$ is itself a probability distribution function. Moreover, $F^J(x)$ is the distribution of the limiting distribution of J_n as $n\to\infty$.[2]

The restriction (10) on the kernel function, $K(x, \xi)$, is not severe. Since f_d and f_i are probability density functions, the integral in (10) cannot exceed unity. It may be shown that (10) is satisfied whenever

$$F_d(C/R_0)F_i(C/R_i) < 1.$$

This inequality implies that it is possible for the duration of a transmission period to exceed C/R_0 or that an interval between transmissions may be greater than C/R_i. C/R_0 and C/R_i are the times required to empty and fill the store, respectively.

Note that $K(x, \xi)$ is a continuous function of x which has a finite jump in its first derivative at $x=\xi$. Thus, $K(x, \xi)$ has the properties of a Green's function for a linear second-order differential equation. If $K(x, \xi)$ satisfies a second-order differential equation as a function of x, then it is possible to find a second-order equation satisfied by $F(x)$.

[2] H. Cramer, "Mathematical Methods of Statistics," Princeton University Press, Princeton, N. J., p. 59; 1946.

Determination of Mean Rate

It will now be assumed that the distribution function $F^J(x)$ is known and applies at all times. This means that effects due to the initial condition of the system are neglected and that $F^J(x)$ is the probability that the amount of information in the store at the end of a transmission period is less than or equal to x.

The mean rate of transfer of information is easily calculated once the fraction of time when the transmitter store is full is known. Let $\bar{d}$ be the mean duration of a transmission period and $\bar{i}$ the mean duration of the interval between transmissions. Then, since it was assumed that the duration of the transmission period and the duration of the interval between transmissions are independent, the mean time between beginnings of successive transmissions is $\bar{d}+\bar{i}$. Also, let $\bar{t}_f$ be the mean time that the store is full in one interval between transmissions. Then the fraction of time, D, that the store at the transmitter is full is given by

$$D = \frac{\bar{t}_f}{\bar{d} + \bar{i}}\cdot \tag{16}$$

The mean durations, $\bar{d}$ and $\bar{i}$, are given simply by

$$\bar{d} = \int_0^\infty xf_d(x)dx \tag{17}$$

and

$$\bar{i} = \int_0^\infty xf_i(x)dx. \tag{18}$$

The mean time that the store is full is derived from $F^J(x)$. Suppose that there is a quantity J of information in the store at the end of a transmission period and that the interval between the end of this transmission and the beginning of the next is i. Then, the length of the interval, t_f, that the store is full during this interval between transmissions is given by

$$t_f = \begin{cases} 0 & (J + R_i i \le C), \\ (J + R_i i - C)/R_i & (J + R_i i > C). \end{cases} \tag{19}$$

Thus, $t_f \le x$ if $J \le C + R_i x - R_i i$ for $x \ge 0$. Therefore, the probability that $t_f \le x$, $G(x)$ say, is given by

$$G(x) = \begin{cases} 0 & (x<0), \\ \displaystyle\int_0^{(C+R_i x)/R_i} F^J(C+R_i x - R_i u) f_i(u)du & (x \ge 0). \end{cases} \tag{20}$$

The upper limit of the integral in (20) arises from the fact that $F^J(x)$ vanishes for $x<0$. The mean value of t_f, $\bar{t}_f$, is then given by

$$\bar{t}_f = \int_0^\infty xG'(x)dx, \tag{21}$$

where the dash denotes the first derivative.

Once the system has reached a state of equilibrium, the mean rate of transmission of information must equal the mean rate at which information is fed to the transmitter store. Whenever the store is not full, information is inserted in it at the rate R_i; when the store is full, no information is inserted. Since the store is not full for a fraction $1-D$ of the time, the mean rate at which information is fed to the store, R_m, is given by

$$R_m = (1 - D)R_i. \tag{22}$$

III. Application to JANET Systems

Calculation of $F^J(x)$

In order to obtain explicit expressions for R_m, the probability distributions for the intervals between transmissions and durations of transmission periods must be specified. These distributions must be derived from experimental observations on the particular system in question. In the present JANET system, it is found that reasonable approximations are the Poisson distributions:

$$F_d(x) = \begin{cases} 0 & (x < 0), \\ 1 - e^{-x/\bar{d}} & (x \geq 0), \end{cases} \tag{23}$$

and

$$F_i(x) = \begin{cases} 0 & (x < 0), \\ 1 - e^{-x/\bar{i}} & (x \geq 0). \end{cases} \tag{24}$$

The corresponding density functions are

$$f_d(x) = \bar{d}^{-1}e^{-x/\bar{d}} \qquad (x \geq 0), \tag{25}$$

and

$$f_i(x) = \bar{i}^{-1}e^{-x/\bar{i}} \qquad (x \geq 0). \tag{26}$$

It is easily verified that inequality (10) and (17) and (18) hold.

The assumption of a Poisson distribution for intervals implies that transmissions occur randomly and independently. As far as can be determined, the meteor trails, which support communication in the JANET system, form independently of one another. The rate at which they form is known to undergo a diurnal and seasonal variation. However, the periods of these variations are relatively long compared with the intervals between formation of successive trails. Thus, it may be assumed that the rate at which trails form is constant over the time of interest. The assumption of a Poisson distribution for durations is more difficult to justify either theoretically or experimentally. However, the Poisson distribution seems to fit the data as well as any other distribution which has so far been proposed.

Only the principal steps in the derivation of R_m for the distributions (23) and (24) will be given. From (6)

$$H(x) = e^{-A(C-x)} \tag{27}$$

where

$$A = (R_0\bar{d})^{-1}. \tag{28}$$

From (8),

$$K(x, \xi) = \begin{cases} \dfrac{AB}{A+B}\left[e^{B(\xi-x)} - e^{-(A+B)C+Ax+B\xi}\right] \\ \qquad\qquad (0 < \xi < x), \\ \dfrac{AB}{A+B}\left[e^{-A(\xi-x)} - e^{-(A+B)C+Ax+B\xi}\right] \\ \qquad\qquad (x < \xi < C), \end{cases} \tag{29}$$

where A is given by (28) and

$$B = (R_i\bar{i})^{-1}. \tag{30}$$

A solution of the integral equation

$$F(x) = H(x) + \int_0^C F(\xi)K(x, \xi)d\xi, \tag{9}$$

where $H(x)$ and $K(x, \xi)$ are given by (27) and (29), must be found. Note that $H(x)$ and $K(x, \xi)$ for $x \neq \xi$ both satisfy the differential equation

$$L[y] \equiv \frac{d^2y}{dx^2} + (B - A)\frac{dy}{dx} - ABy = 0. \tag{31}$$

The kernel, $K(x, \xi)$, is a continuous function of x and ξ in the interval $(0, C)$. However, its first derivative has a finite jump at $x=\xi$. The size of this jump is given by

$$\left[\frac{\partial K}{\partial x}(x, \xi)\right]_{\xi=x-0} - \left[\frac{\partial K}{\partial x}(x, \xi)\right]_{\xi=x+0} = -AB. \tag{32}$$

When $L[F(x)]$ is calculated from (9) and account is taken of this jump, the result is

$$L[F(x)] = -ABF(x). \tag{33}$$

Hence, $F(x)$ satisfies the differential equation

$$\frac{d^2F}{dx^2} + (B - A)\frac{dF}{dx} = 0. \tag{34}$$

The general solution of this equation is

$$F(x) = \alpha_1 + \alpha_2 e^{(A-B)x}. \tag{35}$$

The constants α_1 and α_2 are determined by substituting (35) into (9). The final result is that

$$F^J(x) = \begin{cases} 0 & (x < 0), \\ \dfrac{B - Ae^{(A-B)x}}{B - Ae^{(A-B)C}} & (0 \leq x < C), \\ 1 & (x \geq C). \end{cases} \tag{36}$$

This is the probability distribution of the amount of information in the store at the end of a transmission period.

Calculation of R_m

If the probability distribution of the time the store is full during an interval between transmissions is calculated from (20), the result is

$$G(x) = 1 - \frac{(A - B)e^{(A-B)C - BR_i x}}{Ae^{(A-B)C} - B} \qquad (x \geq 0). \qquad (37)$$

The mean value of the time that the store is full in one interval between transmissions is, from (21),

$$\bar{t}_f = \int_0^\infty xG'(x)dx = \frac{(A - B)e^{(A-B)C}}{BR_i[Ae^{(A-B)C} - B]}. \qquad (38)$$

Hence, the fraction of the time that the transmitter store is full, D, is, from (16),

$$D = \frac{\bar{t}_f}{\bar{d} + \bar{i}} = \frac{AR_0}{AR_0 + BR_i} \cdot \frac{(A - B)e^{(A-B)C}}{Ae^{(A-B)C} - B}, \qquad (39)$$

where A and B are given by (28) and (30).

Thus, according to (22), the mean rate of information transfer, R_m, is given by

$$R_m = \frac{BR_i[Ae^{(A-B)C}(R_0 + R_i) - (AR_0 + BR_i)]}{(AR_0 + BR_i)(Ae^{(A-B)C} - B)}. \qquad (40)$$

Discussion of Results

Eq. (40) reduces to a simpler form when $A = B$. For this special case,

$$R_m = \frac{R_i}{R_0 + R_i} \cdot \frac{AC(R_0 + R_i) + R_i}{1 + AC}. \qquad (41)$$

The parameters A and B represent, respectively, the reciprocal of the mean net decrease of information which could occur during a single transmission and the reciprocal of the mean net increase of information in the store in a single interval between transmissions, provided the store is neither filled nor emptied during the transmission and the interval between transmissions. The JANET system parameters are chosen to make A and B roughly equal.

The limiting values approached by R_m as $C \to \infty$ are given by

$$\lim_{C \to \infty} R_m = \begin{cases} R_i & (A \leq B), \\ \dfrac{\bar{d}}{\bar{d} + \bar{i}}(R_0 + R_i) & (A \geq B). \end{cases} \qquad (42)$$

In the first case ($A \leq B$), $R_i\bar{i} \leq R_0\bar{d}$ and therefore, the input between transmissions does not, on the average, supply enough information to the store to make full use of the transmission periods. In this case, as would be expected, the mean rate tends to the input rate as the store capacity increases indefinitely. In the second case ($A \geq B$), the input rate is more than enough to keep up transmission. Thus, the output rate becomes the controlling factor and the mean rate of transfer of information tends to the instantaneous rate of transmission multiplied by the fraction of time that transmission is possible. (Recall that the instantaneous rate of transmission is $R_0 + R_i$.)

The normalized mean rate, R_m/R_i, is plotted in Fig. 1 as a function of AC for $B = 2A$, $B = A$, and $B = A/2$. In each case it is assumed that the ratio of input to transmission rate, $R_i/(R_0 + R_i)$, is 0.05. The general shape of the curves will remain the same for other values of this ratio. As mentioned above, the parameters of the present JANET system are adjusted so that $A = B$ on the average. However, the diurnal and other variations in the rate of occurrence of meteor trails cause $\bar{i}$ and hence B to fluctuate. The values $B = 2A$, $B = A$, $B = A/2$ correspond, respectively, to duty cycles (fraction of time available for transmission) of 0.0953, 0.05, and 0.0256. In Fig. 2, R_m/R_i is plotted as a function of duty cycle, $\bar{d}/(\bar{d} + \bar{i})$, for $AC = 1$, 2, 4, 8, and ∞. This figure shows how the mean rate varies with duty cycle for fixed values of storage capacity and mean duration. The parameter AC, which appears in both figures, is equal to $C/R_0\bar{d}$. Since $R_0\bar{d}$ is the net decrease in amount of information in the store in a transmission of average duration, AC is the number of successive transmissions required, on the average, to empty a full store.

IV. Conclusion

The general expression (40) gives the mean rate of transfer of information, R_m, as a function of the parameters of the JANET system, provided that the exponential distributions (23) and (24) describe the duration and interval distributions adequately. When the distributions (23) and (24) must be replaced by other distributions, the theory of Section II shows how the corresponding expression for R_m is obtained.

Fig. 1 shows how the mean rate is increased as the storage capacity is increased. Since an increase in storage capacity also increases the delay which a message undergoes in the system, it may often be necessary to compromise between high mean rate and low mean delay time. Alternatively, if delays of twelve hours or more are acceptable, a very large storage capacity may offer greater advantages than are indicated by (40) or Fig. 1. This possibility arises because of the diurnal variation in the rate of formation of trails. With a very large storage unit, information could be inserted in the store faster than it is transmitted during periods of low meteor activity. The excess would then be transmitted during periods of high activity.

Fig. 2 shows how the mean rate varies with the duty cycle for fixed storage capacity and fixed mean duration. This figure must be used with caution since very often a change in duty cycle is accompanied by a change in the mean duration. For example, there appears to be a definite variation in mean duration throughout the day, although the extent of the variation is not as great as the variation in rate of formation of trails.

Finally, it should be pointed out that more information is required about the interval and duration distribu-

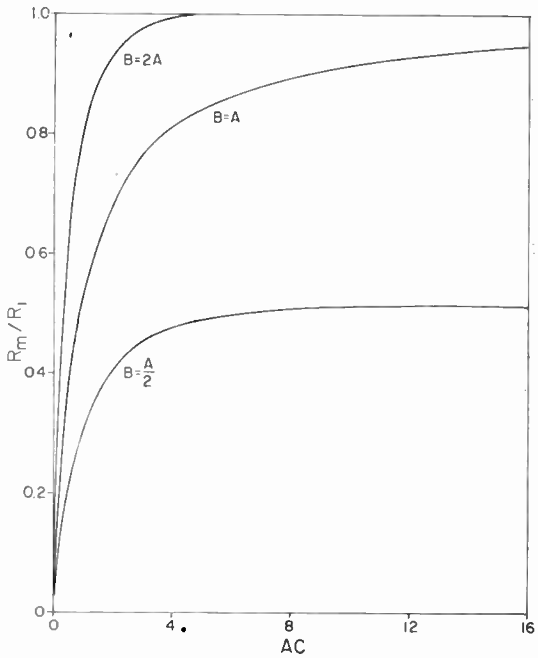

Fig. 1—Normalized mean rate of transfer of information as a function of normalized storage capacity for $R_i/(R_0+R_i)=0.05$ and $B=2A$, A, $A/2$.

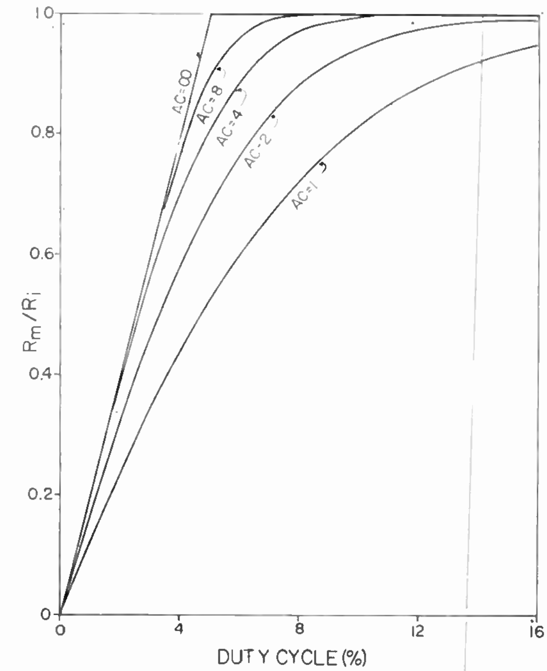

Fig. 2—Normalized mean rate of transfer of information as a function of duty cycle (fraction of time available for transmission) for $R_i/(R_0+R_i)=0.05$ and $AC=1, 2, 4, 8, \infty$.

tions. If overdense trails can be ignored, there is theoretical justification for the use of the exponential distributions (23) and (24). However, the presence of overdense trails will almost certainly alter the distribution of durations and may alter the apparent distribution of intervals. The interval distribution may be altered because signals reflected from overdense trails are more subject to fading and may appear as several short, closely spaced signals. This effect will increase the number of short intervals.

V. Acknowledgment

The author is particularly indebted to Dr. P. A. Forsyth for suggesting the problem, to D. R. Hansen for much information on the operation of the experimental JANET system, and to Dr. C. O. Hines for detecting a serious error in an earlier draft of this manuscript. In addition, the author has benefited from many discussions with the above mentioned people and with many others connected with the JANET project.

The Canadian JANET System*

G. W. L. DAVIS†, MEMBER, IRE, S. J. GLADYS‡, MEMBER, IRE, G. R. LANG‡, MEMBER, IRE, L. M. LUKE‡, MEMBER, IRE, AND M. K. TAYLOR‡, SENIOR MEMBER, IRE

***Summary*—JANET is a point-to-point communication system based on the forward scattering of radio waves from meteor trails. The properties of the transmission medium are such that special methods are required to take full advantage of them. Factors influencing system design have been discussed elsewhere;[1] it is the purpose of this paper to describe a data handling equipment which has been designed for use on a single channel radio teletype link operating on the JANET principle. The equipment is designed for use with double sideband AM radio links having 3-kc bandwidths. Standard 60 wpm teletype machines are used for input and output, and the instantaneous transmission rate is 1300 wpm.**

* Original manuscript received by the IRE, May 6, 1957.

† Ferranti Electric Ltd., Electronics Div., Toronto, Canada.
‡ Ferranti Electric Ltd., Research Div., Toronto, Canada.

[1] P. A. Forsyth, E. L. Vogan, and D. R. Hansen, "The principle of JANET—a meteor-burst communication system," this issue, p. 1642.
L. L. Campbell and C. O. Hines, "Bandwidth considerations in a JANET system," this issue, p. 1658.
L. L. Campbell, "Storage capacity in burst-type communications systems," this issue, p. 1661.

Outline of the System

Gating

THE essential elements of a two-way single channel teletype system are shown in Fig. 1. Information is to be transferred in both directions be-

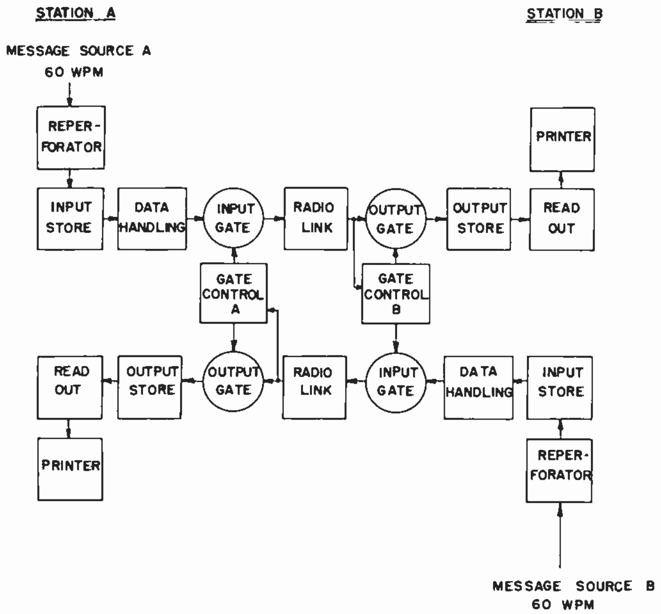

Fig. 1—JANET meteor communication system.

tween A and B at an average rate of 60 wpm via two radio links operating on closely-spaced frequencies. The nature of these links is such that a reciprocal radio path between A and B is available only in short randomly timed intervals, and the average link duty cycle is about five per cent. Gate control circuits establish when reciprocal conditions exist, and input-output gates limit the flow of information to these times.

To maintain an average rate of 60 wpm with a link duty cycle of five per cent, transmission rates of 1300 wpm are used, and the flow of information through the system is smoothed by means of stores. Information is fed to the input stores continuously at 60 wpm. During a transmission burst, information from the input stores is transferred via the radio link to the ouput stores at 1300 wpm. Read out mechanisms remove information from the output stores continuously at 60 wpm.

The error rate in the JANET system is largely dependent on accurate operation of the information gates. Ideally, the radio paths should be very nearly reciprocal. However, in practice it is necessary to ensure that the signal at the remote receiver is above the detection threshold before the input gate to the transmitter is opened. This is done in the following way: both stations radiate unmodulated carrier continuously on separate frequencies. At each station, the output of a sensitive receiver tuned to the frequency of the remote transmitter is monitored continuously by the gate control circuits. If the received carrier to noise ratio exceeds the detection threshold at a station, a 650 cps tone is transmitted. When the incoming carrier is above the detection threshold and is modulated by a 650 cps tone, a closed loop exists between the stations, and information can be transferred in both directions.

The transmission loop may be broken by either station as a result of either of two conditions:

1) The signal-to-noise ratio falls below the detection threshold.
2) The output store fills.

A third condition which might be used to break the transmission loop occurs when the input store is empty. However, if this condition is enforced, transmission time will be lost because both input stores will not necessarily be empty at the same time. To prevent this loss, a dummy message consisting of blanks is transmitted when the input store is empty.

When the transmission loop must be broken, the station initiating the break closes its input gate and sends a stop code, which causes the remote station to close both its input and output gates. Following this, the remote station sends a stop code which closes the output gate of the first station to complete the break. It is particularly important to minimize the delays involved in breaking the loop to enable the system to handle fast fading signals accurately. Part of this delay is unavoidable because of the time required for signals to traverse the loop; the remainder is due to the data handling equipment itself. The JANET equipment is capable of handling fading rates up to 60 db per second satisfactorily.

Data Handling

As the message progresses through the system, it assumes a variety of forms. In the input store, it appears in parallel on paper tape in standard five digit teletype form. On the radio link, it appears as a ppm code having two pulse positions for each digit of the teletype code. A synchronous tone superimposed on the ppm is transmitted as a time reference. At the receiver, the message is reconverted from ppm to pcm and written in parallel on magnetic tape, together with a character sync pulse. The read out mechanism, operating continuously at 60 wpm, removes the message from the store, reads it character by character, and converts it into a standard $7\frac{1}{2}$ digit serial code to operate the printer.

Signaling

The choice of pulse shape on the link is influenced by the following considerations:

1) method of pulse detection,
2) link bandwidth,
3) method of modulation,
4) choice of information codes.

A cosine squared pulse shape has been adopted with two position ppm coding.

The pulse detector determines which of two pulse positions in the frame is occupied, by sampling both pulse positions and comparing the sample amplitudes in a difference amplifier. For a cosine squared signaling function, the link bandwidth is minimum when the base width of the pulse is maximum. In the present system, the maximum base width of the pulse is deter-

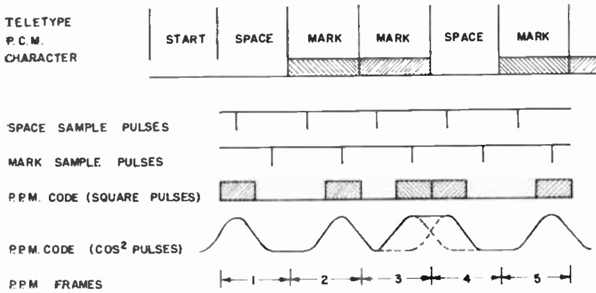

Fig. 2—Code signals.

mined by the consideration that the pulse amplitude must be zero at the sample point of a pulse in the adjacent position. The coding and shaping operation for a single teletype character is illustrated in Fig. 2. The start-stop portions of the teletype signal are not transmitted. Each character on the link is made up of five ppm frames, corresponding to the pulses of a pcm teletype character. Each ppm frame has two pulse positions, but only one is occupied. The absence of a pulse in the pcm code corresponds to a pulse in the first position of a ppm frame: the presence of a pulse in the pcm code corresponds to a pulse in the second position.

Pulse synchronizing information for the ppm receiver is provided by adding a tone of frequency equal to twice the frame rate to the transmitted signal. Frame and character sync pulses at the receiver are obtained by counting cycles of this tone and are synchronized at the beginning of each transmission burst by means of a special code.

The advantages of this signaling technique may be summed up as follows:

1) The comparison of sample amplitudes in the pulse detector renders the circuit insensitive to low-frequency noise components in the receiver output. As a result, dc drift and calibration problems commonly encountered in pulse detecting circuits are avoided.
2) The power spectrum of the signaling function is almost entirely limited to the frequency range 30 to 1300 cps. In this band a signaling rate of 650 bits per second is achieved.
3) The average level in each frame of the ppm signal is constant, and peak positive and negative signal excursions from the average level are equal. Such a signal can be handled by conventional ac coupled modulators.
4) The use of two-position coding in conjunction with digital circuit techniques results in simple coding and pulse-detecting circuits.

The Data Handling Equipment

A block diagram of the equipment used at one terminal of a two-way teletype link is shown in Fig. 3. Units associated with the transmission of the input message are shown in the upper half of the diagram, and units associated with the reception of the output message are shown in the lower half. The gate control unit is shared by both transmitter and receiver circuits.

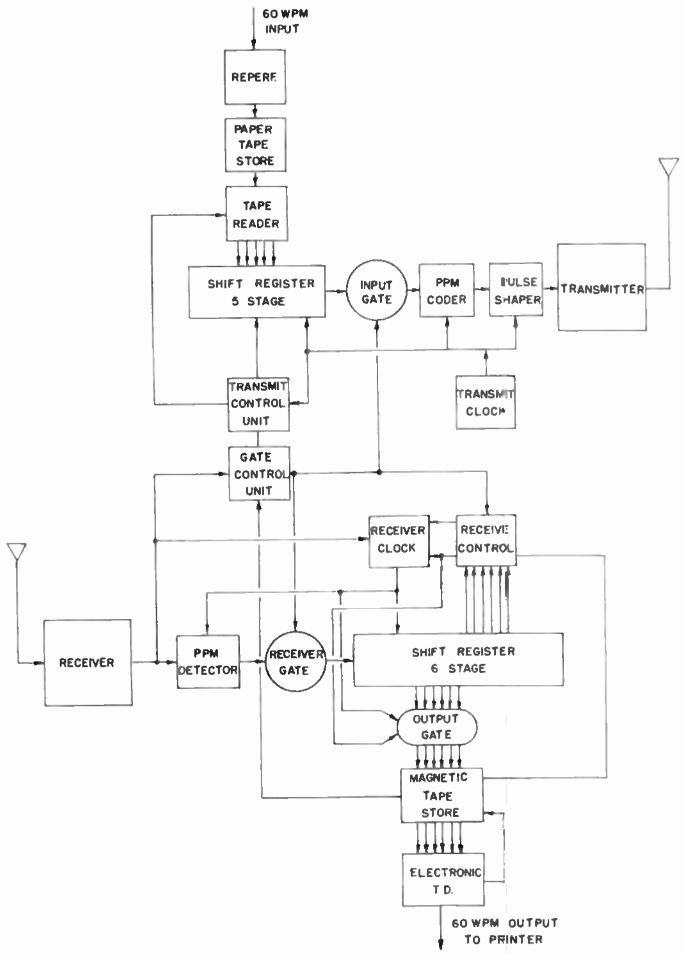

Fig. 3—Data handling equipment.

When there is no radio path between the two stations of the JANET link, the situation at each station is as follows:

1) The transmitter radiates carrier continuously.
2) The input to the receiver, which is tuned to the frequency of the remote transmitter, is below the system detection threshold.
3) The gate control unit holds the input and output gates closed.
4) The transmit control unit causes the transmitter shift register to shift marks continuously. Since the input gate is closed, these pulses are not transmitted.
5) The next character to be transmitted is in position in the tape reader, but is not transferred to the register because drive pulses from the transmit control unit are inhibited.
6) The ppm detector is producing a random output due to noise, but the receiver gate, which passes the detector output to the receiver shift register, is held closed by the gate control unit. Under these conditions the receiver register shifts spaces continually.

When the received carrier level rises above the detection threshold, the transmitter input gate is opened by the gate control unit, and mark pulses from the transmitter shift register are transmitted. Because of the combination of two-position coding and pulse shaping used in the system, the signal transmitted is identical with a 650-cps sinusoid. When reciprocal conditions obtain, a similar 650-cps signal from the remote transmitter will be detected in the gate control unit. This has two effects:

1) The transmit control unit allows about 30 more mark pulses to be transmitted, then inserts a character sync code in the transmitter shift register. When character sync has been transmitted, a pulse from the transmit control unit transfers the first character of the message from the tape reader to the transmitter shift register. The tape advances and stops with the next character in the reading position. Meanwhile, the character read is shifted out of the register, passing through the input gate in serial form. After being processed by the coder and shaper, it is fed to the modulator and transmitted. This process is repeated for the duration of the transmission.
2) The gate control unit opens the receiver gate, allowing the output of the ppm detector to pass into the receiver shift register. The first part of the received signal, consisting of a series of mark pulses followed by a sync character, is detected in the receiver control unit and used to synchronize the receiver clock. When the sync character is received, the receive control unit opens the output gate and energizes the input drive of the magnetic tape store. When the next character of the incoming message has entered the shift register, it is transferred through the output gate by a clock pulse and recorded in five parallel tracks on the magnetic tape. The clock pulse is stored in a sixth track. The process repeats until a stop code is detected in the gate control unit. This resets the receive control unit, which closes the output gate and stops the input drive of the magnetic tape store.

The transmission may be stopped for any of three reasons:

1) A stop code is received.
2) The received signal falls below the detection threshold.
3) The magnetic tape store fills.

The shut-off procedure in the first case differs from that of the second and third. When a stop code is received, the output gate is closed immediately, and the input gate is closed as soon as the last character to be read has been passed to the coder. The transmit control unit shuts off drive pulses to the tape reader and fills up the transmitter register with mark pulses.

In cases two and three, the same shut off procedure applies at the transmitter, but the receiver output gate remains open until a stop code is received. In all cases, the transmission of the stop code begins as soon as the input gate closes.

The choice of stop codes for the system is limited by the fact that all possible combinations of five digits are used for teletype characters. It is necessary to violate the rules of the two-position ppm code in some easily detectable manner to provide a stop code for the system. The code adopted here is produced simply by stopping the transmission of pulses, and might in fact be regarded as no code at all except for the fact that it can be distinguished from the remainder of the transmission.

The transmission is timed by a moderately stable oscillator in the transmitter clock, operating at a frequency of 1300 cps. A portion of the oscillator output is added to the transmitted signal at the pulse shaper to provide pulse synchronization at the receiver. Shift pulses at 650 pps for the transmitter shift register are obtained by division of the oscillator output in a binary counter, and the shift pulse rate is divided by five to obtain letter timing pulses at 130 pps.

At the data receiver, the 1300 cps synchronizing component of the received signal is recovered by means of a filter in the receiver clock. Two sets of clock pulses are derived by counting cycles of the filter output. One of these sets, at a frequency of 650 pps, times the operation of the ppm detector and the receiver shift register; the second set, at a frequency of 130 pps, operates the output gate. The phase of both sets is ambiguous and must be corrected by means of a sync code preceding each transmission, which is detected in the receiver control unit. Once established, synchronization of the receiver clock is maintained by counting cycles of the synchronizing tone.

The received message must be read out of the magnetic tape store at 60 wpm and converted into a $7\frac{1}{2}$-bit code. This function is performed by the electronic transmitter distributor operating in conjunction with a start-stop tape drive in the store output. In operation, the output drive is energized regularly by start pulses from the electronic transmitter-distributor. As tape advances over the read head, a character is read in parallel, and a pulse from the tape sync track stops the drive. Meanwhile, start and stop digits are added to the character code and the resulting $7\frac{1}{2}$-bit code is serialized and passed to the printer via the output line. The process is repeated for each start pulse, and operation of the electronic transmitter-distributor is continuous as long as information is available in the magnetic tape store.

Input information to the transmitter is punched on paper tape by a chad reperforator and placed in the paper tape store. During a transmission, tape is removed from the store and read by the paper tape reader. As in the case of the magnetic tape store read out drive, start-stop operation is used to simplify the problem of synchronization. In the case of the tape reader, start pulses are provided by the transmit control unit at 130 pps, and stop pulses are derived from the tape sprocket hole. Reading is accomplished by means of photocells.

Although this prototype JANET system is designed for single-channel operation, there appears to be no difficulty in providing multiplex operation when adequate bandwidth and transmitter power are available. The design of the data handling equipment can be modified readily to accommodate several teletype channels by means of time division multiplex. This would require the addition of a paper tape reader and an input store for each additional channel, as well as some additional control circuits. Since much of the gating and timing circuitry in a time division multiplex system would be common to all channels, a multiplexed data handling equipment should be attractive economically.

The Experimental Radio Link

A conventional double sideband AM radio link has been used in the present JANET development program. Test sites in Ontario near Toronto and Port Arthur were set up during the summer of 1955. The approximate geometric parameters of the path are: length, 600 miles; bearing from Toronto, 308°; mean latitude, 46°N. A photograph of the Toronto site appears in Fig. 4.

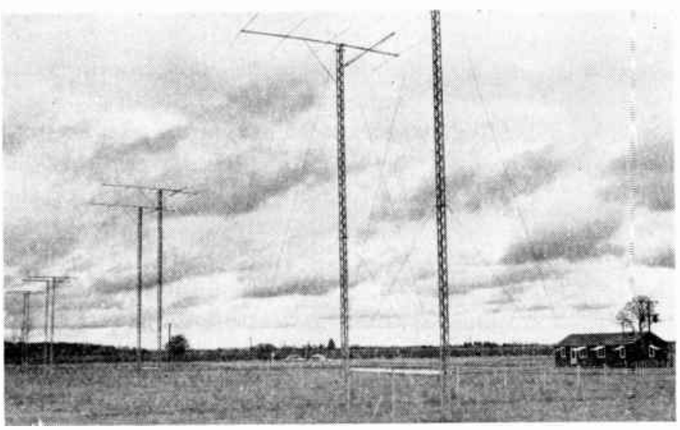

Fig. 4—Toronto station site.

Separate antenna arrays are used for transmitting and receiving. Each array consists of four five-element yagis, spaced and driven so as to produce a horizontal split beam pattern with a null on the great circle bearing between the stations, and with the major lobes lying $7\frac{1}{2}°$ to each side of the path. The vertical angle of the major lobes is about 8°.

Transmitters of conventional design having a 750-watt carrier output (500 watts radiated) and high level modulation are used. The modulators are designed to cover a frequency band of 30 to 4000 cps with a gain variation of less than 4 db. RF preamplifiers followed by communications receivers with IF bandwidths of 3 kc between the 6 db points provide adequate sensitivity with an over-all noise figure of about 2.5 db. Both transmitters and receivers are crystal controlled. Experimental work at the test site has been confined to frequencies of about 40 mc, with a separation of one megacycle between the receiving and transmitting frequencies.

Some Experimental Observations

The operation of the JANET circuit between Toronto and Port Arthur began in November of 1955. Since that time, two continuous test runs, each of about 30 days duration, have been completed; and in addition, numerous short term tests have been made. The first major test, extending from March 22 to April 17, 1956, included a period of low meteor shower activity. Antenna arrays consisting of four five-element yagis were used. At this time, the carrier detector circuit was operated directly by the receiver avc voltage, and a carrier detection occurred when the avc voltage exceeded a calibrated level. At hourly intervals, the received noise level was checked and the carrier detector adjusted to trigger at 12 db above noise. This method of controlling the trigger level proved to be impractical because of large fluctuations in the average noise. When the noise level dropped after calibration, the information rate suffered because the trigger level was higher than necessary; when the noise level rose, the error rate suffered because the system worked in an inadequate snr.

The second major test, extending from July 17 to August 17, 1956, included a period of high meteor shower activity. For this test, single five-element yagis were used as transmitting antennas, and two five-element yagis were used for receiving. The carrier detector circuit was modified to maintain the trigger level at 12 db above noise automatically. Noise levels and trigger calibration were checked every hour, and the calibration of the circuit was found to hold over periods in excess of one month without readjustment.

The diurnal variation of information rate during this test is shown in Fig. 5(a). Fig. 5(b) shows data obtained from carrier gate time totalizers, which recorded at hourly intervals the total time in seconds during which the received carrier was greater than 12 db above noise. Points in this figure were obtained by plotting the data for each hour in histogram form and estimating the location of the peak. It is clear from these figures that a considerable discrepancy exists between the achieved information rate and the carrier gate totals, since 180 seconds of transmission time per hour corresponds to a five per cent duty ratio. Two possible explanations for this discrepancy appear reasonable:

1) The start up and synchronization of the data handling receiver consumed an appreciable part of the transmission time, particularly for short transmission bursts.
2) Reciprocity was not obtained on many signals.

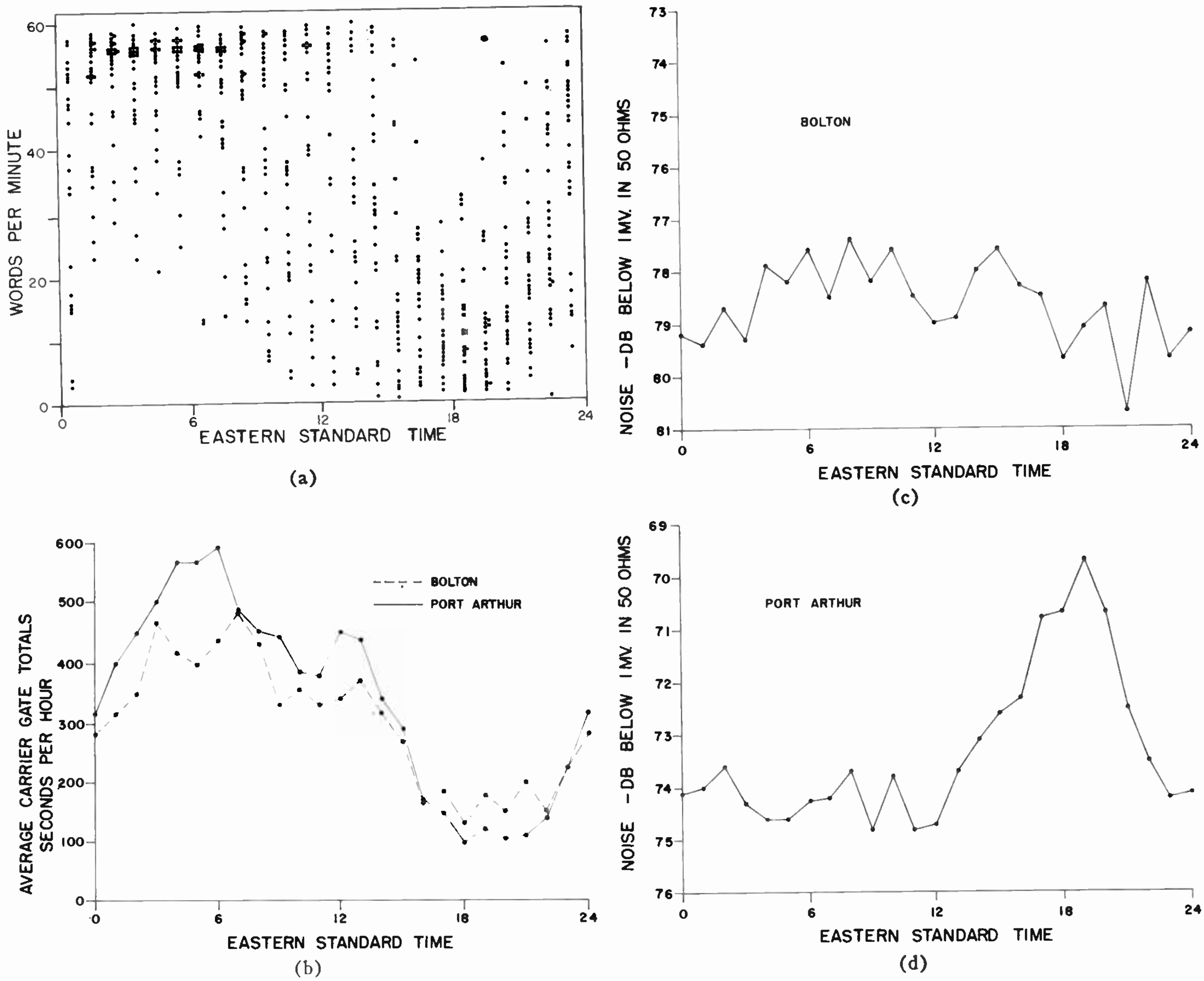

Fig. 5—Test results from the Toronto-Port Arthur link; July 17–August 17, 1956. (a) Diurnal variation of information rates. (b) Diurnal variation of carrier gate totals. (c) Diurnal variation of noise—Toronto side. (d) Diurnal variation of noise—Port Arthur site.

The length of individual transmissions ranged from one character to several hundred characters, with an average length in the region of 30 characters. In practice, several transmissions may occur with a single trail due to deep fades. In view of these facts, it is desirable to reduce the start-up and recycling delays of the link as far as possible, and recent work has reduced these delays by about 50 per cent. Sufficient evidence to establish the effect of this modification has not yet been accumulated. The question of reciprocity is still under investigation.

Fig. 5(c) and 5(d) shows the results of hourly noise measurements made at both stations. Points on these curves were obtained by averaging the data for each hour. The orientation of the Port Arthur antenna is such that the beam sweeps near the center of the galaxy, producing an increase of several db in the received noise level.

Character error rates on the link during these tests ranged from 0.1 per cent in good conditions to four per cent in poor conditions, with the peak of the distribution lying near one per cent. The major part of the errors were due to inaccurate gating, and if these were eliminated, it appeared that error rates of better than 0.1 per cent could be achieved. Part of the gating difficulty was found to be due to interfering carriers, a condition which is aggravated at present by unusually high sun spot activity. This difficulty has been partly overcome by the use of a code character which identifies the incoming signal, which must be received before any message can be transmitted.

Short tests carried out in January of 1957 indicate that the reduction of start-up time and the use of a signal identification facility has reduced error rate considerably. During a 3-hour test on the afternoon of January 22, an average information rate of 60 wpm and an error rate of 0.09 per cent were achieved. Of these errors, the majority were still due to inaccurate gating.

It has been observed that some blackouts on the Toronto-Port Arthur hf link have no apparent effect on JANET signals. However, on other relatively rare occasions, signals have been blanked out for two to three hours by unusually strong atmospheric noise. During local storms, noise due to lightning is not as pronounced as in the case of hf, but, of course, nearby flashes will result in errors. On nights of visible auroral activity, no unusual effects have been observed.

The link duty cycle is influenced strongly by meteor shower activity. Results so far obtained on the Toronto-Port Arthur link are too meager to give a reliable indication of the annual variation of the duty cycle, but it appears that the magnitude of the variation may be in the order of two- or three-to-one.

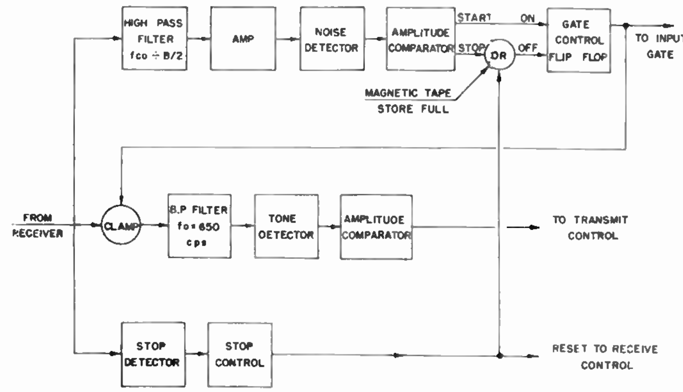

Fig. 6—Gate control unit.

Appendix I

Some System Details

The Gate Control Unit

The gate control unit performs three functions.

1) carrier detection,
2) reciprocity testing,
3) stop signal detection,

The carrier detection circuit operates by measuring the signal-to-noise ratio in the receiver input. The sn measuring circuit depends on efficient avc action in the receiver, and is based on the assumption that the receiver output remains constant for a considerable range of input signal levels. Thus, while the ratio of rms signal to rms noise varies widely, their sum at the receiver output is assumed to remain constant. Subject to this assumption a measure of the noise alone, taken at the receiver output, is sufficient to determine the snr.

In addition, the frequency spectrum of noise in the output of an envelope detector contains components up to B cps, where B is the receiver bandwidth. For a receiver operating on a double sideband AM signal, the modulating signal is confined to the band zero to B/2 cps. Accordingly, it is convenient to examine the detector output in the range B/2 to B cps to obtain a measure of the snr.

The application of this principle to a carrier detection circuit is shown in the upper section of Fig. 6. A high-pass filter with a cutoff at about B/2 cps selects high-frequency noise components in the receiver output. The filter output is amplified and the positive noise peaks are rectified and filtered in the noise detector to produce an output voltage inversely proportional to the snr. When this voltage falls below a calibrated reference level, an amplitude comparator circuit sets the gate control flip-flop to "on"; when it exceeds the reference level, the gate control flip-flop is reset to "off." The reference level in the amplitude comparator circuit is set so that the gate control flip-flop triggers when the input snr is slightly above the detection threshold.

The test for reciprocity on the link requires the detection of 650-cps modulation on the incoming carrier. In the tone detection circuit, a band-pass filter selects the 650-cps component in the receiver output. The filter output is rectified and filtered in the tone detector circuit. When the tone detector output exceeds a calibrated reference level, an amplitude comparator triggers the transmit control unit to initiate the transmission of the message. Calibration of the amplitude comparator is such that the probability of an output due to noise is negligible. A clamp circuit at the input to the band-pass filter, operated by the gate control flip-flop, prevents excitation of the filter when the snr is below the detection threshold.

Since the stop code at the end of a transmission is produced by stopping the transmission of pulses, the stop detector is required to distinguish quickly between the presence or absence of pulses. This is accomplished by a modified version of the ppm detector circuit which recognizes a pulse only if the difference between the two sample amplitudes in a ppm frame exceeds half the nominal value. If fewer than two pulses out of five are recognizable by this criterion, a stop detection occurs and the stop control circuit resets the receiver control unit, closing the output gate.

The gate control flip-flop may be reset when the received snr falls below the detection threshold, or when a stop detection occurs. It may also be reset when the magnetic tape store fills, and in this case retriggering of the system is prevented until the store can accept more tape.

Coding and Shaping

The conversion from pcm to two position ppm coding is accomplished in two "and" gates A1 and A2, and "or" gate O1 of Fig. 7. Opposite phases of the pcm message are fed to A1 and A2. When the pcm digit is space, a clock pulse D1, timed to occur during the first half of the pcm digit, is allowed through A1; when the pcm digit is mark, clock pulse D2, occurring during the second half of the pcm digit, is allowed through A2. The output of O1 contains a pulse for every pcm digit period which occupies one of two possible positions depending

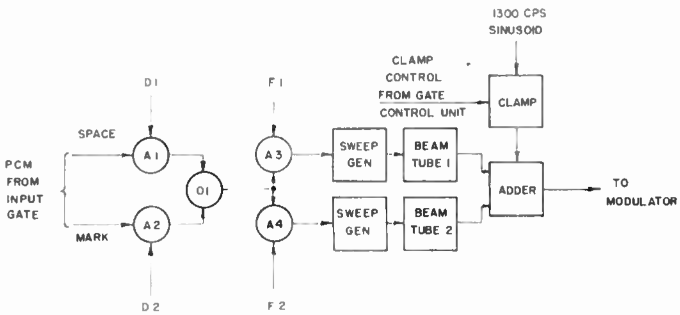

Fig. 7—Coding and shaping circuit.

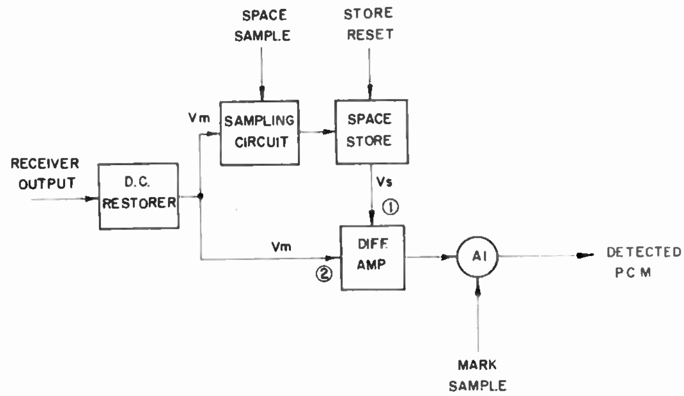

Fig. 8—PPM detector.

on whether the pcm digit is mark or space. This fulfills the requirements of a two-position ppm code.

A linear sweep generator triggered by ppm pulses and a type 6218 beam deflection tube are used for pulse shaping. In this application, the usefulness of the beam tube derives from its ability to produce a good approximation to a $\cos^2$ output when the beam is swept across the collector aperture.

Since pulses in adjacent positions of the signalling function overlap, it is necessary to use two pulse shapers triggered alternately. Message pulses in the output of O1 are shared alternately between the two shapers by "and" gates A3 and A4, which are controlled by clock waveforms F1 and F2. After shaping, the pulses are mixed in a linear adder and fed out to the modulator. An additional input is provided on the mixer for the addition of a 1300-cps synchronizing tone obtained from the transmitter clock. Tone transmission is controlled by a clamp circuit operated by the gate control unit.

The PPM Detector

The ppm detector determines which of two pulse positions is occupied in each frame of the received message. Details of the circuit operation are illustrated by Fig. 8.

After dc restoration, the incoming signal is sampled in the first half of each frame by a narrow space sampling pulse derived from the receiver clock. This charges a storage capacitor (the space store) to a voltage Vs equal to the message amplitude at the space sample time. The store output voltage Vs and the signal Vm are fed to a differential amplifier, with circuit polarities arranged so that an "and" gate A1 connected to the amplifier output is opened when Vm is greater than Vs. The mark sample pulse occurring in the second half of each frame is accordingly allowed to pass through A1 only when the second pulse position of the frame is occupied; *i.e.* when a mark is received. Thus, in the output of A1 the ppm input signal is converted to pcm coding. After the mark sample time, a store reset pulse discharges the space store.

In the absence of noise the ppm detector will operate satisfactorily with input signal amplitudes ranging from 2 to 50 volts peak-to-peak. With a nominal input of 30 volts peak-to-peak and a double sideband AM link, detection errors are in the order of 0.1 per cent in characters at a carrier-to-noise ratio of 10 db.

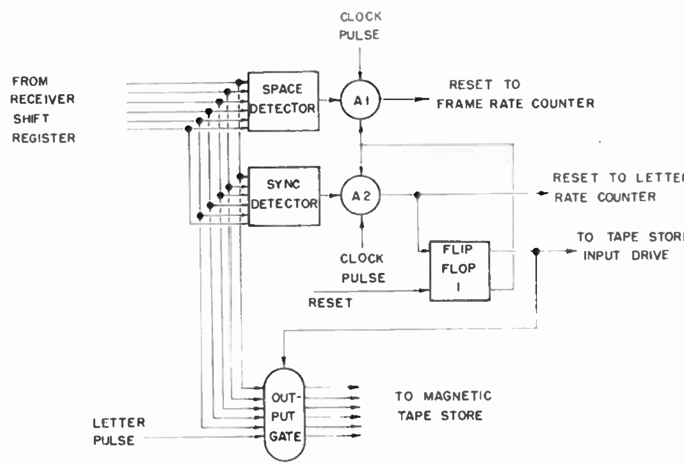

Fig. 9—Receive control unit.

The Receiver Control Unit and Output Gating

An earlier portion of this paper discusses the synchronization of the receiver clock by means of an introductory signal consisting of a series of marks followed by a sync letter. Details of the method are illustrated in Fig. 9.

All six stages of the receiver shift register are continually scanned by space and sync detectors. If the receiver clock is incorrectly phased at the start of a transmission, mark and space sample pulses at the ppm detector will be reversed, and the introductory marks will be recognized as spaces. The detection of six consecutive spaces causes the space detector to open "and" gate A1 of Fig. 7, which allows a clock pulse to correct the phase of the frame counter in the receiver clock. When the sync letter is received, the sync detector opens "and" gate A2 of Fig. 7, and a clock pulse from A2 corrects the phase of the letter counter in the receiver clock and triggers flip-flop 1. One of the flip-flop outputs closes A1 and A2 to prevent the generation of further reset pulses during the course of the message; the other opens the output gate and energizes the input drive to the magnetic tape store.

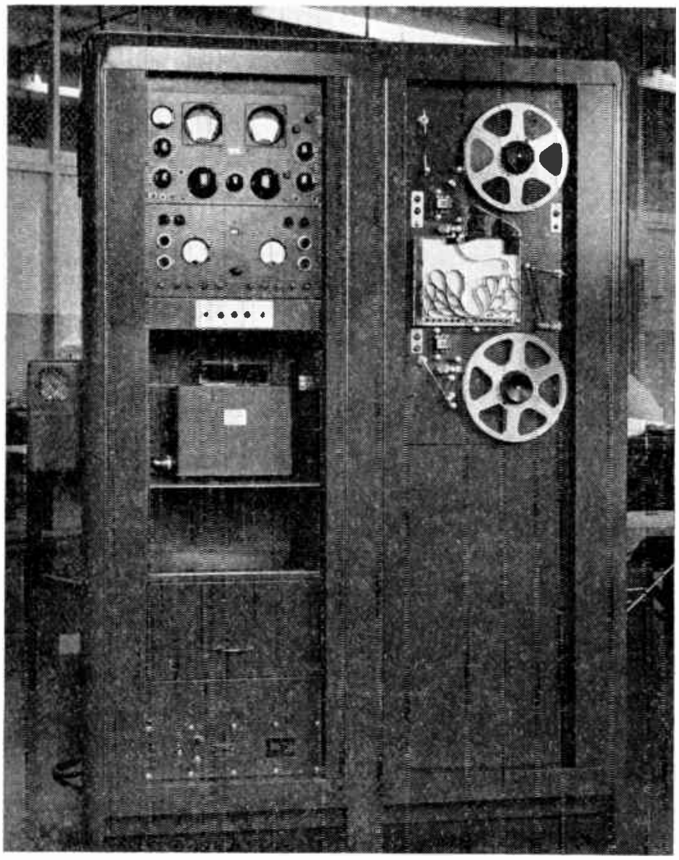

Fig. 10—Equipment cabinet—front view.

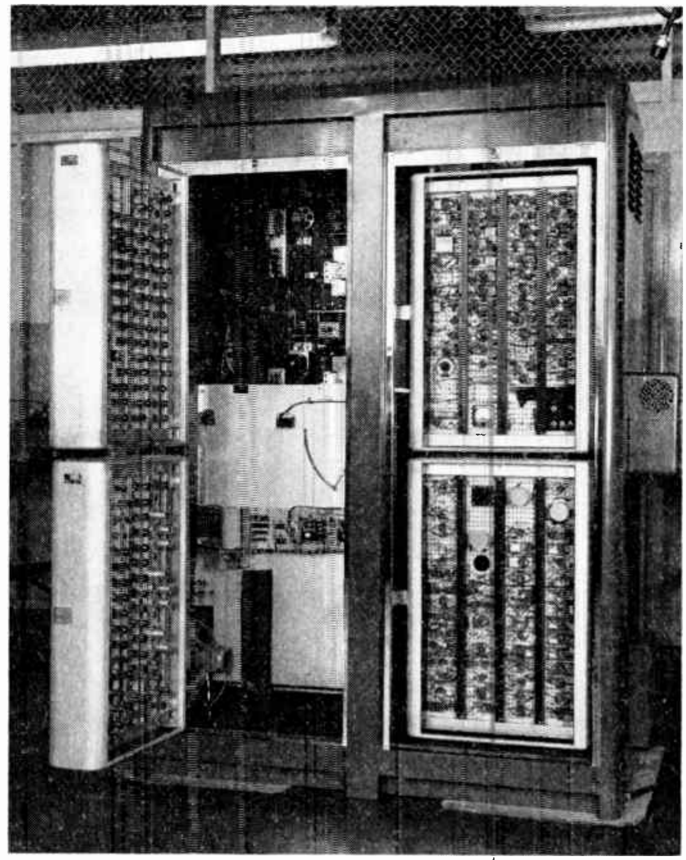

Fig. 11—Equipment cabinet—rear view.

The first five stages of the receiver register are connected to the output gate. Characters are read out of the register in parallel by a letter pulse on the output gate which is generated in the receiver clock when all five digits of a character are simultaneously presented to the gate inputs.

When a stop signal is detected, the gate control unit resets flip-flop 1, closing the output gate and preparing the receiver control unit for the next transmission.

Tape Handling and Storage

The magnetic tape handler and store is shown in a front view of the equipment (Fig. 10). In operation, tape is pulled off the upper reel by a drive capstan located just above the store, passing the erase magnet and the write head en route. Tape is removed from an aperture at the bottom of the store and pulled over the read head by a second drive capstan. Slack tape is taken up by the lower reel.

The tape drives are designed for a tape speed of five inches per second. About 35 feet of tape can be accommodated in the store, giving a capacity of 11,000 characters. A "store full" indication is obtained when a loop of tape rises into a hooded enclosure on the upper right-hand corner of store, interrupting a light beam. When the store is empty, a tension arm to the right of the store is pulled down, operating a microswitch which stops the lower drive capstan.

The read-out drive is required to stop on each character in order to simplify the problem of synchronizing the store read-out rate with the printing rate. Acceleration and braking times of 5 milliseconds or better are required, and these are achieved by means of a differential gear drive mechanism similar in principle to that used in the Ferranti High Speed Tape Reader. The input shaft of the drive rotates continuously, and the output is transmitted via a differential gear to two output shafts. Each output is provided with a brake drum and two brake shoes operated by electromagnets. In operation, the output shafts are braked alternately. One of these shafts carries the tape drive capstan, and the tape can be either braked or driven by energizing the appropriate electromagnet.

Because the tape speed is relatively slow, servo control of the tape reels is unnecessary. The supply reel is controlled by a band brake which is released by a tension arm as the input drive takes up tape, and take-up reel is controlled by a slipping clutch. Standard $10\frac{1}{2}$-inch NAB reels having a capacity of 2000 feet of tape give a minimum of 27 hours uninterrupted operation.

The input store for paper tape is located inside the equipment cabinet and can be seen in Fig. 11. It is physically much larger than the magnetic tape store, having a capacity of about 300 feet of paper tape, but is provided with similar devices for sensing store full and store empty conditions. Tape is fed directly into the paper tape store from a reperforator located on a shelf on the right of the cabinet and is removed by the high-speed tape reader drive during transmission. As in the case of the magnetic tape store, a start-stop drive is used in the tape reader to simplify synchronization of the reader with the link transmission rate. The reader is located in a recess in the front of the cabinet and can be seen in Fig. 10.

During transmission, tape passes through the reader at a rate of about 13 inches per second. A rotary cutter located on the left side of the cabinet disposes of the used tape by cutting it into quarter-inch segments which fall into a removable drawer.

The Electronic Transmitter Distributor

Information in the magnetic tape store is converted into a teleprinter line signal by the electronic transmitter distributor. This unit controls the magnetic tape read-out drive, adds start and stop pulses to the character codes as they are read from the tape, and converts the message into serial form. It is designed for 60-wpm operation, but can readily be modified for any of the standard printing speeds. A block diagram of the unit is shown in Fig. 12.

The output pulses from the read heads are amplified in six read amplifiers and set the first six stages of a seven-stage shift register simultaneously. By virtue of a continuous mark pulse input to this register, all seven stages contain marks just prior to the reading operation. After reading, the seventh stage of the register contains a mark, corresponding to the printer stop pulse; the sixth stage contains a space, corresponding to a printer start pulse; and the remaining stages contain the five digits of a character code.

During the read operation, the timing generator is inhibited. This inhibit is removed by the sync pulse as a character is read, and the timing generator begins producing shift pulses which cause the register contents to pass serially through the seventh stage, and thence via a line relay to the printer. When the last digit has cleared the register, the seventh stage will again contain a stop, and the timing generator will be inhibited.

The movement of tape past the read head is controlled by the tape control flip-flop. At the beginning of a stop period, this flip-flop is set by a pulse from the timing generator and the tape drive is energized. With normal character stacking on the tape, a character will be read about 10 milliseconds later, and the tape stops when a character sync pulse resets the tape control flip-flop. In order to provide an adequate stop pulse for the printer, however, the timing generator is inhibited until 31 milliseconds have elapsed from the beginning of the stop period. When large gaps exist between characters on the tape, reading will not occur within 31 milliseconds, and in this case the timing generator inhibit is removed when a sync pulse is read. If the tape store is empty, operation of the transmitter distributor is inhibited by a sensing switch mounted on the tape handler panel.

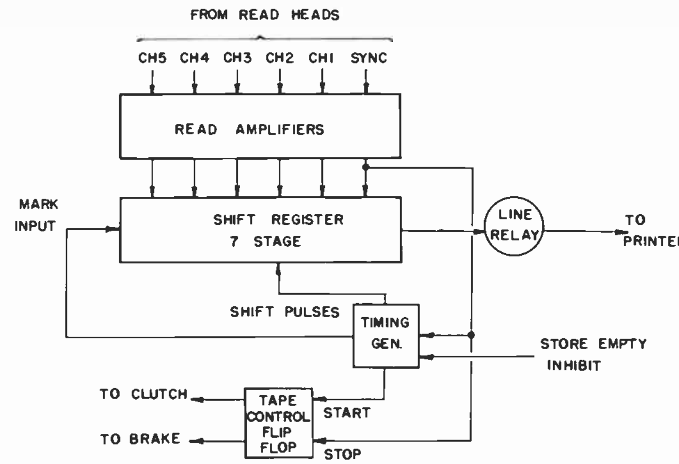

Fig. 12—Electronic transmitter distributor.

Power Supplies

Five dc supplies are used, providing output voltages of ± 67.5 volts, ± 135 volts, and $+360$ volts. The 360-volt supply is a conventional tube rectifier type delivering 200 ma and provides power for operating electromechanical tape drives. The remaining voltages are obtained by series connecting four supplies, each capable of providing an output of 67.5 volts at 1 amp. In these supplies, bridge rectifiers employing high efficiency germanium diodes are used in conjunction with transformers and filter chokes having low dc resistance. The internal resistance of the supply for dc is small, and the regulation from half to full load is about three per cent. Since the load is relatively constant, adequate stability of the supply voltages is obtained by ac regulation of the input, together with high over-all power efficiency and good reliability.

Test Facilities

Routine maintenance of the data handling equipment is considerably simplified by internal test switching facilities. The modulation output signal can be switched into three circuits, as follows:

1) to the modulator, providing normal operation;
2) to the ppm detector, providing internal operation without reference to any of the link components;
3) to a test jack, for convenience in modulating a signal generator. When a suitable signal generator is available the radio receiver can be included in an internal test.

Test signals may originate from a special tape loop in the high-speed reader, or from a set of five code switches. Individual teletype characters, coded manually on these switches, can be read and transmitted at link rates. This facility affords a check on the operation of the tape reader and also provides repetitive signals which are useful in fault tracing.

Normal gating operation is simulated on internal test by means of a manually operated switch.

Physical Details

The JANET data handling equipment and the radio receiver are housed in a single cabinet about 75 inches high, 63 inches wide, and 28 inches deep, and having a total weight of about 1200 pounds. Fig. 10 shows the front panel layout. The tape handler and power supplies are located on the right side: on the left are the radio receiver, power control unit, high-speed reader, and ac regulator.

Most of the circuitry is mounted on four easily accessible swing-out units at the rear of the cabinet, as shown in Fig. 11. Important circuit points on these units can be readily identified by means of a geometric reference system used in the circuit diagrams. These two features simplify the servicing problem considerably. The rear of the cabinet can be completely closed by two roller doors.

Of a total of 295 tubes in the cabinet, 22 are used in the radio receiver and preamplifier. Eighty-two per cent of the remaining tubes are type 5965—a twin triode designed for computer service. In about 3000 hours operation, tube failures in the prototype equipment have occurred at an average rate of approximately one per cent per thousand hours.

Although tube circuits are used, no difficulty is anticipated in converting much of the design to transistor and magnetic circuits, and the saving in size, weight, and power input which can be achieved by such a conversion is considerable. The power input to the cabinet of the present equipment is approximately 1700 watts, of which about 1000 watts are dissipated by the tube heaters. It has been estimated that the power consumption can be reduced to about 350 watts by the use of transistors and magnetics.

Appendix II

Equipment Circuits

Most of the machine circuits are of the on-off or two-state type and have been designed on the basis of a negative-going signal convention. The presence of a pulse or control waveform is recognized by a negative excursion from the normal or quiescent state, and, as a result, "and" gates are composed of triodes having a common cathode load and "or" gates of diodes having a common anode load. Signals having amplitudes between 10 and 30 volts and edge speeds of about 10 volts per microsecond will provide satisfactory operation in most of the circuits. DC coupling is used extensively.

Since the JANET equipment is relatively complex, considerable emphasis was placed on reliability in the design. The high-speed data handling circuits operate at rates which are relatively slow compared with modern computing circuits so that it was possible to design circuits for low power dissipation and to operate the tubes very conservatively. In most circuits, a tolerance of ± 10 per cent from nominal values of resistances and applied voltages has been assumed, and the dc design is such that satisfactory performance will be obtained if all the resistance values and voltages lie simultaneously at the worst tolerance limit. In critical circuits close tolerance high quality components are used for additional reliability.

About 75 per cent of the machine circuitry is made up of 10 basic circuits shown in schematic form in Fig. 13. Two standard resistor divider chains, shown in the inverters of Fig. 13(a) and 13(b), are used in dc coupled circuits throughout the machine. In some circuits speed-up capacitor C has been omitted, and the value of R is chosen to limit grid current to a safe value in cases where the input waveform has a large positive excursion. Crystal diodes are used to limit the positive excursion of the output waveform at ground; the negative excursion depends on the voltage drop across a tube in its conducting state.

The standard flip-flop circuit, shown in Fig. 13(c) uses the same resistor chain as the inverter of Fig. 13(a). DC triggering via germanium diodes is used, and the output is normally taken off the grid tap points on the resistor chain. In this circuit, the positive excursion of the output waveform is limited at ground level by grid current in the tube. The counter circuit of Fig. 13(d) uses the same resistor chain as the inverter of Fig. 13(b). AC triggering with a differentiating network and two germanium diodes is used. The circuit is designed so that the output waveform at the plate tap has characteristics suitable for triggering another counter.

The shift register stage of Fig. 13(e) is derived from the standard flip-flop by adding a trigger tube V1. The delay of a shift register stage of this type is determined by the interval between shift pulses. The circuit is designed so that the input to the grids of V1 can be taken directly from the flip-flop grid taps of a preceding shift register stage.

Several versions of the cathode coupled one shot are used: one version for generating shift pulses is shown in Fig. 13(f). In this circuit, a triode V1 is used to plate trigger the one shot, and the output is taken from the cathodes of V2 and V3. The positive dc level of the output is defined by a diode clipper V4 on the grid of V3, and the negative level by a divider chain on the grid of V2. Other circuits of this type differ in dc levels and widths of the output pulse, and in the method of triggering.

Cathode followers are used extensively for their impedance transformation properties. A standard circuit is shown in Fig. 13(g). This circuit is designed to operate from the grid tap of a flip-flop, and the design is a compromise between economy of power and negative edge speed. With 250-pf shunt capacity across the output, the response to a negative step of 20-volts amplitude has a fall time of about 2 μsec. Cathode follower outputs are run via unshielded wire throughout the machine, with no difficulties arising due to pick-up from adjacent wires.

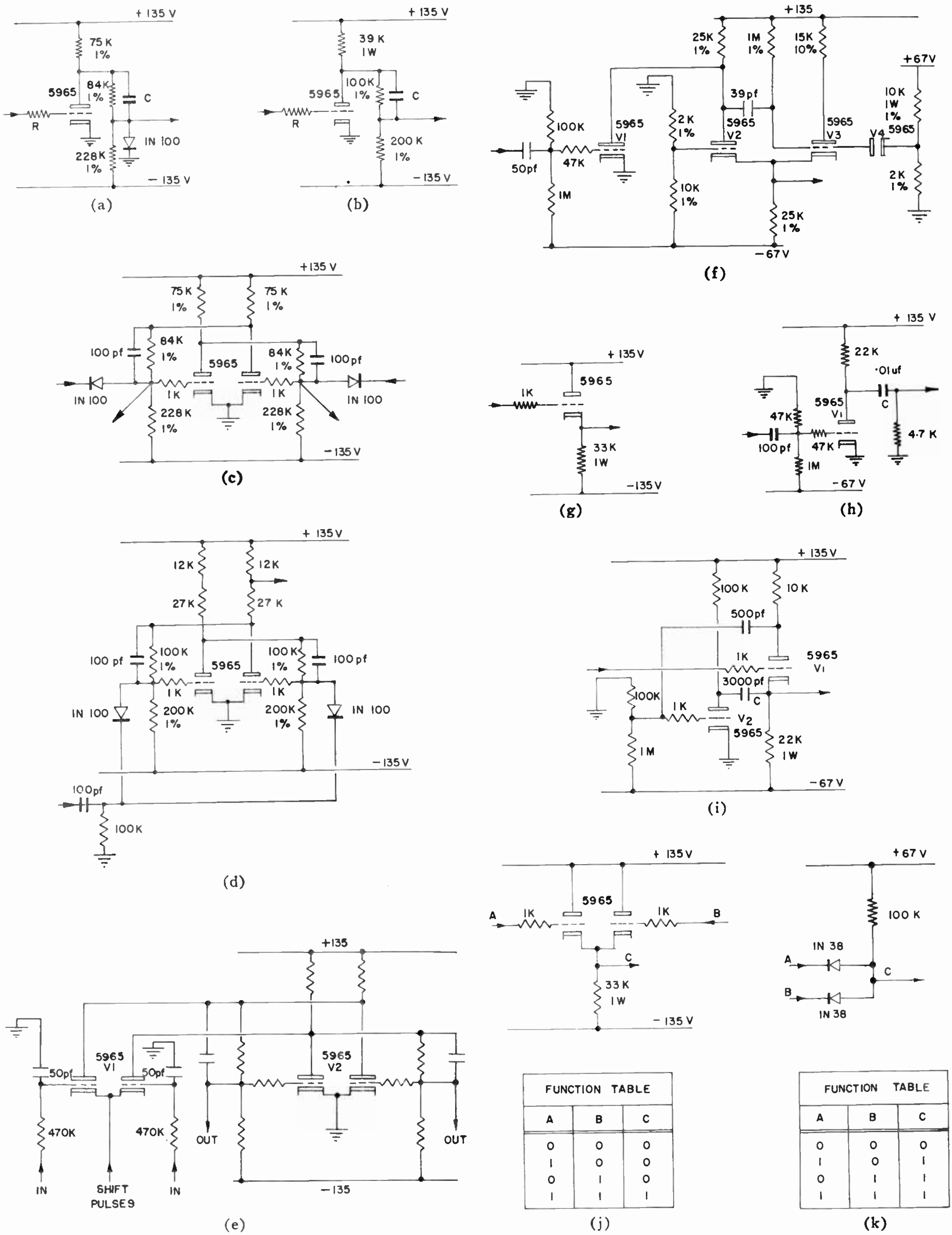

FUNCTION TABLE (j)

A	B	C
0	0	0
1	0	0
0	1	0
1	1	1

FUNCTION TABLE (k)

A	B	C
0	0	0
1	0	1
0	1	1
1	1	1

Fig. 13—(a) and (b) Inverter. (c) Flip-flop. (d) Counter. (e) Shift register. (f) Cathode coupled one shot. (g) Cathode follower. (h) Buffer amplifier. (i) Pulse driver. (j) Triode "and" gate. (k) Diode "or" gate.

Many of the timing waveforms in the machine are negative-going spikes produced by the circuit of Fig. 13(h). The operation of this circuit is similar to that of hard tube pulser circuits. V1 is normally cut off, and the storage capacitor C is charged to the full power supply voltage. When a positive step is applied to the input, a spike appears at the grid of V1, causing it to conduct heavily for a period of about 10 μsec, and generates a negative spike at the output. The storage capacitor C is only partially discharged during the pulse and recharges in the interval between pulses. The circuit is economical of power, is inherently capable of generating fast negative edges, and is not damaged by accidental shorts on the output.

The pulse driver circuit in Fig. 13(i) combines the best features of the cathode follower and buffer amplifier circuit and is used when the dc level and shape of the input signal must be preserved approximately. In this circuit, the amplifier tube V2 is normally cut off. With heavy capacity loading on the output line, V1 will tend to cut off when a fast negative edge is applied to the input grid, and a positive pulse will be generated in the plate circuit of V1 which will cause V2 to conduct. Consequently, the cathode of V1 will be pulled down via the coupling capacitor C. The circuit will reproduce a flip-flop grid waveform with a fall time of about 2 μsec and 500 pf of shunt loading.

A triode "and" gate is shown in Fig. 13(j). The operation of the gate as a logical element is illustrated by the associated function table, in which a signal level of zero volts corresponds to 0 in the binary code and a negative signal level corresponds to 1. The gate output will be 1 only when both inputs are 1. Although a two-input gate is shown, the number of triodes operating into a common cathode load can be increased to provide more inputs.

In the diode "or" gate of Fig. 13(k), the output is 1 if either or both inputs are 1. The number of inputs on a diode gate of this type is limited by the back resistance of the diodes.

ACKNOWLEDGMENT

Development of the JANET equipment was sponsored by the Defence Research Board, Ottawa, Canada, under contract No. P69-8-479, and was directed by Dr. P. A. Forsyth and D. R. Hansen of the DRB. The design, construction, and testing of the equipment was carried out in the Research Division of Ferranti Electric Limited, Toronto, Canada.

Intermittent Communication with a Fluctuating Signal*

G. FRANKLIN MONTGOMERY†, SENIOR MEMBER, IRE

Summary—**Intermittent transmission is proposed as a method to combat the effects of signal fading. Message error and average transmission rate are functions of operating bandwidth and threshold signal-to-noise ratio. The method is evaluated for Rayleigh-fading signals, using binary frequency modulation and phase modulation. One variable-bandwidth system is examined. The theoretical advantage (power gain>40 db for a binary error$=10^{-6}$) is reduced by practical limitations but should be nearly realized for some systems.**

Definition of Symbols

B = bandwidth of the signal at carrier frequency, cps.

B_m = bandwidth for an intermittent system of maximum capability, cps.

B_0 = characteristic bandwidth, that for which the mean signal-to-noise power ratio is unity, cps.

B_{0c} = characteristic bandwidth for a continuous system, cps.

B_u = limit of bandwidth above which the signal is not coherent, cps.

dp_s/dr = relative probability of a specified signal amplitude or signal-to-mean noise power ratio.

f_n = fraction of total transmission initiated by noise.

G = intermittent power gain, the reduction in power permitted by operating a system intermittently instead of continuously.

${}_{FM}G_m$ = intermittent power gain of a binary fm system of maximum capability.

${}_{PM}G_m$ = intermittent power gain of a binary pm system of maximum capability.

G_v = power gain of a variable-bandwidth system.

${}_{FM}G_v$ = power gain of a variable-bandwidth binary fm system.

h = time rate of erroneous message elements, elements per second.

$I(x)$ = the probability integral.

M = average transmission rate, message elements per second.

* Original manuscript received by the IRE, April 16, 1957; revised manuscript received August 20, 1957. This work was supported by the AF Cambridge Research Center, Bedford, Mass.

† National Bureau of Standards, Washington 25, D. C.

M_m = average transmission rate for an intermittent system of maximum capability, message elements per second.

N_0 = rms noise amplitude.

p = average probability of an erroneous message element.

p_i = probability of an erroneous message element at a specified signal-to-mean noise power ratio.

p_s = probability that the signal amplitude, or the signal-to-mean noise power ratio, exceeds a specified value.

r = ratio of the signal power to the mean noise power.

r_t = threshold signal-to-noise power ratio above which transmission occurs.

r_{tm} = threshold signal-to-noise power ratio for an intermittent system of maximum capability.

r_u = upper limit of the possible signal-to-noise power ratio for a practical system.

R = a constant signal-to-noise power ratio.

S = signal amplitude.

S_0 = rms signal amplitude.

Introduction

We are nearly always forced to communicate with signals whose received amplitudes vary in time, and our ability to communicate precisely is impaired by this fluctuation. When the signal amplitude is large compared with the system noise, the received message can be interpreted with great certainty; when the amplitude is small, the message will be uncertain and perhaps useless.

Intermittent transmission, which has often been used in manual operation, is one method of reducing the fading error. Suppose, for example, that A is signaling to B. If A's signal fades so that B cannot copy accurately, B signals A to stop sending. A waiting period follows until A's signal has grown stronger, whereupon B signals A to resume, and so on. By restricting A's transmission to intervals when the signal amplitude is relatively large, B increases the probability that he will copy the message correctly. In addition, it may be possible for A to signal more rapidly during the active intervals than would be expedient in continuous transmission, so that the time required to transmit a complete message shall be no greater than before.

The intermittent method should be particularly useful when it is effected by automatic means. Provision must be made, of course, for a command link from receiver to transmitter, for message storage at the transmitter, and, if the message is to be delivered at a continuous rate, for message storage at the receiver.

It is the purpose of this paper to examine the method quantitatively and to evaluate its benefit for a particular type of signal and signal fluctuation. It is assumed that the interference is band-limited Gaussian noise and that the maximum frequency of the signal amplitude variation is less than the maximum signaling rate, *i.e.*, that the signal amplitude remains substantially constant for at least the duration of one element in the message.

Analysis

Any message can be considered a time sequence of elements. For any type of signal modulation we can define a probability $p_i(r)$ that an element of the message will not be copied with the required precision, where r is the signal power, during the interval when the element is received, divided by the average noise power. If the fluctuation of signal amplitude can be specified, we can define a relative probability $dp_s/dr(B, r)$ for this power ratio; *i.e.*, dp_s is the probability that the ratio is contained in the interval $(r, r+dr)$, and B is the system bandwidth. Knowing these probabilities, we can calculate the average probability that a message element will not be copied with the required precision.

$$p = \int_{r_1}^{r_2} p_i \frac{dp_s}{dr}\, dr \tag{1}$$

where r_1 and r_2 are the limits within which we choose to observe r.

The intermittent system of practical interest is one in which transmission occurs whenever r exceeds a predetermined threshold r_t, so that

$$p(B, r_t) = \int_{r_t}^{\infty} p_i \frac{dp_s}{dr}\, dr. \tag{2}$$

For most modulation systems, the active transmission rate in message elements per second is approximately equal to the bandwidth B in cps. The average transmission rate, therefore, is

$$M(B, r_t) = B \int_{r_t}^{\infty} \frac{dp_s}{dr}\, dr. \tag{3}$$

Eqs. (2) and (3) are the defining equations for the intermittent system. If intermittent operation is to yield an improvement over continuous operation, the probabilities p_i and dp_s/dr must satisfy certain conditions; for example, the functions (2) and (3) must be such that, if p is chosen constant, an increase in B yields an increase in M. It is shown in the Appendix that a sufficient condition for improvement is[1]

$$\frac{d}{dB} \int_0^{\infty} p_i \frac{dp_s}{dr}\, dr < \frac{p_i(0)}{B}. \tag{4}$$

[1] The integral in (4) is the probability of error when the system is operated continuously. Improvement (*i.e.*, a smaller p for a given M, or a larger M for a given p) will be obtained if the rate of change of the continuous error $p(B, 0)$ with bandwidth is less than the reciprocal of the bandwidth times a constant, $p_i(0)$. Let $h = Bp(B, 0)$ be the number of incorrectly received message elements per unit time. Then, if p is small, (4) is approximately equivalent to $\delta h < p_i(0)\delta B$, or the increase in error rate is less than $p_i(0)$ times the increase in bandwidth required to generate the additional error. For binary transmission, this reduces to $\delta h < \frac{1}{2}\delta B$. Condition (4) is sufficient for improvement but not necessary, for we can postulate p_i and dp_s/dr such that (4) is not satisfied and such that improvement is obtained for $r_t > R$, where R is a constant >0.

In principle, it should be possible to operate intermittently using any type of modulation, but it will be technically simpler to use a system wherein the message is independent of amplitude variation, *i.e.*, some form of angle modulation. For specific evaluation, therefore, we choose narrow-band frequency modulation and phase modulation, and a message constituted by a sequence of binary symbols.

An important class of signals consists of those (*e.g.*, ionospheric and tropospheric scatter signals) whose amplitudes are distributed according to the Rayleigh formula[2]

$$p_s(S) = e^{-(S^2/S_0^2)} \tag{5}$$

where p_s is the probability that the signal amplitude exceeds S, and S_0^2 is the mean-square signal amplitude. We define the characteristic bandwidth B_0 of the system as the bandwidth for which the average signal-to-noise power ratio is unity. If N_0^2 is the mean-square amplitude of the system noise, then

$$\frac{S_0^2}{N_0^2} = \frac{B_0}{B} \tag{6}$$

and

$$p_s(r) = e^{-(B/B_0)r}. \tag{7}$$

Frequency Modulation

It has been shown[3] that for a binary fm signal, the probability of a symbol error is

$$p_i = \tfrac{1}{2}e^{-r}. \tag{8}$$

From substitution of (7) and (8) in (2), the average binary error is

$$\begin{aligned} p &= \frac{1}{2}\int_{r_t}^{\infty} \frac{B}{B_0} e^{-(1+B/B_0)r}\, dr \\ &= \frac{1}{2(1+B_0/B)} e^{-(1+B/B_0)r_t} \end{aligned} \tag{9}$$

and from substitution of (7) in (3), the average rate in binary symbols per second is

$$M = Be^{-(B/B_0)r_t}. \tag{10}$$

But we can eliminate r_t in (9) and (10), so that

$$M = B[2p(1 + B_0/B)]^{1/(1+B_0/B)}. \tag{11}$$

Now, for a constant p, M will be a function of transmission bandwidth generally like that in Fig. 1, where M/B_0 has been plotted against B/B_0 for $p=10^{-3}$. Inspection of (11) shows that if p is sufficiently small, the function M has two inflection points and for various ranges of B reduces to the following approximations:

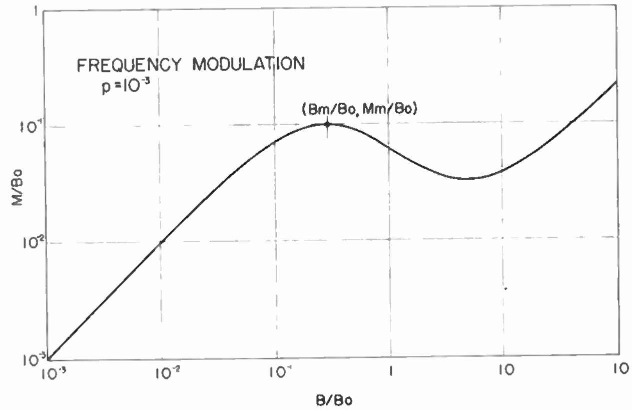

Fig. 1—Variation of average transmission rate M with operating bandwidth B for binary frequency modulation; constant average error $p=10^{-3}$.

$$M \approx B, \qquad B \ll B_0 \tag{12}$$

$$M \approx 2Bp^{1/2}, \qquad B \approx B_0 \tag{13}$$

$$M \approx 2Bp, \qquad B \gg B_0. \tag{14}$$

Evidently there will be practical advantage in operating at the maximum shown in Fig. 1 as $(B_m/B_0, M_m/B_0)$. If, for a constant p in (11), $dM/dB=0$, then

$$1 + \frac{B_0}{B} + \frac{B}{B_0} + \ln 2p\left(1 + \frac{B_0}{B}\right) = 0 \tag{15}$$

where ln indicates the natural logarithm. If $p \ll 1$, the solution B_m of (15) corresponding to the maximum will satisfy $B_m/B_0 < 1$. With this condition,

$$p = \frac{1}{2(1 + B_0/B_m)} e^{-(1+B_0/B_m+B_m/B_0)} \tag{16}$$

and

$$\frac{M_m}{B_0} = \frac{B_m}{B_0} e^{-(1+B_0/B_m+B_m/B_0)/(1+B_0/B_m)} \tag{17}$$

which are plotted in Fig. 2. The operating parameter

$$r_{tm} = \frac{1 + B_0/B_m + B_m/B_0}{1 + B_m/B_0} \tag{18}$$

is plotted on the same grid.[4]

Phase Modulation

It has been shown[3] that for a binary pm signal, the probability of a symbol error is

$$p_i = \tfrac{1}{2}[1 - I(r^{1/2})] \tag{19}$$

where

$$I(x) = \frac{2}{\pi^{1/2}}\int_0^x e^{-x^2} dx$$

[2] Lord Rayleigh, "The Theory of Sound," Dover Publications, New York, N. Y., vol. 1, pp. 35–42; 1945.

[3] G. F. Montgomery, "A comparison of amplitude and angle modulation for narrow-band communication of binary-coded messages in fluctuation noise," PROC. IRE, vol. 42, pp. 447–454; February, 1954.

[4] As $p \to 0$ for this case, $B_m \to 0$, $r_{tm} \to \infty$, and the duty factor $M_m/B_m \to 1/e$ from below. Transmission is therefore inactive for at least 63 per cent of the time.

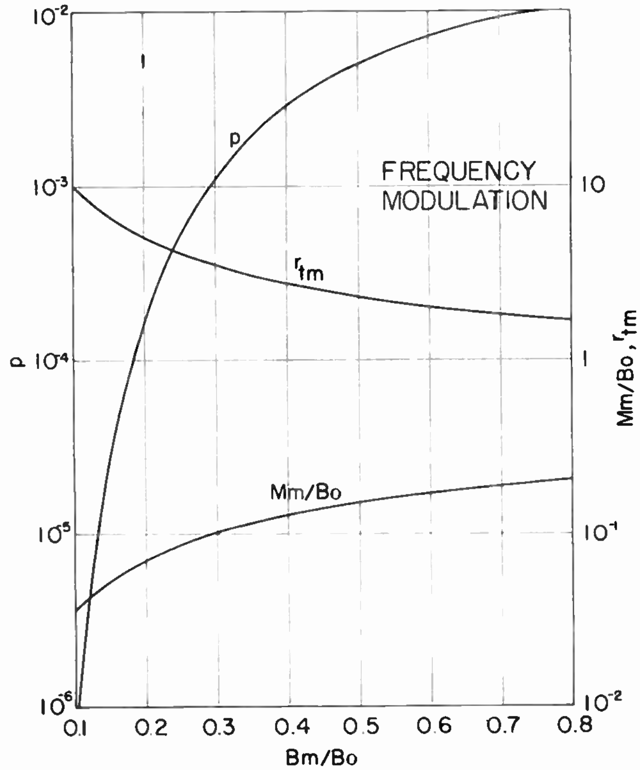

Fig. 2—Intermittent system parameters for binary frequency modulation at maximum capability.

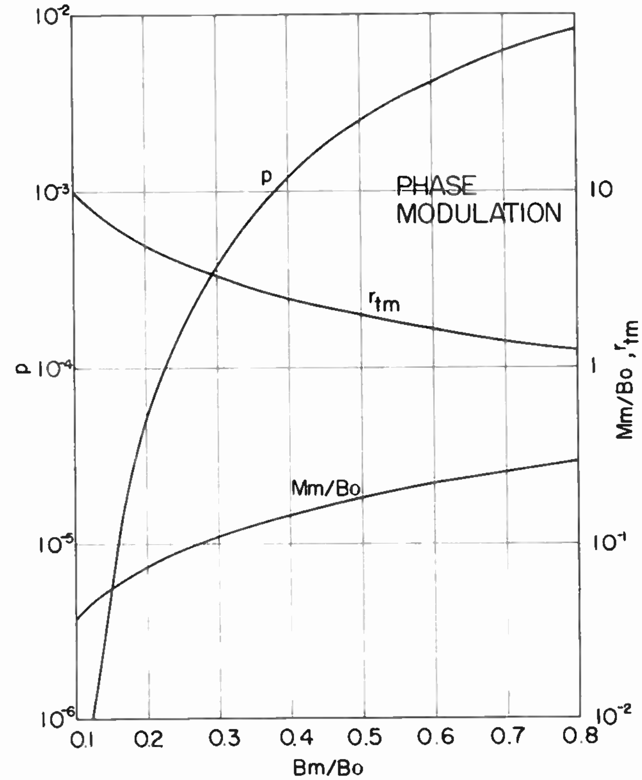

Fig. 3—Intermittent system parameters for binary phase modulation at nearly maximum capability.

the tabulated[5] probability integral. From substitution of (7) and (19) in (2), the average binary error is

$$p = \frac{1}{2}\int_{r_t}^{\infty} [1 - I(r^{1/2})] \frac{B}{B_0} e^{-(B/B_0)r} dr. \qquad (20)$$

After integration by parts,

$$p = \tfrac{1}{2}[1 - I(r_t^{1/2})]e^{-(B/B_0)r_t} - \frac{1}{2(1 + B/B_0)^{1/2}}\{1 - I[(1 + B/B_0)^{1/2}r_t^{1/2}]\} \qquad (21)$$

and

$$M = Be^{-(B/B_0)r_t} \qquad (10)$$

as before. We can eliminate r_t in (10) and (21), but M is not obtained explicitly by doing so. Note, however, that if $B/B_0 < 1$ and $r_t > 1$, p changes less rapidly with B than with r_t. Let us then hold r_t constant in (10) and find a maximum M by differentiating with respect to B alone. This maxinium will not be as large as could be obtained by maintaining p constant rather than r_t, but it will be close enough for engineering purposes. Then, for $dM/dB = 0$,

$$r_{tm} = \frac{B_0}{B_m} \qquad (22)$$

$$p = \frac{1}{2e}\{1 - I[(B_0/B_m)^{1/2}]\} - \frac{1}{2(1 + B_m/B_0)^{1/2}}\{1 - I[(1 + B_0/B_m)^{1/2}]\} \qquad (23)$$

and

$$\frac{M_m}{B_0} = \frac{B_m}{B_0 e} \qquad (24)$$

which are plotted in Fig. 3.

Intermittent Power Gain

It will be useful to calculate the power advantage of intermittent over continuous operation. The comparison is made easily on the basis of system gain, which is proportional to the characteristic bandwidth B_0. We shall assume that the reference continuous system has the same average binary error p and transmission rate M as the intermittent system and a characteristic bandwidth B_{0c}. Then, we define the intermittent power gain

$$G = \frac{B_{0c}}{B_0} \qquad (25)$$

which is the ratio of continuous system gain to intermittent system gain required for equal performance.

For continuous frequency modulation,

$$p = \frac{1}{2(1 + B_{0c}/B)} \qquad (26)$$

which is obtained by setting $r_t = 0$ in (9). Since $M = B$,

$$B_{0c} = M\left(\frac{1}{2p} - 1\right) \qquad (27)$$

[5] B. O. Peirce, "A Short Table of Integrals," Ginn and Co., Boston, Mass., pp. 116–120; 1929.

which is the required characteristic bandwidth for the continuous system. If the intermittent system is operated at its maximum,

$$ {}_{FM}G_m = \frac{B_{0c}}{B_0} = \frac{M_m}{B_0}\left(\frac{1}{2p} - 1\right) \tag{28} $$

which can be calculated from the data of Fig. 2. A graph of (28) as a function of p is given in Fig. 4.

For continuous phase modulation,

$$ p = \frac{1}{2}\left[1 - \frac{1}{(1 + B/B_{0c})^{1/2}}\right] \tag{29} $$

from setting $r_t = 0$ in (21). But $M = B$. Then,

$$ B_{0c} = \frac{M(1-2p)^2}{4p(1-p)}. \tag{30} $$

If the intermittent system is operated at its maximum,

$$ {}_{PM}G_m = \frac{B_{0c}}{B_0} = \frac{M_m}{B_0}\cdot\frac{(1-2p)^2}{4p(1-p)} \tag{31} $$

which can be calculated from the data of Fig. 3 and is plotted in Fig. 4.

An Example

Suppose that a communication circuit using frequency-shift keying is to support one 60-word-per-minute teletype channel with a binary error of 10^{-4}. If the circuit is to operate continuously using a bandwidth $B = 50$ cps, the required characteristic bandwidth is, from (27),

$$ B_{0c} = (50)(4999) = 2.5 \times 10^5 \text{ cps}. $$

If the system is operated intermittently at its maximum rate, then, from Fig. 2,

$$ M_m = 0.065 B_0 = 1.6 \times 10^4 \text{ binary symbols per second.} $$

This system now has 320 times the required capacity. The operating bandwidth is

$$ B_m = 0.18 B_0 = 4.5 \times 10^4 \text{ cps} $$

and the duty factor is

$$ \frac{M_m}{B_m} = 0.36. $$

If we return to the original specification ($M_m = 50$, $p = 10^{-4}$), the intermittent power gain from Fig. 4 is 25 db, or 316, and

$$ B_0 = \frac{B_{0c}}{{}_{FM}G_m} = 7.9 \times 10^2 \text{ cps} $$

is the required characteristic bandwidth for the intermittent system. The operating bandwidth is

$$ B_m = 0.18 B_0 = 1.4 \times 10^2 \text{ cps}. $$

The threshold signal-to-noise ratio, from Fig. 2, is

$$ r_{tm} = 5.6 $$

and the duty factor is 0.36 as before.

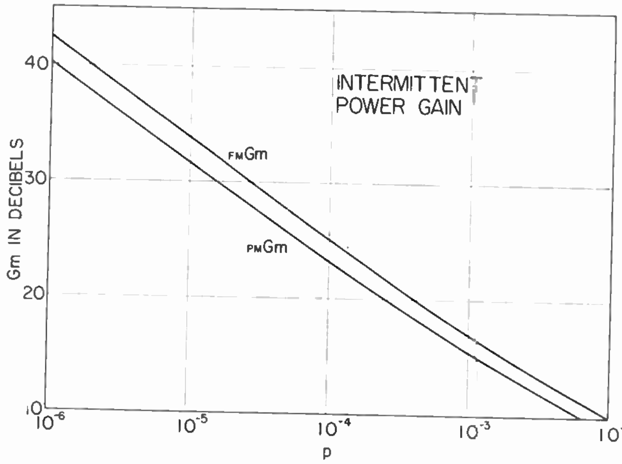

Fig. 4—Power gain of intermittent frequency and phase modulation referred to continuous frequency and phase modulation.

Variable-Bandwidth Systems

So far, we have found that intermittent operation with a fixed transmission bandwidth yields an improvement over continuous operation. This finding suggests that a system using a bandwidth and transmission rate that vary continuously with received signal-to-noise ratio might be superior to both of the simpler systems. Such a variable-bandwidth system will be difficult to realize, but it is interesting at least to calculate its superiority.

We must recognize that there are an infinite number of possible specifications for the variation of bandwidth with the power ratio r. We shall choose only one of these and, in combination with Rayleigh fading and binary frequency modulation, evaluate the defining equations. Let us assume that the error probability is to be independent of the transmission bandwidth; then, $r = R$ (constant), and from (8),

$$ p = p_i = \tfrac{1}{2}e^{-R}. \tag{32} $$

If B_0 is the characteristic bandwidth,

$$ p_s(B) = e^{-(B/B_0)R} \tag{33} $$

so that

$$ M(B_0, R) = \int_0^\infty \frac{BR}{B_0} e^{-(B/B_0)R} dB = \frac{B_0}{R}. \tag{34} $$

But

$$ R = \ln\frac{1}{2p} \tag{35} $$

so that

$$ \frac{M}{B_0} = \frac{1}{\ln\left(\frac{1}{2p}\right)} \tag{36} $$

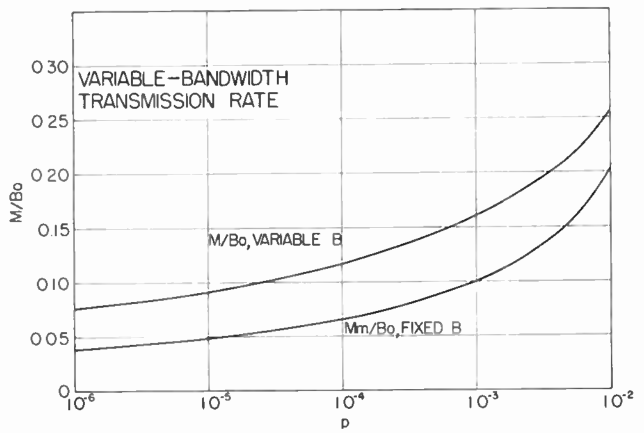

Fig. 5—Comparison of average transmission rates for variable-bandwidth and intermittent, fixed-bandwidth frequency modulation.

which is plotted in Fig. 5. A graph of M_m/B_0 for intermittent frequency modulation is shown on the same grid for comparison.

A power gain G_v can be defined as the ratio of characteristic bandwidths for a continuous system and a variable-bandwidth system having the same modulation and equal average transmission rates and average errors. For frequency modulation with $p \ll 1$,

$$_{FM}G_m \approx \frac{1}{2p \ln\left(\frac{1}{2p}\right)}. \tag{37}$$

If $p = 10^{-6}$,

$$_{FM}G_m = 45.8 \text{ db}$$

compared with 42.5 db for the intermittent system.

Discussion

The practical limitations of three assumptions made in the analysis should now be noted. First, the infinite limits used in preceding integrals are a mathematical convenience; the Rayleigh amplitude distribution is based on the assumption that the signal is the sum of an infinite number of infinitesimal signals of random phase. Consequently, the mathematical probability $p_s(r)$ that the signal-to-noise ratio will exceed r, however large, is always greater than zero. This statement will not be true in practice. Whatever the transmission medium may be, there will be a finite r_u, depending upon system gain, for which $p_s(r_u) = 0$. The ratio r_u may often be much greater than unity, but its limitation should be held in mind, particularly for wide-band systems.

Second, we have assumed that it will always be possible to determine precisely whether the signal-to-noise ratio is greater or less than the threshold r_t. Actually, this measurement can be made only with a certain probability; it is generally impossible to measure the signal amplitude with whatever precision we may choose.[6]

The practical range of parameters for intermittent operation is such, however, that this deficiency should contribute little to system malfunction. In the numerical example, for instance, operating at maximum capability, the threshold ratio is

$$r_{tm} = 5.6.$$

Now, suppose that the maximum frequency of the fading variation does not exceed $B/5$. Then, by simple filtering, it is possible to increase the signal-to-noise ratio at the input to the threshold detector by $\sqrt{5}$, and the fraction of total transmission that is initiated by noise rather than signal becomes

$$f_n = \frac{(1 - M_m/B_m)}{M_m/B_m} e^{-\sqrt{5}r_{tm}} = 6.6 \times 10^{-6}$$

which represents an almost negligible increase in error.

The third assumption is implicit in the idea that whatever amplitude we choose to measure does, in fact, represent the amplitude of the signal within the limitation of the second assumption. In many systems, the amplitude actually measured will be either a smoothed (averaged) amplitude of the total signal or the amplitude of a small band of signal components, perhaps including the signal carrier. Whatever is measured, the relative phases and amplitudes of the measured components may vary so rapidly under certain conditions that it will be impossible to determine the amplitude within the required interval of one message element. The assumption will fail, therefore, when the received signal lacks coherence over a sufficient interval. Lack of coherence is often described as "multipath propagation" or "selective fading," and, practically, there will always be a transmission bandwidth B_u above which coherence is no longer maintained.

These considerations are especially important for the alternate, but probably impractical, mode of intermittent operation corresponding to the conditions of (14). In this case, the theoretical average transmission rate increases without limit as the bandwidth is increased. In the numerical example, for instance, an average rate of 1.6×10^4 binary symbols per second can also be obtained by choosing

$$B = \frac{M}{2p} = 8 \times 10^7 \text{ cps}$$

with a threshold

$$r_t = \frac{B_0}{B} \ln \frac{B}{M} = 2.8 \times 10^{-2}$$

and a duty factor

$$\frac{M}{B} = 2 \times 10^{-4}.$$

The obvious practical disadvantages are the need for a large bandwidth, the possible difficulty in measuring a small r_t, and the long transmission delay.

[6] G. F. Montgomery, "Message error in diversity frequency-shift reception," Proc. IRE, vol. 42, pp. 1184–1187; July, 1954.

Conclusion

We have shown that operating a communication system intermittently, under proper conditions, reduces the message error caused by a fluctuating signal amplitude. Several practical limitations may trim the theoretical advantage of such a system, but in any case a theoretical power gain of over 40 db, for binary angle modulation with an error of 10^{-6}, is not easily discounted. At least one system of continuously variable bandwidth has been shown to yield still greater power advantage over continuous, fixed-bandwidth operation. The practical advantages of such systems have not yet been shown, and any of those discussed will be more difficult to realize technically than a continuous system of comparable performance. Economic advantage, however, may well outweigh technical difficulty with the passage of time.

Appendix

We wish to determine a condition that intermittent operation will yield a greater average transmission rate than continuous operation for the same average error.

Let p be constant. Then, from (2),

$$\frac{\partial p}{\partial B} dB + \frac{\partial p}{\partial r_t} dr_t = 0$$

and

$$\frac{dr_t}{dB} = -\frac{\frac{\partial p}{\partial B}}{\frac{\partial p}{\partial r_t}} = \frac{\frac{\partial p}{\partial B}}{p_i(r_t)\frac{\partial p_s}{\partial r_t}(B, r_t)}. \tag{38}$$

Now, from (3),

$$\frac{dM}{dB}(B, r_t) = \frac{\partial}{\partial B}\left[B\int_{r_t}^{\infty}\frac{dp_s}{dr}dr\right] - B\left[\frac{\partial p_s}{\partial r_t}(B, r_t)\right]\frac{dr_t}{dB}. \tag{39}$$

From substitution of (38),

$$\frac{dM}{dB} = \frac{\partial}{\partial B}\left[B\int_{r_t}^{\infty}\frac{dp_s}{dr}dr\right] - \frac{B}{p_i(r_t)}\cdot\frac{\partial p}{\partial B}. \tag{40}$$

If there is to be improvement, then it is sufficient that $dM/dB(B, 0) > 0$; *i.e.*,

$$1 - \frac{B}{p_i(0)}\frac{\partial p}{\partial B}(B, 0) > 0 \tag{41}$$

or

$$\frac{d}{dB}\int_0^{\infty} p_i\frac{dp_s}{dr}dr < \frac{p_i(0)}{B}. \tag{4}$$

The Utility of Meteor Bursts for Intermittent Radio Communication*

G. F. MONTGOMERY†, SENIOR MEMBER, IRE, AND G. R. SUGAR†, MEMBER, IRE

Summary—**It has been suggested that the transient vhf signal produced by meteor ionization be used for communication, and several groups have been investigating this possibility. Analysis of the meteor bursts measured on the 49.8-mc transmissions from Cedar Rapids, Iowa, to Sterling, Va., implies that useful intermittent communication can be achieved. Transmission experiments in a 100-kc band have not realized the theoretical capacity of the signal, mostly because of multipath propagation. About half of the meteor bursts observed are unaffected by this distortion, however, so that a useful system of this bandwidth may yet be possible.**

Introduction

Consider a vhf radio transmitter and receiver at the earth's surface, separated from each other by several hundred kilometers and using directive antennas that illuminate a common volume of the atmosphere about one hundred kilometers above the ground. If the transmitter power is sufficient, a signal of moderately slow fluctuation will be observed at the receiver, propagated, as is now well known, by ionospheric forward scatter.[1,2] But superimposed on the scatter signal is another signal of different kind, and with a transmitter power considerably less than that required for an observable scatter signal the second signal will still be received. The signal is intermittent, occurs in short bursts that last generally for less than a few seconds, and occasionally produces bursts of sur-

* Original manuscript received by the IRE, April 17, 1957. This work was supported by Air Force Cambridge Res. Center, Bedford, Mass.

† National Bureau of Standards, Washington, D. C.

[1] D. K. Bailey, *et al.*, "A new kind of radio propagation at very high frequencies observable over long distances," *Phys. Rev.*, vol. 86, pp. 141–145; April 15, 1952.

[2] D. K. Bailey, R. Bateman, and R. C. Kirby, "Radio transmission at vhf by scattering and other processes in the lower ionosphere," Proc. IRE, vol. 43, pp. 1181–1231; October, 1955.

prisingly large amplitude. Its propagation is attributed to the transient columns of ionization generated by meteors as they are consumed in the upper atmosphere.[3–5]

In 1951, while investigating radar reflections from meteor trails, Pineo[6] suggested that these signal bursts might be used for intermittent but high-speed communication between separated stations, particularly where other forms of propagation were impractical or inconvenient. It is the purpose of this paper to describe a partial investigation of this idea. The first section of the paper concerns the extent and frequency of measured meteor-signal fluctuation; the second evaluates the communication capability of an ideal signal modeled on the measurements; and the third summarizes the results of experiments in transmitting a test signal via meteor bursts.

Meteor-Signal Characteristics

A system[1] used ordinarily for forward-scatter research provided the meteor data. The 49.8-mc continuous-wave transmitter operated by the Collins Radio Company at Cedar Rapids, Iowa, delivered about 30 kw to a rhombic antenna directed toward the National Bureau of Standards field station at Sterling, Va. The calculated power gain of the antenna was 18 db referred to a half-wave dipole at the same height above ground. A nearly identical antenna of 600-ohms impedance was used for reception at Sterling. The antennas were designed so that their main lobes intersected at a point midway between the stations and 100 km in height.

The detector output of a linear receiver of 3-kc bandwidth was used to run a pen recorder whose amplitude response was constant from zero frequency to approximately 100 cps. Instrument gain settings were adjusted to give full-scale pen deflection with an induced (open-circuit) antenna voltage of 300 μv. A continuous record was made for a 28-minute interval during each hour of three 24-hour periods. The first period began at 1500 EST on May 6, 1953, a date on which it is presumed that the *Eta Aquarid* meteor shower was in progress; the second began at 1500 EST on June 18, 1953, a date for which no unusual meteor activity has been noted; and the third began at 1500 EST on August 11, 1953, during the annual *Perseid* shower.

Typical records with calibrations in terms of induced antenna voltage are shown in Figs. 1 and 2. Only those meteor bursts whose peak amplitudes exceeded 25 μv were considered part of the data. Total number of bursts in each 28-minute period, converted to an average rate

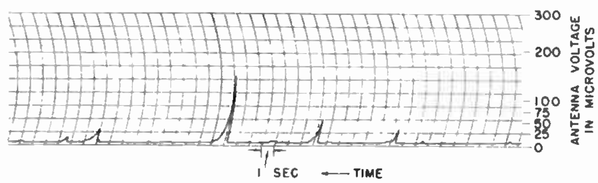

Fig. 1—Typical meteor burst oscillogram.

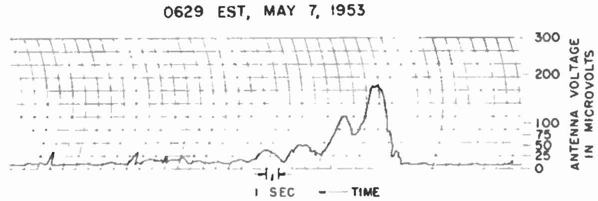

Fig. 2—Diffused meteor burst oscillogram.

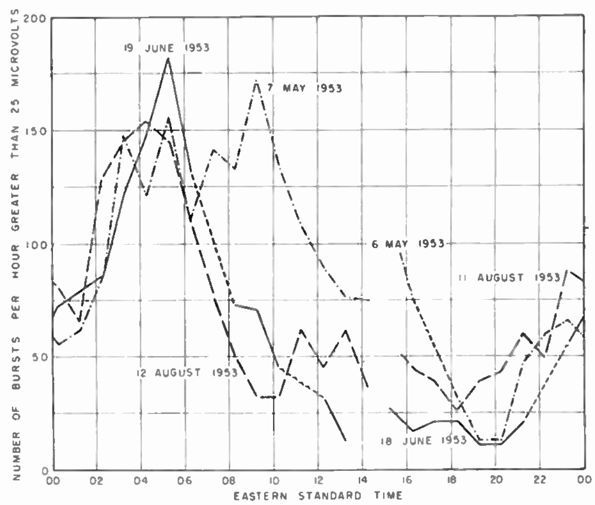

Fig. 3—Average meteor burst rate.

in bursts per hour, is plotted in Fig. 3. Dashed lines indicate loss of data during periods of atmospheric interference, sporadic-E transmission, or equipment failure.

The peak amplitude of each burst was scaled to the nearest 5 μv, and the distributions of peak amplitude for the three test periods are shown in Fig. 4. The duration of each burst was scaled at several amplitudes, where duration is defined as the time interval during which the amplitude of the burst exceeds a specified value. The amplitudes chosen for scaling were 300, 200, 100, 50, and 25 μv, and $1/e$ times the peak amplitude. Durations were scaled to the nearest tenth of a second. If there are N bursts in period T, and if $\delta_S(i)$ is the duration at amplitude S of the ith burst, then

$$p_s = \frac{1}{T} \sum_{i=1}^{N} \delta_S(i) \tag{1}$$

where p_s is the fraction of the time that the signal amplitude due to meteor bursts exceeds S. The distributions obtained in this way for the three 24-hour periods are plotted in Fig. 5. (The average transmitter output power was about 30 kw during the first period, 24 kw

[3] J. A. Pierce, "Abnormal ionization in the E region of the ionosphere," Proc. IRE, vol. 26, pp. 892–908; July, 1938.
[4] G. R. Abell, Jr., correspondence, *QST*, vol. 30, p. 48; November, 1946.
[5] E. W. Allen, Jr., "Reflections of very high frequency radio waves from meteoric ionization," Proc. IRE, vol. 36, pp. 346–352; March, 1948.
[6] V. C. Pineo, private communication, Natl. Bureau of Standards; November, 1951.

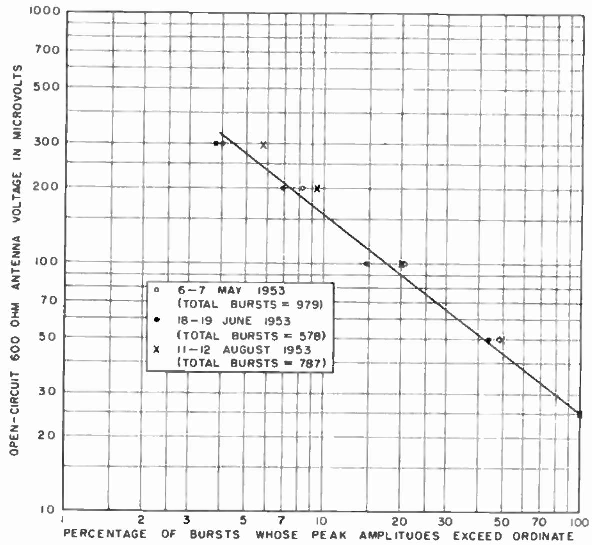

Fig. 4—Peak amplitude distribution of meteor bursts.

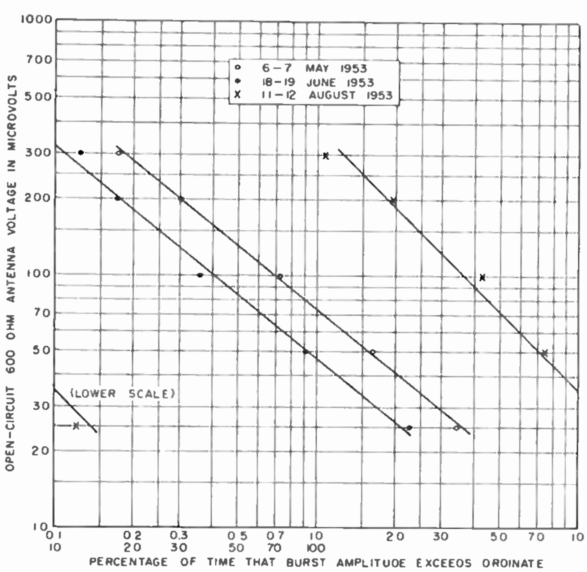

Fig. 5—Meteor burst amplitude distribution.

during the second, and 26 kw during the third. The difference in the first two distributions is greater than can be accounted for by the difference in transmitter power alone.)

The time distribution for the August 11–12 experiment (during the *Perseid* shower) does not fit a straight line as well as the first two distributions, and large-amplitude durations are relatively more frequent events. The amplitude distribution for the first two periods is approximated over the measured range by

$$p_s = (S_1/S)^a \tag{2}$$

where $a = 1.2$, and

$$S_1 \text{ (May 6–7)} = 1.59\ \mu\text{v}$$

$$S_1 \text{ (June 18–19)} = 1.02\ \mu\text{v}.$$

Let $\Delta(i)$ be the duration of the ith burst at an amplitude $1/e$ times its peak amplitude; we can call this duration the time constant of the burst. The average time constant is

$$\langle\Delta\rangle = \frac{1}{N}\sum_{i=1}^{N}\Delta(i), \tag{3}$$

but the significance of this average should not be overestimated. While the majority of the bursts were approximately exponential in form as shown in Fig. 1, an appreciable fraction were of the type shown to the right in Fig. 2, and these, having relatively large values of Δ, contribute to the average out of proportion to their number. With this reservation established, the values of $\langle\Delta\rangle$ for the three test periods are:

$\langle\Delta\rangle$ (May 6–7) = 1.1 seconds

$\langle\Delta\rangle$ (June 18–19) = 1.4 seconds

$\langle\Delta\rangle$ (August 11–12) = 2.2 seconds.

There are limitations on the distribution (2). First, even if (2) holds for all $S \geq S_1$ (which cannot be confirmed by the measurements because of their restricted range), it is evident that the signal in the range $0 \leq S < S_1$ will be constituted by a number of overlapping bursts. Thus the amplitude distribution in this range will approximate a Rayleigh distribution. Second, there must be a finite upper limit S_2 for the range in which (2) is valid. This limitation is evident from the fact that

$$\langle S^2\rangle = \lim_{S\to\infty}\int_{S_1}^{S} S^2\frac{dp_s}{dS}\,dS \tag{4}$$

does not converge. A sufficient condition for convergence is that $a > 2$ for $S > S_2 = \text{constant}$. Campbell[7] finds that a changes from time to time and has measured values in the range from 1.14 to 1.92, using a relatively low-power system.

From extrapolation of Fig. 4, it is found that if $a = 1.2$, about one per cent of the bursts should have peak amplitudes greater than one millivolt. From the June 18–19 data, the average interval between bursts is 58.1 seconds, corresponding to about one burst per minute. Consequently, a waiting period of at least 100 minutes is required, on the average, for a burst exceeding one millivolt. For a practical communication system, we shall therefore assume that $p_s = 0$ for $S > 10^3 S_1$, and this upper amplitude limit will be used in calculations that follow.

Theory of Communication

A system using meteor bursts for communication is presumed to be one in which message information is transmitted and received only during the burst. The system is therefore intermittent and can be analyzed by a method described previously.[8] We shall assume narrow-band binary frequency modulation and develop the

[7] L. L. Campbell, "Further Considerations on a Variable Information Rate Janet System," Defence Res. Telecommunications Establishment, Radio Phys. Lab. Rep. No. 12-3-17; February, 1956.

[8] G. F. Montgomery, "Intermittent communication with a fluctuating signal," Proc. IRE, this issue, p. 1678.

relations between average transmission rate, average error, and bandwidth.

Let the relative probability of the signal amplitude S due to a meteor burst be

$$\frac{dp_s}{dS} = \frac{aS_1^a}{S^{1+a}}, \qquad S_1 \leq S \leq S_2 \tag{5}$$

where a, S_1, and S_2 are positive constants. We now define the signal-to-noise power ratio $r = S^2/N_0^2$, where N_0^2 is the mean-square amplitude of the system noise, and a reference bandwidth B_1 such that

$$\frac{B_1}{B} = \frac{S_1^2}{N_0^2} \tag{6}$$

where B is the system bandwidth. B_1 is thus the bandwidth at which the signal-to-noise ratio is unity for a signal amplitude S_1. Then,

$$\frac{dp_s}{dr} = \frac{a}{2(B/B_1)^{a/2}r^{1+a/2}}, \quad (B_1/B) \leq r \leq (B_1/B)(S_2/S_1)^2 \tag{7}$$

is the relative probability of the ratio r; *i.e.*, dp_s is the probability that r is contained in the interval $(r, r+dr)$.

For frequency modulation, it has been shown[9] that the probability of a binary symbol error is

$$p_i = \tfrac{1}{2}e^{-r}. \tag{8}$$

The average binary error for reception above a threshold $r_t \geq (B_1/B)$ is therefore

$$p = \int_{r_t}^{r_2} p_i \frac{dp_s}{dr}\, dr = \frac{a}{4(B/B_1)^{a/2}} \int_{r_t}^{r_2} e^{-r} r^{-(1+a/2)} dr \tag{9}$$

where $r_2 = (B_1/B)(S_2/S_1)^2$. It is shown in the Appendix that the second integral of (9) can be approximated by a function $F(a, r_t)$ which is plotted in Fig. 6. Then,

$$p = \frac{a}{4(B/B_1)^{a/2}} F(a, r_t). \tag{10}$$

During transmission, the binary symbol rate is approximately equal to the bandwidth B, so that the average transmission rate is

$$M = B \int_{r_t}^{r_2} \frac{dp_s}{dr}\, dr \tag{11}$$

and if $r_2 \gg r_t$,

$$\frac{M}{B_1} = \frac{(B/B_1)^{1-a/2}}{r_t^{a/2}}. \tag{12}$$

Eqs. (10) and (12) allow us to calculate the capacity of a system for a given error p if the constants a and B_1 are given. A bandwidth B is assumed, and $F(a, r_t)$ is calculated from (10). The threshold ratio r_t is then found from a graph such as Fig. 6. It must be verified

[9] G. F. Montgomery, "A comparison of amplitude and angle modulation for narrow-band communication of binary-coded messages in fluctuation noise," Proc. IRE, vol. 42, pp. 447–454; February, 1954.

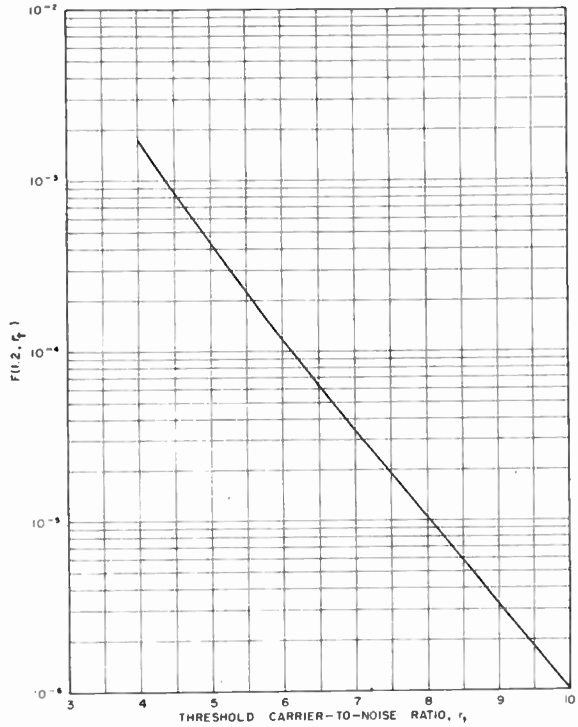

Fig. 6—Error function $F(a, r_t)$ for $a = 1.2$.

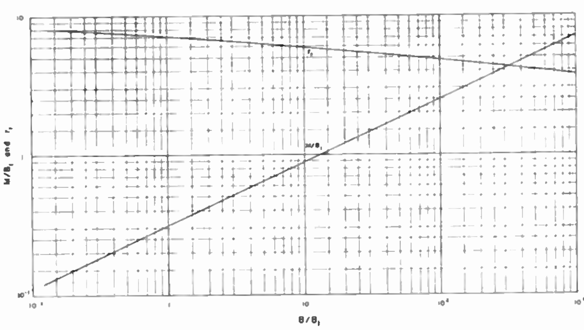

Fig. 7—Average transmission rate and threshold power ratio as functions of system bandwidth.

that $r_t \geq (B_1/B)$; if this is not so, a smaller p or a larger B should be chosen to begin with. With r_t established, the average transmission rate M is calculated from (12). A graph of M/B_1 as a function of B/B_1 is shown in Fig. 7, for $p = 10^{-5}$. Ratio r_t; shown in the same figure, varies slowly with bandwidth, and therefore M varies approximately as $B^{1-a/2}$. It is evident that unless $a < 2$, approximately, there will be no advantage in operating a meteor-burst system intermittently; *i.e.*, at a bandwidth $B > B_1$.

For the system on which the measurements were made, B_1 (June 18–19) $= 1.3 \times 10^4$ cps. If $B = 10^6$ cps, and $p = 10^{-5}$, then from Fig. 7,

$$M = 0.78\, B_1 = 1.0 \times 10^4 \text{ binary digits/second}$$

$$r_t = 6.0$$

and the duty cycle is

$$M/B = 0.10.$$

Interpolation from the constants of one system to another is not a simple matter. We can certainly assume that B_1 is proportional to transmitter power, but it will also be a function of the range, the antenna directivities, the geographical station latitudes, and the position of the illuminated atmosphere relative to the stations. Of particular importance is Eshleman's finding[10] that the number of observable bursts should be increased by displacing the illuminated volume laterally from a point directly above the great-circle path between transmitter and receiver. In order to produce a signal burst the path of the meteor must be tangent to one of a family of ellipses defined by the station positions. The probability of such a meteor trajectory is a function of both latitude and relative station orientation.[10,11]

Additional measurements were made to determine the practical effect of these conclusions. The results show that if the antennas at Cedar Rapids and Sterling had been suitably directed off the great-circle path, the number of meteor bursts observed would have increased by a factor of about 4. The average duration of the bursts would have decreased by a factor of about 2. The combination of these two factors would have approximately doubled the capacity of a communication system.

B_1 is not directly proportional to antenna gain, for although the signal amplitude from a given meteor within the illuminated volume increases with gain of the transmitting and receiving antennas, the total volume illuminated, and thus the number of meteors intercepted per unit time, decreases because of the reduced beamwidth.

The theory given here applies only to operation of a meteor-burst communication system with a fixed signal threshold. A variable-bandwidth system, in which the transmission rate is varied continuously with the received signal amplitude, is an additional possibility.[7,12,13] Campbell[7] concludes, however, that this refinement offers a small advantage over fixed-threshold operation in view of its technical complexity.

Transmission Experiments

Transmission experiments were made with the Cedar Rapids-Sterling system on 49.8 mc. Simultaneously, other investigators,[14] including amateurs,[15] have been experimenting with meteor-burst communication, usually with relatively low power and at moderate transmission speeds.

A preliminary experiment, intended to verify technique rather than theory, was made on September 18, 1953. One line of teletype test symbols, at the normal speed of 60 words per minute, was recorded on magnetic tape using a conventional audio-frequency recorder with a tape speed of 7.5 inches per second. The recorded signal consisted of a keyed 100-cps tone, with the presence of tone indicating "mark." The tape record was formed into a continuous loop which was then played back at 15 inches per second, yielding a series of test lines at twice normal speed. The reproduced signal was re-recorded on a second machine at 7.5 inches per second. This process was successively repeated to produce a record of a keyed 6400-cps tone, at 7.5 inches per second, representing teletype signals at 64 times normal speed. The output of this record was used to frequency-modulate the Cedar Rapids transmitter with a deviation of about 50 kc.

A frequency-modulation receiver with a bandwidth of about 200 kc was used at Sterling. The audio output of the receiver was fed to a tape recorder that was arranged to record only during those intervals when the receiver antenna voltage exceeded 30 μv. The speed of the recorded signals was subsequently reduced by the reverse of the process used in making the transmitted program, after which the reduced signal was used to operate a printer.

The results obtained in this experiment were adequate to show that transmission speeds at least as great as 3200 binary digits per second could be achieved with the proposed propagation mechanism. Although printed errors were frequent, most could be traced to deficiencies of the conventional recording equipment when used for this purpose and to unavoidable signal distortions introduced in the tape processing.

System performance using more nearly optimum modulation is of greater significance. In the preceding section, it is shown that, ideally, an average transmission rate of 10^4 binary digits per second with an error of 10^{-5} should be obtained with a bandwidth of 10^5 cps using narrow-band frequency modulation. We should expect actual performance to fall short of this specification because of equipment limitations; in addition, however, it was appreciated that multipath or other interference effects might limit the communication results obtained theoretically and that the severity of these effects, if present, probably would depend on the transmission speed.

The object was to measure received errors at a transmission speed of 10^5 binary digits per second; accordingly, the periodic test signal in Fig. 8 was provided. During interval marked a, the signal consists of 50-kc waves of nearly sinusoidal form; exactly 1000 complete cycles are included in this interval. Interval b is a constant-amplitude signal equal in duration to interval a. The test signal was transmitted continuously by fre-

[10] V. R. Eshleman and L. A. Manning, "Radio communication by scattering from meteoric ionization," Proc. IRE, vol. 42, pp. 530–536; March, 1954.

[11] O. G. Villard, Jr., V. R. Eshleman, L. A. Manning, and A. M. Peterson, "The role of meteors in extended-range vhf propagation," Proc. IRE, vol. 43, pp. 1473–1481; October, 1955.

[12] D. R. Hansen and L. L. Campbell, "A Proposed Variable Information Rate Janet System," Defence Res. Telecommunications Establishment, Radio Phys. Lab. Rep. No. 12-3-13; July, 1955.

[13] D. K. Weaver, Jr., "Applied Research on Meteor-Burst Communications," Stanford Res. Inst., Sci. Rep. 2; May, 1956.

[14] P. A. Forsyth and E. L. Vogan, "Feasibility Trials of System Janet," Defence Res. Telecommunications Establishment, Radio Phys. Lab. Rep. No. 12-3-7; May, 1954.

[15] "ARRL Merit Award for 1955 Goes to W4HHK and W2UK," QST, vol. 40, p. 62; October, 1956.

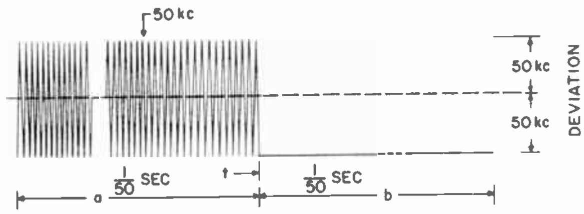

Fig. 8—Test signal waveform.

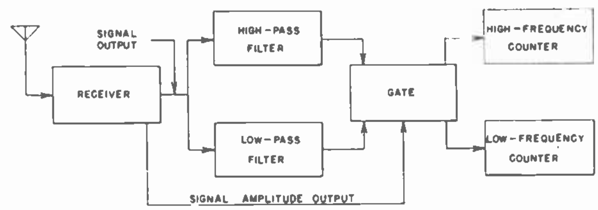

Fig. 9—Block diagram of error-counting receiver.

quency-modulating the transmitter, with the positive peak of the 50-kc wave corresponding to a positive deviation of 50 kc and the negative peak of the 50-kc wave and the b interval corresponding to a negative deviation of 50 kc. The signal was received on a frequency-modulation receiver of approximately 100-kc bandwidth. The output of the receiver discriminator was fed to two pulse counters through a filter and gating circuit, the block diagram of which is shown in Fig. 9. Filtering was such that one counter responded only to frequencies of the order of 50 kc, while the other responded only to the low-frequency (25-cps) modulation of the received signal. The developed grid voltage of the receiver limiter, a voltage that increases with signal amplitude, was also connected with the gate. The gate was arranged to operate in the following way.

As long as the signal amplitude remains below a predetermined threshold, the gate remains closed, and no input is delivered to either counter. When the amplitude rises above the threshold, the gate remains closed until the end of a 1000-cycle group is received, corresponding to point t in Fig. 8, whereupon the gate is opened and remains open for as long as the amplitude exceeds the threshold. During this interval, the 50-kc component is delivered to the high-frequency counter, and the 25-cps component is delivered to the low-frequency counter. When the amplitude falls below the threshold, the gate remains open until the end of a 1000-cycle group is received; it is then closed, and the counter inputs are interrupted.

If there are no errors in transmission during the time that the gate is open, the high-frequency counter will register exactly n thousand counts, n being the number of groups received, and the low-frequency counter will register n counts. In general, transmission errors will cause a deviation, either positive or negative, from exactly n thousand counts. Multipath propagation can be expected to produce several effects, all of which can be explained as a variation in amplitude or phase of the propagated signal as a function of frequency. The first is the relative change in phase of the carrier and side frequencies. This effect appears either as attenuation of the 50-kc modulation or as slight distortion of the 50-kc waveform; severe distortion of the 50-kc waveform is not visible in the receiver output because of restricted intermediate-frequency and post-discriminator bandwidths. Appreciable attenuation of the 50-kc modulation will cause loss of count in the high-frequency counter. The second effect is selective fading. Loss of signal may occur differentially during the a and b parts of the test signal, possibly for only fractions of either interval. Signal attenuation during the b interval will generate noise spikes that increase the count of the high-frequency counter.

A number of experiments have been made using this equipment, but two made on May 9–10 and May 16–17, 1955, will be the only ones discussed, since each of these covered a 24-hour period and their data have been analyzed in detail. Measurements were made during two 14-minute intervals in each hour of the two periods, and two amplitude thresholds (17.5 and 35 μv induced antenna voltage) were used for the two intervals in each hour. Throughout the tests, counter readings were recorded after each burst. The operator observed received signal on an oscilloscope connected to the receiver discriminator output. It has been found that multipath distortion of some bursts can be detected in this way. Such distortion as did not escape the operator's attention was noted in the data. Presence of occasional interference from an adjacent-channel radio-telephone transmitter and from automobile ignition was also noted.

Fig. 10 shows the variation in average burst rate at the two thresholds for both tests; the variations are similar to those given in Fig. 3. Figs. 11 and 12 are graphs of the total number of received binary digits during each 14-minute test interval. These numbers are proportional to the sum of the burst durations less a small number of bursts that were discarded because of radio or ignition-noise interference. The totals of the durations for each 24-hour period agree closely with those found for June 18–19, 1953, but the totals for other dates have been found to vary by from one-third to three times those given here.

Since some of the multipath distortion was observable, the data were analyzed in two sets. The first set consisted of all data except that eliminated because of interference; the second set consisted of the data of the first with all bursts that showed observable multipath distortion excluded. In Figs. 11 and 12, the total ordinate height represents the first set, or all data. The dashed portion of the ordinate represents that portion of the data affected by observable multipath distortion. Table I displays calculations from both sets of data.

There is some uncertainty concerning the calculation of average error. The procedure has been to sum the count deviations for a series of bursts regardless of sign, to divide this sum by the total of the burst durations converted to equivalent binary digits (4000 digits per

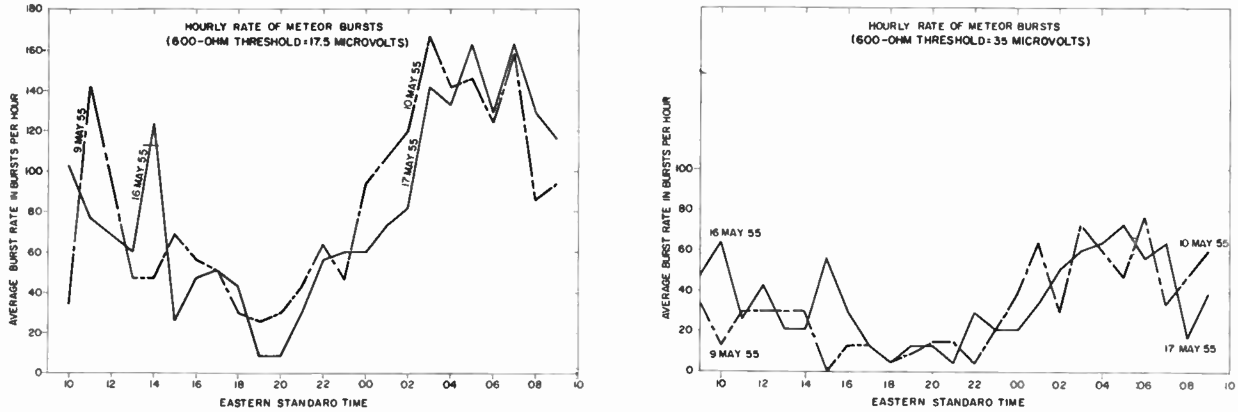

Fig. 10—Average meteor burst rate during test periods.

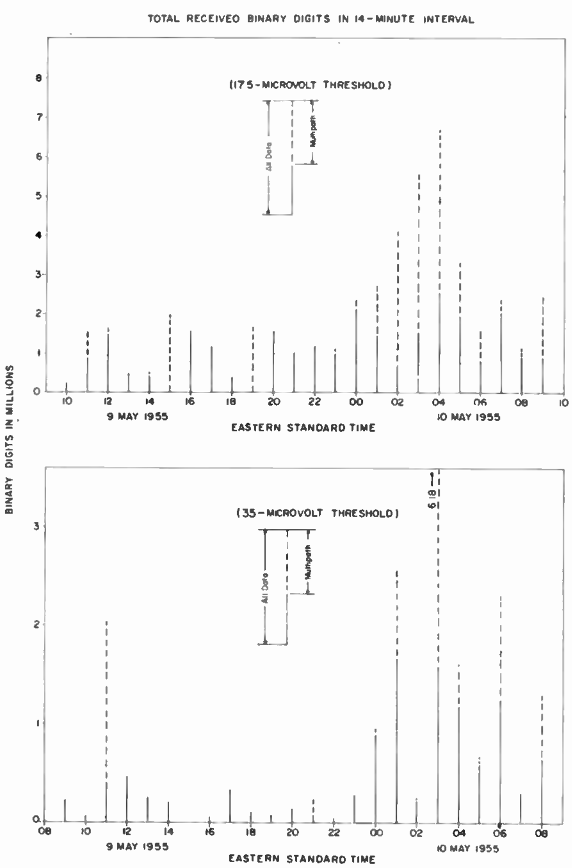

Fig. 11—Integrated burst duration, May 9–10, 1955.

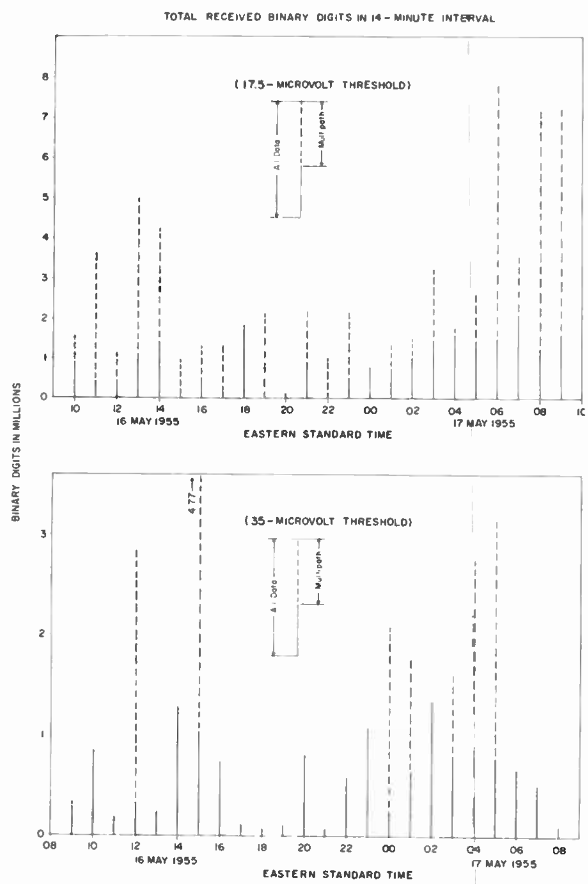

Fig. 12—Integrated burst duration, May 16–17, 1955.

TABLE I
METEOR BURST DATA FOR TWENTY-FOUR 14-MINUTE INTERVALS

May 1955	Threshold in microvolts (600 ohms)	All Data					Data with Observable Multipath Distortion Excluded				
		Total number of bursts	Average frequency in bursts per minute	Average burst length in seconds	Average transmission rate in binary digits per second	Binary error in per cent	Total number of bursts	Average frequency in bursts per minute	Average burst length in seconds	Average transmission rate in binary digits per second	Binary error in per cent
9–10	17.5	472	1.40	1.02	2383	0.249	387	1.15	0.692	1328	0.0665
16–17	17.5	455	1.35	1.44	3251	0.411	364	1.08	0.633	1143	0.0679
9–10	35	170	0.506	1.22	1028	0.0986	155	0.461	0.716	551	0.00414
16–17	35	198	0.589	1.40	1378	0.0649	183	0.545	0.740	672	0.000642

test cycle), and to label this quotient the average binary error. Now, this fraction equals the true average error only under the condition that the deviation increases (or decreases) monotonically within any one burst. This condition is not always met in practice. If the count deviation for any one burst of a set of bursts were the sum of random errors (positive or negative, with equal probability), a best measure of the average error would be found only by calculating the probabilities of the sums as a function of the error and then by finding the most probable error yielding the given set of sums. For a given set, the error calculated in this way is larger than the error calculated by the simpler procedure, but the calculation is prohibitively long.

A method has been found, however, that permits a rough evaluation of the randomness of the deviation. Pen oscillograms are made of the output of the units register in the high-frequency counter. A record is thus obtained of the rest position of this register at the end of each cycle of the received test signal. If less than ten (monotonic) errors occur within any one cycle, the progress of the deviation within a burst can be tracked in the oscillogram. The conclusion reached from examination of such pen records is that the deviation within most bursts is neither monotonic nor random but tends more to the first than the second; indeed, error of this sort might be expected if the error source were other than random noise. The error has therefore been calculated using the simpler procedure, and the reported error is smaller than the real error. From the fact that many deviations appear to be nearly monotonic, however, it is concluded that the underestimate of the real error given by the calculations is probably not serious.

The error is considerably larger than that expected from meteor bursts of the observed power but without multipath distortion and with cosmic noise as the only interference. During the tests, the cosmic noise in a 100-kc band varied from 1 db to 8 db above one microvolt at 600 ohms. For a theoretical error of 0.01 per cent, the required noise using a 17.5-μv threshold is about 20 db above one microvolt. The difference between theoretical and experimental noise powers required for approximately the same error indicates the presence of unobserved multipath distortion or other interference (not cosmic noise) or both.

Multipath distortion may be present but not obvious because of the speed of its occurrence. Unfortunately, there was no equipment available at the time that would permit recording the meteor-burst signal so that its fine structure could be examined in detail; a high-speed magnetic tape recorder recently completed should permit such examination. The second probable interference source is the more-or-less steady background signal provided by ionospheric scatter propagation. During the tests, the median amplitude of the scatter signal varied from 1 db to 23 db above one microvolt. Strictly speaking, the scatter signal provides a kind of multipath interference, but the observable multipath distortion considered here occurs when the burst amplitude is much larger than the scatter signal and is therefore assumed to be characteristic of the burst alone. Since the phase of the scatter signal is almost certainly random with respect to the burst signal, and since the scatter signal fades with a nearly Rayleigh amplitude distribution,[16] it seems logical to consider the scatter signal as an interfering random noise.

As a test of the effect of the scatter signal on the received error, the individual 14-minute errors were plotted against the median scatter-signal amplitude for the half-hour nearest the 14-minute test. The results of this plot, including and excluding observable multipath distortion, are shown in Figs. 13 and 14. Both 17.5- and 35-μv threshold data are shown in these figures; the scatter-signal abscissas are exact for the 17.5-μv points, but the 35-μv points were shifted 6 db to the left in plotting in order to compare both sets of data with the same threshold-to-scatter amplitude ratio. The curve in each of the figures is the error curve for a 17.5-μv threshold with random noise interference whose rms amplitude equals the abscissa. It was plotted by calculation from (10), with $a=1.2$, $B_1=1.3\times10^4$ cps, and $B=10^5$ cps.

In Fig. 13, which includes all of the burst data, there is little, if any, apparent correlation between error and scatter-signal amplitude. In Fig. 14, where the observable multipath distortion has been excluded, there is definite correlation between the two. The conclusion is that the influence of observable multipath distortion is large enough to obscure other contributions to error; when those bursts affected by observable multipath distortion are excluded, the error of the remaining bursts is influenced in part by the scatter signal and in part by as yet unidentified effects.

It is possible, of course, that this correlation is fictitious. If the remaining unidentified effects include distortion of the fine structure of the signal and if this distortion varies diurnally as does the scatter-signal amplitude, then the correlation will appear even though the errors are not, in fact, influenced by the scatter signal. But the possibility seems unlikely. If the theoretical error curve of Fig. 14 is moved only 4 db to the left as a reasonable allowance for, say, the nonideal signal-capture performance of the receiver, then the curve begins to intersect experimental points. Not even all of the observable multipath effects can have been removed from the data of Fig. 14, and therefore the general agreement of the experimental plot with the theoretical curve must be considered good.

The process of excluding bursts affected by observable multipath distortion reduced the average transmission rate by a factor of about 2 and reduced the error by a factor of from 4 to 100, depending mainly upon threshold amplitude. This fact suggests that automatic means

[16] G. R. Sugar, "Some fading characteristics of regular vhf ionospheric propagation," Proc. IRE, vol. 43, pp. 1432–1436; October, 1955.

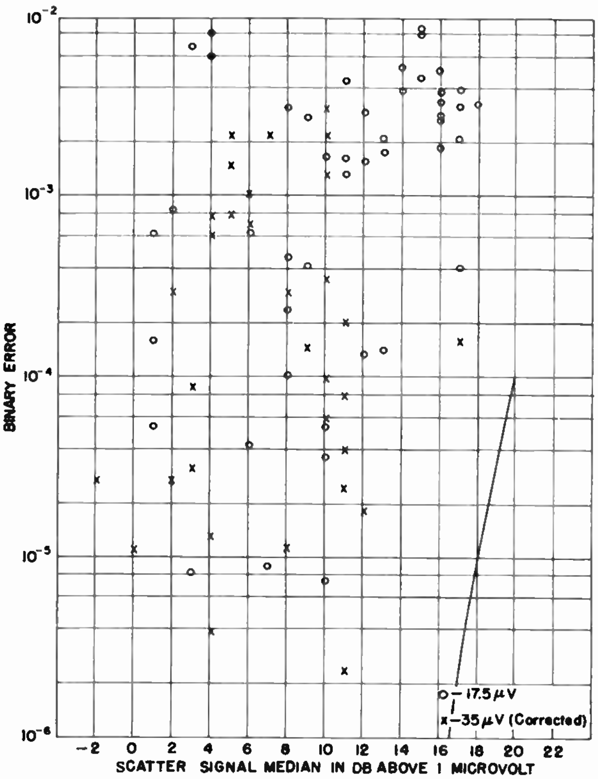

Fig. 13—Variation of error with scatter-signal amplitude, observable multipath distortion included.

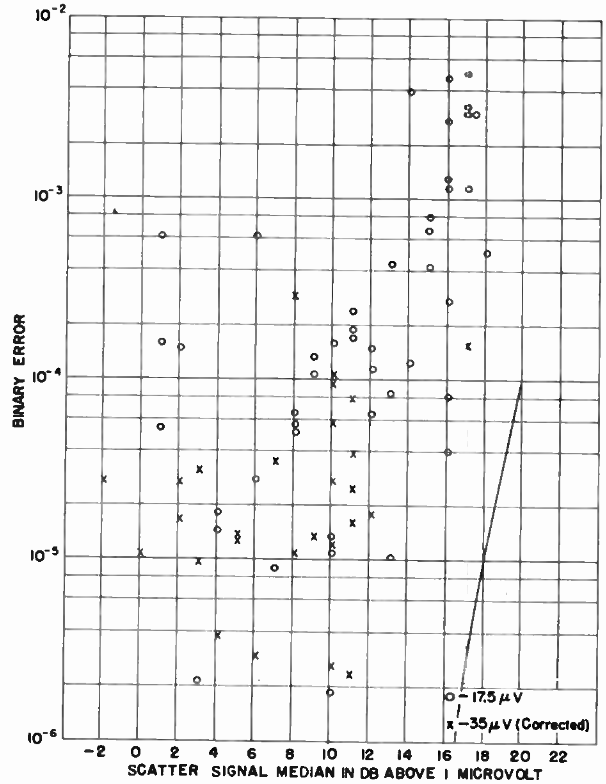

Fig. 14—Variation of error with scatter-signal amplitude, observable multipath distortion excluded.

to eliminate "bad" bursts would be helpful and might be devised if a suitable distinguishing characteristic of such bursts (*e.g.*, amplitude variation) can be found upon which to base the automatic rejection. Operation at the 35-μv threshold with observable multipath distortion excluded gave an error less than the 0.01 per cent figure generally accepted as satisfactory for reliable teleprinter operation. The average transmission capacity under these conditions corresponded to 11 sixty-word-per-minute channels on one date and to 13 channels on the other, representing average meteor activity. As we have noted previously, the capacity on any one day may vary from one-third to three times this average, and the average capacity itself can probably be doubled by orienting the antennas more favorably.

Conclusion

The vhf radio signal propagated by meteors is a possible means for intermittent, high-speed communication. Meteor bursts have been measured on the 49.8-mc transmissions from Cedar Rapids to Sterling, and their amplitude distribution can be specified by a simple formula in a restricted amplitude range. The theory developed for meteor-burst communication indicates that a moderately high information rate can be achieved if a large bandwidth is used, or that more usual information rates can be achieved with relatively low power. Error-counting experiments show the largest source of error in a 100-kc bandwidth signal at 49.8 mc to be the multipath signal distortion that can be observed with an oscilloscope. Other sources of error, not yet firmly identified, maintain the error at values considerably above theoretical prediction based on cosmic noise interference. Included in these error sources is the signal propagated by ionospheric scatter. Transmission may be improved by automatic means to reject bursts affected by multipath distortion if a technique can be developed to differentiate these from unaffected bursts. Present error and average transmission rates are useful in practice.

Appendix

We wish to evaluate the integral

$$Q(r_t, r_2) = \int_{r_t}^{r_2} e^{-r} r^{-(1+a/2)} dr = Q(r_t, \infty) - Q(r_2, \infty). \quad (13)$$

Successive integration by parts gives

$$Q(x, \infty) = e^{-x} x^{-(1+a/2)} \sum_{i=0}^{n} \frac{\left(i + 1 + \frac{a}{2}\right)}{\left(1 + \frac{a}{2}\right)} \left(-\frac{1}{x}\right)^i + \frac{(-1)^{n+1}\Gamma\left(n + 2 + \frac{a}{2}\right)}{\Gamma\left(1 + \frac{a}{2}\right)} \cdot \int_x^{\infty} e^{-r} r^{-(n+2+a/2)} dr. \quad (14)$$

With $n=0$,

$$Q(x, \infty) < e^{-x}x^{-(1+a/2)} \tag{15}$$

and with $n=1$,

$$Q(x, \infty) > e^{-x}x^{-(1+a/2)}\left(1 - \frac{2+a}{2x}\right). \tag{16}$$

Now, suppose that $r_2=kr_t$, $k>1$. Then, from (15),

$$Q(r_2, \infty) < e^{-kr_t}r_t^{-(1+a/2)}k^{-(1+a/2)} \tag{17}$$

and from (16),

$$Q(r_t, \infty) > e^{-r_t}r_t^{-(1+a/2)}\left(1 - \frac{2+a}{2r_t}\right). \tag{18}$$

Therefore,

$$\frac{Q(r_2, \infty)}{Q(r_t, \infty)} < \frac{1}{e^{(k-1)r_t}k^{1+a/2}\left(1 - \dfrac{2+a}{2r_t}\right)}. \tag{19}$$

If $a=1.2$, $r_t \geq 2$, $k>3$,

$$\frac{Q(r_2, \infty)}{Q(r_t, \infty)} < 0.016$$

and

$$Q(r_t, r_2) \approx Q(r_t, \infty) = F(a, r_t). \tag{20}$$

The summation of (14) does not form a convergent series, but

$$\int_x^\infty e^{-r}r^{-(n+2+a/2)}dr < e^{-x}x^{-(n+2+a/2)} \tag{21}$$

so that

$$F(a, r_t) = e^{-r_t}r_t^{-(1+a/2)}\left[\sum_{i=0}^{n} \frac{\left(i+1+\dfrac{a}{2}\right)}{\left(1+\dfrac{a}{2}\right)}\left(-\frac{1}{r_t}\right)^i + \frac{(-1)^{n+1}\Gamma\left(n+2+\dfrac{a}{2}\right)}{\Gamma\left(1+\dfrac{a}{2}\right)}D\right] \tag{22}$$

where $D<r_t^{-(n+1)}$, can be calculated to a useful approximation by proper choice of n if r_t is sufficiently large. The function $F(1.2, r_t)$ is plotted in Fig. 6.

A Meteor-Burst System for Extended Range VHF Communications*

W. R. VINCENT†, ASSOCIATE MEMBER, IRE, R. T. WOLFRAM†, B. M. SIFFORD†, MEMBER, IRE, W. E. JAYE†, AND A. M. PETERSON†

Summary—**A low-power burst communication system has been designed and tested, utilizing the intermittent propagation path provided by ionized meteor trails. A test circuit has been installed between Bozeman, Mont. (Montana State College), and Palo Alto, Calif. Details of the burst control techniques and storage devices used to handle the intermittent information flow are discussed along with the over-all system design.**

Introduction

THE reflection of radio signals from meteor-ionization trails offers a number of attractive characteristics as a propagation mode for communication circuits. Such trails are capable of reflecting incident vhf signals for distances up to 1500 miles between transmitter and receiver. The paths are unaffected by ionospheric variations and other disturbances which occur in the hf band. They can also provide a certain measure of security of information and resistance to jamming.

Stanford Research Institute has constructed an experimental meteor-burst system now in operation between Bozeman, Mont., and Palo Alto, Calif. The great circle distance between these points is 820 miles. The frequencies used are 40 and 32 mc. Both teletype and voice information have been successfully transmitted over the link. This paper describes the over-all teletype and voice systems and the special system components developed for this type of communication.

Some Unique Design Considerations

Meteor particles enter the E region of the ionosphere in great numbers. The signals propagated to a remote receiver via reflection from the individual ionized meteor trails can also be very numerous, but they differ

* Original manuscript received by the IRE, September 16, 1957. The work described in this paper was sponsored by the Air Force Cambridge Res. Center, Cambridge, Mass., Contract No. AF 19(604) 1517.
† Stanford Research Institute, Menlo Park, Calif.

greatly in intensity, duration, and frequency of occurrence. The number of signals of usable intensity and duration is proportional to transmitter power, receiver sensitivity, and, within certain limitations, antenna gain. If these equipment parameters were made sufficiently high the received signal could be essentially continuous. Even with moderate power and antenna gain a fraction of the signals will be of sufficient intensity and duration to effect an appreciable transfer of information. With equipment designed to synchronize transmission with appropriate meteor trails between sending and receiving stations, it is possible to convey messages in the vhf band over distances completely beyond normal line-of-sight ranges.

The amplitude-vs-time characteristic of a typical meteor-reflected signal is shown in Fig. 1. The maximum amplitude may be as high as 50 db above receiver noise, and the rate at which signals are received may vary from 10 to many thousands per hour. The usable duration of an individual burst can fluctuate in a random manner from a few milliseconds to whole minutes.

The most efficient way to make use of this varying-amplitude signal would be to transmit information at the highest rate consistent with the signal power received. This would require a variable rate and variable bandwidth system. It is simpler but less efficient to transmit at a fixed information rate and only during those portions of bursts when the received signal does not fall below a specified intensity level. The over-all information transfer rate in this case will be the product of the transmission rate during bursts and duty cycle, *i.e.*, the percentage of time the received signal is above a preset threshold level. The latter system (referred to as a threshold system) implies that the transmitting terminal must know when a usable path exists, so that it can control the flow of information and synchronize it with these signal bursts. This in turn requires a recognition signal to indicate that a signal path exists. As meteor-reflected signals follow reciprocity laws the existence of a path can be determined from a signal originating at either terminal.

Also, since information can be transmitted at a higher than normal rate during bursts, special data-storage and rate-changing components are required if information is to be put in and taken out of the system at its normal rate.

The Bozeman-Palo Alto Link

The present Bozeman-Palo Alto system is designed as a one-way communication link; *i.e.*, information other than that required for operation of the link is transmitted only one way—from Bozeman to Palo Alto. In this paper the information-sending station at Bozeman is designated T, and the receiving station at Palo Alto is designated R.

Operation of a meteor-burst system must comprise at least four functions in addition to those required in a continuous communication system. It must:

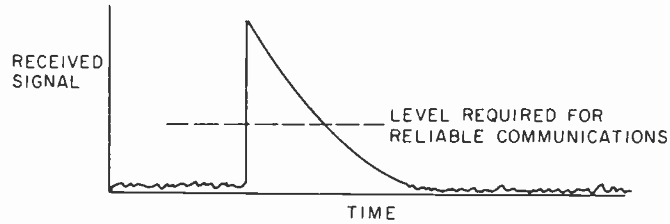

Fig. 1—Sketch of typical meteor-reflected signal.

1) Determine when a path exists; *i.e.*, when a suitable signal is being received.
2) Control transmission of information at T coincident with bursts.
3) Speed up the information transmission rate at T during bursts, and slow down the rate at R after reception.
4) Store information at a conventional rate and read it out intermittently at T; store received information intermittently at R and read it out at normal speed.

In the Bozeman-Palo Alto link, cw signals are transmitted continuously from both T and R. When R determines that a usable signal is being received, it modulates its transmitter and notifies T to begin sending.

The Teletype System

General System Characteristics: In the design of this initial meteor-burst teletype link proved methods and standard circuits are used except where the nature of the meteor channel requires special techniques. Standard 60-wpm teletype equipment is used as the information source and termination. Conventional frequency-shift, binary-keying modulation was selected, which allows the use of standard Class C power amplifiers in the transmitters. The equipment has initially been designed to transmit information during bursts at 10 times the normal 60-wpm teletype rate or 600 wpm. A block diagram of the teletype system is shown in Fig. 2.

A closed loop circuit is utilized to determine when a useful meteor path exists and to relay control information to T. A 2-kw, fsk modulated transmitter at T transmits continuously on one of its two frequencies. When a path exists, this signal is received at R by a conventional superheterodyne receiver having two narrow band filters (650 cps) to select the two-fsk frequencies before detection. At signal levels below the desired threshold, the signal reaches the filters without limiting. The output of the two filters is rectified and added destructively. When the output of one filter exceeds that of the other by a predetermined amount, indicating an acceptable signal level, a signal is generated—the *link start control*—which notifies T that transmission of information may begin. An fsk transmitter at R, duplicate of the one at T, also transmits continuously. The link start control signal generated by the detector output

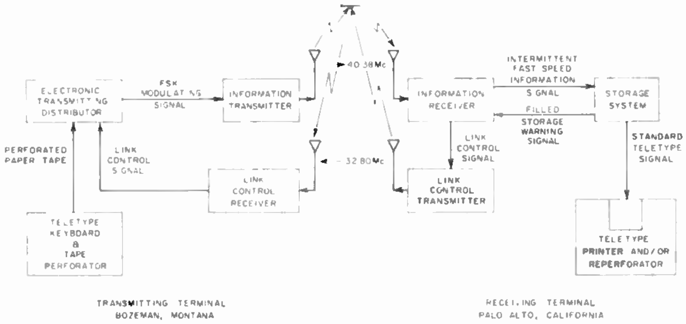

Fig. 2—Block diagram of teletype system.

causes this transmitter to shift its transmitting frequency. A receiver at T (exactly like the one at R) detects this shift and begins transmitting information. The fsk transmitter at T and receiver at R, used to determine a suitable meteor path, also transmit and receive teletype information. Hence the detectors in the receiver at R perform the normal fsk function as well as indicate when the signal is at a suitable level for communication.

Once the transmission of information is begun, the detector output follows the fsk signal within the response of the filters. This information signal is regenerated and sent to the storage system. To detect the end of the burst the rectified outputs of the filters are constructively combined. As one of the two frequencies is always transmitted, this signal will be independent of the fsk modulation and will be a function of the received signal strength only. Another decision circuit operates on this combination to generate a link stop control order when the signal has faded below a usable level. Thus when the transmitter frequency at R is shifted back, transmission of information is stopped at T. This method allows the receiving terminal to control the starting and stopping of information according to signal-to-noise conditions at the receiving site. It also enables R to stop information if the storage systems become filled or if there is a malfunction at R.

The operating frequency of the information transmitter at T is 40.38 mc and the frequency of the control transmitter at R is 32.8 mc. These frequencies are close enough to give good path correlation yet far enough apart to avoid cross-coupling problems.

Two 3-element Yagi antennas are used at each terminal for receiving and transmitting. These antennas are spaced about 200 feet apart in a direction normal to their line of directivity and supported on poles 30 feet above the ground.

Conventional perforated paper tape is used as a buffer storage at the transmitting terminal. From the perforated tape a Ferranti high-speed tape reader and electronic distributor generate a sequential keying signal which modulates a 2-kw transmitter during bursts. This keying signal is the normal, nonsynchronous teletype code in which each character is represented by a sequentially transmitted start pulse, five information pulses, and a stop pulse. During a burst the information is transmitted at 600 wpm. The fsk deviation at the transmitted frequency is 2.5 kc.

Two novel information storage and speed-changing components have been developed for use at R. One uses a continuous loop of magnetic recording tape on which the fast-speed teletype signal is recorded. After this recorded information is played back, the tape is erased and returned to the bin of tape available for recording. The other is a magnetic core storage component where the fast-speed information is stored in magnetic core matrices and read out at slow speed into standard printing equipment.

Both systems can be adapted to operate in reverse as a storage system at T; *i.e.*, store slow-speed information and read out at fast speed during bursts.

Fig. 3 shows the receiving terminal equipment at Palo Alto. The information receiver rack is on the left and includes preamplifier, converters, filters, and detector circuits. The other two racks contain the magnetic tape storage system and associated circuits. The equipment was designed and built with evaluation testing and ease of modification in mind. Unit chassis construction was used throughout and many standard plug-in circuits employed in the digital portions of the equipment. The chassis are mounted on standard relay racks and patched together with connecting cables. Each terminal operates one of the duplicate transmitters of the type shown in Fig. 4. The fsk oscillator and a 60-watt driver unit are contained in the cabinet on the right. A lab-constructed, 2-kw, Class C power amplifier and power supply are shown to the left. Fig. 5 is a photograph of the transmitting terminal equipment at Bozeman. Preamplifiers, converters, and control circuits, etc., similar to the equipment at Palo Alto, are included in the rack to the left of the Model 19 teletype equipment. The electronic transmitting distributor is in the rack to the right with the Ferranti high-speed tape reader on the bench beside it.

Signal Fading Rates: In contrast to continuous systems, where the signal must be used throughout a fade, a burst system needs to tolerate signal fading only until the information transmission can be halted. Certain irreducible time delays are encountered in controlling the starting and stopping of information transmission from a remote terminal. Approximately 17 mμsec after a start signal is generated in the receiver at R, the first information pulse should arrive. Starting delays cause only a slight reduction in duty cycle. However, an additional 16 mμsec may be required before the information cuts off at R; the transmitter distributor cannot stop in the middle of a character.

Stopping the link is a more serious problem, especially when rapidly fading signals are encountered, because of the increased probability of end-of-burst errors. Meteor-signal fading rates as high as 500 db/second have been observed on this circuit. To compensate for the effect

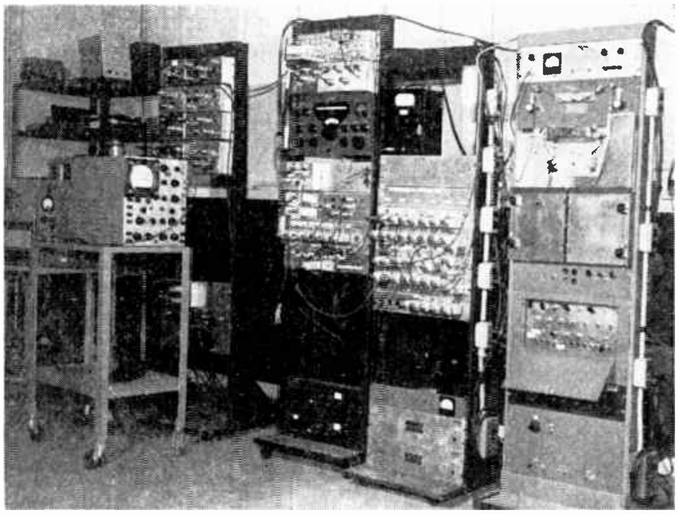

Fig. 3—Teletype system receiving terminal.

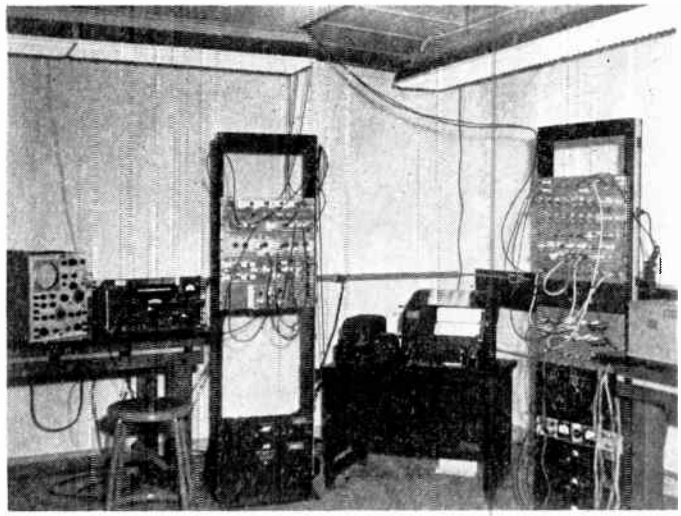

Fig. 5—Teletype system transmitting terminal.

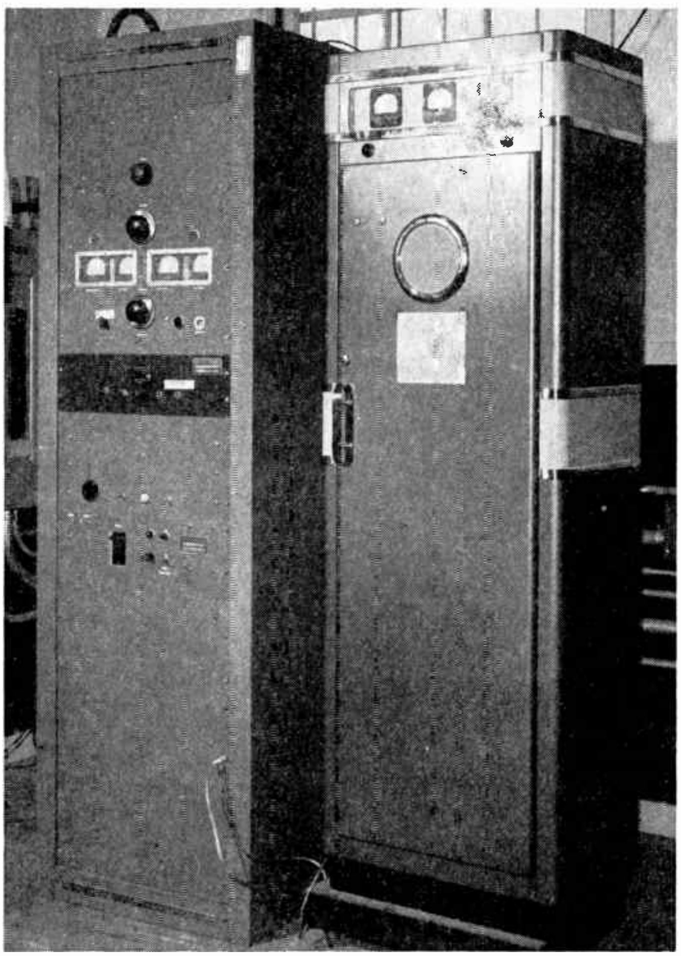

Fig. 4—FSK transmitter.

of such high fading rates in this system, the stop threshold level (received signal level at which link stop control signal is given) has been set higher than the information detectors call for at a given error rate. This again is at the expense of duty cycle. With a constant signal-to-noise ratio of about 9 db at the input of the detector in this system, character errors can be held to one per cent. The stop threshold level is generally set at about 15 db above the noise level. This will accommodate fading rates up to about 200 db/second. However, the fading-rate problem is far from solved, and it will undoubtedly receive further attention in design of future meteor-burst systems.

The Electronic Transmitting Distributor: At the transmitting terminal, information in the form of perforated paper tape is converted to a fast-speed serial modulating signal and transmitted by the information transmitter when *R* signals the presence of a meteor burst. This operation is performed by the electronic transmitting distributor which consists of a Ferranti high-speed tape reader, tape control circuits, register and counter, master oscillator, and a pulse generator.

The perforated tape is fed into the Ferranti tape reader. This commercially built unit reads the tape perforations by means of light beams and photocells. The tape is friction-driven by a rotating shaft started and stopped by a magnetically operated clutch and brake. The tape control circuits regulate the currents in the brake and clutch coils to advance the tape after each read operation. The 5-hole positions for each character are read simultaneously and these signals are then fed to the vacuum tube register and counter unit.

The timing of the information bits from the distributor is controlled by the master oscillator and pulse generator which produces timing pulses for the register and counter. The register and counter unit accepts the timing pulses and the information signals from the tape reader, plus the link control signal from the receiver, and delivers the serial output signal. This modulates the information transmitter during bursts. When the link control signal indicates the presence of a burst, the register accepts and stores the parallel input information bits, and the counter uses the timing pulses to read out the stored bits serially. A signal is then fed to the tape control circuits and the tape is advanced to the next character. When this occurs, the tape control circuits signal the register and counter and the character is then either transmitted or not, according to the position of the link control signal.

By varying the frequency of the master oscillator, information can be transmitted at any rate from 0 to 2000 wpm. However, the receiving terminal equipment was designed specifically for a 600-wpm rate. Tests at other rates have not been attempted.

The Magnetic Tape Storage System: The fast-speed teletype information from the receiver detector is recorded on magnetic tape in the form of an on/off modulated 13-kc carrier. The tape is played back at one-tenth the recorded speed and the signal, now a 1.3-kc carrier, is detected and used to operate a Model 19 teletype page printer and tape reperforator.

The magnetic tape storage system includes the delay shift register, the tape control circuits, and the magnetic tape storage unit. As illustrated in Fig. 6, the latter consists of a dual-speed, continuous-loop tape transport mechanism, record and playback amplifiers, and mechanism control circuits. A continuous loop of one-fourth inch magnetic tape runs successively through the fast-speed drive mechanism, where the tape is erased and recorded at 48 inches per second; into a storage bin; then out of the bin and through the slow-speed drive mechanism, where it is played back at 4.8 inches per second; and finally into the blank tape storage bin to await further recording. The storage bins can each hold approximately 120 feet of tape providing about 30 seconds of fast-speed recording time or 5 minutes at standard teletype speed. Because the average burst length with the power and threshold levels used is much shorter than this, the loss in duty cycle owing to lack of storage space is negligible. The enclosed tape bins and narrow filler-tube arrangement, shown in Fig. 6, proved to be a very satisfactory solution to a perplexing problem involving static-charge accumulation. This caused sticking of the magnetic tape and consequent trouble in keeping the tape in the bins. The tape mechanisms utilize synchronous motor-driven capstans and magnetically actuated pinch rollers. The fast-speed mechanism, using thyratron actuator drive circuits, has a tape starting time of less than 2 mμsec. Standard heads and amplifiers are used for tape recording and playback and a permanent magnet for tape erasure.

A fundamental design objective required that the storage system be controlled by received information only, so that storage would not be wasted when the message was for some reason not transmitted during a burst. Therefore, the received information signals are also applied to the tape drive control circuits where they are processed and used to start and stop the recording and playback tape drive mechanisms in the tape storage unit. Upon receiving the fast-speed information signal, the tape control circuits start both tape drive mechanisms. At the end of the information burst the

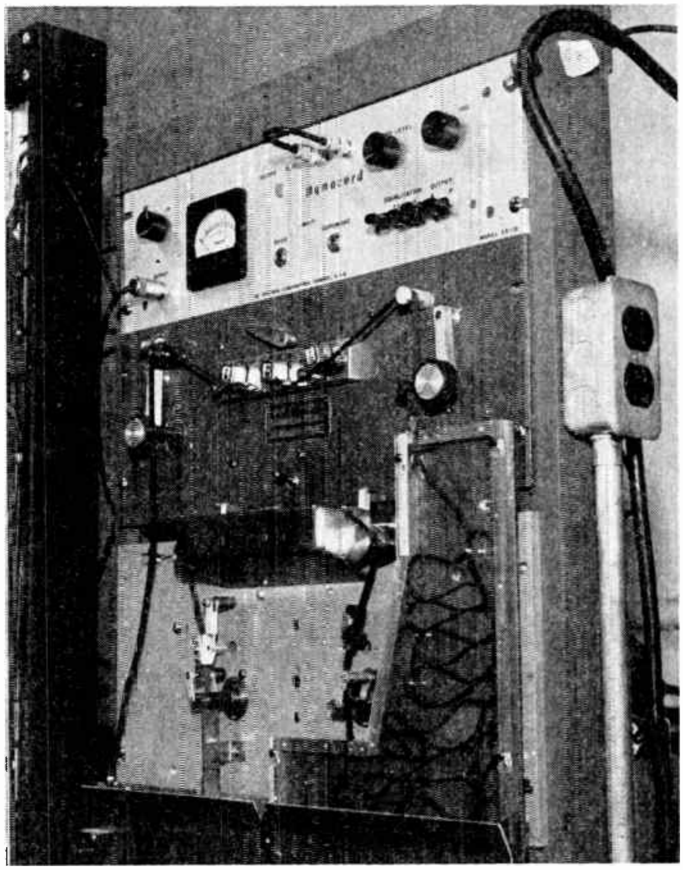

Fig. 6—Magnetic tape storage unit.

fast-speed drive is stopped but the slow-speed drive continues running until all the recorded information has been played back. If the end of the blank tape in storage is approached during a burst, a warning signal is sent to the link control circuits and the remote information transmitter is signalled to stop the information flow until additional blank tape is made available. Because the tape starting circuits receive no advance warning of information arrival and the tape needs a relatively long time to get up to speed, the fast-speed information must be delayed before being fed to the tape unit for recording. This delay is provided by a vacuum tube shift register that delays the information by one fast-speed character (16 mμsec).

The tape storage system has proved highly reliable in this application, though the tape unit itself can undoubtedly be much improved as to size, weight, and operating efficiency. The storage capacity may be increased to almost any desired size by adding more magnetic tape and larger storage bins. The tape system has a further advantage in its ability to accept information at the same time information is being read out. Because of mechanical considerations, operation of the present tape system with input information rates much over a few thousand words per minute would be difficult to attain. Also, considerable modification would be required to provide convenient control of the input-output speed ratio.

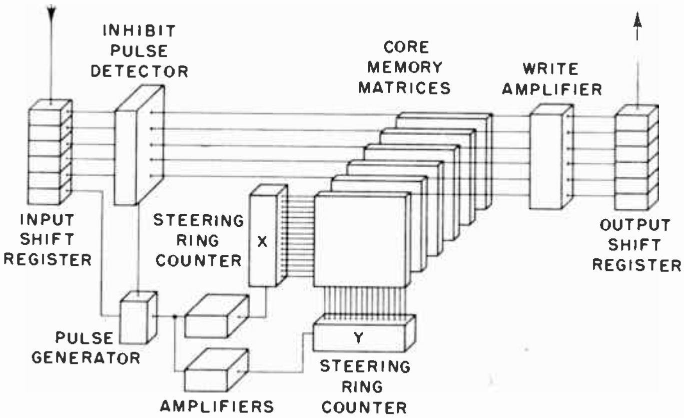

Fig. 7—Block diagram of magnetic core storage system.

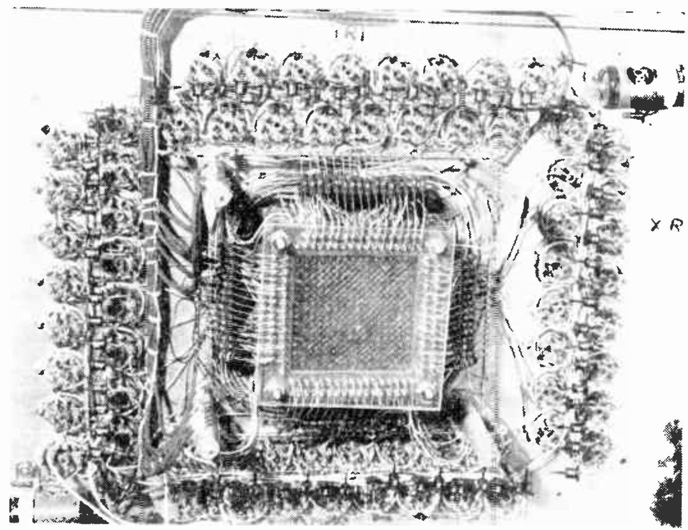

Fig. 8—Magnetic core matrices.

The Magnetic Core Storage System: A block diagram of this system is shown in Fig. 7. The fast-speed serial teletype information from the receiver detector is first fed into a vacuum tube shift register where it is converted to a parallel output signal. The start pulse and the five information bits of each teletype character are then fed out of the shift register, each going to one of six magnetic core storage matrices (see Fig. 8). At the end of the burst the stored information is read out of the matrices in parallel, one character at a time, into an output shift register. This register converts the parallel signals to a normal speed serial output signal for operation of standard teletype printing equipment.

Each of the six storage matrices consists of a rectangular plane of 240-toroidal memory cores arranged 15 by 16 Such cores have two permanent magnetic states and are thus ideally suited to store binary information Each core is traversed by two lines, the X line and the Y line. During switching of a core a current of half the amplitude necessary to switch the core from one state to the other flows in one X line and one Y line, respectively. Only the core at the intersection of these two lines will have enough drive to switch. This system is called the coincident-current method of switching.

The matrices are driven from a unit composed of memory cores and diodes, called a magnetic steering ring counter. This receives input pulses, resets itself, and steers the input pulses to the desired output lines. A circuit of this kind requires only two drivers, instead of one driver per line, or 31 drivers in all.

The read operation is triggered by the start pulse of the teletype character, which triggers a pulse generator. The short duration pulse thus generated follows two distinct paths. The first path is split into what are called the X channel and the Y channel. In each of these the pulse is amplified separately. The X and Y pulses are then fed to the X and Y magnetic steering ring counter respectively, then to the rows and columns of the matrices. The second path leads to the inhibit pulse detector. There, each of the five remaining information bits from the shift register is fed to an electronic gate together with the pulse generated by the start pulse of the character. Depending on the information in the shift register, each gate opens or remains closed. If it opens, the pulse is allowed to pass, amplified, and fed to the corresponding matrix on an inhibit line. This line traverses every core, but in such a manner that the half-current pulse it carries will subtract from the half-current pulses on the X and Y lines and prevent switching of the core.

The write operation is essentially identical with the read operation except that the inhibit gates are inoperative and the X and Y pulses now have a reverse polarity. Each core switched during the read operation will now be switched back and switching signals will be generated. These signals are detected by the write line in each matrix, a line which also traverses every core. The signals are then amplified and fed to the output shift register.

The memory used in this system is capable of storing 240 complete characters, the equivalent of 40 seconds of normal teletype speed. The memory characteristics of the magnetic steering ring counters are such that each burst of information received is stored in the area immediately following that used by the previous burst. For example, when a short burst of information is received, it may fill, say, only 60 cores of each matrix. The device then switches to the write operation. When the next burst of information comes, the device switches back to read and stores this burst, beginning at the stopping point of the previous burst, *i.e.*, starting in the sixty-first core of each matrix. This process can go on indefinitely to full storage capacity.

The same phenomenon holds for write operations. The interval of time between the two incoming bursts, mentioned in the example above, may be too short to allow the matrices to be emptied completely in one operation. In this event the write process, starting again at the end of the second incoming burst, will begin where it stopped previously.

Both the read and write triggers are connected to a counter which adds the number of characters read into the matrix and subtracts the number of characters read out. When it reaches a count of 240, a filled-storage warning is given which stops the information transit. When it reaches a count of zero, an empty-storage warning is given which stops the read-out of information. Since it requires no mechanical moving parts, the magnetic core system can be made to operate with extremely high input information speeds; *i.e.*, over a million words per minute. In addition, the read/write speed ratio can be easily changed for various system requiremen ts Chief limitations of the present magnetic core storage unit are the small storage capacity and the inability to perform the read and write operations simultaneously.

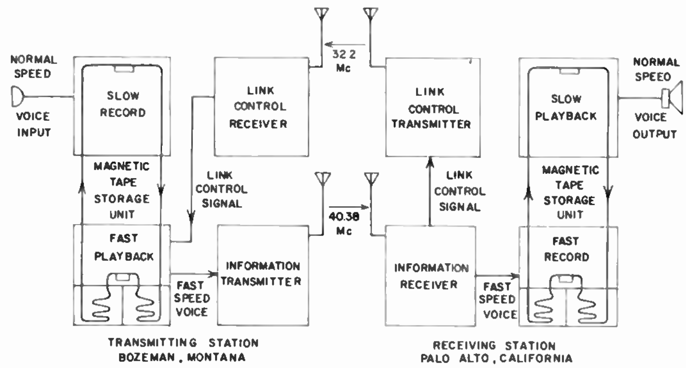

Fig. 9—Block diagram of voice system.

The Voice System

General System Characteristics: In the design of the initial voice system equipment it was decided to limit the transmission bandwidth to a maximum of 20 kc. For this reason SSB modulation is used and the voice information is transmitted during bursts at five times the normal rate, the actual bandwidth of the transmitted signal being 16.5 kc.

A block diagram of the voice system is shown in Fig. 9. A closed loop circuit similar to that used in the teletype system is employed to detect a useful meteor path and to relay control information to T. A 1-kw SSB transmitter at T sends out a continuous 100-watt recognition signal. When a path exists this signal is received at R by a duplicate of the fsk teletype receiver. When the receiver output indicates an acceptable signal level, a link control signal is generated which signals T to begin sending information. The return control link from R to T utilizes the same equipment as the teletype system, *i.e.*, a 2-kw fsk transmitter at R and an fsk receiver at T. A shift in frequency of the signal transmitted from R, initiated by the link control signal, is detected at T and information transmission from T is started.

The spoken message goes into a microphone at T and thus enters the system. The microphone output is fed to a magnetic tape storage unit and recorded and stored on a continuous loop of magnetic tape. When T is signalled to transmit information, the recorded voice signal plays back at five times the recording speed and feeds into the SSB transmitter. After playback the tape is erased and stored in a bin for further recording. The transmitter radiates a single sideband having a bandwidth of 15 kc and conveying normal voice frequencies from 300 to 3300 cps multiplied by five.

When transmission of this signal is started the 100-watt recognition signal is shifted 2.5 kc to a frequency corresponding to the carrier frequency of the voice sideband. This shift is detected by the fsk receiver at R and a signal generated which starts a second magnetic tape storage unit. The voice sideband is received at R with the same preamplifiers and first converter used with the fsk receiver. After conversion the voice signal is amplified in a special wideband IF amplifier and demodulated by a product detector. The audio output from the detector is fed to the magnetic tape storage unit. The fast-speed voice signal from the detector is recorded on a continuous loop of recording tape and played back at one-fifth the recording speed to produce a normal-speed voice output signal. This signal is fed to an audio amplifier and loudspeaker for aural monitoring and to a standard tape recorder for permanent recording of the voice information.

The SSB transmitter at T consists of an exciter, a power converter, and a 1-kw linear power amplifier. The linear amplifier utilizes 4X250B power tetrodes in a push-pull parallel Class B_1 circuit. The exciter uses the Weaver method of SSB generation.[1]

The operating frequencies of the transmitters at T and R are the same as the teletype system frequencies. Also, the same antennas are used for both systems.

The Magnetic Tape Storage Units: The magnetic tape storage unit at R is the same unit used with the teletype system at R except that the speed ratio between the record and playback operations is now 5:1, the playback tape speed being changed to 9.6 inches per second. This unit has been described in detail above and is illustrated in Fig. 5.

During voice tests the slow-speed playback at R is controlled manually to reduce the number of breaks in the voice output signal. In a practical voice system it would be desirable to provide for continuous uninterrupted playback of each individual message received.

At R the fast-speed tape drive is started when reception of voice information begins. Because of the inherent lag in starting the tape, a loss of information might presumably result unless the information were delayed before being recorded, as is done in the teletype system. In addition, fast-fading meteor trails, which reduce the received signal below a usable level before information transmission can be stopped, might also cause informa-

[1] D. K. Weaver, Jr., "A third method of generation and detection of single-sideband signals," Proc. IRE, vol. 44, pp. 1703–1705; December, 1956.

tion loss if not properly compensated. However, tests have shown that loss of short intervals of information—up to 50 mμsec or so—from the voice signal has almost no effect on intelligibility. For this reason no attempt was made to compensate for either tape starting time or fast-fading trails.

The tape storage unit at T is similar to the unit at R. In this case the information is recorded at a slow speed and played back at a fast speed. The recording operation is normally controlled by a voice operated relay. The fast playback is controlled by the link control signal received from R. If desired, a recorded message may be transmitted repeatedly without being erased. A speech processing circuit is used in the slow-speed record amplifier and serves to reduce amplitude variations and increase the average energy content of the signal fed to the SSB transmitter.

System Results and Possible Improvements

Operation of this system to date has definitely proved the feasibility of long range vhf communications via meteor-reflected signals. Reliable teletype and voice messages have been consistently received and much insight into both the theoretical and, more particularly, the practical aspects of meteor-burst communications has been gained. As the propagation method became more familiar, improvements in the system and its operation have continually been made. Additional improvements can, of course, be achieved, particularly in the over-all communication rate and reliability. A number of possibilities lies open for investigation. The most obvious, of course, are higher transmitter powers and more elaborate antenna arrays. Beneficial gains may be realized by diversity reception techniques. It is also possible that there is a transmission rate more efficient than the 600 wpm used in these tests. Investigations of multiple threshold systems and continuously variable bandwidth systems might be made. The duty cycle undoubtedly can be improved by using more advanced modulation and detection methods. Reliability of station recognition methods in the presence of both intentional and unintentional interference will require further consideration.

Some Potential Applications of the System

The future of burst techniques—meteor-burst systems in particular—seems very promising. As a consequence of the inherent anti-interference and anti-jamming characteristics it may be possible to operate a number of space-separated, meteor-burst systems on the same frequency, using coded recognition signals. Also, it is conceivable that burst-communication techniques could be used in conjunction with existing continuous systems which employ a propagation mode having large signal variations. For instance, when the received signal is greater than required for the continuous channel, a portion of the transmitted power might be routed to a parallel-burst channel with an appreciable increase in the over-all information transfer efficiency.

Acknowledgment

The authors wish to acknowledge the many contributions to the success of this project by the Special Techniques Group at Stanford Research Institute, under direction of Dr. A. M. Peterson. Special thanks are owed to Prof. D. K. Weaver and his staff at Montana State College for efficient operation of the transmitting terminal and for his assistance in the preparation of this report.

Analysis of Oblique Path Meteor-Propagation Data from the Communications Viewpoint*

W. R. VINCENT†, ASSOCIATE MEMBER, IRE, R. T. WOLFRAM†, B. M. SIFFORD†, MEMBER, IRE, W. E. JAYE†, ASSOCIATE MEMBER, IRE, AND A. M. PETERSON†, MEMBER, IRE

Summary—The characteristics of signals reflected from meteor trails have been extensively measured and analyzed to determine their usefulness in communications. The random nature of meteor sizes, radiants, velocities, time of striking the upper atmosphere, showers, etc., make precise determination of the various desirable propagation parameters difficult; however, gross characteristics such as duration, interval between usable signals, antenna direction effects, diurnal rate and duty cycle, and rate of signal decay are presented in a form usable to the design of communications circuits.

Introduction

THE PURPOSE of this report is to summarize a series of measurements undertaken at Stanford Research Institute in the field of radio signal propagation supported by ionized meteor trails. The information has been developed in a way to make it usable to the designer of communications systems. The data presented here summarize approximately two years' findings and provide a basis for determining design parameters applicable for a meteor burst communications system now in operation between Bozeman, Mont., and Stanford. Oblique propagation via reflection from meteor trails is illustrated in Fig. 1 [1–3].

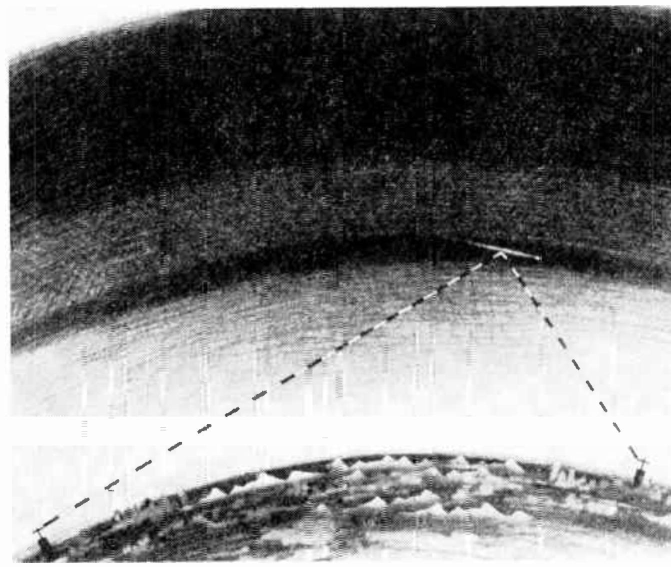

Fig. 1—Sketch of oblique meteor burst propagation.

Test Facilities

Owing to the limited level of received signal when low-power transmitters (one to two kw) are used, low-noise receiving sites are essential to meteor-burst communications. A receiving site was built in the hills beyond Stanford University and was used for the collection of data presented in this paper.

Receiving equipment consisted of various types of antennas (Yagi, 30-foot linear arrays, 61-foot parabolic dish, and dipoles), low-noise preamplifiers, converters, and standard communications receivers set up as IF amplifiers. Television stations transmit in the frequency range (55 to 85 mc) usable for meteoric propagation and therefore were used extensively as remote transmitters. Transmitting equipment operating on 40.38 mc in use on the meteor-burst communications link between Montana State College, Bozeman, Mont., and Palo Alto, Calif., was also used for the collection of signal propagation data.

Amplitude Time Functions

A specular underdense reflection results in a signal which suddenly rises and then falls in an exponential manner as illustrated in Fig. 2. Upper atmospheric winds may cause the trail to become distorted resulting in signal fading as shown in Fig. 3. Specular overdense trails will result in signals which rise rapidly and then become distorted due to the action of upper atmospheric winds. Occasionally a trail will be oriented in a way that inhibits propagation between two chosen points. Such a trail can be moved by upper atmospheric winds into a position capable of supporting signals. Trails blown into a usable orientation usually continue to fade up and down until the trail is dissipated. This produces what is called a *nonspecular overdense signal.* An example of a nonspecular overdense trail is given in Fig. 4.

An analysis of the number of each type of received signal recorded at 61 mc gave the following results. It is

Type	Percentage of Received Signals
Specular Underdense	44 per cent
Specular Overdense	37 per cent
Nonspecular Overdense	19 per cent
	100 per cent

* Original manuscript received by the IRE, September 16, 1957. The work described in this paper was sponsored by the Air Force Cambridge Research Center, Contract No. AF 19(604)-1517.
† Stanford Research Institute, Menlo Park, Calif.

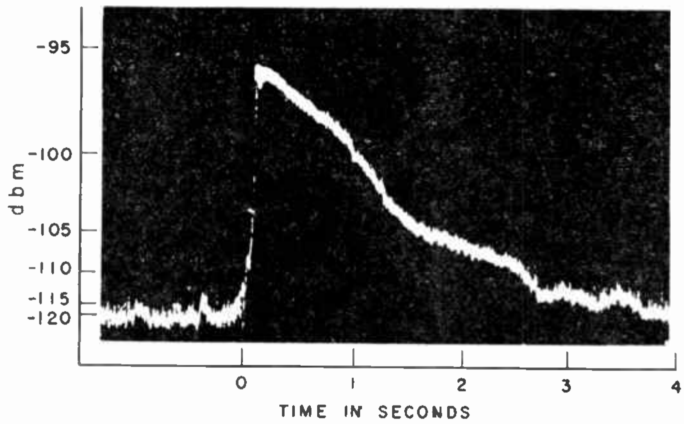

Fig. 2—Signal from specular underdense trail.

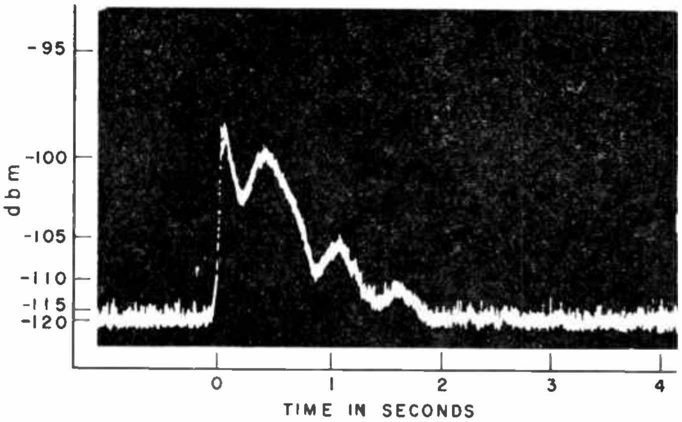

Fig. 3—Signal from specular overdense trail with wind distortion.

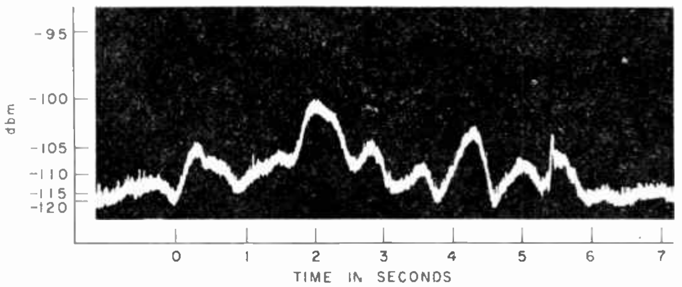

Fig. 4—Signal from nonspecular overdense trail with wind distortion.

apparent that overdense trails with their variety of amplitude time wave shapes are very important to a meteor burst communications system.

Diurnal Rate and Diurnal Duty Cycle

The varying number of meteor reflections [4] observed as a function of time of day interested investigators of meteoric phenomena for many years, and the literature contains many examples of diurnal rate obtained from radar data. Fig. 5 and Fig. 6 show examples of diurnal rate over an oblique path between Phoenix, Ariz., and Stanford, Calif. Note, in Fig. 6, the effect

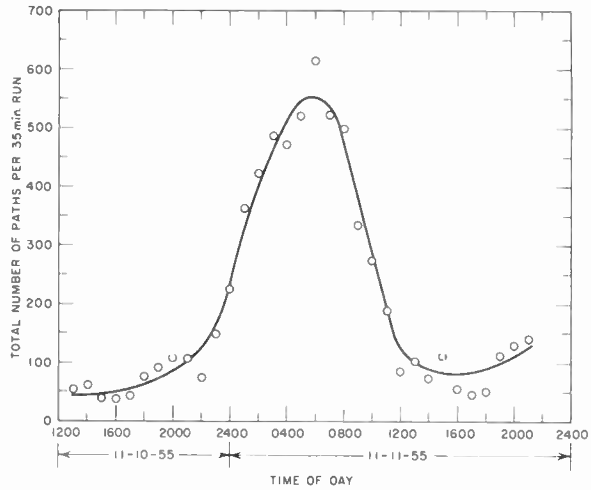

Fig. 5—Diurnal rate.

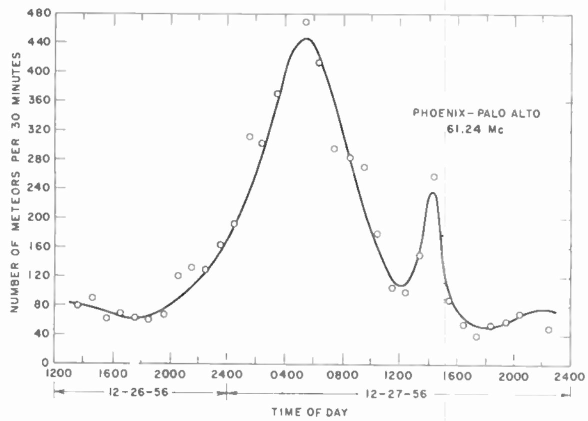

Fig. 6—Diurnal rate showing effect of shower.

of an unpredicted short lived shower at 1400 hours. Such showers are occasionally observed while propagation data are being collected. They enhance the possibility of oblique propagation.

The diurnal rate data obtained for the east-west path between Stanford, Calif. and Phoenix, Ariz. consistently have given excellent results of the form shown. Diurnal rate data for a north-south path consistently have shown a scatter of data points with only a gradual and erratic increase in meteor rate during early morning hours. The reason for this large scatter in data for a north-south path is not yet understood. Also, there appears to be a three to one change in the diurnal rate from day to day.

An example of the variation in *duty cycle* (the percentage of time a usable signal is available) throughout a 24-hour period is given in Fig. 7.

Effect of Decision Level on Duty Cycle

Duty cycle is perhaps the most important factor in the design of a communications system which makes use of ionized meteor trails. It should be pointed out here that information can be transmitted reliably only during those portions of bursts when signal-to-noise ratio

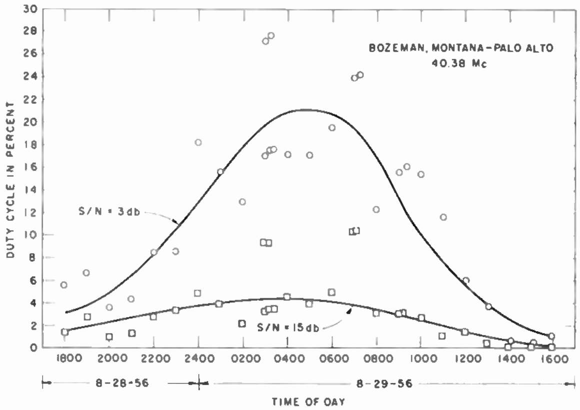

Fig. 7—Duty cycle vs time of day.

snr is adequate. The equipment starts the flow of information when snr reaches a specified value, called the *decision level*, and stops the information when snr falls below that level. Since a finite time is required for the rise and fall of signal, the duration of transmission during a burst depends on the decision level. snr is also a function of transmitter power and antenna gain. Thus, duty cycle depends on a combination of the receiver decision level, antenna gain, and transmitter power.

The data in Fig. 8 and Fig. 9 show results of duty cycle vs receiver decision level measurements made with a fixed receiver bandwidth and constant transmitter power. Fig. 9 shows how this curve changes from morning to evening; Fig. 8 indicates how the data vary with the distance between transmitter and receiver. A 3-db increase in transmitter power or antenna gain would have the same effect on duty cycle as a 3-db decrease in decision level, hence the duty cycle vs decision level curves can be translated conveniently to show the performance of systems requiring different threshold levels, different transmitter powers, and different bandwidths. This can be done merely by adding or subtracting the required db change from the abscissa of the examples shown.

The information capacity [5, 6] of a meteor burst communications system and its relation to bandwidth can be expressed in the following form

$$I = KB^{2-k/2}$$

where I = information, B is system bandwidth, k is slope of the duty cycle vs decision level curves, and K is a factor lumping several constant terms. Fig. 10 (p. 1704) is a plot of information vs bandwidth for several values of k. Several items of importance to burst systems immediately become apparent and are listed as follows.

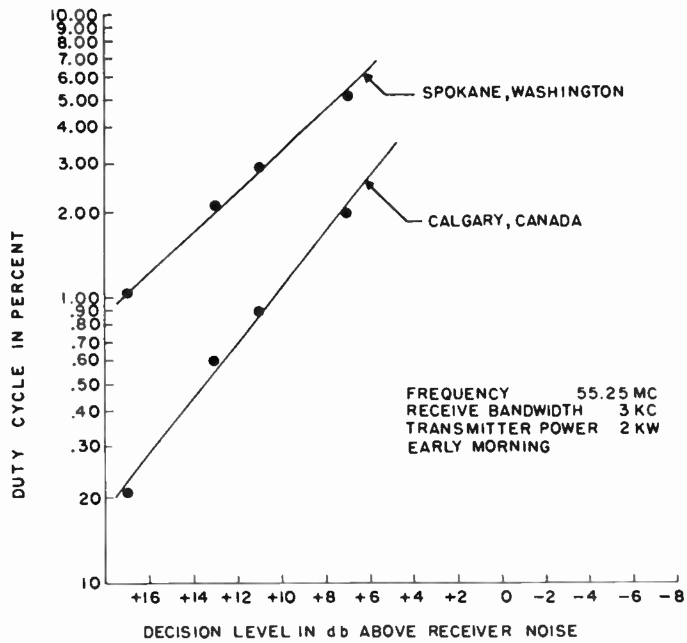

Fig. 8—Duty cycle vs receiver decision level showing effect of distance.

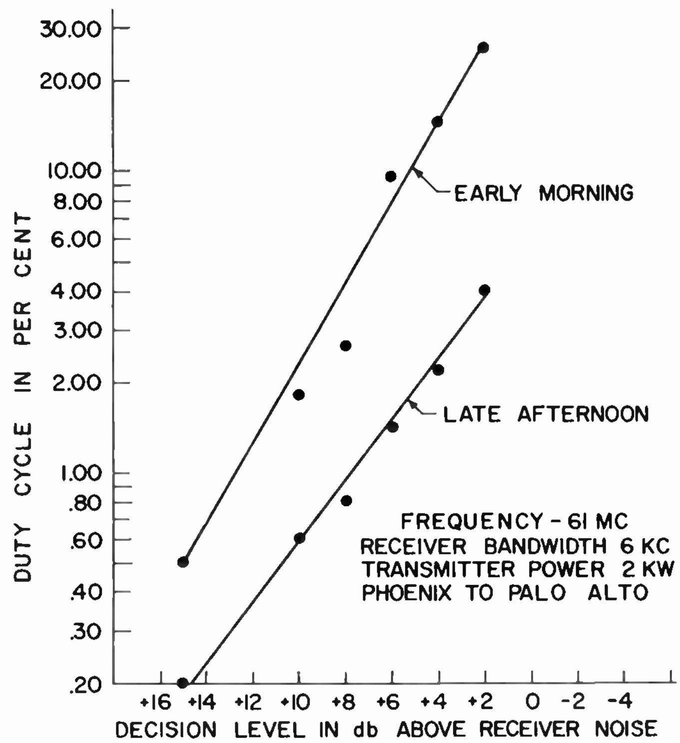

Fig. 9—Duty cycle vs receiver decision level showing effect of time of day.

1) If the slope of the duty cycle vs decision level curve is less than 2, more information can be passed over a burst system by increasing the bandwidth to the maximum value consistent with present equipment designs and sending at a fast rate consistent with this bandwidth.
2) If the slope of the duty cycle vs decision level curve is greater than 2, the information transfer can be maximized by using very narrow bandwidths and transmitting at a low rate.
3) If the slope of the curve is 2, the system bandwidth and the transmission rate are unimportant.
4) Fig. 10 shows that the information transfer is quite dependent upon the slope of this curve and that system design should be in accordance with the best estimate of this slope.

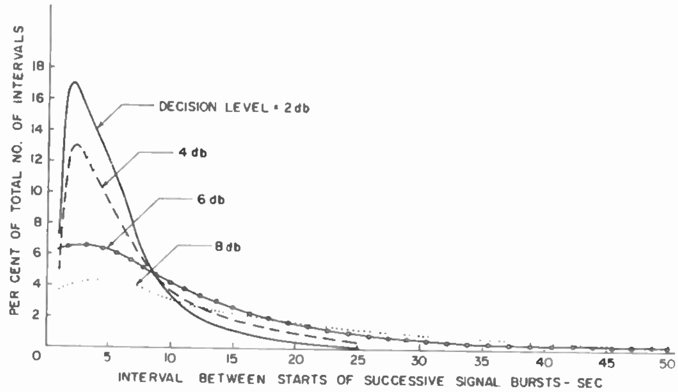

Fig. 10—Variation of mean information rate with bandwidth.

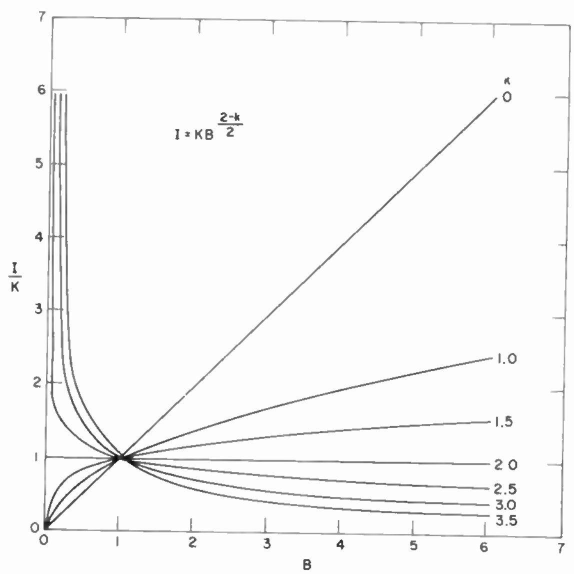

Fig. 11—Distribution of interval between usable signals—early morning.

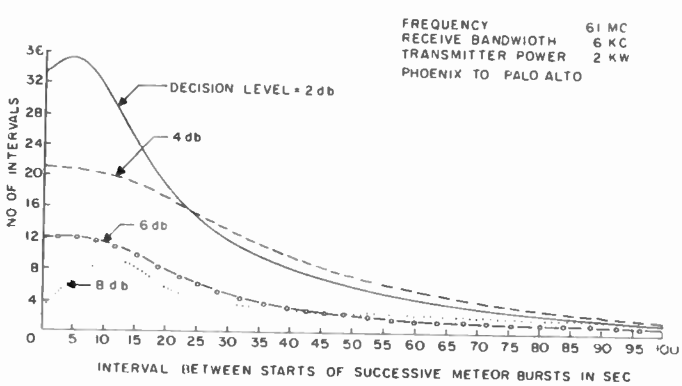

Fig. 12—Distribution of interval between usable signals—late evening.

Measured values for the slope of duty cycle vs decision level curves have ranged from 1.3 to 2.7. Present measurements have not clearly defined a precise range of slopes. An extensive series of measurement is currently under way to better define parameters affecting slopes of the duty cycle vs decision level curves.

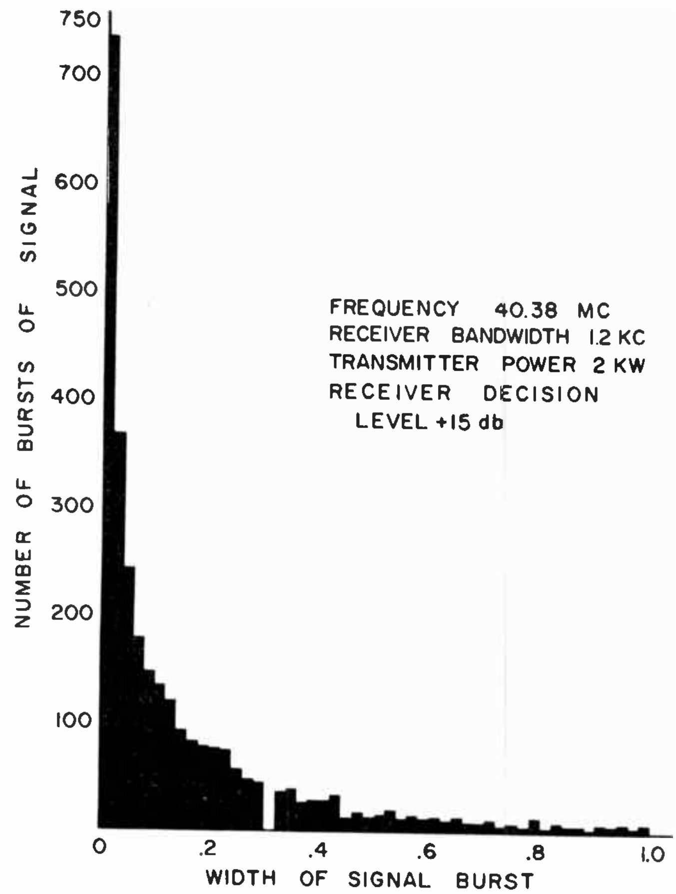

Fig. 13—Duration of usable signals.

The Interval Between Usable Signals and the Duration of Usable Signals

A frequent question—and an important one to the designer of communications equipment—is, "How long do I wait before a meteor forms a usable trail?" The occurrence of meteors is random in time and one meteor as a result of fading often supplies many usable signals (as indicated in Fig. 4). The interval between usable upswings of signal is illustrated by the distributions shown in Fig. 11 and Fig. 12. These distributions illustrate how the interval changes from the early morning maximum in the diurnal rate to the evening minimum. Fig. 11 and Fig. 12 also indicate the effect of varying the decision level of the receiving equipment while the transmitter power and receiver bandwidth are held constant.

The duration of a meteor signal is dependent upon the size of the meteor, the speed at which it enters the upper atmosphere, its orientation with respect to transmitter and receiver, and the action of upper atmosphere winds. The net effect is to make possible a series of received signals having random duration. An example showing the duration distribution [7] of usable received signals is given in Fig. 13. The example shows that the signal received is likely to be one of very short duration. In fact, experience with the Stanford Research Institute meteor-burst teletype communication system shows that the largest number of signals received are

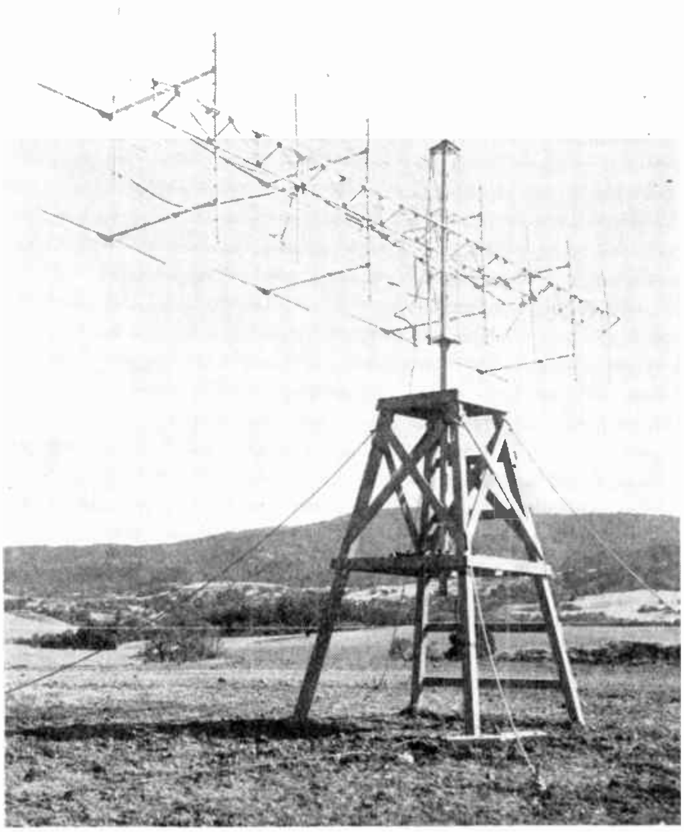

Fig. 14—Antenna array.

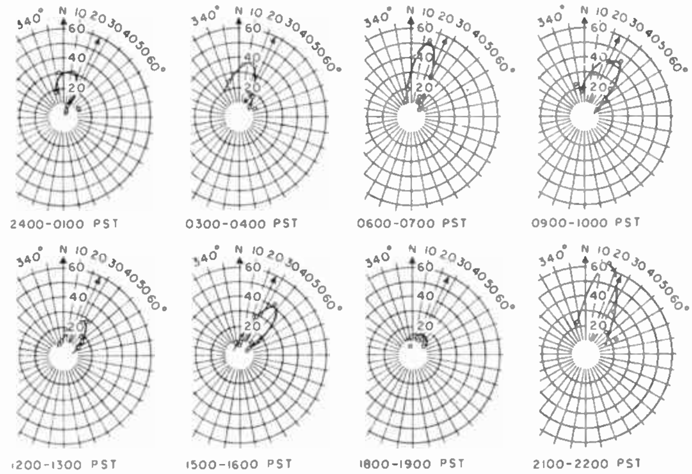

Fig. 15—Polar plots showing north-south directional effects.

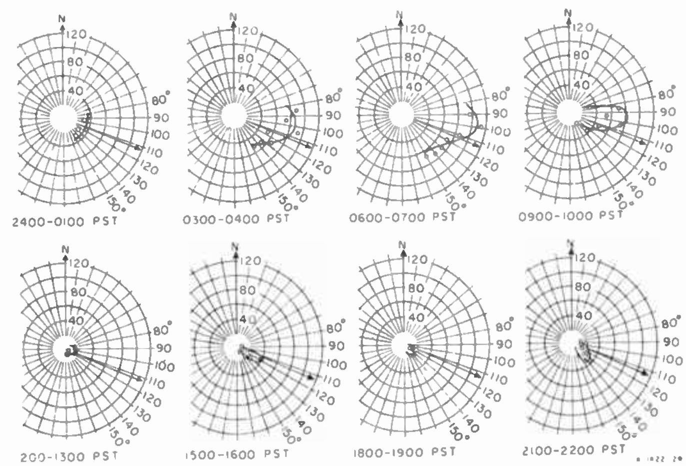

Fig. 16—Polar plots showing east-west directional effects.

but one character in length. Fortunately, the distribution also shows that signal duration of several seconds is reasonably probable. The average duration of the example shown is approximately 0.2 seconds.

Optimum Azimuth Antenna Direction

As a result of the investigation of meteor radiants at Stanford University [8], Eshleman predicted that the performance of communications systems utilizing ionized meteor trails could be improved by directing the antennas first to one side of the great circle path between receiver and transmitter and then to the other side of the great circle. Theoretical considerations indicated that directing antennas along the great circle path would reduce considerably the number of meteors detected, particularly if high-gain antennas were used. Eshleman's predictions are shown in an accompanying paper, this issue, p. 1710.

A series of tests were undertaken to measure the effect of the "active areas" and to determine the extent of the off-great-circle azimuth prediction. For these measurements, a rotatable antenna array was constructed which provided a horizontal beamwidth of 20° at 60 mc. This array was used to receive meteor reflected signals over east-west and north-south paths from suitably located television transmitters. The antenna (see Fig. 14) was programmed as follows (0° is the great circle path from Stanford to the transmitter):

Direction	Duration of Sample
0	5 minutes
10° R	5 minutes
10° L	5 minutes
20° R	5 minutes
20° L	5 minutes
30° R	5 minutes
30° L	5 minutes
40° R	5 minutes
40° L	5 minutes

The sampling was repeated each hour throughout a 24-hour period. The number of meteors detected during each 5 minutes was recorded in tabular form from automatic counters or Brush recorder data. The data were then plotted in polar form showing the directional effects indicated in Fig. 15 and Fig. 16. An estimate of the best angle for each hour throughout a run was made and the results are shown in Fig. 17 and Fig. 18.

The results clearly show that, for an east-west path, the antenna should be directed to the south of path during afternoon and to the north of path during morning hours. For a north-south path, the antenna should be directed to the east of path in daylight and to the west of path at night. Experimental results further in-

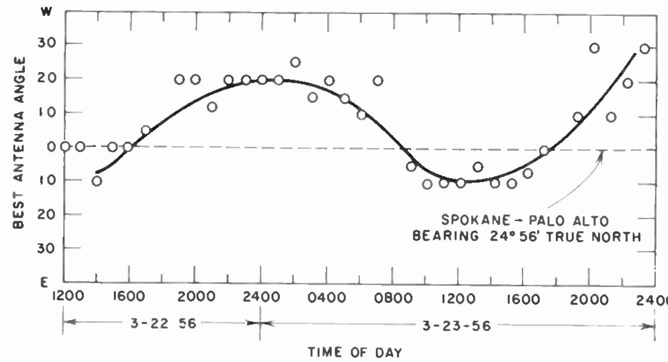

Fig. 17—Best antenna angle vs time of day—north-south.

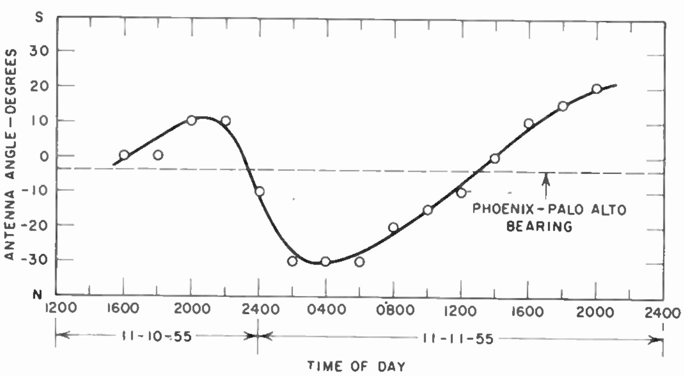

Fig. 18—Best antenna angle vs time of day—east-west.

dicated the off-path phenomena to be as large as 30°. The experimental data appear to confirm Eshleman's prediction and tend to support the assumed spherically-uniform heliocentric distribution of meteor orbits.

Additional data displaying the extent of the off-path effect are given in Fig. 19 and Fig. 20, where the percentage increase in meteors received on the favorable side is also shown.

Fading Rates of Received Signals

Operation of the Stanford-Bozeman meteor burst teletype system and the examination of amplitude-time records indicated that very rapid decreases in received signal occurred occasionally. To investigate this occasional high fading of signals, an oscilloscope was connected to the receiver detector and the sweep triggered each time the signal faded below a preset threshold. A photograph was made of several hundred successive sweeps, and the rate of fall of the signal examined. Fig. 21 gives an example of such a measurement, where the threshold is set at 0 db and decreasing signals go in the downward direction. Signal fades in excess of 400 db per second are shown.

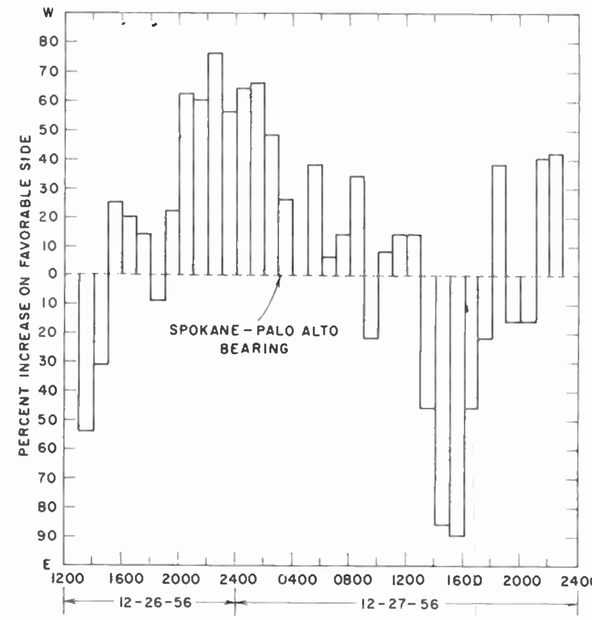

Fig. 19—Best side of path vs time of day—north-south.

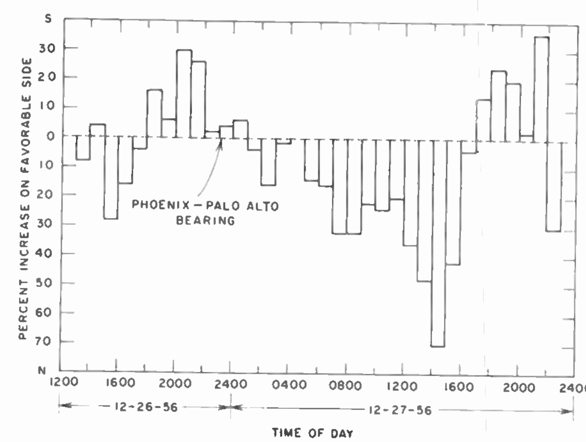

Fig. 20—Best side of path vs time of day—east-west.

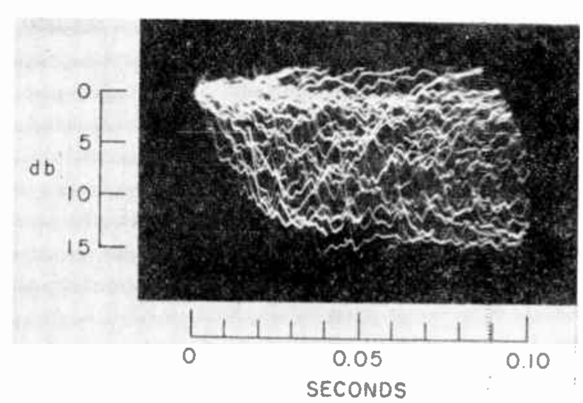

Fig. 21—Fading rate photograph.

Maximum Range Tests

If conventional calculating methods are used and a reflection height of 100 km assumed, the maximum ground-to-ground communication range is found to be 2400 km (1500 miles). To check this, distant television stations were monitored at various ranges up to 2900 km. Meteor reflected signals were received from one station at 2200 km, but not from another station at 2400 km. The maximum usable range for a ground-to-ground communications system using antennas relatively close to sea level is thus considered to be 2200 km.

Conclusion

The results presented are samples taken from data accumulated over the past two years. It should be pointed out that meteor rates vary from day to day, diurnally, seasonally, and, to some extent, with the location on the earth. Therefore, some caution should be used in attempts to interpret precisely or to scale the results. The gross characteristics of a communications path supported by ionized meteor trails is described and may be of value to those interested in the advantages of communications by this method.

Bibliography

[1] Eshleman, V. R. *Meteors and Radio Propagation*. Stanford: Stanford University, Radio Propagation Laboratory, Part A, Technical Report No. 44, February, 1955.

[2] Hines, C. O. *The Efficiency of Meteor Scattering over Short and Long Ranges*. Ottawa, Canada: Defence Research Tele-Communications Establishment, Radio Physics Laboratory, August, 1955.

[3] McKinley, D. W. R. "Meteor Echo Duration and Radio Wavelength," *Canadian Journal of Physics*, vol. 31 (November, 1953), pp. 1121–1135.

[4] Lovell, A. C. B. *Meteor Astronomy*. New York: Oxford University Press, 1954.

[5] Weaver, D. K. *Applied Research on Meteor-Burst Communications*. Menlo Park: Stanford Research Institute Scientific Report No. 2, May, 1956.

7] Hines, C. O. *Information Transfer in Janet Systems of Fixed and/or Variable Bandwidths*. Ottawa, Canada: Defence Research Telecommunications Establishment, Radio Physics Laboratory, July, 1955.

[7] Wirth, H. J. *Preliminary Observations of Forward Scattering of Electromagnetic Waves by Meteor Trails*. San Diego: U. S. Naval Laboratory, Research Report 690, March, 1956.

[8] Eshleman, V. R. and Mlodnosky, R. F. "Directional Characteristics of Meteor Propagation Derived from Radar Measurements," Proceedings of the IRE, this issue, p. 1715.

An Investigation of Storage Capacity Required for a Meteor-Burst Communications System*

ROBERT A. RACH†

***Summary*—The storage capacity requirement of a burst-type communications system is analyzed. Two main categories of storage devices, which correspond to the magnetic tape and magnetic core type units currently in use on burst circuits, are considered. Storage units used in the present Stanford Research Institute meteor-burst system are analyzed to determine the loss in over-all systems efficiency imposed by limited capacity of these devices. The equations developed provide a convenient method of assessing the storage requirements of any burst system provided certain of its measured parameters are available.**

Introduction

All existing and planned[1–3] meteor-burst communications systems operate on the basis of the rapid transmission of information while a usable signal is present. Since terminal equipment cannot operate at rates consistent with most system designs, buffer storage devices are required to: 1) receive the message from the originating source at the normal generating rate of that source, store the message, and transmit it at a high rate of speed during periods of usable signals; 2) to receive the information transmitted during a usable signal at high speed, store this information, and supply it to a recording or presentation device.

Two types of storage devices are currently used in the Stanford-Bozeman meteor-burst communication system.[1] The capacity of such storage devices is very important in the design of burst systems.

Storage with Simultaneous Read-In and Read-Out

Consider a usable signal with sufficient duration for a total of N_{max} characters to be transmitted over a meteor burst system. Because of a finite storage capacity at the receiver, N_{max} characters might not be transmitted because of a filled storage device. The following development will provide an upper bound on the number of characters or bits of information per second which can be approached in a practical system based on the assumption of an empty storage at the start of operation. The development uses terminology applied to a teletype signal.

If we have a distribution of burst lengths (here assumed to be in characters rather than time), we can say that the number of characters received with a storage of infinite capacity is:

$$N_{max} = \sum_{c=1}^{w} cF(c)$$

* Original manuscript received by the IRE, September 16, 1957. The work described in this paper was sponsored by the Air Force Cambridge Research Center, Contract AF 19(604)-1517.

† Stanford Research Institute, Menlo Park, Calif.

[1] W. R. Vincent, R. T. Wolfram, B. M. Sifford, W. E. Jaye, and A. M. Peterson, "A meteor-burst system for extended range vhf communication," Proc. IRE, this issue, p. 1693.

[2] P. A. Forsyth, "The Characteristics of a Novel Communications Technique," Radio Phys. Lab., Defense Res. Estab., Ottawa, Canada, April, 1953.

[3] R. J. Carpenter, "Equipment for an Experimental Meteor-Burst Communications Systems," Natl. Bureau of Standards, CRPL Boulder, Colo., Rep. 6CB101.

where c = number of characters per burst, w = a number larger than the largest number of characters per burst observed, and $F(c)$ = number of bursts with "c" characters. With simultaneous read-in read-out, characters will be removed from the storage device both during read-in and after read-in or after filled storage. The number of characters which can be passed through the storage in a finite time is dependent upon the speed-up; *i.e.*, the ratio of read-in rate to read-out rate. If S is the speed-up ratio, then while S characters are read into the memory, one character is being read out. This process continues as the storage fills.

Defining C as the actual storage and considering a 100-character storage with a speed-up ratio of 10. When we read in 10 characters, we read out 1, leaving 9. At 100 characters read-in we have 90 stored. Reading in 10 more allows us to read out 1, so a total of 111 characters actually is required to fill a storage of 100. Defining the effective storage as C', then:

$$C' = C \sum_{n=0}^{L} \frac{1}{S^n}$$

where $n = 0, 1, 2, \cdots L$, and L is chosen only large enough to obtain an integral value of C'.

Now let us consider the case of a finite storage with no read-out until storage is filled, where the total number of characters received is N'. Such a storage will handle all accumulated characters during bursts where the total is less than or equal to the storage capacity, or the number of characters equal to the storage capacity if a burst duration exceeds the capacity. Then

$$N' = \sum_{c=1}^{C} cF(c) + \sum_{c=C+1}^{w} CF(c).$$

Now by similar reasoning, considering the case where we can read-out during a burst, then the number of characters received, N'', can be expressed as

$$N'' = \sum_{c=1}^{C'} cF(c) + \sum_{c=C'+1}^{w} C'F(c).$$

The difference between an infinite capacity system and the system described for N'' becomes $N_{\max} - N''$.

$$\begin{aligned} N_{\max} - N'' &= \sum_{c=1}^{w} cF(c) - \sum_{c=1}^{C'} cF(c) - \sum_{c=C'+1}^{w} C'F(c) \\ &= \sum_{c=C'+1}^{w} cF(c) - \sum_{c=C'+1}^{w} C'F(c) \\ &= \sum_{c=C'+1}^{w} (c - C')F(c). \end{aligned}$$

The number of characters defined by $N_{\max} - N''$ is number lost due to filled storage where we cannot yet feed in more characters as storage is read-out. Actually, the system described will read-out characters making additional storage available for read-in. Since the read-out rate is $1/S$ as fast as the read-in rate, a time of S is required to read-out one character and read-in an additional character. Thus, the receiver will actually handle $n' = 1/S(N_{\max} - N'')$ of the characters in excess of storage capability, where

$$n' = \frac{1}{S} \sum_{c=C'+1}^{w} (c - C')F(c).$$

The total number of characters N the system will handle is

$$N = N'' + n' = \sum_{c=1}^{C'} cF(c) + \sum_{c=C'+1}^{w} C'F(c) + \frac{1}{S} \sum_{c=C'+1}^{w} (c - C')F(c).$$

The first term of this equation describes the performance of a system when the number of characters per burst is less than C'. The second term expresses the case where the burst is longer than C' characters resulting in the storage of C' characters. The third term describes the additional capacity resulting from storage made available by read-out after fill storage. The efficiency of the system can be defined as $N/N_{\max}$.

Storage System without Simultaneous Read-In and Read-Out

Since this type of storage cannot read-out while reading in, then C is the actual capacity instead of C' in the previous example. Then as developed before

$$N' = \sum_{c=1}^{C} cF(c) + \sum_{c=C+1}^{w} CF(c).$$

Thus, the difference between an infinite capacity and this system is $N_{\max} - N'$.

$$N_{\max} - N' = \sum_{c=C+1}^{w} (c - C)F(c).$$

In order to read a character out and one in, the time of $S+1$ characters is required or

$$n' = \frac{1}{S+1} \sum_{c=C+1}^{w} (c - C)F(c).$$

The total number of characters the storage will handle again is $N = N' + n'$

$$N = \sum_{c=1}^{C} CF(c) + \sum_{c=C+1}^{w} CF(c) + \frac{1}{S+1} \sum_{c=C+1}^{w} (c - C)F(c).$$

Loss of Characters Due to Equipment Considerations

Practical equipment designs do not use all of the burst time due to propagation path delays, recognition of signals, desirability of eliminating the last character of a burst of usable signal to improve error rates, etc. The following analysis will permit an estimate of system performance degradation as a result of such causes.

Defining the number of characters available as

$$N_{\max} = \sum_{c=1}^{w} cF(c).$$

Omitting i characters from each burst will: 1) eliminate all bursts i characters or less in duration, and 2) reduce the durations of all other bursts by i characters. Thus, the usable number of characters N can be defined as

$$N = \sum_{c=i+1}^{w} cF(c) - \sum_{c=i+1}^{w} iF(c) = \sum_{c=i+1}^{w} (c-i)F(c).$$

The efficiency of the system, as shown in Fig. 1 and Fig. 2, is then $N/N_{\max}$. The degradation in performance created by not using all the burst time can be obtained from this type curve. The curve shown was based on an experimental determination of $F(c)$ for the communications system described in an accompanying paper.[1]

Conclusion

An example of the storage system first defined with simultaneous read-in and -out is the closed loop magnetic tape unit currently used on the Stanford, Calif.—Bozeman, Mont. meteor-burst communications system. This system has a storage capacity of approximately 900 characters and operates on a speed up ratio $S=10$. The accompanying curves show that very little loss of information handling capacity should exist due to the storage capacity being exceeded. Practical experience indeed shows this to be the case.

An example of the second storage system described is a magnetic-core storage system which is also currently used on the Stanford, Calif.—Bozeman, Mont. meteor-burst communications system. This system has a storage capacity of 240 teletype characters and presently operates at a speed-up ratio $S=10$, although S may be easily varied. The accompanying curves show that the limited capacity of this unit does slightly degrade teletype system performance. Practical experience shows that occasionally the storage is unable to handle bursts of long duration; however, the loss of efficiency is not appreciable and can be reduced by the addition of cores.

Fig. 1 which shows the capacity of a storage system vs efficiency of storage, was based on an experimental determination of $F(c)$ for the meteor-burst communications system described in an accompanying paper.[1]

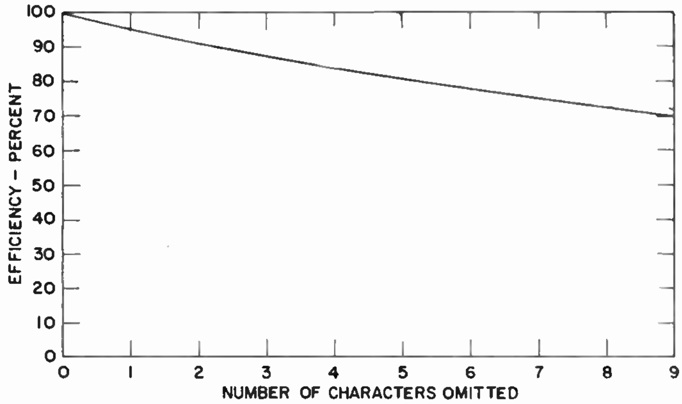

Fig. 1—Efficiency of meteor system as a function of number of characters omitted.

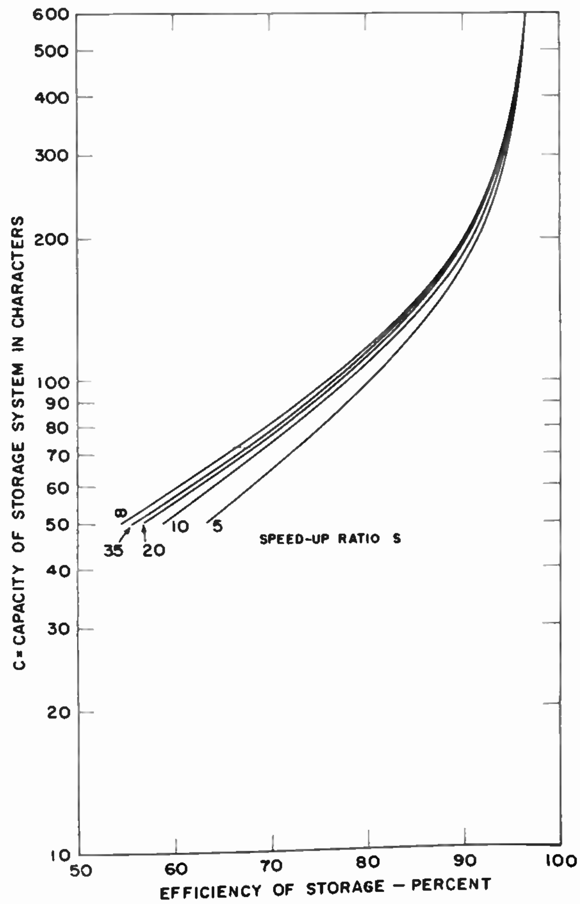

Fig. 2—Efficiency as a function of storage capacity.

On the Wavelength Dependence of the Information Capacity of Meteor-Burst Propagation*

VON R. ESHLEMAN†, SENIOR MEMBER, IRE

Summary—**The discontinuous vhf signal, propagated over ranges up to 2000 km by reflections from meteor ionization trails, makes possible an important new technique for radio communication. With this technique, the required transmitter power and antenna sizes are considerably less than for communication by the continuous vhf scatter signal supported by smaller meteors and other scattering sources in the lower E region. The wavelength dependence of the information capacity of meteor-burst propagation is approximately $\lambda^{2.7}$, which may be compared to approximately $\lambda^{4.7}$ for the continuous signal. Thus, by adding the complexity in the terminal equipment needed for discontinuous operation, meteor-burst communication can fill an important need at the same wavelengths that are used in ionospheric-scatter communication, and can be used at shorter wavelengths than are feasible with continuous scatter. This extension to shorter wavelengths should make it possible to reduce the interference problem now being encountered in the lower vhf band, and to greatly increase the number of channels available for reliable long-range communication.**

INTRODUCTION

A NEW mode of radio propagation shows promise of making additional channels available for reliable, long-range radio communication. This mode of propagation depends upon radio reflections from the columns of ionization left in the wake of meteors as they speed into the earth's upper atmosphere.

Radio studies of meteoric ionization have been conducted at various laboratories since the end of World War II. Perhaps the most extensive studies of this type have been carried out by investigators at the University of Manchester, Eng., at the National Research Council, Can., and at Stanford University, Stanford, Calif. From these studies, much has been learned about meteors and about that region of the upper atmosphere in which they form ionized trails.

It was suggested several years ago that scattering from meteoric ionization plays an important, if not the dominant, role in extended-range vhf ionospheric scatter propagation.[1–8] While the relative contribution to continuous scatter of meteors and other scattering sources is still being debated, it is agreed that the relatively large meteors are responsible for the discontinuous, high-amplitude vhf signals, or "bursts," which can be propagated over distances up to about 2000 km.

In the early 1950's, many propagation specialists were acquainted with proposals to use meteor bursts for useful radio communication. Such a proposal was initiated by Pineo of the National Bureau of Standards. When the author first came to Stanford University in 1949, Villard, Manning, and Peterson were discussing the possible utility of meteor-burst communication, based on the results obtained that summer in a series of oblique-path meteor tests. Some of the earliest investigations of radio reflections from meteor trails involved the monitoring of distant, short-wave transmitters.[9–12] Often, program material was being transmitted, and short passages of apparently undistorted speech and music were heard. The monitoring of bursts of fm broadcast transmission from Boston, Mass. at Grand Island, Neb. (a distance of 1370 miles) by Allen, in 1943, is especially worthy of note.[12] While many early investigators may have forseen the possible utility of meteor burst propagation, the research group at the Radio Physics Laboratory of the Canadian Defense Research Board, under the direction of Dr. P. A. Forsyth,[13] clearly was responsible for appreciating not only the potentialities but also the practical importance of this method of communication. Credit is due this group for devising the closed loop technique and for providing the first demonstration of a working system.

* Original manuscript received by the IRE, September 13, 1957. The research in this paper was supported by the Electronics Res. Dir., Air Force Cambridge Res. Ctr., Air Res. and Dev. Com., under contract with Stanford University.

† Radio Propagation Lab., Stanford University, Stanford, Calif.

[1] D. K. Bailey, R. Bateman, L. V. Berkner, H. G. Booker, G. F. Montgomery, E. M. Purcell, W. W. Salisbury, and J. B. Wiesner, "A new kind of radio propagation at very high frequencies observable over long distances," *Phys. Rev.*, vol. 86, pp. 141–145; April, 1952.

[2] O. G. Villard, Jr., A. M. Peterson, L. A. Manning, and V. R. Eshleman, "Extended-range radio transmission by oblique reflection from meteoric ionization," *J. Geophys. Res.*, vol. 58, pp. 83–93; March, 1953.

[3] V. R. Eshleman and L. A. Manning, "Radio communication by scattering from meteoric ionization," PROC. IRE, vol. 42, pp. 530–536; March, 1954.

[4] D. W. R. McKinley, "Dependence of integrated duration of meteor echoes on wavelength and sensitivity," *Can. J. Phys.*, vol. 32, pp. 450–467; July, 1954.

[5] W. J. Bray, J. A. Saxton, R. W. White, and G. W. Luscombe, "VHF propagation by ionospheric scattering and its application to long-distance communication," *Proc. IEE*, vol. 103B, pp. 236–260; March, 1956.

[6] D. K. Bailey, R. Bateman, and R. C. Kirby, "Radio transmission at vhf by scattering and other processes in the lower ionosphere," PROC. IRE, vol. 43, pp. 1181–1231; October, 1955.

[7] O. G. Villard, Jr., V. R. Eshleman, L. A. Manning, and A. M. Peterson, "The role of meteors in extended-range vhf propagation," PROC. IRE, vol. 43, pp. 1473–1481; October, 1955.

[8] P. A. Forsyth and E. L. Vogan, "Forward-scattering of radio waves by meteor trails," *Can. J. Phys.*, vol. 33, pp. 176–188; May 1955.

[9] J. A. Pierce, "Abnormal ionization in the E-region of the ionosphere," PROC. IRE, vol. 26, pp. 892–902; July, 1938.

[10] C. Chamanlal and K. Venkatamaran, "Whistling meteors-doppler effect produced by meteors entering the ionosphere," *Electrotechnics*, vol. 14, pp. 28–40; November, 1941.

[11] O. G. Villard, Jr., "Listening in on the stars," *QST*, vol. 30, p. 59, January, 1946.

[12] E. W. Allen, Jr., "Reflections of very-high-frequency radio waves from meteoric ionization," PROC. IRE, vol. 36, pp. 346–352, March, 1948. See also, discussion of this paper by L. A. Manning and O. G. Villard, Jr., PROC. IRE, vol. 36, pp. 1255–1257; October, 1948.

[13] P. A. Forsyth, E. L. Vogan, C. O. Hines, D. R. Hansen, and others in various Radio Physics Lab. Reps., Defence Res. Telecomm. Estab., Defence Research Board, Ottawa, Can.; 1953 *et. seq.*

In this paper, the wavelength dependence of the information capacity of meteor propagation is reviewed and discussed. The discussion is based only on first-order effects, with no attempt being made to outline completely all that presently is known about meteor echo characteristics. The primary aim is to show that, while meteor-burst communication can fill an important need at the radio wavelengths which are used for vhf ionospheric-scatter communication, its potential utility at appreciably shorter wavelengths (where continuous-scatter communication is not feasible) may be of prime importance. In comparing meteor-burst with ionospheric-scatter communication, it should be stressed that the same region of the ionosphere is used in the two systems for propagating the radio waves, and that the differences are primarily in the method of utilizing the fluctuating received signal. The advantages of meteor-burst communication over continuous ionospheric-scatter communication (lower power, smaller antennas, wider usable spectrum, less interference, greater security) are due to the fact that the scattered signals are more efficiently used when provisions are made to send and receive information discontinuously. It might be said that the terminal equipments are then better matched to the propagating medium.

Why Bursts?

But how does it come about that the use of a discontinuous signal offers advantages over the use of a continuous vhf scatter signal propagated over the same path? The answer to this question involves considerations of the relative transmitter power requirements, antenna size requirements, and practicable operating wavelengths for the same information flow in the two systems. Other factors which must be taken into account are terminal equipment complexity, circuit reliability (including freedom from interference), and the required degree of immediacy of the message.

Average Information Capacity

The peak power of the echoes from most meteor ionization trails varies as $P_T G_T G_R \lambda^3 q^2$, where P_T is the transmitted power, G_T and G_R are the gains of the antennas used at transmitter and receiver, λ is the radio wavelength, and q is the number of electrons per meter of trail length formed at the reflection point by the meteoric particle. The average duration of the individual echoes is approximately proportional to λ^2. The number of detectable meteor trails is proportional to the area A of the relatively thin meteor region common to both antenna beams. Assuming the above expression for echo intensity, it has been found, from short-term measurements on the number-amplitude distribution over limited ranges of echo amplitudes, that the number of trails formed with line densities greater than q electrons per meter is proportional to q^{-k}. (The measured values of k may vary from about one to two depending upon time of day, season, path geometry, and system parameters.) Thus the total number of echoes is proportional to Aq^{-k}.

Now suppose that in a meteor burst system, the operating level (the signal-power level above which information is sent at constant bandwidth B and below which no information is sent) exceeds the receiver noise level by a fixed factor. For the radio wavelengths of interest, the minimum receiver noise level is determined by cosmic noise. This noise is proportional to $B\lambda^n$, where n has been measured[14] for scaled antennas to be approximately 2.3. Let us assign a value of $q=q_0$ for a meteor trail whose peak echo intensity is just equal to the operating power level. Then the fractional time that information will be transmitted (the circuit duty cycle D) is proportional to the product of the number of echoes having $q>q_0$ and the average echo duration, or

$$D \sim \lambda^2 A q_0^{-k}. \tag{1}$$

Since the operating level is proportional to the receiver noise, $P_T G_T G_R \lambda^3 q_0^2 \sim B\lambda^n$, or

$$B \sim P_T G_T G_R \lambda^{3-n} q_0^2. \tag{2}$$

The average rate of information flow in the meteor burst system described above is proportional to the bandwidth and the duty cycle, or $I \sim BD$. From the relationships given above,

$$I \sim P_T G_T G_R \lambda^{5-n} A q_0^{2-k}. \tag{3}$$

Since the operating power level is proportional to q_0^2, the q_0^{2-k} factor in (3) implies that the average information rate is directly proportional to the value of the operating power level raised to the $(2-k)/2$ power.

This last statement contains part of the answer to the question, "Why bursts?," since it indicates that for $k<2$ (in which range most of the measured values lie), more average information can be sent by raising the operating level and thereby reducing the circuit duty cycle. That is, the gain in information capacity due to the increased bandwidth is greater than the loss of information capacity due to decreased duty cycle.

For several reasons the choice of operating level cannot be made arbitrarily high to obtain an arbitrarily large information capacity. First, the relationship given above for the number of meteors and their line densities does not extend to indefinitely large values of q. Second, the relationships given above for echo amplitude and duration are valid only when $q<10^{14}$ electrons per meter; *i.e.*, only for the low-density[7] trails. Information capacity probably does not increase as the threshold level is increased beyond the point corresponding to $q_0=10^{14}$. Third, the operating level should not be made so high that the time between useful bursts is so great that short, high priority messages are delayed more than is desired. Other limitations may be imposed by the maximum bandwidth of meteor echoes and the delays

[14] H. V. Cottony and J. R. Johler, "Cosmic radio noise intensities in the vhf band," Proc. IRE, vol. 40, pp. 1053–1060; September, 1952.

encountered in starting and stopping the flow of information. However, the conclusion given in the previous paragraph still should be valid over a wide range of parameters. It is expected that the maximum information rate will be obtained with a duty cycle which is considerably less than unity, the precise value depending upon the circuit parameters and the changing meteoric characteristics.

Antenna Gain Considerations

Let us assume that the antennas used at each end of the path have the same gain, and that they are directed so as to illuminate the same area in the meteor ionization region. Then, $G_R = G_T = G$ and $G \sim A^{-1}$, so that (1)–(3) become $D \sim \lambda^2 G^{-1} q_0^{-k}$, $B \sim P_T G^2 \lambda^{3-n} q_0^2$, and $I \sim P_T G \lambda^{5-n} q_0^{2-k}$.

Suppose that G is increased and the operating level is held constant. Since the operating level is proportional to $P_T G^2 \lambda^3 q_0^2$, the value of q_0 is decreased by the same amount that G is increased, assuming that the other parameters are held constant. Thus D will vary as G^{k-1}, B will remain constant, and I will vary as G^{k-1}. If $k = 1$ (the value which is believed to be applicable to the smaller meteors),[15] duty cycle and average information capacity are independent of antenna gain. That is, the loss in number of meteors caused by reducing the area illuminated by the antenna beam is exactly compensated by the increase in the number of detectable trails accompanying the greater system sensitivity.[3] For k between one and two, increasing the antenna gain at both ends of the circuit increases the average information capacity.

In the above discussion, it tacitly is assumed that all areas of the meteor-ionization region are equally useful in terms of the number and duration of detectable trails. But certain areas are better than others, as described in a companion paper on the directional characteristics of meteor propagation.[16] Thus, in addition to the factors outlined above, information capacity can be increased by adjusting the antenna gains and directions so as to illuminate only those parts of the meteor ionization region which are most favorable for meteor propagation.

The optimization of the antenna characteristics for maximum information capacity also should lead to less interference and greater security in meteor-burst communication circuits. Full appreciation of the factors which can be controlled by antenna considerations makes possible a great many special antenna configurations for special operating characteristics. For example, by using two separate receivers connected to two separate antenna beams directed toward different halves of the meteor area illuminated by the transmitting antenna, the information capacity with the same operating level can be increased as much as 41 per cent over what it would be if only one receiver and one antenna beam were used, this antenna illuminating the same area as the transmitting antenna. Interference also could be reduced with this arrangement. This technique might be called "h-plane diversity," to differentiate it from the ground plane diversity encountered in more conventional communication. (Here the h plane refers to the plane at the average height h—approximately 100 km—of the meteor ionization trails.)

Wavelength Dependence

In order to discuss the effects of the operating radio wavelength, it is desirable to decide which parameters are to be held constant as the wavelength is varied. It appears logical to assume that antenna beams of the same gain and orientation are used, so that the same area of the meteor plane is illuminated at all wavelengths. Answers to the following questions are then sought: should the same meteors be used at each wavelength; should the threshold level be held constant; should the duty cycle be held constant; or should the bandwidth be the same at each wavelength? Each of these circumstances leads to a different wavelength dependence for the average information rate.

The comparison that will be made here is on the basis of using the same meteors for communication at the various wavelengths. Thus q_0 is assumed to be constant. There can be no difficulty in extrapolating the number-density law to higher or lower-density meteors, since the same meteors are used at each wavelength. Also, with this criterion, the average time between useful bursts is invariant, as is the information per burst for the same average information rate.

With scaled antennas and constant q_0, the operating level is proportional to $P_T\lambda^3$, the duty cycle is proportional to λ^2, the bandwidth is proportional to $P_T\lambda^{3-n}$, and the average information rate is proportional to $P_T\lambda^{5-n}$. For example, with $n = 2.3$, the average information rate at a wavelength of 4 meters is less by a factor of 6.5 than at 8 meters for the same P_T and using the same meteors. The duty cycle is less by a factor of 4, and the bandwidth is less by a factor of 1.6 under the above conditions.

Alternatively, the information rate at 4 meters may be made the same as at 8 meters by increasing P_T by a factor of 6.5, reducing the duty cycle by a factor of 4, and increasing the bandwidth to 4 times its value at 8 meters. These changes are illustrated in Table I, where the parameters at $\lambda = 8$ m and $P_T = 1$ kw are used as a starting point for comparison. Note that the increase in P_T is accompanied by a decrease in D for the same information rate, so that the average power during the time that information is being sent is up only by a factor of $6.5/4 = 1.6$ in halving the wavelength. That is, if the transmitter power during the rest of the time is only a small fraction of the power during the time of transmission of information, not much more than 60

[15] P. B. Gallagher and V. R. Eshleman, "Radar studies of meteors down to 15th magnitude," presented at the joint URSI-IRE meeting, Washington, D. C.; May 24, 1957.

[16] V. R. Eshleman and R. F. Mlodnosky, "Directional characteristics of meteor propagation derived from radar measurements," this issue, p. 1715.

per cent greater average power is required for the same average information rate when the wavelength is halved. While this may be considered a serious loss, we shall see that a considerably greater loss is encountered in continuous-scatter communication when the wavelength is halved.

TABLE I

EXAMPLES OF SYSTEM PARAMETERS FOR METEOR-BURST COMMUNICATION, WHERE THE SAME METEORS ARE USED AT WAVELENGTHS OF 8 AND 4 METERS.

	Radio Wavelength	
	8 m	4 m
P_T (peak watts)	1000	1000
I (wpm)	60	9.2
B (cps)	100	61.5
D (per cent)	10	2.5
P_T (average watts)	100	25
P_T (peak watts)	6500	6500
I (wpm)	390	60
B (cps)	650	400
D (per cent)	10	2.5
P_T (average watts)	650	162

Comparison with Continuous-Scatter Communication

If the signal is to be continuous, the duty cycle is a constant; namely, unity. The duty cycle defined above was the product of number of echoes exceeding the reference level times their average duration. This is adequate when the duty cycle is small, but for values more than a few tenths, the statistical overlapping of echoes implies that the true duty cycle[3] is $1-\exp(-D)$. Considering only meteors, it is not possible to obtain a truly continuous signal. But when the product of number and duration is large, the signal virtually is continuous.

The details of the above considerations are not important in what is to be emphasized here. The important factor is that, for a "continuous" signal, D is constant. For scaled antennas and constant D, q_0 is proportional to $\lambda^{2/k}$, so that

$$I \sim P_T \lambda^{3-n+4/k}. \tag{4}$$

For any value of $k<2$ in the expression for average information rate, the exponent of λ for continuous meteor communication is greater than for burst communication.

For the smaller meteors, it is believed that $k \cong 1$ so that information rate is proportional to $P_T\lambda^{7-n}$. This last wavelength dependence is particularly interesting since it is about the same as the average value measured in continuous, extended-range vhf ionospheric scatter propagation.[6] Thus, whether or not this scatter signal largely is due to meteors, the following arguments based on the wavelength dependence of meteor propagation should be valid, since the same wavelength dependence is obtained from measurements on the continuous signal.

It was shown above that for burst-communication, information capacity could be held constant when the wavelength is halved by increasing peak transmitter power by a factor of 6.5, or the average power by a factor of 1.6. For continuous propagation, with $k=1$ and $n=2.3$, the average transmitting power must be increased by a factor of 26 to maintain constant information flow when the wavelength is halved. In Table II a comparison is made between meteor burst and ionospheric-scatter communication, where it is assumed that a peak power of 1 kw is sufficient for a 60-wpm meteor burst channel at 10 per cent duty cycle and 8 meter wavelength, while an average power of 10 kw is required for 60 wpm at 8 meters using continuous scatter. This ratio of required powers for the same average information is a rough estimate, the actual ratio being determined in practice by the relative role of meteors and other scatterers in supporting the continuous signal. In any event, in comparing meteor burst with ionospheric-scatter communication, the former starts from a lower required power at the long wavelengths and has a lower rate of loss of information as the wavelength is shortened.

TABLE II

COMPARISON OF METEOR-BURST AND IONOSPHERIC-SCATTER COMMUNICATION

	Average Information Rate (wpm)			
	Meteor Burst		Ionospheric Scatter	
P_T (kw)	8 m	4 m	8 m	4 m
1	60	9.2	6	0.2
6.5	390	60	39	1.5
10	600	92	60	2.3
260	15,600	2400	1560	60

The above arguments on the wavelength dependence appear to be of great significance in considerations of the potential importance and utility of meteor burst communication.

Continuous ionospheric scatter propagation is filling an important requirement for more spectrum space and more reliable long-range communication. It appears to be most useful in the 35 to 45 mc region (8.5 to 6.5 meters). Even at these wavelengths, very high transmitter power and large antennas are required for modest information rates. Because of the strong wavelength dependence of signal strength or information rate, operation at wavelengths considerably shorter than 6 meters does not appear feasible for continuous ionospheric-scatter communication. At the wavelengths now being used, there is a considerable amount of interference to and from other short-range users of adjacent channels. Also, the current high F-layer critical frequencies make it possible for a circuit to experience self-interference from long-delay ground backscatter echoes.

Meteor-burst communication may have an important role to play in this same wavelength range. By adding the complexity required in the terminal equipment for discontinuous operation, it is possible to obtain the same information rate as in continuous circuits with less power and simpler antennas. Thus the meteor burst communication technique would be well suited where power and area for antennas are at a premium. Also, the burst technique could be incorporated in existing ionospheric scatter systems to provide a considerable increase in their capacity.

However, it is believed that the most important potential application of meteor-burst communication is at the shorter wavelengths where there is more spectrum space, where there is less likelihood of interference to and from other users of the same or adjacent channels, where it is highly unlikely that ionospheric-layer-supported ground backscatter will cause self-interference, and where the information security is greater. It is believed that wavelengths at least as short as 3 meters will prove very useful for meteor-burst communication.

Conclusion

In the comparisons made above between meteor-burst and ionospheric-scatter communications, it tacitly is assumed that in each case a constant bandwidth is used when information is being transmitted and received. In both systems, the same propagating medium is used and the same signal is available. This signal fluctuates widely. The principal difference in the two communication techniques is in the use of this fluctuating signal. In one system only the large signal enhancements are used. This is called meteor-burst communication, because it is known that these large short-lived bursts are due to reflections from meteor trails. In the other system, information is sent continuously at a constant rate which is determined by the lowest signal levels. This is called ionospheric-scatter communication, the total signal being due to meteors and other scattering sources in the E region of the ionosphere.

But the optimum use of the fluctuating signal would require a system with a continuously variable information bandwidth. With continuous feedback between transmitter and receiver, the information bandwidth could be varied to follow the fluctuating signal strength. Until such a system becomes practicable, it is evident from the previous discussion that the ideal system is better approximated by large bandwidths and small duty cycles than by narrow bandwidths and unity duty cycle. That is, the fluctuating signal is used more efficiently in meteor-burst communication than in ionospheric-scatter communication. Alternatively, it might be said that the terminal equipments are better matched to the propagating medium when provisions are made to send and receive information discontinuously.

The advantages of meteor-burst communication over ionospheric-scatter communication (less power, smaller antennas, less interference, more security, spectrum extending to shorter wavelengths) are due to the more efficient use of the fluctuating signal.

The disadvantages of meteor-burst communication as compared with ionospheric-scatter communication (more complex equipment, greater delay in starting messages) are due to the difficulties encountered in utilizing the fluctuating signal more efficiently.

Directional Characteristics of Meteor Propagation Derived from Radar Measurements*

V. R. ESHLEMAN†, SENIOR MEMBER, IRE, AND R. F. MLODNOSKY†, STUDENT MEMBER, IRE

Summary—The directivity of radio reflections from meteor trails and the distribution of trail orientations (radiants) control the directional properties of meteor propagation. Because of the geometrical correspondence between radar and oblique path detection of meteors, the directional properties of meteor propagation can be determined from the range and azimuth distributions of the echoes detected by a radar system. The gross features of these directional properties for an east-west path in northern temperate latitudes are such that—for maximum circuit duty cycle (product of number of echoes and their average duration)—the antenna beams at the transmitter and receiver should be pointed north of the great circle bearing during the morning hours and south of this bearing during the evening. The optimum off-path angle may vary from a few degrees to greater than 20°. For a north-south path, the beams should be pointed west of the path at night and east of the path during the day, for maximum duty cycle. These gross features appear to repeat each day. In addition, short-term fluctuations in the radiant distribution have been noted, some of these fluctuations presumably being due to heretofore undetected meteor showers of very short duration. It appears that the information capacity of meteor burst and ionospheric scatter communication systems could be markedly increased by varying the bearings of the antenna beams according to the known diurnal variations in meteor radiants. In addition, it may be possible to utilize the short-term fluctuations in the radiant distribution by means of a radar which can monitor continuously the changing radiant distribution and "instantaneously predict" the optimum antenna bearings for the communication circuit.

Introduction

THE radio energy reflected from a newly formed meteor ionization trail is highly directive. The reflection is specular, the angles of incidence and reflection (relative to the straight axis of the trail) being supplementary. As the trail ages it is contorted into a sinuous shape by wind shears. Because of this distortion, several specular reflection points (glints)[1] are formed, and the total reflected energy is less directive than for the newly formed trail. However, some degree of directivity of the reflected radio energy relative to the original line of the trail persists for an average of ten seconds after trail formation.[2]

The diameter of the meteor trail increases with time due to diffusion. This expansion controls the strength of the radio reflections and limits the time during which they are strong enough to be detected. Most meteor echoes are less than one second in duration. Only a very small fraction of the trails is sufficiently dense to produce echoes which last as long as ten seconds. Thus, most of the radio energy reflected from meteor trails is confined near those directions corresponding to specular reflections from the original axes of the trails.

Because of the directivity of the radio reflection from the straight column of ionization formed by a meteoric particle, the paths of propagation from transmitter to receiver via meteor trails depend upon the directions of travel of the particles. (The direction of travel is perhaps best described by the meteor's radiant, the point on the celestial sphere from which it appears to emanate. Two angles serve to define the radiant. Particles of a given meteor shower have the same radiant. However, most of the signals used in meteor burst propagation are from sporadic meteors, so that it is necessary to consider the distribution of meteor radiants on the celestial hemisphere.)

The purpose of this paper is to outline briefly what is presently known about the directional characteristics of meteor propagation and to show how a radar system can be used to measure these directional characteristics. (As used here, the term radar inplies that the transmitter and receiver are at the same location.) Some preliminary results are presented of radar measurements applied to an east-west and a north-south meteor propagation path. Certain features of these derived results are compared with simultaneous measurements of the directions of arrival of meteor echoes over the E-W and N-S paths.[3]

Theoretical Predictions

It has been predicted that relatively few meteor echoes will be obtained when high-gain antennas at the transmitter and receiver are beamed to intersect in the meteor region (approximately 100 km high) over the midpoint of the great circle path between transmitter and receiver. (At the midpoint, the trails must be horizontal to satisfy the geometrical conditions for reflection. There are few such trails since the number of meteors crossing a unit horizontal area is proportional to the cosine of the angle between the normal to the area and the direction of the trails.) If there were a uniform distribution of meteor radiants over the celestial hemisphere, the area in the meteor region from which the largest number of echoes could be obtained would lie

* Original manuscript received by the IRE, September 13, 1957. The research in this paper was supported by the Electronics Res. Directorate of the Air Force Cambridge Res. Ctr., Air Res. and Dev. Command, under contract with Stanford University.

† Radio Propagation Lab., Stanford University, Stanford, Calif.

[1] L. A. Manning, "The Fading of Meteoric Radio Echoes," presented at the joint URSI-IRE meeting, Washington, D. C.; May 24, 1957.

[2] D. W. R. McKinley and P. M. Millman, "A phenomenological theory of radar echoes from meteors," Proc. IRE, vol. 37, pp. 364–375; April, 1949.

[3] W. R. Vincent, R. T. Wolfram, B. M. Gifford, W. E. Jaye, and A. M. Peterson, "Analysis of oblique path meteor propagation data from the communications viewpoint," this issue; p. 1701.

along the periphery of an ellipse centered over the path midpoint. The major axis of this ellipse lies along the direction between transmitter and receiver and is slightly greater than the transmitter-receiver distance. The minor axis is equal to twice the average height of the meteor region.

But the usefulness of meteor echoes for communication depends upon their individual durations as well as upon their number. Echo duration varies approximately as $\sec^2\phi$, where 2ϕ is the included angle between the rays from the trail to the transmitter and receiver. This factor is maximum for trails directly over the path midpoint. As a result, the product of number and duration is maximum in two areas in the meteor region to either side of the point over the path midpoint. The lateral deviation of these two "hot-spot" areas from the midpoint is somewhat less than the average meteor height. (See Fig. 1). Thus, the product of number of echoes and their durations (circuit duty cycle) can be increased by directing high-gain antennas to one side of the path instead of along the great circle path.

The above theoretical characteristics of meteor propagation have been treated in several publications under somewhat different sets of assumptions.[4–8] Usually, it was assumed that the radiants were uniformly distributed. This was the obvious initial assumption for the theoretical development since complete information on the radiant distribution was lacking. Such complete information is still lacking, but the results of recent experiments and theoretical investigations now make it possible to discuss some of the more important directional characteristics of meteor propagation. That is, the diurnal and seasonal variations in the radiant distribution on the celestial hemisphere above a particular meteor circuit control the relative magnitude and position of the two "hot spots" of the product of meteor number and duration.

From considerations of the manner in which the earth sweeps through interplanetary space, it is not difficult to see why more meteors are incident within an observer's horizon during the morning hours, when he is on the forward side of the earth, than during the evening hours, when he is on the trailing side of the earth. The concentration of meteor radiants towards the apex of the earth's way is perhaps the strongest factor affecting the directional characteristics of meteor propagation.

In an effort to understand better the factors which

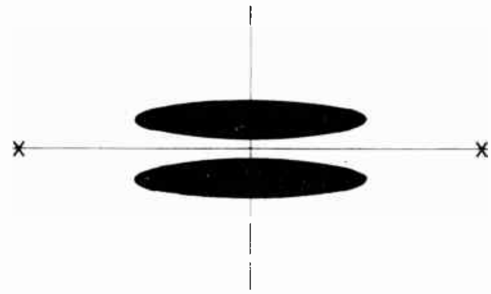

Fig. 1—Plan view of those areas of the meteor plane most favorable for meteor propagation over a 1000-km path between the points marked by X's. It is assumed that the meteor radiants are distributed uniformly over the celestial hemisphere.

control meteor rates and radiants, computations were made[9] based on several simple models. On the assumption that all meteor orbits are parabolic and that they are uniformally distributed relative to the sun, the following gross characteristics would be expected in temperate latitudes: 1) there is an approximate sine wave distribution of the number of trails formed above an observer's horizon with time of day, the maximum being at 0600 and the minimum at 1800 daily; 2) the number of trails is greater during the autumnal equinox than during the vernal equinox; and 3) the amount of the daily variation in number decreases with latitude, while the amount of the seasonal variation increases with the latitude of the observer. On the assumption that the meteor orbits were confined to the plane of the ecliptic, the predicted morning maximum is shifted to after 0600 for the summer solstice, and to before 0600 for the winter solstice. It is still at 0600 during the autumnal equinox, but it splits into two maxima which occur before and after 0600 during the vernal equinox.

The above characteristics are for the total number of trails formed above an observer's horizon. The number of trails which can be detected by a radio system depends not only on the influx rate of meteors, but also upon their radiants and upon the antenna patterns. For the uniform distribution of orbits relative to the sun, it was found[8,9] that the maximum number of meteor echoes for a radar in northern temperate latitudes would be obtained by directing the radar antenna north at 0600, east at 1200, south at 1800, and west at 2400 local time. (For southern temperate latitudes, interchange north and south in the above statement.) For optimum meteor propagation over long paths, these same geometrical considerations lead to diurnal variations in the strength of the "hot spots" of meteor activity. For north temperate latitudes, it was predicted[9] that: 1) for an east-west path, the antennas at transmitter and receiver should be beamed to intersect north of the path midpoint from 2400 to 1200, and south of the midpoint from 1200 to 2400; and 2) for a north-south path, the antennas should be beamed west of the path from 1800

[4] V. R. Eshleman and L. A. Manning, "Radio communication by scattering from meteoric ionization," Proc. IRE, vol. 42, pp. 530–536; March, 1954.

[5] R. E. Pugh, "The number density of meteor trails observable by the forward-scattering of radio waves," *Can. J. Phys.*, vol. 34, pp. 997–1004; October, 1956.

[6] C. O. Hines and R. E. Pugh, "The spatial distribution of signal sources in meteoric forward-scattering," *Can. J. Phys.*, vol. 34, pp. 1005–1015; October, 1956.

[7] J. C. James and M. L. Meeks, "On the Relative Contributions of Various Sky Regions to Meteor-Trail Communication," Georgia Inst. Tech., Atlanta, Ga., Tech. Rep. No. 1; June 30, 1956.

[8] O. G. Villard, Jr., V. R. Eshleman, L. A. Manning, and A. M. Peterson, "The role of meteors in extended-range vhf propagation," Proc. IRE, vol. 43, pp. 1473–1481; October, 1955.

[9] V. R. Eshleman, "Meteors and Radio Propagation: Part A," Stanford University, Stanford, Calif., Radio Propagation Lab., Tech. Rep. No. 44; February 1, 1955.

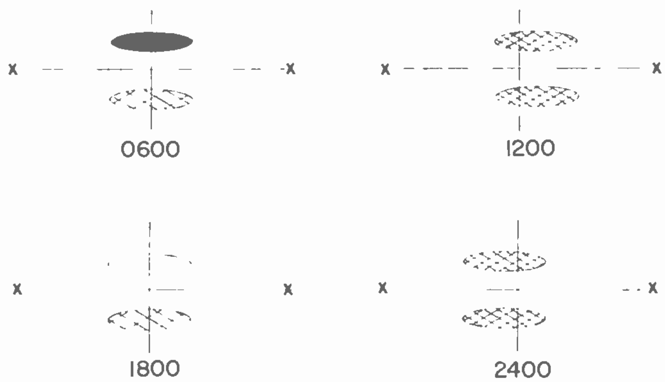

Fig. 2—Plan view of those areas of the meteor plane most favorable for meteor propagation at various times of day for an east-west 1000-km path in northern temperate latitudes. These gross theoretical features are predicted from a uniform distribution of meteor orbits relative to the sun. The shading indicates the approximate relative importance of the areas.

to 0600, and east of the path from 0600 to 1800, for maximum duty cycle. These diurnal variations are illustrated in an elementary manner in Figs. 2 and 3. Similar theoretical conclusions for oblique meteor propagation have been reached by Hines,[10] who also considered uniform heliocentric meteor orbits.

However, the results of these computations are based upon a highly idealized model. Experimental determinations of the radiants of relatively large meteors have been made by both photographic and radar techniques. From photographic data on 144 meteors, Whipple[11] found that 30 per cent of the sporadic meteors were in orbits inclined less than 10° from the ecliptic plane. About 90 per cent of these had direct motion; *i.e.*, they moved in the same direction around the sun as the earth. Hawkins[12] determined statistical information on meteor radiants from single-station radar measurements, using antenna beams directed north and south of west at low elevation angles. He concluded that meteor orbits are strongly concentrated toward the ecliptic plane, and that there are concentrations of radiants toward the helion and anti-helion, as well as toward the apex. Similar measurements have been made in the southern hemisphere by Ellyett and Keay.[13] The radiants of individual sporadic meteors have been measured by a three-station radio technique by Gill and Davies.[14] McCrosky has analyzed a large number of the Harvard photographic records to obtain sporadic meteor radiants. The results of these last two sets of measurements are not yet generally available.

The above experimental determinations of meteor

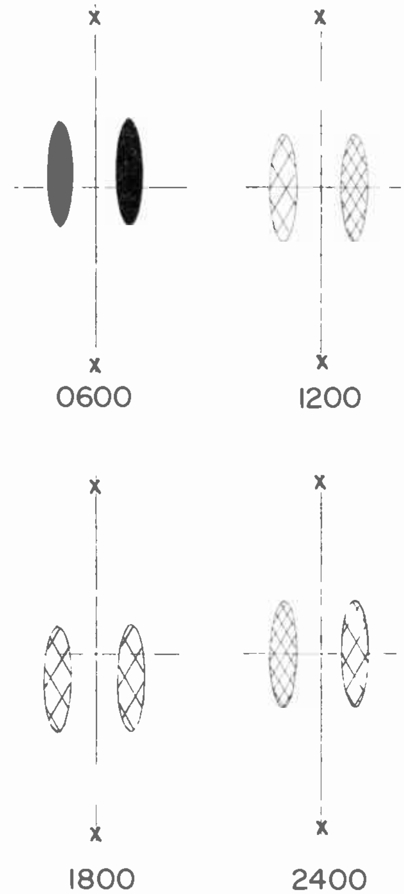

Fig. 3—Plan view of those areas of the meteor plane most favorable for meteor propagation at various times of day for a north-south 1000-km path in northern temperate latitudes. These gross theoretical features are predicted from a uniform distribution of meteor orbits relative to the sun. The shading indicates the approximate relative importance of the areas.

orbits and radiants apply to meteors which are somewhat larger than the average meteor normally used in meteor-burst propagation. The main features of the directional characteristics of meteor propagation may be controlled by the degree of the ecliptic concentration of radiants and the velocities of the smaller meteors. The gross directional characteristics as predicted in Figs. 2 and 3 for all times of day except near 1800, are not expected to be affected materially by a modest degree of ecliptic concentration. Near 1800, however, the south side of an east-west path in northern temperate latitudes is optimum assuming random heliocentric meteors, while the north side would be better at all times of day, if the ecliptic concentration were sufficiently pronounced.[7]

This last uncertainty has been resolved by a series of oblique-path tests performed under the direction of Peterson of the Stanford Research Institute,[3] and a series of radar tests made at Stanford University. For from 6 to 12 hours centered on 1800, it is found that more meteor echoes are obtained from the south side of an east-west path and from the south of a radar site, than from the north. This indicates that the degree of ecliptic concentration is not strong enough to control

[10] C. O. Hines, "Diurnal variations in forward-scattered meteor signals," *J. Atmos. Terr. Phys.*, vol. 9, pp. 229–232; October, 1956.
[11] F. L. Whipple, "Photographic meteor orbits and their distribution in space," *Astron. J.*, vol. 59, pp. 201–217; July, 1954.
[12] G. S. Hawkins, "A radio echo survey of sporadic meteor radiants," *Monthly Notices of the Royal Astron. Soc.*, vol. 116, no. 1, pp. 92–104; 1956.
[13] C. D. Ellyett and C. S. L. Keay, "Radio echo observations of meteor activity in the southern hemisphere," *Aust. J. Phys.*, vol. 9, pp. 471–480; December, 1956.
[14] J. C. Gill and J. G. Davies, "A radio echo method of meteor orbit determination," *Monthly Notices of the Royal Astron. Soc.*, vol. 116, no. 1, pp. 105–113; 1956.

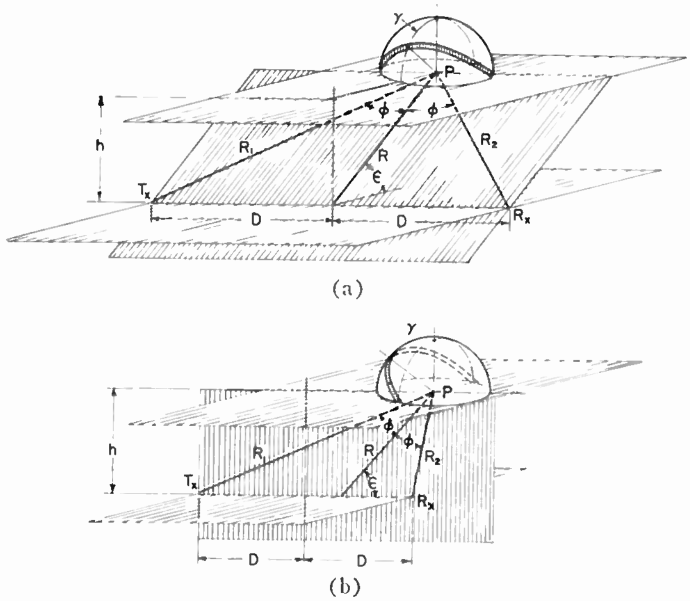

Fig. 4—Illustration of the geometrical correspondence between radar and oblique path detection of meteors.

the directivity of meteor propagation at these times of day. Thus, the gross diurnal directional features, as determined by the oblique-path and radar measurements, are similar to those illustrated in Figs. 2 and 3.

Geometrical Correspondence

One technique of studying the changing directional properties of meteor propagation depends upon the geometrical correspondence between radar and oblique-path detection of meteors. This geometrical correspondence is illustrated in Fig. 4.

Consider Fig. 4(a). The horizontal plane containing the transmitter T_x and receiver R_x is the ground plane. The parallel plane at height h is the meteor plane, where the midpoints of all meteor ionization trails are assumed to be located. The tilted plane is the plane of propagation. This illustration is for the point P in the meteor plane which is equidistant from T_x and R_x, and is to one side of the point over the path midpoint by the distance h. For meteors formed at P to be detected over the T_x–R_x path, they must lie in a plane which is perpendicular to the bisector of the angle T_x–P–R_x. This plane (not shown) intersects the celestial hemisphere in a semicircle. Because of the finite length of the trails, their radiants need not be exactly on this semicircle. In Fig. 4(a), the shaded band on the hemisphere is centered on the semicircle and covers those radiants whose meteors produce echoes over the oblique path. But meteors from the same band of radiants would produce radar echoes at range R, elevation angle ϵ, and at the azimuth which is perpendicular to the line T_x–R_x.

The correspondence between radar and oblique-path detection of meteors is illustrated for a different point in the meteor plane in Fig. 4(b). Similar relationships exist for all points in the meteor region. Thus, by measuring with a radar system the range and azimuth distributions of meteor echoes, the directional characteristics of meteor propagation over any oblique path located in the same geographical area as the radar can be determined. (It is assumed that the meteor trails are formed in a fairly narrow height range, so that the range measurement also determines the elevation angle ϵ.)

Note that if the radar is physically located at the ground end of the line R (Fig. 4), not only are the meteors it detects from the same radiants as those detected over the oblique path, but they are also the same meteors. However, there is no single ground station where this condition would apply for all points in the meteor plane, since the bisector of the forward scattering angle meets the ground at different points for different points in the meteor plane. It is assumed here that the meteor statistics, as defined by their radiant distribution, are constant over dimensions larger than the earth. Thus, the radar site physically need not be very near the midpoint of the oblique path to which it is to be compared. If the radar site is too far distant, however, its horizon will be markedly different from the horizon of the oblique path, so that the two systems cannot be compared directly. If this spacing is in longitude, the comparison can still be made with the proper adjustment for the differences in local time, if the radiant distribution in heliocentric coordinates does not vary during this time. If this spacing is in latitude, the radar cannot measure meteors from some of the radiants which may be important over the oblique path. For a reasonably good comparison between a radar and an oblique circuit, they should be within 10° of each other in latitude. The relative longitude spacing is less stringent.

[While the determination of radar echo rate at a given azimuth and range yields only one measure of the total radiant activity within a band, in theory it is possible to deduce a principal solution for the actual two-dimensional distribution of meteor radiants from many such band measurements. A similar problem has been encountered and solved in radio astronomy, where the two-dimensional brightness distribution of an extended source is determined from many one-dimensional (strip) measurements.[15]]

The correspondence in position of the radiant strips for radar and oblique-path meteor detection was described above. In order to complete the procedure for relating radar measurements to oblique path propagation, it is also necessary to consider the widths of these bands, echo intensities and durations, system parameters for the two meteor detecting systems, and also the number distribution of meteors of various masses and the characteristics of the trails which they produce (*e.g.*, line densities and lengths). While the details of these considerations will not be developed here, some of the principal problems are outlined below.

[15] R. N. Bracewell, "Two dimensional aerial smoothing in radio astronomy" *Aust. J. Phys.*, vol. 9, pp. 297–314; September, 1956.

The main difficulty encountered in relating radar and oblique paths is due to the differences in the width of the radiant bands and the differences in the echo intensities. The radian half widths ψ of the radiant bands are[4]

$$\psi_R = \frac{L}{2R} \tag{1}$$

and

$$\psi_0 = \frac{L(R_1 + R_2)}{4R_1R_2 \cos\phi}(1 - \sin^2\phi \cos^2\beta) \tag{2}$$

where the subscript R refers to radar and 0 refers to oblique path. In these expressions, L is the trail length (assumed much less than the ranges), and β is the angle between the trail axis and the plane of propagation. Because β changes with position along the radiant band, the distribution of meteor radiants must be known before the relative number of meteors emanating from the two radiant bands can be determined. But radiant distribution is the principal unknown in this problem.

The difficulty with these widths is not so important when echo intensities are included. They are[4]

$$P_R = K\frac{q^2}{R^3} \tag{3}$$

and

$$P_0 = K\frac{2q^2 \sin^2\alpha}{R_1R_2(R_1 + R_2)(1 - \sin^2\phi \cos^2\beta)} \tag{4}$$

where K is a constant (for present purposes), q is the electron line density at the reflection point, and α is the polarization angle between the electric vector of the incident wave at the trail and R_2. Note that the product of echo intensity and number (radian width) no longer contains the troublesome β factor. Thus, for every point in the meteor region, $P_R\psi_R$ is related to $P_0\psi_0$ by known factors.

The product considered above is proportional to the energy propagated by meteor trails, and, ideally, signal energy should be proportional to the information capacity of the communication system. However, the fluctuating signal is not used in an optimum manner in present meteor burst communication systems. The important consideration in meteor burst communication is the product of number of echoes and their duration above a threshold level. For the smaller meteors, the number of trails of line density greater than q is approximately inversely proportional to q, and their echo power is proportional to q^2, so that the number of echoes above a threshold level is inversely proportional to the square root of this power threshold. Thus, the product of number and duration (circuit duty cycle) is proportional to the product of the width of the radiant band, the square root of the expression for echo intensity, and the expression for average echo duration. The β factor remains, but its effect is reduced because of the square root.

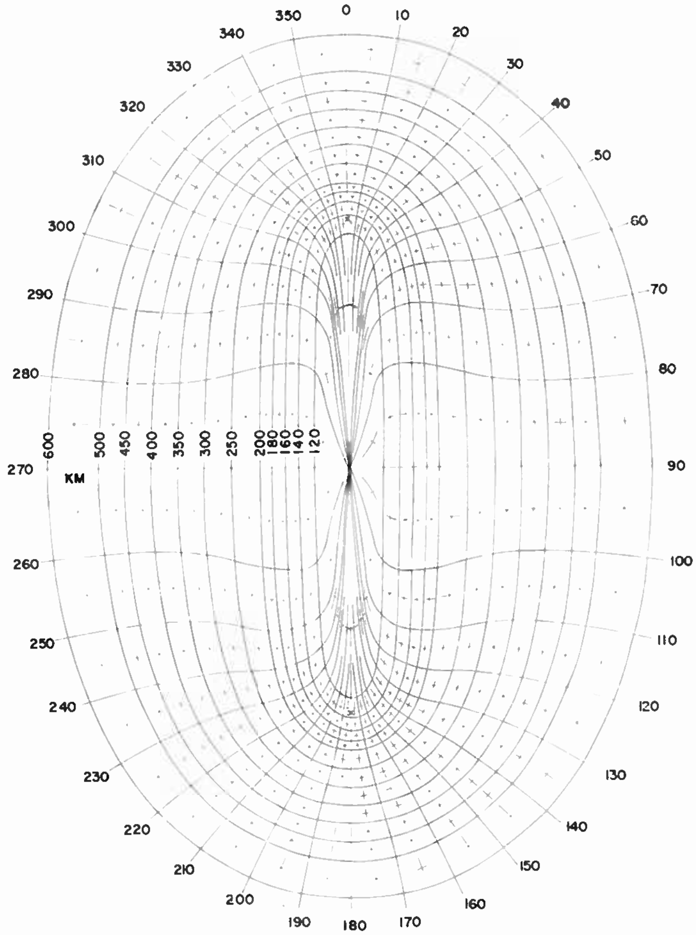

Fig. 5—Plan view of a 1000-km oblique path between the points marked by X's, showing for each point in the meteor plane the radar range and azimuth at which the same meteor radiants are detected as are detected over the oblique path.

While a complete correspondence between radar and oblique paths can be found for meteor-reflected radio energy, the correspondence is not perfect for meteor-burst duty cycle. In effect, the answer must be known before the problem can be solved. However, it has been found, from computations using assumed radiant distributions, that the errors introduced in the duty cycle by neglecting the β factor probably will be less than 10 per cent in practice. Since there are other uncertainties which may be comparable to this magnitude, it appears legitimate to neglect the β factor. (In a more ambitious approach to this problem, it would be possible, at least in principle, to obtain the two-dimensional radiant distribution from the radar measurements, and hence solve the duty cycle problem completely.)

In the contour charts presented in the next section, the geometrical correspondence of the radar and oblique paths is determined as in Fig. 5. Here a plot on the plan view of a 1000-km oblique path shows the correspondence between the various areas of the meteor plane with radar measurements made at the indicated ranges and azimuths relative to the line of the oblique path. (It is assumed that the meteor trails are formed at a height of 100 km.) To compute a relative measure of

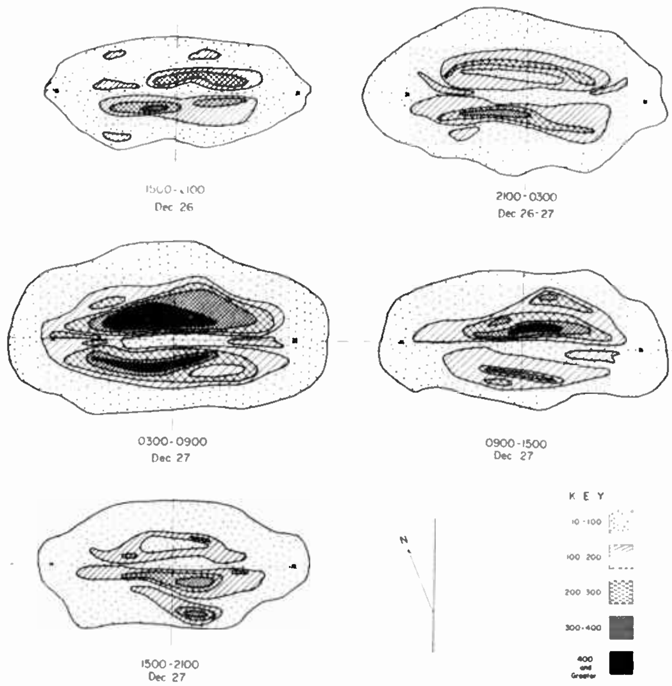

Fig. 6—Plan view of a 1000-km path of the same bearing as the Phoenix-Stanford path, showing from radar measurements the predicted relative importance of the various meteor plane areas for oblique propagation.

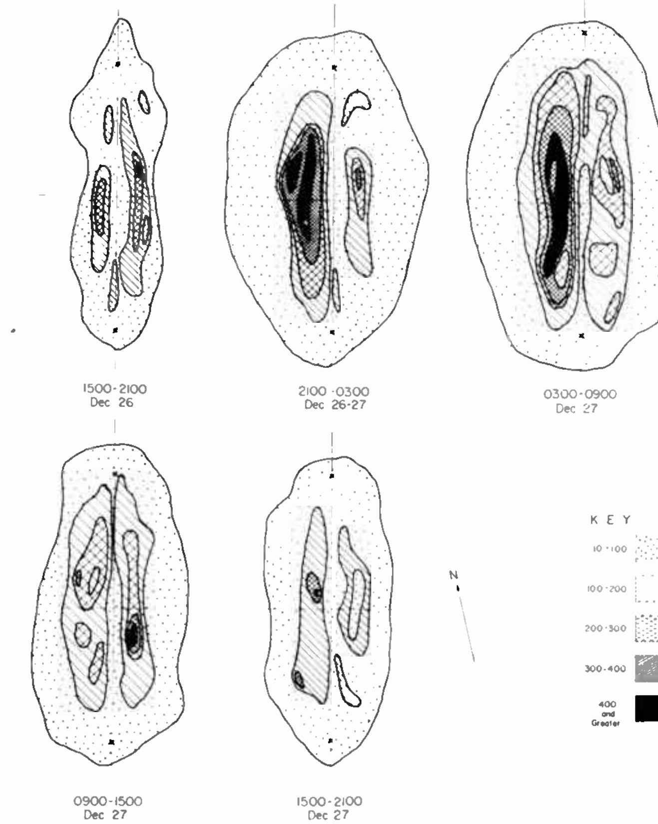

Fig. 7—Plan view of a 1000-km path of the same bearing as the Spokane-Stanford path, showing from radar measurements the predicted relative importance of the various meteor plane areas for oblique propagation.

the potential contribution of these areas to the oblique-path duty cycle, the β factor is neglected, and only those terms which change with position in the meteor plane are used. The expression which is used is

$$\frac{D_0}{(G_{R0}G_{T0})^{1/2}\sin\alpha} \sim N_R\left[\frac{R^{3/2}\cos\epsilon}{\Delta R G_R}\right]_{\text{RADAR}} \cdot \left[\frac{\left(\dfrac{R_1+R_2}{2}\right)^{1/2}\sec^3\phi}{R_1^{3/2}R_2^{3/2}}\right]_{\text{OBLIQUE}} \quad (5)$$

where the left side of the proportionality is the oblique-path duty cycle per unit meteor plane area, normalized by antenna gains and the polarization factor. This is the term that is plotted on the contour maps. On the right side of the proportionality, N_R is the number of radar echoes received in a directive beam in the range interval ΔR. The terms in the first bracket are radar parameters, while those in the second are oblique path parameters, at the position in the meteor plane under consideration. The expression does not check dimensionally because of the omission of dimensional factors which do not change with position in the meteor plane. A detailed evaluation of the required radar antenna beamwidth and range interval ΔR for a given scale of definition in the oblique path contour plots has not been attempted here.

It should be noted that in the technique described above, it is assumed that the radar echo statistics (number-amplitude and number-duration distributions) do not vary with range and azimuth; *i.e.*, the radiant distribution of the large and small meteors are assumed to be similar. If there are appreciable differences, radar echoes in various amplitude groups should be related separately to the oblique paths.

Radar Measurements Applied to Oblique Paths

On December 26–27, 1956, the directional properties of meteor echoes propagated to Stanford from television stations in Phoenix, Ariz., and Spokane, Wash., were measured by Vincent, *et al.*[3] At the same time, a 38-mc radar system was operated at Stanford University to determine the range and azimuth distributions of meteor echoes occurring during this period. The radar system employs a rotating antenna beam consisting of four three-element Yagi antennas fed in phase. The beam width is approximately 25° in azimuth and 55° in elevation angle, with the center of the lobe at an elevation angle of 45°. The beam makes one complete revolution every 30 minutes. The beam pattern supplied by the antenna manufacturer was used to determine G_R in (5).

From 1500 on December 26 to 2100 on December 27, the radar data were divided into five six-hour periods and analyzed to predict oblique path characteristics for the Phoenix-Stanford (approximately east-west) and the Spokane-Stanford (approximately north-south) paths. The results are shown in the contour charts of

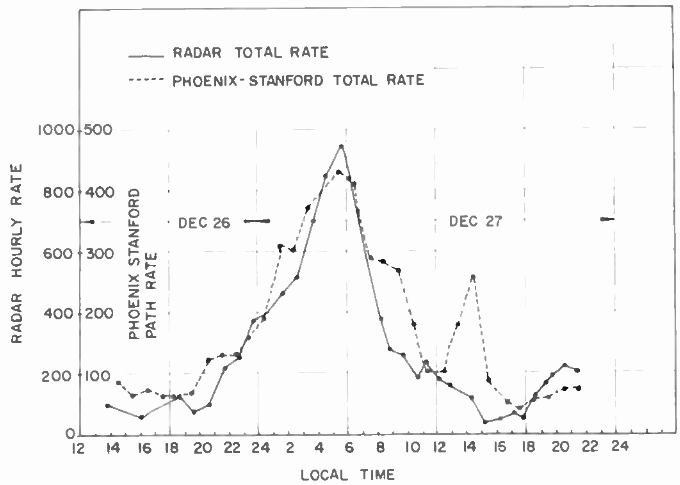

Fig. 8—Comparison of the diurnal variation of the total meteor echo rate measured with a radar and measured over an east-west oblique path.

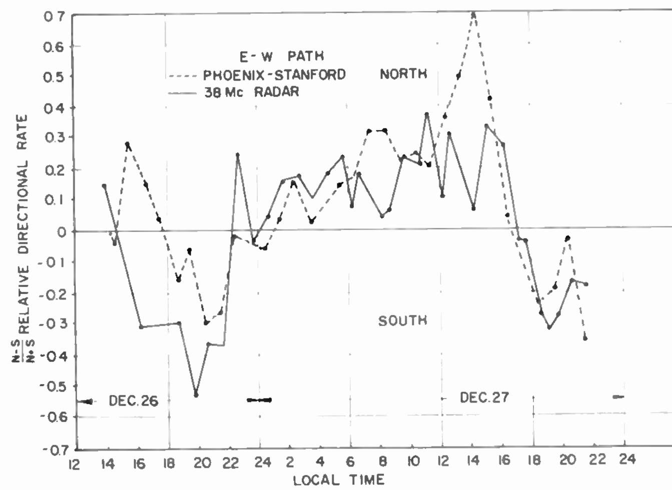

Fig. 9—Comparison between back scatter and forward scatter measurements of the diurnal variation in the $(N-S)/(N+S)$ ratio. N and S refer to the total number of echoes received from the north and south, respectively, of the radar station and the north and south sides, respectively, of the east-west oblique path.

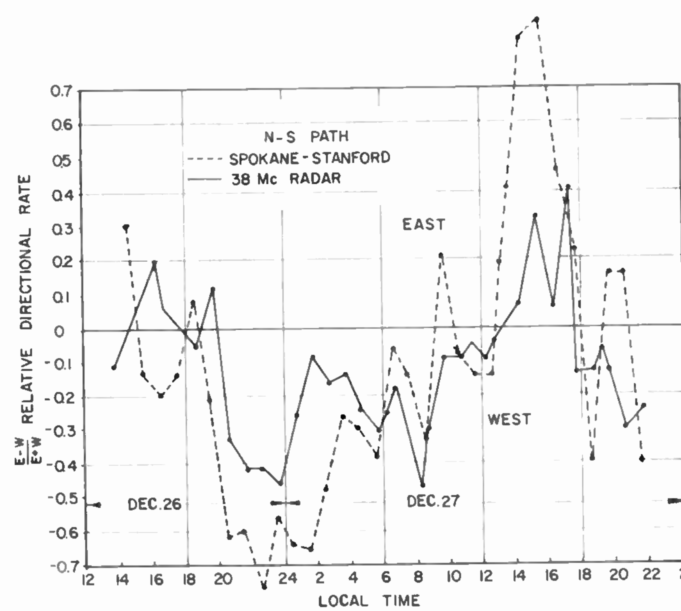

Fig. 10—Comparison between back scatter and forward scatter measurements of the diurnal variation in the $(E-W)/(E+W)$ ratio. E and W refer to the total number of echoes received from the east and west, respectively, of the radar station, and the east and west sides, respectively, of the north-south oblique path.

Figs. 6 and 7. In the analysis it is assumed that the oblique paths are 1000 km in length, a reasonable approximation for the two actual paths. The factor which is plotted is the expression in (5), which might be called the potential circuit duty cycle per unit area of the meteor plane. The numerical values for the various shadings used in the figure are relative and cannot be used alone to find actual duty cycles. If this potential duty cycle factor were constant over all regions of the meteor plane, the actual duty cycle would be approximately independent of the gains of the transmitting and receiving antennas, assuming that they cover the same area in the meteor plane.[4] Since the factor which is plotted does vary with position, the maximum duty cycle would be obtained with antennas designed to illuminate only those areas of the meteor region where the contours are maximum.

From Figs. 2 and 6 it can be seen that the gross features of the diurnal changes in the predicted directional properties of meteor propagation are obtained from measurement. In particular, the north side of the E-W path is better for meteor propagation during the morning hours, while the south side is better during the evening hours, as was predicted. Similarly, for the N-S path (Figs. 3 and 7), antennas should be pointed west of the direct path at night and east of the direct path during the day, for maximum duty cycle. An important difference between theory and experiment is the relative intensity of the hot spots at midnight and noon. Theory predicts that the total meteor rate would be the same at these times of day, but the measurements indicate more activity at midnight than at noon.

Note that the measurements for the same time of day (1500–2100) on the two consecutive days show the same gross features, but there are differences in detail. Other radar measurements of meteor activity also have shown considerable day-to-day variation.

The measurements that were taken over the two oblique paths consisted of the meteor echo rate as a function of azimuth relative to the great-circle path. First-order comparisons between the radar and oblique path measures of echo numbers are shown in Figs. 8–10. A more detailed comparison based on duty cycle was not made for this test, but is planned for future tests. In Fig. 8, the total echo rates observed on the radar and on one of the oblique paths are compared. The radar rate was about twice as high as the rate over the oblique path (indicating that the radar was sensitive to smaller meteors), but the diurnal variation of echo rates were similar, except for a period near 1400 on December 27.

In Fig. 9, simple measures of the directional properties of meteor propagation are plotted for comparison between the radar and the east-west path. In this figure the ordinate is the factor $(N-S)/(N+S)$, where N is the number of echoes obtained from the north of the radar site and from the north side of the east-west oblique path. With an analogous definition for S, it follows that when the ordinate is positive, the north side of the east-west path is better for meteor propagation, while the south side is better when the ordinate is negative. The amount by which the ordinate goes positive or negative is a measure of the degree by which one side of the path is better than the other. A similar comparison between radar and oblique-path measurements is presented in Fig. 10 for the north-south path.

The agreement between the radar and oblique-path measurements shown in Figs. 8–10 is reasonably good, considering the cursory nature of the comparison. It would be desirable to have accurate vertical angle of arrival information as well as azimuthal angle, so that a more detailed comparison could be made with radar predictions, such as those pictured in Figs. 6 and 7.

While the general trends of the two sets of measurements given in Figs. 8–10 are similar, there is a very marked difference near 1400 on December 27. Here the oblique-path rate suddenly increased, while the radar rate continued on its normal diurnal variation. Over the two oblique paths, a sudden increase in the rate over the north side of the E-W path and over the east side of the N-S path was observed. This sudden increase in activity over the oblique paths endured less than two hours and did not occur on the previous or following day at the same hour. This sudden change was presumably due to a heretofore undetected meteor shower of very short duration; one in which the particles evidently were very closely bunched in the orbit. However, this increased activity did not show up on the radar. Based on the angles at which this increased activity was maximum over the oblique paths, it has been computed that the radar should have detected this shower at a minimum radar range of approximately 700 km. This distance is greater than was being used on the radar display at that time (550 km). Thus, it appears that the discrepancy between the radar and oblique path measurements at 1400 was due to a factor that easily can be corrected. For this shower, it appears that the optimum off-path angle was approximately 30° at the receiver and 90° at the transmitter for both the E-W and N-S paths.

Conclusion

The directional characteristics of meteor propagation have important application in the design of the antenna systems used for meteor-burst communication. Recent measurements[16,17] of the angle of arrival of the continuous signal of vhf ionospheric scatter propagation show gross diurnal variations for an east-west path which are similar to those predicted and measured for meteor bursts. Thus it appears that continuous ionospheric scatter in the temperate latitudes is supported during most of the day primarily by the overlapping in time of many small meteor echoes; the same antenna considerations may be as applicable to ionospheric scatter as to meteor-burst communication during those hours when the meteoric component is dominant.

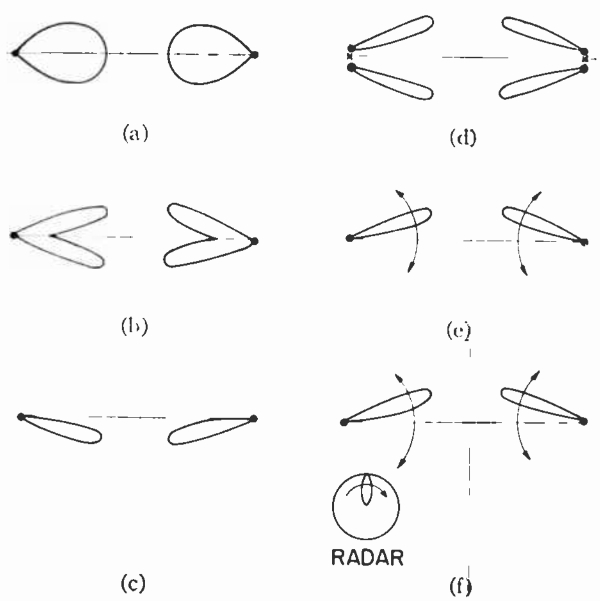

Fig. 11—Plan view illustrations of various suggested antenna configurations for meteor-burst and ionospheric scatter propagation.

From the previous discussion on the directional properties of meteor propagation, several possible antenna beam configurations are evident for meteor-burst and ionospheric scatter communication. These are discussed below in order of their complexity and are illustrated in Fig. 11.

The antenna beams at transmitter and receiver may be made so broad that they cover most of the important meteor scatter region [Fig. 11(a)]. While the meteor mode would not be used to best advantage, this arrangement would be preferred where very small and simple antennas are desired.

Split beams might be used at the transmitter and receiver, in recognition of the fact that little meteor energy is reflected along the great circle path [Fig. 11(b)]. Both "hot spots" are used at all times, regardless of their relative intensity.

One off-path beam could be used, directed so as to maximize the duty cycle at the time of day when meteor activity is minimum; *e.g.*, beams directed to the south side of an east-west path in northern latitudes [Fig. 11(c)]. This arrangement would minimize the diurnal variation in the capacity of the circuit. Alternatively, it may be desired to maximize the duty cycle at some other time of day, because of known nonuniform demands for the transmission of information.

[16] V. C. Pineo, "Experimental observations of the contribution of meteoric ionization to the propagation of vhf radio waves by ionospheric forward scatter," in publication.
[17] K. L. Bowles, "Ionospheric forward scatter," *Ann. IGY*, vol. 3, part 4, pp. 346–357; 1957.

Two off-path beams at each terminal could be employed to advantage, where only one set would be used at a time [Fig. 11(d)]. From the known diurnal variations in the average directional characteristics of meteor propagation, the particular set of beams would be used which would illuminate the hotter of the two hot spots.

In Fig. 11(e), the previous method is carried one step further by using a beam which can be swung (mechanically or electrically) to any off-path angle. Thus, not only the favored side can be used, but also the optimum off-path angle.

The above techniques depend upon prior knowledge of the changing radiant distribution. Certain gross features repeat each day and each year, but hour-to-hour and day-to-day variations can occur, as indicated above. Some of these variations from the normal diurnal and seasonal pattern are due to the well-known meteor showers. These showers repeat each year, but with varying and somewhat unpredictable intensity. Other short-term variations are presumably due to short duration but high intensity showers, such as described above and in a companion paper.[3] Whereas the earth will pass through the orbit of this shower each year, it probably will not hit the highly concentrated group of particles again for some years hence. A short-term change in the radiant distribution could also be caused by a random confluence of sporadic meteors into a configuration that never would be repeated in future years.

The question arises, can the fluctuation from the normal trend be put to use to increase the capacity of meteor-burst and ionospheric-scatter communication systems? Some of these changes could be predicted if we had more nearly complete information on the distribution of meteor orbits. It also appears possible and feasible to make use of the geometrical correspondence between radar and oblique propagation to "instantaneously predict" from radar measurements the optimum antenna configurations for communication over the oblique path. As illustrated in Fig. 11(f), a radar system could be installed near one end of the oblique path to monitor continuously the changing radiant distribution. The optimum direction for the movable beams used at the two ends of the communication circuit could then be determined from the radar data. It may be worth noting that radar measurements made only at azimuths which are normal to the direction of the oblique path usually would suffice to show the most important directional characteristics.

By making better use of the changing meteor radiant distribution in oblique propagation, the circuit becomes more efficient and the interference to and from other services is reduced. The desirability of using highly directive and rotatable antennas makes it important to use as short a radio wavelength as feasible, so that the antennas are not too large. Other reasons for using a relatively short wavelength (6 to 3 meters) in meteor-burst communication are presented in a companion paper.[18]

It appears that the principle of predicting the directional characteristics of oblique-path meteor propagation from radar measurements has been successfully demonstrated. However, considerably more work is needed to determine the limits of accuracy and utility of this technique.

Acknowledgment

The authors gratefully acknowledge the assistance of the following persons in the research reported here: T. V. Harroun and P. B. Gallagher, who built and helped to maintain the radar equipment; O. G. Villard, Jr. and L. A. Manning, whose helpful discussions and suggestions were invaluable; and A. M. Peterson and W. R. Vincent of the Stanford Research Institute, who made available the results of their measurements of oblique-path meteor propagation for comparison with the radar predictions. Credit is also due Dr. P. Newman of the Air Force Cambridge Research Center, for recognizing at an early stage the importance of this research and for helping to make it possible.

[18] V. R. Eshleman, "On the wavelength dependence of the information capacity of meteor burst propagation," this issue, p. 1710.

On the Influence of Meteor-Radiant Distributions in Meteor-Scatter Communication*

M. L. MEEKS† AND J. C. JAMES†

Summary—**The relative effectiveness of various regions of the atmosphere in furnishing usable meteor trails is examined on the basis of several distributions of meteor radiants. An idealized distribution in which the radiants lie near the ecliptic is analyzed and the results compared with previous calculations for a uniform radiant distribution. Experimental data on a 250-km link between Knoxville, Tenn., and Atlanta, Ga., show evidence of a rather diffuse concentration of radiants near the ecliptic. A method for predicting the contributions of meteor showers to forward-scatter propagation is developed. As an example the August Perseid shower is studied on the Knoxville-Atlanta link. Experimental data show good agreement with the shower analysis.**

I. Introduction

ONE of the fundamental problems in meteor-scatter communication is that of determining the relative usefulness of various portions of the sky as a function of time. Questions concerning how antenna beams should be shaped and oriented for a given communication link need to be settled on the basis of a detailed understanding of the relative effectiveness of various regions of the atmosphere in furnishing usable meteor trails.

Meteor trails are known to occur in a region lying roughly between 80 km and 120 km above the earth's surface. Whether or not a given meteor trail can scatter a signal in the desired direction depends on its orientation and position in space and on the number of free electrons initially formed per unit of trail length. If the distribution of these quantities were accurately known, then the problem of interest here could be solved in principle, although the calculation would be long and tedious on account of purely geometrical difficulties. However, at the present time these distributions are not known with precision. The information[1,2] which is available indicates that for sporadic meteors the radiants tend to be concentrated near the ecliptic with the strongest concentrations toward the apex of the earth's way and roughly toward the sun and antisun. In addition, radiants of the principal meteor showers have been determined[3] with considerable precision by visual and photographic techniques.

The distribution of free electron line densities have been measured for both shower and sporadic meteors,[4] and the results can be fitted by an empirical expression of the form

$$N_0(q) = \frac{K}{q^k}, \tag{1}$$

where $N_0(q)$ is the number of meteor trails having electron densities greater than q which pass through unit area per second, and K and k are constants. The best fit to experimental data on sporadic meteors is obtained for $k=1$. While for the major showers, k has been estimated to be somewhat less than 1.

The distribution of electron densities given by (1) together with the assumption of a uniform distribution of radiants, have been used by Eshleman and Manning[5] in an analysis of the forward-scatter problem. More recently, Pugh and Hines[6,7] have studied the uniform distribution and have made a number of refinements in the previous calculation.[5]

In view of the considerable discrepancy between the observed sporadic radiant distribution and the uniform distribution, it has seemed desirable to examine the effect of a radically different distribution which at the same time has some resemblance to the observed one. In the present paper, an ecliptic distribution of radiants has been analyzed, and the two oversimplified distributions (uniform and ecliptic) have been studied for a short-range link between Knoxville, Tenn., and Atlanta, Ga. This link lies roughly north-south with a station separation of 250 km.

The effects of meteor showers on a forward-scatter link have also been examined in the present paper by assuming that meteor radiants are concentrated at a single point on the celestial sphere. Previously, this problem has been studied theoretically by Hines,[8] who

* Original manuscript received by the IRE, September 5, 1957. The work was supported principally by the Office of Naval Research under Contract No. NONR-991(02) and also by the Air Force Cambridge Research Center under Contract No. AF 19(604)-1593. This work forms a portion of a thesis to be submitted to the Graduate School, Georgia Inst. of Tech., by J. C. James in partial fulfillment of the requirements for the Ph.D. degree.

† Eng. Experiment Station, Georgia Inst. Tech., Atlanta, Ga.

[1] G. S. Hawkins, "Variations in the occurrence rate of meteors," *Astronomical J.*, vol. 61, pp. 386–391; November, 1956.

[2] G. S. Hawkins and J. P. M. Prentice, "Visual determination of the radiant distribution of sporadic meteors," Harvard Univ., Cambridge, Mass., Radio Meteor Res. Program, under Air Force Contract No. AF 19(122)-458, Progress Rep. No. 19; March, 1957.

[3] A. C. B. Lovell, "Meteor Astronomy," Oxford University Press, London, Eng.; 1954.

[4] T. R. Kaiser, "Radio echo studies of meteor ionization," *Phil. Mag. Suppl.*, vol. 2, pp. 495–544; October, 1953.

[5] V. R. Eshleman and L. A. Manning, "Radio communication by scattering from meteoric ionization," Proc. IRE, vol. 42, pp. 530–536; March, 1954.

[6] R. E. Pugh, "The number density of meteor trails observable by the forward-scattering of radio waves," *Can. J. Phys.*, vol. 34, pp. 997–1004; April, 1956.

[7] C. O. Hines and R. E. Pugh, "The spatial distribution of signal sources in meteoric forward-scattering," *Can. J. Phys.*, vol. 34, pp. 1005–1015; April, 1956.

[8] C. O. Hines, "Diurnal variations in the number of shower meteors detected by the forward scattering of radio waves," *Can. J. Phys.*, vol. 33, pp. 493–503; September, 1955.

assumed a separation of more than 1000 km between transmitter and receiver. The present calculation places no such restriction on station separation. As an example, the Perseid shower has been observed and analyzed on the Knoxville-Atlanta link.

II. Uniform Distribution of Meteor Radiants

A purely geometrical condition must be satisfied if a meteor trail is to produce a usable signal over a communication link. The condition[5] is that the trail be tangent to one of a family of prolate spheroids having the transmitter and receiver as common foci. This condition applies particularly to the underdense trails that produce scatter signals which decay exponentially as the ionized trail diffuses. Exceptions may be found in the case of overdense trails which are capable of producing scatter signals of long duration. These overdense trails may be twisted and broken up by upper-atmosphere winds so that the scattered wave is broadly distributed. However, the number of overdense trails in any case is comparatively small, and they are neglected in the present calculation as they have been in previous ones.[5-7]

Once the geometrical condition for scattering has been satisfied, the received power as a function of time $P_R(t)$ may be expressed in terms of the transmitted power P_T by means of the forward-scatter equation of Eshleman and Manning.[5] This expression, including the antenna polarization factor given by Hines,[8] may be written as a product involving a function $A(G_T, G_R, \lambda)$, depending on the antenna gains G_T, G_R, and the wavelength λ; and a function $H(R_1, R_2, \mu, \beta, \phi)$, depending on the distances R^1 and R_2, respectively, from the meteor trail to the transmitter and receiver; a polarization parameter μ; and on the angles β and ϕ which are shown in Fig. 1. This equation[9] is then

$$P_R(t) = P_T A(G_T, G_R, \lambda) H(R_1, R_2, \mu, \beta, \phi) q^2 \exp(-t/\tau) \quad (2)$$

where q is the number of free electrons per meter in the trail, and the decay constant τ is given by

$$\tau = \frac{\lambda^2 \sec^2 \phi}{32\pi^2 d}.$$

Here d is the diffusion coefficient for the electrons in the trail, and the functions A and H are

$$A(G_T, G_R, \lambda) = (\text{const})\lambda^3 G_R G_T \quad (3)$$

and

$$H(R_1, R_2, \mu, \beta, \phi) = \cos^2 \mu [R_1 R_2 (R_1 + R_2)(1 - \cos^2 \beta \sin^2 \phi)]^{-1}. \quad (4)$$

The polarization parameter μ requires further discussion. It is the angle between the electric vector of the incident wave and the electric vector accepted by the receiving antenna.

[9] The notation here is consistent with that of Eshleman and Manning, *op. cit.*

It is possible, by a suitable choice of the polarization emitted by the transmitting antenna and accepted by the receiving antenna, to make the polarization factor optimum ($\mu = 0$) for any point in the meteor trail zone.[10] This optimum choice of polarizations may be described with Fig. 1. If the polarizations associated with the transmitter and receiver are both made perpendicular to the TRO plane, then the angle μ will be zero for any point O, and there will be no loss in signal strength at this point due to polarization. Clearly, for large station separations, where the portion of the meteor-trail zone common to both antennas lies near the path midpoint, the choice of horizontal polarization is practically optimum. However, for station separations less than 1000 km, other choices of polarization may have advantages.

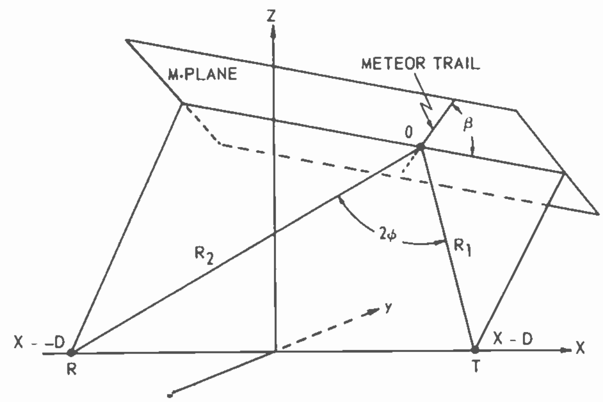

Fig. 1—Geometry for forward scatter by a meteor trail. The meteor trail at point O lies in the M plane which is tangent at this point to one of the family of spheroids with foci at transmitter T and receiver R. The origin of the cartesian system is taken midway between T and R with the x axis vertically upward.

To complete the analysis, following Hines,[7,8] it is necessary to consider the theory of meteoric ionization.[4] This theory gives the free electron density per meter of trail q in terms of the atmospheric pressure p, the meteor mass m, the meteor velocity v, and the angle ζ (the zenith angle) which the trail makes with the vertical. The expression for q is

$$q = m f(p, v) \cos \zeta, \quad (5)$$

where $f(p, v)$ represents the functional dependence of q on pressure p and velocity v. Since q is found to depend on the zenith angle ζ, it is assumed that the distribution of meteor masses is more fundamental than the observed distribution of electron densities in (1), which represents some kind of average over ζ. The mass distribution is taken to be

$$F_1(m) = \frac{\text{const}}{m^k} \quad (6)$$

where $F_1(m)$ is the fraction of all meteors with masses

[10] We are indebted to Dr. W. E. Deeds of the University of Tennessee for pointing out this fact to us.

greater than m, and k is here taken to be one. Using (5) after a suitable average over p and v, one obtains from (6) the fraction $F(q)$ of all meteors with electron densities exceeding q as follows:

$$F(q) = C\frac{\cos\zeta}{q}. \tag{7}$$

Here the value of the constant C is unimportant since we are not concerned with absolute values.

The forward-scatter equation (2), now permits a determination of the threshold values of q in terms of the system parameters and the geometry. The fraction of all meteor trails with a particular orientation and position in space which are capable of producing scatter signals above some amplitude level L_0 at $t=0$ is then proportional to $\sqrt{H}\cos\zeta\sqrt{A}/L_0$. All parameters describing the meteor-scatter system, except for polarization, are contained in the function A. The location of the trails in space and their orientation are contained in the function H. To determine the relative meteor signal rate for two different antenna systems, one must perform two integrations of this expression for the fraction of usable trails: 1) an integration over all possible meteor-trail orientations, taking into account the radiant distribution, and 2) an integration over the illuminated region in space where meteor trails occur.

In analyzing the uniform distribution of radiants the procedure has been to perform integration 1) for points on a surface at some height h above the earth and to present the results in the form of contours plotted on a map of the meteor-trail zone. This plot is made to apply to antennas of arbitrary beam shape by taking G_T and G_R to be equal to one. In a particular case, the factor $\sqrt{G_TG_R}$ can then be put back in when integration 2) is performed for a given system of antennas. The meteor-trail zone is considered relatively thin so that the volume integration is replaced by an integration over a surface at a height $h=100$ km over the surface of the earth.

The method of performing integration 1) for the uniform radiant distribution has been shown in detail by Pugh.[6] The result of this integration may be described by a function $n(x, y)$ in the cartesian coordinate system of Fig. 1. Here $n(x, y)dxdy$ is the relative number of usable meteor trails per second which one associates with an area element $dxdy$ at a vertical height of 100 km above the earth, assuming isotropic unit gain for the transmitting and receiving antennas. The number of meteor trails observed per second by a given system will then be proportional to $\iint n(x, y)\sqrt{G_TG_R}\,dxdy$. The integration 1) to determine $n(x, y)$ may be written as

$$n(x, y) = \int \sqrt{H(\beta)}(\cos\zeta/L_0)J(\beta)d\beta \tag{8}$$

where $J(\beta)d\beta$ is the total number of meteor trails contributing to unit area per second between the angles β and $\beta+d\beta$. The integration must be carried out over the angular region above the horizon. The resulting contour plot of $n(x, y)$ may be regarded as the distribution of observable scatter sources.

In the problem of meteor-scatter communication the meteor signal rate may be less important than the duty cycle, which is defined as the fraction of time that the meteor-scatter signal is above a specified level. The distribution $n(x, y)$ may be modified to obtain the corresponding distribution of sources of signal duration. This may be done simply by multiplying $n(x, y)$ by the weighting factor[11] $\sec^2\phi$ which in effect weights each meteor signal by a factor which is proportional to the mean duration to be associated with it. A detailed justification of this factor is given by Hines and Pugh.[7]

Computations of the distribution of sources of signal duration have been performed for a meteor-scatter link between Knoxville, Tenn., and Atlanta, Ga.—distance of 250 km. The computation, while equivalent to that of Hines and Pugh,[6,7] was performed and reported[12] independently. The numerical computations for this distribution were sufficiently involved to justify the use of a digital computer,[13] and a general program was prepared for the solution of this problem. Figs. 2–4 show the distribution $n(x, y)\sec^2\phi$ for three different assumptions concerning the antenna polarizations. The contour values in these three figures have no absolute significance, but all three figures have been worked out on a consistant basis so that they may be compared. As the polarizations are changed from optimum in Fig. 2 to horizontal in Fig. 4, the contributions at the two maxima (near $x=0$, $y=\pm 60$ km) are cut almost in half. These maxima in Fig. 2 are reduced by roughly a quarter in Fig. 3 where one polarization is horizontal and the other is optimum. Along the x axis all three combinations of polarizations give the same values for the distribution of sources of signal duration, but well off the x axis, where the uniform radiant distribution predicts the highest duty cycle and signal rate, the choice of polarization becomes important. When the station separation is relatively small as it is in the present case, the difference between the optimum polarization and horizontal polarization is significant. Fig. 4 shows a null on the circle passing through the transmitter and receiver with its center at the path midpoint. This null circle is the locus of points where the polarizations are mutually perpendicular, if each point on the xy plane is assumed to be illuminated and observed with horizontal polarization. The discontinuity which appears in Fig. 4 at $x=125$ km, $y=0$ is a consequence of

[11] The absolute value of this weighting factor which converts the distribution of signal sources to the distribution of signal durations above the same level is $\lambda^2\sec^2\phi\,(16\pi^2kd)$.

[12] Jesse C. James and M. L. Meeks, "On the relative contributions of various sky regions to meteor-trail communication," Georgia Inst. Tech., Atlanta, Ga., Eng. Experiment Station, under Office of Naval Research Contract No. NONR-991(02), Tech. Rep. No. 1; June, 1956.

[13] The Univac Scientific ERA 1101 at the Rich Electronic Computer Center was used.

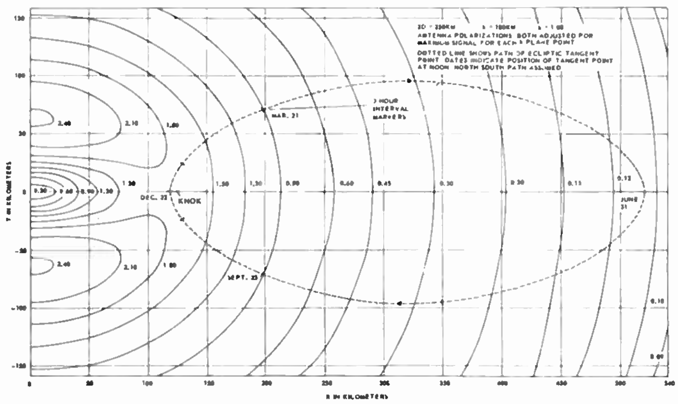

Fig. 2—The distribution of sources of signal duration above a given amplitude level with optimum polarization for each illuminated point. The orbit of the ecliptic tangent point, which is discussed in Section III, is shown by the dotted curve.

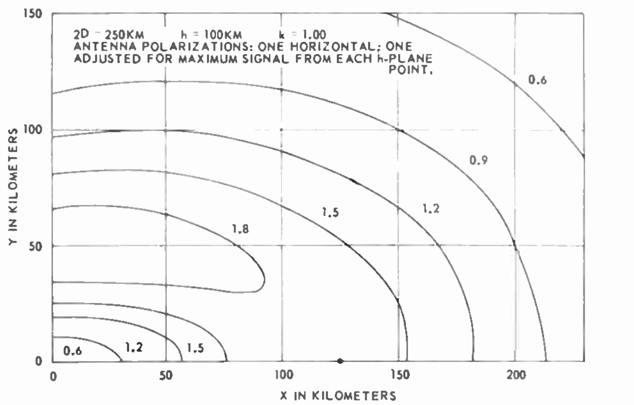

Fig. 3—The distribution of sources of signal duration with optimum polarization on one antenna and horizontal polarization on the other. It is assumed that polarizations are adjusted separately for each point.

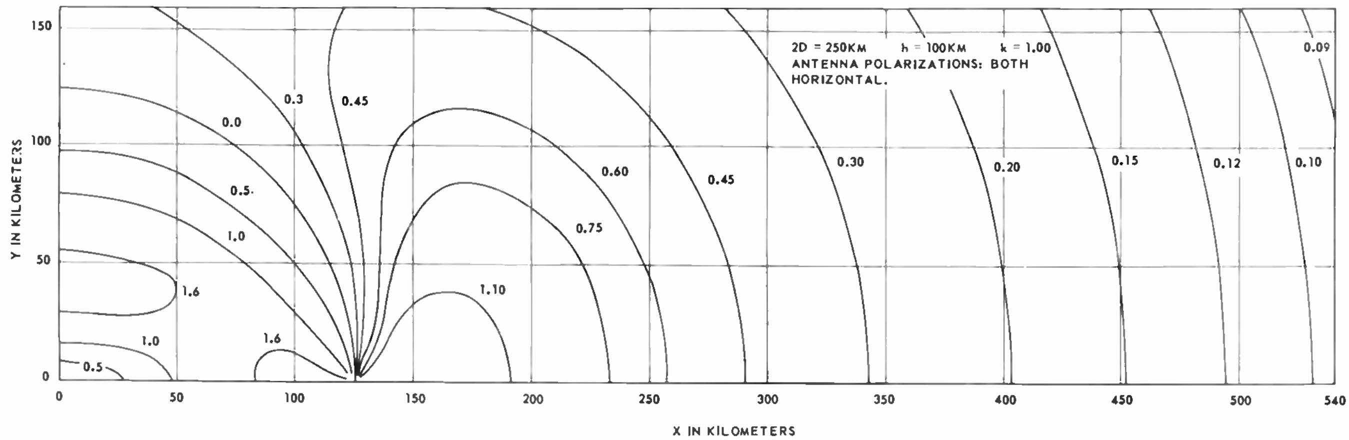

Fig. 4—The distribution of sources of signal duration with horizontal polarization on both antennas. It is assumed that polarizations are adjusted separately for each point.

the fact that horizontal polarization is not uniquely defined for an antenna directed vertically upward.

III. Ecliptic Distribution of Meteor Radiants

The uniform distribution of radiants, which was assumed in the previous section, serves as a good starting point in the analysis of forward scattering by meteor trails. In particular the regions of sky that are most useful for meteor-scatter communication from the standpoint of geometry alone are indicated by the previous analysis. However, the uniform radiant distribution must evidently be incorrect in detail because it fails to predict the characteristic diurnal variations in meteor signal rate which have been observed experimentally. Thus the need for analysis based on other radiant distributions is clearly indicated.

A distribution in which the radiants are concentrated near the ecliptic provides an alternative which can be handled analytically. Recent studies[1,2] indicate an ecliptic concentration for sporadic meteors on the basis of radio, visual, and photographic observations. But the observed ecliptic concentration is not sufficiently strong to justify a distribution which is confined precisely to the ecliptic. Thus the strict ecliptic distribution is viewed here as an approximation in much the same sense that the uniform distribution is itself an approximation from a different point of view.

The effect of an ecliptic distribution may be seen by considering again the geometrical requirement for forward scatter. If all radiants are distributed evenly around the ecliptic and if the ecliptic plane[14] itself coincides with the M plane in Fig. 1, then all trails will be properly oriented to produce reflections. This situation occurs when the ecliptic plane is tangent to a spheroid having the transmitter and receiver as foci. The point of tangency occurring at some specified height h will be referred to as the *ecliptic tangent point*. If h is chosen at the center of the meteor trail zone ($h=100$ km), then every meteor trail in the neighborhood of the ecliptic tangent point will be properly oriented.

With a strongly ecliptic distribution of radiants, the ecliptic tangent point will be the best point in the sky to illuminate, unless polarization or geometrical factors intervene. The contours in Figs. 2–4 indicate roughly

[14] Any plane that intersects the earth and is parallel to the ecliptic is here referred to as an ecliptic plane.

the combined influence of these factors.[15] For radiant distributions, which are less strongly concentrated in the ecliptic plane, one would expect the ecliptic tangent point to have less significance; and other regions with more favorable geometry might become more active than the ecliptic tangent point. This question can be examined by tilting the ecliptic plane slightly in various directions and observing how far the ecliptic tangent point moves from its true position.

The ecliptic plane moves with respect to a fixed observer on the earth in such a way that the ecliptic tangent point describes a simple closed orbit on each sidereal day. The computation of this tangent-point orbit is most easily performed in the cartesian coordinate system of Fig. 1. The family of prolate spheroids is described by

$$R_1 + R_2 = \sqrt{(x-D)^2 + y^2 + z^2} + \sqrt{(x+D)^2 + y^2 + z^2} = \text{const},$$

and the unit vector $\hat{n}$ for this family is given by

$$\hat{n} = \frac{\text{grad } (R_1 + R_2)}{|\text{grad } (R_1 + R_2)|}. \tag{9}$$

The unit normal $\hat{n}$ is used to find the ecliptic tangent point by requiring that $\hat{n}(x, y, z)$ coincide with a unit vector $\hat{m}(t)$ which is normal to the ecliptic plane at a time t. As the earth rotates and moves in its orbit around the sun, the normal to the ecliptic, referred to an earth-fixed coordinate system, nutates about a line pointing approximately toward the north star. The angle between $\hat{m}$ and this line is 23°27 minutes, the tilt angle of the earth's axis. The period of the nutation is one sidereal day. Since the length of a sidereal day is about four minutes less than a mean solar day, the direction of the ecliptic normal is a function of both the time of day and the day in the year.

The determination of the orbit of the ecliptic tangent point for height h above the earth is straightforward but numerically very involved.[16] The components of the spheroid normal are given explicitly by

$$\hat{n}_x = \frac{1}{2\cos\phi}\left[x\left(\frac{1}{R_1}+\frac{1}{R_2}\right) + D\left(\frac{1}{R_1}-\frac{1}{R_2}\right)\right]$$
$$\hat{n}_y = \frac{1}{2\cos\phi}\left[y\left(\frac{1}{R_1}+\frac{1}{R_2}\right)\right]$$
$$\hat{n}_z = \frac{1}{2\cos\phi}\left[z\left(\frac{1}{R_1}+\frac{1}{R_2}\right)\right] \tag{9a}$$

in the coordinate system of Fig. 1. The corresponding components of the ecliptic normal $\hat{m}(t)$ are determined by a straightforward calculation in the cartesian coordinate system of the forward-scatter link. Now, if the condition that $\hat{m}$ and $\hat{n}$ coincide is enforced, one obtains the following independent equations:

$$\frac{\hat{m}_y}{\hat{m}_z} = \frac{y}{z}$$
$$\frac{\hat{m}_x}{\hat{m}_z} = \frac{x}{z} + \frac{D}{z}\left(\frac{R_2 - R_1}{R_2 + R_1}\right). \tag{10}$$

These equations must be solved for x and y with the appropriate value of z inserted to obtain the ecliptic tangent point location for a height h above the earth. In the plane-earth approximation z is equal to h, but to take into account earth curvature, z must be taken as a function of h, x, and y. In this analysis, as well as others in the present paper, the approximate expression

$$z = h + \frac{D^2 - x^2 - y^2}{2R_e}, \tag{11}$$

where R_e is the earth radius, is used to take earth curvature into account.

Solutions to (10) and (11) for x and y cannot be easily obtained in closed form, and it was found necessary to use a numerical method of successive approximations to obtain the orbit of the ecliptic tangent point. These computations were also performed on a digital computer.[13]

For the Knoxville-Atlanta link, the orbit of the ecliptic tangent point is shown in Fig. 2. This orbit was computed on the assumption that the link is exactly north-south, when in fact the line from Atlanta to Knoxville lies 8° east of north. However, the assumption of a north-south path introduces negligible error. The position of the ecliptic tangent point for an arbitrary time and date may be obtained by interpolation on the dotted path shown in Fig. 2. The contours shown in that figure indicate roughly the effectiveness of the ecliptic tangent point from a geometrical point of view. The effect of spreading out the radiant concentration to within ±10° of the ecliptic has been considered[12] by tilting the ecliptic by this amount in various directions and observing the calculated displacement of the ecliptic tangent point. The resulting displacements depend strongly on the distance of the ecliptic tangent point from Knoxville ($x=125$ km, $y=0$). For $x<200$ km in Fig. 2, the displacement for a tilt of ±10° is seldom greater than 50 km. However, far out on the path for $x>300$ km, the displacement is frequently greater than 100 km. Thus one may regard the ecliptic tangent point as reasonably well defined during the 9-hour period each day when $x<200$ km.

When the line joining transmitter and receiver is rotated from the north-south direction, the orbit of the ecliptic tangent point is moved over the xy plane and changed in shape. The orbit, however, remains centered roughly north of the midpoint of the transmitter-receiver axis. Fig. 5 shows four computed orbits of the ecliptic tangent point for a short link (250 km between

[15] The exact measure of the influence of polarization and geometry could be obtained for radiants spread uniformly around the ecliptic by setting $J(\beta)$ in (8) equal to a constant.

[16] A detailed description of this calculation is given in James and Meeks, *op. cit.*

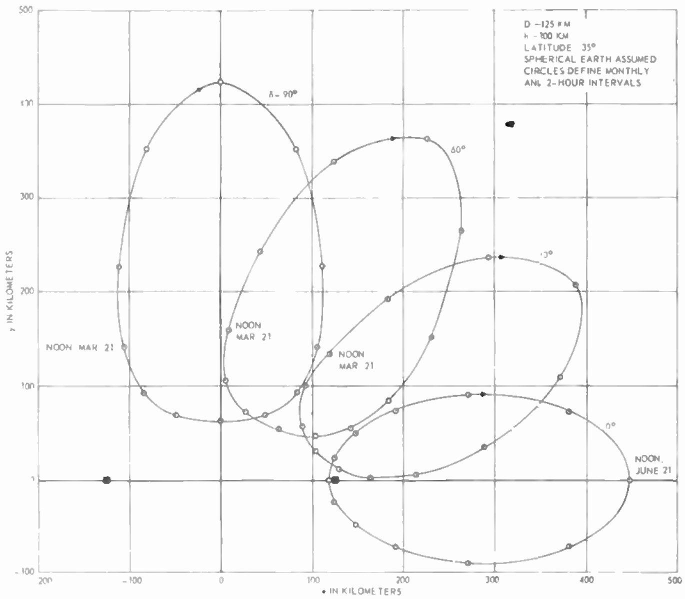

Fig. 5—Ecliptic-tangent-point orbits for various azimuth orientations of the x axis.

stations) with the transmitter-receiver axis at four different angles δ measured east of north. Fig. 6 shows a similar group of orbits for a much longer link (1000 km between stations). A latitude of 35° N was assumed in both of these examples. Increasing the latitude to 45° N moves and distorts these orbits by a distance which is generally less than 100 km.

The extent to which the ecliptic tangent point may be regarded as a strong source of scatter signals depends on its position on the orbit. A rough gauge of the effect of broadening the radiant distribution about the ecliptic may be obtained by observing the distance that the tangent point moves during a 2-hour interval. Where this distance is smallest, the assumptions of this section may be expected to remain most appropriate if the radiant distribution spreads out about the ecliptic.

An experimental test of the preceding analysis has been conducted on the Knoxville-Atlanta link over a period of three days, June 18, 20, and 22, 1957. The test was conducted at a frequency of 41.94 mc with a radiated power of 500 watts. The antennas were identical 7-element Yagis, which were oriented to obtain optimum polarization at the intersection of the axes of the antenna beams. The antennas were directed alternately toward two points on the orbit of the ecliptic tangent point at a height of 100 km. These points were $A(x=200$ km, $y=75$ km) and $B(x=200$ km, $y=-75$ km). From the standpoint of scattering geometry these points are mirror images about the path axis, and any difference in counting rate can therefore be assigned to the radiant distribution. Points A and B were observed alternately every thirty minutes. Data were collected for each point during a twenty-five minute interval, five minutes being required to rotate the antennas and check the receiver adjustment and calibration. The results of these tests are shown in Fig. 7, which represents the average

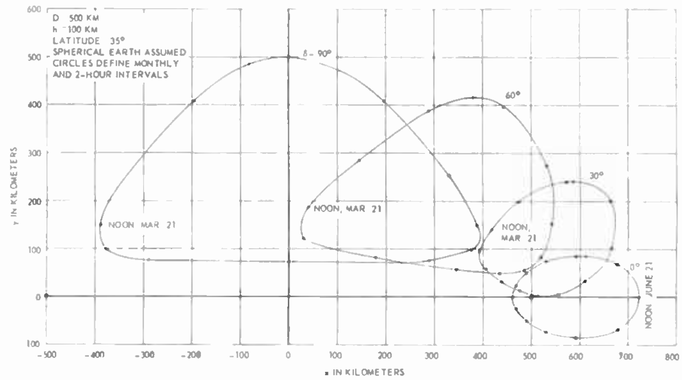

Fig. 6—Ecliptic-tangent-point orbits for various azimuth orientations of the x axis.

meteor signal rate for a period of three days. When the antenna beam widths are taken into account, one would expect on the basis of the orbit shown in Fig. 2 that A should receive a contribution from the ecliptic tangent point from about 0500 until 1000, and B should receive a contribution from about 1500 until 2000. Fig. 7 shows a significantly higher counting rate for A from roughly 0530 until 0900. The degree to which the two counting rates differ may be judged by observing the 95 per cent confidence limits which have been indicated for each counting period. The meteor signal rate for B in Fig. 7 shows higher values during the entire afternoon period until roughly 1930. The data show clearly a higher activity for B from 1530 until 1730 as predicted. The low counting rate during the period 1730–2000 does not permit a clear statistical distinction between the rates at A and B. Thus, one finds good agreement between the measurements and predictions based on a rather diffuse concentration of radiants near the ecliptic. The comparatively high counting rate observed at B during the interval 1330–1400 is, however, not expected on this basis.

During the days June 17, 19, and 21, tests similar to those described previously were performed by illuminating areas directly east and west of the path midpoint. These should be the most active areas for a uniform distribution. The average counting rate for these three days is shown in Fig. 8. The antennas were directed alternately toward each of two points: $A(x=0,\ y=60$ km) and $B(x=0,\ y=-60$ km).

On the basis of a purely qualitative prediction by Eshleman,[17] these should be the best points to illuminate for a north-south path. Eshleman predicts that A should be stronger around 0000, B should be stronger around 1200, and A and B should have about equal strength near the times 0600 and 1800. Fig. 8 shows good agreement with these predictions. During the 12-hour period centered on 0000, the counting rate is considerably higher for A which is west of the path midpoint. For the 12-hour period centered on 1200, the region asso-

[17] See, for example, V. R. Eshleman, P. B. Gallagher, and R. F. Mlodnosky, "Meteor Rate and Radiant Studies," Stanford Univer., Stanford, Calif., under Contract AF-19(604)-1031, final report to AFCRC; February, 1957.

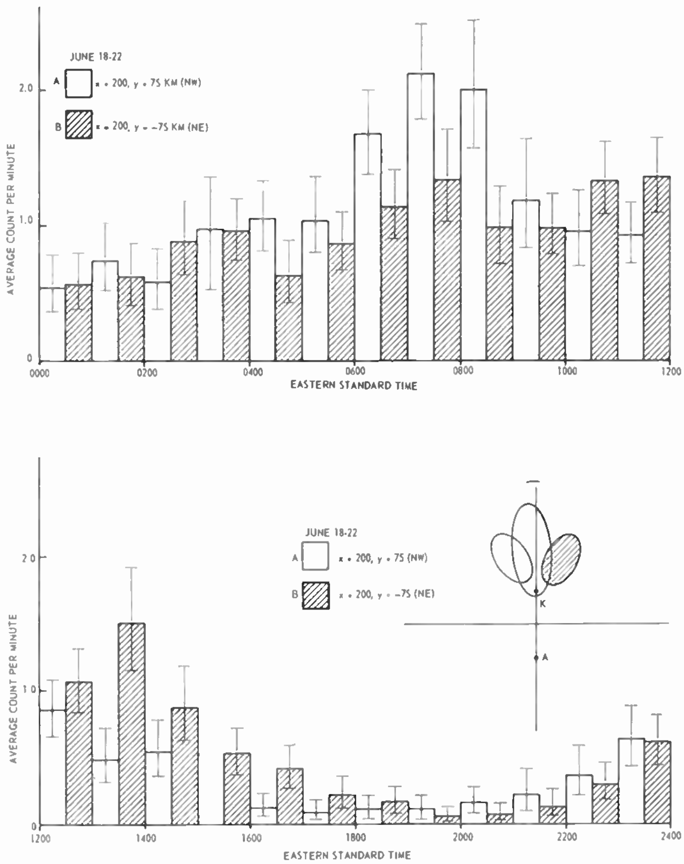

Fig. 7—The average value of the meteor echo rate observed over the Atlanta-Knoxville path on June 18, 20, and 22, 1957. The 40° antenna beam axes were oriented to intersect the h plane at $X=200$, $y=\pm 75$ km.

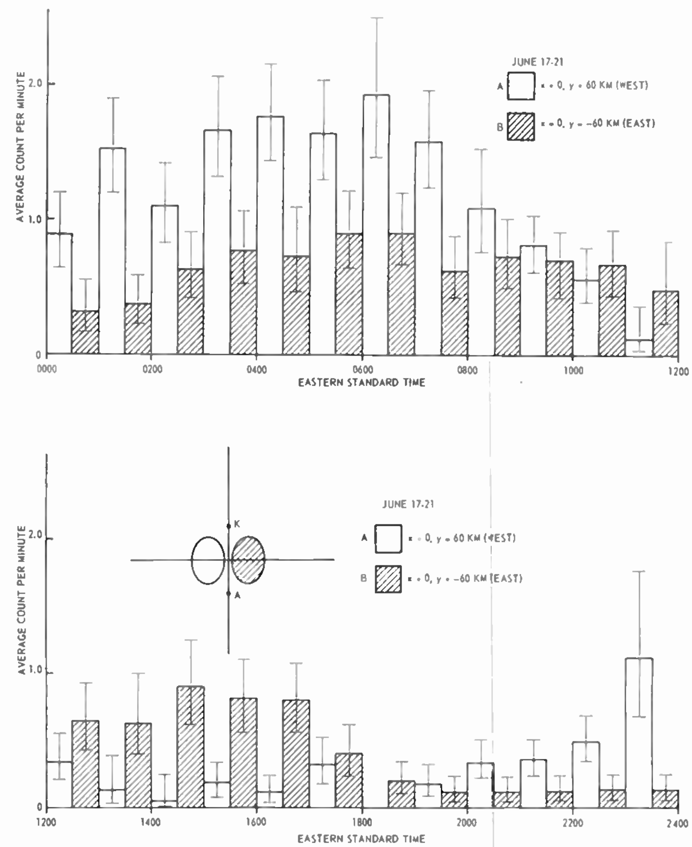

Fig. 8—The average value of the meteor echo rate observed over the Atlanta-Knoxville path on June 17, 19, and 21, 1957. The 40° antenna beam axes were oriented to intersect the h plane at $x=0$, $y=\pm 60$ km. Ninety-five per cent confidence limits are shown. No useful data were taken from 1800 to 1830.

ciated with B is generally stronger—except for the period 0600–0830. Around 0600, when Eshleman predicts roughly equal strength for A and B, Fig. 8 shows A (westward illumination), to be significantly stronger than B (eastward illumination).

A comparison of the data in Fig. 7 and Fig. 8 does not show any very significant differences in meteor signal rate for illumination of the ecliptic tangent point when it is near Knoxville and illumination of the better east or west point predicted by Eshleman. However, choice of the better of the two illuminations in either Fig. 7 or Fig. 8 does in most cases make a significant difference.

IV. Meteor-Shower Radiants

Roughly 5 per cent of the total meteor influx appears in showers which consist of meteors that strike the atmosphere in a number of well-defined streams.[1] The meteors in a given stream all move with nearly the same velocity and in nearly the same direction. The stream direction is specified by the shower radiant, which is the point on the celestial sphere from which the shower appears to come. From the standpoint of meteor-scatter communication these showers offer a number of interesting possibilities. Even though the shower meteors form a small fraction of the total meteor influx during the year, they may provide signal rates that are several times the sporadic background at certain intervals when the showers are near their maximum. The shower radiants and periods of occurrence are well known for the larger showers, so it is possible to predict for a given meteor-scatter link the times when showers would make large contributions to the signal rate. Furthermore it is possible to predict the most favorable areas in the sky to illuminate in order to make maximum use of a given shower.

Forward scatter by meteor showers over long transmission paths has been studied experimentally by Canadian workers.[18,19] The associated theoretical treatment[8] has been worked out using an approximation which breaks down if the transmission path is much shorter than 1000 km. It, therefore, has seemed desirable, to generalize the theoretical analysis so that it might be applied to transmission paths of arbitrary length. Theoretical computation of the locations and relative usefulness of reflection points for showers have been made. Because of the complex geometry in such calculations it was again necessary to make use of a high-

[18] P. A. Forsyth, C. O. Hines, and E. L. Vogan, "Diurnal variations in the number of shower meteors detected by the forward-scattering of radio waves," *Can. J. Phys.*, vol. 33, pp. 600–606; October, 1955.

[19] C. O. Hines and E. L. Vogan, "Variations in the intrinsic strength of the 1956 Quadrantid meteor shower," *Can. J. Phys.*, vol. 35, pp. 703–711; June, 1957.

speed digital computer.[13] The computer code was written in such a way that the geographical position and length of the transmission path for an arbitrary communication link can be inserted. Arbitrary celestial coordinates of the radiant can also be used. The total running time for a typical computation like the one shown as an example here is about 20 minutes.

The analysis may be summarized briefly as follows. The problem of scattering by meteor showers is viewed within the framework of previous calculations for sporadic meteors based on uniform and ecliptic distributions of radiants. The regions in which shower meteors are properly oriented for the desired forward scatter are determined, and the relative effectiveness within these regions is calculated. The results can then be plotted on a series of maps which show the regions of sky which should be illuminated at successive times during the day or, alternatively, the times when a shower will contribute to a given arrangement of antenna beams.

The details of the calculation of the forward scatter from meteor showers proceeds as follows. Consider a system of axes like the one shown in Fig. 1. Let $\hat{T}$ be a unit vector directed toward the radiant, so that $\hat{T}_x$, $\hat{T}_y$, $\hat{T}_z$ are the direction cosines of a line toward the radiant. The condition that the shower trails be properly oriented for reflection can now be expressed in terms of the unit normal $\hat{n}$ to the spheroid family which is given in (9). This condition is

$$\hat{T} \cdot \hat{n}(x, y, z) = 0, \qquad (12)$$

or

$$\hat{T}_x x + \hat{T}_y y + \hat{T}_z z + \frac{R_2 - R_1}{R_1 + R_2} \hat{T}_x D = 0. \qquad (12a)$$

The coordinates x, y, z are the components of a vector extending from the origin to the reflection point on a meteor trail. In the flat-earth approximation z would be the height of the meteor trail above the earth and hence z could be set equal to mean height at which the trails occur. In the present calculation a spherical earth is assumed, so z becomes a function of x, y and the assumed height of the trail. This function is given in (11). If h is specified, (11) and (12a) may be combined so that an implicit function of the form $g(x, y) = 0$ is obtained, which gives a value of y for each value of x, or *vice versa*.

Now it can be seen that a given shower radiant-point gives rise to a line at a height h above the earth's surface, this line specified by $g(x, y) = 0$ being the locus of points at which shower meteors are properly oriented for the desired forward scatter. If h is allowed to vary between 80 km and 120 km, then a family of loci will result. These curves may be drawn on the xy plane so that a map of the scattering region is obtained. A map such as this is shown in Fig. 9. This map would apply to a given link and a given shower at a particular time.

To make the preceding analysis more useful, it is necessary to know something about the relative effectiveness of points along a shower locus. The measure of effectiveness that has been chosen is proportional to the number of observable shower meteors to be associated with the unit length of locus.

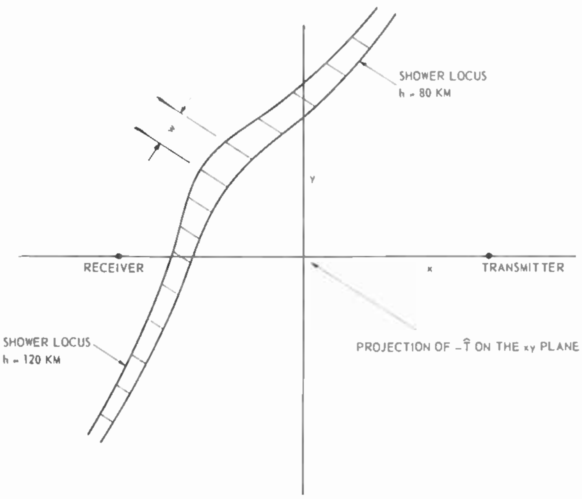

Fig. 9—An example of shower loci plotted on the xy plane. The loci for meteor trails with reflection points lying between 80 km and 120 km will fall between the limiting curves shown. The band between limiting loci is broken into segments of width w (measured perpendicular to the trail direction). These segments illustrate the lengths into which this band is divided in establishing a measure of the relative effectiveness of various portions of the band.

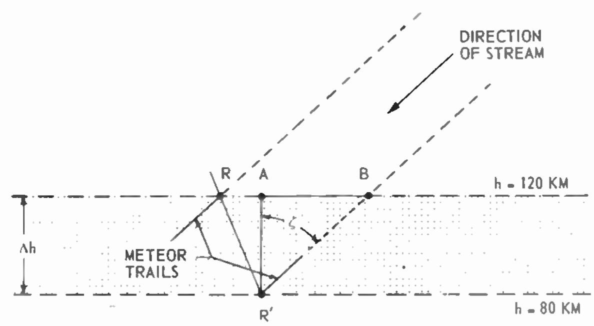

Fig. 10—Diagram showing the surface through which shower meteors must pass to produce signals. The line segment RA represents a portion of the edge of this surface. R and R' are reflection points.

Calculation of the measure of effectiveness involves many of the same considerations that were used to analyze the uniform distribution of radiants in Section II. The number of observable meteors to be associated with a segment of the scattering band shown in Fig. 9 is proportional to the area, lying parallel to the xy plane, through which shower meteors can pass with the proper orientation to produce a scattered signal within this segment. The width of this area will clearly be the width of the band segments measured perpendicular to the meteor trails. As shown in Fig. 9 this width is designated w. The depth of this area varies along the band. Fig. 10 illustrates the method used in determining this depth, which is labeled $\overline{RB}$. The distance $\overline{RA}$ can be measured directly on an xy projection like the one in Fig. 9. The distance $\overline{AB}$ can be calculated knowing the zenith angle

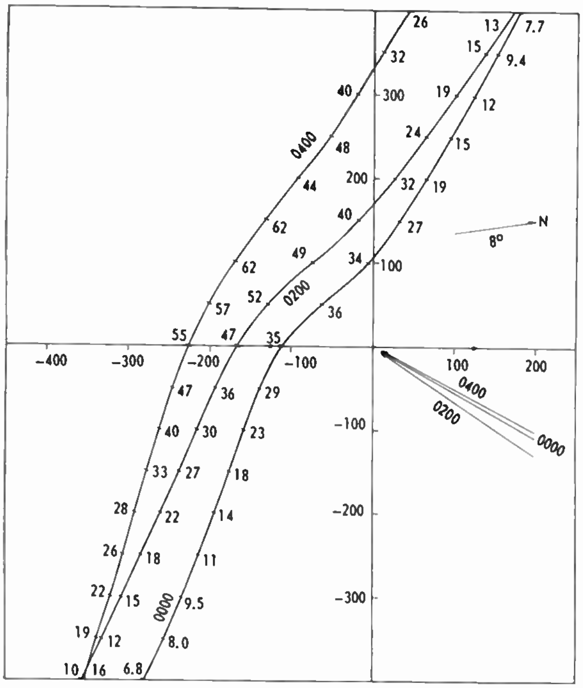

Fig. 11—Loci of properly oriented Perseid-shower meteors for the Knoxville-Atlanta link at the times 0000, 0200, and 0400. The numbers on the lines, when adjusted for antenna gains and polarization loss, are proportional to the number of meteor echoes per minute per unit length of locus.

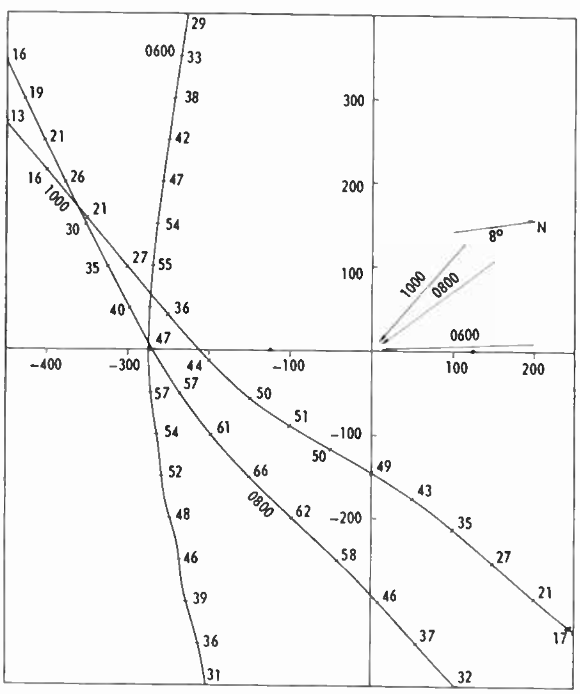

Fig. 12—Shower loci as in Fig. 11 for times 0600, 0800, and 1000.

ζ of the shower radiant and the distance Δh (equal to 40 km in the present case). The result is

$$\overline{RB} = \overline{RA} + \Delta h \tan \zeta. \tag{13}$$

The area A_e through which meteors are captured for a given sement is

$$A_e = w(\overline{RB}), \tag{14}$$

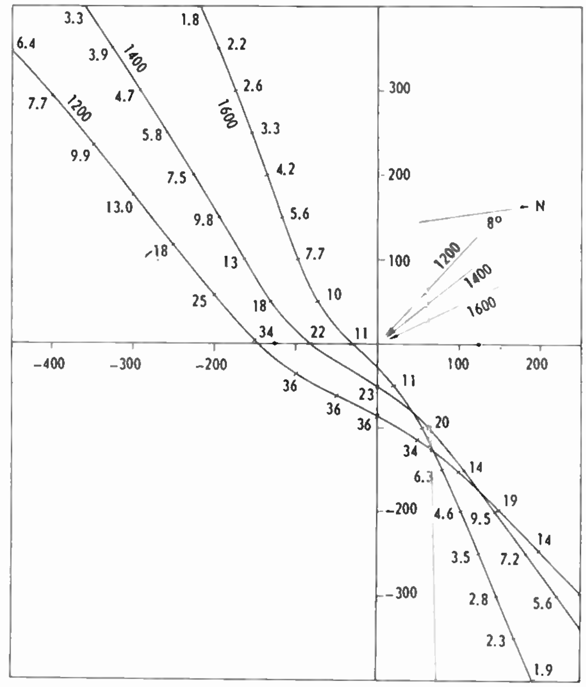

Fig. 13—Shower loci as in Fig. 11 for times 1200, 1400, and 1600.

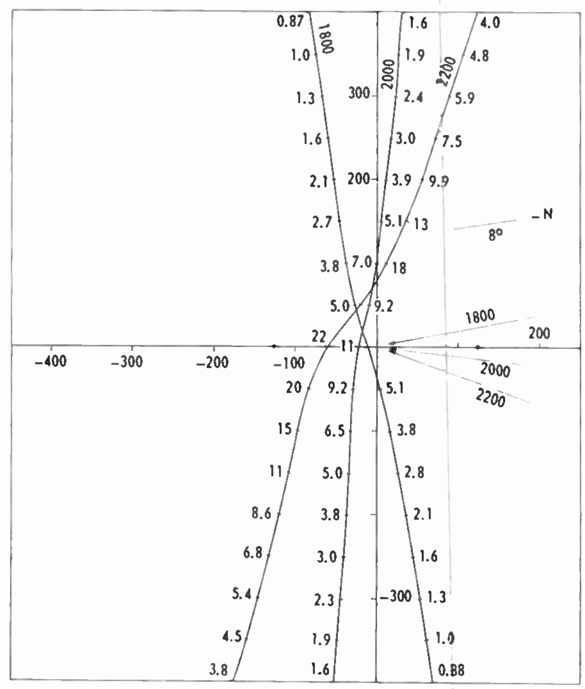

Fig. 14—Shower loci as in Fig. 11 for times 1800, 2000, and 2200.

and the number of meteor signals per second from the segment is then given by $N_S A_e \cos \zeta$, where N_S is the number of detectable shower meteors passing through a unit area normal to the stream in one second. If it is assumed that (6) for the mass distribution applies to the showers with $k=1$, then N_S can be obtained as a function of position in space through the use of (2), the forward-scatter equation. In this way one obtains the following expression for M_w, the number of meteor sig-

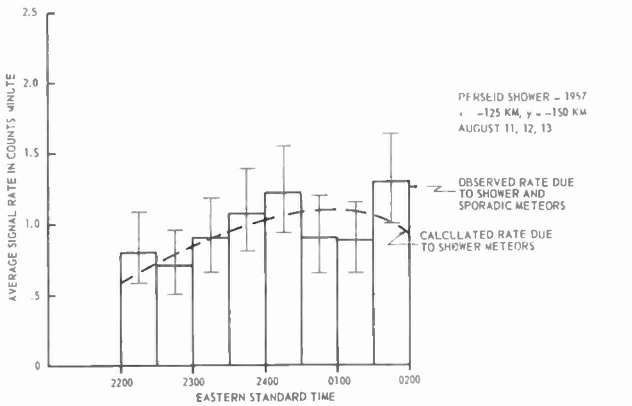

Fig. 15—Experimental meteor signal rates for the Atlanta-Knoxville path averaged for two four-hour intervals from August 11 to August 13, 1957, shown plotted with 95 per cent confidence limits. The computed curve is proportional to the theoretical component of the signal rate due to Perseid meteors.

nals above a specified level coming from a width w of shower band,

$$N_w = (\text{const}) A_c \cos^2 \zeta \sqrt{G_T G_R} H(R_1, R_2, \beta, \phi). \quad (15)$$

A measure of effectiveness F_g which is independent of antenna gains and polarizations can be obtained by writing the preceding equation as

$$N_w = (\text{const}) \cos \mu \sqrt{G_T G_R} F_g, \quad (15a)$$

where

$$F_g = \frac{A_c \cos^2 \zeta}{\sqrt{R_1 R_2 (R_1 + R_2)(1 - \cos^2 \beta \sin^2 \phi)}}. \quad (16)$$

The measure of effectiveness F_g does not take into account the properties of the transmitting and receiving antennas so that it is quite general. Values of F_g can therefore be indicated at intervals along the shower locus. The meteor signal rates for shower meteors with a given arrangement of antennas can be determined by inserting the appropriate values of G_T, G_R and μ in (15) and performing a numerical integration along the shower locus.

As an example, computations based on this analysis have been made for observation of the August Perseid shower with the Knoxville-Atlanta link. Figs. 11–14 (p. 1732) show the loci of properly oriented shower-meteor trails in the Perseid stream for a height $h = 100$ km at two-hour intervals. Values of the measure of effectiveness F_g are indicated at points along each locus. These loci for $h = 100$ km actually represent roughly the center of narrow bands lying between similar loci for $h = 80$ km and $h = 120$ km. The depth of these bands, measured parallel to the projection of the shower direction on the xy plane, varies between zero and 80 km for the loci shown in Figs. 11–14.

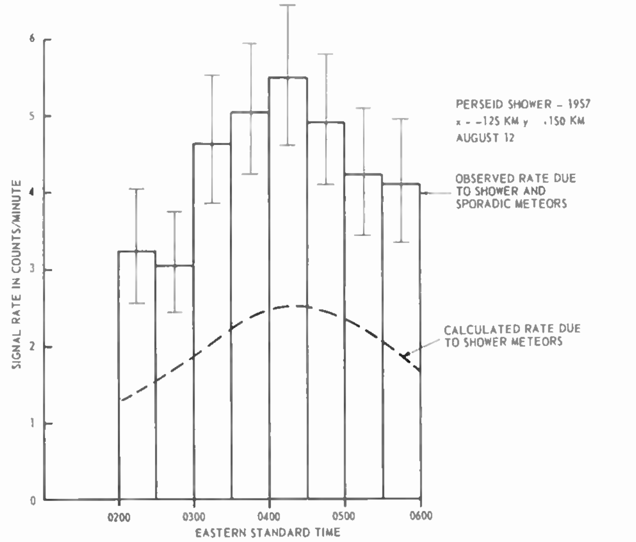

Fig. 16—Experimental meteor signal rates for the Atlanta-Knoxville path observed on August 12, 1957, shown plotted with 95 per cent confidence limits. The computed curve is proportional to the theoretical component of the signal rate due to Perseid meteors.

To calculate the contribution of the shower to the meteor signal rate, one must sum the contributions N_w in (16) along the shower loci. The signal rates have been calculated in this way for two points: ($x = -125$ km, $y = -150$ km) and ($x = -125$ km, $y = +150$ km). The results of these computations together with experimental data are shown in Figs. 15 and 16 for the periods during which the shower loci pass through the beams. Since the computation is only a relative one, the observed data in Fig. 15 have been used to normalize the results. Fig. 16 uses this same normalization to predict the shower contributions to the signal rate at a different location. Fig. 16, in particular, shows good agreement between theory and experiment. The predicted and observed maximum counting rates coincide nicely. The sporadic contribution shows up clearly in Fig. 16, which covers a time interval when the sporadic component could be expected to be large.

These rather preliminary results that have been obtained with the August Perseid shower are encouraging, and plans are under way to extend this analysis to other showers in the near future.

V. Acknowledgment

The authors wish to acknowledge the advice and assistance that they have received from Dr. J. Taylor on all aspects of this study and from Dr. W. F. Atchison on the many computational problems encountered. Thanks are also due the staff on the University of Tennessee who operated the transmitter; in particular the authors wish to thank G. H. Mottern and H. P. Neff.

Correspondence

Experimental Facsimile Communication Utilizing Intermittent Meteor Ionization*

Preliminary tests of facsimile transmission over a 910-mile path have been made at 40 mc by means of intermittent meteor ionization. Printed material was scanned at a rate of 2 frames per second with a resolution of 67 elements per inch. Frequency modulation with a deviation of ±4.5 kc was employed at the transmitter, while a 27-kc bandwidth was used at the receiver. An all-electronic facsimile system recorded a picture when the received signal rose above a preset threshold. Although insufficient data are available to draw any conclusions, the initial results are encouraging.

General

Preliminary tests have been made in the transmission of facsimile over a 910-mile path by means of reflection from meteor ionization. Transmissions were at a frequency of 40 mc, with a transmitter power of 20 kw. The program, which included the design and fabrication of special equipment, is being conducted by the Radio Corporation of America under the sponsorship of the Air Force Cambridge Research Center.

A considerable amount of theoretical and experimental investigation has been going on for several years and this has yielded a number of conclusions about meteor-path propagation. This type of path is characterized by its random intermittency with a low duty cycle. The optimum distance for transmission is roughly 600 to 1200 miles and considerable power is required if a wide bandwidth is used. Frequencies in the vicinity of 40 to 60 mc are advantageous for propagation by this means. Multipath delays during any given meteor burst appear to be in the order of a few microseconds.

The burst duration varies over a range of less than 0.1 second to several minutes. In one test of 159 samples the average length was 0.33 second. In addition to a strong diurnal variation with an optimum near 6 A.M. local time, the duty cycle may vary with path latitude, season, and other factors. Experimental results to date indicate, however, that the received signal is usually solid and reliable for meteor bursts of less than one second duration.

It appeared that the experimental transmission of intelligence by facsimile via meteor ionization would be an excellent way in which to explore further the properties of this medium. Several methods of facsimile transmission were considered and their possibilities examined. As a basic premise it is obvious that a whole picture must be transmitted per meteor burst or the picture must be sent in broken sections. With such a short transmission time, the bandwidth must be high for a whole picture of reasonable size and detail. This requires excessive power. If the picture is sent in sections, the problem of matching the pieces together to produce an acceptable result may be difficult.

Mode of Operation

In view of the importance of getting test transmissions under way at an early date the decision was made to design and build a facsimile system of the simplest possible type for one frame-per-burst operation. Consequently, the system that was produced and is now in its experimental trials has the following characteristics and mode of operation.

The scanner and transmitter run continuously during test periods, sending a picture over and over at a rate of two complete scans per second. A resolution of 67 picture elements per inch, both vertically and horizontally, was selected as suitable for reproducing the copy used in these tests. (The reproduction of average typewritten copy requires somewhat greater resolution.) For a 3-inch by 4-inch picture a transmission bandwidth of 106 kilocycles is required. Several different bandwidths may be used and the picture information content is adjusted accordingly. Black and white signals only are developed with no attempt to handle halftones. Horizontal or line sync pulses are combined into the composite signal as a super black level. No vertical sync pulses are transmitted. Frequency modulation of the carrier is used to help overcome the inevitable amplitude variations encountered in the propagation path. The receiver is also on continuously during tests with the recorder in standby condition. When a passing meteor closes the transmission path, the incoming signal trips the recorder, which then 1) produces a 0.5-second vertical sweep and 2) unblanks the cr-tube beam to permit picture reproduction on the phosphor screen. The circuit then resets for the next burst.

Facsimile Equipment

The facsimile system is all-electronic. The subject matter is recorded as a frame of 35-mm film. The film is scanned by a flying-spot cathode-ray tube scanner and the transmitted light is picked up by a secondary-emission phototube. The output of the phototube is the picture or video signal. The dc component of the signal is carried all the way to the transmitter output.

At the recorder the incoming picture is reproduced on a similar cathode-ray tube and a permanent record is made by photographic techniques. The proper dc picture level is restored automatically and the sync pulses are extracted from the composite signal to control the horizontal sweep.

Transmitting Equipment

The transmitter is frequency modulated by the composite picture signal with its three levels of amplitude, corresponding to sync, black, and white. The transmitter exciter is capable of providing frequency deviations up to ±50 kc for operation with various bandwidths at the receiver.

The transmitter final amplifier has an output power of approximately 20 kw. The transmitting antenna is a rhombic having approximately 22 wavelengths per leg with a half side angle of 80.25°. Its height is 79 feet above ground, making the maximum radiation in the vertical plane at 4.5° above the horizon.

Transmission Path

The transmitter is located at the transmitting facility of the National Bureau of Standards, Havana, Illinois. The Great Circle distance to the receiving site at Riverhead, New York is 1465 km (910 miles).

The transmitting and receiving antennas are oriented on a common volume approximately 6° north of the Great Circle path to favor reflections from meteor trails during normal working hours.

Receiving Equipment

The receiving antenna is a duplicate of the transmitting antenna already described. The characteristics of the receiver are as tabulated below:

RF:

Three fixed-tuned stages centered at 40 mc.
Noise figure about 4 db.

Conversion Oscillator:

Crystal controlled.

IF:

Centered at 13 mc.
27-kc, 55-kc, 110-kc, or 220-kc bandwidths are available by means of panel switching.

Outputs:

FM with four choices of video bandwidth.
AM monitoring and threshold voltage.
Logarithmic recording.
Direct from the IF at 13 mc.

AGC:

Adjustable delayed agc. Four time constants 0.1 millisecond, 1 millisecond, 1 second, and 10 seconds, are available.

Results and Discussion

The pictures presented in Fig. 1(a) through 1(d) were taken during the operational shakedown of the equipment and were part of the results obtained during a half-hour test period. The original subject copy size in this case was 1.5 inches by 2 inches and the horizontal sweep rate was 200 lines per second. The total frequency shift at the transmitter was 9 kc and the receiver bandwidth was 27 kc. An individual picture represents the results obtained in the half-second interval after the receiving scanning circuitry has been triggered by a signal rising above a preset threshold. Consequently, the vertical blanking or framing band may ap-

* Received by the IRE, September 6, 1957. This work was sponsored by the Cambridge Air Force Research Center under Contract AF 19(604)-1922.

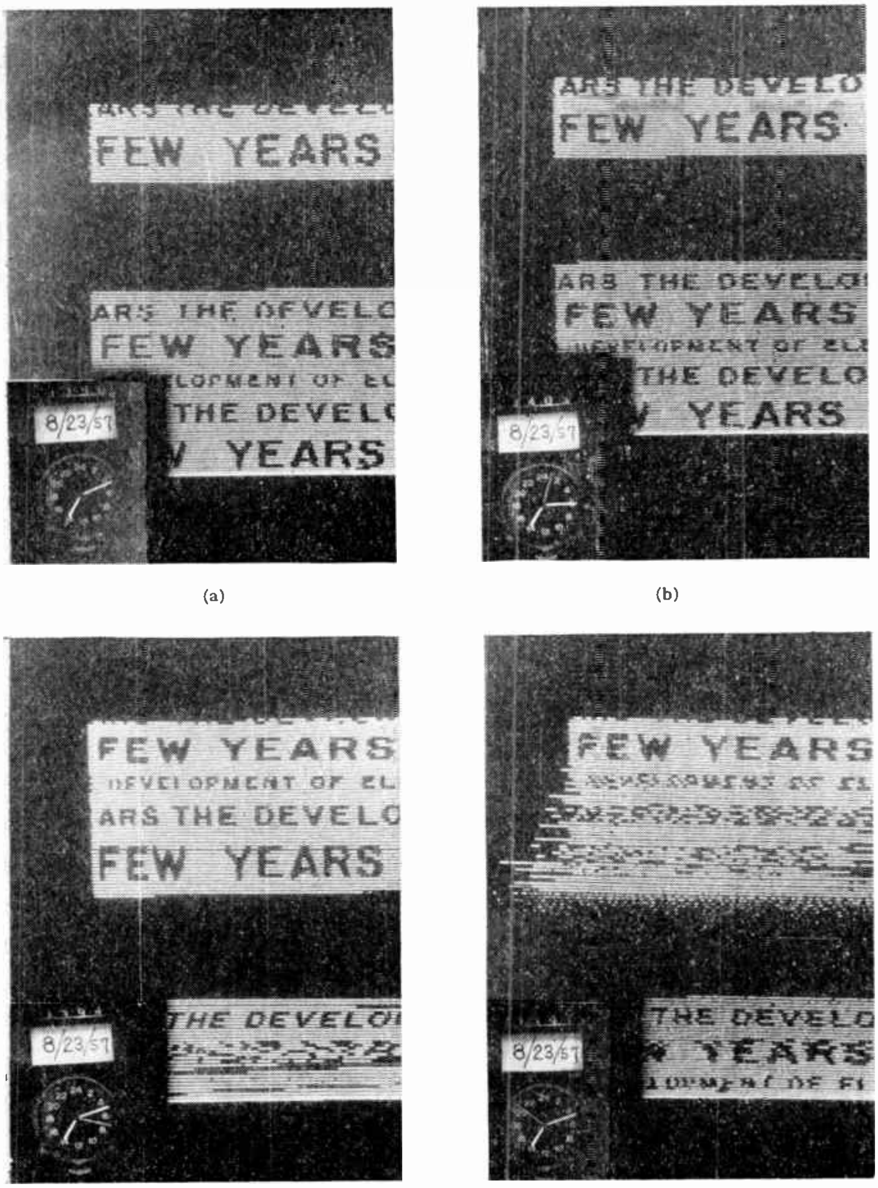

(a) (b) (c) (d)

Fig. 1—Facsimile pictures transmitted by means of intermittent meteor ionization.

pear at any location on the picture due to the lack of vertical synchronism. In the example shown, the receiver threshold was approximately 6 μv across 50 ohms. Fig. 1(a) and 1(b) represent typical results when the meteor ionization has a duration equal to at least one-half second. After triggering the scanning mechanism, the receiving equipment scans upward from the bottom of the picture for one-half second or the time to transmit one frame. In all the accompanying illustrations it is apparent that the vertical scanning time in the receiving equipment is about 25 per cent too long, thus showing more than one transmitted frame. Purely by chance, the recorder was triggered at the beginning of a frame in Fig. 1(a) and 1(b). These two samples are among the best transmissions made thus far and the quality is judged to be only slightly impaired by the radio propagation path. (Previous back-to-back scanner-recorder operation produced essentially the same results.)

Fig. 1(c) and 1(d) are examples of received copy when the propagation path becomes poor for a part of the time interval required for transmission of one frame. The signal apparently dropped into the noise during the middle of Fig. 1(d) with resultant loss of sync and picture information. The initial deterioration seems to come from loss of line synchronization stability, a result frequently encountered in facsimile operation when the synchronizing information is transmitted with the picture signal.

These pictures are among the first results obtained with the automatic recording equipment. Future tests with wider bandwidths and higher information rates may yield data on multipath limitations and duty cycles that may be expected with this method of information transmission.

Conclusion

At the present time only preliminary tests have been made on the equipment before starting a planned research program. Although no extensive conclusions can be made at this time regarding this mode of communication, the results are encouraging.

W. H. Bliss
RCA Laboratories
Princeton, N. J.
R. J. Wagner, Jr.
and G. S. Wickizer
RCA Laboratories
Riverhead, L. I., N. Y.

Some Airborne Measurements of VHF Reflections from Meteor Trails*

In the course of a program to determine the feasibility of transhorizon communication by means of reflections from meteor trails (that is, meteor bursts), it was indicated that measurements from an aircraft would be useful in establishing the probability of simultaneous reception of meteor bursts by separated receivers as a function of their separation. High-power cw vhf transmissions already were directed from Cedar Rapids, Iowa, toward South Dartmouth, Mass., for another purpose and were suitable for this investigation.

All signals were monitored simultaneously in the aircraft and by duplicate receiving equipment set up at the Air Force Cambridge Research Center (AFCRC), Bedford, Mass. Bedford is located just outside the 3-db points on the transmitting antenna beam pattern, but this was not considered detrimental for this investigation. Accurate synchronization was maintained between the airborne and ground-based recorders.

The transmitting equipment produced 49.6-mcps cw at about 30-kw output into a rhombic antenna having a nominal gain of 18 db over a half-wave dipole.

Five-element yagi antennas delivered the signals to the receivers.

The Bedford antenna was fixed in position, directed at Cedar Rapids; the airborne antenna was rotatable (and retractable for landings and take-offs), and always was manually positioned to point at Cedar Rapids.

Flights were set up both along and transverse to the Cedar Rapids-Bedford path. The method finally adopted, for determining simultaneity of the received bursts, consisted in recording the WWV audio directly on one channel of a Brush recorder and recording the signal on the other. Clear-cut, unambiguous markers were obtained, even through considerable variation in the WWV signal strength. Interpolation to a small fraction of a second was possible. The recorders operated from the avc voltages of the receivers and were calibrated in terms of the rf input voltages to the receivers.

Most of the good data resulted from one 24-hour flight in which the aircraft reached a point 250-statute miles due east of AFCRC, approximately off Halifax, Nova Scotia.

* Received by the IRE, September 3, 1957.

A burst was considered to have occurred every time the signal level exceeded an arbitrary threshold established just above the normal continuous scatter signal. A correlated burst was considered to have occurred whenever there was an overlap in time of the bursts as detected at the separated receivers; that is, information could be passed from the transmitter to both receivers simultaneously.

An effort was made to distinguish between overdense and underdense bursts.[1] Duration was the primary criterion, but the personal judgment of the analyst was a factor when the shape characteristics indicated one overdense burst rather than a group of closely spaced underdense bursts. Since the reflections from the overdense trails were not nearly so specular as those from the underdense, the two types are reported separately.

In general, more bursts were detected with the airborne than with the ground-based equipment. This can be attributed to the fact that the volume of space in which reflections may occur, within the beams of both the transmitting and the receiving antennas and within the "meteor layer," is larger for the airborne equipment than for the ground station beneath it. The meteor layer here is defined as the volume of space in which satisfactory meteoric trail formation occurs. This is a shell about 10-miles thick, completely enclosing the earth and about 70 miles away from the earth's surface.

Because of the greater number of airborne bursts, the correlation in any given area must be reported as two ratios, one relating to the number of bursts detected on the ground, the other relating to the number detected in the air. For the eastbound leg of the flight, the ratios for underdense bursts are plotted in Fig. 1. (Included in the same

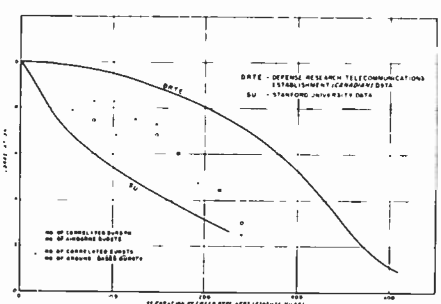

Fig. 1.

figure are both the Canadian[2] and the Stanford[3] computed curves, which are based on a separation between transmitter and receiver of 1000 *kilometers*, whereas the Cedar Rapids to Bedford separation is about 1000 *miles*.) The correlation ratios for the overdense bursts (not plotted) remained 1.0 out to a separation of 150 miles between receivers, when they started to drop and reached about 0.6 at the maximum range, a separation of 275 miles.

J. P. Casey
and J. A. Holladay
Propagation Laboratory
Air Force Cambridge Res. Center
Bedford, Mass.

[1] For discussions of trail density, see Von R. Eshleman, "On the wavelength dependence of the information capacity of meteor burst propagation," this issue, p. 1710, and W. R. Vincent, *et al.*, "Analysis of oblique path meteor propagation from the communications viewpoint," this issue, p. 1701.

[2] C. O. Hines, "Privacy in a JANET System of Communication," Rad. Phys. Lab., Defence Res. Telecommun. Estab., Ottawa, Project Rep. 12-3-16; December, 1935.

[3] O. G. Villard, Jr., A. M. Peterson, L. A. Manning, and V. R. Eshleman, "Some Properties of Oblique Radio Reflections From Meteor Ionization Trails," Rad. Propagation Lab., Stanford Univ., Stanford, Calif., Tech. Rep. No. 85; May, 1955.

Mobile Single-Sideband Equipment*

The paper by Richardson *et al.*[1] presents a somewhat depressing piecture, and one is forced to the conclusion that the general feeling among Motorola engineers is that mobile vhf SSB installations are not worthwhile except from the viewpoint of spectrum economy which the writer considers not to be the true position.

While the tests described were well-engineered, some of the premises on which they were based are only partly true, and closer examination would have led to different design considerations.

There are few locations where *throughout a season* critical circuit component temperature is likely to vary from $-30°C$ to $+85°C$ in normal use, so that the maximum frequency deviation for most installations may be considerably less than the ± 638 cycles postulated; indeed, such components could be temperature-controlled.

The complete equipment design, however, has been based on the ideas behind the statement that the carrier generated in the receiver must be within 50 cycles of the correct frequency to give the detected voice signal the proper tonal qualities. The writer's experience, on the other hand, is that good intelligibility is obtained with the carrier generated in the receiver in excess of 300 cycles off frequency (and with an SSB experienced operator up to 600 cycles), provided no frequency lower than 600 cycles is allowed to voice-modulate the transmitter. We may say that the tone changes, but up to this limit the speech does not commence to become garbled until the carrier deviation exceeds the lowest speech frequency transmitted.

The fact must be faced that good SSB equipment will be considerably more complicated than normal AM or fm equipment. Considerable speech processing to obtain the best intelligibility and rms to peak voice modulation ratio (for highest final amplifier efficiency) is very much worthwhile.

For most users at vhf a manually operated, speech clarifier, trimmer on the receiver would be acceptable and, with amended design, is practicable. However, for stringent services requirements, controlled reduced dual pilots, one above and one below the converted voice frequencies, operating only on speech pauses and controlling afc electromechanically, would be almost immune from capture effects.

Listening on the experimental hf bands during rather poor long-range communication conditions will show the ease with which intercontinental SSB contacts can be made when normal AM and nbfm dx stations cannot be heard, and though this is hardly a fair comparison with SSB vs fm at vhf, better range, if required, can be produced by mobile SSB equipment over fm for equal primary power; but the real battle between the systems, from the mobile users point of view, will inevitably again focus around ignition disturbance suppression.

R. E. Morrow
Worth Communications Services
Birmingham, England

* Received by the IRE, July 22, 1957.

[1] R. Richardson, O. Eness, and R. Dronsuth, "Experience with single-sideband mobile equipment," Proc. IRE, vol. 45, pp. 823–829; June, 1957.

Author's Comment[2]

Our paper[1] was intended as information concerning what we consider a possible solution to the application of SSB to the uhf mobile services. We did not intend or attempt to give a depressing picture. Our intention was to present the technical background for what is presently an experimental approach to the problem. When SSB can supply the same standards of performance as presently achievable with fm equipment, the saving of frequency spectrum in and of itself will result in universal acceptance of SSB for the mobile services. Any advantages over and above this main advantage the industry would happily accept.

Although Mr. Morrow has indicated that we have focused, in his opinion, too much attention upon spectrum economy, he has failed to indicate what he considers as "the true position."

I would perfer, at this time, to give close examination to those premises of our paper which he has indicated as being only partly true.

The first point in question was to the circuit component operating temperature which we have indicated as being from $-30°C$ to $+85°C$. Our organization has produced a considerable amount of fm two-way equipment during the last decade. It must be realized that we manufacture equipment which must operate anywhere within the continental limits of the United States, as well as throughout the world. There are many locations in the United States alone where the winter temperature can be as low as $-30°C$ and since, in general, the majority of two-way equipment is installed in the trunks of vehicles, the ambient temperature to be expected during the summer can be considerably higher than the outside air

Received by the IRE, August 7, 1957.

temperature because of the heating effect of the sun. For these reasons, the fm two-way equipment which we produce at present is required to operate over the ambient temperature range of −30°C to +85°C. It is well to point out that military specifications for this type of service are from −40°C to +65°C. There is no reason for not assuming the same operating temperature range when considering SSB equipment.

The next point in question was the frequency error of the reinserted carrier which could be tolerated. It was stated in the paper that the frequency error must be within 50 c to give the detected signal the proper tonal quality. In Mr. Morrow's experience, good intelligibility is obtained up to frequency errors of 300 c and even 600 c. But here we are comparing different standards of performance, *i.e.*, proper tonal quality vs intelligibility. Is there any doubt that an error of 300 c does not give the proper tonal quality? It is our opinion that any SSB system for uhf mobile application must give the proper tonal quality in addition to good intelligibility. This is based on what industry is willing to accept today. In fact the trend is toward better tonal quality than now exists.

The third point in question was the use of a "speech clarifier." At present, it is only necessary to provide the user of fm mobile radio with an audio volume control and a squelch adjustment control. These two controls are usually made available at a dashboard mounted control head. It must be realized that the people who use mobile equipment are not experienced radio operators. For this reason, it is preferable to provide a communication means which requires a minimum of adjustment over and above that required to use a telephone. A taxi cab driver cannot be expected to manipulate a "speech clarifier" while driving through city traffic. In addition, the rapid rate of exchange of communication on the mobile services would be slowed down considerably if a "speech clarifier" were required. A "speech clarifier" would not be of much use when ten cab companies share the same channel and where the length of individual messages is from 1 to 10 seconds. For these reasons, we feel that a "speech clarifier" is totally impractical for mobile application of SSB.

One of the main advantages of SSB over AM is realized in the hf band where long range communication is required. Under these conditions the phenomenon, which has become known as selective fading, takes place. This is a well-known phenomenon, but at the frequency of operation of this equipment (160 mc) this phenomenon is not evidenced. For this reason, no advantage of SSB over fm for uhf mobile application based on selective fading is anticipated.

To obtain a realistic performance comparison between the two equipments, the SSB equipment was designed to use the same final amplifier tube and have the same physical size as the fm transmitter. As indicated in our paper, the primary power required for the SSB transmitter is 30 per cent less than the primary power required for the fm transmitter. For the same primary power the SSB equipment would probably out-perform the fm equipment by a small extent. I say small extent because an increase of power of 15 db or so will only double the communication range for the services being considered here. Hence a few db increase in power results in very little increase in communication range.

If the standard of comparison had been equal primary power, it is clear that a larger transmitter using a larger final amplifier tube, having a higher plate dissipation and a higher maximum plate voltage, would be required for the SSB system. We believe it is more realistic to use the same final amplifier in the same size transmitter as a standard of comparison than to use the same primary power.

In closing let me make a few comments about ignition noise. I am in agreement with Mr. Morrow that ignition noise will be more deleterious to a SSB receiver than to an fm receiver because of the decrease in receiver bandwidth and because the SSB receiver is basically an AM receiver. However, we have been working on this problem and have arrived at a solution which we feel is satisfactory. Basically, the solution is to blank out the ignition disturbance prior to the main selective elements of the receiver and hence avoid ringing caused by the impulse noise interference. Since the disturbance is very short in time at the blanking point and since the main selective element following this point will continue to provide energy to the receiver during the blanking time, ignition disturbance can be eliminated from the output of the receiver without any loss to the desired voice signal.

Roy A. Richardson
Motorola, Inc.
Chicago, Ill.

Gain Bandwidth and Noise in Maser Amplifiers*

A cavity-type maser,[1,2] or any similar resonant negative-resistance device can serve as an amplifier in two ways: either by having a single external coupling line with a circulator to separate input and output signals (*circulator maser*); or by having separate external coupling lines for the input and output signals (*two-port maser*). The purpose of this note is to compare the two types with respect to gain-bandwidth product and noise figure. While the expressions presented are not new, the specific comparison does not seem to have been made previously.

The conclusions reached here are: 1) the optimum gain-bandwidth product of the two-port maser is only one-half that of the circulator maser for the same basic maser cavity and is obtained in the two-port case only at the sacrifice of low noise figure. 2) The optimum noise figure of the two types of maser is the same, but it can be achieved in the two-port maser only by sacrificing some of the bandwidth. 3) Despite the theoretical superiority of the circulator maser, certain practical considerations may still make the two-port maser competitive.

To demonstrate these statements, consider the cavity equivalent circuit of Fig. 1

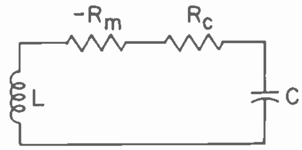

Fig. 1—Equivalent circuit of the maser cavity.

where

R_c = ohmic losses in the cavity walls and the maser material, all at temperature T_c.

$-R_m$ = negative resistance of the maser-material spin system with negative spin temperature $-T_m$.

$-R_m' = R_c - R_m$ = effective negative total resistance of cavity-plus-spin system.

We then define

$Q_c = \omega_0 L/R_c$ = unloaded cavity Q due to ohmic losses.

$-Q_m = -\omega_0 L/R_m$ = negative Q of spin system.

$-Q_m' = -\omega_0 L/R_m'$ = effective negative total unloaded Q of cavity-plus-spin system.

In the circulator maser a single external line of impedance R_e couples the cavity, through a circulator, to matched generator and load resistances $R_g = R_L = R_e$, as shown in Fig. 2, where the resistance values refer to

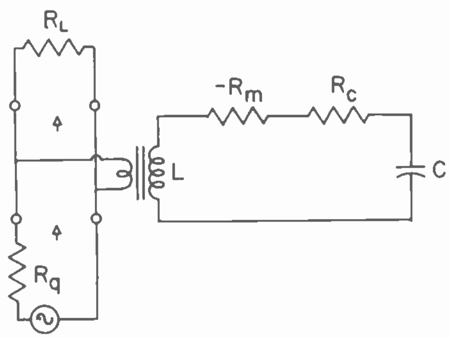

Fig. 2—Equivalent circuit of the circulator maser.

the values as transformed into the cavity by the coupling transformer. The temperatures of the resistances R_g and R_L are T_g and T_L, respectively. We also define

$Q_e = \omega_0 L/R_e$ = external Q of the coupling line.

We will characterize the noise generated in the maser by an amplifier noise temperature T_{ampl}, defined so that the additional noise generated in the maser amplifier is equivalent to an additional noise source at tem-

* Received by the IRE, August 5, 1957.

[1] J. P. Gordon, H. J. Zieger, and C. H. Townes, "The maser," *Phys. Rev.*, vol. 99, pp. 1264–1274; August 15, 1955.

[2] N. Bloembergen, "Proposal for a new type solid state maser," *Phys. Rev.*, vol. 102, pp. 324–327; October 15, 1956.

perature T_{ampl} connected to the input of the maser. The noise figure of the amplifier is then $F=1+T_{ampl}/T_g$. We will assume that the bandwidth of the spin system is much larger than the bandwidth of the resonant cavity and that the noise due to spontaneous emission in the spin system can be considered to be Johnson noise in a negative resistance $-R_m$ at a negative temperature $-T_m$.[3] Then for the circulator maser the gain bandwidth and noise temperature are

$$G^{1/2}B = 2f_0/Q_e$$

$$T_{ampl} = \frac{Q_e}{Q_c}\,T_c + \frac{Q_e}{Q_m}\,T_m. \tag{1}$$

The condition for high gain in a circulator maser is that the external loading should just slightly overcome the negative resistance of the cavity, or that $1/Q_e \approx 1/Q_m'$. Under this condition, the above expressions become

$$G^{1/2}B \approx 2f_0/Q_m'$$

$$T_{ampl} = \frac{Q_m'}{Q_c}\,T_c + \left(1+\frac{Q_m'}{Q_c}\right)T_m. \tag{2}$$

In the two-port maser the source and load have separate coupling lines, as shown in Fig. 3.

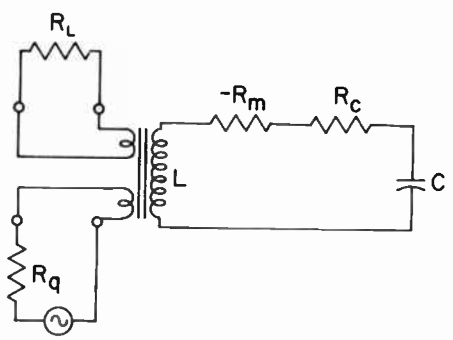

Fig. 3—Equivalent circuit of the two-port maser.

We define

$Q_{eg} = \omega_0 L/R_g$ = external Q of the input coupling line.

$Q_{eL} = \omega_0 L/R_L$ = external Q of the output coupling line.

For a given maser cavity with a given Q_m', the circulator maser must have a fixed output coupling Q_e to achieve a certain gain, and the noise figure and gain bandwidth are then fixed. However in the two-port maser, the input and output couplings Q_{eg} and Q_{eL} can be separately varied to adjust the gain, and different ratios of input to output coupling will give different noise figures and gain bandwidths for the same gain. Furthermore, the load can never match the negative resistance of the maser cavity, and so noise from the load resistance is reflected back from the cavity and must be taken into account in the noise temperature.

In general, the noise temperature and gain bandwidth of the two-port maser are given by the expressions

$$G^{1/2}B = 2f_0/(Q_{eg}Q_{eL})^{1/2}$$

$$T_{ampl} = \frac{Q_{eg}}{Q_c}\,T_c + \frac{Q_{eg}}{Q_m}\,T_m + \frac{(1/Q_{eg} - 1/Q_{eL} - 1/Q_m')^2}{4/Q_{eg}Q_{eL}}\,T_L. \tag{3}$$

The condition for high gain in a two-port maser is that the *total* external coupling should just barely overcome the negative cavity resistance, or $1/Q_{eg}+1/Q_{eL}\approx 1/Q_m'$. For high gain, the two-port noise temperature and gain bandwidth become

$$G^{1/2}B \approx (2f_0/Q_m')\left[\epsilon(1-\epsilon)\right]^{1/2}$$

$$T_{ampl} \approx \left(\frac{1}{1-\epsilon}\right)\left\{\frac{Q_m'}{Q_c}\,T_c + \left(1+\frac{Q_m'}{Q_c}\right)T_m\right\} + \left(\frac{\epsilon}{1-\epsilon}\right)T_L \tag{4}$$

where the parameter $\epsilon = Q_m'/Q_{eL}$ tells how the coupling is distributed between the input and output lines. In practice, ϵ would vary between the limits 0 and $\frac{1}{2}$. Eq. (4) shows that for $\epsilon=0$, which means that $Q_{eg}\approx Q_m'$ and $Q_{eL}\gg Q_m'$, *i.e.*, heavy input and light output coupling, the noise temperature of the two-port maser has a minimum value just equal to the value for the circulator maser. Unfortunately, this case also reduces the bandwidth to zero. For the limit $\epsilon=\frac{1}{2}$, which means equal input and output coupling, $Q_{eg}\approx Q_{eL}\approx 2Q_m'$, the gain bandwidth is maximum and equal to one-half the value for the circulator. The noise temperature, however, is at least doubled, plus the contribution due to the load resistance noise.

That the gain bandwidth of the two-port is only one-half as large as the circulator maser can be explained as being due to the fact that one-half of the amplified output is lost by being fed back down the input line, since the input and output are coupled equally to the cavity. However, once one accepts the initial loss of $\frac{1}{2}$ the bandwidth or 6 db in gain in going from the circulator to the two-port, the situation is not as bad as it may seem. Fig. 4 shows a plot of noise temperature and bandwidth vs ϵ for the two-port maser, where the load resistance noise term has been ignored. The *opt* subscripts refer to the values for the circulator case. As ϵ is reduced, the noise temperature falls off much more rapidly than the bandwidth, so that nearly optimum noise figure can be achieved with very little further loss in bandwidth.

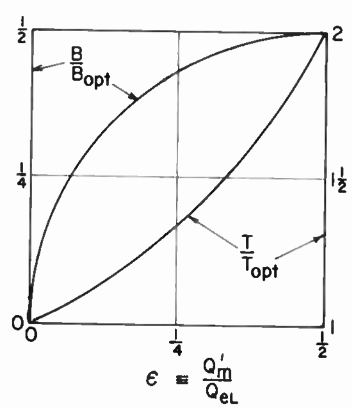

Fig. 4—Noise temperature and bandwidth of a two-port maser vs the output coupling parameter.

If presently proposed solid-state[2] or molecular-beam[1] masers are to achieve anything approaching their optimum potential noise temperatures, it is apparent that in the two-port case the load line will have to be cooled to very low temperatures. However, this can probably be done in practice by use of a cooled ferrite isolator in the output line with the additional benefit of stability to load fluctuations. Furthermore, the noise performance of the system will not be too badly degraded by various types of nonideal performance of this isolator. In the circulator case, on the other hand, nonideal performance in the form of forward loss in the circulator will have a serious effect on the optimum noise figure even when the circulator is cooled. This is because the circulator comes *before*, not *after*, the amplifier.

If one is not really pushing the maser to its ultimate noise figure, then the circulator maser is probably better, as well as simpler. To approach the ultimate noise figure in practice, however, it may be necessary to go to the two-port maser.

The author is grateful to P. N. Butcher and H. Heffner of this laboratory for their suggestions and discussions.

A. E. SIEGMAN
Stanford Electronics Labs.
Stanford, Calif.

[3] R. V. Pound, "Spontaneous emission and the noise figure of maser amplifiers," *Ann. Phys.*, vol. 1, pp. 24–32; January, 1957.

Improvements to the High-Accuracy Logarithmic Receiver*

Chambers and Page have described a high-accuracy logarithmic receiver.[1] Fig. 1 (opposite) shows a single stage of this amplifier. Each IF tube acts as an infinite impedance detector and supplies a detected signal to its associated video amplifier. A cathode capacitor is required in each IF stage to keep the IF out of the video section and to avoid excessive degeneration. This capacitor unavoidably causes some attenuation of the higher frequency components of the video signals. To balance off the video response a similar capacitor is used in the video amplifier cathode so that the high-frequency components receive maximum video amplification while the lower frequencies are heavily degenerated.

We have had occasion to construct a matched pair of these receivers for precision comparison of two pulse trains. It was found that for exact pulse reproduction, each set of IF and video cathode capacitors required critical adjustment so as to make matching of the pulses from two logarithmic amplifiers nearly impossible. It was found possible to replace each IF cathode capacitor and its associated isolating resistor with a π-section constant κ low-pass filter. This filter was designed to match the approximately 200-ohm cathode impedance of the 6AK5 IF tube and to have a cutoff frequency of 15

* Received by the IRE, June 24, 1957.
[1] T. H. Chambers and I. H. Page, "The high-accuracy logarithmic receiver," PROC. IRE, vol. 42, pp. 1307–1314; August, 1954.

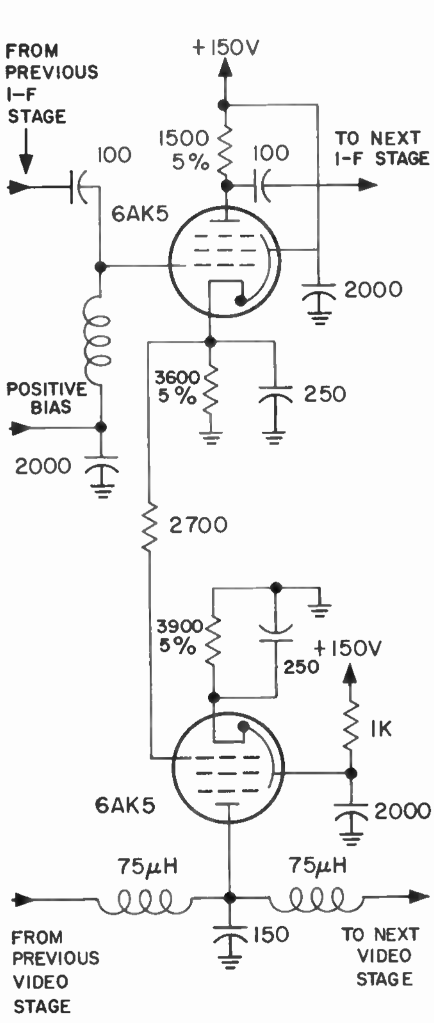

Fig. 1.

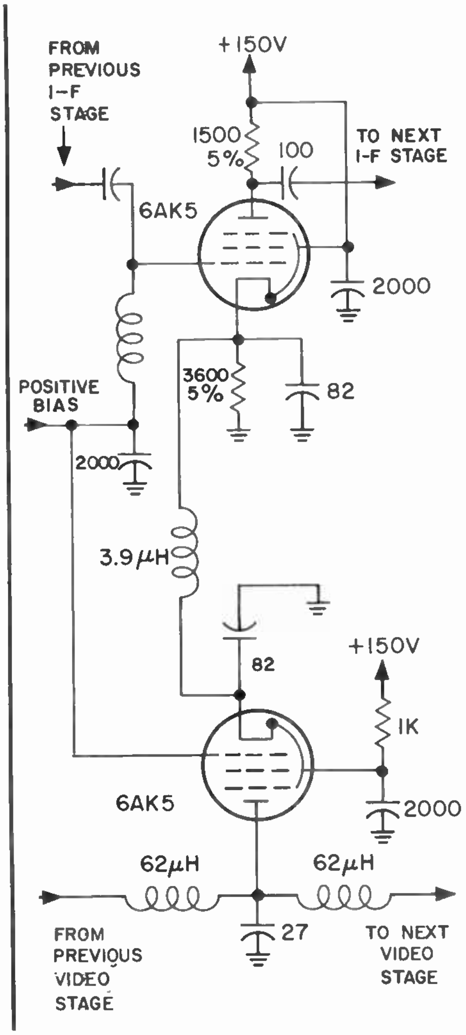

Fig. 2.

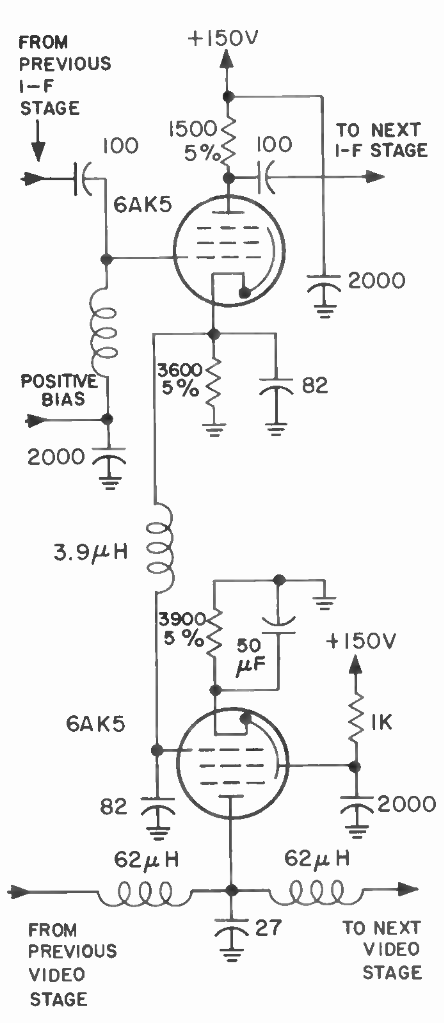

Fig. 3.

mc. Video signals below this frequency are passed unaltered while the IF is efficiently blocked and IF cathode bypassing is nearly as good as the original circuit.

This method of coupling to the video tubes offers two interesting possibilities. Fig. 2 shows a cathode-driven video stage. This circuit produces the most faithful pulse reproduction since the constant κ section is properly terminated at both ends. Moreover, the output pulse now has the positive polarity which is conventional in radar IF strips. It should be pointed out, however, that since the two tubes are working from a common dc cathode resistor, some of the dc current stabilization advantages of the original circuit are lost. Fig. 3 shows a grid-driven version which is suitable if no dc video signals are anticipated. This circuit utilizes the full gain of the video amplifier tubes and is capable of maximum outputs in excess of 40 volts. A modification of this circuit could conceivably be used to cathode-drive a cathode ray indicator tube without the use of an additional video amplifier.

Roger T. Stevens
Electronic Systems, Inc.
Boston 11, Mass.
Formerly with Avco Mfg. Co.
Boston, Mass.

Accurate Measurement of r_c and α_0 for Transistors*

At low frequencies the dynamic collector resistance, r_c, and the common-base short-circuit current gain, α_0, are the only important transistor r parameters for most small-signal computations. The purpose of this note, however, is to present a method whereby both r_c and α_0 can be directly and accurately measured.

Consider the circuit diagram of Fig. 1.

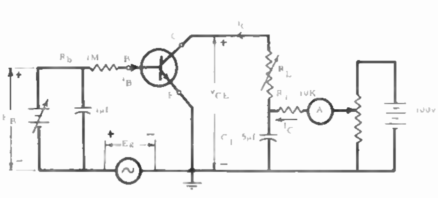

Fig. 1—Circuit diagram used for measuring the low-frequency current gain of an n-p-n transistor as a function of the collector load, R_L.

The base bias current, I_B, is very nearly E_B/R_b. The input (rms) ac component of the base current, I_b, is very nearly E_g/R_b.

* Received by the IRE, July 8, 1957

In the collector circuit, however, the (rms) ac component of the collector current, I_c, is very nearly V_{ce}/R_L, since the ac voltage across the capacitor, C_1, is negligibly small. The quiescent collector current, I_C, is measured directly by the dc ammeter, A. If the transistor parameters are to be maintained constant while R_L is varied, I_C should be kept constant by properly adjusting the potentiometer.

It can be shown that if the input signal is small enough for linear operation, at low frequencies the current gain, A_i, is given by

$$A_i = \frac{r_e - \alpha_0 r_c}{r_e + r_c(1-\alpha_0) + R_L} \cong \frac{-\alpha_0 r_c}{R_L + r_c(1-\alpha_0)}$$

from which it follows that

$$\left|\frac{1}{A_i}\right| = \frac{1-\alpha_0}{\alpha_0} + \frac{1}{\alpha_0 r_c} R_L = \frac{|I_b|}{|I_c|}. \qquad (1)$$

Both I_b and I_c can be computed once $|E_g|$, $|V_{ce}|$, R_b, and R_L are known.

If R_L is varied and the transistor parameters are held constant as indicated above, according to (1), a plot of $|1/A_i|$ vs R_L gives a straight line whose slope and y intercept are, respectively, $1/\alpha_0 r_c$ and $(1-\alpha_0)/\alpha_0$. Hence, the parameters r_c and α_0 can be calculated.

From the graph of Fig. 2, it is found that for the given transistor $\alpha_0 = 0.9922$ and $r_c = 1.136 \times 10^6$ ohms.

It can be shown that the magnitude of α_{0fe}, the low-frequency short-circuit current gain of the common-emitter transistor amplifier, is $\alpha_0/(1-\alpha_0)$. Hence, $|\alpha_{0fe}|$ is the inverse of the y intercept of the graph of Fig. 2. For the transistor used here, $|\alpha_{0fe}| = 128.2$.

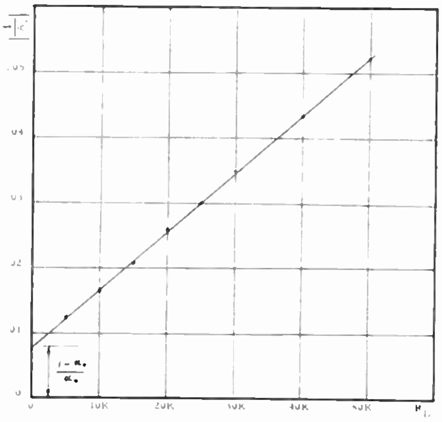

Fig. 2—A plot of $|1/A_i|$ vs R_L at 1000 cps for a p-n-p transistor (GE 2N192) with $I_B = 20$ µa, and $I_C = -2.5$ ma.

To improve further the accuracy of measurement, the voltage V_{ce} and E_g can be compared by a precision attenuator rather than by measuring their absolute values. Moreover, since a relatively large increment of the quiescent collector-to-emitter voltage corresponds to a much smaller relative increment of the quiescent collector current, maintaining the transistor parameters constant can be more accurately achieved by means of a dc voltmeter across C and E rather than by the dc ammeter, A.

M. A. Melehy
Elec. Eng. Dept.
Michigan State University
East Lansing, Mich.

A Further Note on Differentiability of Autocorrelation Functions*

In a recent communication appearing in this journal, Brennan[1] has given conditions under which an autocorrelation function of a stationary process is differentiable at the origin. It was shown that any one of the following three conditions is sufficient to insure differentiability:

1) $f(t)$ satisfies a uniform Lipschitz condition of order $p > \frac{1}{2}$.
2) $f(t)$ is uniformly differentiable and has a finite mean square derivative $\langle (f')^2 \rangle$.
3) $f(t)$ is uniformly differentiable and the limit $\langle ff' \rangle$ exists and is equal to zero.

Here $\langle\ \rangle$ denotes a time average. The autocorrelation $\rho(\tau)$ of f is defined in terms of this time average.

If time and ensemble averages are equal, differentiability of the autocorrelation is assured under conditions much weaker than the above. Let the prefix E denote ensemble average or expectation. Then we have: $\rho(\tau)$ is twice differentiable only if there exists a random process $f'(t)$ such that given any $\epsilon > 0$ there is a $\delta > 0$ for which

$$E\left\{\left|\frac{f(t+h)-f(t)}{h} - f'(t)\right|^2\right\} < \epsilon \qquad (1)$$

whenever $|h| < \delta$. If (1) holds, there also follows

$$E(ff') = \langle ff' \rangle = \frac{d}{d\tau}\rho(\tau)\Big|_{\tau=0} = 0 \qquad (2)$$

and also

$$E[f'(t)f'(t+\tau)] = \frac{d^2}{d\tau^2}\rho(\tau). \qquad (3)$$

The above theorem is a standard result in probability theory[2] and will not be proved here.

To show that (1) is weaker than the uniform convergence required by Brennan, we note that the stationarity of $f(t)$ implies that if (1) holds for any t, it holds for all t. Furthermore, convergence in the ordinary sense implies (1) but not conversely.

It does not appear that Brennan's condition one can be sharpened readily. However, a partial converse of condition one is that if (1) holds, there is a modified Lipschitz condition of the form

$$E\{|f(t+\tau) - f(t)|\} = o(|\tau|^p) \qquad (4)$$

for sufficiently small τ and all $0 \leq p < 1$ independently of t. The proof of (4) is a result of Schwarz inequality and the finiteness of $E\{|f'(t)|^2\}$.

F. J. Beutler
Dept. of Aeronautical Eng.
University of Michigan
Ann Arbor, Mich.

* Received by the IRE, August 5, 1957.

[1] D. G. Brennan, "Smooth random functions need not have smooth correlation functions," Proc. IRE, vol. 45, pp. 1016–1017; July, 1957.

[2] A proof may be found in Loeve, "Probability Theory," D. Van Nostrand Co., Inc., New York, N. Y., pp. 470–471; 1955.

An Improved Operational Amplifier*

The recent proposal suggested by Mr. Nitzberg in these columns[1] for the use of low-gain amplifiers to perform mathematical operations appears to overlook the implications of the use of positive feedback. In fact "adjustment of the parameters of the circuit to perform exactly the required mathematical operations" calls for the use of a feedback amplifier of infinite external gain [Z_a, Z_b, k_2 in Fig. 2 of Mr. Nitzberg's note, with $Z_b = Z_a(k_2 - 1)$]; this is, therefore, impracticable. Although static accuracy may be improved through an increase in loop gain, this need not be so for dynamic accuracy.[2] In fact no improvement would result for adders, whereas integrator performance may improve, subject to consideration of input-signal frequencies. Instability problems are not avoided or simplified by the proposed scheme.

If positive feedback is used it will, in general, be good to avoid it around the last stage of the amplifier because of output impedance requirements. Finally, positive feedback in operational amplifiers has been in use for many years, the best example known to me being the Boeing analog computer.

Amos Nathan
Technion, Israel Institute of Technology,
Haifa, Israel

* Received by the IRE, July 25, 1957.

[1] R. Nitzberg, "An improved operational amplifier," Proc. IRE, vol. 45, p. 880; June, 1957.

[2] A Nathan, "Dynamic accuracy as a design criterion of linear electronic differential analyzers," IRE Trans., vol. EC-2, pp. 74–86; June, 1957.

The Junction Transistor as a Charge Controlled Device*

Explanations of transistor action in most publications hitherto have centered around the basic concept of the transistor being a current controlled current source. It is the purpose of this note to emphasize the fact that such an explanation essentially is valid only for the equilibrium conditions obtained during dc or low-frequency operation and that a more fundamental description, as well as a more powerful one, involves a description in terms of *charge* control.

It is well known, of course, that for a current to flow between emitter and collector in a junction transistor, a density gradient of minority carriers must exist in the base region (see Fig. 1) and that a corresponding number of majority carriers must also exist there (in excess of the equilibrium number of impurity carriers) in order to maintain space charge neutrality. For transistors in which the current gain approaches unity, the relationship between this base charge Q_B and the gradient of this charge from emitter to collector is almost linear and since the emitter-collector current is proportional to the charge gradient, the ratio Q_B/I_E which has the dimensions of a time constant, but is conveniently expressed in pico-coulombs per microamp, is a fundamental parameter of a transistor.

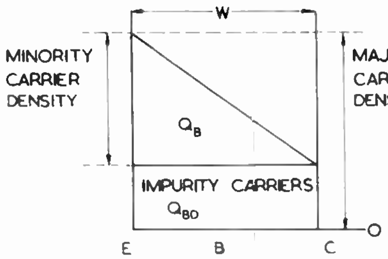

Fig. 1—Charge distribution in the base region.

* Received by the IRE, August 13, 1957.

Evidently, since narrow base regions permit a particular gradient to be set up with a smaller total base charge, it is to be expected that Q_B/I_E is a function of base width and hence of cutoff frequency. Indeed, it can be shown that when base width W is very small compared with the minority carrier diffusion length L and when emitter efficiency γ is equal to one:

$$Q_B/I_E = W^2 I_E/2D \qquad (1)$$

where D is the minority carrier diffusion constant.

Moreover, since for

$$W \ll L,\ \omega_N = 2.43D/W^2 \qquad (2)$$

$$Q_B/I_E = 1.215/\omega_N \qquad (3)$$

where ω_N is the common base current gain angular cutoff frequency. It can readily be shown that (3) [although not (1) and (2)] is valid to within about 2 per cent even for $W=L$.

If, however, $\gamma<1$ and W is not very much less than L, two time constants must be defined which have the values shown in (4) and (5).

Emitter-time constant

$$T_E = Q_B/I_E = 1.215\gamma/\omega_N. \qquad (4)$$

Collector-time constant

$$T_C = Q_B/I_C = 1.215/\beta\omega_N, \qquad (5)$$

where β is the emitter-to-collector minority carrier transport factor.

It is of interest that (4) and (5) offer a method of measuring (somewhat inaccurately) β and γ separately, a separation which cannot be achieved when currents only are measured. Furthermore, it may be noted that T_C is independent of emitter efficiency so that even at current levels at which γ decreases[1] the base charge control of I_C remains linear.

An "ideal" transistor now may be described. It is one in which both β and γ are unity (*i.e.*, no minority carrier recombination either in the base or the emitter) and in which the extrinsic base resistance is zero. Such a transistor could be "turned on" by a lossless injection of Q_B into the base region (by discharging a capacitor into it) and a steady emitter-collector current would then flow until the base charge was removed. It is this process which constitutes the fundamental operation of the transistor. Such an ideal transistor would draw no base current and base current control of the transistor output current would not be possible. Indeed it is only as a result of "imperfections" in the transistor that current control becomes a practical possibility. Nevertheless recombination does occur and it becomes necessary to supply a steady current to the base region in order to maintain the level of Q_B. A third time constant therefore becomes of significance, namely:

Base-time constant

$$T_B = \frac{Q_B}{I_B} = \frac{1.215\gamma}{\omega_N(1-\alpha_N)}, \qquad (6)$$

[1] W. M. Webster, "On the variation of junction transistor current amplification factor with emitter current," PROC. IRE, vol. 42, pp. 914–921; June, 1954.

where $\alpha_N=\beta\gamma$. [The collector cutoff current has been neglected in (5) and (6) for simplicity.]

The measurement of these time constants can be achieved readily by driving the transistor from a square wave generator through a parallel resistance capacitance network and adjusting the resistance and capacitance for square wave current output. For example, if the transistor is in the common emitter connection and the drive is applied to the base then T_B is equal to the time constant of the driving network.

An equivalent circuit representation of the transistor in its basic form (neglecting I_{CO} again) is shown in Fig. 2. S_B represents

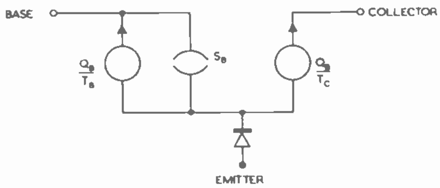

Fig. 2—Ideal large signal equivalent circuit.

the "base charge store" and is analogous to an infinite capacitance in that for a finite charge upon it no voltage appears across it.

If the transistor is driven from the constant current source I_B, say, this current has not only to provide the recombination current and the emitter majority carrier current but also the majority carriers, comprising Q_B (the minority carriers comprising Q_B enter through the emitter). Evidently, while Q_B is being set up to its equilibrium value, I_B/I_C is greater than its normal value of $(1-\alpha_N)/\alpha_N$, and linear current control of the output current is lost. During this period the behavior can be expressed as follows:

$$I_B = \frac{q_B}{T_B} + \frac{dq_B}{dt} \qquad (7)$$

where q_B is the instantaneous charge on the base store.

Since also

$$I_C = \frac{q_B}{T_C}, \qquad (8)$$

(7) can be solved for the rise time t_0, required for the collector current, starting from zero to reach, say, 90 per cent of its final value I_{C1}.

Thus

$$t_0 = T_B \ln\left[I_B T_B/(I_B T_B - 0.9 I_{C1} T_C)\right]. \quad (9)$$

This rise time has been evaluated by Ebers and Moll,[2] starting from somewhat different premises, and substitution from (5) and (6) in (9) leads directly to (40) of Ebers and Moll with the exception of the numerical factor 1.215.

Expressions can be derived similarly for the rise time or fall time in the common base and common collector configurations of the transistor and also for the storage time of the transistor operating in the saturation region. For the latter case a saturation time constant T_S is required and can readily be evaluated (and measured), thus

[2] J. J. Ebers and J. L. Moll, "Large signal behavior of junction transistors," PROC. IRE, vol. 42, pp. 1761–1772; December, 1954.

$$T_S = \frac{Q_{BS}}{I_{BS}} = \frac{1.215(1/\omega_{NO} + 1/\omega_{IO})}{1 - \alpha_{NO}\cdot\alpha_{IO}} \qquad (10)$$

where Q_{BS} is the base charge in excess of Q_B, and Q_B here is the base charge corresponding to the "just bottomed" state of the transistor. I_{BS} is the base current in excess of Q_B/T_B.

ω_{NO} and ω_{IO} are the current gain angular cutoff frequencies in the normal and inverse connections of the transistor, and α_{NO} and α_{IO} are the corresponding values of the dc or low-frequency current gain. The suffix zero indicates that the values of the last four parameters refer to the condition in which the collector-base voltage is approximately zero. [This qualification can be of importance. It was not emphasized by Ebers and Moll, in connection with their (42) to (44)].

If, as is normal, the collector-base voltage falls during turn-on, the collector depletion layer is reduced in thickness and the effective base width is increased. This, of course, accounts for the difference between cutoff frequency values at different collector voltages, but it also implies that a larger base charge must be injected in order to set up the charge gradient corresponding to the required collector current. The extra charge involved is illustrated by the shaded areas in Fig. 3. It will be noticed that it is necessary

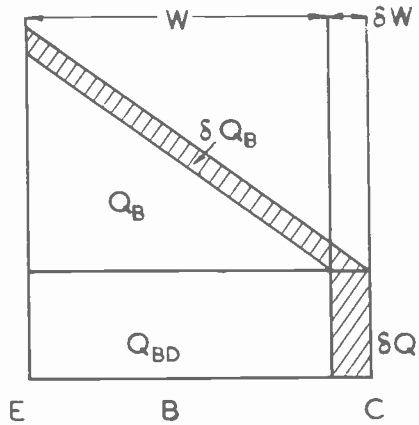

Fig. 3—Change in base charge arising from a change of collector-base voltage.

not only to inject a larger control charge Q_B but also to inject majority carriers to neutralize the impurity centers which have emerged from the collector depletion layer during turn-on. These two additional charges are labeled respectively, δQ_B and δQ_{BD}, and can be associated with the discharge of the collector storage and depletion layer capacitances; their presence increases the effective values of the time constants.

By considering small increments of voltage and charge the characteristic small signal equations can be set up readily from which the element values of either the hybrid-π equivalent circuit proposed by Giacoletto[3] or the equivalent T circuit proposed by Early[4] can be derived.

[3] L. J. Giacoletto, "A study of p-n-p alloy junction transistors from dc through medium frequencies," *RCA Rev.*, vol. 15, pp. 506–562; December, 1954.

[4] J. M. Early, "Effect of space charge layer widening in junction transistors," PROC. IRE, vol. 40, pp. 1401–1406; November, 1952.

It can be seen from the foregoing that the charge control concept provides a relatively simple means of relating the small and large signal response of the transistor. The time constants T_B, T_C, and T_S are particularly simple to evaluate experimentally and offer a convenient alternative to the measurement of current gain and cutoff frequency. Indeed, in our view the description of the transistor in terms of charge control is not only useful but is in fact the fundamental description of transistor action. In view of this, a fully analysis of the problem of charge control has been written.[5]

J. J. Sparkes
and R. Beaufoy
British Telecomm. Research Ltd.
Taplow, Berks, England

[5] R. Beaufoy and J. J. Sparkes, "The junction transistor as a charge controlled device," *ATE J.*, pp. 310–327; October, 1957.

FM Noise Spectra*

While the writer was investigating fm noise in cw magnetrons, there appeared correspondence[1] from Mullen and Middleton on this and related subjects. The purposes of the present letter are: 1) to point out that the principal result presented by them (the need for a correction to the previously published form[2] for the tails of the fm noise spectrum) can also be obtained by a simpler, albeit less elegant, calculation; 2) to give some details of interest not included explicitly by Mullen and Middleton; and 3) to comment on a crude but useful "quasistatic" model for the type of wave studied.

Consider a sinusoidal wave $v(t)$ of amplitude A_0 and mean (angular) frequency ω_0 which is corrupted in frequency by a stationary, Gaussian, random wave $v_n(t)$ according to the relation

$$\omega(t) = \omega_0 + D_0 v_n(t). \qquad (1)$$

Let $W_n(\omega')$, the power-density spectrum (pds) of $v_n(t)$, be practically independent of $|\omega'|$ from zero to a frequency far in excess of $D_0{}^2W_n(0)$ and then decrease monotonically to zero before $|\omega'|$ reaches, say, $\omega_0/10$. We thus study "low-index" noise of the type treated by Stewart,[2] not that discussed by Medhurst.[3] Although by elementary methods (see below) one can estimate the pds of $v(t)$, a careful treatment[4] employs the Wiener-Khintchine relation between spectra and correlation functions. The pds of $v(t)$ is found to be

$$W(\omega) = (2/\pi)\int_0^\infty R(t')\cos\omega t' dt', \qquad (2)$$

where $R(t')$ is the autocorrelation function (acf) of $v(t)$, given in terms of $W_n(\omega')$ by

$$R(t') = (A_0{}^2/2)\cos\omega_0 t' \cdot \exp\left\{\int_{-\infty}^{\infty}(1/\omega'^2)D_0{}^2W_n(\omega')\cdot[\cos(\omega' t') - 1]d\omega'\right\}. \qquad (3)$$

For convenience, we let the argument of $W_n(\omega')$ take on negative values as well as positive ones but restrict the arguments of $R(t')$ and $W(\omega)$ to nonnegative values.

As a simple example, consider the "rectangular" modulating spectrum, in which $W_n(\omega')$ equals W_{n0} for $|\omega'| < \omega_M$ and is zero elsewhere, with $\omega_M \gg D_0{}^2W_{n0}$. Use of the apparently excellent approximation

$$R(t') = (A_0{}^2/2)\cos\omega_0 t' \exp(-\pi D_0{}^2W_{n0}t') \qquad (4)$$

leads readily to the result[2]

$$W(\omega) = \frac{(A_0{}^2/2)D_0{}^2W_{n0}}{(\pi D_0{}^2W_{n0})^2 + k^2}, \qquad (5)$$

where $k = \omega - \omega_0$. Since the difference between (5) and the exact result can easily be shown to be very small compared to $W(0)$, a better approximation need be made only for the tails of the spectrum of $v(t)$. It is recommended by Mullen and Middleton that further approximations to $W(\omega)$ be made by their (1b), an expression for $R(t')$ in terms of the acf of $v_n(t)$ rather than in terms of its pds. It seems worth mentioning here that a good approximation can also be obtained by a calculation based on (3). The analysis is straightforward once a well-hidden (to this writer) mathematical pitfall is sidestepped. Combination of (2) and (3) and neglect of the term involving the rapidly oscillating factor $\cos(\omega+\omega_0)t'$ lead to the relation

$$W(\omega) = (A_0{}^2/2\pi)\int_0^\infty \cos kt' J(t')dt', \qquad (6)$$

where $J(t')$, the exponential in (3), decreases slowly and monotonically from unity at $t'=0$ to zero. The cosine term in (6) oscillates rapidly when k is appreciable. Then the contribution to $W(\omega)$ made by a positive lobe of the oscillating integrand is almost exactly cancelled by the succeeding negative lobe, and the value of the integral is very small. More important, it is highly sensitive to the slope of the slowly varying function $J(t')$ at and near its maximum. A serious error thus arises when the accurate $J(t')$ is replaced by the exponential in (4), for their slopes at $t'=0$ are not the same. (One wonders whether similar errors have been made by other workers in other problems.) It is found that a better approximation than (5) is that $W(\omega)$ is given by (5) for $|k| < \omega_M$ and is zero elsewhere.

For a general $W_n(\omega')$ (subject to the restrictions stated in the second paragraph), one obtains by an approximation similar to (4) an estimate good for ω close to ω_0:

$$W(\omega) \approx \frac{(A_0{}^2/2)D_0{}^2W_n(0)}{[\pi D_0{}^2W_n(0)]^2 + k^2}. \qquad (7)$$

To calculate the tails of the spectrum, one integrates (6) twice by parts to arrive at

$$W(\omega) = (A_0{}^2D_0{}^2/k^2)(I_1 - I_2), \qquad (8)$$

where

$$I_1 = (1/2\pi)\int_0^\infty \cos kt' J(t')\cdot\left[\int_{-\infty}^{\infty}W_n(\omega')\cos\omega' t' d\omega'\right]dt' \qquad (9)$$

and

$$I_2 = (D_0{}^2/2\pi)\int_0^\infty \cos kt' J(t')\cdot\left[\int_{-\infty}^{\infty}W_n(\omega')(1/\omega')\sin\omega' t' d\omega'\right]^2 dt'. \qquad (10)$$

One can show that, except for small $|k|$, the contribution of I_2 can be ignored at any value of k for which $W_n(\omega')$ is not negligible with respect to $W_n(0)$; specifically,

$$|I_2(k)/I_1(k)| < [W_n(0)/W_n(k)][\pi D_0{}^2W_n(0)/|k|]. \qquad (11)$$

Since in (9) the integral over ω' decays much more rapidly with t' than does $J(t')$, one may set $J(t')=1$ for all t' without introducing appreciable error in the integrand or in the slope of the monotonic portion of the integrand near its maximum. Then comparison of I_1 with the Fourier-integral identity yields the important result

$$W(\omega) \approx (A_0{}^2/2)D_0{}^2W_n(k)/k^2, \quad |k| \gg D_0{}^2W_n(0). \qquad (12)$$

Eqs. (7) and (12) may be combined in the form, valid for all k,

$$W(\omega) = r(k)\frac{(A_0{}^2/2)D_0{}^2W_n(0)}{[\pi D_0{}^2W_n(0)]^2 + k^2}, \qquad (13)$$

where $r(k) \approx W_n(k)/W_n(0)$.

A further calculation of interest may be made if the modulating spectrum is rectangular. Evaluation of I_1, with the help of a transformation from t' to the sine integral of $\omega_M t'$, shows that the discontinuity in $W_n(\omega')$ is rounded off in $W(\omega)$ to an extent dependent on the bandwidth of the spectrum of the modulated wave. Specifically,

$$|dr(k)/dk| \approx (\pi^2D_0{}^2W_{n0})^{-1}, \quad |k| = \omega_M. \qquad (14)$$

This function $r(k)$ behaves much as does the Fermi-Dirac probability function $[1+\exp(E-E_m)/kT]^{-1}$, the bandwidth $D_0{}^2W_{n0}$ playing the same role as T.

Some important properties of a noisy wave of the type discussed above are indicated by a simple "quasistatic" model of the wave. Although it is quite unlikely that this model is original with the writer, it has evidently not appeared in the literature. Despite its limitations, such as the absence of explicit information concerning phase correlation, it seems worth comment.

* Received by the IRE, August 26, 1957. The study leading to this letter was begun under the sponsorship of the General Electric Co. and has been continued under the sponsorship of the Wright Air Development Center.

[1] J. A. Mullen and D. Middleton, "Limiting forms of fm noise spectra," Proc. IRE, vol. 45, pp. 874–877; June, 1957.

[2] J. L. Stewart, "The power spectrum of a carrier frequency modulated by Gaussian noise," Proc. IRE, vol. 42, pp. 1539–1542; October, 1954.

[3] R. G. Medhurst, "RF bandwidth of frequency-division multiplex systems using frequency modulation," Proc IRE, vol. 44, pp. 189–199; February, 1956.

[4] D. Middleton, "The distribution of energy in randomly modulated waves," *Phil. Mag.*, ser. 7, vol. 62, pp. 689–707; 1951.

Consider first a carrier subjected to sinusoidal fm at high modulation index (low rate of frequency deviation, relatively high deviation). It can be represented by the sum of a carrier (much reduced in amplitude) and many sidebands, or it can be considered simply as a carrier whose frequency varies slowly with time. If the carrier is now also subjected to low-index fm by a sinusoid of high frequency, ω_m, the wave can still be represented completely in terms of a carrier and sidebands. The relatively large sidebands near the carrier remain, and "small-scale models" of the group close to the carrier appear near $\omega = \omega_0 \pm \omega_m$. Higher-order spectra are present, but they can usually be ignored. Alternatively, one can think of the wave as a carrier of slowly varying frequency plus a pair of small antisymmetric sidebands which vary slowly in frequency so as to remain just ω_m from the carrier. Modulation in amplitude at the rate ω_m can be represented by symmetric sidebands whose frequencies vary similarly.

It is possible to use a similar quasistatic description of the wave if more than one slow, high-index modulation and/or more than one fast, low-index modulation are present; and the idea may be extended to fm and AM arising from a combination of "low-frequency" and "high-frequency" noise. The frequency of the carrier of such a noisy wave fluctuates slowly in a relatively narrow frequency band centered at ω_0; it is accompanied by a continuous sideband distribution which shifts slowly in frequency to keep in step with the carrier. Elementary fm theory indicates that the power in an fm-noise sideband separated from the carrier by ω_m is proportional to $\omega_m^{-2} W_n(\omega_m)$, where $W_n(\omega')$ is the pds of the process causing fm noise. These crude ideas thus lead to the correct form (12) for the tails of the pds of the modulated wave.

It also follows from this model that a discontinuity in $W_n(\omega')$ such as that at the outer edge of the rectangular modulating spectrum will not give rise to a discontinuity in $W(\omega)$, for the sidebands corresponding to ω_M fluctuate in frequency about $\omega_0 \pm \omega_M$. The degree of smoothing depends on the extent of the fluctuations of the carrier frequency about ω_0. This prediction is consistent with (14), which shows that the smoothing of the discontinuity increases with the half-power bandwidth of the spectrum $W(\omega)$.

Because the spectrum of the random process causing fm of the carrier is continuous from zero to a high frequency, there is no natural demarcation between low- and high-frequency modulating terms. A "separation" frequency, ω_s, must be chosen rather arbitrarily. In order that the amplitude of the quasistatic carrier be practically the same as that of the unmodulated carrier, ω_s should be chosen high enough that practically all of the energy of the pds (13) lies in the range $\omega_0 - \omega_s < \omega < \omega_0 + \omega_s$. On the other hand, in order that little error be introduced by treating the slow fluctuations in a quasistatic manner, ω_s should be small compared to the bandwidths of all of the circuit elements involved.

A mathematical representation of the noisy wave which is convenient for the calculation of such effects as the conversion of fm to AM by frequency-dependent circuit elements is

$$
\begin{aligned}
i(t) = \operatorname{Im} \Big\{ & A_0 \exp(j\phi_q(t)) \\
& \cdot \Big\{ 1 + \int_0^{\omega_s} A(\omega') \big[\exp j(\omega' t + \theta_a(\omega')) \\
& + \exp j(-\omega' t - \theta_a(\omega')) \big] d\omega' \\
& + \int_{\omega_s}^{\infty} \exp(j\omega' t) \big[A(\omega') \exp(j\theta_a(\omega')) \\
& + (1/\omega') D_0 F(\omega') \exp(j\theta_f(\omega')) \big] d\omega' \\
& + \int_{\omega_s}^{\infty} \exp(-j\omega' t) \big[A(\omega') \\
& \exp(-j\theta_a(\omega')) - (1/\omega') D_0 F(\omega') \\
& \exp(-j\theta_f(\omega')) \big] d\omega' \Big\} \Big\}.
\end{aligned} \tag{15}
$$

Here $A(\omega')$ and $F(\omega')$ are proportional to the square roots of the pds of the processes causing AM and fm, respectively. The phases $\theta_a(\omega')$ and $\theta_f(\omega')$ may be thought of as varying randomly in time; correlation between AM and fm exists if some values of $\theta_a(\omega') - \theta_f(\omega')$ occur more often than others. The low-frequency components of fm cause the random phase $\phi_q(t)$ to fluctuate relatively slowly about $\omega_0 t$. One can also include in $\phi_q(t)$ the effect of nonrandom fm such as that caused by power-supply ripple or by mechanical vibrations. In general, a quasistatic model such as (15) seems useful as a semiquantitative representation of a wave in which the low-frequency portion of the modulating spectrum is unpleasantly complicated. Thus it is complementary in a way to the exact analysis based on the idealization that the modulating spectrum is flat to zero frequency.

Roy C. Ward
Ohio State University
Columbus, Ohio

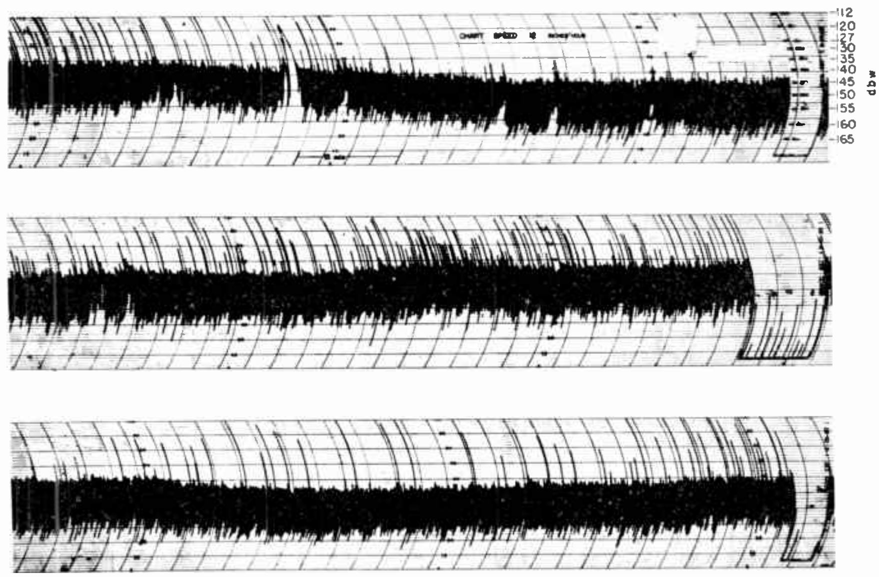

Fig. 1.

UHF Forward Scatter from Lightning Strokes*

Examination of records obtained by monitoring a 400-mile distant 915-mc transmitter has disclosed an apparent close correlation between a form of anomalous propagation and the occurrence of thunderstorms near the midpoint of the propagation path. This type of propagation is characterized by short duration "spikes" rising from the median signal level to power levels two to three orders of magnitude (20–30 db) above the median level. Fig. 1 (above) is an example of such propagation. Similar spike-like signals are received during the transmitter bi-hourly silence period, but the amplitude received during these periods is from 30 to 40 db less than the amplitudes obtained when the transmitter is on. Correlation between this type of signal and thunderstorm activity is obtained only with thunderstorms near the midpoint of the propagation path. The behavior of the spike amplitudes and the lack of correlation with local thunderstorms indicate that this phenomenon is distinct from the "sferics" recorded by Hay and Hartz[1] at 492 mc. It is suggested that our records when examined in the light of back scatter data obtained by Marshall,[2] Ligda,[3] and others, offer evidence of forward scattering from ionized regions caused by cloud-to-cloud discharges.

L. H. Bauer
and W. A. Flood
Applied Physics Dept.
Cornell Aeronautical Lab., Inc.
Buffalo, N. Y.

* Received by the IRE, August 20, 1957. This work was carried out under Contract AF19(604)-1835 with Air Force Cambridge Res. Center.

[1] D. R. Hay, and T. R. Hartz, "Thunderstorm signals at very high and ultra high frequency," *Nature*, vol. 175, pp. 949–950; May 28, 1955.

[2] J. S. Marshall, "Frontal precipitation and lightning observed by radar," *Can. J. Phys.*, vol. 31, pp. 194–203; February, 1953.

[3] M. G. H. Ligda, "The radar observation of lightning," *J. Atmos. Terr. Phys.*, vol. 9, pp. 329–346; November, 1956.

A Proposed Technique for the Improvement of Range Determination with Noise Radar*

In certain radar systems continuous wide-band noise signals are transmitted and target-range determination is made by cross correlating the returned signal with a delayed duplicate of the transmitted signal. The target range corresponds to the delay time giving the maximum in the resulting cross correlation. For white noise the cross correlation is of the form of a delta function and the maximum is easily located. In practice, however, a white power spectrum is inconvenient even to approximate since it requires occupying the entire radio band. It is possible to use a rectangular power spectrum in order to avoid this, but this has the disadvantage of producing a cross correlation function with many local maxima which, in the presence of interfering signals especially, may be difficult to distinguish from the absolute maximum. This may be shown as follows.

If the transmitted signal is $f(t)$, its power spectrum $\Phi(\omega)$, its total power P, and its autocorrelation function $R(\tau)$, then from the Wiener-Khintchine relation

$$R(\tau) = \int_0^\infty \Phi(\omega) \cos \omega\tau d\tau \qquad (1)$$

we can determine the autocorrelation[1] function of a signal which has the rectangular power spectrum

$$\Phi(\omega) \begin{cases} P/(\omega_2 - \omega_1) & \omega_1 \le \omega \le \omega_2 \\ 0 & \text{otherwise} \end{cases} \qquad (2)$$

to be given by the expression

$$R(\tau) = \frac{P}{\omega_2 - \omega_1} \frac{(\sin \omega_2\tau - \sin \omega_1\tau)}{\tau} \qquad (3)$$

whose near periodicity over short intervals in τ for large ω_2 and ω_1 produces the ambiguity described.

In the problem of making a target-range determination by the use of the correlation function between transmitted and received signals we are interested in knowing the probability of the true delay being at a particular point under the correlation curve. Woodward[2] has described how, for Gaussian signals with equivalent temperature T, the probability density of the true delay lying between τ and $\tau + d\tau$ is proportional to

$$\exp \frac{2}{kT} R(\tau - \tau_0) \qquad (4)$$

where τ_0 is the delay in the comparison signal and $R(\tau - \tau_0)$ is the cross correlation between the received and delayed signals. (Here it is assumed that we have no prior knowledge of the likelihood of various target distances.) It can be shown that this probability distribution represents *all* the information available about the probable location of the true delay. Thus, although this curve cannot be improved upon as a source of information about target distance, in practice one must finally choose a single value of τ as that corresponding to the true delay, rightly or wrongly. For this reason it would seem justifiable to use any method to reduce the ambiguity inherent in the correlation function alone. The following[3] is such a method.

We choose a bell-shaped power spectrum of the form[4]

$$\Phi(\omega) = \frac{P\beta/\pi}{\beta^2 + (\omega - \omega_0)^2} \qquad (5)$$

where P is the total power as before, ω_0 is the pulsatance at maximum power density, and β is the distance on either side of ω_0 to the half power-density point. Using (1) we obtain the correlation function

$$R(\tau) = P \cos \omega_0\tau e^{-\beta|\tau|}. \qquad (6)$$

This curve, because of the appearance of the absolute value in it, is concave upward near the origin for both positive and negative values of τ. At the origin it has a sharp apex which corresponds to a discontinuity in the first derivative of $R(\tau)$. It is this feature which can be used to advantage in locating the origin of $R(\tau)$ where its absolute maximum occurs. This is so because at the origin there is infinite curvature or *buckle* which may be exhibited as a delta function singularity in the second derivative. We take the second derivative of $R(\tau)$ with the aid of the relation

$$\frac{d|\tau|}{d\tau} = 2U(\tau) - 1 \qquad (7)$$

where $U(\tau)$ is the unit step function whose additional properties we use.

$$\frac{dU(\tau)}{d\tau} = \delta(\tau) \quad \text{and} \quad U^2(\tau) = U(\tau). \qquad (8)$$

The result is

$$R''(\tau) = (\beta^2 - \omega_0^2) \cos \omega_0\tau e^{-\beta|\tau|} - 2\beta\delta(\tau). \quad (9)$$

The delta function peak can be used to locate the origin providing the derivatives of $R(\tau)$ can be conveniently obtained. Since, in most practices known to the writer, $R(\tau)$ is presented as a spatial variation of light intensity, the differentiation would seem to call for optical means. Fortunately, however, the fact that it is formed by the integration

$$R(\tau - \tau_0) = \frac{1}{2T} \int_{-T}^{T} f(t - \tau) f(t - \tau_0) dt \quad (10)$$

we may form the second derivative by first differentiating the delayed comparison signal $f(t - \tau_0)$ with respect to time in view of the relation

$$R''(\tau - \tau_0) = \frac{1}{2T} \int_{-T}^{T} f(t - \tau) f''(t - \tau_0) dt. \quad (11)$$

Thus, given a bell-shaped power spectrum for the signal (or a truncated approximation thereto) we can obtain a sharp maximum in the resulting cross correlation function by interposing a double differentiation circuit between the delay line and the correlator as shown in Fig. 1.

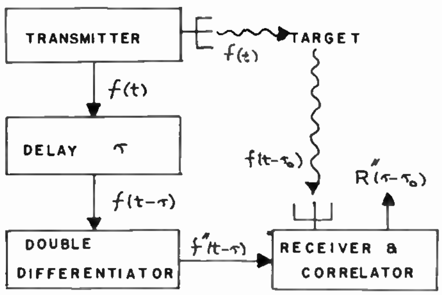

Fig. 1.

Richard Bourret
University of Miami
Coral Gables, Fla.

* Received by the IRE, September 5, 1957.

[1] It is permissible here to speak of the autocorrelation and cross correlation almost interchangeably since, neglecting target filtering action, they are of the same form.

[2] P. M. Woodward, "Probability and Information Theory, With Applications to Radar," McGraw-Hill Book Co., Inc., New York, N. Y.; 1955.

[3] A similar procedure was recently described by A. E. Martin as a means for improving the resolution of spectral lines. See: "Difference and derivative spectra," *Nature*, vol. 180, pp. 231–233; August 3, 1957.

[4] More accurately

$$\Phi(\omega) = \frac{P\beta/\pi}{\beta^2 + (\omega - \omega_0)^2} + \frac{P\beta/\pi}{\beta^2 + (\omega + \omega_0)^2}$$

since this does not change the physical meaning and the power spectrum must be symmetric on account of its definition.

Serendipity

From time to time, serendipity is mentioned in these columns. Without backing this as a method of research, I would like to comment on the origin of the word for it. *Webster's New International Dictionary* of 1952 describes it as: "The gift of finding valuable or agreeable things not sought for, a word coined by Walpole in allusion to a tale *The Three Princes of Serendip* who in their travel were always discovering, by chance or sagacity, things they did not seek."

Now I note in Edward Gibbon, *The Decline and Fall of the Roman Empire*, ch. XXIV (about Julian, A.D. 361) the following passage and footnote: "The ambassadors of the East, from the continent of India and the isle of Ceylon,[6] had respectfully saluted the Roman people . . . " and footnote 6: "Inde nationibus Indicis certatim cum donis optimates mittentibus . . . ab usque Divis et Serendivis. Ammian XXII, 7. This island to which the names of Taprobana, Serendib, and Ceylon have been successively applied, manifests how imperfectly the seas and lands to the East of Cape Comorin were known to the Romans.

"1. Under the reign of Claudius, a freedman who farmed the customs of the Red Sea, was accidentally driven by the winds upon this strange and undiscovered coast: he conversed six months with the natives; and the King of Ceylon, who heard for the first time of the power and justice of Rome, was persuaded to send an embassy to the emperor (Plinius, Hist. Nat. VI, 24).

"2. The geographers (and even Ptolemy) have magnified above 15 times the real size of this new world which they extended as far as the equator, and the neighbourhood of China." [Diva gens or Divorum regio = India East Coast, Ganges to Ceylon.]

I think Walpole (1717–1797)—or the author of that tale—would have read Gibbon's work when it appeared 1776–1788; and I like to think that the footnote 6, with the word and the classical example juxtaposed, suggested the name for the concept.

H. E. Kallmann
New York, N. Y.

Contributors

William Ross Aiken (S'46–A'48–M'55) was born on February 19, 1919, in the Territory of Hawaii. He graduated from the University of California with a degree in electrical engineering and is the inventor of the flat cathode-ray tube. During the war, he supervised electronic activities at the Kaiser Richmond Shipyards, and after the war, he organized the Ross Radio Corp. which specializes in custom-made radios, tv sets, and industrial electronics.

W. R. Aiken

In 1948, Mr. Aiken joined the staff of the University of California Radiation Laboratory, where he developed electronic controls for large nuclear accelerators. In 1951, he participated in a classified project for the Atomic Energy Commission overseas as group leader. Upon his return he assumed charge of the special problems group at the Radiation Laboratory. He has held his present position as Director of Research for the Kaiser Aircraft and Electronics Corp., West Coast Electronics Lab., since 1953.

❖

L. Lorne Campbell (M'56) was born on October 20, 1928, in Winnipeg, Canada. He received the B.Sc. degree in mathematics and physics from the University of Manitoba in 1950. In 1951, he was awarded the M.S. degree in physics from Iowa State College, and in 1955, the Ph.D. degree in mathematics from the University of Toronto. Since 1954, Dr. Campbell has been employed at the Radio Physics Lab., Defence Research Board, Ottawa, Canada.

L. L. Campbell

He is a member of the American Mathematical Society and the Canadian Mathematical Congress.

❖

John S. Cross was born in Birmingham, Ala., on September 18, 1904. In 1923, he received the B.S.E.E. degree from the Alabama Polytechnic Institute, Auburn, Ala.

J. S. Cross

He served in the state highway departments of South Carolina and Michigan, from 1927 to 1930, as assistant resident engineer and survey chief, respectively. Since that time he has worked on a number of government engineering projects. From 1935 to 1941, he was Chief of the Survey, Design, and Road Division in Washington, D. C., for the National Park Service, Dept. of Interior, From 1941 to 1946, he was with the U. S. Navy as a line officer in Naval Communications, attaining the rank of Captain. He is currently the Assistant Chief of the Telecommunications Division of the State Department in charge of technical radio services and maritime and postal services. In this capacity he has served as U. S. delegate to numerous conferences on communications, the most recent being the Maritime VHF Telephone Conference at The Hague in January, 1957.

Mr. Cross is a member of Kappa Alpha and the Washington Society of Engineers.

❖

G. W. L. Davis (M'55) was born in Leigh-on-Sea, England, in 1921.

During the war he was a radar officer on destroyers and aircraft carriers. He then joined Metropolitan Vickers in Manchester, England, working on commercial marine radar and other projects.

G. W. L. Davis

In 1952, Mr. Davis came to Canada and went to work on digital data processing at Ferranti Electric Ltd., in Toronto, Ontario. In 1954, he became project engineer in charge of the JANET development and in 1955, was appointed Chief Engineer of the newly formed Electronics Division.

He is an associate member of the IEE, and a member of the Association of Professional Engineers of the Province of Ontario.

❖

Francis Colt de Wolf was born on October 28, 1894 in Aix-la-Chapelle, Germany. In 1918, he received the A.B. degree from Harvard University, Cambridge, Mass. and the LL.B. degree from Columbia University, New York, N. Y. in 1922.

F. C. de Wolf

He has served as an official to the League of Nations Secretariat in Geneva, Switzerland from 1931 to 1934, and has been with the State Department since 1922 in the treaty and international communications divisions. Since 1944, he has served as Chief of the Telecommunications Division, and in 1941 also, began lectures in international law at George Washington University.

Mr. de Wolf is a member of the American Society of International Law.

Von R. Eshleman (S'48–A'53–SM'55) was born in Darke County, Ohio, on September 17, 1924. After serving three years in the United States Navy, he attended George Washington University, Washington, D. C., where he received the B.E.E. degree in 1949. He received the M.S. and Ph.D. degrees in electrical engineering from Stanford University in 1950 and 1952, respectively. From 1951 to 1952, he held an Atomic Energy Commission Fellowship in the physical sciences. He was appointed research associate in 1952, lecturer in 1956, and assistant professor in 1957, in the Electrical Engineering Department at Stanford University, Stanford, Calif. He also holds the position of Consultant at Boulder Laboratories, National Bureau of Standards, Boulder, Colo., and at the Stanford Research Institute, Menlo Park, Calif.

V. R. Eshleman

Dr. Eshleman is a member of Sigma Tau, Sigma XI, and the U.S.A. Commission III of URSI.

❖

Peter A. Forsyth was born in Prince Albert, Saskatchewan, Canada, on March 20, 1922. He attended the University of Saskatchewan and received the B.A. degree in 1942. He was commissioned in the Canadian Navy in 1941, and from 1942 to 1945, was loaned to the British Navy, during which time he spent two years at the Telecommunications Research Establishment working on the development of airborne radar equipment. He then returned to the University of Saskatchewan where he obtained the M.A. degree in physics in 1947. In 1951, he received the Ph.D. degree from McGill University, Montreal, P. Q., his research being in the field of radio studies of aurora. In the same year he joined the Defence Research Telecommunications Establishment where he has continued his studies of upper atmospheric phenomena, including meteors and aurora. For several years, he has been Head of the Upper Atmospheric Physics section and is now acting superintendent of the Radio Physics Wing.

P. A. Forsyth

Dr. Forsyth is a member of the Canadian Association of Physicists, the Canadian Associate Committee on Geodesy and Geophysics, and the Canadian Commission III of URSI.

S. J. Gladys (S'49–A'51–M'56) was born in Winnipeg, Manitoba, Canada, on July 25, 1917. He served four years with the radar division of the Royal Canadian Air Force. He then was graduated from the University of Western Ontario, London, with the B.S. degree in honor mathematics and physics in 1950.

S. J. GLADYS

Mr. Gladys then joined the Research Division of the Ferranti Electric Ltd., in Toronto, Ontario, where he has been engaged mainly in research and development of data handling systems.

❖

Delos R. Hansen (A'56) was born at Viscount, Saskatchewan, Canada, on August 5, 1920. After a brief period in 1941, as announcer-control operator at CFQC, Saskatoon, he joined the monitoring service of the Department of Transport, where he was employed as a commercial radio operator from 1941 to 1947. Following this, Mr. Hansen joined the staff of the Defence Research Board where he is still employed. His work has been concerned mainly with the development of instrumentation for use in ionospheric research. He has been associated with the JANET meteor-burst communications system development as DRB project officer since 1954.

D. R. HANSEN

❖

Colin O. Hines was born in 1927, in Toronto, Ontario, Canada. He received the B.A. degree in physics and the M.A. degree in applied mathematics from the University of Toronto in 1949 and 1950, respectively. After a year with Defence Research Board of Canada, he continued his post-graduate studies in England, first at the University of Cambridge where he received the Ph.D. degree in mathematics in 1953, and then at the University of London. He returned to the Radio Physics Laboratory of the Defence Research Board in 1954 and has continued his researches there. His investigations have been concerned primarily with the theory of electromagnetic and hydromagnetic wave propagation with particular reference to the ionosphere. His recent work has included studies of the radio signals which are forward-scattered from ionized meteor trails.

C. O. HINES

Dr. Hines is a member of the Canadian Association of Physicists.

Jesse C. James was born in Florence, Ala., on February 29, 1924. He received the Bachelor's degree in electrical engineering in 1945, and the Bachelor's degree in engineering physics in 1946, both from the Alabama Polytechnic Institute, Auburn, Ala.

J. C. JAMES

From 1946 to 1948, he was a research assistant for the Southern Research Institute, Birmingham, Ala. He attended Rice Institute from 1948 to 1950 and received the M.A. degree in physics in 1950. He then was employed as a physicist for the U. S. Navy Mine Defense Lab., Panama City, Fla., and later as an electronic engineer at Redstone Arsenal. In 1952, he was employed by the Engineering Experiment Station at the Georgia Institute of Technology, where he simultaneously began working for the Ph.D. degree in electrical engineering. At Georgia Tech. he has worked on radar systems and meteor-scatter communications; he plans to write his dissertation in meteor-scatter propagation.

Mr. James is a member of Tau Beta Pi and Sigma Xi.

❖

Walter E. Jaye (S'50–A'53) was born in Berlin, Germany on October 21, 1905. He received the B.S. degree in electrical engineering from the University of Rhode Island, Kingston, R. I. in 1951, and the M.S.E.E. degree from Stanford University, Stanford, Calif., in 1952. He worked on upper-atmosphere wind investigations and meteor research equipment design while a research assistant at the Radio Propagation Laboratory of Stanford University. From 1953 to 1956, he was employed as an electronics engineer at Sierra Electronic Corporation. While at Sierra, he worked on rf transformer research, transmitter control circuitry design, and vhf filter design. He also developed an impedance meter for carrier systems. He joined the Stanford Research Institute in 1956, and is presently working on magnetic core memory devices as research engineer for the Special Techniques Group.

W. JAYE

Mr. Jaye is a member of Tau Beta Pi.

❖

Ernest S. Kuh (S'49–A'52) was born on October 2, 1928, in Peiping, China. He received the B.S. degree in electrical engineering from the University of Michigan in 1949, the M.S. degree from the Massachusetts Institute of Technology, Cambridge, Mass., in 1950, and the Ph.D. degree from Stanford University, Stanford, Calif. in 1952.

He then joined the technical staff of Bell Telephone Laboratories, where he engaged in the basic development of networks for the coaxial line and submarine cable systems. He also devoted some time to teaching in the Communication Development Training Program at the Bell Laboratories. In 1956, he joined the Electrical Engineering Department of the University of California at Berkeley and is now Associate Professor.

E. S. KUH

Dr. Kuh is a member of Eta Kappa Nu, Tau Beta Pi, Phi Kappa Phi, and Sigma Xi.

❖

Hiroji Kurokawa (A'51) was born in Tokyo, Japan, on March 10, 1914. He received the B.S. degree in electrical engineering from Tokyo Imperial University in 1937. He was employed by the Nippon Telegraph and Telephone Public Corporation (formerly the Ministry of Communication), in the design and installation of various radio equipments and systems. In 1949, he received the degree of Doctor of Engineering for research on distortion of fm radio relay systems. Thereafter, he was appointed Chief of the Radio and Investigation Section, where he was engaged in the development and installation of Japanese public communications systems. At present, he is Director of the Microwave Division, working on the rapid expansion of the Japanese microwave relay system.

H. KUROKAWA

Dr. Kurokawa is a member of several committees of electrical engineering in Japan.

❖

G. R. Lang (S'46–A'50–M'55) was born on September 17, 1922, in London, Ontario, Canada. He enlisted with the Royal Canadian Corps of Signals in 1939, and served with them in England and the European Theatre from 1940 to 1945. In 1946, he enrolled at the University of Western Ontario, London, Ontario, graduating in 1949, with the B.S. degree in honor mathematics and physics, radio physics option.

G. R. LANG

In 1949, he joined the Research Division of Ferranti Electric Ltd., in Toronto, Ontario, and has remained with this firm.

His special fields are those of communication and information theory and the design of related systems.

Mr. Lang is an associate member of the Institution of Electrical Engineers.

❖

L. M. Luke (S'46–A'49–M'55) was born on June 27, 1922, in Albinston, Ontario, Canada. During World War II, he served three years as a flying instructor with the Royal Canadian Air Force. In 1949, he was awarded the B.S. degree in honor mathematics and physics from the University of Western Ontario, London, Ontario.

L. M. Luke

From 1949 to 1950, he was employed by the Dominion Government on Shoran survey work in the Canadian north. In 1950, Mr. Luke joined the Research Division of Ferranti Electric Ltd., and in 1955, was appointed project engineer of the JANET development group.

❖

M. L. Meeks was born in Gainesville, Ga., in 1923. He received the B.S. degree from the Georgia Institute of Technology Atlanta, Ga., in 1943. He served in the Navy until 1947, and received the Ph.D. degree from Duke University, Durham, N. C., in 1951.

M. L. Meeks

Dr. Meeks has been a member of the faculty at the Georgia Institute of Technology since 1951, on the staffs of the School of Physics and the Engineering Experiment Station. He is now an associate professor of physics, and has worked in the fields of nuclear physics, operations research, and electromagnetic theory.

Dr. Meeks is a member of Sigma Xi and the American Physical Society.

❖

Robert F. Mlodnosky (S'54) was born in Shenandoah, Pa., on October 5, 1932. He received the B.S. degree in electrical engineering in 1955 from the Drexel Institute of Technology, Philadelphia, Pa., and the M.S. degree from Stanford University, Stanford, Calif., in 1956. He is presently in the doctoral program at Stanford.

R. F. Mlodnosky

At Stanford he was an International Business Machines Company Fellow and later a research assistant at the Radio Propagation Laboratory. He is now engaged in research on the characteristics of radio reflections from meteor ionization trails.

Mr. Mlodnosky is a member of Eta Kappa Nu, Tau Beta Pi, and Sigma Xi.

❖

G. Franklin Montgomery (M'48–SM'56) was born in Oakmont, Pa., on May 1, 1921. After receiving the B.S.E.E. degree from Purdue University in 1941, he joined the Naval Research Laboratory, where he worked on radar and counter-measures devices until 1944. He served in the U. S. Army Signal Corps for two years, first as an instructor and later as an engineer in antenna design and ionospheric research. In 1946, he joined the National Bureau of Standards, where he has been engaged in instrumentation, propagation research, and communication theory.

G. F. Montgomery

Mr. Montgomery has been a licensed radio amateur since 1935. He is a member of Tau Beta Pi, Eta Kappa Nu, Sigma Xi, and Sigma Pi Sigma. He is a registered professional engineer in the District of Columbia.

❖

Masasuke Morita (A'54) was born in Utsunomiya, Japan, on December 6, 1915. He graduated from the electrical engineering department of Tokyo University in 1939, and received the Ph.D. degree in engineering in 1950, also from Tokyo University. During World War II, he designed and developed radar equipments in the Nippon Electric Co. At the close of the war, Dr. Morita worked on the research and development of microwave communication equipments. In 1956, he won official commendation from the president of the Nippon Telegraph and Telephone Public Corporation for his contribution to the development of the microwave repeater used in nationwide long distance lines. At the present time, he is Chief of the development section of the Radio Engineering Department in the Nippon Electric Co.

M. Morita

He is a Councilor of the Institute of Electrical Communication Engineers of Japan.

❖

Allen M. Peterson was born on May 22, 1922, in Santa Clara, Calif. He attended San Jose State College from 1939 to 1942. From 1942 to 1944, he was associated with the Electronics Group of Sacramento Air Service Command, and from 1944 to 1946, he was on active duty with the U. S. Army Air Force. He received the B.S. degree in 1948, the M.S. degree in 1949, and the Ph.D. degree in 1952, all in electrical engineering, from Stanford University, Stanford, Calif.

A. M. Peterson

Since 1947, Dr. Peterson has been a staff member of the Radio Propagation Laboratory at Stanford; he is an associate professor of the Electrical Engineering Department.

In June 1953, Dr. Peterson joined Stanford Research Institute where he has been engaged in research on radio propagation, communications, and radio systems design. He is Head of the Special Techniques Group.

Dr. Peterson is a member of Sigma Xi, RESA, the Society for Industrial and Applied Mathematics, and URSI.

❖

Robert A. Rach was born in Elmhurst, Ill. on May 29, 1927. He received the A.B. degree in astronomy from the University of California, Berkeley, Calif., in 1950. He worked at Lick Observatory from 1950 to 1951, as an observer. From 1951 to 1953, he served with the U. S. Army as a Field Instrumentation Officer and later in Korea as Commanding Officer of a topographic and meteorological unit. From 1953 to 1956, he was a graduate student and later Lick Observatory Fellow in astronomy at the University of California. While at Lick Observatory, he was concerned with position measurement and spectrographic studies.

R. A. Rach

In May 1956, Mr. Rach joined the staff of Stanford Research Institute. He is engaged in research on meteoric and high-frequency propagation.

❖

Willmar K. Roberts was born in Jacksonville, Florida on August 26, 1918. He studied at the University of Florida, where he received the Bachelor degree in electrical engineering in 1941. Since that time he has been a member of the staff of the Federal Communications Commission, beginning as an inspector in the Baltimore Field Office. Since 1946, he has been associated with the Commission's Laboratory at Laurel, Md.

W. K. Roberts

Mr. Roberts is a member of Phi Eta Sigma and Phi Kappa Phi.

J. L. Salpeter was born in 1886, in Poland. He studied science at the Universities of Vienna and Göttingen where he published some papers on atmospheric electricity. His early work included one of the first theories on the reflection coefficient of an ionized gas for electromagnetic waves. He also has published a textbook on calculus for natural scientists.


J. L. SALPETER

Upon completion of his university studies, Dr. Salpeter entered industry, working on the incandescent lamp and radio tubes, first in Hungary and then in Austria. He invented a new process for manufacturing small grain coiled tungsten filaments which is still in use today in Europe for vibration proof lamps.

In 1939, he traveled to London and eventually to Australia where he joined Philips Electrical Industries Pty, Ltd., as a research physicist. He is engaged in studies in fluorescent lighting, television optics, and magnetic materials and their applications.

Dr. Salpeter is a member of the Illuminating Engineering Societies of Great Britain and of Australia.

❖

Bruce M. Sifford (S'50–A'51–M'56) was born in Des Moines, Ia., on May 2, 1926. He received the B.S.E.E. degree from the University of Minnesota, in 1950. He worked at the Engineering Research Associates, St. Paul, Minn. from 1950 to 1953, as an electrical engineer, where he was primarily concerned with the design and development of an automatic antenna coupler. He joined Stanford Research Institute, Menlo Park, Calif., where, as a research engineer, for the Special Techniques Group, he has been concerned with measurement of dielectric properties of structural materials, antenna couples, and the design and evaluation of meteor burst communications systems.


B. M. SIFFORD

Mr. Sifford is a member of RESA.

❖

Isao Someya was born in Okayama, Japan on March 23, 1915. He attended Tokyo University, where he received the Ph.D. degree in electrical engineering in 1952. During 1938–1941, he was employed by the Electro Technical Lab., working on research of television transmission on the coaxial cable. In 1942, he was engaged in the development of radar. Since 1945, he has been with the Electrical Communication Lab. of the Nippon Telegraph and Telephone Public Corp., working in the field of development of vhf and microwave relay systems.


I. SOMEYA

He is a member of the Institute of Electrical Communication Engineers of Japan.

❖

George R. Sugar (A'45–S'48–M'53) was born in Winthrop, Mass., on October 12, 1925. He received the B.S. degree in physics from the University of Maryland in 1950. From 1950 to 1951, he was a graduate assistant at the Institute for Fluid Dynamics and Applied Mathematics at the University of Maryland where he attended graduate courses in mathematics and electrical engineering and developed electronic, optical, and mechanical instrumentation for a shock tube research program.


G. R. SUGAR

Since 1951, he has been a member of the staff of the Central Radio Propagation Laboratory of the National Bureau of Standards where he is engaged in experimental research in specific aspects of ionospheric radio propagation.

Mr. Sugar is a member of Sigma Pi Sigma and Phi Kappa Phi.

❖

M. K. Taylor (SM'44) was born on June 26, in Scotland. He has been continuously with Ferranti Electric Co., Ltd. since 1931, joining the radio department as a laboratory assistant. He then took charge of experimental work on a new air bearing textile machine, which had been started by the late Dr. S. Z. de Ferranti. Afterwards Mr. Taylor started and became head of the company's television activities, marketing a 12-inch tube receiver as early as 1936. He made improvements to mechanical A. A. fuses before the war and became chief research engineer. With the early installation of radar in 1937, Mr. Taylor was responsible for the design and manufacture in Great Britain of identification (iff) equipment of various types used by the Allied air forces during the war.


M. K. TAYLOR

Then he started the company's electronic laboratory at Edinburgh, Scotland and worked there on analog computation, particularly in connection with air navigation. He went to Canada in 1949, to start the present Research Division. He went to Edinburgh in 1950, and returned again in 1951, becoming Head of the Division on the return to Great Britain of Dr. A. Porter in 1955.

Mr. Taylor holds about seventy patents, mainly in the electronics and electromechanical fields. He received the Page Prize for a thesis on pulse amplitude modulation. He is a Professional Engineer and an associate member of the IEE.

Wilbur R. Vincent (S'47–A'49) was born in Saginaw, Mich., on August 1, 1922. He received the B.S. degree in 1947, and the M.S. degree in 1951, both in electrical engineering from Michigan State University. He was a radio technician in the U. S. Signal Corps installing and servicing radioteletype installations in the Pacific from 1943 to 1946. In 1948, he joined the electronics staff of the Bell Aircraft Corp., as a unit leader in charge of missile communications equipment development. He is now project engineer on the meteor burst program. In October, 1955 he joined the Stanford Research Institute, where he is an Assistant Group Head in the Special Techniques Group of the Radio Systems Lab., engaged in work on the meteor-burst communication problem.


W. R. VINCENT

❖

Eric L. Vogan (S'44–A'53) was born in London, Ontario, Canada, on September 3, 1924. He received the B.S. and M.S. degrees in physics from the University of Western Ontario, London, Ontario, in 1946 and 1947, respectively. In 1952, he received the Ph.D. degree in physics from McGill University, Montreal, P. Q. Dr. Vogan joined the Radio Physics Laboratory of the Defence Research Board in Ottawa in 1952. From 1952 to 1957, he worked in the field of vhf long-distance propagation at this laboratory. In the summer of 1957, he was appointed resident Canadian Liaison Officer at Lincoln Lab., Massachusetts Institute of Technology.


E. L. VOGAN

Dr. Vogan is a member of the Canadian Association of Physicists.

❖

Russell Wolfram was born in Windsor, Wis. on October 10, 1906. After serving as a Navy electronics technician during World War II, he attended San Jose State College, San Jose, Calif., receiving the B.S. degree in engineering with great distinction in 1950.


R. WOLFRAM

He was employed by the Philco Corp. from 1950 to 1955, as a technical representative of the U.S.A.F. Air Defense Command, acting as operational consultant for heavy ground radar and associated equipment.

He joined Stanford Research Institute in 1955, and is presently engaged in radio propagation studies as research engineer for the Special Techniques Group.

IRE News and Radio Notes

Joint Winners of Ballantine Medal Recently Announced

The Stuart Ballantine Medal of The Franklin Institute, presented in recognition of outstanding achievement in fields of communications or reconnaissance which employ electro-magnetic radiation, was awarded this year to two navy scientists who developed the first U.S. pulse radar system.

R. M. Page (SM'45–F'47) and L. C. Young (A'19–M'29–SM'43–F'43), of the U. S. Naval Research Laboratory, Washington, D. C., received the Ballantine Medal.

Mr. Young, who has been engaged in communications research for the Navy since 1917, first discovered the radio-reflecting action of ships in 1922 while he was associated with the Naval Aircraft Radio Laboratory in Anacostia, D. C.

Dr. Page has worked in close collaboration with Mr. Young on the pulse generation problem for almost a quarter of a century. Following Mr. Young's suggestion that a system using the pulse method be tried for the detection and ranging of aircraft and other objects by radio, Dr. Page built the first pulse radar system and with it detected aircraft in flight in December, 1934.

In April, 1937, experimental radar systems were installed and tested on a naval vessel and, in January, 1939, the first naval radar set was installed aboard the battleship USS *New York* for extensive sea trials.

Dr. Page was head of the Radar Research Section from 1938 to 1945; superintendent of Radio III Division from 1945 to 1952; associate to the director of Research from 1952 to 1954, and, in 1954, he became the first associate director of Research for Electronics, the position he presently holds.

Mr. Young was an associate superintendent of the Radio Division of the Laboratory for several years prior to and during World War II. One of his outstanding accomplishments was the establishment and development of the Chesapeake Bay Annex of the Naval Research Laboratory, which has made a contribution to the advancement of radar and its adaptation to naval operations. He is presently an electronic consultant for the Naval Research Laboratory.

Microwave Convention Planned

The Committee of the Radio and Telecommunication Section of the Institution of Electrical Engineers, London, England, have arranged an international convention on microwave valves during May 19–23, 1958. The convention will survey present knowledge and discuss future trends; particular attention will be paid to work in progress or recently completed. The whole field of microwave devices and their technology and applications will be covered.

The complete proceedings of the convention will be published as a supplement to the Proceedings of the Institution.

Further information may be obtained from W. K. Brasher, The Institution of Electrical Engineers, Savoy Place, London, W.C. 2, England.

Transistor Issue of Proceedings Set for June

To mark the tenth year of transistor progress, the June, 1958 issue of the Proceedings of the IRE will be devoted to transistors and related subjects. The IRE-AIEE Committee on Solid State Devices is assisting the Editorial Board in organizing the scientific content of the issue. The purpose of this announcement is to indicate the type of papers desired for the issue and to call for contributions.

Significant progress has been made since the 1952 transistors issue in the understanding of semiconductor materials and devices. The central theme, therefore, will be lasting contributions to the understanding of the transistor art. Papers relating to research and development of materials and devices, and significant contributions to the application of semiconductor devices are suitable.

Please send manuscripts to E. K. Gannett, Managing Editor, Institute of Radio Engineers, 1 East 79th Street, New York 21, New York, noting that the contribution is intended for the 1958 transistors issue. The closing date for manuscripts is March 1, 1958. Suggestions and comments concerning content and emphasis in the issue should be sent to the organizers of the issue, Stephen J. Angello and James E. Early, in care of E. K. Gannett.

National Science Foundation Fellowships Now Available

The National Science Foundation recently announced that applications are now being accepted in four National Science Foundation fellowship programs for advanced study and research in the natural sciences. The four fellowship programs are: a predoctoral fellowship program for which college seniors and graduate science students may apply; a postdoctoral fellowship program for scientists who have already received the doctoral degree; a senior postdoctoral fellowship program for candidates who have held the science doctorate for a minimum of five years; and a science faculty fellowship program for college teachers of science seeking to increase their competence.

Applications for the 1958–1959 National Science Foundation graduate and regular postdoctoral fellowship program may be obtained from the Fellowship Office, National Academy of Sciences-National Research Council, 2101 Constitution Ave., N. W., Washington 25, D. C. The closing dates for receipt of applications are December 23, 1957, for postdoctoral applicants, and January 3, 1958, for graduate students working towards advanced degrees in science. Selections will be announced March 15, 1958.

Applications for the senior postdoctoral and the science faculty fellowships may be obtained from the Division of Scientific Personnel and Education, National Science Foundation, Washington 25, D. C. Completed material must be received not later than January 13, 1958. Selections will be announced on March 18 and 20, 1958.

Calendar of Coming Events and Authors' Deadlines

Human Factors in Systems Eng., Penn-Sherwood Hotel, Phil., Pa., Dec. 3–4

PGVC Conf., Hotel Statler, Wash., D. C., Dec. 4–5

Eastern Joint Computer Conf., Park-Sheraton Hotel, Wash., D. C., Dec. 9–13

EIA Conf. on Maintainability of Elec. Equip., U.S.C., Los Angeles, Calif., Dec. 18–19

1958

Nat'l Symp. on Reliability & Quality Control, Statler Hotel, Wash., D. C., Jan. 6–8

Scintillation Counter Symp., Shoreham Hotel, Wash., D. C., Jan. 27–28

Transistor-Solid State Circuits Conf., Phil., Pa., Feb. 20–21

Nuclear Eng. and Science Congress, Palmer House, Chicago, Ill., Mar. 16–21

IRE Nat'l Convention, N. Y. Coliseum and Waldorf-Astoria Hotel, New York City, Mar. 24–27 (DL*: Nov. 1, G. L. Haller, IRE Headquarters, New York City)

Instruments & Regulators Conf., Univ. of Del., Newark, Del., March 31–Apr. 2

SW Regional Conf. & Show, Mun. Audit., San Antonio, Tex., Apr. 10–12

Conf. on Automatic Techniques, Statler Hotel, Detroit, Mich., Apr. 14–16

Elec. Components Symp., Ambassador Hotel, Los Angeles, Calif., Apr. 22–24 (DL*: Nov. 15, E. E. Brewer, Convair, Pomona, Calif.)

Seventh Region Conf. & Show, Sacramento, Calif., Apr. 30–May 2

PGMTT Symp., Stanford Univ., Stanford, Calif., May 5–7 (DL*: Jan. 15, K. Tomiyasu, G. E. Microwave Lab., 601 California Ave., Palo Alto, Calif.)

Western Joint Computer Conf., Ambassador Hotel, Los Angeles, Calif., May 6–8 (DL*: Jan. 15, Tech. Program, Chairman, P. O. Box 213, Claremont, Calif.)

Nat'l Aero. & Nav. Elec. Conf., Dayton, Ohio, May 12–14

* DL = Deadline for submitting abstracts.

(Continued on page 1751)

Left to right are: J. W. Worthington, PGCS National Chairman; A. C. Gunn; William Morrow, M.I.T. Lincoln Labs.; S. R. McConoughey, past chairman of the Syracuse Chapter of PGCS; and I. T. Corbell, present Syracuse Chapter Chairman at meeting. Mr. Morrow presented a paper on SSB scatter communications.

Activities of IRE Sections and Professional Groups

Dignitaries attending the WESCON All-Industry luncheon were (left to right): Meyer Leifer, San Francisco Section chairman; J. K. Gossland, Los Angeles Section chairman; J. T. Henderson, IRE President; Earl Goddard, San Francisco Section vice-chairman; and I. N. Whitaker, Los Angeles Section vice-chairman.

IRE President J. T. Henderson, and IRE Vice-President Yasujiro Niwa, meet at the Twelfth URSI Assembly in Boulder, Colo., August 29, 1957.

The Santa Barbara Subsection began its official existence when J. K. Gossland (left), Los Angeles Section chairman, welcomed Walter Hausz as the Santa Barbara subsection's first chairman.

Committee members of the Symposium on Long Haul Communications held by the Hawaii Section are *left to right* F. James, Field Trips; G. Grubb, Sec'y-Treas.; R. Hughes Facilities; R. R. Hill, Chairman; H. Turner, Hospitality; D. Dashiell, Facilities; R. Arden, Vice Chairman; V. Kelly, Section Chairman; and V. Vaughn, Sessions.

AVAILABLE BACK ISSUES OF IRE TRANSACTIONS

The following issues of TRANSACTIONS are available from the Institute of Radio Engineers, Inc., 1 East 79 Street, New York 21, New York, at the prices listed below:

Sponsoring Group	Publications	Group Members	IRE Members	Non-Members*
Aeronautical & Navigational Electronics	PGAE-5, October, 1952	$0.30	$0.45	$0.90
	PGAE-6, December, 1952	.30	.45	.90
	PGAE-8, June, 1953	.65	.95	1.95
	PGAE-9, September, 1953	.70	1.05	2.10
	ANE-1, No. 2, June, 1954	.95	1.40	2.85
	ANE-1, No. 3, September, 1954	1.00	1.50	3.00
	ANE-2, No. 1, March, 1955	1.40	2.10	4.20
	ANE-2, No. 2, June, 1955	1.55	2.30	4.65
	ANE-2, No. 3, September, 1955	.95	1.45	2.85
	ANE-3, No. 2, June, 1956	1.40	2.10	4.20
	ANE-4, No. 1, March, 1957	1.50	2.25	4.50
	ANE-4, No. 2, June 1957	1.10	1.65	3.30
	ANE-4, No. 3, September, 1957	1.25	1.85	3.75
Antennas & Propagation	PGAP-1, February, 1952	3.00	4.50	9.00
	PGAP-4, December, 1952	2.20	3.30	6.60
	AP-1, No. 1, July, 1953	1.20	1.80	3.60
	AP-1, No. 2, October, 1953	1.20	1.80	3.60
	AP-2, No. 1, January, 1954	1.35	2.00	4.05
	AP-2, No. 2, April, 1954	2.00	3.00	6.00
	AP-2, No. 3, July, 1954	1.50	2.25	4.50
	AP-3, No. 4, October, 1954	1.50	2.25	4.50
	AP-3, No. 1, January, 1955	1.60	2.40	4.80
	AP-3, No. 2, April, 1955	1.60	2.40	4.80
	AP-4, No. 4, October, 1956	2.10	3.15	6.30
	AP-5, No. 1, January, 1957	3.20	4.80	9.60
	AP-5, No. 2, April, 1957	1.75	2.60	5.25
	AP-5, No. 3, July, 1957	2.00	3.00	6.00
Audio	PGA-6, March, 1952	0.80	1.20	2.40
	PGA-7, May, 1952	.90	1.35	2.70
	PGA-8, July, 1952	.80	1.20	2.40
	PGA-10, November, 1952	.70	1.05	2.10
	AU-1, No. 6, November, 1953	.90	1.35	2.70
	AU-2, No. 1, January, 1954	1.20	1.80	3.60
	AU-2, No. 3, May, 1954	.95	1.40	2.85
	AU-2, No. 4, July, 1954	.95	1.40	2.85
	AU-2, No. 5, September, 1954	.95	1.40	2.85
	AU-2, No. 6, November, 1954	.80	1.20	2.40
	AU-3, No. 1, January, 1955	.60	.90	1.80
	AU-3, No. 3, May, 1955	.85	1.25	2.55
	AU-3, No. 5, September, 1955	.90	1.35	2.70
	AU-3, No. 6, November, 1955	.95	1.40	2.85
	AU-4, No. 1, January, 1956	.75	1.10	2.25
	AU-4, No. 2, March, 1956	.55	.80	1.65
	AU-4, No. 3, May, 1956	.80	1.20	2.40
	AU-4, No. 5, September, 1956	.60	.90	1.80
	AU-4, No. 6, November, 1956	.80	1.20	2.40
	AU-5, No. 1, January, 1957	.45	.65	1.35
	AU-5, No. 2, March, 1957	.70	1.05	2.10
	AU-5, No. 3, May, 1957	.60	.90	1.80
Broadcast Transmission Systems	PGBTS-2, December, 1955	1.20	1.80	3.60
	PGBTS-4, March, 1956	.75	1.10	2.25
	PGBTS-5, September, 1956	1.05	1.55	3.15
	PGBTS-6, October, 1956	.80	1.20	2.40
	PGBTS-7, February, 1957	1.15	1.70	3.45
	PGBTS-8, June, 1957	.90	1.35	2.70
Broadcast & Television Receivers	PGBTR-4, October, 1953	1.00	1.50	3.00
	PGBTR-5, January, 1954	1.80	2.70	5.40
	PGBTR-7, July, 1954	1.15	1.70	3.45
	PGBTR-8, October, 1954	.90	1.35	2.70
	BTR-1, No. 1, January, 1955	1.25	1.85	3.75
	BTR-1, No. 2, April, 1955	.95	1.45	2.85
	BTR-1, No. 3, July, 1955	.95	1.45	2.85
	BTR-1, No. 4, October, 1955	.95	1.40	2.85
	BTR-2, No. 1, April, 1956	1.10	1.65	3.30
	BTR-2, No. 2, July, 1956	.85	1.25	2.55
	BTR-2, No. 3. October, 1956	1.05	1.55	3.15
	BTR-3, No. 1, June, 1957	1.40	2.10	4.20
	BTR-3, No. 2, October, 1957	1.70	2.55	5.10
Circuit Theory	PGCT-1, December, 1952	1.95	2.90	5.58
	CT-2, No. 4, December, 1955	1.85	2.75	5.55
	CT-3, No. 2, June, 1956	1.60	2.40	4.80
	CT-3, No. 4, December, 1956	1.90	2.85	5.70
	CT-4, No. 1, March, 1957	.65	.95	1.95
	CT-4, No. 2, June, 1957	.70	1.05	2.10
	CT-4, No. 3, September, 1957	2.50	3.75	7.50
Communications Systems	CS-2, No. 1, January, 1954	1.65	2.50	4.95
	CS-4, No. 2, May, 1956	2.90	4.35	8.70

* Colleges, subscription agencies and all libraries, may purchase at IRE member rate.

(Continued on page 1752)

Calendar of Coming Events and Author' Deadlines Continued

IEE Convention on Microwave Valves, Savoy Place, London, England, May 19–23

PGME Meeting, Wash., D. C., May

PGPT Symp., Hotel New Yorker, New York City, June 5–6

PGMIL Convention, Wash., D. C., June 15–18

WESCON, Ambassador Hotel and Pan-Pacific Audit., Los Angeles, Calif., Aug. 19–22 (DL* May 1, D. A. Watkins, Stanford Univ., Stanford, Calif.

Nat'l Electronics Conf., Chicago, Ill., Oct. 13–15

PGCS Symp. on Aero. Communications, Utica, N. Y., Oct. 20–22

Nat'l Simulation Conf., Dallas, Tex., Oct. 23–25

EIA-IRE Radio Fall Meeting, Sheraton Hotel, Rochester, N. Y., Oct. 27–29

East Coast Aero. & Nav. Elec. Conf., Lord Baltimore Hotel and 7th Regiment Armory, Baltimore, Md., Oct. 27–29

PGED Meeting, Shoreham Hotel, Washington, D. C., Oct. 30–Nov. 1

Instrumentation Conf., Atlanta-Biltmore Hotel, Atlanta, Ga., Nov. 17–19

Eastern Joint Computer Conf., Bellevue-Stratford Hotel, Philadelphia, Pa., Dec. 3–5

1959

IRE Nat'l Convention, New York City, Mar. 23–26

Nat'l Aero. & Nav. Elec. Conf., Dayton, Ohio, May 11–13

WESCON, San Francisco, Calif., Aug. 18–21

Nat'l Electronics Conf., Chicago, Ill., Oct. 12–14

East Coast Aero. & Nav. Conf., Baltimore, Md., Oct. 26–28

PGED Meeting, Shoreham Hotel, Washington, D. C., Oct. 29–31

Radio Fall Meeting, Syracuse, N. Y., Nov. 9–11

* DL = Deadline for submitting abstracts.

Philadelphia Hosts Symposium On Systems Engineering

A joint symposium, sponsored by the IRE Philadelphia Section and the Professional Group on Military Electronics, and the Human Factors Society of America, will be held in Philadelphia, Pa. at the Penn-Sherwood Hotel Dec. 3–4, 1957.

The symposium is entitled "Human Factors in Systems Engineering." Brig. Gen. D. D. Flickinger, Chief of the Directorate of Human Factors, ARDC, Baltimore, will be the keynote speaker. The program is to be divided into four half-day sessions.

On the morning of December 3 engineering approaches to systems synthesis will be discussed. J. G. Truxal, Brooklyn Polytechnic Institute, and W. K. Linvill, MIT, will be among the speakers for this session. In the afternoon, the topic will be human factors approaches to systems synthesis. F. V. Taylor, NRL, will be a speaker. The next morning's session will feature a panel of engineers and human factors experts on development of a space ship control system. This panel will include, among others, P. M. Fitts, Ohio State Univ.; D. T. McRuer, Control Specialists, Inc.; and George Long, Douglas Aircraft. J. W. Brady, of Ramo-Wooldridge, will serve as chairman. That afternoon human factors information will be discussed. Walter Grether, Director of Operations, Aeromedical Laboratory, Wright Air Development Center; R. B. Miller, IBM; and R. L. French, Air Force Personnel and Training Research Center, will speak.

Advance registration fee will be $2.50. Mail registrations to Conrad Fowler, Amer. Elec. Labs., 121 N. 7 St., Philadelphia, Pa.

NBS Studies Earth Satellite

The Boulder Laboratories of the National Bureau of Standards has mobilized and set up a crash program to make use of the Russian satellite as long as it circles the world or until its radio batteries go dead.

Since radio waves are bent more by the ionosphere at 20 than at 40 mc, the satellite appears to be at different locations at the same time at each of these frequencies. By studying this effect, the Boulder Laboratories expects to gain much knowledge about the amount of ionization the satellite is passing through as well as other characteristics of this ion media which is all important to the transmission of radio waves.

In order to determine the satellite's exact velocity and the time at which it is closest to the receivers, another Bureau team is measuring shifts in its transmission frequency. When the satellite enters the radio horizon of the receiver, the frequency of its transmitter is upped as much as 1000 cycles per second and as it leaves the frequency is lowered by the same amount. This means that by comparing the actual frequency recordings with the standard tones of frequency and time issued regularly by the NBS radio standard station WWV, the scientists will be able to find the satellite's exact velocity and the time it is closest to us.

Other teams are recording any details of the individual pulses broadcast by the "moon" and making phase measurements that will indicate such things as the presence and location of clouds of ion density in the ionosphere.

AVAILABLE BACK ISSUES OF IRE TRANSACTIONS (Continued)

Sponsoring Group	Publications	Group Members	IRE Members	Non-Members*
	CS-4, No. 3, October, 1956	$1.05	$1.55	$3.15
	CS-5, No. 1, March, 1957	2.30	3.45	6.90
	CS-5, No. 2, September, 1957	.70	1.05	2.10
Component Parts	PGCP-3, April, 1955	1.00	1.50	3.00
	CP-3, No. 2, September, 1956	1.75	2.60	5.25
	CP-4, No. 1, March, 1957	1.35	2.00	4.05
	CP-4, No, 2, June, 1957	1.20	1.80	3.60
Electronic Computers	EC-4, No. 4, December, 1955	.90	1.35	2.70
	EC-5, No. 2, June, 1956	.90	1.35	2.70
	EC-5, No. 3, September, 1956	1.05	1.55	3.15
	EC-6, No. 1, March, 1957	1.15	1.70	3.45
	EC-6, No. 2, June, 1957	1.05	1.55	3.15
Electron Devices	ED-1, No. 3, August, 1954	1.40	2.10	4.20
	ED-1, No. 4, December, 1952	3.20	4.80	9.60
	ED-2, No. 2, April, 1955	2.10	3.15	6.30
	ED-2, No. 3, July, 1955	1.10	1.65	3.30
	ED-3, No. 2, April, 1956	1.10	1.65	3.30
	ED-3, No. 3, July, 1956	1.35	2.00	4.05
	ED-3, No. 4, October, 1956	1.45	2.15	4.35
	ED-4, No. 1, January, 1957	2.60	3.90	7.80
	ED-4, No. 2, April, 1957	2.05	3.10	6.15
	ED-4, No. 3, July, 1957	2.00	3.00	6.00
Engineering Management	PGEM-1, February, 1945	1.15	1.70	3.45
	EM-3, No. 1, January, 1956	.95	1.40	2.85
	EM-3, No. 2, April, 1956	.55	.80	1.65
	EM-3, No. 3, July, 1956	.90	1.35	2.70
	EM-4, No. 1, March, 1957	1.00	1.50	3.00
	EM-4, No. 2, June, 1957	1.00	1.50	3.00
	EM-4, No. 3, September, 1957	.60	.90	1.80
Industrial Electronics	PGIE-1, August, 1953	1.00	1.50	3.00
	PGIE-2, March, 1955	1.90	2.85	5.70
	PGIE-3, March, 1956	1.70	2.55	5.10
Information Theory	PGIT-3, March, 1954	2.60	3.90	7.80
	PGIT-4, September, 1954	3.35	5.00	10.00
	IT-1, No. 2, September, 1955	1.90	2.85	5.70
	IT-1, No. 3, December, 1955	1.55	2.30	4.65
	IT-2, No. 2, June, 1956	1.65	2.45	4.95
	IT-2, No. 3, September, 1956	3.00	4.50	9.00
	IT-2, No. 4, December, 1956	1.85	2.75	5.55
	IT-3, No. 1, March, 1957	2.20	3.30	6.60
	IT-3, No. 2, June, 1957	2.45	3.65	7.35
Instrumentation	PGI-3, April, 1954	1.05	1.55	3.15
	PGI-4, October, 1955	2.70	4.05	8.10
	I-6, No. 1, March, 1957	1.50	2.25	4.50
	I-6, No. 2, June, 1957	1.85	2.75	5.55
Medical Electronics	PGME-2, October, 1955	.85	1.25	2.55
	PGME-4, February, 1956	1.95	2.90	5.85
	PGME-7, December, 1956	1.00	1.50	3.00
	PGME-8, July, 1957	.95	1.40	2.85
Microwave Theory & Techniques	MTT-2, No. 3, September, 1954	1.10	1.65	3.30
	MTT-3, No. 1, January, 1955	1.50	2.25	4.50
	MTT-3, No. 4, July, 1955	1.60	2.40	4.80
	MTT-4, No. 1, January, 1956	1.65	2.45	4.95
	MTT-4, No. 3, July, 1956	1.25	1.85	3.75
	MTT-4, No. 4, October, 1956	1.85	2.75	5.55
	MTT-5, No. 1, January, 1957	1.75	2.60	5.25
	MTT-5, No. 2, April, 1957	1.90	2.85	5.70
	MTT-5, No. 3, July, 1957	1.15	1.70	3.45
	MTT-5, No. 4, October, 1957	1.20	1.80	3.60
Military Electronics	MIL-1, No. 1, March, 1957	.90	1.35	2.70
Nuclear Science	NS-1, No. 1, September, 1954	.70	1.00	2.00
	NS-2, No. 1, June, 1955	.55	.85	1.65
	NS-3, No. 1, February, 1956	.90	1.35	2.70
	NS-3, No. 2, March, 1956	1.40	2.10	4.20
	NS-3, No. 3, June, 1956	1.00	1.50	3.00
	NS-4, No. 1, March, 1957	1.80	2.70	5.40
Production Techniques	PGPT-2, April, 1957	2.85	4.25	8.55
Reliability & Quality Control	PGQC-2, March, 1953	1.30	1.95	3.90
	PGQC-3, February, 1954	1.15	1.70	3.45
	PGQC-4, December, 1954	1.20	1.80	3.60
	PGRQC-5, April, 1955	1.15	1.75	3.45
	PGRQC-6, February, 1956	1.50	2.25	4.50
	PGRQC-7, April, 1956	1.10	1.65	3.30
	PGRQC-10, June, 1957	1.20	1.80	3.60
	PGRQC-11, August, 1957	1.35	2.00	4.05
Telemetry & Remote Control	PGRTRC-1, August, 1954	.85	1.25	2.55
	PGRTRC-2, November, 1954	.95	1.40	2.85

* Colleges, subscription agencies and all libraries, may purchase at IRE member rate.

(Continued on page 1753)

AVAILABLE BACK ISSUES OF IRE TRANSACTIONS (Continued)

Sponsoring Group	Publications	Group Members	IRE Members	Non-Members*
	TRC-1, No. 2, May, 1955	$ .95	$1.40	$2.85
	TRC-1, No. 3, August, 1955	.70	1.05	2.10
	TRC-2, No. 1, March, 1956	1.00	1.50	3.00
	TRC-3, No. 1, April, 1957	2.70	3.60	7.20
	TRC-3, No. 2, May, 1957	1.15	1.70	3.45
Ultrasonics Engineering	PGUE-1, June, 1954	1.55	2.30	4.65
	PGUE-5, August, 1957	1.50	2.25	4.50
Vehicular Communications	PGVC-5, June, 1955	1.50	2.25	4.50
	PGVC-6, July, 1956	1.55	2.30	4.65
	PGVC-8, May, 1957	1.40	2.10	4.20
	PGVC-9, June, 1957	.75	1.10	2.25

* Colleges, subscription agencies and all libraries, may purchase at IRE member rate.

W. L. Everitt Wins AIEE Medal

W. L. Everitt (A'25–M'29–F'38), dean of the College of Engineering, University of Illinois, has been awarded the American Institute of Electrical Engineers' Medal in Electrical Engineering Education for outstanding service as a teacher in electrical engineering. Dean Everitt, the second recipient of the Medal, received it at the five-day Fall General Meeting of AIEE at Chicago, October 7.

W. L. Everitt

The Medal was awarded Dr. Everitt "in recognition of his distinguished service as a teacher of electrical engineering and as evidence of the high esteem in which his contributions to engineering education are held by his fellow members of the American Institute of Electrical Engineers."

Dr. Everitt has devoted most of his life to education, except for two years as engineer in charge of P.B.X. development for the North Electric Manufacturing Company at Galion, Ohio and a war stint. He was an instructor in electrical engineering at Cornell University during 1920–1922 and an instructor in charge of communications courses at the University of Michigan in 1924–1926. He then joined the staff of Ohio State University where he remained until 1942. From then until 1945 he was director of the Operational Research Staff Office of the Chief Signal Officer, War Department. He became professor and head of the Department of Electrical Engineering at the University of Illinois in 1945 and was named dean of engineering in 1949.

An alumnus of Cornell University, the University of Michigan and Ohio State University, Dean Everitt is noted for inventions in the fields of automatic telephony, radio altimeters for aircraft, directional antenna systems, speech compression and radio tuning systems.

He is a Fellow of AIEE and a former IRE president in 1945. He was an IRE Director from 1942 to 1947, and 1949 to 1951. He won the IRE Medal of Honor in 1954. He also has served on a number of IRE and technical committees, and he is presently on the Editorial Review committee.

D. A. Watkins Wins 1957 IRE Annual Western Region Award

D. A. Watkins (A'47–M'48–S'49–A'51–SM'55) of Stanford University has been named recipient of the 1957 Electronic-Achievement Award of the IRE Seventh Region.

D. A. Watkins

The award is given annually as recognition for outstanding contributions to electronic activities in the Western Region of the IRE, which embraces nine western states. The citation for Dr. Watkins' award is for "his basic contributions in reducing noise in microwave electron tubes." Dr. Watkins is also the inventor of the "Helitron" tube, which permits instantaneous radar tuning over a prodigious range of microwave frequencies.

Achievement Award winners are chosen by secret ballot of a regional committee representing more than 7,000 members of the IRE in the Seventh Region. Members of the Awards Committee for 1957, who chose the nominees, are Clayton Clark, Utah State University, chairman; Prof. H. J. Hendricks, California Polytechnic Institute, and Eugene French, Albuquerque, N. M.

The presentation of the award was made at WESCON.

Dr. Watkins holds a B.S. degree from Iowa State College (1944), an M.S. from California Institute of Technology (1947) and the Ph.D. degree (1951) from Stanford.

Early in his career he was a design engineer for Collins Radio Co. of Cedar Rapids, Iowa. He then spent a year on the staff of Los Alamos Scientific Laboratories. In early 1951 Dr. Watkins joined the Research and Development Laboratories of Hughes Aircraft Co., Culver City, Calif., where he became head of the Microwave Tube Section. Dr. Watkins' faculty association with Stanford began in the spring of 1954, when he was appointed an associate professor of electrical engineering.

He was advanced to a full professorship in June, 1956 and has since been engaged in teaching and direction of research in microwave tubes. He was named an associate director of Stanford Electronics Laboratories in September, 1954, his present position.

He is a member of the American Physics Society and he was chairman of the technical program committee for WESCON this year.

Color TV Proceedings Printed

The journals *Optica Acta* and *Acta Electronica* have undertaken the joint publication of the full proceedings, mostly in English, of the International Symposium on the Physical Problems of Color Television, held last July in Paris. The volume consists of 400 pages and more than 450 illustrations. The number of copies available to non-subscribers of either journal, however, is limited. Persons interested should send $10 post-paid to either *Optica Acta*, 3 boulevard Pasteur, Paris, 15, France, or *Acta Electronica*, 23 rue du Retrait, Paris 20, France, before Jan. 1

The Buenos Aires IRE Section held lectures and a radio equipment show during its tenth annual Electronics Week. Shown above is the Argentina Minister of Communications as he cuts the ribbon to open the radio show.

Symposium on Scintillation Counters Set for Jan. 27–28

The Sixth Scintillation Counter Symposium, sponsored by the IRE, AIEE, Atomic Energy Commission and the National Bureau of Standards, is scheduled for January 27–28 at the Hotel Shoreham, Washington, D. C.

The program will include both invited and contributed papers on components, equipment and applications. There will be four sessions, each a half day in length, covering phosphor and Cerankov scintillators, photomultipliers, energy and time resolution, and scintillation counter applications. An additional evening program on January 27 will be held to show films on the latest techniques for low-level counting. At this time papers dealing with the approach to the scintillation counter problem taken by other countries will be delivered, too.

Professional Group News

The following chapters were approved by the Executive Committee on October 10: PG's on **Aeronautical & Navigational Electronics, Broadcast Transmission Systems,** and **Communications Systems,** Florida West Coast Section; PG's on **Communications Systems,** and **Military Electronics,** San Francisco Section; PG on **Military Electronics,** Tucson Section; PG on **Microwave Theory & Techniques,** Denver Section; and PG on **Telemetry & Remote Control,** Washington, D. C. Section.

An award to be known as the Scott Helt Memorial Award has been established by the Administrative Committee of the IRE Professional Group on **Broadcast Transmission Systems.** This is the first Professional Group Award of the PGBTS and is established in memory of Mr. Helt who died in an airplane collision on August 9, 1956. It will be awarded annually for the best paper published in the Transactions of the Group.

The Professional Group on **Instrumentation** announces that its 1956–57 prize has gone to E. S. Gordon, D. C. Maxwell, Jr. and N. E. Alexander for their paper, "Electronic Instrumentation of a Device to Automatically Count and Size Particles in a Gas," published in the issue of March, 1957, IRE Transactions on instrumentation.

The January, 1958 issue of the IRE Transactions on **Microwave Theory & Techniques** will be completely devoted to the papers given at the recent 1957 annual PGMTT meeting covering microwave ferrites and related devices, and their applications.

This issue of the Transactions, and subsequent issues, can be obtained by all IRE members upon joining the PGMTT and payment of the annual assessment of $3.00.

The 1958 National PGMTT Symposium will be held May 5–7 at Stanford University.

Authors should submit, *in triplicate*, prior to January 1958, both a 100-word abstract, title of paper, name and address; and a 500-word summary, title of paper, name and address. Papers related to microwave physics and applications, microwave components and microwave techniques are considered appropriate. Submit papers to Kiyo Tomiyasu, Technical Program Chairman, 601 California Ave., Palo Alto, Calif.

Current IRE Standards

Please order by number from IRE Headquarters, 1 E. 79 St., N. Y. 21, N. Y. A 20% discount will be allowed on order for 100 or more copies mailed to one address.

	PRICE
48 IRE 2., 11., 15.S1 Standards on Antennas, Modulation Systems, and Transmitters: Definitions of Terms, 1948	$0.75
53 IRE 2.S1 Standards on Antennas and Waveguides: Definitions of Terms, 1953. Adopted by ASA. (ASA C16.21-1954). Reprinted from the December, 1953, Proceedings	$0.75
55 IRE 2.S1 Standards on Antennas and Waveguides: Definitions for Waveguide Components, 1955. Reprinted from the September, 1953, Proceedings	$0.25
48 IRE 2.S2 Standards on Antennas: Methods of Testing. 1948. Adopted by ASA. (ASA C16.11-1949)	$0.75
54 IRE 3.S1 Standards on Audio Techniques: Definitions of Terms, 1954. Reprinted from the July, 1954, Proceedings	$0.50
56 IRE 3.S1 Standards on Audio Systems and Components: Methods of Measurement of Gain, Amplification, Loss, Attenuation, and Amplitude-Frequency-Response, 1956. Adopted by ASA. (ASA C16.29-1957). Reprinted from the May, 1956, Proceedings	$0.80
53 IRE 3.S2 Standards on American Recommended Practice for Volume Measurements of Electrical Speech and Program Waves, 1953. Adopted by ASA. (ASA C16.5-1954). Reprinted from the May, 1954, Proceedings	$0.50
50 IRE 4.S1 Standards on Circuits: Definitions of Terms in Network Topology, 1950 Reprinted from the January, 1951, Proceedings	$0.50
53 IRE 4.S1 Standards on Circuits: Definitions of Terms in the Field of Linear Varying Parameter and Nonlinear Circuits, 1953. Reprinted from the March, 1954, Proceedings	$0.25
42 IRE 6.S1 American Recommended Practice for Loudspeaker Testing. Adopted by ASA. (ASA C16.4-1942)	$0.40
51 IRE 6.S1 Standards on Electroacoustics: Definitions of Terms, 1951. Reprinted from the May, 1951, Proceedings	$1.00
52 IRE 7.S1 Standards on Magnetrons: Definitions of Terms, 1952. Reprinted from the May, 1952, Proceedings	$0.25
53 IRE 7.S1 Standards on Electron Devices: Methods of Measuring Noise, 1953. Adopted by ASA (ASA C60.13-1954). Reprinted from the July, 1953, Proceedings	$0.75
54 IRE 7.S1 Standards on Electron Devices: Definitions of Terms Related to Phototubes, 1954. Reprinted from the August, 1954, Proceedings	$0.25
56 IRE 7.S1 Standards on Electron Devices: Definitions of Terms, Related to Microwave Tubes (Klystrons, Magnetrons, and Traveling Wave Tubes), 1956. Reprinted from the March, 1956, Proceedings	$0.50
57 IRE 7.S1 Standards on Electron Tubes: Physical Electronics Definitions, 1957. Reprinted from the January, 1957, Proceedings	$0.50
50 IRE 7.S2 Standards on Electron Tubes: Methods of Testing, 1950. Part I reprinted from August, 1950, Proceedings; Part II reprinted from September, 1950, Proceedings	$1.25
52 IRE 7.S2 Standards on Gas-Filled Radiation Counter Tubes: Methods of Testing, 1952. Adopted by ASA. (ASA C60.11-1954). Reprinted from the August, 1952, Proceedings	$0.75
54 IRE 7.S2 Standards on Electron Devices: Definitions of Semiconductor Terms, 1954 Reprinted from the October, 1954, Proceedings	$0.50
56 IRE 7.S2 Standards on Electron Devices: Definitions of Terms Related to Storage Tubes, 1956. Reprinted from the April, 1956, Proceedings	$0.25
57 IRE 7.S2 Standards on Electron Tubes: Definitions of Terms, 1957. Reprinted from the July, 1957, Proceedings	$1.00
52 IRE 7.S3 Standards on Gas-Filled Radiation Counter Tubes: Definitions of Terms, 1952. Reprinted from the August, 1952, Proceedings	$0.50
56 IRE 7.S3 Standards on Electron Tubes: TR and ATR Tube Definitions, 1956. Reprinted from the August, 1956, Proceedings	$0.50
56 IRE 8.S1 Standards on Electronic Computers: Definitions of Terms, 1956. Reprinted from the September, 1956, Proceedings	$0.60
43 IRE 9.S1 Standards on Facsimile: Temporary Test Standards, 1943	$0.20
56 IRE 9.S1 Standards on Facsimile: Definitions of Terms, 1956. Adopted by ASA. (ASA C16.30-1957). Reprinted from the June, 1956, Proceedings	$0.60
55 IRE 10.S1 Standards on Industrial Electronics: Definitions of Industrial Electronics Terms, 1955. Reprinted from the September, 1955, Proceedings	$0.50
53 IRE 11.S1 Standards on Modulation Systems: Definitions of Terms, 1953. Reprinted from the May, 1953, Proceedings	$0.50
54 IRE 12S.1 Standards on Radio Aids to Navigation: Definitions of Terms, 1954. Adopted by ASA. (ASA C16.26-1955). Reprinted from the February, 1955, Proceedings	$1.00
49 IRE 14.S1 Standards on Piezoelectric Crystals, 1949. Adopted by ASA. (ASA C83.3-1951, R 1954). Reprinted from the December, 1949, Proceedings	$0.80
57 IRE 14.S1 Standards on Piezoelectric Crystals—The Piezoelectric Vibrator: Definitions and Methods of Measurement, 1957. Reprinted from the March, 1957, Proceedings	$0.60

(Continued on page 1755)

Current IRE Standards

Please order by number from IRE Headquarters. 1 E. 79 St., N. Y. 21, N. Y. A 20% discount will be allowed on order for 100 or more copies mailed to one address.

	PRICE
55 IRE 15.S1 Standards on Pulses: Methods of Measurements of Pulse Quantities, 1955. Adopted by ASA. (ASA C16.28-1956). Reprinted from the November, 1955, PROCEEDINGS	$0.60
49 IRE 16.S1 Standards on Railroad and Vehicular Communications: Methods of Testing, 1949. Reprinted from the December, 1949, PROCEEDINGS	$0.50
47 IRE 17.S1 Standards on Radio Receivers: Methods of Testing Frequency-Modulation Broadcast Receivers, 1947. Adopted by ASA. (ASA C16.12-1949)	$0.50
48 IRE 17.S1 Standards on Radio Receivers: Methods of Testing Amplitude-Modulation Broadcast Receivers, 1948	$1.00
49 IRE 17.S1 Tests for Effects of Mistuning and for Downward Modulation. 1949 Supplement to 47 IRE 17.S1 reprinted from the December, 1949, PROCEEDINGS	$0.25
51 IRE 17.S1 Standards on Radio Receivers; Open Field Method of Measurement of Spurious Radiation from Frequency Modulation and Television Broadcast Receivers, 1951. Reprinted from the July, 1951, PROCEEDINGS	$0.50
52 IRE 17.S1 Standards on Receivers: Definitions of Terms, 1952. Reprinted from the December, 1952, PROCEEDINGS	$0.60
54 IRE 17.S1 Standards on Receivers: Methods of Measurement of Interference Output of Television Receivers in the Range of 300 to 10,000 KC, 1954. Adopted by ASA. (ASA C16.25-1955). Reprinted from the September, 1954, PROCEEDINGS	$0.60
55 IRE 17.S1 Standards on Radio Receivers: Method of Testing Receivers Employing Ferrite Core Loop Antennas, 1955. Reprinted from the September, 1955, PROCEEDINGS	$0.50
53 IRE 19.S1 Standards on Sound Recording and Reproducing: Methods of Measurement of Noise, 1953. Reprinted from the April, 1953, PROCEEDINGS	$0.50
53 IRE 19.S2 Standards on Sound Recording and Reproducing: Methods for Determining Flutter Content, 1953. Adopted by ASA. (ASA Z57.1-1954). Reprinted from the March, 1954, PROCEEDINGS	$0.75
51 IRE 20.S1 Standards on Pulses: Definitions of Terms—Part I, 1951. Reprinted from the June, 1951, PROCEEDINGS	$0.50
52 IRE 20.S1 Standards on Pulses: Definitions of Terms—Part II, 1952. Reprinted from the May, 1952, PROCEEDINGS	$0.50
51 IRE 20.S2 Standards on Transducers: Definitions of Terms, 1951. Reprinted from the August, 1951, PROCEEDINGS	$0.50
49 IRE 21.S1 Standards on Designations for Electrical, Electronic and Mechanical Parts and Their Symbols, 1949. Reprinted from February, 1950, PROCEEDINGS	$0.60
51 IRE 21.S1 Standards on Abbreviations of Radio-Electronic Terms, 1951. Reprinted from the April, 1951, PROCEEDINGS	$0.50
54 IRE 21.S1 Standards on Graphical Symbols for Electrical Diagrams, 1954. Reprinted from the June, 1954, PROCEEDINGS	$1.25
57 IRE 21.S1 Standards on Letter Symbols and Mathematical Signs, 1948 (Reprinted 1957). Reprinted from the August, 1957, PROCEEDINGS	$0.60
57 IRE 21.S2 Standards on Reference Designations for Electrical and Electronic Equipment, 1957. Reprinted from the November, 1957, PROCEEDINGS	$0.70
57 IRE 21.S3 Standards on Graphical Symbols for Semiconductor Devices, 1957. Reprinted from the December, 1957, PROCEEDINGS	$0.60
48 IRE 22.S1 Standards on Television: Methods of Testing Television Receivers, 1948. Adopted by ASA. (ASA C16.13-1949)	$1.00
55 IRE 22.S1 Standards on Television: Definitions of Color Terms, 1955. Reprinted from the June, 1955, PROCEEDINGS	$0.60
50 IRE 23.S1 Standards on Television: Methods of Measurement of Television Signal Levels, Resolution, and Timing of Video Switching Systems, 1950. Reprinted from the May, 1950, PROCEEDINGS	$0.70
54 IRE 23.S1 Standards on Television: Methods of Measurement of Aspect Ratio and Geometric Distortion, 1954. Adopted by ASA. (ASA C16.23-1954). Reprinted from the July, 1954, PROCEEDINGS	$0.60
55 IRE 23.S1 Standards on Television: Definitions of Television Signal Measurement Terms, 1955. Reprinted from the May, 1955, PROCEEDINGS	$1.00
50 IRE 23.S2 Standards on Television: Methods of Measurement of Time of Rise, Pulse width, and Pulse Timing of Video Pulses in Television, 1950. Reprinted from the November, 1950, PROCEEDINGS	$0.75
50 IRE 23.S1 Standards on Television: Methods of Measurement of Electronically Regulated Power Supplies, 1950. Reprinted from the January, 1951, PROCEEDINGS	$0.75
45 IRE 24.S1 Standards on Radio Wave Propagation: Definitions of Terms Relating to Guided Waves, 1945	$0.20
50 IRE 24.S1 Standards on Wave Propagation: Definitions of Terms, 1950. Reprinted from the November, 1950, PROCEEDINGS	$0.60
55 IRE 26.S1 Standards on Graphical and Letter Symbols for Feedback Control Systems, 1955. Reprinted from the November, 1955, PROCEEDINGS	$0.25

(Continued on page 1756)

Obituary

J. D. Southwell (A'47–M'48–SM'53), longtime worker in various city departments and director of the Division of Public Safety since it was organized in November, 1956 in Beaumont, Tex., died recently.

He was a native of New Iberia, La., and came to Beaumont in 1902 at the age of six. He attended Millard School and old Beaumont High School before beginning his mechanical career as a chauffeur.

He became a mechanic in the White Steamer Automobile Co. shops in 1909 and joined the Beaumont Fire Department in 1917 as an electrician and maintenance mechanic.

Mr. Southwell, as city electrician, designed and installed the city's first traffic signal system in 1926. He also designed and installed the underground cable for the telegraph system of the police department. He designed and built the police department's radio communications system and, the seventh in the nation, it was the first to go into operation south of St. Louis, Mo.

For the local fire department, he designed the searchlight truck which includes a self-contained power plant, reel-out cables and elevators for lights atop the truck. It was copied by fire departments in a number of cities, including London, England.

A key figure in the city's water department, he had been in charge of electrical and maintenance work for the department and worked with other engineers in designing the pumping plant as well as the raw water supply system which guarded the city against salt water encroachment.

He installed the original power distribution system and more recently worked on the design for a diesel generating plant for an emergency power supply at the plant. He also supervised installation of electric power equipment at the new sewage disposal plant.

He was president of Local 183, International Alliance of Theatrical Stage Employes and Motion Picture Machine Operators and of the International Brotherhood of Electrical Workers for 19 years. He was a member of the American Institute of Electrical Engineers, Texas Society and Sabine Chapter of Professional Engineers.

Technical Committee Notes

The following Technical Committees held meetings this past month:

Sept. 17—Feedback Control Systems Committee, J. E. Ward, Chairman, MIT Faculty Club.
Video Techniques Committee, S. Doba, Jr., Chairman, IRE Headquarters.

Sept. 23—Industrial Electronics Committee, J. A. Eiselein, Chairman, Morrison Hotel, Chicago.

Sept. 24—Audio Techniques Committee, I. M. Kerney, Chairman, IRE Headquarters.

Sept. 27—Information Theory and Modulation Systems Committee, J. G. Kreer, Jr., Chairman, IRE Headquarters.
Electron Tubes Committee, G. Espersen, Chairman, IRE Headquarters.

Facsimile Committee, D. Frezzolini, Chairman, Times Building, New York.

Oct. 2—Antennas and Waveguides Committee, G. Deschamps, Chairman, IRE Headquarters.

Oct. 3—Standards Committee, M. W. Baldwin, Jr., Chairman, IRE Headquarters.

Oct. 4—Circuits Committee, W. A. Lynch, Chairman, IRE Headquarters.

Oct. 9—Recording and Reproducing Committee, D. E. Maxwell, Chairman, IRE Headquarters.

Oct. 11—Radio Transmitters Committee, H. Goldberg, Chairman, IRE Headquarters.

Current IRE Standards

Please order by number from IRE Headquarters, 1 E. 79 St., N. Y. 21, N. Y. A 20% discount will be allowed on order for 100 or more copies mailed to one address.

	PRICE
55 IRE 26.S2 Standards on Terminology for Feedback Control Systems. 1955. Reprinted from the January, 1956, Proceedings	$0.50
56 IRE 27.S1 Standards on Methods of Measurement of the Conducted Interference Output of Braodcast and Television Receivers in the Range of 300 KC to 25 MC, 1956. Adopted by ASA. (ASA C16.25a-1957). Reprinted from the August, 1956, Proceedings	$0.50
56 IRE 28.S1 Standards on Letter Symbols for Semiconductor Devices, 1956. Reprinted from the July, 1956, Proceedings	$0.50
56 IRE 28.S2 Standards on Solid-State Devices: Methods of Testing Transistors, 1956. Reprinted from the November, 1956, Proceedings	$0.80

Books

Television Engineering, Volume Three by S. W. Amos and D. C. Birkinshaw

Published (1957) by Philosophical Library, Inc., 15 E. 40 St., New York 16, N. Y. 224 pages+2 index pages. 132 figures. 8¾×5¾. $15.00.

This is an exceptionally valuable book for all those interested in the generation of television signals. Adequately illustrated with clearly defined schematic diagrams and figures, it is equally useful in the fields of research, development and operation. The precise tabulation and detailed analysis of an unusually wide variety of techniques for waveform generation is a brilliant illustration of the high quality of engineering of the British Broadcasting Corporation.

Commencing with an analysis of the waveforms used in the synthesizing of television synchronizing, blanking, scanning and shading signals, the mathematical relationship between rectangular, sawtooth and parabolic waveforms is derived and shown graphically. The authors describe in detail the operation, the derivation of the basic equations and the optimum component values for numerous circuits employed in generating sine, rectangular, sawtooth and parabolic waveforms. Following a spectrum analysis, the generation of rectangular waveforms covers diode limiting, amplifier limiting, bi-stable, monostable and astable multivibrators, transitron, phantastron and Miller-transitron circuits.

The generation of sawtooth waveforms is given a similarly detailed treatment. It includes blocking oscillator, multivibrator and Miller-integrator circuits together with methods of linearizing the output waveforms. A comprehensive study of methods of synchronization of the various types of generators, together with the associated development of counting circuits, is included.

W. B. Whalley
CBS Television Inc.
New York 22, N. Y.

Semiconductor Surface Physics ed. by R. H. Kingston

Published (1957) by Univ. of Pennsylvania Press, 3436 Walnut St., Philadelphia 4, Pa. 405 pages +7 index pages+xvi pages. Illus. 8½×5¾. $8.00.

The study of semiconductor surface phenomena is very much in an early stage in spite of the great importance of the role of surfaces in many fields of physics, chemistry, and electrical engineering. This volume contains a collection of invited papers and contributed discussion pertaining to a conference held during June, 1956. The book is divided into four sections: clean surfaces, real surfaces, adsorption and catalysis, and oxidation.

The first section, dealing with experiments designed toward exploring the physical nature of ideal surfaces together with some of the theories involved, contains only two papers; however, the value of this work more than makes up for its brevity. The electron diffraction experiments by the Farnsworth group are described, and cover the difficult techniques involved in obtaining clean surfaces. Some of the techniques include alternate heating of germanium to 700°C and argon ion bombardment, followed by annealing at 500°C, then probing by electron diffraction. Results are not yet fully conclusive, but the approach is excellent. This report is followed by a survey article by Handler. The recorded discussion is provocative and thought stimulating.

The second part deals with real surfaces or surfaces more readily attainable. Most of the emphasis is related to surface conductivity experiments and subsequent deductions. Field-effect mobilities are discussed with some repetition. This, in turn, is related to surface recombination velocity, surface potential studies, photovoltaic effects, and inversion layers induced by surface contaminants. The redundancy in these presentations is not without value, since each investigator expresses his own sense of values, providing the reader with a broader perspective.

For example, each paper in this section is concerned with "fast" surface states and "slow" surface states. The "fast" surface states are attributed to traps at the semiconductor surface, and can result in a rapid change in conductivity after application of a transverse electric field. The "slow" states are attributed to traps relating to an oxide layer or other thick coatings. Little is really known as to the source of these traps, yet it is interesting and instructive to compare the interpretations of the experimental data.

The third group of papers, dealing with adsorption and catalysis, offers a challenge to the physical chemist. It is pointed out that the band structure of the surface and the energy level structure of surrounding molecules is intimately connected with the rates of reaction.

Although this field is relatively unexplored, Garrett and Brattain point out that some of these concepts may have already been verified in that it has been found that hole density plays a major part in anodic oxidation of germanium. Brattain further indicates possibilities in the use of illumination to control reaction rates at the surface of germanium.

The fourth part, dealing with oxidation, is also of interest to the physicist and chemist. In one of the experiments, fresh surfaces of germanium are created by crushing the semiconductor in vacuum and then measuring the oxygen adsorption as a function of time and temperature. In another experiment, the oxidation rate of the (110), (111), and (100) faces has been measured at elevated temperatures and at various pressures of oxygen. These data when combined with future electrical measurements offer new approaches to gaining more information about surfaces of semiconductors.

Since this book is a collection of papers rather than a textbook, certain aspects are lacking. First, more work is needed in linking the physical, chemical, and electronic aspects of surfaces. Secondly, there is a lack of contact with monumental work in the past such as that performed by DeBoer, Langmuir, Nottingham, Becker and others. Thirdly, any collection of papers must be somewhat lacking in continuity.

However, the volume is fairly well edited and includes references and discussions. This book will be of great value to the research specialist studying semiconductors and semiconductor surface phenomena. The ideas presented are rich in experience, technical detail and, with very little effort on the part of the reader, will point out new areas of exploration and experimentation. The physicist, chemist, or engineer concerned with the design and construction of transistors and other semiconductor devices will find the book useful and interesting.

The volume comprises the thinking developed in the past few years and is a valuable contribution to the semiconductor field.

H. A. ZAHL and HAROLD JACOBS
U. S. Army Signal Eng. Labs.
Fort Monmouth, N. J.

Digital Computer Programming by D. D. McCracken

Published (1957) by John Wiley & Sons, Inc., 440 Fourth Ave., N. Y. 16, N. Y. 216 pages+5 index pages+16 appendix pages+vii pages. 9¼×6¼. $7.75.

This book can best be described as a text for an elementary course in programming digital computers for numerical problems in the field of scientific and engineering computation. The author, who evidently has considerable experience, both in applying and in teaching the art of programming, has written a book which should prove extremely useful to the teacher and the student of this fast-growing subject. Many illustrations of short programs are given, and each chapter concludes with exercises for the student.

The basic concepts of number systems, computer arithmetic, addressing, and programming in machine language are treated extensively. Relative, interpretive, and automatic programming concepts are introduced. A touch of reality is added by discussions of common mistakes in programming and of checkout techniques; the author occasionally asks the reader to find errors left in the sample programs.

The author has chosen to devise on paper his own computer to provide an instruction set for use in the sample programs. As a result, he is able to streamline and even omit some of the more complex features of actual computers, although he has retained others, such as indexing and floating point features, which are gradually becoming standard items.

Making up a paper computer is a controversial approach which considerably simplifies the exposition and avoids singling out any one commercial product. On the other hand, the student preparing to program a specific machine may find the treatment of many topics inadequate, particularly in the input-output area. The author suggests referring to manufacturers' literature for additional information. This information is sufficiently complex, however, that the reader may wish for another textbook instead of the usual compilations found in machine manuals.

In the treatment of the more advanced topics, the author has wisely chosen to introduce the ideas, even though the scope of the book prohibits giving more than brief illustrations. A bibliography leads the reader to what information is published. The need for more published material is evident. In particular, a companion book covering the area of programming computers for business data processing would be desired.

The choice of a simplified though practical treatment of a complex subject will appeal to many readers. The style is clear and concise. The book should fill a great need in the expanding educational efforts on programming digital computers.

WERNER BUCHHOLZ
IBM Corp.
Poughkeepsie, N. Y.

Transistor Circuit Engineering, ed. by R. F. Shea

Published (1957) by John Wiley & Sons, Inc., 440 Fourth Ave., N. Y. 16, N. Y. 433 pages+10 index pages+9 appendix pages+13 bibliography pages+xx pages. Illus. 9¼×6¼. $12.00.

The coverage of this new book on transistors is quite complete, starting with a description of the solid state physics of the transistor and going all the way to a completely transistorized television receiver. The text is clearly written and studded with design equations and numerical examples. The problems are intriguing. There is a great variety of circuit techniques representing a judicious selection and editing from the literature.

Two criticisms which can be offered of the book is that it suffers from the fault of any design book within a fast moving field in that it must be out of date at the time it is published. The second comment is that the switching circuit area is sparse in comparison with the rest of the book.

The book represents the maturing of the transistor art. It is design-oriented with much less emphasis on physics and transistor characteristics than the earlier volumes and devotes most of its coverage to actual circuit design problems. The space devoted to point contact transistors, as a further example, is minimized.

The material on small signal amplifiers is excellent and is sufficient to execute specific designs. Of particular value to design engineers are the sections on temperature stabilization and high frequency amplifier neutralization.

Although a compilation the book reads as though written by one man. The comprehensive bibliography should be of great value.

KNOX MCILWAIN
Burroughs Corp.
Paoli, Pa.

Electrical Engineering Circuits by H. H. Skilling

Published (1957) by John Wiley & Sons, Inc., 440 Fourth Ave., N. Y. 16, N. Y. 694 pages+12 index pages+18 appendix pages+xi pages. 9¼×6¼. $8.75. Illus.

To write a generally acceptable book for the basic course in a-c circuits for electrical engineering students has long been a challenge, and a number of persons have addressed themselves to this challenge. The result has been a continuous stream of new books in the field. These efforts have usually been only partially successful in satisfying the "using" public, and I see no reason for expecting Prof. Skilling's book to be any more satisfying than the many similar books which predate his.

The content and presentation of the material of this book are largely traditional, with only minor basic differences between the content of this book and that by other authors. Of course, the choice of material may better meet the needs of some schools than do other books. If Prof. Skilling had really carried out in detail the statement made in his preface, that "we wanted a book in touch with modern thought," this reviewer might have been somewhat enthusiastic, but unfortunately the "touch" has been much too light. The accepted modern text for present-day needs must still be written.

Prof. Skilling's book is generally well-written, and appears to be a carefully presented development of a-c circuit theory. Many topics are included which often are found in somewhat more advanced texts. The balance between the order of difficulty of the subject matter and the time and space devoted to the material is usually good. There are a number of cases where new ideas are presented, but nothing is really done with them; and unfortunately most of the "modern" aspects of network theory get completely inadequate treatment. Thus the treatments of duality, network topology, and the complex s-plane, which could have distinguished this book from most others, are never really carried anywhere.

There are several specific points with which this reviewer disagrees. The use of the term phasor (which is a complex number) to represent a rotating line, requires that such complex numbers be distinguished from the complex numbers which represent impedance. This situation is further confused on pps. 80 and 253 by the effort to classify the phasor as a "transform." In its normal use, the phasor is not the "transform" of anything in a mathematical sense; it might conceivably be an heuristic transform, but it is not presented as such. The phasor contains only amplitude and phase information, and this may be related to a sinusoid, but no concept of a rotating line is essential.

In discussing the number of nodes and loops on pg. 285 a method is given for determining the number of independent loops of a network. This is a topological approach, but without any topological basis for the development. Much more should have been done with this topic.

The introduction to Chap. 17 begins with the statement that "The Laplace transformation method turns transients problems into steady-state problems." This is a very misleading statement, as the Laplace transformation transforms an integrodifferential equation into an algebraic equation, thereby permitting algebraic methods to be employed in the solution of the differential equation. Furthermore, no mention appears to be made that this is not the only transform that accomplishes this.

Chapters 18 and 19, which discuss two-terminal pair networks, and electric filters, are detailed considerations of rather special classes of network problems. Such detail almost seems out of place in such a general textbook, and these chapters could well have been omitted without any damage to the continuity of the book.

In summary, it appears that this book will take its place in the literature of a-c circuits, as a presentable and teachable book. It is a personal disappointment that Prof. Skilling chose a very traditional presentation, when he might really have led the way with a sorely needed "modern" book on a-c circuits.

SAMUEL SEELY
Case Inst. of Technology
Cleveland 6, Ohio

Fourth National Symposium on Reliability and Quality Control

Hotel Statler, Washington, D.C., January 6–7, 1958

The symposium will consist of 46 speakers and two panel sessions, a banquet, and ladies' program.

The keynote speaker will be Major Gen. F. L. Ankenbrandt, U.S.A.F. Rtd., Defense Electronic Products, RCA. Lawrence N. Hyland, Vice-President and General Manager of Hughes Aircraft Co., will deliver the major address at the banquet on Tuesday, January 7th at 7:00 p.m. His topic will be "The Challenge of Reliability to Management." At the same time the National Reliability Award will be presented by M. M. Tall; the IRE-PGRQC Award will be presented by Dr. Victor Wouk, Chairman of the IRE-PGRQC; the American Society for Quality Control in Electronics Division Award will be presented by I. W. Schoeninger.

There will be nine tours; one to the Naval Ordnance Laboratory, to the Potomac Railroad yard at Alexandria, Va., and to the NBC radio and TV station at 8 a.m. each morning.

January 6—10:00 a.m.

Ageing Effects in Transistors, R. M. Ryder, Bell Telephone Co.

Simplified Reliability Evaluation, C. M. Ryerson, RCA.

Deterioration and Failure as a Stochastic Process, M. L. Norden, NYU.

The Effects of Maintenance on Part Reliability, R. L. Madison, Aeronautical Radio Inc.

Current Military Reliability Specifications, D. W. Pertschuk, American Bosch Arma Corp.

Military Reports on Reliability, T. M. Child, U.S. Army; J. L. Miller, U.S. Navy; Lt. Col. J. S. Lambert, U.S.A.F.

2:00 p.m.

Mathematics and Statistics Used in Reliability, N. A. Woodbury, NYU.

Reliable System Design by Part Engineering, C. G. Walance, Hughes Aircraft Co.

Systematic Methods in Missile Seeker System Design, H. V. Cooper, Bendix Aviation Corp.

Reliable Design and Development Techniques, J. E. McGregor, IBM.

Panel on System Reliability Measurement, G. M. Armour, Moderator, G.E. Co.

7:30 p.m.

Reliability Definitions Panel—Open Discussion, C. M. Ryerson, Moderator, RCA.

January 7—9:00 a.m.

Accelerated Life Test in Airframe Manufacture, M. H. Simpson, General Dynamics Corp.

Accelerated Life Testing to Predict Failure Rate, B. Hecht, Sprague Electric Co.

Study of Accelerated Life Test Versus Field Operation, Joseph Kimmel, RCA.

Accelerated Light Test of Precision Resistors, H. S. Herrick, Erie Resistor Co.

Mechanical Airline Equipment Reliability Analysis, A. M. Hull, United Airlines, Inc.

Improved Reliability by Stabilizing the Transistor, O. R. Baker, IBM.

Some Reliability Factors of Electrical Insulation, N. M. Bashara, Univ. of Nebraska.

Large Digital Computer Dependability Measurements, G. B. McCarter, IBM.

2:00 p.m.

Reliability Versus Cost of Failure, G. A. Raymond, Remington Rand.

The Price of Reliability, A. L. Lambert, The Martin Co.

Significances of R & D—Reliability & Dollars, E. T. Welmers, Bell Aircraft Corp.

Reliability Costs for Spares at Remote Locations, R. J. Herman, Bell Telephone Lab.

Report on Northrop's Tube Surveillance Program, Dwight Hawley, Northrop Aircraft Co.

Design and Analysis of Comparison Tests on Parts, R. P. Bosley, American Bosch Arma Corp.

Evaluating Component Parts bythe Box Technique, R. Glaser, General Electric Co.

The Mechanisms of Failure of Tantalum Capacitors, M. E. Krasnow, Inland Testing Lab.

January 8—9:00 a.m.

Reason—Reliability and Reality, L. J. Jacobson, Electronic Industries Assoc.

Vendor Certification Program, D. A. Hill, Hughes Aircraft Corp.

Test Program Design for a Missile Guidance System, R. P. Grant, American Bosch Arma Corp.

Commercial Aspects of Guaranteed Reliability, W. A. MacCrehan, Bendix Radio Co.

Organization for Reliability, H. Knapp, Federal Telephone and Radio.

Talos Missile Data System Contributes to Management, R. R. Wendt, Bendix Aviation Corp.

Organizing Reliability in Airborne Equipment Manufacture, J. J. Crowley, General Dynamics Corp.

Organizing for Reliability at Westinghouse, Trevor Clark, Westinghouse Elec. Corp.

2:00 p.m.

Techniques & Relationships of Quality Control and Reliability, J. J. Riordan, Office of Secretary of Defense.

Controls for Reliability and Quality Assurance, H. G. Romig, Summers Gyroscope Co.

Propagation of Error Techniques in Electronic Circuits, M. Racite, IBM.

Vendor and Subcontractor Liaison for High Reliability, J. A. Rice, American Bosch Arma Corp.

Talos Reliability and Quality Education Program, W. H. Johnson, Bendix Aviation Corp.

Education and Engineering Reliability, A. B. Credle, IBM.

Training Evaluation Engineers for Reliability Programs, L. W. Ball, Stellardyne Lab.

Training Through Design Reviews, H. C. Bryson, Jr., RCA.

On the management committee of the Fourth Symposium on Reliability and Quality Control are (*left to right*): C. M. Ryerson, program; R. M. Jacobs, publicity; I. W. Schoeninger, vice-chairman; J. J. Mackey, arrangements vice-chairman; M. M. Tall, general chairman; M. Raphelson, secretary; J. W. Greer, vice-chairman; J. Kaufman, arrangements; and P. K. McElroy, Transactions. The symposium will be held at the Hotel Statler, Washington, D. C., January 6–8.

Abstracts of IRE Transactions

The following issues of "Transactions" have recently been published, and are now available from the Institute of Radio Engineers, Inc., 1 East 79th Street, New York 21, N. Y. at the following prices. The contents of each issue and, where available, abstracts of technical papers are given below.

Sponsoring Group	Publication	Group Members	IRE Members	Non-Members*
Antennas & Propagation	Vol. AP-5, No. 3	$2.00	$3.00	$6.00
Communications Systems	Vol. CS-5, No. 2	.70	1.05	2.10
Electron Devices	Vol. ED-4, No. 3	2.00	3.00	6.00
Engineering Management	Vol. EM-4, No. 3	.60	.90	1.80

*** Public libraries and colleges may purchase copies at IRE Member rates.**

Antennas & Propagation

Vol. AP-5, No. 3, July, 1957

News and Views (p. 245)

Contributions—An Interferometer for Radio Astronomy with a Single-Lobed Radiation Pattern—A. E. Covington and N. W. Broten (p. 247)

The 150-foot slotted wave guide antenna for operation on a wavelength of 10 centimeters at the National Research Council, Ottawa, Canada, is now in operation as one element of an interferometer. The other element is itself a simple interferometer with element separation equal to that of the long array and is placed to the west on the common E-W axis. A rotary phase shifter in the arm between the array and simple interferometer is used, after Ryle, with a phase-sensitive detector. The resultant pattern consists of the product of three terms: 1) the single-lobe pattern of the long array; 2) the interference pattern of the simple interferometer, and 3) the interference pattern between the simple interferometer and array. This configuration gives a twofold increase in E-W resolving power over a uniformly collecting aperture of equal dimension. The presence of two interference patterns suggests the name, "compound interferometer," and the new antenna produces a fan-shaped beam 2′ E-W×2° N-S. The instrument has been used to obtain daily drift curves of the sun.

Statistical Data for Microwave Propagation Measurements on Two Oversea Paths in Denmark—P. Gudmandsen and B. F. Larsen (p. 255)

Measurements were carried out on 6.4-cm and 17-cm wavelength on two optical paths, 54-km and 82-km long, stretching over sea nearly east-west and starting at the same point. For the greater part of the measurements, height-spaced receivers were used. The bulk of the statistical data comprises distributions of field strengths for every day of measurement. Curves for single receivers and diversity combinations of two receivers have been worked out. Distributions for every hour of a day as well as distributions of fade durations for a few days with special propagation conditions were obtained. A study of special fading phenomena with almost coinciding fades on the receivers in operation has been made.

The data reveal that the field strength distribution for single receivers on days with a great number of fades generally approximates the Rayleigh distribution irrespective of wavelength, path, and antenna height within the range of height considered. The field strength distributions for diversity systems approximate the diversity Rayleigh distribution, which is derived from two uncorrelated Rayleigh distributed signals. Deviations from appropriate Rayleigh distribution towards more serious fading conditions seem to be more frequent and more pronounced for diversity systems than for single receivers. Distributions of fade durations are found to be log-normal. Measurements on three-height-spaced receivers on 17-cm wavelength indicate that the simple two-ray theory is insufficient to describe the fadings on a path over sea.

Some Observations of Antenna-Beam Distortion in Trans-Horizon Propagation—A. T. Waterman, Jr., N. H. Bryant, and R. E. Miller (p. 260)

3000-mc signals from a rotating narrow-beam transmitting antenna have been observed at distances from 92 to 177 miles. The manner in which the received power builds up and falls off as the transmitting beam sweeps past the receiver shows a variety of shapes instead of merely reflecting the transmitting-antenna pattern, as would be expected on a line-of-sight path. From a series of these received-power patterns, mean received power as a function of transmitting-antenna azimuth is obtained and, from this, an angular scattering function is derived. This angular scattering function, which is a characteristic of the path only, is used to predict the optimum antenna size for this path. These observations are also used to predict the improvement provided by a diversity system employing two identical receiving beams separated in azimuth only.

Back-Scattering Cross Section of a Thin, Dielectric, Spherical Shell—M. G. Andreasen (p. 267)

The back-scattering cross section of a thin, dielectric, spherical shell is calculated on the basis of simplified boundary conditions at the shell. These conditions approximate the correct conditions at the shell better, the higher the dielectric constant of the shell, and the less the variation of the normal component of the electric field along the surface of the shell. Numerical results are added for a shell, whose electrical radius $kr_1 < 5$, and whose thickness d and dielectric constant χ_e obey the relation $(\chi_e - 1)kd = 0.4$. A comparison is made, with the results obtained, by applying Rayleigh's scattering law to objects that are small as compared to the wavelength.

Serrated Waveguide—Part I: Theory—R. S. Elliott (p. 270)

A corrugated waveguide in which the corrugations pierce the broad wall, permitting leakage, is called a serrated waveguide. Controlling the size and spacing of the serrations will permit the design of a practical traveling-wave antenna.

In this paper, an analysis is presented for the case of serrations which have a transverse dimension equal to the width of the broad wall, and longitudinal dimension and spacing that are small compared to a wavelength.

The analysis yields an expression for the complex propagation constant of the leaky hybrid mode in the serrated guide, and computations reveal an adequate range of leakage.

Serrated Waveguide—Part II: Experiment—K. C. Kelly and R. S. Elliott (p. 276)

Groups of nonresonant closely-spaced slots, cut in the broad wall of a rectangular waveguide, have been studied in a series of experiments. The name "serrated waveguide" has been applied to such structures. The complex propagation constant of the fundamental mode in a serrated waveguide has been measured as a function of slot size and spacing. The results have been used in the design of traveling-wave antennas with various aperture distributions. These antennas can be used for flush-mounted applications.

A Technique for Controlling the Radiation from Dielectric Rod Waveguides—J. W. Duncan and R. H. DuHamel (p. 284)

This paper describes a technique for controlling the radiation from a dielectric rod waveguide by placing obstacles or antenna elements at appropriate points along the waveguide. The HE_{11} mode on a dielectric rod was used to excite concentric rings and radial wires. The coupling of the obstacles to the HE_{11} mode was determined by constructing an image line with a slotted section for impedance measurements. This information was used to design several antenna arrays with different types of patterns. The measured patterns were very satisfactory.

A Circularly-Polarized Corner Reflector Antenna—O. M. Woodward, Jr. (p. 290)

Unidirectional, circularly-polarized radiation may be obtained by tilting a dipole in a corner reflector. Inherent advantages of this antenna are the simplicity of both the construction and adjustment. The theory of images is employed to develop the basic theory of the antenna for the cases of greatest practical interest. An experimental investigation has been made on the radiation characteristics of a practical-sized antenna as a function of its geometric parameters. From this data, an antenna producing unidirectional, circularly-polarized radiation has been designed and constructed.

Corner Reflector Antennas with Arbitrary Dipole Orientation and Apex Angle—R. W. Klopfenstein (p. 297)

This paper is concerned with the determination of corner reflector characteristics for reflectors of arbitrary apex angle excited by any infinitesimal dipole source which is tangent to a circular cylinder having the reflector axis as its axis. Use is made of the dyadic Green's functions for the perfectly conducting wedge recently given by Tai, and the results are obtained as infinite series of Bessel functions.

The quantities of interest are the relative phase and magnitude of vertical and horizontal components of electric field, the directive gain of the antenna, and the radiation resistance of the dipole source. These have been computed for a continuous range of apex angles from 30° to 180° for dipole-to-axis spacings up to about a wavelength.

The results of this general analysis are useful not only for the determination of reflector characteristics for apex angles not subject to image analysis, but also for the obtaining of certain limiting forms for small apex angles which are not readily apparent from the image analyses.

Mutual Impedance of Unequal Length Antennas in Echelon—H. E. King (p. 306)

The expression is developed for the mutual impedance between two staggered parallel center-fed, infinitely thin antennas of unequal lengths. Heretofore unpublished curves are presented here which display the mutual impedance characteristics for a variety of unequal antenna lengths in echelon.

Corrections (p. 313)

Communication—Determination of HF Skywave Absorption—G. L. Pucillo (p. 314)

A graphical method is employed as a means for facilitating the determination of hf skywave absorption for any given transmission path at any given time.

Abstracts of Papers From the IRE-URSI Symposium Held May 22–25, 1957—Washington, D. C. (p. 316)

Contributors (p. 333)

Communications Systems

Vol. CS-5, No. 2, September, 1957

Growth of Communications—G. T. Royden (p. 1)

A 60 KW Transmitter for Ionospheric Scatter Communications—J. L. Hollis, W. H. Collins and A. R. Schmidt (p. 3)

Some Properties of a Frequency Stabilizing Circuit—L. L. Campbell (p. 10)

J. B. Rudd has described a double-mixing circuit which transfers a signal of unstable frequency to a new frequency determined by a stable local oscillator. It is shown that the signal-to-noise ratio at the output of this circuit is related to the signal-to-noise ratio at the input in about the same way as these ratios are related in a square-law detector. The choice of one of the circuit parameters for arbitrary input noise spectrum is also discussed.

Generations of Oscillations with Equally Spaced Frequencies in a Given Band—D. Makow (p. 13)

One or two crystal oscillators determine the lowest and the highest frequency of the band, f_a and f_b, respectively. A self-excited oscillator is stabilized to the mean frequency, f_1, of the band by comparison of the difference frequencies f_1-f_a and f_b-f_1. A second oscillator stage can then be stabilized similarly, either to the midfrequency between f_1 and f_a or between f_1 and f_b. In each further stage the number of frequencies to which the corresponding oscillators can be stabilized is doubled. Thus, for example, ten stages make any of 1047 frequencies available. Further methods are described where each stage triples or quadruples the capacity of the system.

Design Considerations in a Wideband Microwave Mixer and IF Preamplifier—J. C. Rennie (p. 21)

Practical and Theoretical Design Considerations for Bridge Negative Feedback Amplifiers in Carrier Telephony—M. J. Cotterill and J. W. Halina (p. 26)

The problem of providing proper impedance matching for interconnecting circuitry in carrier telephony systems is of first-order importance.

Transmission branches that contain nonpassive elements, such as amplifiers, are of particular concern and thus require special treatment. Bridge feedback amplifiers employing a hybrid output transformer offer outstanding advantages as a solution.

Basic design formulae and a practical example with measured results are presented for such an amplifier.

Contributors to This Issue (p. 32)

Correction Notice (p. 34)

Electron Devices

Vol. ED-4, No. 3, July, 1957

Point Contact Rectifier Theory—Melvin Cutler (p. 201)

Point contact rectifiers have long been reputed to be unsusceptible to analysis. Although some features of their behavior are still poorly understood, there are a number of aspects which probably can be described quantitatively. In these cases, the difficulties are due to the complexity of the mathematical analysis rather than a lack of basic understanding.

The approaches used in the theoretical analysis of two aspects of point contacts are discussed: the forward characteristics at moderately high currents, and the breakdown in the reverse direction. For the former, a theoretical solution is obtained for a hemispherical *p-n* junction. The computed curves agree qualitatively with experimental ones; a quantitative check is complicated by the need to compute curves for many different parameters. The breakdown properties of a point contact diode are compared with the theory for avalanche breakdown in a junction where heating occurs.

Again, quantitative comparisons have not yet been made, but qualitative agreement encourages one to use the theory for obtaining design criteria in developmental work.

Junction Capacitance and Related Characteristics Using Graded Impurity Semiconductors—L. J. Giacoletto (p. 207)

The transition capacitance of a junction of semiconductors with constant impurity density is well-known and varies inversely with the square root of the bias voltage. This paper analyzes the variation of transition capacitance with bias voltage of a junction of semiconductors with graded impurity densities; *i.e.*, densities which are an arbitrary function of position. It is found that the transition capacitance can be simply related to a depletion width and that, in turn, depletion width can be related to the bias voltage. An analysis is also carried out for the impurity grading to produce a specified transition capacitance variation, as for instance, a linear variation of capacitance with bias voltage. It is also possible to determine impurity gradings to satisfy certain special conditions. An example of this type that is considered in some detail is the determination of the impurity grading which will produce avalanche breakdown simultaneously throughout the semiconductor. An important result of the analysis is that the capacitance vs bias voltage relation can be favorably modified by suitable choice of impurity grading. The practical realization of the various characteristics considered in this article is contingent upon techniques for fabricating semiconductors with specified impurity gradings.

A Three-Dimensional Analytic Solution for Alpha of Alloy Junction Transistors—A. J. Wahl (p. 216)

A three-dimensional analytic solution for the alpha of junction transistors with extended base region is presented in terms of arbitrary volume and surface recombination. The method also accommodates emitter and collector junctions of different size, as commonly encountered in high alpha alloy junction transistors. In principle, the solution can be carried to any desired degree of accuracy, but the large amount of labor involved in numerical evaluation of useful examples seriously impairs the practical value and for this reason the solution in its present form may well be largely of academic interest only.

The Transient Response of Photoconductive Camera Tubes Employing Low-Velocity Scanning—R. W. Redington (p. 220)

The transient signal which results from the characteristics of a low-velocity electron beam and the capacitance of the scanned surface has been calculated. A very slow transient of the hyperbolic type can result if the scanned surface is stabilized at a retarding field potential. The calculations have been verified by tests on a 6198 Vidicon, which was taken as an example. For this tube, the relative contributions of the "electronic transient" and the photoconductive decay to the observed transient response were determined. They make comparable contributions to the total transient.

Noise Wave Excitation at the Cathode of a Microwave Beam Amplifier—W. R. Beam (p. 226)

General equations are derived, giving the amplitudes of noise current and velocity for the many modes of space-charge wave propagation in an electron beam. The properties of the cathode taken into consideration are the current density and the emission velocity distribution as a function of position. Simplified cases are considered which show the order of magnitude of effects due to cathode nonuniformity and magnetic field strength. From present evidence, it can be shown that high noise figure in low noise tubes is almost certainly due to excess noise velocity, brought about by cathode nonuniformities. Suggestions are given for reducing these undesirable effects.

Design and Calculation Procedures for Low-Noise Traveling-Wave Tubes—L. D. Buchmiller, R. W. Degrasse, and G. Wade (p. 234)

A step-by-step procedure for designing low-noise traveling-wave tubes is presented in this paper. The procedure permits the rapid calculation of the significant design parameters corresponding to the conditions for minimum noise figure. The procedure includes the use of a special transmission-line type chart which facilitates the calculations and aids in understanding the principles involved in achieving low-noise behavior.

By using the chart in connection with a second procedure, noise figure variation with frequency and with the tube parameters can be predicted for arbitrary electron gun design.

Measured noise figures for two X-band low-noise tubes designed essentially by these procedures agree with the theoretically predicted noise figures to within 1.5 db.

High-Voltage Regulator Tubes for Color Television Receivers—R. E. Byram (p. 243)

With the advent of color television, it became very important to regulate the high-voltage supply in the receiver. This paper describes the RCA-6BD4-A and the RCA-6BK4 low-current beam triodes of the sharp cutoff type designed specifically for this purpose. Typical operation of the tubes is described, and the results of an analysis of the regulator circuit are given. When the 6BD4-A is used, the output of a regulated 20,000-volt supply does not drop more than 300 v as the load current is increased from 0 to 1 ma. For the same increase in load current, the output of a regulated 27,000-v supply does not drop more than 500 v. When the 6BK4 is used, the output of a regulated 25,000-v supply does not drop more than 500 v for a similar increase in load current. A feature of the regulator circuit is that variations in output voltage may be kept within plus or minus 1 per cent for input-voltage changes of plus or minus 10 per cent, or the compensation for input-voltage changes may be eliminated while the above compensation for load-current changes is maintained. The requirements of a high-voltage supply for use with the RCA color kinescopes are outlined, and the 6BD4-A and 6BK4 are shown to satisfy the desired specifications.

Traveling-Wave Amplifiers and Backward-Wave Oscillators for VHF—D. A. Dunn (p. 246)

An important aspect of the design of traveling-wave amplifiers and backward-wave oscillators for frequencies below 500 mc is the problem of obtaining a tube of reasonably small physical dimensions. Hollow beams of greater perveance than is obtainable with solid beams offer one method of reducing the size of such tubes by permitting operation at a lower voltage and greater gain per wavelength, for a specified beam power, than is possible in a solid beam tube. Some aspects of the design of minimum size hollow-beam forward-wave amplifiers using single helix circuits and backward-wave oscillators using bifilar helix circuits are presented. Several tubes of these types for operation below 500 mc have been built. Amplifier bandwidths and oscillator tuning ranges in excess of four to one in frequency have been obtained experimentally. Amplifier efficiencies in excess of 20 per cent and oscillator efficiencies in excess of 10 per cent have been achieved.

Beam Perturbations in Confined Flow Electron Beams With Planar Symmetry—D. A. Dunn and W. R. Luebke (p. 265)

An analysis of the perturbations in a confined flow beam from a two-anode gun as a result of lens effects at the gun apertures is presented for the case of parallel flow with planar symmetry. The results are presented in the form of plots of the amplitude of the perturbation as a function of the ratio of the final beam voltage at the second anode to the voltage of the first anode. The parameters are the magnetic field and the ratio of spacings between cathode and the first and second anodes. For magnetic fields greater than about twice the Brillouin field corresponding to the first anode voltage, the result is a very broad minimum of perturbation extending over a voltage ratio of the order of thirty to one up to a maximum voltage determined by the spacing ratio. The conditions for exact cancellation of the perturbation introduced at the first anode by the lens action of the second anode are considered, and a convenient chart for determination of these conditions is presented. The lens effect perturbation amplitude is shown to be much greater than that resulting from space charge in the absence of lens effects, except at or very near the voltage and spacing ratio that is correct for cancellation and at relatively low voltages and magnetic fields. It is also shown how these results can be applied to hollow cylindrical beams with and without center conductors.

The Development of a Tunable CW Magnetron in the *K*-Band Region—Z. Feev Fraenkel (p. 271)

The development of a low field, *K*-band, tunable cw magnetron is described. The major characteristics of the device are presented. The research leading towards the development of the magnetron is outlined. This research program had two major objectives: 1) the study of cathode back-bombardment in cw magnetrons, 2) the study of low field operation. The cathode back-bombardment was found to be closely related to two voltage regions at which large anode currents were drawn without any connection to magnetron operation. The close study of these effects made it possible to eliminate them in cw magnetrons through a particular choice of magnetron parameters. The research program culminated in the development of a low field, *K*-band, tunable cw magnetron, utilizing capacitive crown of thorns tuning. At a fixed operating point, an output power exceeding 10 watts at an efficiency exceeding 5 per cent can be obtained over a tuning range of 7 per cent. The tuning range can be doubled by lowering the output power requirements and making use of two operating points.

On the Performance of High Perveance Electron Guns—L. E. S. Mathias and P. G. R. King (p. 280)

A design of high perveance electron gun has recently been proposed by Müller.

An experimental investigation has been made of the electron beams produced from: 1) a gun designed directly from Müller's charts, and 2) a gun whose design is a modification of the Müller design to make it more suitable for high-voltage operation. The perveance in each case was about 2×10^{-6}. The distribution of the current density and the profile of the beam were examined, either by allowing the beam to fall on a plate coated with carbon, or by measuring the current passing through a pinhole in a screen which could be moved across the beam at a number of axial positions.

Electrostatic experiments showed that the beams were initially annular, but further along the axis the current density became highest at the center. This is attributed to crossing trajectories resulting from lens aberrations in an anode aperture whose diameter is comparable with the cathode-anode spacing.

With magnetic focusing, the current density distribution across the beam varied periodically along the axis to an extent which depended critically on the magnetic field conditions in the accelerating region of the gun.

Experimental Notes and Techniques (p. 287)

Contributors (p. 287)

Engineering Management

Vol. EM-4, No. 3, September, 1957

Views on Decentralization—E. U. DaParma (p. 85)

Management of a Navy Laboratory—Capt. J. M. Phelps, USN (p. 90)

Planning of Research Work at Westinghouse Electric—Clarence Zener (p. 94)

Management of a Dispersed Research and Development Facility—Thomas Meloy (p. 96)

Research Center in an Institute of Technology—J. E. Boyd (p. 99)

Motivating Engineers in a Balanced Military-Commercial Industry—R. S. Bell (p. 101)

The Public Relations Function in an Engineering Organization—T. E. Garrigan (p. 103)

The Project Overlay System of Research Organization—R. M. Bowie (p. 105)

Correction (p. 108)

Abstracts and References

Compiled by the Radio Research Organization of the Department of Scientific and Industrial Research, London, England, and Published by Arrangement with that Department and the *Electronic and Radio Engineer*, incorporating *Wireless Engineer*, London, England

NOTE: The Institute of Radio Engineers does not have available copies of the publications mentioned in these pages, nor does it have reprints of the articles abstracted. Correspondence regarding these articles and requests for their procurement should be addressed to the individual publications, not to the IRE

The Index to the Abstracts and References published in the PROC. IRE from February, 1956 through January, 1957 is published by the PROC. IRE, May, 1957, Part II. It is also published by *Electronic and Radio Engineer*, incorporating *Wireless Engineer*, and included in the March, 1957 issue of that journal. Included with the Index is a selected list of journals scanned for abstracting with publishers' addresses.

The number in heavy type at the upper left of each Abstract is its Universal Decimal Classification number and is not to be confused with the Decimal Classification used by the United States National Bureau of Standards. The number in heavy type at the top right is the serial number of the Abstract. D.C numbers marked with a dagger (†) must be regarded as provisional.

ACOUSTICS AND AUDIO FREQUENCIES

534.133-8 **3369**

Excitation of Ultrasonic Oscillations in Quartz—K. N. Baranski. (*C.R. Acad. Sci. U.R.S.S.*, vol. 114, pp. 517–519; May 21, 1957. In Russian.) A variable frequency oscillator of 5–10-w output was used to drive a 240-kc X-cut quartz plate to oscillate at frequencies up to 2 kmc. Diffraction measurements on the velocity of longitudinal waves in quartz have shown that, in the range of frequencies examined, this remains constant at 5750 m.

534.143:621.317.39 **3370**

Measurement of Longitudinal Vibrations in the Mc/s Frequency Range by means of Electrostatic Excitation and a F.M. System of Detection—P. G. Bordoni and M. Nuovo. (*Ricerca sci.*, vol. 27, pp. 695–706; March, 1957.) Description of apparatus with results of measurements on Al disks resonating at frequencies ranging from 0.5 to 5.5 mc.

534.2-14 **3371**

On the Propagation of Ultrasonic Waves of Finite Amplitude in Liquids—V. A. Krassilnikov, V. V. Shklovskaya-kordy and L. K. Zarembo. (*J. Acoust. Soc. Amer.*, vol. 29, pp. 642–647; May, 1957.) The dependence of the ultrasonic absorption coefficient on intensity was measured at 1.5 mc for water, ethyl and methyl ethers, toluene, transformer oil and glycerine by means of thermocouples.

534.2-8 **3372**

Action of Infrared Radiation on an Ultrasonic Stationary-Wave Field—C. Rossetti. (*C.R. Acad. Sci., Paris*, vol. 244, pp. 3038–3040; June 17, 1957.) Measurements made with an interferometer (1223 of 1953) show that infrared radiation is absorbed by a gas in which stationary ultrasonic waves are generated. Two different mechanisms are indicated, one purely thermal, the other of molecular origin.

534.232:534.641 **3373**

The Electrical and Mechanical Impedance of Electroacoustic Transducers—R. Bierl. (*Nachr. Tech. Z.*, vol. 10, pp. 160–167; April, 1957.) Equivalent electromechanical circuits are considered which take account of impedance changes during oscillations. The mechanical impedance of resonators with distributed mass and elasticity can be represented approximately by a combination of single-frequency resonators. Theory is confirmed by measurements on an electrodynamic system coupled to 1) a cylindrical tube, 2) an exponential horn.

534.232-8 **3374**

Research on the Acoustic Air-Jet Generator: a New Development—E. Brun and R. M. G. Boucher. (*J. Acoust. Soc. Amer.*, vol. 29, pp. 573–583; May, 1957.) Modifications which substantially increase the efficiency and available power output of the Hartmann air-jet ultrasonic generator are described.

534.232-8:538.652 **3375**

Performance of Magnetostrictive Transducers Made of Aluminium-Iron Alloy or Nickel-Copper Ferrite—Y. Kikuchi. (*J. Acoust. Soc. Amer.*, vol. 29, pp. 569–573; May, 1957.) Both Ni and the alloy Alfer (13.5 per cent Al) have as high a coupling factor as is necessary for transducers operating at resonance. Improvements in efficiency can be obtained by elimination of eddy currents, *e.g.*, by the use of ferrites such as $(NiO)_{0.85}(CuO)_{0.15}Fe_2O_3$. Details are given of ferrite transducers with electroacoustic efficiency 90 per cent suitable for high-intensity ultrasonic radiation in water at powers up to 3 w/cm². See also 904 of 1955 (Thiede).

534.232.001.4 **3376**

A Method for Measuring Solvent Resistance of Crystal-to-Crystal Adhesive Bonds—B. J. Faraday and D. J. G. Gregan. (*ASTM Bull.*, no. 222, pp. 42–45; May, 1957.) The apparatus described is suitable for testing bonds in butt-jointed crystals used for lf transducers.

534.75 **3377**

Effect of Time on Pitch Discrimination Thresholds under Several Psychophysical Procedures; Comparison with Intensity Discrimination Thresholds—E. König. (*J. Acoust. Soc. Amer.*, vol. 29, pp. 606–612; May, 1957.) See also 1237 of 1955 (Pollack).

534.75:621.3.108.7 **3378**

How Little Distortion Can We Hear?—M. Lazenby. (*Wireless World*, vol. 63, pp. 435–440; September, 1957.) The smallest amount of nonlinear distortion that can be detected by the ear is calculated from known nonlinear hearing effects and compared with existing measurements.

534.78 **3379**

Word Intelligibility as a Function of Time Compression—G. Fairbanks and F. Kodman, Jr. (*J. Acoust. Soc. Amer.*, vol. 29, pp. 636–641; May, 1957.) "An experiment is described in which words were automatically compressed in duration and presented to observers for identification. The effects of time compression and of time sampling are assessed and compared with those of periodic interruption. The results of an analogous nonauditory study of the effects of phonemic sampling are presented."

534.79 **3380**

Concerning the Form of the Loudness Function—S. S. Stevens. (*J. Acoust. Soc. Amer.*, vol. 29, pp. 603–606; May, 1957.) Results of experiments based on halving and doubling the loudness of 1-kc tone at different levels tend to confirm irregularities in the loudness function.

534.79 **3381**

Critical Bandwidth in Loudness Summation—E. Zwicker, G. Flottorp., and S. S. Stevens. (*J. Acoust. Soc. Amer.*, vol. 29, pp. 548–557; May, 1957.) The critical bandwidth at which loudness summation begins to depend on the spread of energy is approximately the critical bandwidth determined previously by methods involving thresholds, masking, and phase. See also 2944 of 1956 (Bauch).

534.84:621.395.623.8 **3382**

System of Sound Amplification in the Congress Hall of the Palace of Culture and Science in Warsaw—W. W. Furdujew (Furduev). (*Nachr. Tech.*, vol. 7, pp. 112–117; March, 1957.)

534.845 **3383**

On Standard Methods of Measurement in Architectural Acoustics—R. V. Waterhouse. (*J. Acoust. Soc. Amer.*, vol. 29, pp. 544–547; May, 1957.) The sound absorption of acoustical materials and the sound transmission loss of partitions are discussed.

621.395.623.7 **3384**

On the Low-Frequency Radiation Load of a

Bass-Reflex Speaker—R. H. Lyon. (*J. Acoust. Soc. Amer.*, vol. 29, p. 654; May, 1957.) The radiation load on the port-cone combination of a bass-reflex system near the fundamental resonance involves a coupling between the radiators which is calculated.

621.395.625.3:681.84.083.84 3385

Noise in a Magnetic Recording Tape—P. A. Mann. (*Arch. elekt. Übertragung*, vol. 11, pp. 97–100; March, 1957.) Magnetic domains arranged at random along the tape give rise to noise voltages when passing the reproducing head. Assuming a statistical distribution of domain position and orientation, the relation of noise voltage and frequency is expressed in an equation and plotted. After erasure a tape is noisier than an unused tape because the size of the domains cannot be reduced sufficiently.

ANTENNAS AND TRANSMISSION LINES

621.372.8 3386

The Scattering Effect of a Junction between Two Circular Waveguides—V. Papadopoulos. (*Quart. J. Mech. Appl. Math.*, vol. 10, pt. 2, pp. 191–209; May, 1957.) "The exact solution is found for the electromagnetic problem of the scattering effect of a junction between two semi-infinite circular pipes of radius a and b, respectively, $(a>b)$ and having the same axis. The solution involves constants which satisfy an infinite set of equations."

621.372.8 3387

Reflection at the Transition from Rectangular Waveguide to Sectoral Horn—G. Piefke. (*Arch. elekt. Übertragung*, vol. 11, pp. 123–135; March, 1957.) The reflection coefficient is calculated for a junction of waveguide and horn flared in the E plane or H plane. Curves of the coefficient are plotted for flare angles up to 90° for the range $1 \leq 2a/\lambda_0 \leq 2$, where a is the width of the waveguide and λ_0, the free-space wavelength. For horns flared in the H plane the reflection coefficient is independent of waveguide height. An approximate formula for very small flare angles is derived.

621.372.8:621.3.017.71 3388

Heat Loss in Grooved Metallic Surface—E. A. Marcatili. (PROC. IRE, vol. 45, pp. 1134–1139; August, 1957.) A theoretical method of evaluating the conduction-current losses in certain parallel periodic grooves in waveguide walls.

621.396.67:621.397.62 3389

Antenna-Multiplex System Design—H. K. Schlegelmilch, O. K. Nilssen, and W. Y. Pan. (*Electronics*, vol. 30, pp. 148–151; July 1, 1957.) A description of a distribution network giving an average isolation of 25 db between 256 television receivers connected to a single common antenna.

621.396.67.011 3390

A Reactance Theorem for Antennas—C. A. Levis. (PROC. IRE, vol. 45, pp. 1128–1134; August, 1957.) A rigorous expression for the frequency derivative of the input reactance of an arbitrary antenna, used to predict bandwidth properties.

621.396.673 3391

The Measurement of the Efficiency of Shoft Unbalanced Metre-Wave Aerials—M. Lohr. (*Nachr. Tech. Z.*, vol. 10, pp. 120–124; March, 1951.) The method described involves only simple impedance measurements and accuracy within 2 per cent is obtainable; examples are given.

621.396.674.1 3392

Terminated Circular Loop Aerial—S. B. Rao. (*Electronic Radio Eng.*, vol. 34, pp. 347–350; September, 1957.) An expression is derived for the radiation field of a circular loop with a terminating resistance diametrically opposite the feeding point. Experimental results using a small loop at 110 mc are given.

621.396.674.1 3393

Insulated Loop Antenna Immersed in a Conducting Medium—J. R. Wait. (*J. Res. Nat. Bur. Stand.*, vol. 59, pp. 133–137; August, 1957.) "A solution is given for the fields of a circular loop in a conducting medium. The loop is assumed to have a uniform current, and it is enclosed by a spherical insulating cavity. The impedance of the loop is also considered. It is shown that the power radiated from the loop varies approximately as the reciprocal of the radius of the cavity for a specified loop current. Furthermore, if the cavity is electrically small, relative to the external medium, the radiation field is not significantly affected by the presence of the cavity." See also 39 of 1953 (Wait).

621.396.677.43 3394

The Development of Rhombic Short-Wave Aerials for Wide-Band Radiation—M. Jacob. (*Bull. schweiz. elektrotech. Ver.*, vol. 48, pp. 422–428, 445; April 27, 1957.) Design curves and a monogram are given and their use explained by examples.

621.396.677.71 3395

Slotted-Cylinder Antenna with a Dielectric Coating—J. R. Wait and W. Mientka. (*J. Res. Nat. Bur. Stand.*, vol. 58, pp. 287–296; June, 1957.) "Analysis is presented for the fields produced by an arbitrary slot on a circular cylinder which has a concentric dielectric coating. Expressions for the far-zone fields are developed by evaluating the appropriate integrals using a saddle-point method. Numerical results are presented for the case of a narrow axial slot for a range of values of cylinder diameters and electrical constants of the dielectric coating. There is some evidence that the coating provides a trap or a duct for surface waves, resulting in an increase of over-all amplitude of the field in the backward direction."

621.396.677.71:621.398:621.396.934 3396

Beacon Antennas for Guided Missiles—W. E. Barrick and D. L. Brannon. (*Electronics*, vol. 30, pp. 166–168; March 1, 1957.) S-band and X-band antenna arrays consisting of three elements, equally spaced and circumferentially mounted on the missile, are fed in phase with polarization parallel to the missile axis. Three elements appear to be more satisfactory than a higher number.

621.396.677.8 3397

Directional Aerials with Apertures of Special Shape—G. F. Koch. (*Nachr. Tech. Z.*, vol. 10, pp. 175–186; April, 1957.) Side lobes of radiation can be reduced by using apertures of special shape (see also 936 of 1955). Rhombic reflectors are discussed as an example of uniformly illuminated radiator, and radiation patterns for perpendicular and oblique incidence are calculated. Nonuniformly illuminated apertures of paraboloidal reflectors bounded by cosine curves are also considered. Special reflectors of German manufacture are illustrated.

621.396.677.83 3398

Influence of a Dielectric Layer on the Reflecting Properties of a Nonsolid Reflector—V. G. Yampol'ski. (*Radiotekhnika, Moscow*, vol. 12, pp. 59–64; February, 1957.) A theoretical investigation is made of the field distribution at a mesh-type or perforated reflector showing that the reflecting properties are reduced by a covering dielectric layer, such as ice.

AUTOMATIC COMPUTERS

681.142 3399

The Development of a Business Computer System—A. S. Johnston and S. L. H. Clarke. (*J. Brit. IRE*, vol. 17, pp. 351–364; July, 1957.) Describes the Elliott 405 system, incorporating a 1.6-m nickel delay line and a new type of store using 35-mm film coated with magnetic oxide.

681.142 3400

LACE (The Luton Automatic Computing Engine)—(*Electronic Eng.*, vol. 29, pp. 306–312; July, and 380–385; August, 1957.) **Part 1**—R. J. Gomperts and D. W. Righton. The general-purpose analog computer in operation at the Guided Weapons Division ot the English Electric Company was designed to have a high utilization and growth factor. Four separate units called "bricks" are available which may may be operated in combination or separately. **Part 2**—J. C. Jones and D. Readshaw. A description of 1) an electronic multiplier and 2) an electronic general-purpose function generator developed for use with LACE.

681.142 3401

The "Metrovick 950" Digital Computer—R. M. Foulkes. (*Metropolitan Vickers Gaz.*, vol. 28, pp. 111–117; May, 1957.) The computer is a medium-speed general-purpose binary machine designed for application to mathematical and scientific problems. The first model was completed in July, 1956. Transistors are used in the computing circuits and thermionic tubes in the circuits for writing on the magnetic storage drum. The method of operation of the transistors is that described by Chaplin (see 36 of 1955).

681.142 3402

Electronic Computer Study of English Syntax Patterns—(*Tech. News Bull. Nat. Bur. Stand.*, vol. 41, pp. 84–86; June, 1957.) Report of an exploratory study for data-processing purposes.

681.142 3403

Typed Figures Translated into Computer Code: High-Speed Reading by Electric Automaton—(*Engineering, London*, vol. 183, pp. 348–349; March 15, 1957.) Description of a pilot model of the electronic reading automaton (ERA). A flying-spot scanning system provides 100 bits for the recognition of each typed figure. The use of many redundant bits ensures that minor defects in typescript do not affect the accuracy of the information supplied to the computer.

681.142:537.226/.227:546.431.824–31 3404

Barium Titanate and its Use as a Memory Store—Campbell. (See 3501.)

681.142:621.039 3405

The Place of Analogue Computers in Reactor Control—J. Walker. (*J. Electronics Control*, vol. 3, pp. 125–136; July, 1957.)

681.142:621.314.7 3406

Computer Delay Unit Uses Semiconductors—W. A. Seism. (*Electronics*, vol. 30, p. 173; July 1, 1957.) Three point-contact-transistor multivibrators are cascaded to provide a delay of 40 μsec per stage.

681.142:621.374.32:621.314.7 3407

Basic Logic Circuits for Computer Applications—G. W. Booth and T. P. Bothwell. (*Electronics*, vol. 30, pp. 196–200; March 1, 1957. "Digital computer circuits, including flip-flop, gated pulse amplifier, dc amplifier, power amplifier and indicator, use high-frequency junction transistors to obtain high reliability and performance characteristics. Circuits operate over temperature range of $-30°$ to $+60°$C; their low dissipation imposes minimum requirements on power supplies and cooling.

681.142:621.394.3 3408

Morse-to-Teleprinter Code Converter—W. R. Smith-Vaniz and E. T. Barrett. (*Elec-*

tronics, vol. 30, pp. 154–158; July 1, 1957.) An analog-digital computer converting international Morse-code signals into standard five-digit teleprinter code.

681.142:681.176 **3409**
Computer Selects Premium Bond Winners—R. K. Hayward, E. L. Bubb, and H. W. Fensom. (*Electronics*, vol. 30, pp. 138–143; July 1, 1957.) A description of the electronic random number indicating equipment (ERNIE) used to print a list of purely random bond numbers. See also *P.O. Elec. Eng. J.*, vol. 50, pp. 1–6; April, 1957 (Hayward and Bubb).

681.142 **3410**
Electronic Computers [Book Review]—T. E. Ivall (ed.). Publishers: Iliffe & Sons, London, and Philosophical Library, New York, 167 pp.; 1956. (*Nature, London*, vol. 179, p. 1095; June 1, 1957.) A nonmathematical introduction to the principles and applications of digital and analog computers.

CIRCUITS AND CIRCUIT ELEMENTS

621.3.012:[621.3.015.3+621.3.018.4 **3411**
Approximate Method for Determining the Relation between Frequency- and Transient-Response Characteristics in Radio Circuits—S. N. Krize. (*Elektrosvyaz*, no. 1, pp. 11–16; January, 1957.) The analysis is based on an approximate evaluation of the Fourier integral. Experimental results are given.

621.318.5:[681.142+621.316.7 **3412**
A Method of Synthesis of Computing and Control Switching Circuits—G. N. Povarov. (*Avtomatika i Telemekhanika*, vol. 18, pp. 145–162; February, 1957.) The method described is applicable to bridge-type multiple switching circuits, and particularly to symmetrical circuits. Illustrative examples are given. See also 1351 of 1957.

621.318.57:621.3.042 **3413**
Multihole Ferrite Core Configurations and Applications—H. W. Abbott and J. J. Suran. (PROC. IRE, vol. 45, pp. 1081–1093; August, 1957.) Describes applications to gating, memory storage, and miscellaneous switching. With suitable equipment, operation over a temperature of $-50°C$ to $+200°C$ is possible.

621.318.57:621.314.63 **3414**
Fast Switching by Use of Avalanche Phenomena in Junction Diodes—Salzburg and Sard. (See 3682.)

621.318.57:621.314.7 **3415**
Boosting Transistor Switching Speed—R. H. Baker. (*Electronics*, vol. 30, pp. 190–193; March 1, 1957.) The advantages of combining *p-n-p* and *n-p-n* transistors and other switching circuit improvements are briefly outlined.

621.318.57:621.387 **3416**
Counters and Control Circuits with Coincidence Thyratrons—L. Hartmuth. (*Nachr. Tech. Z.*, vol. 10, pp. 141–144; March, 1957.) The application of the thyratron Type ST80T is briefly discussed.

621.372.44:621.314.26 **3417**
Frequency Conversion with Nonlinear Reactance—C. H. Page. (*J. Res. Nat. Bur. Stand.*, vol. 58, pp. 227–236; May, 1957.) "A lossless nonlinear impedance subject to an almost periodic voltage (sum of sinusoids) will absorb power at some frequencies and supply power at other frequencies. Necessary and sufficient relations among these powers are found. It is shown that simple cubic capacitors ($Q \propto V^3$) are sufficient for producing any possible conservative modulation or distortion process." See also 2978 of 1956.

621.372.5 **3418**
The Ideal Power Transformer—a New Element in Electric Circuits—E. V. Zelyakh. (*Elektrosvyaz*, no. 1, pp. 35–47; January, 1957.) The quadripole discussed maintains the voltage ratio equal to the current ratio irrespective of the load. Its application to transistor amplifiers is described.

621.372.5 **3419**
Exact Electronic Integration—H. Wittke. (*Elektron. Rundschau*, vol. 11, pp. 73–74; March, 1957.) The improvement of integrating RC quadripoles by the addition of a feedback amplifier is discussed. See also 3060 of 1957.

621.372.5.012 **3420**
RC Network Analogue—A. K. Choudhury and B. R. Nag—(*Indian J. Phys.*, vol. 31, pp. 121–134; March, 1957.) "An RC analog for obtaining the steady state and transient response of networks is described. The zeros and poles of the network function are realized by a system of cascade feedback amplifiers, the input and feedback networks of the amplifiers being so arranged that the zeros and poles of the transfer function of the system are identical with those of the network function. The root loci of a few basic networks for the feedback amplifiers have been studied. A method of solving polynomial equations using the analog is also described."

621.372.5.012 **3421**
Application of Linear Systems to the Filtering of Complex Oscillations—F. M. Gol'tsman. (*Bull. Acad. Sci. U.R.S.S., Sér. Géophys.*, no. 5, pp. 584–594; May, 1957. In Russian.) A method is developed for deriving expressions for the frequency characteristics of physically realizable linear systems, and examples are given of improving the selectivity of the analytical characteristics of low-pass and high-pass filters. The theory of filters for transforming signals in a specified way is considered. Practical details are not discussed.

621.372.54 **3422**
Tables of Frequency Transformation and Band-Pass Filters—H. Weber and J. Martony. (*Tech. Mitt. schweiz. Telegr.-Teleph. Verw.*, vol. 35, p. 163; April 1, 1957.) Correction to 2366 of 1957: Tables III and V have been reprinted and are enclosed with this issue.

621.372.54:621.317.3 **3423**
Filter Circuits for Measurement Purposes—C. Moerder. (*Arch. tech. Messen*, pp. 95–96; April, pp. 115–118; May, and pp. 161–164; July, 1957.) Survey of methods used for filter calculations. Eighteen references.

621.317.34:621.372.54 **3424**
Wide-Range Analyser Traces Precise Curves—Feldman. (See 3590.)

621.372.54:621.375.13 **3425**
Feedback Filter with Continuously Variable Cut-Off Frequency—K. Posel. (*Trans. S. Afr. Inst. Elec. Eng.*, vol. 47, pt 12, pp. 373–382; December, 1956.) "A feedback filter employing a parallel-T network in the forward loop of a feedback amplifier is described with a cutoff frequency continuously variable over a range of 2.3 to 1. Theory of operation and design equations are presented." See also 1329 of 1956 (Thiele).

621.372.57:621.314.7 **3426**
The Iterative Characteristics of Active Quadripoles and their Equivalent Circuit as Applied to Transistors—C. Kurth. (*Frequenz*, vol. 11, pp. 107–114; April, 1857.) The representation of the general type of active quadripole in the form of two series-connected ideal active quadripoles, one reciprocal and the other nonreciprocal, is derived by the use of matrix methods. The solution is applied to transistor circuits where account must be taken of the internal coupling between output and input.

621.373.012.3 **3427**
Universal Curves for Electrical Oscillatory Circuits in Dimensionless Form—A. Frei and M. J. O. Strutt. (*Bull. schweiz. elektrotech. Ver.*, vol. 48, pp. 233–235; March 16, 1957.) The derivation and application of such curves are briefly outlined.

621.373.4:621.385.029.63 **3428**
On Multimode Oscillators with Constant Time Delay—V. Met. (PROC. IRE, vol. 45, pp. 1119–1128; August, 1957.) A discussion and analysis of high-speed switchable bistable oscillators, analogous to multivibrators. Graphical methods are used to demonstrate switching and threshold phenomena. In an experimental S-band system incorporating a traveling-wave tube, two modes at 2790 and 2985 mc could be established, with a switching time of 7 mμsec.

621.373.42.029.42 **3429**
A Very-Low-Frequency Three-Phase Oscillator—M. D. Armitage. (*Electronic Eng.*, vol. 29, pp. 318–323; July, 1957.) A cathode feedback circuit to increase the time constant of the RC networks in a phase-shift oscillator is discussed. A complete oscillator for the frequency range 0.01–40 c is described. Nonlinear resistors are incorporated in the anode loads for amplitude limiting. A three-phase output of 150 v peak-to-peak per phase is obtainable with total distortion about 1 per cent.

621.373.421:517.43 **3430**
The Periodic Solutions of the Differential Equation of a Resistance-Capacitance Oscillator—A. W. Gillies. (*Quart. J. Mech. Appl. Math.*, vol. 10, pt 1, pp. 101–121; February, 1957.) "The equation is normalized to the form $\{(D^2+1)(D+\sqrt{6}/5)+\epsilon D^3\}x+g(D)\Sigma_{n=2}c_n\mu^{n-1}x^n = g(D)2B\cos\omega t$, where ϵ and μ are small parameters which in the main part of the discussion are related by $\epsilon=\mu^2$, and $g(D)$ is a particular polynomial operator of the third degree. The procedure, previously applied to a second-order equation with unsymmetrical nonlinear damping, is used to obtain the periodic solutions having the period of the forcing term when ω is near to 1, *i.e.*, for the fundamental resonance."

621.373.421.11.076.12:621.316.86 **3431**
New Method of Temperature Compensation for Oscillator Circuits—F. Müller. (*Elektron. Rundschau*, vol. 11, pp. 68–73; March, 1957.) The experimental circuit described uses a thermistor as temperature-dependent device in conjunction with a reactance tube which converts resistance changes into compensating changes of L or C. Some recorded measurements, possible applications, and modifications are discussed.

621.373.52:621.314.7 **3432**
Transistor Oscillator Performance—M. R. E. Bichara. (*Nuovo Cim.*, vol. 5, pp. 702–706; March 1, 1957.) The frequency stability of two crystal-bridge-controlled transistor oscillators was examined. One, operating at 350 kc (see also 3203 of 1955) had its stability improved tenfold to within 0.00057 per cent by stabilizing its input voltage; the other, using different types of transistor and crystal, had a stability within ±0.00107 per cent at 100 kc.

621.373.52:621.314.7 **3433**
Transistor Oscillator Stability—M. G. Scroggie. (*Wireless World*, vol. 63, pp. 443–444; September, 1957.) Describes simple drift tests against the London Light Programme (1214 kc). The superiority of the Gouriet circuit is demonstrated, a temperature coefficient of -50 in $10^6/°C$ being obtained.

621.374.32:53.087 3434
Automatic Counting Techniques Applied to Comparison Measurement—C. C. H. Washtell. (*J. Brit. IRE*, vol. 17, pp. 397–402; July, 1957.) A gated dekatron chain and associated equipment print the ratio of counts of two independent pulse sources.

621.374.32:621.387.4 3435
A Fast Kicksorter Channel—R. D. Amado and R. Wilson. (*J. Sci. Instr.*, vol. 34, pp. 205–206; May, 1957.) A single-channel instrument which responds to pulses of 10^{-8}-seconds duration.

621.374.32:621.387.4 3436
A Multichannel Analyser using a Rectifier Matrix for Channel Selection—P. K. Patwardhan. (*J. Sci. Ind. Res.*, vol. 15A, pp. 439–443; October, 1956.) Description of a pulse-height analyzer using Type-5687 high-current-capacity tubes as buffer amplifiers, which gives a 1:3 voltage discrimination between the selected and the nonselected signal.

621.374.32:621.387.4 3437
Improvements on a Multichannel Pulse Analyser—S. Colombo, C. Cottini, and E. Gatti. (*Nuovo Cim.*, vol. 5, pp. 748–750; March 1, 1957. In English.) For the description of the original analyzer see 2016 of 1954 (Gatti).

621.375.4:621.314.7:546.28 3438
Compensating Silicon Transistor Amplifiers—S. H. Gordon. (*Electronics*, vol. 30, pp. 184–185; July 1, 1957.) Methods of temperature compensation in IF amplifiers using impedance mismatch, feedback, and thermistors.

621.375.9:538.569.4.029.6 3439
Inherent Noise in Quantum-Mechanical Amplifiers—Strandberg. (See 3460.)

GENERAL PHYSICS

535.13:531.51 3440
Influence of the Force of Gravity on the Propagation of Light—G. V. Skrotski. (*C.R. Acad. Sci. U.R.S.S.*, vol. 114, pp. 73–76; May 1, 1957. In Russan.)

537/538 3441
A New Formulation on the Electromagnetic Field—T. Ohmura. (*Progr. theoret. Phys.*, vol. 16, pp. 684–685; December, 1956.) By introducing new scalar and pseudo-scalar fields and a pseudo-vector magnetic current, a set of equations for an em field is combined into a single equation of form similar to the Dirac equation for the electron.

537/538 3442
Stability of the Electron—T. Ohmura. (*Progr. theoret. Phys.*, vol. 16, pp. 685–686; December, 1956.)

537.212:621.38.032.24 3443
Electrostatic Field of a Conducting Grid with Square Mesh—B. Ya. Mol'zhes. (*Zh. Tekh. Fiz.*, vol. 27, pp. 147–155; January, 1957.) An approximate solution for the electrostatic problem of a mesh of thin cylindrical wires is given. The cylinders are replaced by charged wires and an integral equation for the charge density is derived. The equipotential surface of the approximate solution coincides nearly everywhere with the cylinder surface.

537.228:538.63 3444
Behaviour of an Electron in a Periodic Electric and Uniform Magnetic Field: Part 1—G. E. Zil'berman. (*Zh. Eksp. Teor. Fiz.*, vol. 32, pp. 296–304; February, 1957.) The equation of motion of an electron in a weak magnetic field is determined. The broadening of the discrete electron energy levels in a crystal in a magnetic field is considered.

537.523 3445
Glow-Arc Transition in Current-Stabilized Electrical Discharges—J. Jenkins and T. B. Jones. (*J. Appl. Phys.*, vol. 28, pp. 663–668; June, 1957.) Accurate measurements in the unstable transition region were made possible by the use of a current-stabilized power supply and instrumentation for making voltage measurements in 0.02 μsec. Transitions can occur in argon at atmospheric pressure for currents between 0.002 a and at least 1 a. At low currents an oxide film must be present on the cathode.

537.525:535.61–15 3446
Infrared Emission from High-Frequency Discharges in CO_2—D. Cohen, R. Lowe, and J. Hampson. (*J. Appl. Phys.*, vol. 28, pp. 737–741; June, 1957.) The radiation was measured near 2.7μ and 4.3μ in a discharge driven by external electrodes at 10 mc at a pulse recurrence frequency of 5–30 c. The dependence of the emission on pressure and power were studied together with other characteristics of the discharges.

537.525.08:538.566.029.6 3447
Microwave Measurements of the Properties of a D.C. Hydrogen Discharge—B. J. Udelson, J. E. Creedon and J. C. French. (*J. Appl. Phys.*, vol. 28, pp. 717–723; June, 1957.) The measurements were made by exposing thin cross-sectional elements of the discharge in the gap between the cones of an S-band re-entrant cavity magnetron operating in the TM_{010} mode. The variation of electron density with tube current and gas pressure and electron collision frequencies are discussed.

537.533:061.3 3448
Exo-electrons—(*Acta Phys. austriaca*, vol. 10, pp. 313–480; March, 1957.) Texts of seventeen papers presented at the conference of the Austrian Physical Society held in Innsbruck on September 10 and 11, 1956.

537.533.8 3449
On the Theory of Secondary Emission of Metals—J. L. H. Jonker. (*Philips Res. Rep.*, vol. 12, pp. 249–258; June, 1957.) The angular distribution of secondary emission of Ni has been measured for small energy intervals. An explanation is given for this distribution following a cosine law.

537.56:538.56 3450
Plasma Acceleration by a Magnetic Field—A. I. Morozov. (*Zh. Eksp. Teor. Fiz.*, vol. 32, pp. 305–310; February, 1957.) The motion of ions and electrons is investigated assuming collisions, magnetic interaction of the particles, and wave excitation to be negligible. A critical charge density appears to exist in this case.

537.56:538.56 3451
Pulsations of String-Like Plasma—A. G. Kulikovski. (*C.R. Acad. Sci. U.R.S.S.*, vol. 114, pp. 984–987; June 11, 1957. In Russian.) The uniform axially symmetric movements of an unbounded gas with infinite conductivity are examined and equations are derived. A cylinder of finite length and radius is considered with ends in conducting material and with a pressure on its side equal to its internal pressure.

537.56:538.6 3452
Experimental Study of Plasmoids—W. H. Bostick. (*Phys. Rev.*, vol. 106, pp. 404–412; May 1, 1957.) By firing several plasmoids simultaneously across a magnetic field, it is possible to simulate in geometrical form the production of spiral galaxies and barred spirals.

537.56:538.63 3453
Conditions of Discharge in an Electromagnetic Cavity and Progressive Waves in Lorentz-Type Plasmas—R. Jancel and T. Kahan. (*C.R. Acad. Sci., Paris*, vol. 244, pp. 2894–2896; June 24, 1957.) Application of theory developed previously (3104 of 1957 and back references).

538.24 3454
Calculation of the Magnetization of a Prism at Constant Susceptibility—E. N. Mokhova. (*Bull. Acad. Sci. U.R.S.S., Sér Géophys.*, no. 5, pp. 680–682; May, 1957. In Russian.) The demagnetization coefficient for an inductively magnetized prism is calculated making simplifying assumptions for the measurement of the intensity of magnetization by the ballistic method.

538.3 3455
Nonlinear Electromagnetism and Photons—F. Destouches-Aeschlimann. (*C.R. Acad. Sci., Paris*, vol. 244, pp. 3034–3036; June 17, 1957.)

538.566:535.42 3456
The Diffraction of a Dipole Field by a Half-Plane—B. D. Woods. (*Quart. J. Mech. Appl. Math.*, vol. 10, pt 1, pp. 90–100; February, 1957.) A perfectly conducting half-plane is assumed. Solutions for arbitrary orientations of the dipole are determined by extending a method due to Bromwich, which was based on the solution of a scalar problem and valid only when the axis of the dipole is parallel to the edge of the screen. Results are given for an electric dipole with its axis normal to a screen and for an electric dipole with its axis normal to the edge of the screen and lying in a plane parallel to the screen.

538.566:535.42 3457
A Note on the Diffraction of a Dipole Field by a Half-Plane—W. F. Williams. (*Quart. J. Mech. Appl. Math.*, vol. 10, pt 2, pp. 210–213; May, 1957.) "A simple compact solution is given for the diffraction of the field of a dipole by a perfectly conducting half-plane." See also 3456 above.

538.569.4 3458
High-Stability Nuclear Magnetic Resonance Spectrograph—E. B. Baker and L. W. Burd. (*Rev. Sci. Instr.*, vol. 28, pp. 313–321; May, 1957.) Feedback of the error signal from a secondary nuclear resonance probe controls the oscillator driving frequency.

538.569.4.029.6:535.33 3459
Submillimetre-Wave Spectroscopy: Rotation—Inversion Transitions in ND_3—G. Erlandsson and W. Gordy. (*Phys. Rev.*, vol. 106, pp. 513–515; May 1, 1957.) Measurement of the $J=0\rightarrow1$ rotational transition of $^{14}ND_3$ at a wavelength of 0.97 mm.

538.569.4.029.6:621.375.9 3460
Inherent Noise of Quantum-Mechanical Amplifiers—M. W. P. Strandberg. (*Phys. Rev.*, vol. 106, pp. 617–620; May 15, 1957.) The noise figure or limiting sensitivity is derived. See also 1036 of 1957.

538.6 3461
Radiation in Anisotropic Media—F. V. Bunkin. (*Zh. Eksp. Teor. Fiz.*, vol. 32, pp. 338–346; February, 1957.) A general solution is derived for the problem of a field produced by a given current distribution in an infinite homogeneous medium of arbitrary anisotropy. The radiation field is expanded into multipoles and the radiation of a dipole in a magneto-active medium is also examined.

538.65 3462
Oscillations of an Infinite Self-Gravitating Cylinder of Gas in a Magnetic Field—I. M. Yavorskaya. (*C.R. Acad. Sci. U.R.S.S.*, vol. 114, pp. 988–990; June 11, 1957. In Russian.) The problem of radial movements of a gas of

cylindrical shape under a strong gravitational force and an internal magnetic field is considered.

GEOPHYSICAL AND EXTRATERRESTRIAL PHENOMENA

523.16 3463
New Observation of Cosmic Radiation at a Wavelength of 33 cm—J. F. Denisse, J. Lequeux, and É. Le Roux. (*C.R. Acad. Sci., Paris*, vol. 244, pp. 3030–3033; June 17, 1957.) Continuation of previous work (1635 of 1955). Some further localized sources are mentioned. One of these is thought to correspond with the supernova of 1572. Outside the galactic-plane regions no detectable variation in radiation was observed.

523.165:550.385 3464
27-Day Recurrence Tendency in the Daily Variation of Cosmic Ray Meson Intensity—R. P. Kane. (*Proc. Nat. Inst. Sci. India, A*, vol. 22, pp. 398–407; November 26, 1956.) Analysis of data for Huancayo for the period 1937–1945.

523.745:550.385 3465
On the Origin of the Long-Lived Solar Corpuscular Streams which Appeared Last Solar Cycle, 1950 to 1953—K. Sinno. (*J. Radio Res. Labs., Japan*, vol. 4, pp. 25–35; January, 1957.) A statistical study of the recurrence tendency of geomagnetic activity and coronal intensity.

523.75:621.396.822:523.16 3466
Solar-Flare Detection for I.G.Y.—R. H. Lee. (*Electronics*, vol. 30, pp. 162–165; March 1, 1957.) A 27-kc receiver records the sudden enhancements of atmospheric radio noise which accompany flares, while an 18-mc receiver records the simultaneous decrease in cosmic noise due to D-layer absorption. Both receivers have special circuits designed to reject unwanted signals of different kinds. Time-sharing between the two receivers is used and the outputs appear on a pen recorder.

550.3 3467
A Transient Magnetic Dipole Source above a Two-Layer Earth—J. S. Lowndes. (*Quart. J. Mech. Appl. Math.*, vol. 10, pt 1, pp. 79–89; February, 1957.) "The problem of a magnetic dipole acting as a transient current source when situated over a two-layer earth is considered by using the methods of integral transforms. The general expressions have been applied to deduce the induced field at the surface of the earth when the dipole is located on the surface, in the cases when the earth has homogeneous conductivity, and when the conductivities of the two layers are nearly equal." See also 413 of 1956 (Bhattacharyya).

550.38 3468
Electromagnetic Induction in Rotating Conductors—A. Herzenberg and F. J. Lowes. (*Phil. Trans., A.*, vol. 249, pp. 507–584; May 16, 1957.) An experimental and theoretical investigation of induction in a rotating conductor surrounded by a rigid conductor of finite or infinite extent. The results are applied to a discussion of induction in rotating eddies in the fluid core of the earth as a possible origin of the geomagnetic nondipole field.

551.510.52:[621.396.11+535.325 3469
Relation of Radio Measurements to the Spectrum of Tropospheric Dielectric Fluctuations—A. D. Wheelon. (*J. Appl. Phys.*, vol. 28, pp. 684–693; June, 1957.) The size spectrum of isotropic fluctuations is related to quantities which can be directly measured by radio techniques. Two types of experiment are analyzed: 1) line-of-sight phase and amplitude instability, 2) refractometer measurements of dielectric fluctuations.

551.510.535 3470
A Statistical Distribution Arising in the Study of the Ionosphere—M. S. Longuet-Higgins. (*Proc. Phys. Soc.*, vol. 70, pp. 559–565; June 1, 1957.) "An approximate distribution is deduced for the directions of the "lines of maxima" on a random surface. The theoretical distribution is found to be in good agreement with some experimental results obtained previously by Briggs and Page [755 of 1956]."

551.510.535 3471
Sporadic Ionization in the E Region of the Ionosphere at Medium Latitudes—W. Becker. (*Arch. elekt. Übertragung*, vol. 11, pp. 101–104; March, 1957.) With reference to the recommendations made by the Special Committee of U.R.S.I. on World-Wide Ionospheric Soundings, the more detailed classification of E_s layers by type and height is proposed. An analysis of records taken at Lindau shows at least five different causes for sporadic ionization.

551.510.535 3472
Effect of the *Sq* Current System on the Ionospheric E and F_1 Regions—T. Shimazaki. (*J. Radio Res. Labs., Japan*, vol. 4, pp. 37–48; January, 1957.) Departures from the diurnal variation in electron density predicted from Chapman's theory are discussed. They are due to vertical motion caused by a combination of the *Sq* current and the geomagnetic field. Gradients in scale-height and recombination coefficient are considered.

551.510.535 3473
A New Theory of Formation of the F_2 Layer: Part 2—The Effect of the Vertical Movement of Electrons and Ions on the Electron Density Distribution—T. Yonezawa. (*J. Radio Res. Labs., Japan*, vol. 4, pp. 1–14; January, 1957.) The vertical velocity is assumed to increase with height in inverse proportion to the molecular density. Solutions of the resulting equation are considered and typical data given for the height and electron density of the F_2 layer. Part 1: 3049 of 1956.

551.510.535 3474
On Differences of $f0F_2$ between June and December Viewed from a Worldwide Standpoint—M. Mambo. (*J. Radio Res. Labs., Japan*, vol. 4, pp. 59–71; January, 1957.)

551.510.535:523.745 3475
Relationship between the Semi-thickness of F_2 Layer at Tokyo and Solar Activity—I. Kasuya. (*J. Radio Res. Labs., Japan*, vol. 4, pp. 49–57; January, 1957.)

551.510.535:621.395.11 3476
The Proceedings of the International Convention on Radio Propagation in the Ionosphere—(See 3628.)

551.571 3477
Heterogeneity in the Measurements of Humidity Made by the Radiosonde Network of Europe—A. H. Hooper. (*Met. Mag., London*, vol. 86, pp. 13–21; January, 1957.) Discrepancies in the observations made by stations of the network are examined in respect of magnitude and speed of response to low-level moisture discontinuities of large magnitude. The likely causes are differences in the instruments and techniques used.

551.594:621.375.13 3478
Measuring Corona from Radioactive Point—R. W. Hendrick, Jr., F. C. Martin, and S. Chapman. (*Electronics*, vol. 30, pp. 172–173; March 1, 1957.) The amplifier described has logarithmic response and is used in conjunction with a radioactive corona point for atmospheric measurements in fair or disturbed weather.

551.594.21 3479
Leader Stroke Current in a Lightning Discharge According to the Streamer Theory—S. R. Khastgir. (*Phys. Rev.*, vol. 106, pp. 616–617; May 15, 1957.) A value is derived for the pilot leader current which is consistent with the observed electrostatic field change.

551.594.6:621.317.3 3480
Amplitude Probability Distribution of Atmospheric Noise on 10 Mc/s—T. Ishida and M. Higashimura. (*J. Radio Res. Labs., Japan*, vol. 4, pp. 73–75; January, 1957.) See also 3135 of 1956 (Yuhara, *et al.*).

LOCATION AND AIDS TO NAVIGATION

621.396.932 3481
One Year's Trials of a Surveillance Radar Installation for Marine Traffic Control at Bremerhaven—G. Wiedemann, H. Schellhoss, and H. Bruckmann. (*Nachr. Tech. Z.*, vol. 10, pp. 125–134; March, 1957.)

621.396.933.2 3482
Correlation and Phase Methods of Direction Finding—N. F. Barber. (*N. Z. J. Sci. Tech. B*), vol. 38, pp. 416–424; March, 1957.) A comparison of the two methods shows that their resolving powers are equal and their relative merits depend on the conditions of their application.

621.396.96:621.318.57 3483
Problems in Protection of Radar Receivers—G. D. Speake. (*Electronic Eng.*, vol. 29, pp. 313–317; July, 1957.) "The protection of a radio receiver from damage caused either by the associated system transmitter or from external sources is discussed. The main emphasis is placed on tr devices based on a gas discharge, and the advantages and limitations of these components are outlined. The use of other forms of protection, based for example on ferrites, and of traveling wave tubes as receiver components capable of withstanding relatively high pulse powers is briefly described."

621.396.963.3:621.318.57 3484
A Precision Electronic Switch for Fixed Coil Radar Displays—A. P. Young and D. H. Chandler. (*Marconi Rev.*, vol. 20, pp. 94–103; 3rd quart., 1957.) In designing a switching circuit to maintain an accurate correlation between operator-controlled marker positions and radar timebase. residual current in the tubes causes imperfections in switching action and limits the performance of a capacitor store used to counteract dc drift. These effects are overcome 1) by modifying the basic switching circuit so that an alternative source supplies the residual current, and 2) by using a nonlinear SiC resistor in an improved type of storage circuit.

621.396.969.3 3485
Helical Scan Nomograph—C. W. Wood. (*Electronics*, vol. 30, p. 186; July 1, 1957.)

MATERIALS AND SUBSIDIARY TECHNIQUES

535.215+535.376[:537.311.33 3486
Theory of Dynamic Quenching of Photoconductivity and Luminescence—F. Matossi. (*J. Electrochem. Soc.*, vol. 103, pp. 662–667; December, 1956.) A mathematical description of the dependence of quenching effects on time in terms of a simplified model of the energy levels and transitions in a semiconductor. Good agreement with experimental results for conductivity quenching in CdS is shown.

535.215:546.321.51 3487
Photoelectric Emission from Single-Crystal KI—H. R. Philipp and E. A. Taft. (*Phys. Rev.* vol. 106, pp. 671–673; May 15, 1957.)

535.215:546.47 31 3488
Influence of Impurities on the Photoconductance of Zinc Oxide—H. A. Papazian, P. A. Flinn, and D. Trivich. (*J. Electrochem. Soc.*, vol. 104, pp. 84–92; February, 1957.) "The photoconductance of pure ZnO and ZnO with known impurities, both in powder form, has been measured using a capacitor method. When irradiated by light, ZnO undergoes a 'memory mechanism' which depends on the past irradiation history. It is suggested that the memory is caused by formation of traps independent of charge-carrier formation. The concentration of traps is a function of impurity concentration and temperature."

535.215:546.482.21 3489
Hydrothermal Synthesis of Photoconductive Cadmium Sulphide—A. Kremheller and A. K. Levine. (*J. Appl. Phys.*, vol. 28, pp. 746–747; June, 1957.)

535.215:546.482.21 3490
Primary Photocurrent in Cadmium Sulphide—P. J. van Heerden. (*Phys. Rev.*, vol. 106, pp. 468–473; May 1, 1957.) Excitation by light flashes and by S particles produced primary photocurrent of both electrons and holes.

535.215:546.482.21 3491
Absorption of Light by CdS Crystals—V. L. Broude, V. V. Ermenko, and E. I. Rashba.—(*C.R. Acad. Sci. U.R.S.S.*, vol. 114, pp. 520–523; May 21, 1957. In Russain.) The luminescence of CdS at 20.4° K was investigated on samples 1-100 μ thick and with differing surface finishes; 10 absorption lines were found in the range 4875–4920 Å.

535.215:546.482.21:539.166 3492
Preparation of High-Sensitivity Cadmium Sulphide Cells for Gamma-Ray Detection—L. E. Hollander, Jr. (*Rev. Sci. Instr.*, vol. 28, pp. 322–323; May, 1957.)

535.243:546.482.21 3493
Line Spectrum of the Absorption Edge and Structure of Cadmium Sulphide Crystals—E. F. Gross, B. S. Razbyrin, and M. A. Yakobson. (*Zh. Tekh. Fiz.*, vol. 27, pp. 207–209; January, 1957.) Measurements were made at 4° K and lines of $\lambda = 4817$, 4816, and 4815 Å were found. See also 3270 of 1955 (Gross and Yakobson).

535.37:539.234 3494
Formation of Luminescent Films by Evaporation—C. Feldman and M. O'Hara. (*J. Opt. Soc. Amer.*, vol. 47, pp. 300–305; April, 1957.) Luminescent films of ZnS-Mn, Zn_2SiO_4-Mn, $Zn_3(PO_4)_2$-Mn, CaF_2-Mn, and $CaWO_4$-W have been formed by evaporation in vacuum and subsequent heat treatment. The luminescence brightness of fogged films, under cathode-ray excitation, approaches that of the powdered phosphors. Zn_2SiO_2-Mn films show most promise in respect of brightness and transparency. See also 444 of 1956 (Studer and Cusano).

535.37:546.791 3495
The Luminescence of Trivalent Uranium—L. N. Galkin and P. P. Feofilov. (*C.R. Acad. Sci. U.R.S.S.*, vol. 114, pp. 745–747; June 1, 1957. In Russian.) An investigation of CaF_2-U, SrF_2-U, and BaF_2-U with a uranium content of 0.1–0.3 per cent showed that these substances exhibit strong luminescence in the infrared region.

535.376 3496
Contact Electroluminescence—W. Lehman. (*J. Electrochem. Soc.*, vol. 104, pp. 45–50; January, 1957.) "Many powdered crystal phosphors which are normally nonelectroluminescent become electroluminescent if they are simply mechanically mixed with suitable powdered metals, or with some nonmetals of good electrical conductivity. The conclusion is drawn, and supported by many facts, that ordinary electroluminescence in powdered phosphors excited by an alternating electric field (Destriau effect) is also due to substances of relatively high conductivity incorporated as small segregations within the essentially insulating phosphor particles."

535.376 3497
The Light Output of some Phosphors Excited with Electrons of High Current Density—P. A. Einstein. (*Brit. J. Appl. Phys.*, vol. 8, pp. 190–194; May, 1957.) Equipment is described for observing the light output with pulse lengths from 30 to 6000 μsec and current densities from 10^{-5} to 2.7 a/cm². The rise and decay time constants generally increase with current density and empirical laws relating these parameters are given.

535.376:546.47.273 3498
Zinc Borate Phosphors and their Luminescent Properties—Yu. S. Leonov. (*C.R. Acad. Sci. U.R.S.S.*, vol. 114, pp. 976–979; June 11, 1957. In Russian.) Results of tests on the luminescence of $ZnO.B_2O_3$-Mn $3ZnO.B_2O_3$-Mn and $ZnO.B_2O_3$ with light of $\lambda = 2537$ Å and at temperatures ranging from about 170° to 500°K are summarized in graphical form.

535.376:546.472.21 3499
Voltage Dependence of Electroluminescence of Powdered Phosphors—W. Lehmann. (*J. Electrochem. Soc.*, vol. 103, pp. 667–672; December, 1956.) Report of measurements made on ZnS phosphors 1) with applied sinusoidal voltage v up to 600 v at frequencies between about 20 c and 50 kc, and 2) with voltages up to 3000 v at 60 c. The time-average electroluminescent intensity L is found to be in accordance with the equation $L = A \exp[-B/(V+V_0)]$, where A, B, and V_0 are constants.

535.376:546.472.21 3500
Effect of Crystal Disorder on the Electroluminescence of Zinc Sulphide Phosphors—A. H. McKeag and E. G. Steward. (*J. Electrochem. Soc.*, vol. 104, pp. 41–45; January, 1957.) "A blue electroluminescent ZnS phosphor was prepared by prefiring precipitated ZnS at a high temperature, activating with Cu, and refiring at about 700° C. The material was characterized by strong pale blue electroluminescence throughout the body of the crystal. The Cu entered most effectively at that temperature of refiring where the transformation from hexagonal to cubic structure occurred most readily." See also 1736 of 1956 (Short, *et al*).

537.226/.227:546.431.824 31:681.142 3501
Barium Titanate and its Use as a Memory Store—D. S. Campbell. (*J. Brit. IRE*, vol 17, pp. 385–395; July, 1957.) A practical 10×10 unit can be constructed in a square inch. Properties of the material limit the minimum access time to 10 μsec, but transistor drive circuits can be used since large currents are not required.

537.226/.227:546.48.882.5 3502
Dielectric Studies in the System CdO-Nb_2O_5—A. DeBretteville, Jr., F. A. Halden, T. Vasilos, and L. Reed. (*J. Amer. Ceram. Soc.*, vol. 40, pp. 86–89; March, 1957.) Room-temperature measurements in the paraelectric phase at 21 kmc indicate a dielectric constant of 150 with a dissipation factor of less than 0.002 as compared with the high losses of $BaTiO_3$ in this frequency range.

537.226 3503
Electrical Conductivity of Ceramic Materials in Strong Electric Fields—I. E. Balygin and H. T. Plaschchinski. (*Zh. Tekh. Fiz.*, vol. 27, pp. 138–146; January, 1957.) The conductivities of spinel and other ceramic materials for use at radio frequencies were measured and are plotted against temperature.

537.226:537.534.9 3504
Etching of Dielectrics by Ionic Bombardment—G. V. Spivak, A. I. Krokhina, T. V. Yavorskaya, and Yu. A. Durasova. (*C.R. Acad. Sci. U.R.S.S.*, vol. 114, pp. 1001–1003; June 11, 1957. In Russian.) The ionic bombardment of the surface of quartz, NaCl, $CaCO_3$ and Rochelle salt is described and photographs of the resultant etching are shown.

537.226.8 3505
Dependence of the Dielectric Strength of Ionic Crystals on Temperature—V. D. Kuchin. (*C.R. Acad. Sci. U.R.S.S.*, vol. 114, pp. 301–303; May 11, 1957. In Russian.) The dielectric strength of NaCl, KBr, KCl and KI was measured by an oscillographic method over the range −130° to +150°C for constant applied voltage and for pulses of 10^{-4}–10^{-8} sec.

537.227:546.431.811.824 31 3506
Research on the Electrostriction of Ferroelectric Ceramics—T. N. Verbitskaya. (*C.R. Acad. Sci. U.R.S.S.*, vol. 114, pp. 533–536; May 21, 1957. In Russian.) Four solid solutions of Ba (Ti, Sn)O_3 with differing Sn content were investigated. For the samples examined it was found that an increase in Sn content lowered the Curie point from +80° to +25° C. Graphs show the effect of temperature, with and without a dc field, on the coefficient of linear expansion and on capacitance.

537.227:621.318.57 3507
Polarization Reversal and Switching in Guanidinium Aluminium Sulphate Hexahydrate Single Crystals—H. H. Wieder. (PROC. IRE, vol. 45, pp. 1094–1099; August, 1957.) The substance has lower hysteresis losses and electromechanical activity than barium titanate and is easier to grow, but at present its use must be limited to low-speed (<1-kc) switching circuits.

537.228.1:548.0 3508
Piezoelectric Crystal Techniques—H. O. Koch. (*Frequenz*, vol. 10, pp. 373–383; December, 1956; vol. 11, pp. 53–57; February, 72–82; March, 1957.) After a general discussion of piezoelectric properties, methods of measuring piezoelectric constants and of determining flows in natural crystals and their relation to the aging characteristics of a crystal resonator are surveyed. Details and results of the method of etching in an electric field are given and its application in artificially reducing flaws in quartz crystals is indicated.

537.311.1+538.63+537.32+536.2 3509
Electrical Conductivity, Thermal Conductivity, Thermo-e.m.f., Hall Constant and Nernst Constant in Amorphous Bodies with n-Type Conductivity—A. I. Gubanov. (*Zh. Tekh. Fiz.*, vol. 27, pp. 3–11; January, 1957.) The temperature dependence of kinetic coefficients is calculated for amorphous conductors, taking into account the spherical scattering of electrons.

537.311.31:537.311.8 3510
Explosion of a Metal Due to an Electric Current—S. V. Lebedev. (*Zh. Eksp. Teor. Fiz.*, vol. 32, pp. 199–207; February, 1957.) The behavior of metal wires at currents of 5×10^5–5×10^6 a/cm² was investigated.

537.311.33 3511
Some Contributions to the Theory of Electrical Conductivity, Thermal Conductivity and Thermoelectric Power in Semiconductors—J. E. Parrott. (*Proc. Phys. Soc.*, vol. 70, pp. 590–607; June 1, 1957.) It is shown theoreti-

cally that the effects of phonon disequilibrium on electron transport phenomena and of electron disequilibrium on phonon transport phenomena are most noticeable in thermoelectric effects, but they may also be important in electrical and thermal conduction. The theoretical results show general agreement with experimental data.

537.311.33 3512
Radiative Transitions in Semiconductors—H. J. Bowlden. (*Phys. Rev.*, vol. 106, pp. 427–431; May 1, 1957.) Matrix elements are obtained for radiative intraband, and for allowed and forbidden interband transitions.

537.311.33 3513
Field Dependence of Mobility in Semiconductors—B. V. Paranjape. (*Proc. Phys. Soc.*, vol. 70, pp. 628 629; June 1, 1957.)

537.311.33 3514
Electrical Properties of Some Complex Oxide Semi-conductors—B. T. Kolomiets, I. T. Sheftel', and E. V. Kurlina. (*Zh. Tekh. Fiz.*, vol. 27, pp. 51–72; January, 1957.) Two main types of semiconductors, CuO-MnO-O_2 and CoO-MnO-O_2, are considered. The influence of composition, microstructure, or crystal lattice structure on the conductivity of the material is investigated. The conductivity in vacuum, air, or oxygen is also examined.

537.311.33 3515
Preparation and Investigation of Intermetallic Compounds in Thin Layers—V. A. Presnov and V. F. Synorov. (*Zh. Tekh. Fiz.*, vol. 27, pp. 123–126; January, 1957.) The electrical properties of Al-Sb, In-Sb, Ga-Sb compounds in the form of strips about 10^{-5} cm thick were investigated at pressures down to 10^{-6} mm Hg and the Hall constant was measured in an electromagnetic field of up to 7000 oersteds. Results are given in graphical form.

537.311.33:537.226.2/.3 3516
Investigation of Permittivity of Semiconductors—Z. I. Kir'yashkina, F. M. Popov, D. I. Bilenko, and V. I. Kir'yashkin. (*Zh. Tekh. Fiz.*, vol. 27, pp. 85–89; January, 1957.) The permittivity at cm λ was measured by two different methods. The free-wave method was used for materials such as WO_3, PbO, CuO, SnO_2, Ni_2O_3, ZnO, V_2O_5, Cu_2O, Na_2WO_4 of resistivity above 10_3 Ω cm, and semiconductors of lower resistivity, such as ZnS, CdS, ZnSe, ZnTe, CdSe, CdTe, HgS, HgSe, HgTe were tested in powder form in a paraffin dielectric. The results obtained are tabulated.

537.311.33:537.32:621.362 3517
Conversion [Efficiency] of Semiconductor Thermocouples—L. S. Stil'bans. (*Zh. Tekh. Fiz.*, vol. 27, pp. 212–213; January, 1957.) A simple expression is derived for the efficiency of semiconductor devices used for heat generation or refrigeration.

537.311.33:538.63 3518
Nernst-Ettingshausen Effect in Strong Magnetic Fields—I. M. Tsidil'kovski. (*Zh. Tekh. Fiz.*, vol. 27, pp. 12–22; January, 1957.) An experimental investigation on *n*-type HgSe specimens in fields up to about 10^4 oersted at temperatures between about 120 and 440° K is reported. The carrier mobility, u, in the various specimens could be calculated from the relation $(uH/c)=1$, where c is the velocity of light and H is the magnetic field at which the maximum of the E_y (H) curve occurs at the given temperature. These values, calculated from measurements of the transverse Nernst-Ettingshausen effect, were found to be in good agreement with those obtained from Hall-effect measurements. The longitudinal-transverse thermomagnetic effect, predicted by theory, and the longitudinal Nernst-Ettingshausen effect were also investigated.

537.311.33:538.63 3519
Investigation of the Influence of Recombination Processes on Galvanomagnetic Effects—S. A. Poltinnikov and L. S. Stil'bans. (*Zh. Tekh. Fiz.*, vol. 27, pp. 30–34; January, 1957.) Two effects were investigated experimentally in a single crystal of Ge with a resistivity of 27Ω cm: 1) the change in charge carrier concentration at two opposite surfaces of the specimen, and 2) change of resistance in a magnetic field in a specimen with different recombination velocities on opposite surfaces. Results are presented graphically.

537.311.33:538.639 3520
Influence of the Transfer of Electrons by Phonons on the Thermomagnetic Effect in Semiconductors—V. L. Gurevich and Yu. N. Obraztsov. (*Zh. Eksp. Teor. Fiz.*, vol. 32, pp. 390–392; February, 1957.) The influence of electron transfer by phonons on the Nernst-Ettingshausen effect in semiconductors is discussed.

537.311.33:546.23 3521
Equilibrium and Non-Equilibrium Electrical Properties of Polycrystalline Selenium—P. T. Kozyrev. (*Zh. Tekh. Fiz.*, vol. 27, pp. 35–44; January, 1957.) The temperature dependence of the electrical conductivity, thermo-emf, hole concentration, and mobility in the temperature range 40–200° C, the effect of pressure, and the relation between the equilibrium hole concentration, and the mobility at high temperatures were investigated in Se specimens containing 0.001 per cent Te, 0.0008 per cent S and 0.006 per cent other impurities. Results are presented graphically.

537.311.33:546.23 3522
The Influence of Iodine on the Thermal Conductivity of Selenium—G. B. Abdullaev and M. I. Aliev. (*C.R. Acad. Sci. U.R.S.S.*, vol. 114, pp. 995–996; June 11, 1957. In Russian.) Experiments show that the specific heat is independent of I content and is higher in amorphous than in crystalline Se samples: 0.118 cal/g° and 0.0701 cal/g°, respectively. The thermal conductivity decreases with increasing I and passes through a minimum for about 0.2 per cent I.

537.311.33:546.24:538.63 3523
Galvanomagnetic Properties of Tellurium at Low Temperatures: Part 1—S. S. Shalyt. (*Zh. Tekh. Fiz.*, vol. 27, pp. 189–204; January, 1957.) The conductivity and Hall constant of pure single-crystal Te were measured on specimens of differing purity in the temperature range 100°C–1.3° K. At 4.2° K an increase in the field strength produced a decrease of resistance much higher than that predicted by theory. This is explained by assuming that two groups of holes exist with mobilities of about 535 cm²/v sec and 9500 cm²/v sec, respectively.

537.311.33:546.26 1 3524
Magnetoresistance of a *p*-Type Semiconducting Diamond—E. W. J. Mitchell and P. T. Wedepohl. (*Proc. Phys. Soc.*, vol. 70, pp. 527–530; May 1, 1957.) The measured constants of the specimen are related to an equation derived from Seitz's theory. The results are similar to those obtained using *p*-type Ge and *p*-type Si.

537.311.33:[546.28+546.289 3525
Surface States on Silicon and Germanium Surfaces—H. Statz, G. deMars, L. Davis, Jr, and A. Adams, Jr. (*Phys. Rev.*, vol. 106, pp. 455–464; May 1, 1957.) On weakly oxidized surfaces these lie 0.42 and 0.13 ev above the Fermi level for intrinsic material, with approximate densities of 10^{11}–10^{12} cm^{-2} and 10^{10}–10^{11} cm^{-2} for Si and Ge, respectively. Corresponding figures for well oxidized surfaces are 0.44–0.48 and 0.18 ev, and 10^{12} and 10^{11}–10^{12} cm^{-2}. See also 2434 of 1956.

537.311.33:546.28 3526
The Drift Mobility of Carriers in High-Purity Silicon—M. Zerbst and W. Heywang. (*Z. Naturf.*, vol. 11a, pp. 608–609; July, 1956.) Brief report of tests on *p*- and *n*-type specimens derived from *p*-type Si of 200- to 2000-Ω cm resitivity. Results are compared with those of Prince (2421 of 1954). The temperature dependence of drift mobility for *p* and *n* type was found to be proportional to $T^{-2.3}$, electron mobility being about 1400–1450 cm²/v sec and hole mobility about 500 cm²/v sec

537.311.33:546.28 3527
Internal Field Emission in Silicon *p-n* Junctions—A. G. Chynoweth and K. G. McKay. (*Phys. Rev.*, vol. 106, pp. 418–426; May 1, 1957.) The forward and reverse dc characteristics of narrow *p-n* junctions, formed by solid-phase diffusion, have been studied. The interpretation of these involves internal field emission (Zener effect) rather than local avalanche breakdown.

537.311.33:546.28 3528
Thermal and Thermoelectric Properties of Alloys of Silicon with Transition Metals—P. V. Gel'd. (*Zh. Tekh. Fiz.*, vol. 27, pp. 113–118; January, 1957.) The results of investigations on Fe-Si, Cr-Si, and Mn-Si alloys are given in the form of graphs and tables.

537.311.33:546.28:621.314.63 3529
Silicon Diffused-Junction "Avalanche" Diodes—Veloric and Smith. (See 3680.)

537.311.33:546.28:621.314.64 3530
Anodic Formation of Oxide Films on Silicon—P. F. Schmidt and W. Michel. (*J. Electrochem. Soc.*, vol. 104, pp. 230–236; April, 1957.) Dense oxide films can be formed anodically on *p*- and *n*-type single crystal Si using a solution of KNO_3 in *N* methylacetamide and voltages up to 560 v.

537.311.33:546.28:621.793 3531
Electroless Nickel Plating for Making Ohmic Contacts to Silicon—M. V. Sullivan and J. H. Eigler. (*J. Electrochem. Soc.*, vol. 104, pp. 226–230; April, 1957.) The contact may be used on either *n*- or *p*-type Si.

537.311.33:546.289 3532
Field Effect in Germanium at High Frequencies—H. C. Montgomery. (*Phys. Rev.*, vol. 106, pp. 441–445; May 7, 1957.) Changes in conductivity near the surface have been investigated at frequencies up to 50 mc for both *n*- and *p*-type material, and in wet air, dry oxygen, and ozone ambients.

537.311.33:546.289 3533
Excess Noise in *n*-type Germanium—J. J. Brophy. (*Phys. Rev.*, vol. 106, pp. 675–678; May 15, 1957.) Experimental examination for single crystal Ge shows that the phenomena appears as a conductivity modulation caused by fluctuations in carrier density.

537.311.33:546.289 3534
Junctions Induced in Germanium Surfaces by Transverse Electric Fields—J. D. Nixon and P. C. Banbury (*Proc. Phys. Soc.*, vol. 70, pp. 481–485; May 1, 1957.) The surface conductance of Ge may be modulated by an external field produced by electrodes. A boundary effect appears between the field-free and field-applied surfaces near the edge of the electrodes. The transition region acts as a junction and the properties of such junctions are discussed.

537.311.33:546.289 3535
Influence of External Electrostatic Field on the Surface Recombination Velocity in Ger-

manium—V. P. Zhuze, G. E. Pikus, and O. V. Sorokin. (*Zh. Tekh. Fiz.*, vol. 27, pp. 23–29; January, 1957.) Experimental results on single crystals of *n*-type Ge with a resistivity of 30 Ω cm and on *p*-type Ge with 50-Ω cm resistivity indicate that the influence is negligible. This result is discussed.

537.311.33:546.289 3536
Influence of Heating Germanium by an Electric Current on the Thermal Acceptor Concentration—V. G. Alekseeva, B. N. Zobnina, and I. V. Karpova. (*Zh. Tekh. Fiz.*, vol. 27, pp. 215–217; January, 1957.) Specimens heated for 25–30 hours by dc showed no noticeable diminution in the concentration of thermal acceptors below 700°C but above this temperature a change in concentration occurs. The samples changed from *n* type into *p* type with increase in resistance. Graphs show that with ac heating the concentration of acceptors is higher.

537.311.33:546.289 3537
Diffusion and Solubility of Iron in Germanium—A. A. Bugaĭ, V. E. Kosenko, and E. G. Miselyuk. (*Zh. Tekh. Fiz.*, vol. 27, pp. 210–211; January, 1957.) The radioactive isotope ^{59}Fe was used for investigations in the temperature range 750–950°C. The maximum diffusion of $1.5 = 10^{15}$ atoms/cm³ occurred near 850°C.

537.311.33:546.289 3538
The Oxidation of Germanium—O. Rösner. (*Z. Metallkunde*, vol. 48, pp. 137–141; March, 1957.) The oxidation of single-crystal and polycrystalline Ge of various degrees of purity subjected to six different oxidizing agents, including air, water, and CO_2 was investigated. Single crystals are less oxidized than polycrystalline Ge of equal purity; oxidation decreases with increasing purity. See also 3001 of 1955.

537.311.33:546.289 3539
Rates of Oxidation of Germanium—J. T. Law and P. S. Meigs. (*J. Electrochem. Soc.*, vol. 104, pp. 154–159; March, 1957.) "Oxidation rates of the (110), (111), and (100) faces of a Ge crystal have been measured between 450° and 700°C and at various oxygen pressures."

537.311.33:546.289:539.433 3540
Internal Friction and Defect Interaction in Germanium: Experimental—J. O. Kessler. (*Phys. Rev.*, vol. 106, pp. 646–653; May 15, 1957.) The logarithmic decrement of germanium crystals undergoing small-amplitude longitudinal forced vibrations was measured as a function of temperature, frequency and concentration of impurities, and edge dislocations. Results are tentatively interpreted in terms of the stress-induced migration of lattice vacancies.

537.311.33:546.289:539.433 3541
Internal Friction and Defect Interaction in Germanium: Theoretical—J. O. Kessler. (*Phys. Rev.*, vol. 106, pp. 654–658; May 15, 1957.) A model is proposed for the energy dissipation caused by the stress-induced change in the equilibrium distribution of relatively mobile impurities around dislocations and used to derive numerical results corresponding to those derived from experiment. For details of the experimental work, see 3540 above.

537.311.33:[546.3-1.92+546.3-1.59 3542
Intermetallic Compounds of Platinum and Gold with Alkali and Alkaline-Earth Metals—I. L. Sokol'skaya. (*Zh. Tekh. Fiz.*, vol. 27, pp. 127–129; January, 1957.) The electrical properties of Na-Au, Na-Pt, and Ba-Pt were investigated in vacuum.

537.311.33:546.48.86 3543
Electrical Properties of the Intermetallic Compound CdSb—I. M. Pilat. (*Zh. Tekh. Fiz.*, vol. 27, pp. 119–122; January, 1957.) Experimental results based on the investigations of Justi and Lautz (1099 of 1954) show the influence of impurities and temperature changes from −180° to +250°C on the electrical properties of CdSb. Rectifying properties of CdSb produced by the addition of Al, Te, Pb, or Sn impurities are also considered; additions of Al gave the best results.

537.311.33:[546.682.19+546.681.19 +546.682.18 3544
The P-T-x Phase Diagrams of the Systems In-As, Ga-As and In-P—J. van den Boomgaard and K. Schol. (*Philips Res. Rep.*, vol. 12, pp. 127–140; April, 1957.) The maximum melting point for InAs is 943±3°C at an arsenic vapor pressure of 0.33 atm, and for GaAs 1237±3°C at 0.9 atm; that estimated for InP is 1062±7°C at phosphorous vapor pressure of 60 atm.

537.311.33:546.682.86 3545
Diffusion of Indium, Antimony and Tellurium in Indium Antimonide—B. I. Boltaks and G. S. Kulikov. (*Zh. Tekh. Fiz.*, vol. 27, pp. 82–84; January, 1957.) The influence of temperature on the diffusion coefficient in InSb was investigated by means of radioactive isotopes ^{114}In, ^{124}Sb, and ^{127}Te. The coefficients were found to vary exponentially with temperature, the coefficient for In being highest and that for Sb lowest at any given temperature.

537.311.33:546.682.86 3546
The Kinetics and Mechanism of Formation of Anode Films on Single-Crystal InSb—J. F. Dewald. (*J. Electrochem. Soc.*, vol. 104, pp. 244–251; April, 1957.)

537.311.33:546.78-3 3547
Electrical Properties of Some Complex Tungsten Oxides—Z. I. Ornatskaya. (*Zh. Tekh. Fiz.*, vol. 27, pp. 130–137; January, 1957.) The coefficient of specific conductivity and the thermo-emf of specimens of Na_2WO_4 and Li_2WO_4 heated in air and in vacuo were investigated. Their dissociation energies were found to be about 0.94 and 1.43 ev, respectively. The conductivity and mechanical properties of samples stored in air did not alter. Na-W and Li-W bronzes were also examined.

537.311.33:546.817.221 3548
Lifetime of Carriers in Lead Sulphide Crystals—W. W. Scanlon. (*Phys. Rev.*, vol. 106, pp. 718–720; May 15, 1957.) Experiments show that the lifetime is determined mainly by the density of dislocations in the crystals and is independent of crystal resistivity for a high dislocation density.

537.311.33:[546.817.23+546.817.241]:537.32 3549
Investigation of Thermoelectric Properties of Lead Telluride and Selenide—N. V. Kolomoets, T. S. Stavitskaya, and L. S. Stil'bans. (*Zh. Tekh. Fiz.*, vol. 27, pp. 73–81; January, 1957.) The properties of PbTe and PbSe were investigated between 0 and 450°C, and between 100 and 700°K. The effect of temperature and carrier concentration on the thermo-emf was observed. At temperatures below 200°K the thermo-emf deviated from the theoretical characteristics. The influence of different compositions and temperatures on the carrier mobility were also examined.

537.311.33:666.2:546.881.5-31 3550
Semiconducting Properties of some Vanadate Glasses—P. L. Baynton, H. Rawson, and J. E. Stanworth. (*J. Electrochem. Soc.*, vol. 104, pp. 237–240; April, 1957.) "Glasses have been made in the systems $BaO-V_2O_5-P_2O_5$ and $Na_2O-BaO-V_2O_5-P_2O_5$ with V_2O_5 contents ranging between 50 and 87 mole per cent. The glasses were found to be semiconductors, those with the highest V_2O_5 contents having a specific conductivity of the order of $10^{-5}\ \Omega^{-1}\cdot cm^{-1}$ at room temperature."

537.311.33.002.2:338.45 3551
Semiconductor Manufacture—(*Elec. Rev., London*, vol. 160, pp. 969–970; May 24, 1957.) A new Mullard plant at Southampton is to employ between 1500 and 2000 people. About a third is completed. Details of the production of Ge transistors are given.

537.311.33.07 3552
A Miniature Dry-Box for Semiconductor Work—P. R. Rowland and G. W. Whiting. (*J. Sci. Instr.*, vol. 34, p. 207; May, 1957.) Brief descriptive note of arrangement in which the micromanipulator is mounted outside the dry box.

538.22 3553
On a Higher Approximation of the Critical Field Strength for an Antiferromagnetic—K. F. Niessen. (*Phillips Res. Rep.*, vol. 12, pp. 259–269; June, 1957.) "The critical magnetic field strength is derived for an antiferro-magnetic with different anisotropy constants for the two sublattices, account being taken of the field-strength dependence of the parallel and perpendicular susceptibilities and a higher approximation of the anisotropy energy." See also 3015 of 1955.

538.22:546.65 3554
The Magnetic Susceptibilities of Lanthanum, Cerium, Praseodymium, Neodymium and Samarium, from 1.5°K to 300°K—J. M. Lock. (*Proc. Phys. Soc.*, vol. 70, pp. 566–576; June 1, 1957.) At the lowest temperatures cerium, neodymium, and samarium appear to become antiferromagnetic.

538.22:546.657 3555
Magnetic Properties of Neodymium Single Crystals—D. R. Behrendt, S. Legvold, and F. H. Spedding. (*Phys. Rev.*, vol. 106, pp. 723–725; May 15, 1957.)

538.22:546.668 3556
The Magnetic Susceptibility of Ytterbium from 1.3°K to 300°K—J. M. Lock. (*Proc. Phys. Soc.*, vol. 70, pp. 476–480; May 1, 1957.) Conclusions regarding the distribution of electrons are given.

538.22:621.385.833 3557
A New Method of Observing Magnetic Transformations—M. Blackman, G. Haigh, and N. D. Lisgarten. (*Nature, London*, vol. 179, pp. 1288–1290; June 22, 1957.) The focus of an electron diffraction camera was deflected by the use of coils carrying ac near which a specimen of a magnetic material was placed. Solid haematite, magnetite, and pyrrhotite, and powdered maghaemite (γFe_2O_3), magnetite and haematite, and a reversing spinel were examined.

538.221 3558
Critical Size and Nucleation Field of Ideal Ferromagnetic Particles—E. H. Frei, S. Shtrikman, and D. Treves. (*Phys. Rev.*, vol. 106, pp. 446–455; May 1, 1957.) The nucleation field is calculated for an infinite cylinder and a sphere, while the critical size for single-domain behavior is calculated for a prolate ellipsoid.

538.221 3559
Minimum Saturating Fields for Ferromagnetic Crystals—J. S. Kouvel. (*J. Appl. Phys.*, vol. 28, pp. 704–706; June, 1957.) The conditions for magnetic saturation are investigated analytically for a very thin single-crystal disk or spheroid. The applicability of the calculated minimum saturating fields to torque measurements is discussed.

538.221 3560
On the Width and Energy of Domain Walls in Small Multi-Domain Particles—H. Amar. (*J. Appl. Phys.*, vol. 28, pp. 732–733; June, 1957.) It is shown that the inclusion of the magnetostatic energy in the derivation of the wall characteristics in two-domain ferromagnetic particles yields values of these characteristics which differ considerably from those in bulk material.

538.221 3561
On the Mechanism of Magnetite Oxidation—W. I. Arkharov and B. S. Borisov. (*C.R. Acad. Sci. U.R.S.S.*, vol. 114, pp. 293–296; May 11, 1957. In Russian.)

538.221:621.318.134 3562
The Dependence of Coercive Force on Particle Size in Ferrites—W. Holzmüller and G. Rüger. (*Nachr. Tech.*, vol. 7, pp. 118–121; March, 1957.) The coercivity of sintered Ni-Zn and Mn-Zn ferrites was measured before and after grinding. In the resulting powders increases in coercive force by factors up to 60 were noted; after subsequent reheating the coercive force decreased. An interpretation of these results is given.

538.221:621.318.134 3563
The Magnetoresistance of the Nickel-Zinc Ferrite System—R. Parker. (*Proc. Phys. Soc.*, vol. 70, pp. 531–533; May 1, 1957.) Smit's model (*Physica*, vol. 17, pp. 612–627; June, 1951.) is inadequate to account for the observed effects.

538.221:621.318.134 3564
Microwave Properties of some Chromite-Ferrites of Nickel-Zinc—C. Guillaud, R. Vautier, and W. Kagan. (*C.R. Acad. Sci., Paris*, vol. 244, pp. 2781–2784; June 3, 1957.) X-band measurements made at constant static field of Faraday rotation θ and attenuation α on cylindrical specimens of chromite-substituted Ni-Zn ferrites show the ratio θ/α to increase with Cr_2O_3 content for percentages up to 15 or 20 per cent.

538.221:621.318.134 3565
Variation of the Resonance Field in Chromite-Ferrites of Nickel-Zinc—R. Vautier and W. Kagan. (*C.R. Acad. Sci., Paris*, vol. 244, pp. 3040–3043;, June 17, 1957.) See 3564 above. Further measurements show that the resonance field strength decreases with increasing percentage Cr_2O_3 contrary to theory.

538.221:621.318.134 3566
Controlled Crystal Anisotropy and Controlled Temperature Dependence of the Permeability and Elasticity of Various Cobalt-Substituted Ferrites—C. M. van der Burgt. (*Philips Res. Rep.*, vol. 12, pp. 97–122; April, 1957.) "Dynamic elasticity at remanence, piezomagnetic coupling at remanence, and initial permeability of polycrystalline toroids of various cobalt-substituted ferrites are determined in temperatures range from −196°C to +120°C at least. The compositions are represented approximately by $(M_{1-y}Zn_y)_{1-x}Co_xFe_2O_4$, where M stands for one of the divalent metal ions $Li_{\frac{1}{2}}^{1+}Fe_{\frac{1}{2}}^{3+}$, Ni^{2+}, and Mn^{2+}." Forty-eight references.

538.221:621.318.134 3567
Oxidation of Manganese Ferrite—R. S. Weisz. (*J. Amer. Ceram. Soc.*, vol. 40, pp. 139–142; April 1, 1957.)

538.221:621.318.134:538.569.4 3568
Temperature Dependence of the g-Factor and Relaxation Time in Ferromagnetic Resonance of Some Ferrites—A. P. Komar and N. I. Krivko. (*C.R. Acad. Sci. U.R.S.S.*, vol. 114, pp. 64–66; May 1, 1957. In Russian.) The magnitude of the observed decrease of the g factor, in some ferrites, with a decrease in temperature cannot be explained on the basis of existing microscopic theories. The experimental results are tabulated.

538.221:621.318.134:538.66 3569
The Effect of Grain Size on the Magnetothermal Properties of Ferrites—D. A. Christoffel. (*Proc. Phys. Soc.*, vol. 70, pp. 623–625; June 1, 1957.) Measurements on two samples of Ni ferrite show differences which are attributed to different particle sizes in the two cases.

538.652 3570
Magnetostriction of Aluminum-Iron Single Crystals in the Region of 6 to 30 Atomic Per cent Aluminum—R. C. Hall. (*J. Appl. Phys.*, vol. 28, pp. 707–713; June, 1957.) The spontaneous saturation magnetostriction and the forced magnetostriction were measured on slowly cooled single crystals. The results are shown in graphical and tabular form.

539.16/.18:[537.311.3+549.514.51 3571
The Effect of Radiation Damage on the Electronic Properties of Solids—E. W. J. Mitchell. (*Brit. J. Appl. Phys.*, vol. 8, pp. 179–189; May, 1957.) A discussion of the effects of atomic displacements produced by elastic collisions between the nuclei and the incident high-energy radiation, with special reference to electron mobility in metals, carrier concentration in Ge, and optical absorption in quartz and diamond. Fifty references.

539.23:537.311.33:546.492.31.46 3572
Some Peculiarities of the Electrical Properties of HgSe-HgTe Films—O. D. Elpat'evskaya and A. R. Regel'. (*Zh. Tekh. Fiz.*, vol. 27, pp. 45–50; January, 1957.) Investigations on transparent and opaque film show that carrier mobility increases with the thickness of the film. Tables showing the variation of specific conductivity, Hall constant, carrier mobility, and concentration with film thickness are given.

539.23:546.571 3573
Oxide Films on Silver at High Temperatures—D. E. Davies. (*Nature, London*, vol. 179, pp. 1293–1294; June 22, 1957.) It is shown that Ag_2O may exist at temperatures up to 800°C.

548.0:537 3574
Relation between the Electrical Properties of Crystals and the Crystal Lattice Parameters—V. A. Presnov and V. I. Gaman. (*C.R. Acad. Sci. U.R.S.S.*, vol. 114, pp. 67–69; May 1, 1957. In Russian.) A preliminary calculation of the relation for alkalihalide crystals is reported.

621.357.8 3575
Electrolytic Surface Phenomenon and its Application in Precision Engineering—M. Naruse and A. Nannichi. (*Technol. Rep. Tohoku Univ.*, vol. 21, no. 2, pp. 63–69; 1957.) The surface of an anode partially immersed in an electrolyte is more deeply corroded near the liquid/air boundary. Electrolytic polishing, in which this phenomenon is used, can be applied to the production of thin wires and of fine pivots.

666.1.037.5 3576
Fundamentals of Glass-to-Metal Bonding: Part 2—Reactions of Tantalum and Sodium Silicate Glass—S. P. Mitoff. (*J. Amer. Ceram. Soc.*, vol. 40, pp. 118–120; April 1, 1957.) Part 1: 2712 of 1953 (Zackay, *et al.*).

MATHEMATICS

517.43:621.373.421 3577
The Periodic Solutions of the Differential Equation of a Resistance-Capacitance Oscillator—Gillies. (See 3430.)

517.63 3578
A New Method of Inversion of the Laplace Transform—A. Papoulis. (*Quart. Appl. Math.*, vol. 14, pp. 405–414; January, 1957.)

517.9:621–52 3579
On the Solution of a Differential Equation with Nonlinearity appearing in the Second Derivative of Combined Linear and Cubic Terms—Chi-Neng Shen. (*Quart. Appl. Math.*, vol. 15, pp. 11–30; April, 1957.) Physical applications include a feedback control system for a two-capacity process with nonlinear elements.

517.942.82 3580
Connection between Time Function A(t) and Spectral Function ψ(p)—U. Kirschner. (*Elektron. Rundschau*, vol. 11, pp. 87–92; March, 1957.) Amplification of earlier theoretical investigations of transient phenomena (see 3360 of 1952 and 764 of 1953).

517.946.9+[536+537 3581
The General Solution of Boundary-Valve Problems of the Transmission of Heat or Electrical Energy—L. von Szalay and K. H. Löcherer. (*Frequenz*, vol. 11, pp. 97–106; April, 1957.) Solutions are tabulated for the case of a parallelepiped, a cylinder, and a sphere.

519 3582
Diakoptics—the Piecewise Solution of Large-Scale Systems—G. Kron. (*Elec. J.*, vol. 158, pp. 1673–1677; June 7, 1957.) One of a series of articles dealing with a systematic method of analyzing and solving complicated network problems by the method of "tearing." See also 2164 of 1954.

519.2 3583
Stochastic Processes Associated with Integrals of a Class of Random Functions—P. M. Mathews and S. K. Srinivasan. (*Proc. Nat. Inst. Sci. India, A.*, vol. 22, pp. 369–376; November 26, 1956.) Laplace-transform treatment of a random process involving a Poisson distribution with application to shot-effect fluctuations.

MEASUREMENTS AND TEST GEAR

53.087:621.374.32 3584
Automatic Counting Techniques applied to Comparison Measurement—Washtell. (See 3434.)

536.5:621.316.825 3585
Thermistor Thermometer Bridge: Linearity and Sensitivity for a Range of Temperature—K. S. Cole. (*Rev. Sci. Instr.*, vol. 28, pp. 326–328; May, 1957.) Analysis and construction of a measuring circuit incorporating a slide-wire Wheatstone bridge. Linearity of scale and constant sensitivity over a wide temperature range are achieved.

621.3.018.41(083.74):621.396.712 3586
Experimental Standard-Frequency Broadcast on 60 Kilocycles—(*Tech. News Bull. Nat. Bur. Stand.*, vol. 41, pp. 99–100; July, 1957.) A note on the transmission from Boulder under the call sign KK2XEI, which started July 1, 1956, on low power. Comparisons have been made with other standard frequencies including GBR and WWV transmissions, and figures are quoted for most days of January, 1957.

621.317.087.6:681.62 3587
A Printing Method for Measuring Instruments with Digital Indication—J. Hacks and M. Klose. (*Elektron. Rundschau*, vol. 11, pp. 97–99; April, 1957.) Electronic equipment is described which in conjunction with a conventional electric calculating machine prints the results of measurements in digital form. The generation of the requisite step voltages is discussed.

621.317.32:621.396.61.029.62 3588
Intercomparison of the Various Methods of Measuring Spurious Emissions—S. Kurokawa, T. Takahashi, and M. Arai. (*J. Radio Res. Labs., Japan*, vol. 4, pp. 89–93; January, 1957.) Experimental data are quoted for half, twice, and three times the fundamental transmitted frequency in the vhf band.

621.317.328:621.373.421.14 3589
Electrical Field Strength Measurements in Endovibrators [Cavity Resonators] by the Method of Changing the Resonance Frequency with a Dielectric Probe—G. N. Rapoport. (*Radiotekhnika, Moscow*, vol. 12, pp. 51–58; February, 1957.) The field distribution within the cavity is perturbed by the insertion of a small spherical, spheroidal or needle-shaped dielectric probe. Field measurements are simplified as the dielectric probe only reacts to the electric field. See also 2265 of 1952 (Maier and Slater).

621.317.34:621.372.54 3590
Wide-Range Analyser Traces Precise Curves—E. F. Feldman. (*Electronics*, vol. 30, pp. 184–187; March 1, 1957.) The attenuation characteristics of frequency-selective networks may be measured by means of equipment consisting of a swept heterodyne spectrum analyzer used as an indicator for a sweep generator. Stop-band attenuations of 100 db within the range 20 c–20 kc may be measured.

621.317.422 3591
The Rapid and Accurate Measurement of Coercive Force—F. Förster. (*Arch. tech. Messen*, no. 254, pp. 65–66; March and no. 255, pp. 87–90; April, 1957.) The astatic instrument described is insensitive to the effects of the earth's field and other disturbing fields; rapid and accurate coercivity measurements can be carried out in the range 10^{-2}–10^{3} oersteds.

621.317.44:538.614:539.23 3592
A New Method of Measuring the Magnetic Properties of Thin Films by Means of the Faraday Effect—L. Reimer. (*Z. Naturf.*, vol. 11a, p. 611; July, 1956.) The method briefly described uses a magnetizing field parallel to the film and a beam of polarized light incident at 45° to the film. Thus low field strengths suffice to achieve saturation. The magnetization curve obtained for a Ni film 450 Å thick is shown.

621.317.6:621.314.7 3593
A Simple Transistor Beta Tester for Rapid Determination of Transistor Gain—(*Tech. News Bull. Nat. Bur. Stand.*, vol. 41, p. 93; June, 1957.) The circuit diagram is shown of a device designed by G. F. Montgomery for measuring the common-emitter short-circuit current gain of *p-n-p* or *n-p-n* transistors at low af.

621.317.6:621.314.7 3594
Sweeper determines Power-Gain Parameter—W. N. Coffey. (*Electronics*, vol. 30, pp. 201–203; March 1, 1957.) A comparison circuit using a sweep frequency generator, cro, and reference network for determining the gain of junction transistors is described.

621.317.7.029.64:621.396.822:537.54 3595
A Thermal Noise Standard for Microwaves—K. S. Knol. (*Philips Res. Rep.*, vol. 12, pp. 123–126; April, 1957.) A thermal noise source for the 3-cm waveband, consisting of a heated platinum waveguide, terminated with a ceramic wedge, is described. The temperature of the wedge is fixed at the melting point of gold. Using this as a standard, a figure of 21700°K was obtained for the noise temperature of a noise diode Type K50A.

621.317.725.029.62:621.385 3596
A Selective Valve Voltmeter for the V.H.F. Range—H. Mack. (*Elektron. Rundschau*, vol. 11, pp. 102–105; April, 1957.) Description of commercial instrument covering 30–300 mc with a range of 80 db (3μv–30 mv) and a bandwidth of 45 kc.

621.317.729.1:621.317.755 3597
A High-Speed Electronic Analogue Field Mapper—R. B. Burtt and J. Willis. (*J. Sci. Instr.*, vol. 34, pp. 177–182; May, 1957.) A cr tube, the screen of which forms the base of an analog tank, is scanned in 40 msec by using a 100-line raster. The variations in the secondary emission from the screen operate trigger circuits, corresponding to a series of field potentials, which modulate the brilliance of a second cr tube scanned simultaneously.

621.317.73.011.3:621.3.029.65 3598
Measuring Instrument for Very Low Inductances—H. Brand and E. Schuon. (*Elektron. Rundschau*, vol. 11, pp. 65–67; March, 1957.) The instrument described uses a method of impedance transformation. It covers the range 1–500 mμh at λ = 80 cm.

621.317.733 3599
Bridge Sorts Capacitors to Tolerance—S. D. Breskend, J. I. Cooperman, and P. J. Franklin. (*Electronics*, vol. 30, pp. 177–179; July 1, 1957.) A description of production test equipment using a Schering bridge to measure loss factor and capacitance deviation from a standard value.

621.317.75 3600
Undistorted Reproduction of Waveforms of Very Large Bandwidth by Means of Display Units with Narrow Bandwidth: Bandwidth Compression—H. Riedle. (*Nachr. Tech. Z.*, vol. 10, pp. 135–140; March, 1957.) An adaptor circuit is described which by means of a pulse scanning method compresses a frequency spectrum of up to 200 mc of a periodic waveform so that it can be displayed on a cro of about 25-kc bandwidth. Some illustrative oscillograms are shown.

621.317.755 3601
Magnetically Deflected 21-Inch Oscilloscope—H. E. O'Kelley and W. H. Todd. (*Electronics*, vol. 30, pp. 159–161; July 1, 1957.) The deflection-coil waveform is proportional to the input signal voltage. A deflection of 10 inches is achieved at 18.5 kc, falling to 4 inches at 50 kc.

621.317.755:621.385.832 3602
A Precision Electron-Beam Oscillograph with a Spot Diameter of a few Microns—M. von Ardenne. (*J. Sci. Instr.*, vol. 34, pp. 206–207; May, 1957.) Brief description of instrument detailed in 1495 of 1956.

621.317.76 3603
A Modified Periodmeter—V. N. Rao and K. Achyuthan. (*Electronic Eng.*, vol. 29, pp. 338–339; July, 1957.) Modified version of an instrument described by Barker and Cannon (221 of 1954) for observing small changes in the frequency of an af signal of short duration.

621.317.784.029.64:621.316.825 3604
A New Thermistor Power-Measuring Head for λ = 9–20 cm—H. Rieck and F. Panniger. (*Nachr. Tech.*, vol. 7, pp. 101–104; March, 1957.) The device described uses a single thermistor mounted close to an adjustable λ/4 stub line. By selection two thermistors were found to cover the ranges 9–17 cm or 12–20 cm, respectively, with a vswr ≦ 1.1

621.317.794:537.311.33:546.289 3605
Low-Inertia Germanium Bolometers—V. N. Bogomolov, Yu. V. Ilisavski, M. Kornfel'd, L. S. Sochava, and R. I. Strunin. (*Zh. Tekh. Fiz.*, vol. 27, pp. 213–215; January, 1957.) The bolometer described consists of a vacuum-deposited Ge film about 1μ thick, protected by a layer of polystyrene. The sensitivity of this instrument for a modulation frequency of 30 c was 60–70 v/w. The temperature coefficient of resistance of the sensitive layer was estimated to be 25×10^{-2} degrees^{-1}. A section drawing of the bolometer is shown.

621.317.794.029.64:621.317.733 3606
A Self-Balancing Direct-Current Bridge for Accurate Bolometric Power Measurements—G. F. Engen. (*J. Res. Nat. Bur. Stand.*, vol. 59, pp. 101–105; August, 1957.) "A self-balancing dc bridge has been developed that preserves the inherent accuracy of the manual bridge, extends the dynamic range of operation, and greatly simplifies the operating procedure. A general description of the equipment and operating techniques is given, followed by a comprehensive survey of the sources of error accompanying the method and the accuracy achieved."

OTHER APPLICATIONS OF RADIO AND ELECTRONICS

534.1–8:61 3607
Ultrasonics in Medicine and Dentistry—W. Welkowitz. (Proc. IRE, vol. 45, pp. 1059–1069; August, 1957.)

534.1–8:663.4 3608
Ultrasonics Bubbles Beer in Brewery—A. S. Davis. (*Electronics*, vol. 30, pp. 162–164; July 1, 1957.) Unwanted air is expelled from bottles through foam formation resulting from vibration caused by a magnetostrictive transducer.

535.24:621.397.6 3609
Television-Optical Method of Obtaining Equal-Density Contours—A. Lohmann. (*Optik, Stuttgart*, vol. 14, pp. 178–182; April, 1957.) The easily variable nonlinear characteristics of a television system, such as that used for microscopy by Köhler (3837 of 1956), can be used for photometric applications in place of photographic methods.

621–52:621.397.611.2 3610
Television Technique Applied to Observation and Control—McGee. (See 3668.)

621.3.083.7:621.314.7:616 3611
Endoradiosonde—R. S. Mackay and B. Jacobson. (*Nature, London*, vol. 179, pp. 1239–1240; June 15, 1957.) A capsule 2.8 cm long and 0.9 cm in diameter contains a junction transistor and battery for transmitting data such as temperature, pressure, and pH value from within the gastro-intestinal tract of a human body. The frequency used is about 100 kc.

621.316.7.078:616 3612
Muscles control Iron-Lung Operation—L. H. Montgomery. (*Electronics*, vol. 30, pp. 180–181; July 1, 1957.) Potentials picked up from the patient's muscles trigger a control circuit for an artificial respirator.

621.317.39:531.77:621.396.322 3613
Tachometer Noise Reduction—J. C. West. (*Electronic Radio Eng.*, vol. 34, pp. 342–344; September, 1957.) A discussion of the improvements obtainable using a brushless low-noise accelerometer.

621.365.521:621.387 3614
Thyratrons Stabilize Induction Heaters—H. J. Fraser and E. G. Hopkins. (*Electronics*, vol. 30, pp. 152–153; July 1, 1957.) A closed-loop regulator which stabilizes high-power oscillators used for heating receiving tube electrodes during an automatic exhaust process.

621.365.54 3615
Radio-Frequency Energy Transfer Switch—L. E. Bollinger. (*Rev. Sci. Instr.*, vol. 28, pp.

383–384; May, 1957.) The switch can be used at frequencies of 500 kc and higher and has been tested at rf currents of 140 a.

621.374.3:795 3616

Electronic Fruit Machine—G. L. Swaffield. (*Wireless World*, vol. 63, pp. 447–451; September, 1957.) Description of a slot machine in which coincidence in the flashing of neon lamps is controlled by pulse circuits.

621.383.27:621.3.083.722 3617

A Photoelectric Particle Counter for Use in the Sieve Range—T. Beirne and J. M. Hutcheon. (*J. Sci. Instr.*, vol. 34, pp. 196–200; May, 1957.) A suspension of the particles is passed through a capillary tube and the image projected onto a photomultiplier and analyzed by a rate-meter. The size distribution is obtained by plotting count rates against discriminator threshold voltage.

621.383.4:531.787.4 3618

Precise Automatic Manometer Reader—J. Farquharson and H. A. Kermicle. (*Rev. Sci. Instr.*, vol. 28, pp. 324–325; May, 1957.) Electronic and mechanical device registering mercury surface level with a maximum error of ±0.05 mm.

621.384.612 3619

Nonlinear Theory of Betatron Oscillations in a Strong-Focusing Synchrotron—Yu. F. Orlov. (*Zh. Eksp. Teor. Fiz.*, vol. 32, pp. 316–322; February, 1957.)

621.385.3:531.787:616 3620

Movable-Anode Tube—(*Electronics*, vol. 30, pp. 232–238; March 1, 1957.) The RCA Type-5734 transducer consists of a miniature triode having a movable anode with a small extension shaft protruding through the center of a thin air-tight metal diaphragm. Abstract from "Research on Mechano-electronic Transducer Blood Pressure Manometers" read at the 1956 I.S.A. Conference.

621.385.833 3621

Magnetic Electron Lenses—P. Durandeau and C. Fert. (*Rev. Opt.*, vol. 36, pp. 205–234; May, 1957.) A description of design principles with constructional data based on experimental results from the Laboratoire d'Optique électronique, Toulouse. Twenty-one references.

621.385.833 3622

Combination of Emission-Type [Electron] Microscope and Reflection-Type Diffractograph—R. Arnal and C. Gonçalves. (*C.R. Acad. Sci., Paris*, vol. 24, pp. 3139–3141; June 24, 1957.) The diffraction microscope is vertical, the emission-type microscope horizontal. A single sample can be viewed simultaneously by the two instruments.

621.385.833 3623

Condensation of Iron and Platinum on Tungsten Single-Crystal Surfaces in the Field-Emission Electron Microscope at Elevated Temperatures—K. Neubeck. (*Z. Naturf.*, vol. 11a, pp. 587–589; July, 1956.)

621.385.833:621.385.032.213.2 3624

The Bolt Cathode as Object in the Electron-Emission Microscope—E. B. Bas. (*Z. angew. Math. Phys.*, vol. 8, pp. 203–213; May 25, 1957.) The use of this type of cathode (see also 3793 of 1955) in electron microscopes and the method of its preparation are described.

621.396.969:533.6.011.7 3625

A Radio Method of Determining the Velocity of a Shock Wave—J. S. Hey, J. T. Pinson, and P. G. Smith. (*Nature, London*, vol. 179, pp. 1184–1185; June 8, 1957.) The change of frequency caused by the Doppler effect on continuous radio waves reflected from the shock discontinuity in a shock tube is measured.

PROPAGATION OF WAVES

621.396.11 3626

On the Relationship between the Scattering of Radio Waves and the Statistical Theory of Turbulence—K. Tao. (*J. Radio Res. Labs., Japan*, vol. 4, pp. 15–24; January, 1957.) The scattering cross section derived by Villars and Weisskopf (see 244 of 1956) is discussed in terms of a mathematical model of a turbulent element. The cross section can be expressed in terms of the energy spectrum of the turbulence.

621.396.11:551.510.52 3627

The Concept of the Equivalent Radius of the Earth in Tropospheric Propagation—G. Millington. (*Marconi Rev.*, vol. 20, pp. 79–93; 3rd quart.; 1957.) "The concept of the equivalent radius of the earth to take account of a linear variation of refractive index with height in tropospheric refraction is re-examined. It is shown that the transformation is not limited to nearly horizontal rays, but that essentially it reduces the curvature of the earth by that of a ray traveling horizontally and the curvature of the rays by the amount required to straighten them at whatever angle to the horizontal they may be going. The results were obtained geometrically in a previous paper (1637 of 1946) for the angle of elevation at the reflection point; the optical path difference between the direct and indirect rays and the divergence factor are derived by simple analysis, affording a useful check on the method."

621.396.11:551.510.535 3628

The Proceedings of the International Convention on Radio Propagation in the Ionosphere—(*Nuovo Cim.*, vol. 4, supplement no. 4, pp. 1343–1608; 1956.) The text is given of the introductory speeches and the following papers presented at the convention held in Venice August 18–21 1955.

Ionospheric Turbulence and Electromagnetic Wave Propagation—T. Kahan (pp. 1352–1383, discussion, p. 1384. In French.)

The Electrical Conductivity of the Ionosphere (a Review)—S. Chapman. (pp. 1385–1412. In English.)

Some Properties of the Meteoric E Layer Used in Radio Wave Propagation—R. Naismith (pp. 1413–1420, discussion, pp. 1420–1421. In English.)

Some Remarks on the Theory of Self-Demodulation—M. Carlevaro (pp. 1422–1429. In English.)

On the Interaction of Radio Waves—V. A. Bailey (pp. 1430–1448, discussion, pp. 1448–1449. In English.)

Ionospheric Self-Demodulation of Radio Waves—M. Cutolo, G. C. Bonghi, F. Immirzi, and P. Cachon (pp. 1450–1458, discussion, pp. 1458–1459; In English.)

The Blanketing of Paths: an Important Phenomenon of Ionospheric Propagation—K. Rawer (pp. 1460–1476, discussion pp. 1476–1477. In French.)

The Absorption of Short Waves in an Isotropically Ionized Medium—E. Argence (pp. 1478–1510, discussion, p. 1510. In French.)

The Determination of the Number of Collisions Relative to the F_2 Region of the Ionosphere—E. Argence and K. Rawer (pp. 1511–1531. In French.)

Echo Sounding Experiments with Variable Frequency at Oblique Incidence—W. Dieminger and H. G. Möller (pp. 1532–1544, discussion, pp. 1544–1545. In English.)

On a Correlation between the Electronic Density of the E Layer and the 500-mb Surface Position—A. Napoletano (pp. 1546–1551. In English.)

Remarks on the Connection between Mode Theory and Ray Theory—H. Bremmer (pp. 1552–1558. In English.)

On Some Characteristics of the F_2 Region in South America—I. Ranzi (pp. 1559–1560, discussion, p. 1561. In English.)

The Ionized Aurora—N. C. Gerson (pp. 1562–1571. In English.)

Some Observations on the Influence of a Solar Eclipse upon the Ionosphere—P. Dominici (pp. 1572–1578. In English.)

Some Considerations on Temperature Effects in the Upper Atmosphere—F. Mariani (pp. 1579–1585. In English.)

Diffusion in a Not Isothermal Ionosphere—F. Mariani (pp. 1586–1588. In English.)

Some Critical Considerations on the Parameters h′ and f_0 of the Ionospheric Layers—P. Dominici and F. Mariani (pp. 1589–1592, discussion, p. 1592. In English.)

Molecular Spectroscopy of Oxygen by Means of Microwaves. The Form of the Absorption Lines—N. Carrara (pp. 1593–1608. In Italian.)

621.396.11:551.510.535 3629

Propagation of a Plane Electromagnetic Wave Across an Ionospheric Layer—P. Poincelot. (*C.R. Acad. Sci., Paris*, vol. 244, pp. 3045–3047; June 17, 1957.) Short mathematical treatment of propagation of a plane wave incident vertically on a parabolic layer, considering electrons subject to two forces only, due to 1) the em field and 2) viscous resistance. See also 3275 of 1957.

621.396.11:621.396.933 3630

The Application of Radio Frequency Predictions to Aeronautical Communications—Foxcroft. (See 3654.)

621.396.11.029.45/.51 3631

Mixed-Path Ground-Wave Propagation: Part 2—Larger Distances—J. R. Wait and J. Householder. (*J. Res. Nat. Bur. Stand.*, vol. 59, pp. 19–26; July, 1957.) "The theoretical results given in Part 1 [*ibid.*, vol. 57, pp. 1–15; July, 1956. (Wait)] for ground-wave propagation over a mixed path on a flat earth are generalized to a spherical earth. The problem is formulated in terms of the mutual impedance between two vertical dipoles which are located on either side of the boundary of separation. Extensive numerical results are given in graphical form for a mixed land-sea path at frequencies of 10, 20, 50, 100, and 200 kc." See also 3516 of 1956 (Wait and Howe).

621.396.11.029.51 3632

Amplitude and Phase of the Low-Frequency Ground Wave Near a Coastline—J. R. Wait. (*J. Res. Nat. Bur. Stand.*, vol. 58, pp. 237–242; May, 1957.) "A theoretical analysis is given for the amplitude and the phase change of the ground wave, originating from a distant transmitter on land, as it crosses a coastline. The land and sea are assumed to be smooth and homogeneous with a sharp boundary of separation. Attention is focused on the effects that take place near the coastline when it is not permissible to employ arguments based on the principle of stationary phase. A limited comparison is made with the recent experimental work of Pressey, Ashwell, and Fowler (3194 of 1956)."

621.396.11.029.55 3633

Characteristics of H. F. Signals—A. F. Wilkins and F. Kift. (*Electronic Radio Eng.*, vol. 34, pp. 335–341; September, 1957.) Measurements made between 1952 and 1954 of the angles of elevation of both pulsed and cw signals arriving at Slough from India and Ceylon on frequencies between 15 and 19 mc showed that 7°±2° was the predominant angular range. Back-scatter data from Ceylon and Slough were used to interpret the propagation modes concerned.

621.396.812 3634
Variation of the Polarization of Ultra Short Waves due to the Heterogeneity of the Troposphere—G. Eckart. (*C.R. Acad. Sci., Paris*, vol. 244, pp. 3044–3045; June 17, 1957.) A mathematical note explaining the fact that the field radiated from a vertical antenna is often no longer vertically polarized at the receiver. See 1218 of 1957.

RECEPTION

621.376.232:621.396.822 3635
Influence of Fluctuations on a Phase Detector—V. I. Tikhonov and I. N. Amiantov. (*Radiotekhnika, Moscow*, vol. 12, pp. 39–50; February, 1957.) Imperfections of the phase detector are examined and statistical characteristics of output voltage given. Approximate formulas for the average voltage and also a correlation function of voltage fluctuations and phase-detector load are derived.

621.376.33 3636
A New Approach to the Nonlinear Problems of F.M. Circuits—M. A. Biot. (*Quart. Appl. Math.*, vol. 15, pp. 1–10; April, 1957.) "Closed form expressions are developed for the output of a frequency modulation receiver for an arbitrary number of superposed input signals. This corresponds to problems of interference or disturbance due to scatter and multiple reflexions. It is also shown how the Fourier components of the output may be evaluated by methods more direct than the usual Fourier analysis."

621.396.62:621.314.7 3637
Further Notes on the Portable Transistor Receiver—S. W. Amos. (*Wireless World*, vol. 63, pp. 452–453; September, 1957.) Details of practical layout. See 2895 of 1957.

621.396.621:621.396.822 3638
Method of Increasing the Interference Stability of an Autocorrelated Reception of Pulse Signals—M. I. Karnovski and V. I. Chaikovski. (*Radiotekhnika, Moscow*, vol. 12, pp. 22–27; February, 1957.) Better interference stability is obtained by the addition of a synchronized switching unit in one of the channels thus increasing the selectivity of the system. See also 562 of 1957 (Chaikovski).

621.396.621.54 3639
An All-Electronic Signal-Seeking Broadcast Receiver—C. W. Hargens, III. (IRE Trans. vol. BTR-1, pp. 5–9; October, 1955. Abstract, Proc. IRE, vol. 44, p. 434; March, 1956.) See also 555 of 1956 (Chih Chi Hsu).

621.396.81:621.396.621 3640
Probability of Detection of a Signal by a Receiver Having a Finite Recovery Time—A. M. Vasil'ev. (*Radiotekhnika, Moscow*, vol. 12, pp. 28–38; February, 1957.) A general equation is derived for the probability density of signal detection by the receiver. Some illustrative examples and results are given.

621.396.812.3 3641
Characteristics of Fading in H.F. and M.F. Waves at Middle Distances—R. Inoue, M. Ose, and N. Wakai. (*J. Radio Res. Labs., Japan*, vol. 4, pp. 77–87; January, 1957.) The fading characteristics depend on whether pulsed or continuous-wave signals are used and on time of day. The amplitude distribution is presented by automatic equipment.

621.396.82.029.62.63 3642
V.H.F.-U.H.F. Radiation Measurements—A. B. Glenn. (IRE Trans., vol. BTR-1, pp. 15–19; October, 1955. Proc. IRE, *Australia*, vol. 18, pp. 15–19; January, 1957. Abstract, Proc. IRE, vol. 44, p. 435; March, 1956.)

STATIONS AND COMMUNICATION SYSTEMS

621.39.001.11 3643
A System of Signal Reception—A. A. Kharkevich. (*Elektrosvyaz*, no. 2, pp. 5–9; February, 1957.) In the system described the whole of the binary coded signal received is compared, for purposes of error detection, with signals prerecorded in a magnetic-tape memory store. In the case discussed the result of the comparison is displayed on a cr tube screen subdivided into 64 squares for a 32-letter telegraphy code. Half the number of the squares are blank and correspond to an error signal.

621.394/.395:621.396.933 3644
Line Communication Equipment for Air Traffic Control within the German Federal Republic—K. Heidelauf. (*Nachr. Tech. Z.*, vol. 10, pp. 187–194; April, 1957.)

621.394.3:681.142 3645
Morse-to-Teleprinter Code Converter—Smith-Vaniz and Barrett. (See 3408.)

621.396.24.029.62(494) 3646
The Basis, Tasks and Aims of U.S.W. Broadcasting—E. Metzler. (*Tech. Mitt. schweiz. Telegr.-Teleph. Verw.*, vol. 35, pp. 138–148; April 1, 1957.) Particular reference is made to the planned expansion of the Swiss network of vhf stations.

621.396.3 3647
The Correction of Synchronization in Start-Stop Radio Teleprinter Systems—W. Kronjäger, B. Lenhart, and K. Vogt. (*Nachr. Tech. Z.*, vol. 10, pp. 167–174; April, 1957.) Examples illustrate the improvement in transmission quality achieved by generating the synchronizing pulses locally.

621.396.3:621.396.933 3648
An Experimental Airborne Teleprinter Service for North Atlantic Airlines—A. Bickers. (*Marconi Rev.*, vol. 20, pp. 104–112; 3rd quart., 1957.) A ground-to-air teleprinter service for the transmission of weather information in the l-f band would relieve the existing congestion in m-f and h-f bands. Details are given of an airborne teleprinter receiver Type-X2779 which has been designed to test the feasibility of such a service. It is crystal-controlled and is designed for frequency-shift keying in any one of four channels in the range 90–130 kc.

621.396.4:621.376.3:621.3.018.78 3649
Distortion Produced in a Noise-Modulated F.M. Signal by Nonlinear Attenuation and Phase Shift—S. O. Rice. (*Bell Sys. Tech. J.*, vol. 36, pp. 879–884; July, 1957.) An expression derived for the power spectrum of the distortion yields useful approximations for the second- and third-order modulation terms.

621.396.41:534.78 3650
The Use of Speech Clipping in Single-Sideband Communications Systems—L. R. Kahn. (Proc. IRE, vol. 45, pp. 1148–1149; August, 1957.) An analysis of the output waveform produced by a perfect SSB suppressed-carrier transmitter, when fed by a severely clipped af wave, and a discussion of advantages of the system.

621.396.65:621.396.4.029.64 3651
Microwave Remotes Aid Air Traffic Control—E. K. Peterson, H. R. Ulander, R. N. Hargis, and E. Hajic. (*Electronics*, vol. 30, pp. 144–147; July 1, 1957.) Information obtained from a search radar, height-finding radar, and iff equipment is transmitted by a microwave relay system to the control center 250 miles away.

621.396.72:621.396.61/.62 3652
Radiotelephony—Prerequisites and Applications—F. Kruse. (*Telefunken Ztg.*, vol. 30, pp. 5–8, English summary, p. 71; March, 1957.) The use of mobile radiotelephony installations, particularly in Germany, is briefly surveyed with twenty-seven references which include the papers on portable sets discussed earlier [see 1550 of 1956 (Muth and Ulbricht)]. Details of the development, design, and application of some of these installations are given in the following papers.

FuG7—from the Single-Channel to the Multichannel U.S.W. Radiotelephone Set—A. Hagen (pp. 9–20, English summary, p. 71.)

Radiotelephony Antennas with Broad-Band Characteristics—R. Becker (pp. 21–26; English summary, p. 72.)

The Development of the 100-Channel Radiotelephone Set FuG7—H. J. Fründt and F. Sobott (pp. 27–36, English summary, pp. 72–73.)

Automatic Operation for U.S.W. F.M. Radiotelephone Services with Mobile Subscribers—W. Kuehl and J. Schon (pp. 36–43, English summary, p. 73.)

Fortuna Mine—an Example of Fully Automatic Through-Dialling in Both Directions in a Radiotelephony System (pp. 44–46, English summary, p. 74.)

Helicopter with Radiotelephone Communication System for Use by the Police—(pp. 47–49, English summary, p. 74.)

U.S.W. Radiotelephony Installations for the Repair and Maintenance Services of Electric Railway Power Supplies—A. Schepp. (pp. 50–54, English summary, pp. 74–75.)

621.396.91:621.3.018.41(083.74) 3653
Time-Signal Broadcast Sets Electric Clock—R. L. Ives. (*Electronics*, vol. 30, pp. 174–176; July 1, 1957.) A method of setting an electric clock by time signals from WWV.

621.396.933:621.396.11 3654
The Application of Radio Frequency Predictions to Aeronautical Communications—A. Foxcroft. (*Proc. IRE, Australia*, vol. 18, pp. 7–12; January, 1957.) Prediction data available in Australia are reviewed and application of long-term and short-term forecasts to the planning and operation of aviation communication systems is discussed. An example of the use of predictions for a flight from Sydney to Nadi (about 2000 miles) is given.

SUBSIDIARY APPARATUS

621.311.6:621.363 3655
The Problem of Efficiency of Thermoelectric Generators—A. Käch. (*Elektrotech. Z., Edn. A*, vol. 78, pp. 182–187; March 1, 1957.) Thermoelectric transducers of considerably greater efficiency than those based on present-day low output thermoelements appear feasible on theoretical grounds. For pure metals about 80–90 per cent of the Carnot efficiency could be achieved with thermoelectric forces of 2–5 mv/°K.

621.311.62:621.316.722.1 3656
Low-Noise Stabilized D.C. Supplies—D. W. W. Rogers. (*Electronic Radio Eng.*, vol. 34, pp. 320–326; September, 1957.) Sources of hum and low-level noise in power supply units are described, together with methods for greatly reducing their effects. One of the circuits shown (with component values) gives: hum content less than 20 μv rms drift within ± 0.15 per cent over eight hours, and stability within ± 0.1 per cent for ± 6 per cent mains variation.

621.314.634:537.311.33 3657
Structure of the Upper Layer Adjacent to the Electrode of a Selenium Rectifier—V. A. Dorin and D. N. Nasledov. (*Zh. Tekh. Fiz.*, vol. 27, pp. 90–94; January, 1957.) An X-ray investigation of the diffusion in the contact boundaries Sn-S and Sn-Se is described. The products of reactive diffusion of S and Sn were

examined in samples heated to 220°C. When S comes into contact with the electrode containing Cd and Sn hole migration takes place in the Se, which results in rectification.

621.316.722.1:621.385.2 3658
Some Characteristics of Saturated Diodes with A.C. Heating—Benson and Seaman. (See 3716.)

621.318.57:621.396.662.6 3659
A Variable Slow-Speed Uniselector Drive—R. Selby. (*Electronic Eng.*, vol. 29, pp. 326–327; July, 1957.) "A circuit is described which employs a small thyratron to drive a uniselector without the use of relays or auxiliary power supplies."

TELEVISION AND PHOTOTELEGRAPHY

621.397.2 3660
U.S.S.R. Television Standard G.O.S.T. [Government Standard] 7845–55—S. V. Novakovski and D. I. Ermakov. (*Elektrosvyaz*, no. 1, pp. 24–34; January, 1957.) Details of the monochrome 625-line system in use since 1944 are given.

621.397.335:621.314.7 3661
Transistors Synchronize Portable TV Camera—K. Kinoshita, Yasushi, Fujimura, Y. Kihara, and N. Mii. (*Electronics*, vol. 30, pp. 168–169; July 1, 1957.) The sync generator described is of modular design and contains 26 transistors on a chassis $12\times 3\frac{3}{4}\times 1\frac{3}{4}$ inches.

621.397.5:535.623 3662
Monochrome Slides broadcast Colour—E. L. Covington. (*Electronics*, vol. 30, pp. 169–171; March 1, 1957.) "Two complementary colors can be broadcast from a television transmitter using monochrome slides having well-defined transitions. In addition, special circuits permit continuous transmission of a yellow-green color stripe for color receiver adjustment during monochrome broadcasts."

621.397.5:535.623 3663
Sequential Colour Again (*Wireless World*, vol. 63, pp. 426–429; September, 1957.) Description of a new French compatible 819-line system demonstrated at the Paris symposium. It incorporates a delay line and has the advantage that receivers can be simpler and less critical in operation.

621.397.61 3664
The Optimum Ratio between Sound and Vision Transmitter Powers—L. Kedzierski and S. Ogulewicz. (*Nachr. Tech.*, vol. 7, pp. 109–112; March, 1957.) Measurements on several Polish and Russian television receivers show that a vision/sound power ratio of at least 5 is acceptable and that a much higher ratio can be used for some types of receiver. This is in agreement with the 1953 recommendations of the CCIR.

621.397.611 3665
High-Fidelity Frame-Scanning Method—L. L. Santo. (*Radiotekhnika, Moscow*, vol. 12, pp. 18–24; March, 1957.) Report of experimental investigations and discussion of the conditions necessary to ensure the exact overlapping of frames.

621.397.611:621.385.833 3666
Electron-Optical Method of Varying the Scale of a Television Image—I. I. Tsukkerman. (*Radiotekhnika, Moscow*, vol. 12, pp. 4–9; March, 1957.) The electron-optical system described produces variable magnification without image reversal. See also 1598 of 1956.

621.397.611.2 3667
Automatic Level Control for TV Slide Chains—E. W. Lambourne. (*Electronics*, vol. 30, pp. 182–183; July 1, 1957.) A simple three-tube circuit which maintains the peak-to-peak video signal from the iconoscope slide chain at a constant predetermined level.

621.397.611.2:621.-52 3668
Television Technique Applied to Observation and Control—J. D. McGee. (*Trans. Soc. Instr. Technol.*, pp. 26–40, discussion pp. 40–43; March, 1957.) Description of some modern pick-up tubes (see also 3418 of 1955) and outline of suitable equipment for some specialized applications. Twenty-five references.

621.397.62 3669
Ultrasonic Gong Controls TV Sets—R. Adler, P. Desmares and J. Spracklen. (*Electronics*, vol. 30, pp. 156–161; March 1, 1957.) A device for remote control of a set by the viewer.

621.397.62 3670
Interesting Details of the Circuitry of This Year's Television Receivers—W. Taeger. (*Frequenz*, vol. 11, pp. 114–123; April, 1957.) Some improvements and novel features of receivers, mainly of German manufacture, are described.

621.397.62:621.385:621.375 3671
Operating Point and Modulation Range of Video End Stages—W. Sparbier. (*Elektron. Rundschau*, vol. 11, pp. 118–121; April, and 151–153; May, 1957.) General rules are established regarding the operation of video output stages in receivers. The advantages of black-level clamping are discussed and some typical tube operating data are given.

621.397.621:621.318.4 3672
Yoke Development for Standardization of 70° and 90° Deflection Angle—C. E. Torsch. (IRE Trans., vol. BTR-1, pp. 10–15; October, 1955. Abstract, Proc. IRE, vol. 44, pp. 434–435; March, 1956.)

621.397.621:621.318.4 3673
Overcoming Line-Scan Ringing—K. G. Beauchamp. (*Wireless World*, vol. 63, pp. 441–443; September, 1957.) The method described consists in ensuring that the line-scan transformer can resonate simultaneously at several frequencies in a definite relation. This is achieved in a specially designed transformer with the leakage inductance tuned. See also *Tele-Tech.*, vol. 12, pp. 108–110; June, 1953. (Torsch).

621.397.621.2 3674
Improvements in Television Receivers—(*Electronic Applic. Bull.*, vol. 17, no. 2, pp. 41–63; 1956 and 64–71; 1957.) **Part 2—The PL 36 Line Output Pentode**—Three phenomena (the effects of Barkhausen oscillations, "fraying" effect and envelope cracks) which are frequently experienced in line output tubes are treated and methods of elimination given. **Part 3—Stabilization of the Frame Deflection Circuit**—Efficient stabilization is obtained without increasing the conventional tube complement as described earlier (Part 1: 3316 of October).

621.397.8:535.61 3675
The Distortion of Television Image Gradation by Illumination of the Screen—R. Suhrmann. (*Elektron. Rundschau*, vol. 11, pp. 75–77; March, 1957.) The influence of room lighting is investigated and simple circuits for correcting gradation distortion are outlined. See also 3323 of 1957.

TRANSMISSION

621.396.61–71:621.396.933 3676
Fluid Cooling an Airborne Transmitter—J. B. Humfeld. (*Electronics*, vol. 30, pp. 170–172; July 1, 1957.) A 1-kw power amplifier for the range 4–30 is described which employs self-rectification and silicone-oil cooling. The total volume occupied is 500 inches^3.

621.396.61.029.62:621.317.32 3677
Intercomparison of the Various Methods of Measuring Spurious Emissions—Kurokawa, Takahashi, and Arai. (See 3588.)

621.396.712:621.3.018.41(083.74) 3678
Experimental Standard-Frequency Broadcast on 60 Kilocycles—(See 3586.)

TUBES AND THERMIONICS

621.314.63:537.311.33 3679
Surface Discharges at *p-n* Junctions—B. M. Vul and A. P. Shotov. (*Zh. Tekh. Fiz.*, vol. 27, pp. 211–212; January, 1957.) Experiments show that the performance of high-voltage diodes may be limited by breakdown of the air across the *p-n* junction at reverse voltages greater than 400 v at normal pressure.

621.314.63:537.311.33:546.28 3680
Silicon Diffused-Junction "Avalanche" Diodes—H. S. Veloric and K. D. Smith. (*J. Electrochem. Soc.*, vol. 104, pp. 222–226; April, 1957.) The diffusion technique is described and the characteristics of a series of "avalanche" or voltage-limiting diodes made by this method are discussed. The range of breakdown voltages is from 6 v to >200 v, with areas 5×10^{-3} cm^2–5cm^2.

621.314.63:546.289 3681
Design Theory and Experiments for Abrupt Hemispherical *P-N* Junction Diodes—H. L. Armstrong, E. D. Metz, and I. Weiman. (IRE Trans., vol. ED-3, pp. 86–92; April, 1956. Abstract, Proc. IRE, vol. 44, p. 955; July, 1956.)

621.314.63:621.318.57 3682
Fast Switching by Use of Avalanche Phenomena in Junction Diodes—B. Salzburg and E. W. Sard. (Proc. IRE, vol. 45, pp. 1149–1150; August, 1957.) Reduced transients are obtained when switching through avalanche breakdown from low to high current.

621.314.632 3683
Study of Rectifying Characteristics of FeS_2 and Germanium Point-Contact Rectifiers—J. N. Das. (*Indian. J. Phys.*, vol. 31, pp. 172–174; March, 1957.) Results of measurements of contact potential difference, spreading resistance, current amplification factor, and the effect of photo-injection on the reverse current with and without bias are given for commercially available Ge diodes and FeS_2 crystals with tungsten-wire contact, the crystals being embedded in Wood's metal to establish a large-area base contact. Observations can be explained by considering the effect of trapped electrons in the surface states.

621.314.632:546.28 3684
The Silicon "Zener" Diode—P. Dobrinski, H. Knabe and H. Müller. (*Nachr. Tech. Z.*, vol. 10, pp. 195–199; April, 1957.) Description of the characteristics of commercial types of Si reference diode with Zener voltages between 6 and 9 v. A number of applications are discussed. See also 923 of 1956 (Wulfsberg).

621.314.632:546.289 3685
Current/Voltage Characteristic and Hole Injection Factor of Point-Contact Rectifiers in the Forward Direction—K. Lehovec, A. Marcus, and K. Schoeni. (Trans. IRE, vol. ED-3, pp. 1–6; January, 1956. Abstract, Proc. IRE, vol. 44, p. 716; May, 1956.)

621.314.7 3686
An Approximation to Alpha of a Junction Transistor—R. D. Middlebrook and R. M. Scarlett. (Trans. IRE, vol. ED-3, pp. 25–29; January, 1956.) Abstract, Proc. IRE, vol. 44, p. 716; May, 1956.)

621.314.7 3687
A Method of Determining Impurity Diffusion Coefficients and Surface Concentrations of Drift Transistors—L. S. Greenberg, Z. A. Martowska, and W. W. Happ. (Trans. IRE, vol. ED-3, pp. 97–99; April, 1956. Abstract, Proc. IRE, vol. 44, p. 955; July, 1956.)

621.314.7:546.28 3688
High-Frequency Silicon Alloy Transistor—A. D. Rittmann and T. J. Miles. (Trans. IRE, vol. ED-3, pp. 78–82; April, 1956. Abstract, Proc. IRE, vol. 44, p. 955; July, 1956.)

621.314.7:621.317.6 3689
A Simple Transistor Beta Tester for Rapid Determination of Transistor Gain—(See 3593.)

621.314.7:621.317.6 3690
Sweeper determines Power-Gain Parameter—Coffey. (See 3594.)

621.383.5:546.289 3691
Photocell Measures Light Direction—J. T. Wallmark. (*Electronics*, vol. 30, pp. 165–167; July 1, 1957.) The lateral voltage produced on a germanium-indium junction varies with the angle between the photocell axis and the direction of the incident light. Several applications are discussed.

621.384.5:621.385.5:621.387 3692
An Improved Circuit for Reliable Operation of Nomotron Counter Tubes—T. M. Jackson. (*Electronic Eng.*, vol. 29, pp. 324–326; July, 1957.) New operating conditions are given for the nomotron G10/241E cold-cathode multi-electrode counter tube originally described by Hough and Ridler (2933 of 1952).

621.385:621.374.3 3693
A Search for a Pulser of High Output Requiring Small Grid Drive—S. C. Nath and B. M. Banerjee. (*J. Sci. Ind. Res.*, vol. 15A, pp. 444–449; October, 1956.) The pulse characteristics of various receiving-type tubes have been investigated to select a suitable pulse amplifier for frequency-sweep ionospheric sounding equipment. Figures for some 20 types are listed. The performance of a line pentode Type EL81 is superior to any other tube tested. Other types with useful characteristics for fast pulse applications are the Type 6AH6 and Type EFP60.

621.385.029.6 3694
A Small-Amplitude Theory for Magnetrons—O. Bunemann. (*J. Electronics Control*, vol. 3, pp. 1–50; July, 1957.) First publication of a 1944 classified report on magnetron work at the Manchester University CVD group. The impedance of a magnetron electron cloud, defined as the ratio of rf electric and magnetic field components at the surface of the cloud, is calculated. This impedance can exhibit a negative resistance component, or a pure reactance which decreases with frequency. This latter property is shown to be a sufficient condition for the spontaneous start-up of oscillations. Calculated operating conditions as a function of load agree closely with experiment.

621.385.029.6 3695
Space Charge in the Relativistic Magnetron—L. Gold. (*J. Electronics Control*, vol. 3, pp. 87–96; July, 1957.) Three relativistic solutions for the space-charge behavior in a magnetron at high energies are calculated. These correspond to the border of the classical region, the intermediate and the extreme relativistic domain.

621.385.029.6 3696
Kinetic Theory of Space Charge: Part 1—Cut-Off Character of the Static Magnetron—L. Gold. (*J. Electronics Control*, vol. 3, pp. 97–102; July, 1957.) The effect of damping in the magnetron space charge by electron-electron collisions is shown to account for departures from Child's law, and also for the previously unexplained lack of a sharp cutoff.

621.385.029.6 3697
Straight-Field Permanent Magnets of Minimum Weight for TWT Focusing—Design and Graphic Aids in Design—M. S. Glass. (Proc. IRE, vol. 45, pp. 1100–1105; August, 1957.) The validity of the method has been confirmed by tests upon a series of traveling-wave-tube magnets varying in weight from 3 to 20 pounds.

621.385.029.6 3698
Some New Circuits for High-Power Traveling-Wave Tubes—M. Chodorow and R. A. Craig. (Proc. IRE., vol. 45, pp. 1106–1118; August, 1957.) A discussion and description of a new class of propagating circuits for use in pulsed high-power traveling-wave tubes in which the electrons interact with the fundamental space component of the propagating wave, and which are suitable for bandwidths of 10–20 per cent. Operation at 100 kv is envisaged, but greater bandwidths at lower voltages should be possible. The structures consist of sets of magnetically coupled cavities leading to negative mutual impedances in the pass band and a fundamental space wave of forward phase velocity; the lower impedance of this wave enables greater energy storage to be obtained than with the more usual space harmonic mode resulting from conventional circuits.

621.385.029.6 3699
Large Signal Behavior of High-Power Traveling-Wave Amplifiers—J. J. Caldwell, Jr., and O. L. Hoch. (IRE Trans., vol. ED-3, pp. 6–17; January, 1956. Abstract, Proc. IRE, vol. 44, p. 716; May, 1956.)

621.385.029.6 3700
A Large-Signal Analysis of the Traveling-Wave Amplifier: Theory and General Results—J. E. Rowe. (IRE Trans., vol. ED-3, pp. 39–56; January, 1956.) Abstract, Proc. IRE, vol. 44, p. 717; May, 1956.) See also 1270 of 1957 (Tien and Rowe).

621.385.029.6 3701
Small-Signal Power Theorem for Electron Beams—H. A. Haus and D. L. Bobroff. (*J. Appl. Phys.*, vol. 28, pp. 694–704; June, 1957.) The analysis deals with a filament beam in arbitrary dc electric and magnetic fields. The electromagnetic power delivered by the beam is balanced by a decrease of the "generalized ac power" in the beam which involves products of the small-signal beam-excitation amplitudes. The theorem can also be extended to thick beams.

621.385.029.6:537.533 3702
Ion Oscillations in Electron Beam Tubes; Ion Motion and Energy Transfer—R. L. Jepsen. (Proc. IRE, vol. 45, pp. 1069–1080; August, 1957.) A plausible physical picture of some possible positive-ion motions is obtained, and shows that the electric field inside the gridded drift tube may undergo one or more space reversals, leading to a mechanism for transfer of energy between beam and oscillating ions. The occurrence of fluctuating ion oscillations is not predicted.

621.385.029.6:537.533 3703
Effects of Space Charge in Crossed-Field Valves—B. Epsztein. (*C.R. Acad. Sci., Paris*, vol. 244, pp. 2902–2905; June 24, 1957.) Application of previous analysis (2568 of 1956) to the M-type carcinotron and the traveling-wave magnetron, and comparison with experimental results.

621.385.029.6:537.533 3704
Space-Charge Neutralization by Ions in Linear-Flow Electron Beams—N. C. Barford. (*J. Electronics Control*, vol. 3, pp. 63–86; July, 1957.) A theoretical analysis shows that the influence of ions may be represented by a single parameter which is a function of gas pressure, current, and collector potential. The analysis is used to find the effect of gas on the operation of a low-voltage reflection oscillator and a high-voltage klystron amplifier.

621.385.029.6:537.533:538.691 3705
Nonlaminar Flow in Cylindrical Electron Beams—K. J. Harker. (*J. Appl. Phys.*, vol. 28, pp. 645–650; June, 1957.) Experiments show that the flow from magnetically shielded cathodes is very nonlaminar. Many electrons pass periodically very near the axis of the beam and, when the focusing field is strong, at well-defined angles. This results in the distribution of transverse velocities near the axis being composed of discrete classes.

621.385.029.6:537.533:621.396.822 3706
Noise Spectrum of Electron Beam in Longitudinal Magnetic Field—W. W. Rigrod. (*Bell Sys. Tech. J.*, vol. 36, pp. 831–878; July, 1957.) Experimental measurements show that the growing noise pattern results from rippled-beam amplification of noise fluctuations over a wide band of microwave frequencies, due to intermodulation and other nonlinear processes within the gain band. Measurements in the uhf region reveal additional forms of instability.

621.385.029.6:621.3.032 3707
Wave Propagation on Multifilar Helices—H. R. Johnson, T. E. Everhart, and A. E. Siegman. (IRE Trans., vol. ED-3, pp. 18–24; January, 1956. Abstract, Proc. IRE, vol. 44, p. 716; May, 1956.)

621.385.029.63 3708
A UHF Traveling-Wave Amplifier Tube Employing an Electrostatically Focused Hollow Beam—C. B. Crumly. (IRE Trans., vol. ED-3, pp. 62–66; January, 1956. Abstract, Proc. IRE, vol. 44, p. 717; May, 1956.)

621.385.029.63:621.375 3709
Scalloped Beam Amplification—T. G. Mihran. (IRE Trans., vol. ED-3, pp. 32–39; January, 1956. Abstract, Proc. IRE, vol. 44, p. 717; May, 1956.) See also 891 of 1955.

621.385.032.213 3710
Calculation of the Anode Current from a Hollow Cathode—T. N. Chin. (*J. Appl. Phys.*, vol. 28, pp. 744–745; June, 1957.)

621.385.032.213 3711
The Dynamic Characteristics of Tungsten Cathodes—W. Ruppel and H. Seifert. (*Nachr. Tech. Z.*, vol. 10, pp. 115–119; March, 1957.) The directly heated diode is treated as a lf amplifier of heater current fluctuations. Its characteristics and life expectancy are investigated in relation to filament dimensions and operating temperature. The theoretical curves are verified by means of measurements on experimental tubes.

621.385.032.213.2:621.385.833 3712
The Bolt Cathode as Object in the Electron-Emission Microscope—Bas. (See 3624.)

621.385.032.216 3713
Secondary Electron Emission from Barium Dispenser Cathodes—I. Brodie and R. O. Jenkins. (*Brit. J. Appl. Phys.*, vol. 8, pp. 202–204; May, 1957.) A description of measurements of the total secondary electron emission coefficient, under electron bombardment, of various dispenser cathodes. Typical results are given and discussed in detail.

621.385.032.216 3714

Computer Valves and Cathode Interface Impedance—J. Seymour. (*J. Electronics Control*, vol. 3, pp. (107–125; July, 1957.) The measurement of cathode interface impedance in standard tubes and its reduction in special high-quality tubes by the use of improved sleeve materials are described.

621.385.032.24 3715

Studies on Grid Emission—G. A. Espersen and J. W. Rogers. (IRE TRANS., vol. ED-3, pp. 100–107; April, 1956. Abstract, PROC. IRE, vol. 44, p. 955; July, 1956.)

621.385.2:621.316.722.1 3716

Some Characteristics of Saturated Diodes with A.C. Heating—F. A. Benson and M. S. Seaman. (*Electronic Eng.*, vol. 29, pp. 343–347; July, 1957.) "Some characteristics of saturated diodes types 29Cl, AV33, and A2087, when operating with ac filament supplies, have been examined. The investigations have been concerned with the shapes of anode-current/anode-voltage curves, the variations of mean emission currents with the filament supply frequency and the way in which ripples superimposed on the emission currents vary with frequency and emission current. Some information is also included about the variation of response time with emission current." See also 3447 of 1955.

621.385.3:531.787:616 3717

Movable-Anode Tube—(See 3620.)

621.387:621.318.57 3718

Counters and Control Circuits with Coincidence Thyratrons—Hartmuth. (See 3416.)

MISCELLANEOUS

621.3(083.7) 3719

IRE Standards on Letter Symbols and Mathematical Signs, 1948 (Reprinted 1957)—(PROC. IRE, vol. 45, pp. 1140–1147; August, 1957.) Standard 57 IRE 21.S1.

413.164:[53+621.3 3720

The International Dictionary of Physics and Electronics [Book Review]—W. C. Michels (ed.). Publishers: Macmillan and Co., London. (*Engineering, London*, vol. 183, p. 371; March 22, 1957.)